Université de Montréal

Olefin Gateway to Substituted Proline, Lactam, and Indolizidinone Tools for Peptide Mimicry

Par

Ramakotaiah Mulamreddy

Département de chimie

Faculté des arts et des sciences

Thèse présentée à la Faculté des Études supérieures

En vue de l'obtention du grade Philosophiae Doctor (Ph.D.)

en Chimie

March 2022

Université de Montréal

Département de Chimie, Facultés des Arts et des Sciences

This Thesis titled:

Olefin Gateway to Substituted Proline, Lactam, and Indolizidinone Tools for Peptide Mimicry

Presented by

Ramakotaiah Mulamreddy

Was evaluated by a Jury composed of:

Richard Giasson

President of the Jury

William D. Lubell

Research Director

James D. Wuest

Jury Member

Marya Ahmed

External Examiner

Résumé

Les acides aminés hétérocycliques peuvent servir d'outils dans les études des relations structure-activité (RSA). Ils peuvent également jouer le rôle d'initiateurs de structure secondaire peptidique. L'incorporation d'unités d'acides aminés hétérocycliques dans des peptides peut limiter la flexibilité, améliorer l'affinité de liaison au récepteur, améliorer la sélectivité et augmenter l'activité. Parmi les acides aminés hétérocycliques, les prolines substituées, les α-amino-δ-lactames et les dérivés d'acides aminés indolizidine-2-one ont montré une utilité significative. Cependant, leurs synthèses restent difficiles.

Divers acides aminés insaturés ont déjà été synthétisés à l'aide de réactions S_N2' catalysées par le cuivre de zincate à partir de dérivés de β-iodoalanine sur des halogénures allyliques, tels que le (*Z*)-1,4-dichlorobut-2-ène, le 3-chloro-2-(chlorométhyl)prop-1-ène et (*E*)-1,3-dichloroprop-1-ène. En utilisant les oléfines résultantes comme synthons, une variété d'acides aminés hétérocycliques substitués ont maintenant été préparés via les déplacements d'halogénures et oxydations d'oléfines. Par exemple, le 2-*N*-(Boc)amino-4-(chlorométhyl)hexénoate a été utilisé dans les déplacements d'halogénures pour synthétiser la 4-vinylproline (4-Vyp), la 4-vinylornithine (4-Von) et le γ-vinyl-α-amino-δ-lactamines. De plus, des azélates de diamines insaturées ont été utilisés pour synthétiser des dérivés d'acides aminés 6-hydroxyméthyle et 5- et 7-hydroxy indolizidine-2-one (I^2aa) par des voies comportant une oxydation des oléfines. Des études par rayons X ont démontré que les résidus 6-hydroxyméthyle et 7-hydroxy I^2aa peuvent imiter la géométrie du squelette des résidus centraux des tours β de type II idéal. Le remplacement du résidu I^2aa d'un puissant modulateur de la prostaglandine-$F_{2\alpha}$ (récepteur $PGF_{2\alpha}$) (FP) par les homologues substitués en position 5, 6 et 7 a été effectué pour étudier les influences des

substituants et la géométrie du squelette sur les effets inhibiteurs sur la contractilité myométriale chez modèles de souris.

Une passerelle prometteuse pour la préparation de différents acides aminés hétérocycliques a été ouverte en utilisant des acides aminés insaturés comme synthons de départ. Dans ces voies, l'oléfine a servi comme moyen d'élargir la diversité des groupes fonctionnels sur les systèmes cycliques. L'accès à une variété de systèmes cycliques substitués a élargi la boîte à outils pour étudier les structures peptidiques à l'aide d'acides aminés hétérocycliques substitués.

Mots-clés: Catalyse au cuivre, proline 4-substituée, 4-vinylproline, α-amino-δ-lactame γ-substitué, acide aminé azabicyclo[X.Y.0]alkanone, indolizidin-2-one, iodolactonisation, prostaglandine $F_{2\alpha}$, naissances prématurées.

Abstract

Heterocyclic amino acids can serve as tools in structure-activity relationship (SAR) studies. They can also act as peptide secondary structure initiators. Incorporation of heterocyclic amino acid units into peptides can limit flexibility, improve receptor binding affinity, enhance selectivity, and augment potency. Among heterocyclic amino acids, substituted prolines, α-amino-δ-lactams, and indolizidine-2-one amino acid derivatives have shown significant utility; however, their syntheses remain challenging.

Various unsaturated amino acids have previously been synthesized using copper catalyzed S_N2' reactions of the zincate from β-iodoalanine derivatives onto allylic halides, such as (*Z*)-1,4-dichlorobut-2-ene, 3-chloro-2-(chloromethyl)prop-1-ene, and (*E*)-1,3-dichloroprop-1-ene. Employing the resulting olefins as building block, a variety of substituted heterocyclic amino acids have now been prepared by routes featuring halide displacements and olefin oxidation. For example, 2-*N*-(Boc)amino-4-(chloromethyl)hexenoate was employed in halide displacements to synthesize 4-vinylproline (4-Vyp), 4-vinylornithine (4-Von) and γ-vinyl-α-amino-δ-lactams. Moreover, unsaturated diamino azelates were employed to synthesize 6-hydroxymethyl and 5- and 7-hydroxy indolizidine-2-one amino acid (I^2aa) derivatives by routes featuring olefin oxidation. X-ray studies have demonstrated that 6-hydroxymethyl and 7-hydroxy I^2aa residues can mimic the backbone geometry of the central residues of ideal type II' β-turns. Replacement of the I^2aa residue of a potent prostaglandin-$F_{2\alpha}$ ($PGF_{2\alpha}$) receptor (FP) modulator by the 5-, 6- and 7-substituted counterparts was performed to study the influences of substituents and backbone geometry on inhibitory effects on myometrial contractility in mouse models.

A promising gateway for preparing different heterocyclic amino acids has been opened by employing unsaturated amino acid building blocks. In these routes, the olefin has served as a means

for adding functional group diversity onto the ring systems. Access to a variety of substituted ring systems has expanded the toolbox for studying peptide structures using substituted heterocyclic amino acids.

Keywords: Copper catalysis, 4-substituted proline, 4-vinylproline, γ-substituted-α-amino-δ-lactam, azabicyclo[X.Y.0]alkanone amino acid, indolizidin-2-one, iodolactonization, prostaglandin $F_{2\alpha}$, preterm birth.

Author Contributions

This thesis is formatted in the form of publications and author contributions are presented below.

All the following chapters were written by me and edited by Professor William D. Lubell.

Chapter 1 (Introduction).

Chapter 2 (Article1) entitled "4-Vinylproline" was published in The Journal of Organic Chemistry (*J. Org. Chem*., 2018, *83*, 13580–13586). The concept of this project work was designed by Professor W. D. Lubell, with assistance from N. D. Prasad Atmuri and me. All the experiments, analysis, and structural elucidations of all the compounds in this publication were performed in a collaborative way by N. D. Prasad Atmuri and me. The manuscript was written by N. D. Prasad and me and edited by Professor W. D. Lubell.

Chapter 3 (Article2) entitled "Constrained Glu-Gly and Gln-Gly dipeptide surrogates from γ-substituted α-amino-δ-lactam synthesis" was published in the journal of Peptide Science (*Peptide Sci*. 2020, *112*, e24149). The concept of this project was designed by Professor W. D. Lubell and me. All the experiments, analyses, and structural interpretations of all compounds were performed by me. The manuscript was written by me and edited by Professor W.D. Lubell.

Chapter 4 (Article 3) entitled "6-Hydroxymethyl Indolizidin-2-one Amino Acid Synthesis, Conformational Analysis, and Biomedical Application as Dipeptide Surrogates in Prostaglandin-$F_{2\alpha}$ Modulators" was published in the journal Organic Letters (*Org. Lett*. 2021, *23*, 5192-5196). The concept of this project was designed by Professors W. D. Lubell and S. Chemtob, with my contribution. All the syntheses, chemical analyses, and structural interpretations of all compounds were performed by me. Crystals obtained by me were analyzed using X-ray diffractometry by Dr. Thierry Maris at the regional center for X-ray crystallography of the Université de Montreal. Dr.

Xin Hou performed all the biological experiments under the guidance of Professor Sylvain Chemtob in the Département de pédiatrie, Université de Montréal. The manuscript was written by me with contributed text from Dr. Xin Hou and edited by Professors W. D. Lubell and S. Chemtob.

Chapter 5 (Article 4) entitled "Constrained Dipeptide Surrogates: 5-and 7-Hydroxy Indolizidin-2-one Amino Acid Synthesis from Iodolactonization of Dehydro-2, 8-diamino Azelates" was published in the journal Molecules (*Molecules* 2022, *27*, 67). The concept of this project was designed by Professor W. D. Lubell and me. All the experiments, analyses, and structural interpretations of all compounds were performed by me. Crystals obtained by me were analyzed using X-ray diffractometry by Dr. Daniel Chartrand at the regional center for X-ray crystallography of the Université de Montreal. The manuscript was written by me and edited by Professor W. D. Lubell.

Chapter 6, the conclusion, and perspectives of this thesis was written by me and edited by Professor W. D. Lubell.

Table of Contents

List of Figures

List of Schemes

List of Tables

List of Abbreviations

SRIF	somatotrophin release inhibiting factor
IC_{50}	inhibitory concentration
Ki	inhibitor constant
μM	micromolar
m	multiplet (spectral)
LCMS	liquid chromatography mass spectrometry
$[\alpha]_D$	optical rotation
MW	molecular weight
NMR	nuclear magnetic resonance
M	molar
Me	methyl
mg	milligram
min	minutes
MHz	megahertz
mL	millilitre
mmol	millimole
mp	melting point

IR	infrared
J	coupling constant
ppm	parts per million
R_f	retention factor in chromatography
s	singlet
t	triplet
DMSO-d_6	hexadeuterodimethyl sulfoxide
br	broad (spectral)
LHMDS	lithium hexamethyldisilazane
ee	enantiomeric excess
HRMS	high-resolution mass spectrometry
Dmb	2,4-dimethoxybenzyl
PhF	9-(9-phenylfluorenyl)
RCM	ring closing metathesis
FP	prostaglandin-$F_{2\alpha}$ receptor
$PGF_{2\alpha}$	prostaglandin-$F_{2\alpha}$
THF	tetrahydrofuran
TLC	thin layer chromatography

m-CPBA	*meta*-chloroperbenzoic acid
DIEA	diisopropylethylamine
DMF	*N*, *N*-dimethylformamide
Fmoc	9-fluorenylmethyloxycarbonyl
TBTU	2-(1H-benzotriazole-1-yl)-1,1,3,3-tetramethylaminium tetrafluoroborate
Vyp	vinylproline
Von	vinylornithine
I^2aa	indolizidine-2-one amino acid
BTD	β-turn dipeptide
Hyp	hydroxyproline
TBHP	*tert*-butyl hydroperoxide
$(Boc)_2O$	di-*tert*-butyl dicarbonate
COMU	(1-cyano-2-ethoxy-2-oxoethylidenaminooxy)dimethylaminomorpholinocarbenium hexafluorophosphate
TEMPO	(2,2,6,6-tetramethylpiperidin-1-yl)oxyl
TFA	trifluoracetic acid
DIBALH	diisobutylaluminium hydride
KHMDS	potassium bis(trimethylsilyl)amide

Acknowledgements

First and foremost, I would like to thank my research director Prof. William D. Lubell, who has guided me with his valuable suggestions throughout my Ph.D. study at the Université de Montréal. I am very thankful for the opportunity to work in his laboratory and benefit from his expertise. His continuous help in solving research problems was exceptional. Although my graduate studies were not easy, his trust in me allowed me to have the level of confidence and the knowledge I have today. He continues to encourage me to overcome my limits and develop the ability to think about my project as a global aspect. Finally, without his support and encouragement my Ph.D. thesis completion would be not possible. Thank you, Bill, you gave me much advice and many joyful memories which I will never forget.

I would also like to thank my committee members, Professors James D. Wuest and Richard Giasson for their suggestions and guidance throughout my Ph.D. study at the Université de Montréal.

I thank the Department of Chemistry administration staff. My sincere thanks go to the analytical teams: Dr. Alexandra Furtos, Karine Gilbert, Marie-Christine Tang and Louiza Mahrouche for HRMS and LCMS analyses in the Regional Laboratory for Mass Spectrometry, Dr. Pedro Aguiar, Dr. Cedric Malveau, Sylvie Bilodeau and Natalie Baho for NMR analyses in the Regional Laboratory for NMR Spectroscopy, Dr. Thierry Maris, and Dr. Daniel Chartrand for X-ray analyses in the Regional Laboratory for X-ray Diffractometry at the Université de Montréal.

I am grateful for the efforts of my biological collaborators for their contribution in the *ex vivo* studies of my compounds, Professor Sylvian Chemtob, and Dr. Xin Hou.

I thank my current and previous group members, Dr. Prasad Atmuri, Dr. Pradeep Chauhan, Dr. Ayyoub Selka, Yousra Hamdane, Minh Thao, Xiaozheng Wei, Charity Yongo-Luwawa, and others.

My sincere thanks go to Yousra Hamdane and Charity Yongo-Luwawa for their help in the writing of my thesis abstract in French.

I want to extend my thanks to the funding agencies for their support in my research including Natural Sciences and Engineering Research Council (NSERC), the Canadian Institutes of Health Research (CIHR), NSERC-CIHR for funding the collaborative Health Research Project "Treatment of Preterm Birth with Prostaglandin F_{2a} Receptor Modulators", the Fonds de recherche nature et technologie Quebec for the Centre in Green Chemistry and Catalysis (FRQNT-2020-RS4-265155-CCVC), and the Université de Montréal. I am grateful to the Faculté des Etudes Supérieures et Postdoctorales (FESP) of the Université de Montréal for a tuition fee exemption, and to NuChem Sciences in Montréal for an industrial scholarship for the year 2021-2022.

I am forever indebted to my family for their care, moral support, and love during my Ph.D. study. I am especially grateful for the efforts of my parents (Nagireddy and Ramulu), brother Sudhakarareddy, grandmother Venkatamma, Uncle Subbareddy Gujjula, and extended family members. I would like to dedicate my Ph.D. thesis to my beloved wife, Koteswaramma Singam and my son, Gautham Nanda Mulamreddy.

Chapter 1: Introduction

1.0 Introduction

1.1 Peptides and applications

Peptides serve roles in many biological functions. More than 7000 naturally occurring peptides have been identified in the human body.[1] Among biological activities, peptides participate as regulators of transduction, heart rate, food intake, and growth.[1,2] Over the last two decades, peptides have emerged as important tools in several fields including medicine,[3] cosmetics,[4] materials science, [5]and agriculture. [6]

The field of peptide therapeutics started with the treatment of type 1 diabetes using insulin, which was isolated from animal pancreases in 1922.[7] Currently, metabolic diseases and oncology are major areas focussed on the use of peptide based therapeutics. For example, the long-acting insulin Lantus ™ (Sanofi) for treating diabetes, and the peptide-based prostate cancer treatment Lupron ™ (Abbott) gained respectively US $7.9 billion in 2013 and US $2.3 billion in 2011 from global sales.[8] Relative to small molecules and biological therapeutics, peptide medications have taken 5% of the global market.[7] The peptide drug market was valued at US $32.1 billion in 2020.[9] Demand for peptide drugs is likely to increase due to their diverse biological activities, high potency and low cytotoxicity.

1.2. Limitations of peptides as therapeutics

In spite their growing market and approvals in various therapeutic indications, limitations restrict the use of peptides as drugs. Drawbacks inherent in the physical and chemical properties of peptides include: a) low oral bioavailability, b) low metabolic stability, c) low membrane permeability, d) short half-life and e) lack of selectivity.[10] Many of these limitations are due to the intrinsic flexibility of the polypeptide chain.[10] In addition, other factors, such as aggregation, denaturation, and limited surface adsorption, may restrict peptide absorption *in vivo*.[11]

1.3. Peptide secondary structures

Polypeptides in solution and in proteins adopt common motifs stabilized by hydrophobic collapse and intramolecular hydrogen bonding which restrict the backbone conformation.[12] The term secondary structure is used to characterize such motifs, among which the most common are α-helices, β-strands and β-turns. The backbone dihedral angles (ϕ, ψ, and ω, Figure 1.1) serve to define the geometry of such secondary structures, which play important roles in the recognition and activity of peptides. The ω dihedral angle of the peptide bonds that links amino acid residues is typically constrained to a value around 180°, due to amide resonance. Side chain orientation is similarly specified using the torsion angle χ and can also influence peptide biology.[13] As discussed below, the relevance of such polypeptide conformations for biological activity is a key element in the design of molecules that can mimic peptide shape and function.

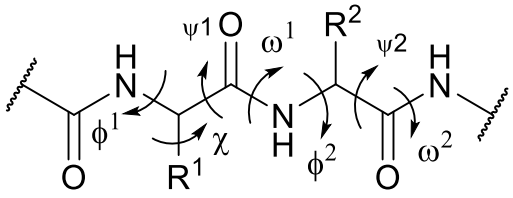

Figure 1.1. Peptide backbone dihedral angles ϕ, ψ, and ω, and side chain torsion angle χ

The α-helix is the most common secondary structure in peptides and proteins. α-Helices account for more than 40% of the conformations of natural polypeptides.[14] The β-strand is the second most abundant secondary structure.[14] α-Helices and β-strands are respectively stabilized by hydrogen bonds within the same peptide strand and between adjacent strands.[15] Turn conformations are the third most prominent secondary structure in peptides and account for 25% of all structural motifs.[16] β-Turns create a loop in the peptide strand that positions the α-carbons

of the first (*i*) and fourth (*i* +3) residues at a distance of less than 7Å.[17] A 10-membered hydrogen bond may exist between the N-H and C=O of the *i* and *i* + 3 residues (Figure 1.2).

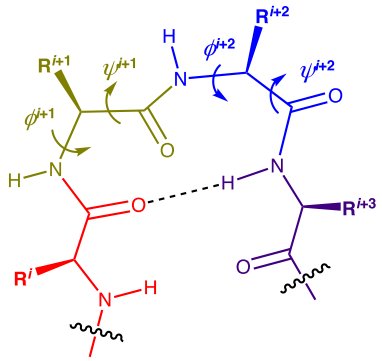

Figure 1.2. β-Turn peptide secondary structure

β-Turns are sometimes referred to as reverse turns.[16] They are key structural motifs in biological processes implicating protein-protein interactions.[14] β-Turns have been classified according to the values of their central residue ϕ and ψ dihedral angles (Figure 1.2 and Table 1.1).[18]

Table. 1.1. β-Turn types and their central residue (*i*+1 and *i*+2) dihedral angles

Type of secondary structure		ϕ^{i+1}, deg	ψ^{i+1}, deg	ϕ^{i+2}, deg	ψ^{i+2}, deg
β-turns	I	-60	-30	-90	0
	I’	60	30	90	0
	II	-60	120	80	0
	II’	60	-120	-80	0
	VIa1	-60	120	-90	0
	VIa2	-120	120	-60	0
	IV	-61	10	-53	17
	VIb	-135	135	-75	160
	VIII	-60	-30	-120	120

1.4. Peptide mimicry

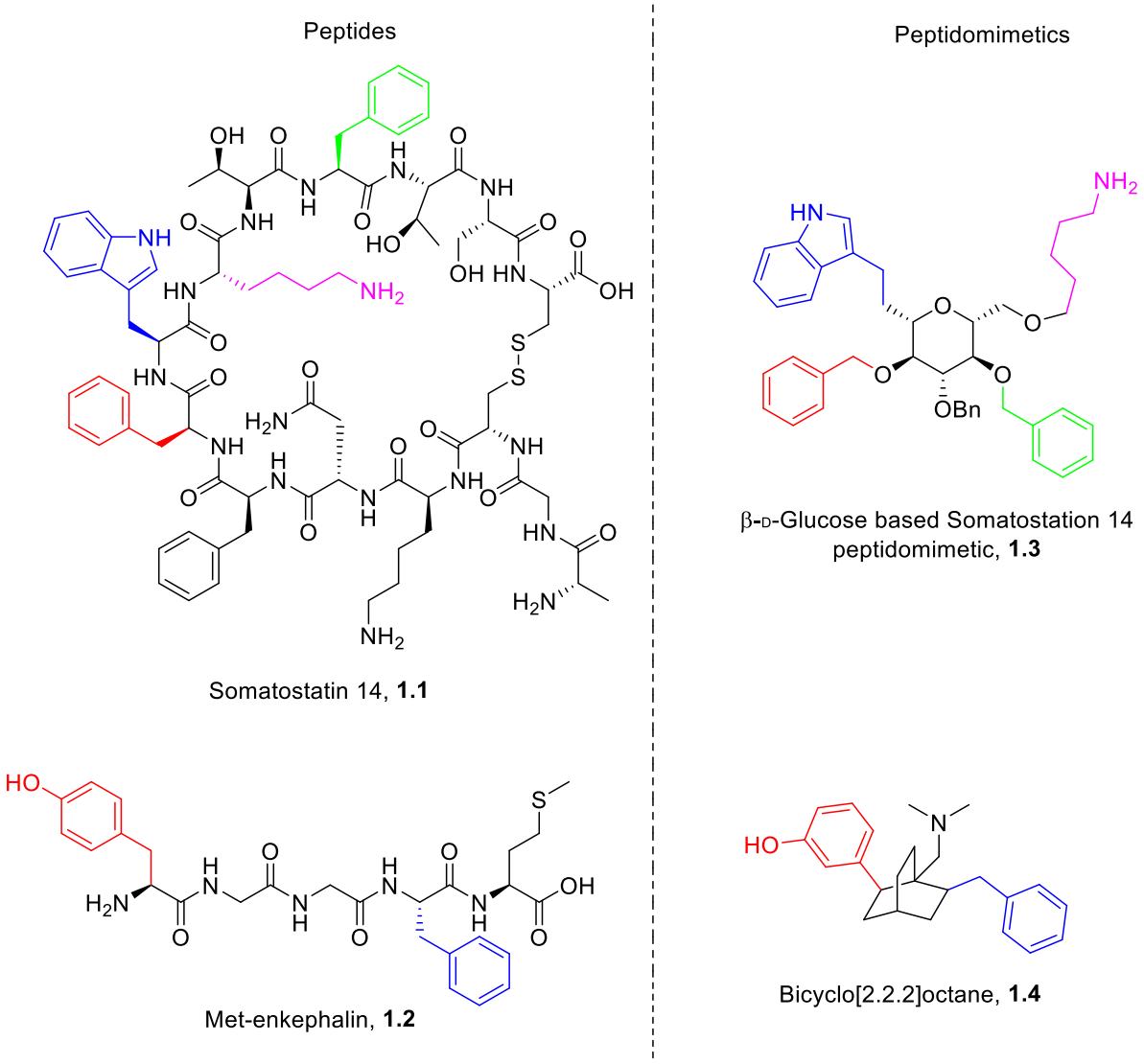

Figure 1.3. Mimicry of whole peptides by small molecule peptidomimetics[19,20]

To overcome limitations for applications in drugs, medicinal chemists have pursued designs of molecules that mimic the form and function of peptide structures. Such peptidomimetics can replicate bioactive conformers, enhance metabolic stability and improve receptor affinity and selectivity.[21] In notable examples, entire peptides have been replaced by small molecule mimics.[19] For example, β-D-glucose derivative **1.3** (Figure 1.3) was created as a mimic of the cyclic

tetradecapeptide hormone somatostatin-14 (**1.1**, somatotrophin release inhibiting factor, SRIF), which exhibits inhibitory activity on the release of growth hormone, gastric acid and insulin.[22] Biological evaluation demonstrated that β-D-glucose derivative **1.3** exhibited lower binding affinity (IC_{50} 15 mM) to AtT20-cells expressing SRIF receptors compared to the parent peptide **1.1** (0.83 nM).[23] At higher concentrations, β-D-glucose derivative **1.3** exhibited binding affinity and antagonized the neurokinin-1 (NK1) receptor for substance P (SP).[24] Moreover, bicyclo[2.2.2]octane **1.4** was conceived by the Merck laboratories in Montréal as a peptide mimic of the naturally occurring opioid pentapeptide Met-enkephalin **1.2** and shown to have analgesic properties.[25] Bicyclo[2.2.2]octane **1.4** exhibited lower binding affinity (IC_{50} of 225 nM) compared to Met-enkephalin **1.2** (IC_{50} of 9.0 nM) in a ^{3}H-naloxone competition assay.[20]

1.5. Covalent constraint in peptide mimic design

Restriction of the flexibility of linear peptides to specific conformers such as β-turns can improve receptor binding affinity.[26] The introduction of heterocyclic motifs into linear peptides has enhanced binding affinity and potency. Such heterocycles could act as pharmacophores as well as stabilize particular secondary structures in polypeptides (Figure 1.4).[27]

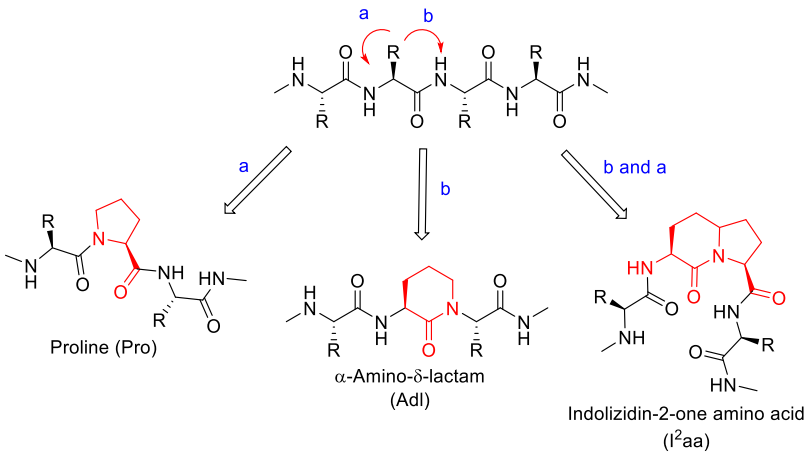

Figure 1.4. Examples of heterocycles that constrain peptide conformation

A common approach for peptide mimicry entails joining specific portions of the peptide using covalent constraints which favour specific conformers. For example, the natural amino acid proline restricts the peptide backbone to specific orientations. In proline, the side chain and amine are cyclized in a pyrrolidine ring which constrains the ϕ dihedral angle to values around –60°.[28] Proline is favoured at the *i*+1 and *i*+2 position of β-turn conformations in peptides. In the natural antibiotic Gramicidin S (**1.5**, Figure 1.5), proline adopts the *i*+1 position of a type II' β-turn.[16,29] Moreover, several peptide-based pharmaceutical products possess proline components, such as in the angiotensin converting enzyme (ACE) inhibitor Lisinopril 1.6.[30,31]

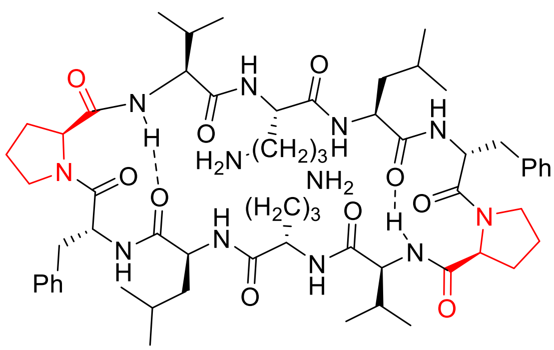

1.5, Gramicidin s
Antibiotic

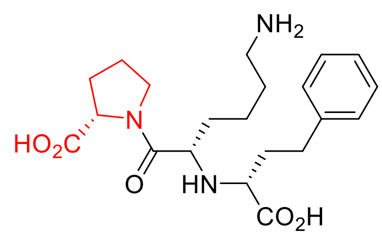

1.6, Lisinopril
ACE inhibitor

Figure 1.5. Importance of proline in turn conformation and as therapeutic drug in small molecule

Cyclization of an amino acid side chain to the amine of the *C*-terminal residue in a peptide introduces an α-amino-lactam residue which restricts the ψ dihedral angle. α-Amino lactams of different ring sizes have served as a conformationally rigid dipeptide surrogates in the study of various biologically active peptides.[32] For example, a series of α-amino lactam dipeptides were used in the development of inhibitors of interleukin-1β (IL-1β) converting enzyme (ICE), which cleaves a precursor protein to provide the proinflammatory cytokine.[33] Targeting the treatment of inflammatory diseases such as arthritis, the tetrapeptide acetal **1.7** (L-709,049) was shown to

inhibit ICE with 0.0046 mM activity against the murine ICE. Towards the synthesis of small molecule ICE inhibitors, the *N*-Ac-Tyr-Val-Ala portion of peptide **1.7** was replaced with rigid dipeptides possessing 5-7-membered *N*-(Cbz)amino-lactams (e.g., **1.7a-e**, Figure 1.6).[34] The 5- and 6-membered α-amino-lactams **1.7a-c** had reduced inhibitory activity (>10, 3.7, 37.0 mM respectively) against ICE relative to the linear tetrapeptide **1.7**. In the case of azepinones **1.7d** and **1.7e** better inhibitory activity (1.68 and 0.186 mM respectively) was demonstrated than 5- and 6-membered counterparts.

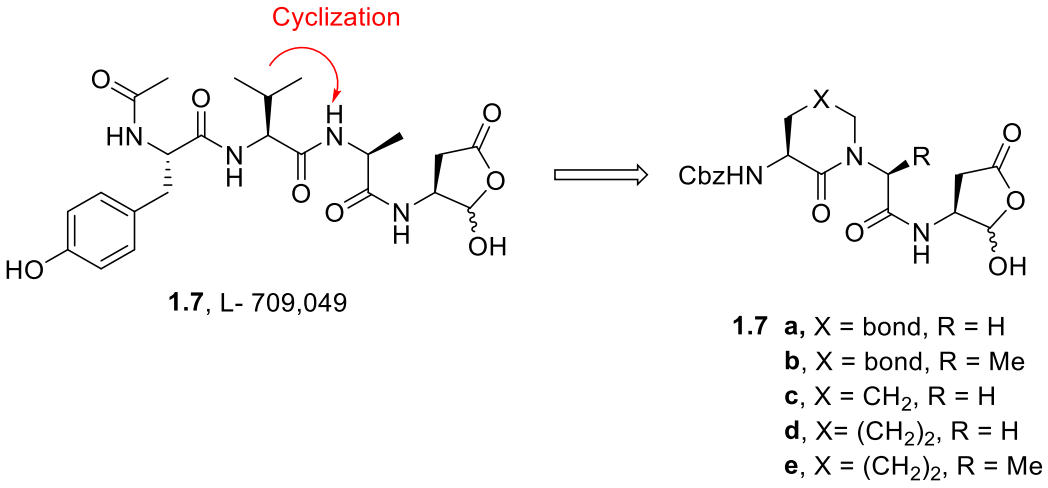

Figure 1.6. Role of different ring size lactams in ICE inhibitors

The combination of proline-like and lactam constraints in a dipeptide has been used to create azabicyclo[X.Y.0]alkan-2-one amino acid residues, which restrict the central ψ and ϕ dihedral angles of the neighbouring residues.[35] Azabicyclo[X.Y.0]alkanone amino acids have been similarly used to restrain the backbone conformation of biologically active peptides in analogs with improved selectivity and potency.[35] Contingent on backbone stereochemistry azabicyclo[X.Y.0]alkan-2-one amino acid residues can mimic the central residues of type II' β-

turn secondary structures as demonstrated by X-ray crystallography and NMR spectroscopy (Figure 1.7).

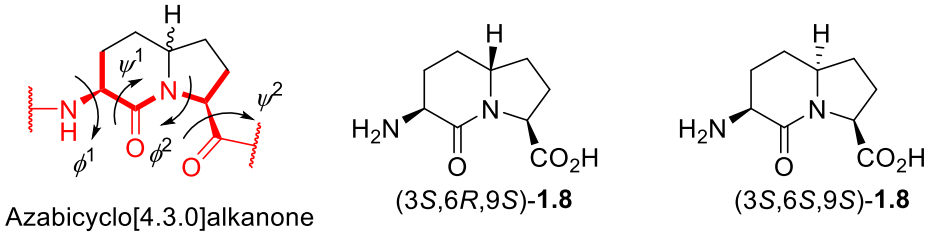

Figure 1.7. Azabicyclo[4.3.0]alkan-2-one amino acids

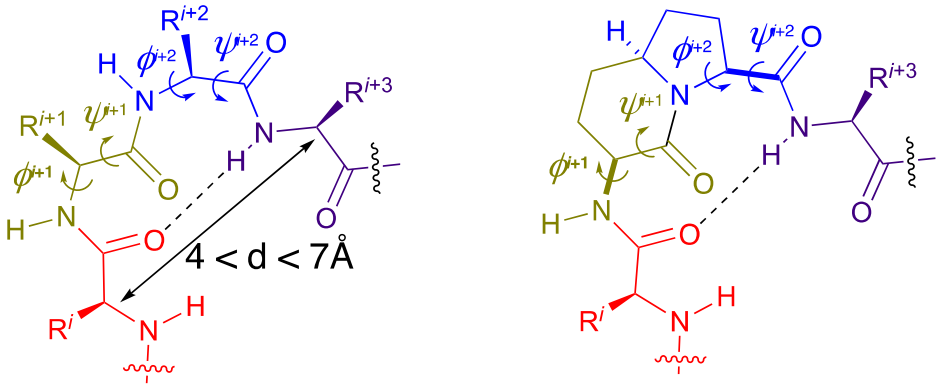

Figure 1.8. β-Turn secondary structure in I^2aa

Azabicyclo[4.3.0]alkan-2-one amino acid residues, so called indolizidin-2-one amino acids (I^2aa) are among the most well studied of this class of dipeptide surrogates. A combination of α-amino δ-lactam and proline moieties, the I^2aa residue can similarly restrict the ψ and ϕ backbone dihedral angles upon introduction into biologically active peptides. Contingent upon stereochemistry, I^2aas residues can fold peptides into β-turn secondary structures (Figure 1.8).[35,36] For example, nociceptin/orphanin FQ **1.9** is a linear neuropeptide which acts as an agonist and binds (*K*i 0.10 nM) on the opioid receptor like 1 (ORL1) receptor.[37] The application of the I^2aa residue as a rigid dipeptide provided hexapeptide **1.10**, which retained binding affinity (*K*i 44 nM) on hORL1 in Chinese hamster ovary cells (Figure 1.9).[38]

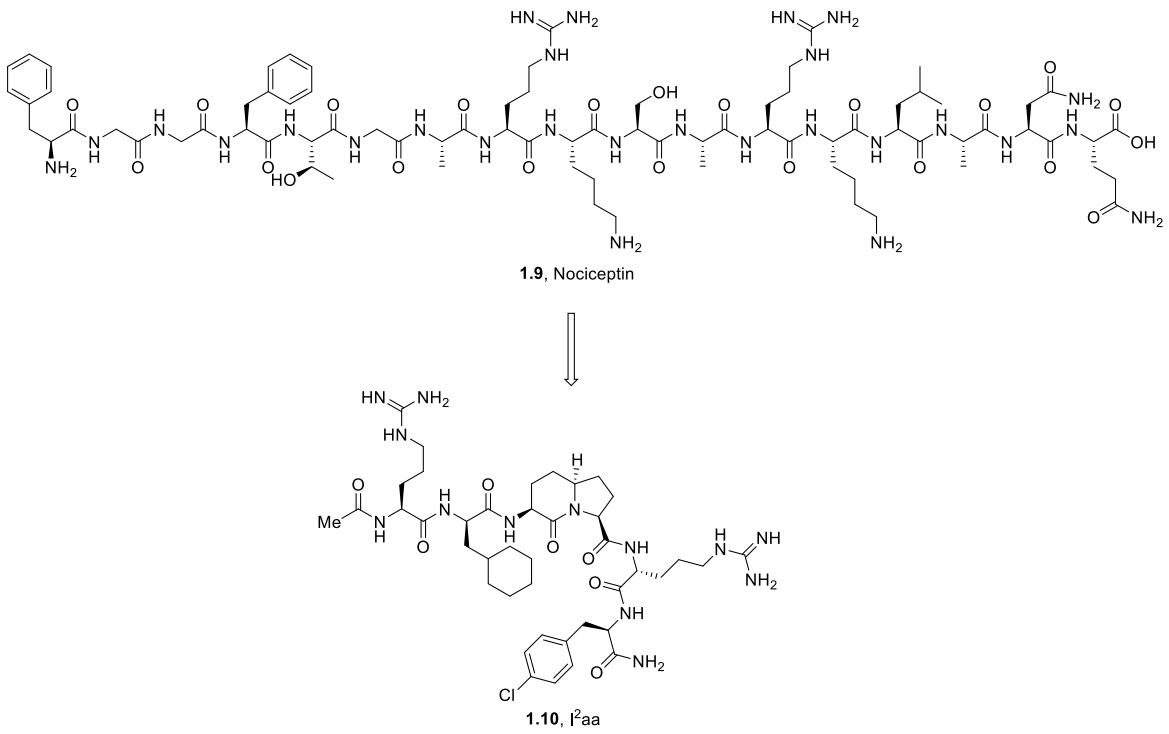

Figure 1.9. Application of I^{2}aa residue to synthesize a mimic of the linear peptide Nociceptin

1.5.1. I^{2}aa analog synthesis

The synthesis of the parent I^{2}aa structure was first accomplished by a diastereoselective approach employing the Schöllkopf alkylation of bis-lactim **1.11** with diiodide **1.12** (Scheme 1.1). Hydrolysis provided diaminoazelate **1.13** as a separable mixture of diastereomers in the ratio of 16:8:1.[39] A mixture of Cbz-I^{2}aa-OMe diastereomers **1.14** was obtained by ketal cleavage, reductive amination under hydrogenation conditions, lactam cyclization and amine protection. Column chromatography afforded Cbz-I^{2}aa-OMe diastereomers (3*S*,6*S*,9*S*)-**1.14** (34%), (3*R*,6*R*,9*R*)-**1.14** (4%), and racemic of **1.14** (28%).[39]

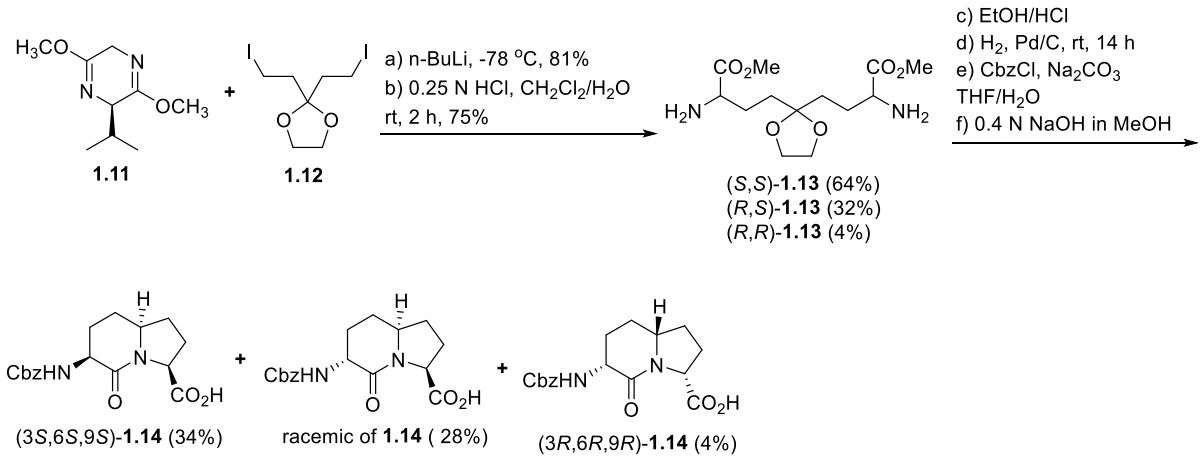

Scheme 1.1. Schöllkopf alkylation approach to I^2aa diastereomers

Selective synthesis of the parent I^2aa diastereomers with control over ring fusion stereochemistry was later achieved by a route employing glutamic acid as chiral educt (Scheme 1.2).[40] Claisen condensation of *N*-(PhF)glutamate diester **1.15a** and **1.15b**, ester hydrolysis and decarboxylation provided symmetrical 5-oxo azelate **1.16a** and **1.16b** after purification with overall yields of 75% and 51%, respectively. Two pathways were used to convert azelates **1.16** into protected I^2aa analogs. In a reductive amination approach, hydrogenation of di-*tert*-butyl 5-oxo azelate **1.16a** using Pd/C in 9:1 EtOH:AcOH gave a 5-substituted proline intermediate. Ester cleavage in 6N HCl, esterification and lactam formation using MeOH/HCl, followed by $(Boc)_2O$ protection and chromatography afforded respectively diastereomeric (3*S*,6*S*,9*S*)- and (3*S*,6*R*,9*S*)-Boc-I^2aa-OMe [(3*S*,6*S*,9*S*)- and (3*S*,6*R*,9*S*)-**1.17**] in 67% and 2% overall yields. A similar route using dimethyl azaelate **1.15b** provided respectively (3*S*,6*S*,9*S*)- and (3*S*,6*R*,9*S*)-**1.17** in 81% and 2% overall yields.

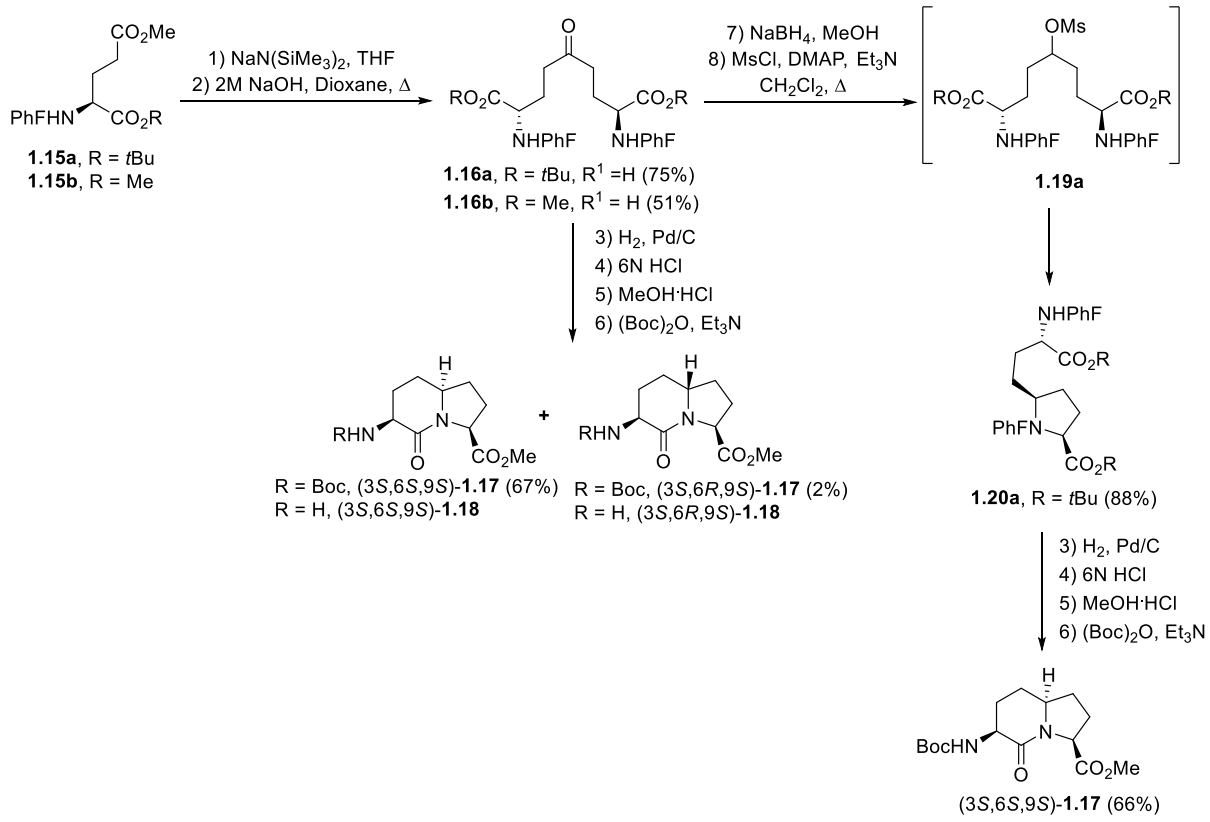

Scheme 1.2. Claisen condensation and intramolecular mesylate displacement approaches to I^2aa diastereomers

Alternatively, (3*S*,6*S*,9*S*)-Boc-I^2aa-OMe [(3*S*,6*S*,9*S*)-**1.17**] was prepared as a single diastereomer by a route featuring intramolecular displacement of mesylate **1.19a**, which was obtained by reduction of 5-oxo azelate **1.16a** using $NaBH_4$ and activation with methanesulfonyl chloride (Scheme 1.2). The resulting 5-substituted proline **1.20a** was converted to I^2aa (3*S*,6*S*,9*S*)-**1.17** by a route similar to that described above involving hydrogenolytic cleavage of the PhF protection, *tert*-butyl ester cleavage, esterification and $(Boc)_2O$ protection .[40]

1.6. Side chain mimicry

The addition of functional groups onto the proline-like, lactam and azabicyclo[4.3.0]alkan-2-one amino acid ring systems has been explored to provide analogs that constrain both the

backbone and side chains of peptide structures.[32] Contingent on location, ring size and stereochemistry, such functional groups can enhance binding affinity of the peptide analogs by improving interactions with sites on the receptor. In the interest of studying structure-activity relationships of peptides, a variety of methods have been developed for the synthesis of such conformationally constrained peptidomimetics.[35]

1.6.1. Substituted prolines

The pyrrolidine ring in proline moiety is key structural motif for initiation of secondary structures in proteins and biologically active peptides. Moreover, the cyclic nature of proline (**1.21**) has impacted on the activity of peptide therapeutic drugs.[41] Proline residues have been designed with substituents at each of the different ring positions. Substituents can give rise to conformational changes with respect to *endo* and *exo* ring puckering as well as *N*-terminal amide (prolyl amide) *cis* and *trans* isomers.[42]

Substituted prolines, such as 4-hydroxyproline, have been isolated as components of natural products.[43] For example, the α-substituted quaternary amino acids are useful scaffolds in peptides to improve the resistance against chemical and enzymatic degradation.[44] (2*R*)-Methyl proline **1.21b** is a key intermediate in the synthesis of Veliparib which is an anti-cancer drug (Figure 1.10).[45] The method involving self-reproduction of chirality, which was developed by Seebach, has been used to add substituents to the 2-position of proline (e.g., **1.21a** and **1.21c-1.21f**).[46]

Among the 3-substituted prolines, 3-methyl examples (3*R*)-**1.21g** and (3*S*)-**1.21j** are found respectively in the natural products Bottromycin A2, which was isolated from *Streptomyces species*,[47] and Roseotoxin B from the fungus *Trichotheceum roseum*.[48] Both *cis*- and *trans*-3-hydroxy prolines (**1.21h** and **1.21k**) are fragments of the cyclic peptide antibiotic Telomycin from

Streptomyces species,[49] and *cis*- 3-amino proline **1.21i** was isolated from the mushroom *Morchella esculenta* (Figure 1.10).[50]

Among the 4-substituted prolines, 4-oxoproline **1.21l** is a component of Actinomycin X_2 which was isolated from *Streptomyces chrysomallus* and exhibits potent activity against methicillin-resistant Staphylococcus aureus (MRSA).[51] After the discovery from a gelatin hydrolysate in 1902, (2*S*,4*R*)-*trans*-4-hydroxyproline (**1.21m**) was shown to be a component of collagen.[52] Isomeric (2*S*,4*S*)- and (2*R*,4*R*)-*cis*-4-hydroxyproline (**1.21n** and **1.21o**) have been respectively shown to be components of the cytotoxic lipopentapeptide Majusculamide D[53] and the cyclic depsipeptide antibiotic Viridogrisein (Figure 1.10).[54]

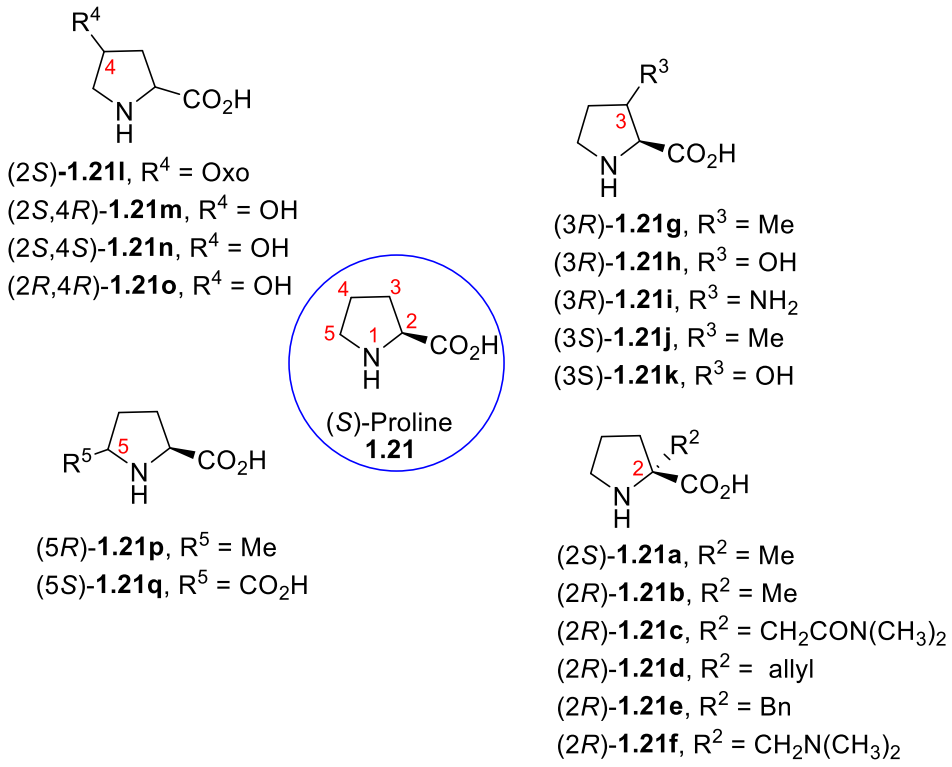

Figure 1.10. Proline derivatives with different ring substituents[46,47-50,51-54,55-56]

Finally, 5-methylproline (**1.21p**) is a component of the chromodepsipeptide antibiotic Actinomycin Z_5 isolated from the *Streptomyces fradiae*.[55] *trans*-5-Carboxylproline (**1.21q**) was isolated from the seaweed *Schizymenia dubyi* (Figure 1.10).[56] In sum, nature has created an abundant variety of substituted prolines.

Among the most well studied of substituted prolines, those with 4-position substituents are in abundance due primarily to the significance of natural (2*S*,4*R*)-*trans*-hydroxyproline.[57] 4-Hydroxyproline (Hyp) is a secondary structure initiator in collagen, a triple helix coiled-coil peptide structure. The importance of collagen in the extracellular matrix found in connective tissues has evoked the synthesis and use of 4-substituted prolines to explore factors influencing the stability and activity of this most abundant mammalian protein.[42]

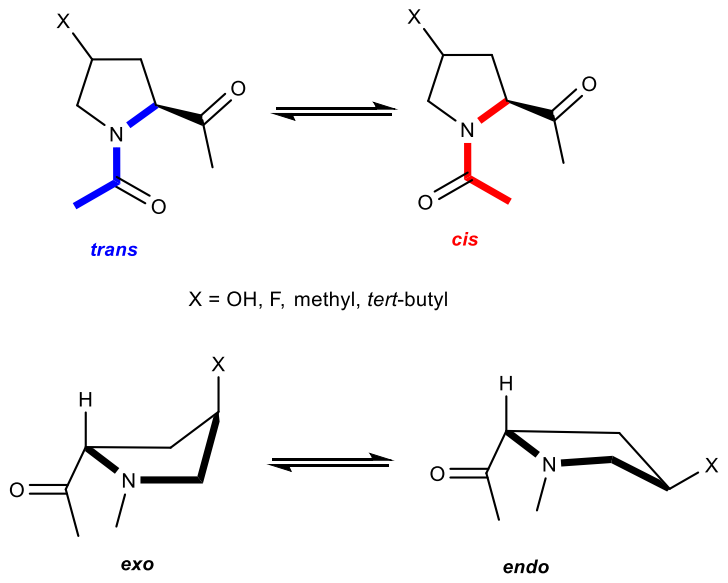

Figure 1.11. Steric and stereoelectronic factors can affect the ring pucker and prolyl amide isomer equilibrium of 4-substituted prolines

4-Substituted prolines alter the *exo* and *endo* ring puckering by steric and stereoelectronic effects contingent on structure and stereochemistry (Figure 1.11).[57] Sterically bulky groups, such

as methyl, *tert*-butyl, on the same or opposite face of the pyrrolidine ring as the α-carboxylate favor respectively the *exo* and *endo* puckering.[58,59] Electron withdrawing groups, such as fluorine and hydroxyl substituents, on the same or opposite face of the pyrrolidine ring as the α-carboxylate cause stereoelectronic effects such that the *endo* and *exo* puckering are respectively favoured.[57] Hyperconjugation from interactions in the *gauche* conformation between the electron withdrawing group and ring nitrogen favour the respective ring puckering contingent on stereochemistry. In addition, the *trans* amide bond was adopted by *exo* ring pucker and in the other case, *cis* amide bond was stabilized by *endo* ring pucker.[42] Similarly, the *endo*/*exo* ring puckering of prolines prefers to have dihedral angle values of $\phi = -75^{o}/-60^{o}$ and $\psi = 164^{o}/152^{o}$ respectively.[60]

1.6.2. Synthesis of 4-substituted prolines

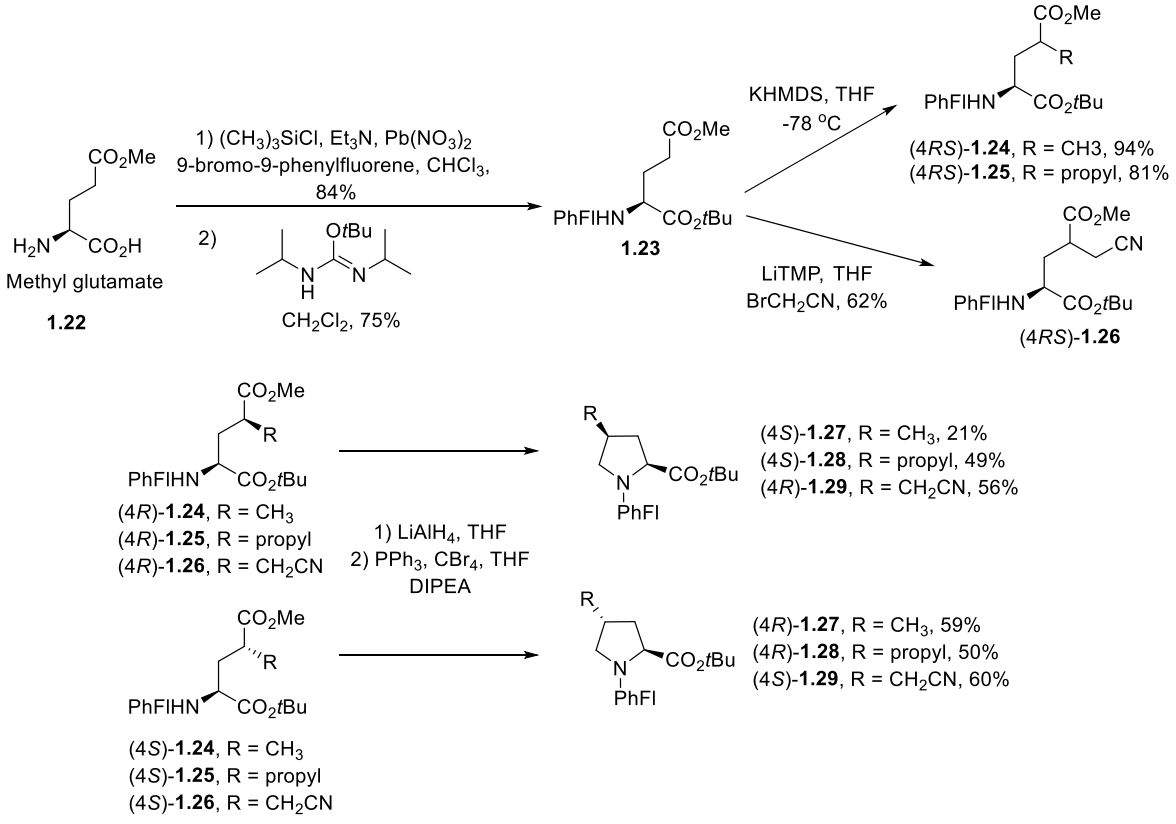

Scheme 1.3. Synthesis of protected 4-alkyl prolines[62]

Many approaches to make 4-substituted prolines have been pursued due in part to the importance of 4-substituted prolines in nature[43] and as conformation controlling elements.[42] Many of these syntheses employ 4-hydroxyproline as chiral educt.[61] Alternatively, glutamic acid was employed as chiral educt in the synthesis of 4-alkyl (2*S*,4*R*)- and (2*S*,4*S*)-proline derivatives (Scheme 1.3). The *N*-9-phenylfluorenyl (PhF) glutamate diester **1.23** was selectively deprotonated to form the γ-ester enolate using KHMDS. Alkylation at the γ-position afforded separable mixtures of diastereomers **1.24-1.25**. Pyrrolidine formation was achieved by a cyclization sequence featuring reduction of the γ-ester using lithium aluminium hydride followed by intramolecular nucleophilic substitution using PPh_3 and CBr_4, which provided 4-substituted prolines **1.27-1.29**.[62] Inspired by this application of an alternative amino acid other than 4-hydroxyproline as chiral educt for making 4-substituted prolines, in Chapter 2, we reported a synthesis of enantiomerically pure 4-vinylprolines using serine as chiral educt.[63]

1.6.3. Substituted α-amino lactams

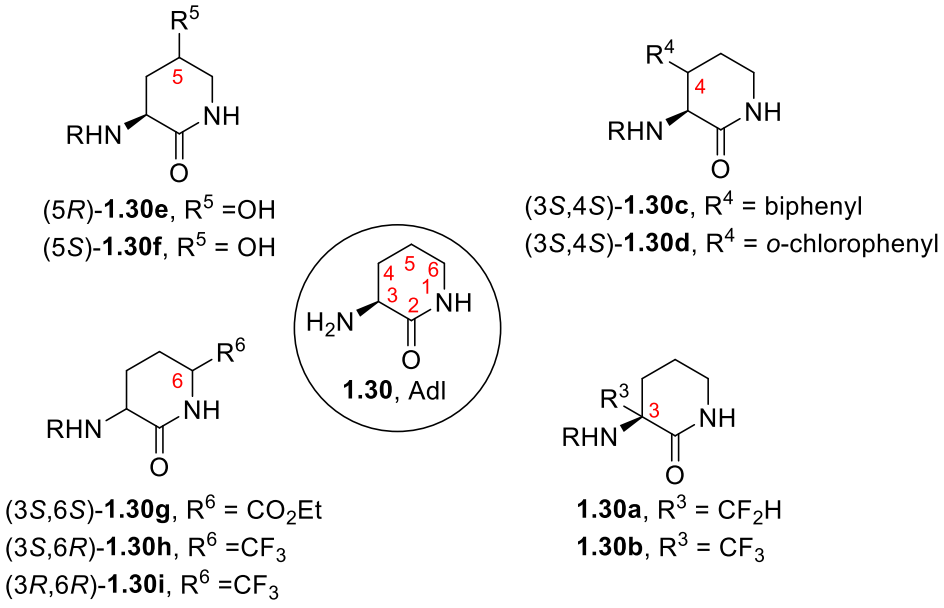

Figure 1.12. Substituted Adl derivatives[68-73]

Like prolines, α-amino lactams have been modified with various ring substituents for various applications.[64] In peptides, substituted α-amino lactams offer potential to restrain both the backbone and side chain of amino acid residues in secondary structures, such as β-turns.[65] The synthesis and importance of substituted α-amino γ- and ε-lactams have been reviewed.[66,67] Examples of the corresponding substituted α-amino δ-lactam (Adl) residues include 3-difluoromethyl analog **1.30a**. Ring opening of δ-lactam **1.30a** provided α-difluoromethylornithine (DFMO), which has been used to treat African sleeping sickness as well as to remove unwanted facial hair.[68] 3-Trifluoromethyl Adl **1.30b** has been used in the core of thalidomide analogs.[69] 4-Substituted Adl derivatives **1.30c-d** have served as constrained phenylalanine analogs in the synthesis of renin inhibitors.[70] 5-Hydroxy Adl diastereomers **1.30e-f** exhibit anthelmintic activity.[71] 6-Ethylcarboxylate **1.30g** was synthesized as a turn mimic,[72] and 6-trifluoromethyl Adl analogs **1.30h-i** have been studied as thalidomide derivatives (Figure 1.12).[73]

Substituted Adl analogs have also been used to study biologically active peptides.[32] For example, 4,5-dihydroxy α-amino-δ-lactam was used to replace the serine residue of the cytostatic cyclic peptide Stylostatin 1 (**1.31**, Figure 1.13) from the marine sponge *Stylostella aurantium sp*.[74] Incorporation of the substituted Adl residue limited the corresponding ψ dihedral angle.[75] In studies against K-652 leukemia cells, Adl surrogate **1.32** retained growth inhibitory activity (GI_{50} 3.59 mM) similar to Stylostatin 1 (**1.31**, 3.42 mM) indicating the biologically active conformer of the natural peptide.[76]

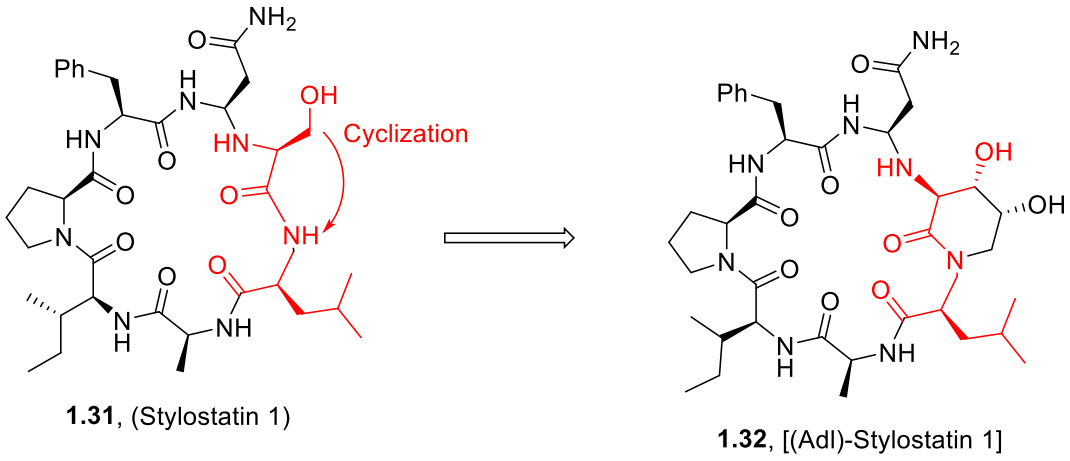

Figure 1.13. Substituted α-amino-δ-lactam analog of natural cyclic peptide[76]

1.6.4. Synthesis of substituted α-amino-δ-lactams

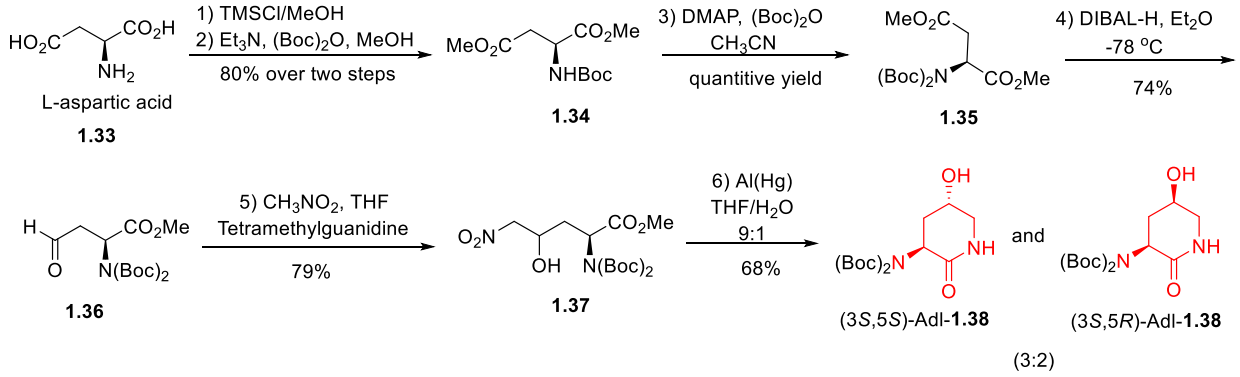

Scheme 1.4. Synthesis of γ-substituted Adl derivatives[77]

Substituted Adl analogs have been used to study the angiogenetic inhibitory activity of thalidomide.[78] In an example of the synthesis of substituted Adl analogs, 5-hydroxy Adl diastereomers were synthesized from L-aspartate semialdehyde **1.36** by nitroaldol reaction and reductive cyclization (Scheme 1.4). Separation of the mixture of diastereomers gave 5*R*- and 5*S*-hydroxy Adl **1.38** in 2:3 ratio.[78]

1.6.5. Substituted indolizidin-2-one amino acids (I^2aa)

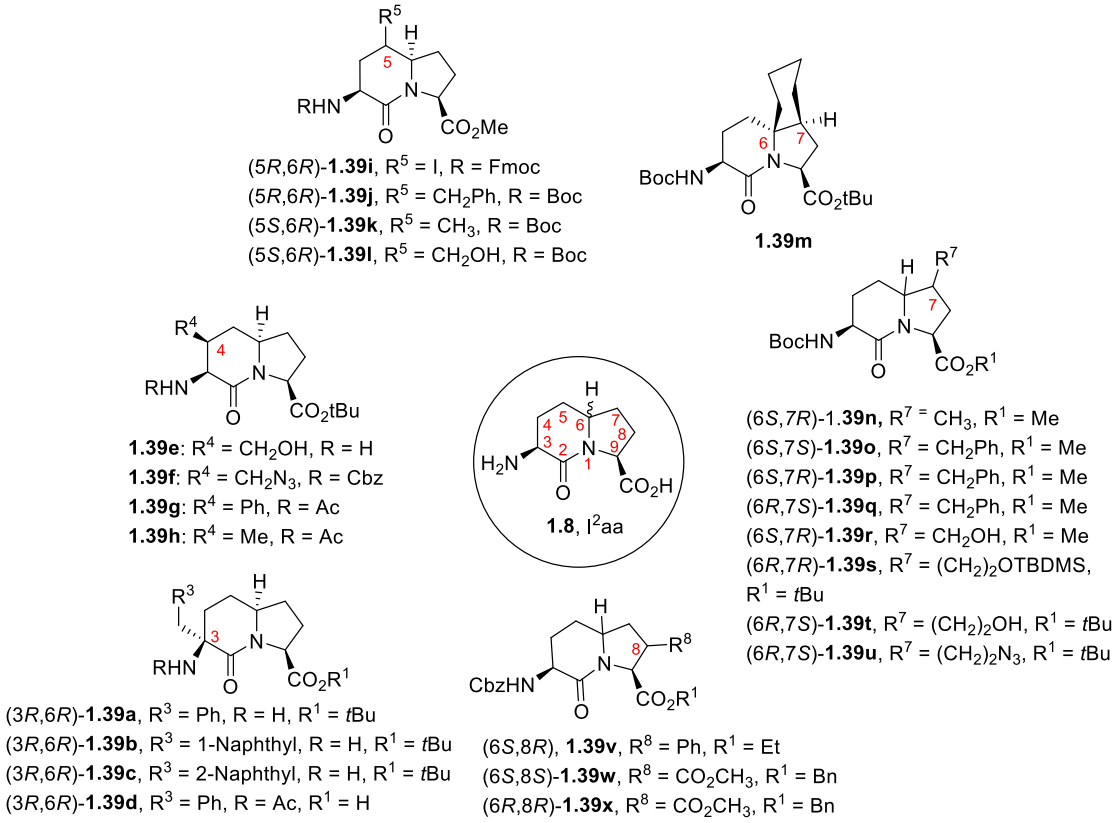

Figure 1.14. Importance of ring substituents on I^2aa[82-92]

Ring substituents on I^2aa residues can influence ring puckering and backbone conformation within the heterocycle.[36] The therapeutic utility of indolizidine-2-one **1.8** and substituted variants as peptide mimics has been demonstrated in the synthesis of thrombin inhibitors,[79] and ligands of the prostaglandin $F_{2\alpha}$,[80] integrin,[81] cholecystokinin and opioid receptors (Figure 1.14).[82] Computational analysis of 3-substituted azabicyclo[4.3.0]alkanones **1.39a-c** suggested utility as conformationally constrained β-turn mimics.[83] The Phe-Pro dipeptide mimic **1.39d** exhibited inhibitory activity on thrombin in *in vitro* studies.[84] Constrained mimics of the Arg–Gly–Asp (RGD) sequence were prepared using 4- and 7-substituted

azabicyclo[4.3.0]alkanones **1.39e-f** and **1.39t-u** and employed as integrin receptor ligands towards tumor blocking αvβ3 and αvβ5 receptor subtype anatgonists.[85,81] 4-Substituted I^{2}aa analogs **1.39g-h** were synthesized by stereoselective radical cyclization of substituted proline derivatives.[86] 5-Iodo I^{2}aa **1.39i** was used in the synthesis of prostaglandin-F$_{2\alpha}$ (PGF$_{2\alpha}$) receptor (FP) modulators that delay preterm birth.[87] Other 5-substituted I^{2}aa derivatives **1.39j-l** have been synthesized by using approaches featuring Claisen condensation of glutamate derivatives.[88,89] Conformational analysis of 6,7-disubstituted cyclohexyl analog **1.39m** in model amides found potential to adopt minimum energy inverse γ- and type II' β-turns.[90] 7-Substituted I^{2}aa derivatives **1.39n-r** were also synthesized using the Claisen condensation approach.[88,89] 7-Silyloxyethyl I^{2}aa **1.39s** was prepared from a 3-allyl pyroglutamic acid derivative and used in conformationally constrained peptide mimics.[91] 8-Phenyl and 8-carboxy I^{2}aa analogs **1.39v-x** were prepared to serve as constrained mimics of Ala-Phe and Ala-Asp dipeptides.[92,82]

1.6.6. Synthesis of substituted indolizidin-2-one amino acids

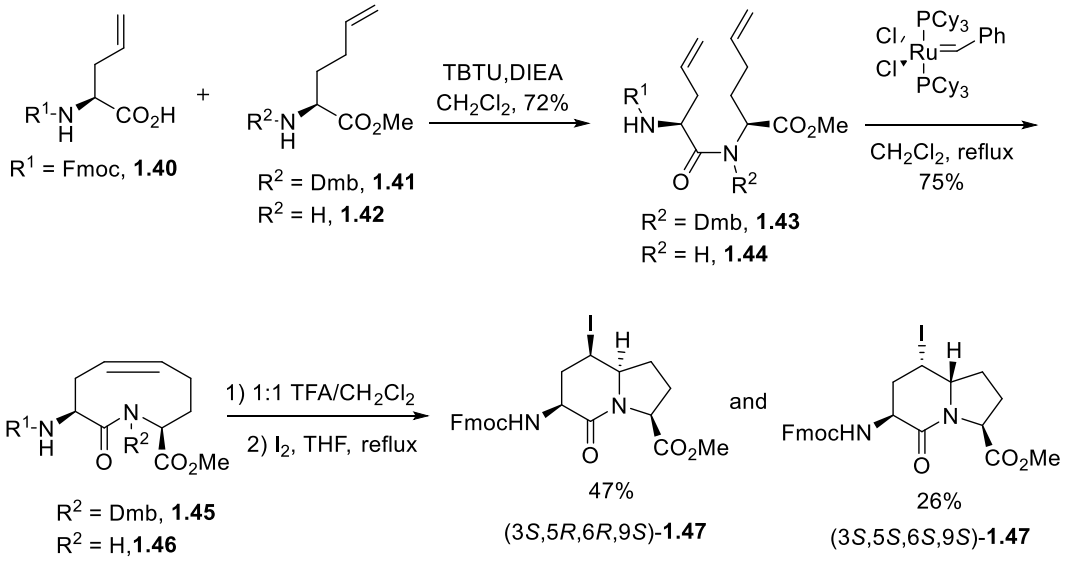

Scheme 1.5. 5-Iodo substituted indolizidin-2-one amino acids synthesis[93]

Among the various approaches for the synthesis of indolizidine-2-one amino acids, ring-closing metathesis and transannular cyclization (RCM-TC) has provided a variety of heterocycles having different ring sizes by employing different ω-olefin amino acid derivatives (e.g., **1.40** and **1.41-1.42**, Scheme 1.5).[93,94] Coupling of the ω-olefin amino acid derivatives using TBTU and DIEA gave various amides (e.g., **1.43** and **1.44**), which were employed in RCM using Grubb's 1st generation catalyst to synthesize different lactams (e.g., **1.45-1.46**). Iodoamination and transannular cyclization of *N*-substituted lactam **1.45** gave 5-substituted I^2aa derivative (3*S*,5*R*,6*R*,9*S*)-**1.47** in 86% yield as a single diastereomer (Scheme 1.5). Unsubstituted lactam **1.46** gave respectively diastereomers (3*S*,5*R*,6*R*,9*S*)-**1.47** and (3*S*,5*R*,6*S*,9*S*)-**1.47** in 47% and 26% yields. 5-Iodo I^2aa diastereomers **1.47** have been employed in the synthesis of prostaglandin-F2α receptor (FP) modulators.[87]

1.7. Copper catalyzed allylic substitution by S_N2' reaction

Transition metal catalyzed asymmetric allylic alkylation is a useful transformation for C-C bond formation in the synthesis of chiral molecules. Among enantioselective allylic substitutions, palladium catalyzed reactions have been well studied,[95,96] but are less common using non-stabilized nucleophiles (pKa > 25).[97]

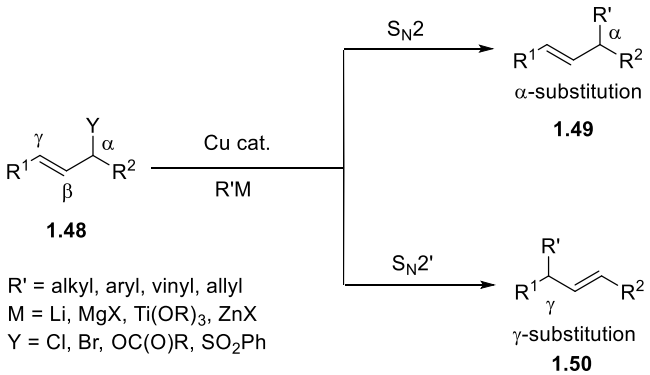

Scheme 1.6. Copper catalyzed allylic substitution may occur by S_N2 and S_N2' pathways[95-97]

Allylic substitutions have two possible reaction pathways (Scheme 1.6). The nucleophile can directly attack the leaving group at α-position carbon in an S_N2 approach. Alternatively, the nucleophile can attack the γ-carbon with double bond migration and leaving group displacement. Regioselective copper-catalyzed allylic substitution was achieved using dialkylzinc nucleophiles and allylchloride electrophiles.[98] Although no enantioselectivity is typically observed using organozinc reagents,[99] enantioselective asymmetric allylic substitution has been achieved using phosphoramidite ligands.[100] The mechanism of the copper catalyzed S_N2' reaction pathway entails initial formation of copper metal π-complex **1.55** upon reaction with allylic halide **1.54** (Scheme 1.7).[101] Oxidative addition on the γ-carbon forms σ-complex **1.56**. Reductive elimination of copper provides S_N2' product **1.57**. Regioselectivity depends on the ligands attached to copper. Electron-withdrawing ligands favor S_N2' product **1.57**. On the contrary, if X is an electron releasing ligand, S_N2 product **1.59** may be formed.

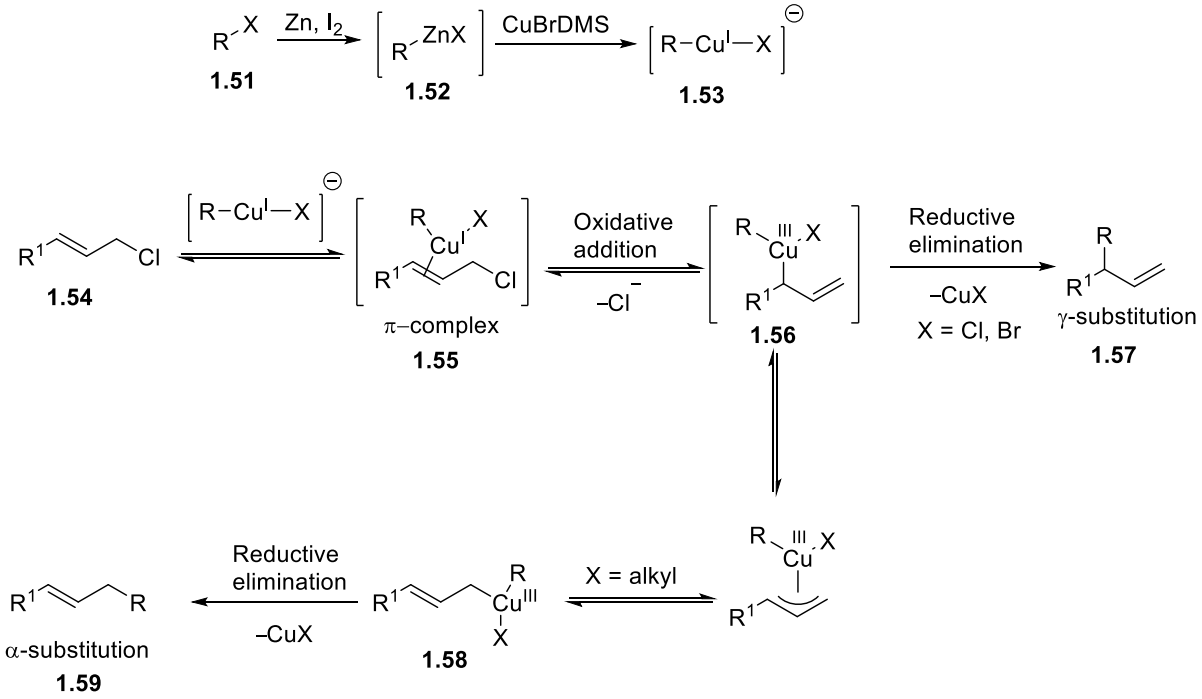

Scheme 1.7. Copper catalyzed S_N2' reaction mechanism[101]

1.8. Synthesis of unsaturated amino acids

Unsaturated amino acids are important building blocks for the synthesis of heterocyclic amino acid derivatives.[94] Strategies to synthesize enantiomerically pure unsaturated amino acids have been developed using L-serine as an inexpensive chiral educt.[94] β-Iodoalaninate **1.61** was previously synthesized in 60% overall yield from L-serine **1.60** in a three-step method featuring esterification, amine protection and alcohol substitution using the Appel reaction (Scheme 1.8).[102] Copper catalyzed S_N2' reactions have previously reacted the zincate from β-iodoalanine **1.61** onto various allylic halides to provide different unsaturated amino acid analogs.[103,104] The utility of such unsaturated amino acid building blocks has however been rarely explored in the synthesis of heterocyclic amino acid derivatives.

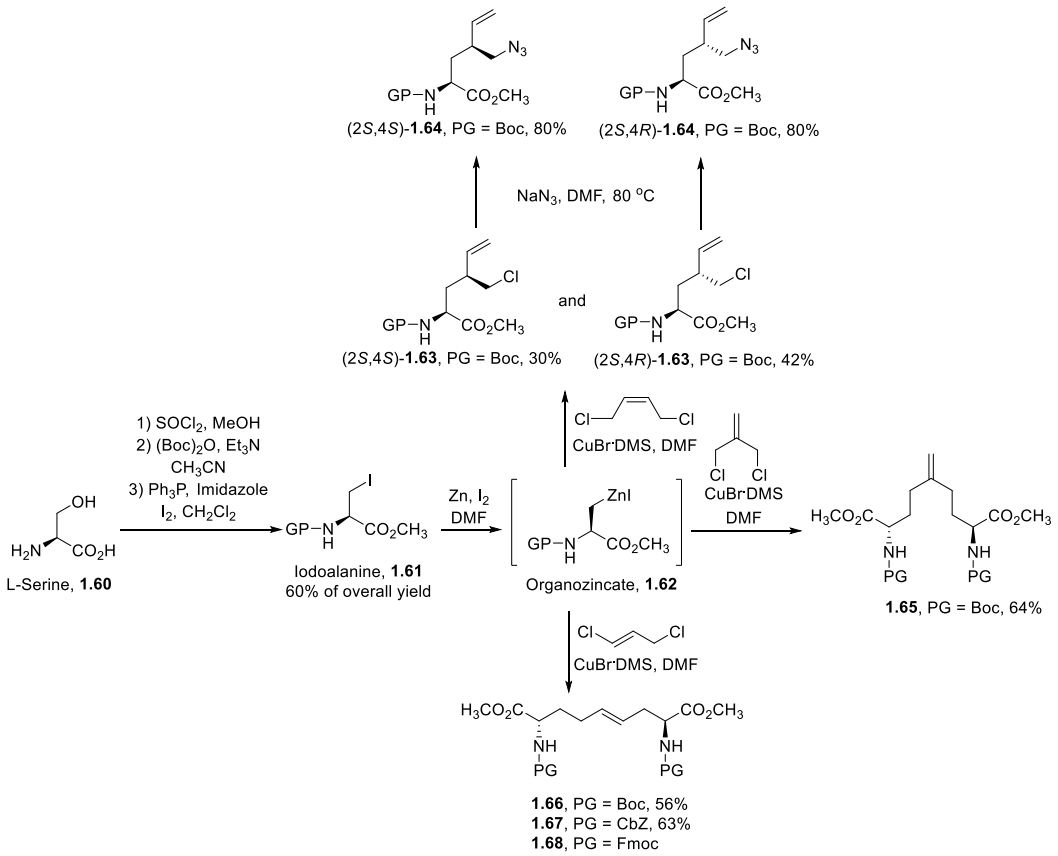

Scheme 1.8. Synthesis of unsaturated amino acid derivatives

1.9. Aims and objectives of the thesis research

The application of heterocyclic amino acids and dipeptides has significant utility for studying peptides to understand conformation-activity relationships. Enantioselective syntheses of unsaturated amino acids has been achieved by copper catalyzed S_N2' reaction of the zincate from β-iodoalanine **1.61**.[105,103,104] The aim of this thesis research was to develop effective synthetic approaches for converting unnatural amino acid derivatives into different heterocyclic amino acids and dipeptides. As demonstrated in the following chapters, access has been opened to prepare 4-substituted prolines, α-amino-γ-substituted-δ-lactam, and 5-, 6-, and 7-substituted fused bicyclic systems.

In Chapter 2, syntheses are described for preparing 4-vinylprolines (4-Vyp) and 4-vinylornithines (4-Von, **1.64**). The copper catalyzed S_N2' reaction of the zincate from β-iodoalanine **1.61** onto (*Z*)-1,4-dichlorobut-2-ene provided separable diastereomers of (2*S*,4*S*)- and (2*S*,4*R*)-2-*N*-(Boc)amino-4-(chloromethyl)hexenoates **1.63**. Intra- and intermolecular displacements of halides **1.63** gave access to 4-Vyp and 4-Von. The utility of 4-Vyp has previously been demonstrated by the synthesis of tricyclic peptide mimic α-helix inducers.[61]

In Chapter 3, 5-vinyl α-amino-δ-lactam (Adl) analogs were prepared from 4-Von **1.64**. The 5-substituted Adl analogs offer potential to place amino acid side chains in an extended *trans* χ-orientation within a β-turn conformation. With ultimate interest in their use to study biologically active peptides possessing glutamate and glutamine residues, effective methods were developed for the assembly, oxidation and functionalization of 5-vinyl Adl diastereomers.[106]

Chapters 4 and 5, describe the syntheses of 5-, 6-, and 7-substituted I^2aa residues by using diamino azelates **1.65** and **1.66** as olefin precursors. The copper catalyzed S_N2' reaction of the

zincate from β-iodoalanine **1.61** onto 3-chloro-2-(chloromethyl)prop-1-ene and (*E*)-1,3-dichloroprop-1-ene gave respectively diamino azelates **1.65** and **1.66**. Different oxidative cyclization methods were explored successfully to deliver 6-hydroxymethyl and 5- and 7-hydroxy I^2aa analogs, which have been employed in the study of prostaglandin-F2α receptor modulators that can delay labor.

In sum, effective methods have been developed for the synthesis of a spectrum of substituted prolines, α-amino-δ-lactams, and indolizidin-2-one amino acids. These heterocyclic amino acids offer potential to restrict backbone and side chain dihedral angles in peptides to study conformation-activity relationships responsible for biological activity. The biomedical application of the substituted indolizidin-2-one amino acids was illustrated by the synthesis of modulators of the prostaglandin-F2α receptor which exhibited inhibitory activity on myometrial contraction. In view of the utility of these heterocyclic peptide mimics and the methods for their synthesis, this thesis offers a range of useful tools and approaches for peptide-based medicinal chemistry.

1.10. References

1. Petrou, C.; Sarigiannis, Y., Peptide synthesis: Methods, trends, and challenges. In *Peptide Applications in Biomedicine, Biotechnology and Bioengineering*, Elsevier **2018**; pp 1-21.

2. Zaky, A. A.; Simal-Gandara, J.; Eun, J.-B.; Shim, J.-H.; Abd El-Aty, A. Bioactivities, Applications, Safety, and Health Benefits of Bioactive Peptides From Food and By-Products: A Review. *Front. Nutr.*, **2022**, *8*, 815640.

3. Recio, C.; Maione, F.; Iqbal, A. J.; Mascolo, N.; De Feo, V. The potential therapeutic application of peptides and peptidomimetics in cardiovascular disease. *Front. Pharmacol.* **2017**, 526.

4. Papini, A. M. Cosmeceutical Peptides in the Framework of Sustainable Wellness Economy. *Front*. *Chem*. **2020**, *8*, 1-8.

5. Pepe-Mooney, B. J.; Fairman, R. Peptides as materials. *Curr. Opin. Struct. Biol.* **2009**, *19*, 483-494.

6. Montesinos, E.; Bardaji, E. Synthetic antimicrobial peptides as agricultural pesticides for plant-disease control. *Chem. Biodiversity* **2008**, *5*, 1225-1237.

7. Muttenthaler, M.; King, G. F.; Adams, D. J.; Alewood, P. F. Trends in peptide drug discovery. *Nat. Rev. Drug Discovery* **2021**, 1-17.

8. Kaspar, A. A.; Reichert, J. M. Future directions for peptide therapeutics development. *Drug Discovery Today* **2013**, *18*, 807-817.

9. Global Peptide Therapeutics Markets, 2021-2026 - Increase Bioavailability of Drugs and Broaden Application of Peptides Therapeutics. **2021**.

10. Fosgerau, K.; Hoffmann, T. Peptide therapeutics: current status and future directions. *Drug Discovery Today* **2015**, *20*, 122-128.

11. Antosova, Z.; Mackova, M.; Kral, V.; Macek, T. Therapeutic application of peptides and proteins: parenteral forever? *Trends Biotechnol.* **2009**, *27*, 628-635.

12. Whitby, L. R.; Ando, Y.; Setola, V.; Vogt, P. K.; Roth, B. L.; Boger, D. L. Design, synthesis, and validation of a β-turn mimetic library targeting protein–protein and peptide–receptor interactions. *J. Am. Chem. Soc.* **2011**, *133*, 10184-10194.

13. Bhuyan, M. S. I.; Gao, X. In *A protein-dependent side-chain rotamer library*, BMC bioinformatics **2011** Springer; pp 1-12.

14. Whitby, L. R.; Boger, D. L. Comprehensive peptidomimetic libraries targeting protein–protein interactions. *Acc. Chem. Res.* **2012**, *45*, 1698-1709.

15. Loughlin, W. A.; Tyndall, J. D.; Glenn, M. P.; Fairlie, D. P. Beta-strand mimetics. *Chem. Rev.* **2004**, *104*, 6085-6118.

16. Gibbs, A. C.; Bjorndahl, T. C.; Hodges, R. S.; Wishart, D. S. Probing the structural determinants of type II 'β-turn formation in peptides and Proteins. *J. Am. Chem. Soc.* **2002**, *124*, 1203-1213.

17. Venkatachalam, C. Stereochemical criteria for polypeptides and proteins. V. Conformation of a system of three linked peptide units. *Biopolymers* **1968**, *6*, 1425-1436.

18. de Brevern, A. G. Extension of the classical classification of β-turns. *Sci. Rep.* **2016**, *6*, 1-15.

19. Lenci, E.; Trabocchi, A. Peptidomimetic toolbox for drug discovery. *Chem. Soc. Rev.* **2020**, *49*, 3262-3277.

20. Bélanger, P. C.; Dufresne, C. Preparation of exo-6-benzyl-exo-2-(m-hydroxyphenyl)-1-dimethylaminomethylbicyclo [2.2.2.] octane. A non-peptide mimic of enkephalins. *Can. J. Chem.* **1986**, *64*, 1514-1520.

21. Avan, I.; Hall, C. D.; Katritzky, A. R. Peptidomimetics via modifications of amino acids and peptide bonds. *Chem. Soc. Rev.* **2014**, *43*, 3575-3594.

22. Hirschmann, R. F.; Nicolaou, K.; Angeles, A. R.; Chen, J. S.; Smith III, A. B. The β-d-Glucose Scaffold as a β-Turn Mimetic. *Acc. Chem. Res.* **2009**, *42*, 1511-1520.

23. Hirschmann, R.; Nicolaou, K.; Pietranico, S.; Leahy, E. M.; Salvino, J.; Arison, B.; Cichy, M. A.; Spoors, P. G.; Shakespeare, W. C. De novo design and synthesis of somatostatin non-peptide peptidomimetics utilizing. beta.-D-glucose as a novel scaffolding. *J. Am. Chem. Soc.* **1993**, *115*, 12550-12568.

24. Prasad, V.; Birzin, E. T.; McVaugh, C. T.; Van Rijn, R. D.; Rohrer, S. P.; Chicchi, G.; Underwood, D. J.; Thornton, E. R.; Smith, A. B.; Hirschmann, R. Effects of heterocyclic aromatic substituents on binding affinities at two distinct sites of somatostatin receptors. Correlation with the electrostatic potential of the substituents. *J. Med. Chem.* **2003**, *46*, 1858-1869.

25. Morley, J. Structure-activity relationships of enkephalin-like peptides. *Annu. Rev. Pharmacol. Toxicol.* **1980**, *20*, 81-110.

26. Bozovičar, K.; Bratkovič, T. Small and simple, yet sturdy: Conformationally constrained peptides with remarkable properties. *Int. J. Mol. Sci.* **2021**, *22*, 1611.

27. Fang, Z.; Song, Y. n.; Zhan, P.; Zhang, Q.; Liu, X. Conformational restriction: an effective tactic in'follow-on'-based drug discovery. *Future Med. Chem.* **2014**, *6*, 885-901.

28. Polinsky, A.; Goodman, M.; Williams, K. A.; Deber, C. M. Minimum energy conformations of proline-containing helices. *Biopolymers* **1992**, *32*, 399-406.

29. Gause, G. F.; Brazhnikova, M. G. Gramicidin S and its use in the treatment of infected wounds. *Nature* **1944**, *154*, 703-703.

30. Fang, W.-Y.; Dahiya, R.; Qin, H.-L.; Mourya, R.; Maharaj, S. Natural proline-rich cyclopolypeptides from marine organisms: Chemistry, synthetic methodologies and biological status. *Mar. Drugs* **2016**, *14*, 194.

31. Natesh, R.; Schwager, S. L.; Sturrock, E. D.; Acharya, K. R. Crystal structure of the human angiotensin-converting enzyme–lisinopril complex. *Nature* **2003**, *421*, 551-554.

32. Perdih, A.; Kikelj, D. The application of Freidinger lactams and their analogs in the design of conformationally constrained peptidomimetics. *Curr. Med. Chem.* **2006**, *13*, 1525-1556.

33. Chapman, K. T. Synthesis of a potent, reversible inhibitor of interleukin-1β converting enzyme. *Bioorg. Med. Chem. Lett.* **1992**, *2*, 613-618.

34. Karanewsky, D. S.; Bai, X.; Linton, S. D.; Krebs, J. F.; Wu, J.; Pham, B.; Tomaselli, K. J. Conformationally constrained inhibitors of caspase-1 (interleukin-1β converting enzyme) and of the human CED-3 homologue caspase-3 (CPP32, APOPAIN). *Bioorg. Med. Chem. Lett.* **1998**, *8*, 2757-2762.

35. Khashper, A.; Lubell, W. D. Design, synthesis, conformational analysis and application of indolizidin-2-one dipeptide mimics. *Org. Biomol. Chem.* **2014**, *12*, 5052-5070.

36. Cluzeau, J.; Lubell, W. D. Design, synthesis, and application of azabicyclo [XY 0] alkanone amino acids as constrained dipeptide surrogates and peptide mimics. *Peptide Sci.* **2005**, *80*, 98-150.

37. Reinscheid, R. K.; Nothacker, H.-P.; Bourson, A.; Ardati, A.; Henningsen, R. A.; Bunzow, J. R.; Grandy, D. K.; Langen, H.; Monsma Jr, F. J.; Civelli, O. Orphanin FQ: a neuropeptide that activates an opioidlike G protein-coupled receptor. *Science* **1995**, *270*, 792-794.

38. Halab, L.; Becker, J. A.; Darula, Z.; Tourwé, D.; Kieffer, B. L.; Simonin, F.; Lubell, W. D. Probing opioid receptor interactions with azacycloalkane amino acids. Synthesis of a potent and selective ORL1 antagonist. *J. Med. Chem.* **2002**, *45*, 5353-5357.

39. Mueller, R.; Revesz, L. Synthesis of 6, 5-fused bicyclic lactams as potential dipeptide β-turn mimetics. *Tetrahedron Lett.* **1994**, *35*, 4091-4092.

40. Lombart, H.-G.; Lubell, W. D. Rigid dipeptide mimetics: efficient synthesis of enantiopure indolizidinone amino acids. *J. Org. Chem.* **1996**, *61*, 9437-9446.

41. Calaza, M. I.; Cativiela, C. Stereoselective synthesis of quaternary proline analogues. *Eur. J. Org. Chem.* **2008**, *20*, 3427.

42. Ganguly, H. K.; Basu, G. Conformational landscape of substituted prolines. *Biophys. Rev.* **2020**, *12*, 25-39.

43. Mauger, A. B. Naturally occurring proline analogues. *J. Nat. Prod.* 1996, *59*, 1205-1211.

44. Vogt, H.; Bräse, S. Recent approaches towards the asymmetric synthesis of α, α-disubstituted α-amino acids. *Org. Biomol. Chem.* **2007**, *5*, 406-430.

45. Kolaczkowski, L.; Barkalow, J.; Barnes, D. M.; Haight, A.; Pritts, W.; Schellinger, A. Synthesis of (R)-Boc-2-methylproline via a memory of chirality cyclization. Application to the synthesis of veliparib, a poly (ADP-ribose) polymerase inhibitor. *J. Org. Chem.* **2019**, *84*, 4837-4845.

46. Seebach, D.; Boes, M.; Naef, R.; Schweizer, W. B. Alkylation of amino acids without loss of the optical activity: preparation of. alpha.-substituted proline derivatives. A case of self-reproduction of chirality. *J. Am. Chem. Soc.* **1983**, *105*, 5390-5398.

47. Nakamura, S.; Chikaike, T.; Yonehara, H.; Umezawa, H. Isolation, characterization and structural elucidation of new amino acids from bottromycin A. *Chem. Pharm. Bull.* **1965**, *13*, 599-602.

48. Springer, J. P.; Cole, R. J.; Dorner, J. W.; Cox, R. H.; Richard, J. L.; Barnes, C. L.; Van der Helm, D. Structure and conformation of roseotoxin B. *J. Am. Chem. Soc.* **1984**, *106*, 2388-2392.

49. Sheehan, J. C.; Mania, D.; Nakamura, S.; Stock, J. A.; Maeda, K. The structure of telomycin. *J. Am. Chem. Soc.* **1968**, *90*, 462-470.

50. Hatanaka, S.-i. A new amino acid isolated from Morchella esculenta and related species. *Phytochemistry* **1969**, *8*, 1305-1308.

51. Brockmann, H.; Manegold, J. H. Actinomycine, XXIII; Antibiotica aus Actinomyceten, XLV. Überführung von Actinomycin X2 in die Actinomycine C1, X0β und X0δ. *Chem. Ber.* **1960**, *93*, 2971-2982.

52. Fischer, E. On a new amino acid from gelatín. *Ber. chem. Ges.* **1902**, *35*, 2660.

53. Moore, R. E.; Entzeroth, M. Majusculamide D and deoxymajusculamide D, two cytotoxins from Lyngbya majuscula. *Phytochemistry* **1988**, *27*, 3101-3103.

54. Bartz, Q. Griseoviridin and viridogrisein: Isolation and characterization. *Antibiotics Ann.* **1955**, *1954*, 777-783.

55. Brockmann, H.; Stahler, E. Composition of Actinomycin-*Z*5. *Tetrahedron Lett.* **1973**, 2567-2570.

56. Impellizzeri, G.; Mangiafico, S.; Oriente, G.; Piattelli, M.; Sciuto, S.; Fattorusso, E.; Magno, S.; Santacroce, C.; Sica, D. Amino acids and low-molecular-weight carbohydrates of some marine red algae. *Phytochemistry* **1975**, *14*, 1549-1557.

57. Pandey, A. K.; Naduthambi, D.; Thomas, K. M.; Zondlo, N. J. Proline editing: a general and practical approach to the synthesis of functionally and structurally diverse peptides. Analysis of steric versus stereoelectronic effects of 4-substituted prolines on conformation within peptides. *J. Am. Chem. Soc.* **2013**, *135*, 4333-4363.

58. Shoulders, M. D.; Hodges, J. A.; Raines, R. T. Reciprocity of steric and stereoelectronic effects in the collagen triple helix. *J. Am. Chem. Soc.* **2006**, *128*, 8112-8113.

59. Koskinen, A. M.; Helaja, J.; Kumpulainen, E. T.; Koivisto, J.; Mansikkamäki, H.; Rissanen, K. Locked conformations for proline pyrrolidine ring: synthesis and conformational analysis of cis-and trans-4-tert-butylprolines. *J. Org. Chem.* **2005**, *70*, 6447-6453.

60. Shoulders, M. D.; Satyshur, K. A.; Forest, K. T.; Raines, R. T. Stereoelectronic and steric effects in side chains preorganize a protein main chain. *Proc. Natl. Acad. Sci.* **2010**, *107*, 559-564.

61. Hack, V.; Reuter, C.; Opitz, R.; Schmieder, P.; Beyermann, M.; Neudörfl, J. M.; Kühne, R.; Schmalz, H. G. Efficient α-Helix Induction in a Linear Peptide Chain by N-Capping with a Bridged-tricyclic Diproline Analogue. *Angew. Chem., Int. Ed. Engl.* **2013**, *52*, 9539-9543.

62. Koskinen, A. M.; Rapoport, H. Synthesis of 4-substituted prolines as conformationally constrained amino acid analogs. *J. Org. Chem.* **1989**, *54*, 1859-1866.

63. Mulamreddy, R.; Atmuri, N. P.; Lubell, W. D. 4-Vinylproline. *J. Org. Chem.* **2018**, *83*, 13580-13586.

64. Muthusamy, S.; Srinivasan, P. Facile chemoselective rhodium carbenoid N–H insertion reactions: synthesis of 3-arylamino-or 3-heteroarylpiperidin-2-ones. *Tetrahedron Lett.* **2005**, *46*, 1063-1066.

65. Kemp, D.; Sun, E. T. Amino acids derivatives that stabilize secondary structures of polypeptides--: I. Synthesis of LL-3-amino-2-piperidone-6-carboxylic acid (LL-Acp), a novel beta-turn-forming amino acid. *Tetrahedron Lett.* **1982**, *23*, 3759-3760.

66. St-Cyr, D. J.; García-Ramos, Y.; Doan, N.-D.; Lubell, W. D., Aminolactam, N-aminoimidazolone, and N-aminoimdazolidinone peptide mimics. In *Peptidomimetics I*, Springer 2017; pp 125-175.

67. Ballet, S.; Guillemyn, K.; Poorten, O. V. d.; Schurgers, B.; Verniest, G.; Tourwé, D., Azepinone-Constrained Amino Acids in Peptide and Peptidomimetic Design. In *Peptidomimetics I*, Springer **2015**; pp 177-209.

68. Zhu, J.; Price, B. A.; Walker, J.; Zhao, S. X. Catalytic hydrogenation of ethyl 2-amino-2-difluoromethyl-4-cyanobutanoate and its Schiff base reaction modes. *Tetrahedron Lett.* **2005**, *46*, 2795-2797.

69. Morisaki, K.; Sawa, M.; Nomaguchi, J. y.; Morimoto, H.; Takeuchi, Y.; Mashima, K.; Ohshima, T. Rh-Catalyzed Direct Enantioselective Alkynylation of α-Ketiminoesters. *Chem. Eur. J.* **2013**, *19*, 8417-8420.

70. Han, L.; Li, K.; Xu, H.; Mei, T.; Sun, Y.; Qu, J.; Song, Y. N-TFA-Gly-Bt-Based Stereoselective Synthesis of Substituted 3-Amino Tetrahydro-2 H-pyran-2-ones via an Organocatalyzed Cascade Process. *J. Org. Chem.* **2019**, *84*, 10526-10534.

71. Gordon, S.; Costa, L.; Incerti, M.; Manta, E.; Saldaña, J.; Domínguez, L.; Mariezcurrena, R.; Suescun, L. Synthesis and in vitro anthelmintic activity against Nippostrongylus brasiliensis of new 2-amino-4-hydroxy-delta-valerolactam derivatives. *Farmaco (Societa chimica italiana: 1989)* **1997**, *52*, 603-608.

72. Kemp, D.; McNamara, P. E. An efficient synthesis of ethyl LL-3-amino-2-piperidone-6-carboxylate. *J. Org. Chem.* **1984**, *49*, 2286-2288.

73. Tolmachova, N. A.; Dolovanyuk, V. G.; Gerus, I. I.; Kondratov, I. S.; Polovinko, V. V.; Bergander, K.; Haufe, G. Catalytic hydrogenation of 3-amino-6-(trifluoromethyl)-5, 6-dihydropyridin-2 (1H)-ones and its use in the synthesis of trifluoromethyl-containing mimetics of ornithine and thalidomide. *Synthesis* **2011**, *2011*, 1149-1156.

74. Pettit, G. R.; Srirangam, J. K.; Herald, D. L.; Erickson, K. L.; Doubek, D. L.; Schmidt, J. M.; Tackett, L. P.; Bakus, G. J. Antineoplastic agents. 251. Isolation and structure of stylostatin 1 from the Papua New Guinea marine sponge Stylotella aurantium. *J. Org. Chem.* **1992**, *57*, 7217-7220.

75. Freidinger, R. M. Design and synthesis of novel bioactive peptides and peptidomimetics. *J. Med. Chem.* **2003**, *46*, 5553-5566.

76. Forns, P.; Piró, J.; Cuevas, C.; García, M.; Rubiralta, M.; Giralt, E.; Diez, A. Constrained derivatives of stylostatin 1. 1. Synthesis and biological evaluation as potential anticancer agents. *J. Med. Chem.* **2003**, *46*, 5825-5833.

77. Luzzio, F. A.; Duveau, D. Y.; Figg, W. D. A chiral pool approach toward the synthesis of thalidomide metabolites. *Heterocycles* **2006**, *70*, 321-334.

78. Luzzio, F. A.; Thomas, E. M.; Figg, W. D. Thalidomide metabolites and analogs. Part 2: Cyclic derivatives of 2-N-phthalimido-2S, 3S (3-hydroxy) ornithine. *Tetrahedron Lett.* **2000**, *41*, 7151-7155.

79. Hanessian, S.; Therrien, E.; Granberg, K.; Nilsson, I. Targeting thrombin and factor VIIa: design, synthesis, and inhibitory activity of functionally relevant indolizidinones. *Bioorg. Med. Chem. Lett.* **2002**, *12*, 2907-2911.

80. Bourguet, C. B.; Goupil, E.; Tassy, D.; Hou, X.; Thouin, E.; Polyak, F.; Hébert, T. E.; Claing, A.; Laporte, S. A.; Chemtob, S. Targeting the prostaglandin F2α receptor for preventing preterm labor with azapeptide tocolytics. *J. Med. Chem.* **2011**, *54*, 6085-6097.

81. Manzoni, L.; Bassanini, M.; Belvisi, L.; Motto, I.; Scolastico, C.; Castorina, M.; Pisano, C., Nonpeptide integrin antagonists: RGD mimetics incorporating substituted azabicycloalkanes as amino acid replacements. *Eur. J. Org. Chem.* **2007**, *2007*, 1309-1317.

82. Ndungu, J. M.; Cain, J. P.; Davis, P.; Ma, S.-W.; Vanderah, T. W.; Lai, J.; Porreca, F.; Hruby, V. J. Synthesis of constrained analogues of cholecystokinin/opioid chimeric peptides. *Tetrahedron Lett.* **2006**, *47*, 2233-2236.

83. Colombo, L.; Di Giacomo, M.; Brusotti, G.; Sardone, N.; Angiolini, M.; Belvisi, L.; Maffioli, S.; Manzoni, L.; Scolastico, C. Stereoselective synthesis of 6, 5-bicyclic reverse-turn peptidomimetics. *Tetrahedron* **1998**, *54*, 5325-5336.

84. Boatman, P. D.; Ogbu, C. O.; Eguchi, M.; Kim, H.-O.; Nakanishi, H.; Cao, B.; Shea, J. P.; Kahn, M. Secondary structure peptide mimetics: design, synthesis, and evaluation of β-strand mimetic thrombin inhibitors. *J. Med. Chem.* **1999**, *42*, 1367-1375.

85. Manzoni, L.; Belvisi, L.; Arosio, D.; Civera, M.; Pilkington-Miksa, M.; Potenza, D.; Caprini, A.; Araldi, E. M.; Monferini, E.; Mancino, M. Cyclic RGD-containing functionalized azabicycloalkane peptides as potent integrin antagonists for tumor targeting. *ChemMedChem* **2009**, *4*, 615-632.

86. Belvisi, L.; Colombo, L.; Manzoni, L.; Potenza, D.; Scolastico, C. Design, synthesis, conformational analysis and application of azabicycloalkane amino acids as constrained dipeptide mimics. *Synlett*. **2004**, *2004*, 1449-1471.

87. Mir, F. M.; Atmuri, N. P.; Bourguet, C. B.; Fores, J. R.; Hou, X.; Chemtob, S.; Lubell, W. D. Paired utility of aza-amino acyl proline and indolizidinone amino acid residues for peptide mimicry: Conception of prostaglandin F2α receptor allosteric modulators that delay preterm birth. *J. Med. Chem.* **2019**, *62*, 4500-4525.

88. Polyak, F.; Lubell, W. D. Rigid dipeptide mimics: synthesis of enantiopure 5-and 7-benzyl and 5, 7-dibenzyl Indolizidinone amino acids via enolization and alkylation of δ-Oxo α, ω-Di-[N-(9-(9-phenylfluorenyl)) amino] azelate esters. *J. Org. Chem.* **1998**, *63*, 5937-5949.

89. Polyak, F.; Lubell, W. D. Mimicry of peptide backbone geometry and heteroatomic side-chain functionality: synthesis of enantiopure indolizidin-2-one amino acids possessing alcohol, acid, and azide functional groups. *J. Org. Chem.* **2001**, *66*, 1171-1180.

90. Belvisi, L.; Colombo, L.; Colombo, M.; Di Giacomo, M.; Manzoni, L.; Vodopivec, B.; Scolastico, C. Practical stereoselective synthesis of conformationally constrained unnatural proline-based amino acids and peptidomimetics. *Tetrahedron* **2001**, *57*, 6463-6473.

91. Artale, E.; Banfi, G.; Belvisi, L.; Colombo, L.; Colombo, M.; Manzoni, L.; Scolastico, C. Synthesis of substituted conformationally constrained 6, 5-and 7, 5-fused bicyclic lactams as dipeptide mimics. *Tetrahedron* **2003**, *59*, 6241-6250.

92. Wang, W.; Yang, J.; Ying, J.; Xiong, C.; Zhang, J.; Cai, C.; Hruby, V. J. Stereoselective synthesis of dipeptide β-turn mimetics: 7-benzyl and 8-phenyl substituted azabicyclo [4.3. 0] nonane amino acid esters. *J. Org. Chem.* **2002**, *67*, 6353-6360.

93. Surprenant, S.; Lubell, W. D. From macrocycle dipeptide lactams to azabicyclo[X.Y.0] alkanone amino acids: A transannular cyclization route for peptide mimic synthesis. *Org. Lett.* **2006**, *8*, 2851-2854.

94. Atmuri, N. P.; Lubell, W. D. Insight into Transannular Cyclization Reactions To Synthesize Azabicyclo[X.Y.Z] alkanone Amino Acid Derivatives from 8-, 9-, and 10-Membered Macrocyclic Dipeptide Lactams. *J. Org. Chem.* **2015**, *80*, 4904-4918.

95. Tsuji, J.; Takahashi, H.; Morikawa, M. Organic syntheses by means of noble metal compounds XVII. Reaction of π-allylpalladium chloride with nucleophiles. *Tetrahedron Lett.* **1965**, *6*, 4387-4388.

96. Trost, B. M.; Crawley, M. L. Asymmetric transition-metal-catalyzed allylic alkylations: applications in total synthesis. *Chem. Rev.* **2003**, *103*, 2921-2944.

97. van Zijl, A. W.; Arnold, L. A.; Minnaard, A. J.; Feringa, B. L. Highly Enantioselective Copper-Catalyzed Allylic Alkylation with Phosphoramidite Ligands. *Adv. Synth. Catal.* **2004**, *346*, 413-420.

98. Dübner, F.; Knochel, P. Copper (i)-Catalyzed Enantioselective Substitution of Allyl Chlorides with Diorganozinc Compounds. *Angew. Chem., Int. Ed. Engl.* **1999**, *38*, 379-381.

99. Goldsmith, P. J.; Teat, S. J.; Woodward, S. Enantioselective Preparation of β, β-Disubstituted α-Methylenepropionates by MAO Promotion of the Zinc Schlenk Equilibrium. *Angew. Chem., Int. Ed. Engl.* **2005**, *44*, 2235-2237.

100. Malda, H.; van Zijl, A. W.; Arnold, L. A.; Feringa, B. L. Enantioselective copper-catalyzed allylic alkylation with dialkylzincs using phosphoramidite ligands. *Org. Lett.* **2001**, *3*, 1169-1171.

101. Stanley, L. M., Hartwig, J. F., "Copper-Catalyzed Allylic Substitution" Organotransition metal chemistry : from bonding to catalysis **2010** p. 999 - 1008.

102. Trost, B. M.; Rudd, M. T. Chemoselectivity of the ruthenium-catalyzed hydrative diyne cyclization: total synthesis of (+)-cylindricine C, D, and E. *Org. Lett.* **2003**, *5*, 4599-4602.

103. Dunn, M. J.; Jackson, R. F.; Pietruszka, J.; Turner, D. Synthesis of Enantiomerically Pure Unsaturated. alpha.-Amino Acids Using Serine-Derived Zinc/Copper Reagents. *J. Org. Chem.* **1995**, *60*, 2210-2215.

104. Reeve, P. A.; Grabowska, U.; Oden, L. S.; Wiktelius, D.; Wångsell, F.; Jackson, R. F. Radical functionalization of unsaturated amino acids: synthesis of side-chain-fluorinated, azido-substituted, and hydroxylated amino acids. *ACS Omega* **2019**, *4*, 10854-10865.

105. Rodríguez, A.; Miller, D. D.; Jackson, R. F. Combined application of organozinc chemistry and one-pot hydroboration–Suzuki coupling to the synthesis of amino acids. *Org. Biomol. Chem.* **2003**, *1*, 973-977.

106. Mulamreddy, R.; Lubell, W. D. Constrained Glu-Gly and Gln-Gly dipeptide surrogates from γ-substituted α-amino-δ-lactam synthesis. *Peptide Sci.* **2020**, *112*, e24149.

Chapter 2: 4-Vinylproline

2.0. Context

2.01. Importance of proline

Proline (Pro, **1.21**) is a non-essential proteogenic heterocyclic amino acid.[1] Employed in the synthesis of proteins, proline restricts the conformations of polypeptide bonds to favour particular secondary structures.[2] An important component of collagen, proline is vital for many physiological processes.[3] Proline deficiency in humans causes soft tissue damage and slower healing.[4]

Among proline containing drugs, Captopril (**2.01**) was the first orally available angiotensin-converting enzyme (ACE) inhibitor used as an antihypertensive agent to treat high blood pressure and heart failure.[5] Enalapril (**2.02**)[6] and Ramipril (**2.03**)[7] were subsequently designed by modifications of Captopril retaining the proline core structure for ACE inhibition (Figure 2.01).

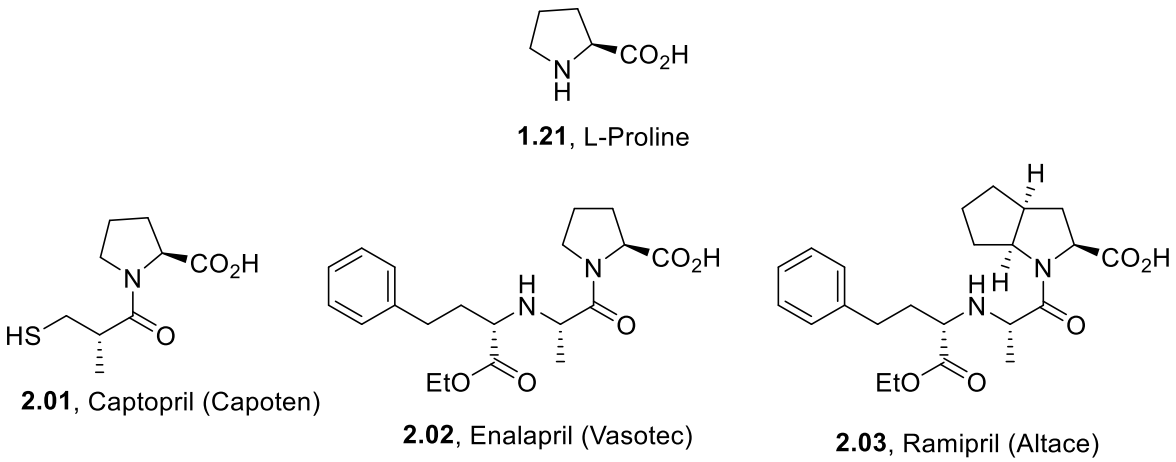

Figure 2.01. Proline and proline containing ACE inhibitors

2.02. 4-Substituted prolines

Among 4-substituted prolines, 4-hydroxyproline (Hyp, **1.22m**) is a key component in collagen (Figure 2.02).[8] 4-Hydroxyproline is prepared by post-translational modification featuring oxidation of proline.[9] The repeating combinations of proline, 4-hydroxyproline and glycine account for the stability and twist of the collagen triple helix.[9] Consequently, 4-fluoroproline diastereomers (**2.07** and **2.010**) have been important building blocks in studies of the folding and conformation of collagen analogs.[10]

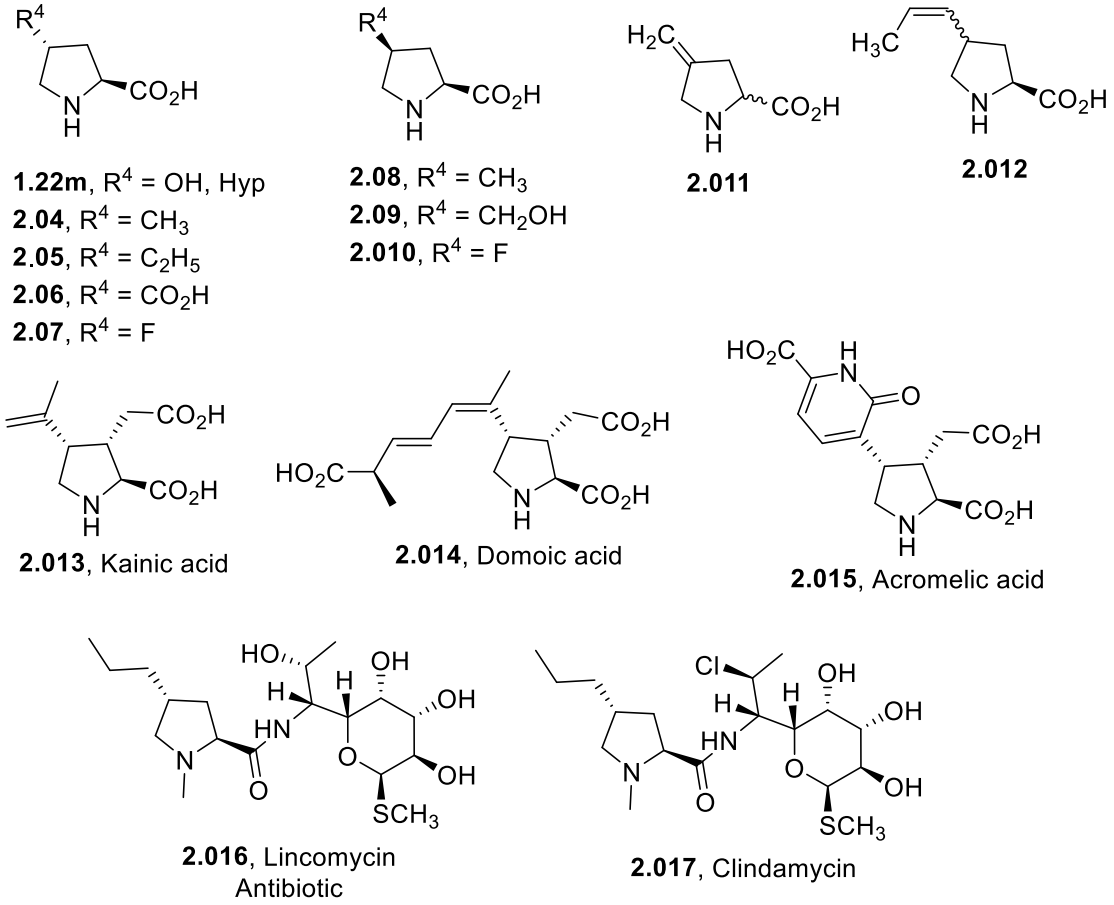

Figure 2.02. 4-Substituted proline derivatives

4-Alkylprolines are found in several natural and synthetic products. *cis*-4-Methyl-L-proline (**2.08**) is found in a number of peptide antibiotics including Leucinostatins A, B, C, and D, which were isolated from *Paecilomyces* strains (Figure 2.02).[11] *trans*-4-Methyl-L-proline (**2.04**) is a component of the antibiotic Monamycin, which was isolated from *Streptomyces jamaicensis*,[12] and has also been isolated from young green apples.[13] 4-Methylene-DL-proline derivatives (e.g., **2.011**) have been identified in the seeds of the loquat tree.[14] *cis*-4-Hydroxymethyl-L-proline (**2.09**) has been identified in many apple species, such a *Malus pumila,*[15] *Pyrus communis*[16] and *Afzelia bella,*[17] from which *trans*-4-carboxy-L-proline (**2.06**) was also characterized.[17] *trans*-4-Ethyl-L-proline (**2.05**) is a component of the depsipeptide antibiotic Mycoplanecin A.[18] Moreover, Lincomysin (**2.016**) and Clindamycin (**2.017**) are a class of antibiotic drugs containing 4-*n*-propylproline and exhibit activity against *streptococcal*, *pneumococcal* and *staphylococcal* infections.[19]

4-Alkenylprolines have also exhibited interesting activity alone and inside peptide analogs. Kainic acid (**2.013**)[20] and Domoic acid (**2.014**),[21] and the related Acromelic acid (**2.015**),[22] all exhibit neuroexcitatory and antiparasitic activities. 4-[(*Z*)-Prop-1-enyl]proline (**2.012**) is a component of the Hormaomycin antibiotics from *Streptomyces griseoflavus*, which are active against Gram negative and positive bacteria and which induce production of aerial mycelia (Figure 2.02).[23]

The vital role in human health and the interesting biological activities of 4-substituted prolines make them important synthetic targets. 4-Hydroxyproline serves commonly as a chiral educt in the synthesis of other 4-substituted proline analogs. Although the (2*S*,4*R*)-isomer of 4-hydroxyproline is abundant in natural peptides such as collagen, other stereoisomers are less readily available. In the interest of providing access to a variety of 4-substituted proline analogs

with opportunity to make all possible stereoisomers, my research has focused on the synthesis of 4-vinylprolines (**2.022**).

4-Vinylproline had previously served as a key building block in synthesis of α-helix inducing scaffold **2.024** (Scheme 2.01).[24] The synthesis of the 4-vinylproline building block was achieved in 12% overall yield and 7 steps from *trans*-(2*S*,4*R*)-hydroxyproline (**1.22m**). The helical nucleator **2.024** was subsequently prepared by a sequence featuring coupling of 4-vinylproline **2.022** to 5-vinylproline **2.023**, ring closing metathesis, and protecting group manipulations.[24]

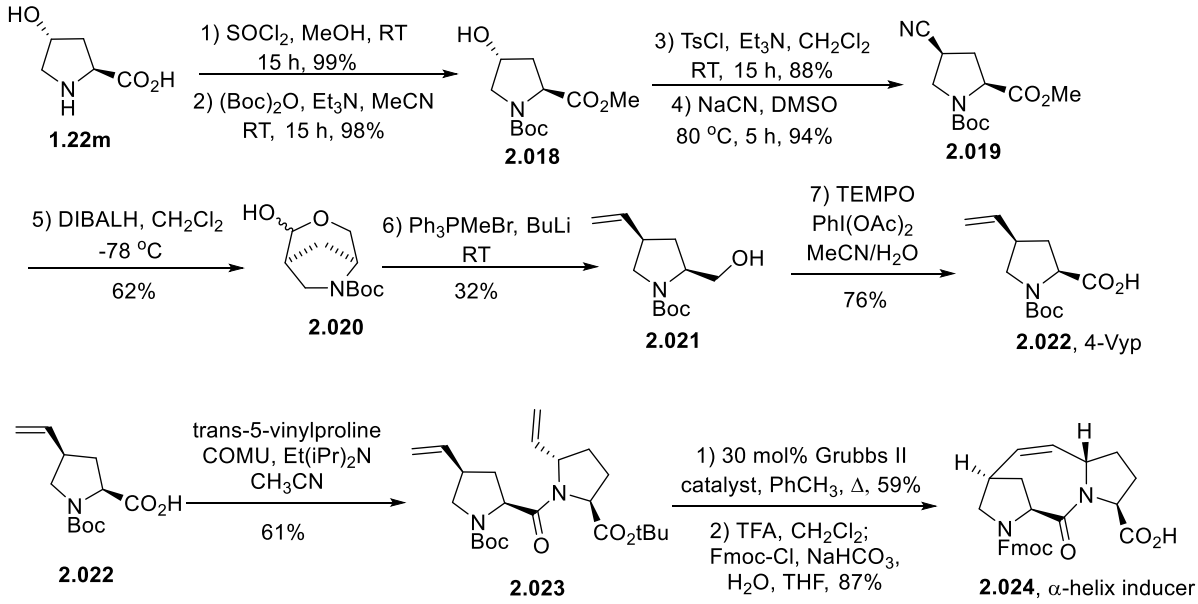

Scheme 2.01. Synthesis of 4-vinylproline and α-helix inducer

Seeking an improved gateway to 4-vinylproline **2.022** and other 4-substituted prolines for research in peptide mimicry, effective syntheses of enantiomerically pure (2*S*,4*R*)- and (2*S*,4*S*)-4-vinylproline diastereomers (2*S*,4*R*)- and (2*S*,4*S*)-**2.022** have been conceived using L-serine as chiral educt.[25] Critical for the synthesis of 4-vinylprolines **2.022** was the copper catalysed S_N2' reaction of (*Z*)-1,4-dichlorobut-2-ene with the organozinc reagent derived from β-iodoalanine

1.61.[25] The S_N2' reaction provided enantiomerically pure linear 2-*N*-(Boc)amino-4-(chloromethyl)hexenoates (2*S*,4*R*)- and (2*S*,4*S*)-**1.63** without diastereoselectivity. Improved selectivity may be achieved by using a phosphoramidite ligand in the presence of copper catalyzed asymmetric allylic substitution.[26] However, these conditions were not explored, due in part to interests in both diastereomers. In addition to 4-vinylproline, 4-vinylornithine derivatives (2*S*,4*S*)- and (2*S*,4*R*)-**1.64** were prepared by intermolecular chloride displacement with azide ion.

In sum, the copper catalyzed S_N2' approach offered access to the synthesis of 4-vinylproline and 4-vinyl ornithine analogs. These residues can be used as building blocks for the synthesis of peptide mimetics, as illustrated by the synthesis of α-helix nucleator.[24] The olefin function offers potential as a handle for diversification to provide other 4-substituted prolines as well as azabicyclo[X.Y.0]alkanone amino acids for introduction into biologically relevant peptides.[27,28]

2.03. References

1. Szabados, L.; Savouré, A., Proline: a multifunctional amino acid. *Trends Plant Sci.* **2010**, *15*, 89-97.

2. Levitt, M., Effect of proline residues on protein folding. *J. Mol. Biol.* **1981**, *145*, 251-263.

3. Wu, G.; Bazer, F. W.; Burghardt, R. C.; Johnson, G. A.; Kim, S. W.; Knabe, D. A.; Li, P.; Li, X.; McKnight, J. R.; Satterfield, M. C., Proline and hydroxyproline metabolism: implications for animal and human nutrition. *Amino Acids* **2011**, *40*, 1053-1063.

4. Mitsubuchi, H.; Nakamura, K.; Matsumoto, S.; Endo, F., Inborn errors of proline metabolism. *J. Nutr.* **2008**, *138*, 2016S-2020S.

5. Cushman, D. W.; Ondetti, M. A., History of the design of captopril and related inhibitors of angiotensin converting enzyme. *Hypertension* **1991**, *17*, 589-592.

6. Todd, P. A.; Heel, R. C., Enalapril. *Drugs* **1986**, *31*, 198-248.

7. Frampton, J. E.; Peters, D. H., Ramipril. *Drugs* **1995**, *49*, 440-466.

8. Jenkins, C. L.; Raines, R. T., Insights on the conformational stability of collagen. *Nat. Prod. Rep.* **2002**, *19*, 49-59.

9. Gorres, K. L.; Raines, R. T., Prolyl 4-hydroxylase. *Crit. Rev. Biochem. Mol. Biol.* **2010**, *45*, 106-124.

10. Newberry, R. W.; Raines, R. T., 4-Fluoroprolines: Conformational analysis and effects on the stability and folding of peptides and proteins. In *Peptidomimetics I*, Springer **2016**; pp 1-25.

11. Kenner, G.; Sheppard, R., α-Amino iso butyric Acid, β-Hydroxyleucine, and γ-Methylproline from the Hydrolysis of a Natural Product. *Nature* **1958**, *181*, 48-48.

12. Hassall, C.; Magnus, K., Monamycin: a new antibiotic. *Nature* 1959, *184*, 1223-1224.

13. Hulme, A.; Arthington, W., Methyl proline in young apple fruits. *Nature* 1954, *173*, 588-589.

14. Gray, D.; Fowden, L., 4-Methyleneproline: a new naturally occurring proline derivative. *Nature* 1962, *193*, 1285-1286.

15. Hulme, A., A New Amino-acid in the Peel of Apple Fruits. *Nature* **1954**, *174*, 1055-1056.

16. Burroughs, L., The amino-acids of apple juices and ciders. *J. Sci. Food Agric.* **1957**, *8*, 122-131.

17. Welter, A.; Marliert, M.; Dardenne, G., Nouveaux acides amines libres de Afzelia bella: trans-Hydroxy-4-L-proline et trans-carboxy-4-L-proline. *Phytochemistry* **1978**, *17*, 131-134.

18. Nakajima, M.; Torikata, A.; Tamaoki, H.; Haneishi, T.; Arai, M.; Kinoshita, T.; Kuwano, H., Mycoplanecins, novel antimycobacterial antibiotics from Actinoplanes awajinensis subsp. mycoplanecinus subsp. nov. III. Structural determination of mycoplanecin A. *J. Antibiot.* **1983**, *36*, 967-975.

19. Mitcheltree, M. J.; Pisipati, A.; Syroegin, E. A.; Silvestre, K. J.; Klepacki, D.; Mason, J. D.; Terwilliger, D. W.; Testolin, G.; Pote, A. R.; Wu, K. J., A synthetic antibiotic class overcoming bacterial multidrug resistance. *Nature* **2021**, 1-6.

20. Murakami, S.; Takemoto, T.; Shimizu, Z., Studies on the effective principles of Digenea-simplex aq. 1. separation of the effective fraction by liquid chromatography. *Yakugaku Zasshi-J. Pharm. Soc. Jpn.* **1953**, *73*, 1026-1028.

21. Clayden, J.; Read, B.; Hebditch, K. R., Chemistry of domoic acid, isodomoic acids, and their analogues. *Tetrahedron* **2005**, *61*, 5713-5724.

22. Konno, K.; Hashimoto, K.; Ohfune, Y.; Shirahama, H.; Matsumoto, T., Acromelic acids A and B. Potent neuroexcitatory amino acids isolated from Clitocybe acromelalga. *J. Am. Chem. Soc.* **1988**, *110*, 4807-4815.

23. Andres, N.; Wolf, H.; Zähner, H.; Rössner, E.; Zeeck, A.; König, W. A.; Sinnwell, V., Stoffwechselprodukte von Mikroorganismen. 253. Mitteilung. Hormaomycin, ein neues Peptid-lacton mit morphogener Aktivität auf Streptomyceten. *Helv. Chim. Acta* **1989**, *72*, 426-437.

24. Hack, V.; Reuter, C.; Opitz, R.; Schmieder, P.; Beyermann, M.; Neudörfl, J. M.; Kühne, R.; Schmalz, H. G., Efficient α-Helix Induction in a Linear Peptide Chain by N-Capping with a Bridged-tricyclic Diproline Analogue. *Angew. Chem., Int. Ed.* **2013**, *52*, 9539-9543.

25. Mulamreddy, R.; Atmuri, N. P.; Lubell, W. D., 4-Vinylproline. *J. Org. Chem.* **2018**, *83*, 13580-13586.

26. Falciola, C. A.; Alexakis, A., 1, 4-Dichloro-and 1, 4-Dibromo-2-butenes as Substrates for Cu-Catalyzed Asymmetric Allylic Substitution. *Angew. Chem. Int. Ed.* **2007**, *119*, 2673-2676.

27. Atmuri, N. P.; Reilley, D. J.; Lubell, W. D., Peptidomimetic synthesis by way of diastereoselective iodoacetoxylation and transannular amidation of 7–9-membered lactams. *Org. Lett.* **2017**, *19*, 5066-5069.

28. Godina, T. A.; Lubell, W. D., Mimics of peptide turn backbone and side-chain geometry by a general approach for modifying azabicyclo [5.3. 0] alkanone amino acids. *J. Org. Chem.* **2011**, *76*, 5846-5849.

Article 1: 4-Vinylproline

Ramakotaiah Mulamreddy, N.D. Prasad Atmuri, William D. Lubell*

Département de Chimie, Université de Montréal, C.P. 6128 Succursale Centre-Ville, Montréal H3C 3J7 QC, Canada.

J. Org. Chem. **2018**, *83*, 13580-13586.

2.1. Abstract

Enantiomerically pure 4-vinylproline (Vyp) was synthesized by a five-step approach from *N*-(Boc)iodo-alanine (**2.2**) featuring copper-catalyzed S_N2' substitution of the corresponding zincate onto (*Z*)-1,4-dichlorobut-2-ene to prepare methyl 2-*N*-(Boc)amino-4-(chloromethyl)hexenoate (**1.63**). Intra- and intermolecular displacement of the chloride provided respectively Vyp and methyl 2-*N*-(Boc)amino-4-(azidomethyl)hexenoate (**1.64**) suitable for the synthesis of constrained peptide analogs.

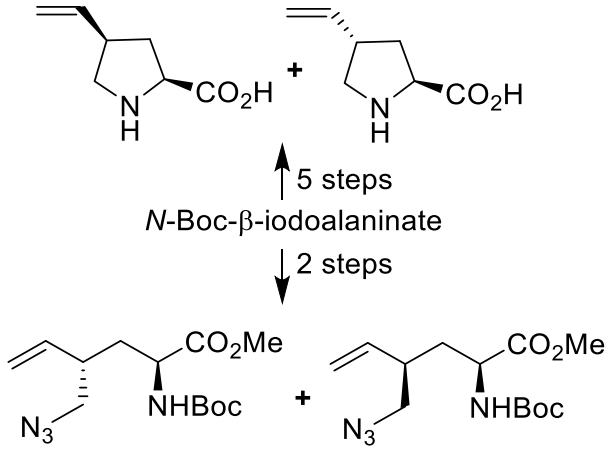

2.2. Introduction

4-Substituted prolines are natural products, peptide components and useful building blocks for a variety of applications (Figure 2.1).[1-6] For example, prolines with methyl, hydroxymethyl, carboxy and methylene 4-position substituents have been isolated from various fruits and seeds.[7] 4-Hydroxyproline is a key component of collagen.[8-10] Moreover, various peptides exhibiting antibiotic, anticancer and immunosuppressant activities contain prolines bearing alkyl,[11] alkenyl,[12] aryl,[13] amine,[14] and thio[15,16] 4-position substituents. 4-Cyclohexylproline is a component of the angiotensin converting enzyme (ACE) inhibitor Fosinopril, which is used to treat hypertension and chronic heart failure.[13] In addition, synthetic peptides possessing prolines with fluoride, amine,

guanidine and various alkyl oxide 4-position substituents have exhibited improved activity, cellular uptake and cell-penetrating ability.[17-20]

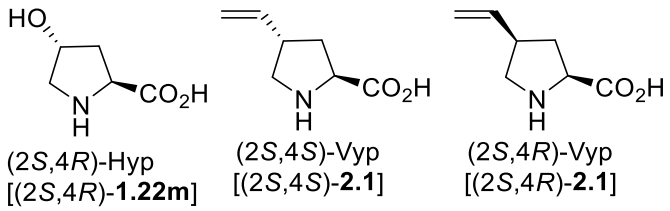

Figure 2.1. 4-Substituted proline derivatives

Natural (*2S*,4*R*)-4-hydroxproline (Hyp) is the principle starting material for the synthesis of enantiopure 4-substituted prolines.[21-25] Unnatural Hyp stereoisomers are however relatively unavailable and expensive, dictating more laborious synthetic routes to procure 4-substituted analogs. In the light of modern methods for olefin modification, 4-vinylproline (Vyp) offers an interesting but rarely used alternative starting material for 4-substituted proline assembly. For example, incorporation of (2*S*,4*R*)-Boc-Vyp-OH into a peptide and olefin metathesis was used to prepare an α-helix inducing *N*-cap bridged-tricyclic diproline analogue.[12] The traditional strategy for the synthesis of (2*S*,4*R*)-Boc-Vyp-OH from (2*S*,4*R*)-Hyp demanded however seven steps to deliver the target in 12% overall yield.[26] Herein, (2*S*,4*S*)- and (2*S*,4*R*)-Vyp-OH were obtained in five steps in 22% and 31% overall yields respectively.

Considering copper catalyzed coupling of various organometallic reagents with allylic halides has given selective S_N2' reactions,[27] the reaction of (*Z*)-1,4-dichlorobut-2-ene with the zincate of *N*-(Boc)iodo-alanine **1.61** has now been explored to provide 2-(Boc)amino-4-(chloromethyl)hexenoate **1.63**. The resulting chloride **1.63** has proven to be an effective precursor for the synthesis of enantiopure (2*S*,4*S*)- and (2*S*,4*R*)-Vyp [(2*S*,4*S*)- and (2*S*,4*R*)-**2.1**]. Moreover, chloride displacement with azide has provided (2*S*,4*S*)- and (2*S*,4*R*)-2-*N*-(Boc)amino-4-(azidomethyl)hexenoates [(2*S*,4*S*)- and (2*S*,4*R*)-**1.64**]. In the context of our program in peptide

mimicry, Vyp (**2.1**) and **1.64**, both represent readily assembled ω-olefin amino acids for the synthesis and application of constrained frameworks.[28-30]

2.3. Results and Discussion

(*2S*)-*N*-(Boc)Iodoalanine **1.61** is a commercially available enantiopure precursor, which can be prepared on multiple-gram scale from L-serine in three steps.[31, 32] Treatment of iodide **1.61** with zinc and iodine in DMF provided the corresponding zincate which was reacted with (*Z*)-1,4-dichlorobut-2-ene in the presence of catalytic copper(I) bromide dimethyl sulfide complex (Scheme 2.1). After aqueous workup and chromatography on silica gel, (2*S*,4*S*)- and (2*S*,4*R*)-2-*N*-(Boc) amino-4-(chloromethyl)hex-5-enoates [(2*S*,4*S*)- and (2*S*,4*R*)-**1.63**] were obtained respectively in 30 and 42% yields on 2 g scale. Although various conditions and chiral catalysts have been employed to achieve stereoselectivity in the Cu-catalyzed addition of organometallic reagents to allylic halides, sulfonates and phosphates,[33-35] no attempts were made to improve diastereoselectivity, because both isomeric chlorides are expected to have value in our research program using ω-unsaturated amino acids for the synthesis of peptide mimics.[28-30, 36] In addition, in contrast to routes from Hyp, effective access to the enantiomeric series is expected by employing D-serine in the sequence.

4-Vinylprolines (**2.1**) were respectively synthesized from chlorides **1.63** by intramolecular cyclization. Although attempts to cyclize carbamate **1.63** to methyl *N*-Boc-4-vinylprolinate **2.2** failed using bases such as sodium hydride and K_2CO_3, after Boc group removal with HCl gas in DCM, cyclization of amine hydrochloride was achieved effectively using K_2CO_3 and silver nitrate. Subsequent, protection with di-*tert*-butyldicarbonate delivered respectively (2*S*,4*S*)- and (2*S*,4*R*)-Boc-Vyp-OMe (2*S*,4*S*)- and

(2*S*,4*R*)-**2.2** in 80% and 82% yields from **1.63** in a one-pot synthesis. Finally, (2*S*,4*S*)- and (2*S*,4*R*)-Vyp [(2*S*,4*S*)- and (2*S*,4*R*)-**2.1**] were respectively prepared as the hydrochloride salts by hydrolysis of Boc-Vyp-OMe (**2.2**) using 6N HCl in 1,4 dioxane in 90% yields. Ion exchange chromatography provided the respective zwitterions as crystalline solids.

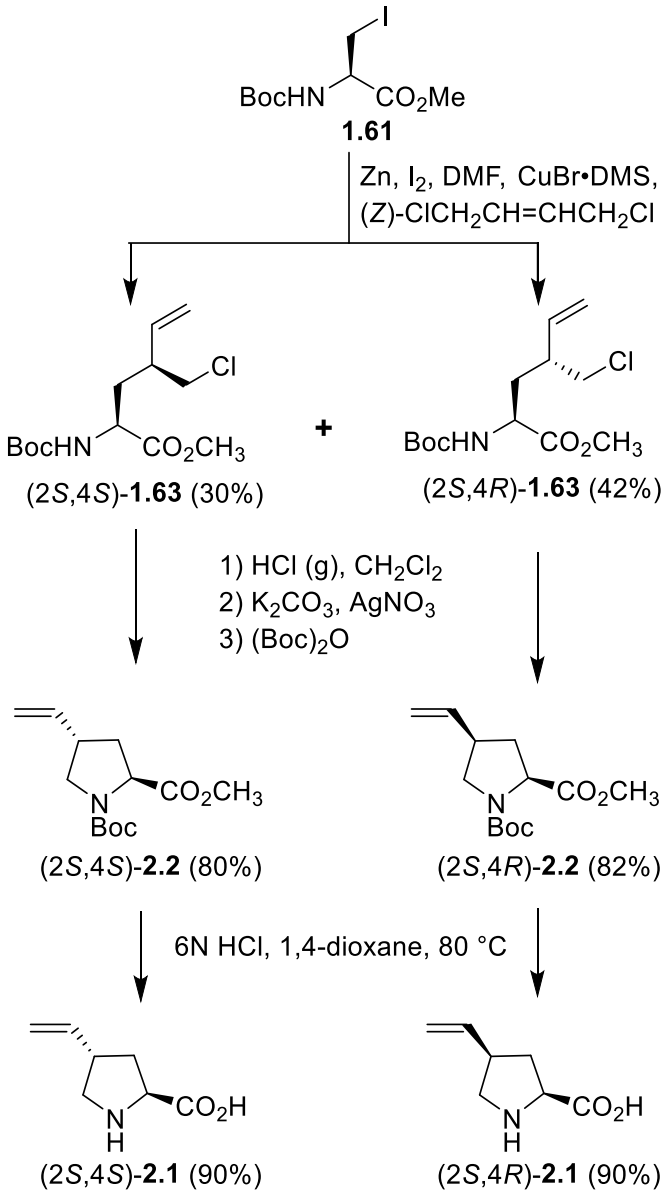

Scheme 2.1. Synthetic strategy to make 4-vinylproline

The enantiomeric purity of aminohexenoates **1.63** was ascertained after conversion to diastereomeric dipeptides by coupling respectively to L- and D-*N*-(Boc)alanine using TBTU, HOBt

and *N*-ethylmorpholine in DCM (Scheme 2.2). Although clean dipeptides were obtained using the above conditions, employment of HBTU under similar coupling conditions gave trace amounts of Boc-Ala-Vyp-OMe due to acylation after intramolecular cyclization. Examination of the diastereotopic methyl ester singlets at 3.208 and 3.222 ppm in the ^{1}H NMR spectra of (2'*S*, 4*S*)- and (2'*R*, 4*S*)-**2.4** in C_6D_6 and incremental additions of the opposite diastereomer to determine the limits of detection demonstrated a >99:1 dr for both peptides. Hence aminohexenoates **1.63** are assumed to be of >98% enantiomeric purity.

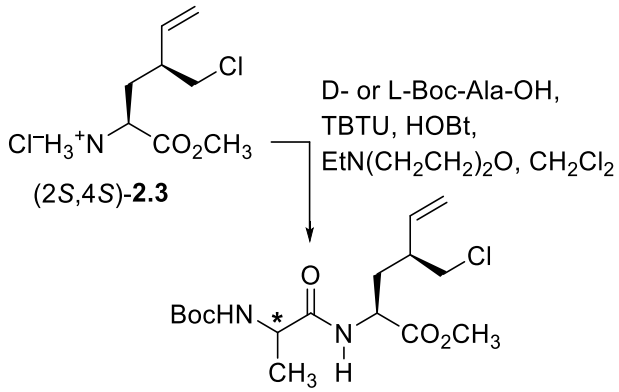

Scheme 2.2. Enantiomeric purity analysis of (2*S*,4*S*)-**2.4** by synthesis and analysis of diastereomeric dipeptides

With enantiopure aminohexenoates **1.63** in hand, chloride displacement was briefly explored to demonstrate potential for preparing novel ω-unsaturated amino acids. (2*S*,4*S*)- and (2*S*,4*R*)-Methyl 2-*N*-(Boc)amino-4-(azidomethyl)hex-5-enoates [(2*S*,4*S*)- and (2*S*,4*R*)-**1.64**] were respectively synthesized by treating the corresponding chlorides **1.63** with sodium azide at 80 °C (Scheme 2.3). Considering the orthogonal azide and olefin functionality, amino acids **1.64** represent intriguing building blocks for exploring peptide cyclization by approaches such as copper-catalyzed azide alkyne cycloaddition (CuACC) reactions,[37] and olefin metathesis.[38] The application of azido olefin **1.64** in such chemistry may be feasible considering ω-unsaturated

azides have been employed in sequential CuACC / ring closing metathesis protocols for constructing fused and bridged triazoles,[39] and that olefin metathesis has been used to release azide-containing sugars from solid supports,[40, 41] and to prepare azido sphingolipid analogs.[41]

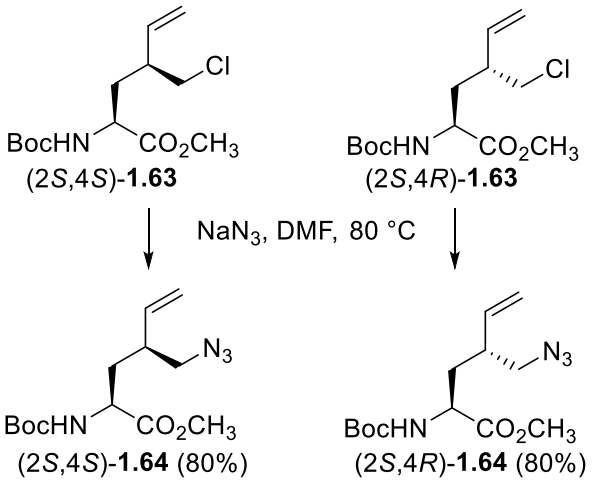

Scheme 2.3. Synthesis of azides **1.64**

The relative stereochemistry of the *cis* and *trans* Vyp diastereomers (2*S*,4*R*)- and (2*S*,4*S*)-**2.5** (Supporting information) were assigned using NOESY spectroscopy, which indicated a long-range transfer of magnetization between the C2 (4.54 ppm) and C4 (3.17 ppm) proton signals of the *cis*-isomer. In contrast, the NOESY spectrum of the *trans* diastereomer exhibited transfer of magnetization only between neighboring protons on the same face of the pyrrolidine ring. Furthermore, hydrolysis of methyl ester (2*S*,4*R*)-**2.2** gave (2*S*,4*R*)-Boc-Vyp-OH, which exhibited identical spectroscopic properties as previously reported.[12]

2.4. Conclusion

Enantiomerically pure vinylprolines **2.1** and 4-azidomethyl-2-aminohex-5-enoates **1.64** were respectively prepared in five and two steps from commercially available L-iodoalanine **1.61**. Copper catalyzed S_N2' reaction of the zincate from **1.61** onto (*Z*)-1,4-dichlorobut-2-ene provided effective access to separable 4-chloromethyl-2-aminohex-5-enoate diastereomers **1.63**, which may

serve in the synthesis of various ω-olefin amino acids by way of chloride displacement chemistry. Application of ω-unsaturated amino acids **2.1**, **1.63** and **1.64** offers potential for synthesizing constrained peptide analogs presently under investigation.

2.5. Experimental Section

2.5.1. General Methods: Unless otherwise specified, non-aqueous reactions were performed under an inert argon atmosphere, glassware was flame dried under argon or stored in the oven and cooled under inert atmosphere prior to use. Anhydrous solvents (DCM and DMF) were obtained by passage through solvent filtration systems (Glass Contour, Irvine, CA) and transferred by syringe. After aqueous workup, organic reaction mixtures were dried over anhydrous Na_2SO_4, filtered, and rotary-evaporated under reduced pressure. Flash chromatography was performed on 230−400 mesh silica gel.[42] Thin-layer chromatography (TLC) was performed on alumina plates coated with silica gel (Merck 60 F254 plates), and visualized by UV absorbance or staining with potassium permanganate solutions. Melting points were obtained on a Buchi melting point B-540 apparatus and are uncorrected. Specific rotations, $[\alpha]_D$ values, were calculated from optical rotation measurements at 25 °C in $CHCl_3$ or MeOH at the specified concentrations (*c* in g/100 ml) using a 0.5-dm cell length (l) on a Anton Paar Polarimeter, MCP 200 at 589 nm, and calculated by the general formula: $[\alpha]_D^{25} = (100 \times \alpha)/(l \times c)$. Accurate mass measurements were performed on an LC-MSD instrument in electrospray ionization (ESI-TOF) mode at the Université de Montréal Mass Spectrometry facility. Sodium adducts $[M + Na]^+$ were used for empirical formula confirmation. Nuclear magnetic resonance spectra (^1H, ^{13}C, COSY, HSQC, NOESY) were recorded on Bruker 400, 500 and 700 MHz spectrometers. ^1H NMR spectra were referenced to $CDCl_3$ (7.26 ppm), CD_3OD (3.31 ppm) or C_6D_6 (7.16 ppm) and ^{13}C NMR spectra were measured in $CDCl_3$ (77.16 ppm), CD_3OD (49.0 ppm), or C_6D_6 (128.06 ppm) as specified below. Coupling

constant *J* values were measured in Hertz (Hz) and chemical shift values in parts per million (ppm). In cases of carbamate isomers, ^{1}H and ^{13}C NMR signals of the minor isomers are respectively presented in brackets and parentheses. Infrared spectra were recorded in the neat on a Perkin Elmer Spectrometer FT-IR instrument and are reported in reciprocal centimeters (cm^{-1}).

2.5.2 Synthetic experimental conditions and characterization data of compounds:

(2*S*,4*R*)- and (2*S*,4*S*)-Methyl 2-*N*-(Boc)amino-4-(chloromethyl)hex-5-enoates (1.63)

In a 100-mL round bottom flask, fitted with three-way tap, CuBr•DMS (160 mg, 0.8 mmol, 0.13 equiv) was weighed, dried gently with a heat gun under vacuum until the powder changed color from white to light green, placed under argon, treated with dry DMF (4 mL), followed by *cis*-2-butene-1,4-dichloride (980 mg, 7.8 mmol, 1.3 equiv, pre-filtered through a plug of silica gel), and cooled to –15 °C. In a second 100-mL round bottom flask with side arm and 3-way tap, zinc dust (1.2 g, 18.2 mmol, 3 equiv) was weighed, treated with iodine (50 mg, 0.18 mmol, 0.03 equiv) and heated with a heat gun under vacuum for 10 min. The flask was allowed to cool, flushed with nitrogen, evacuated, and flushed again with nitrogen (3 x), cooled to 0 °C, treated dropwise with a solution of *N*-(Boc)-3-iodo-L-alanine methyl ester (**1.61**, 2 g, 6.1 mmol, prepared from serine according to ref. 15b) in dry DMF (4 mL), allowed to warm to rt, and stirred for 1 h, when TLC analysis indicated full consumption of the iodide ((R_f = 0.7) and organozinc reagent (R_f = 0.2), 2:1 petroleum ether/EtOAc). Stirring was stopped, the excess zinc powder was let settle and the supernatant was transferred dropwise via syringe (care being taken to minimize the transfer of zinc) into the flask containing the copper catalyst at –15°C. The cooling bath was removed, and the mixture was stirred at rt overnight, diluted with ethyl acetate (35 mL) and stirred for 15 min. The reaction mixture was transferred to a separating funnel and diluted with ethyl acetate (50 mL). The organic phase was washed successively with 1 M $Na_2S_2O_3$ (35 mL), water (2 × 35 mL) and

brine (70 mL), and dried. The volatiles were removed to afford a residue that was purified by chromatography using 4-6% EtOAc in hexane as eluent. First to elute was (2*S*,4*S*)-**1.63** (530 mg, 30%) as light green liquid. (2*S*,4*S*)-1.64:R_f = 0.52 (1:9 EtOAc/hexanes, 3 times eluted, visualized with $KMnO_4$); $[\alpha]_D^{25}$ –20.4 (*c* 1, $CHCl_3$); ^{1}H NMR (700 MHz, $CDCl_3$) δ 5.68-5.74 (m, 1H), 5.19-5.20 (d, 1H, *J* = 1.4), 5.17-5.18 (d, 1H, *J* = 3.2), 5.09-5.10 (br, d, 1H, *J* = 6.7), 4.37-4.38 (d, 1H, *J* = 6.9), 3.75 (s, 3H), 3.59-3.62 (m, 1H), 3.51-3.54 (m, 1H), 2.55-2.58 (m, 1H), 2.11-2.15 (m, 1H), 1.72-1.76 (m, 1H), 1.46 (s, 9H); ^{13}C{^{1}H} NMR (175 MHz, $CDCl_3$) δ 173.0, 155.3, 137.7, 117.8, 80.2, 52.4, 51.5, 48.1, 42.0, 34.9, 28.1; FT-IR (neat) ν_{max} 3368, 2979, 1742, 1707, 1502, 1438, 1391, 1365,1160, 1032 cm^{-1}. HRMS (ESI-TOF) m/z [M+Na]$^+$ calcd for $C_{13}H_{22}ClNO_4Na$ 314.1130 found 314.1130. Second to elute was (2*S*,4*R*)-**1.63** (740 mg, 42%), which solidified on standing: R_f = 0.45 (1:9 EtOAc/hexanes, 3 times eluted, visualized with $KMnO_4$); $[\alpha]_D^{25}$ –0.2 (*c* 1, $CHCl_3$); ^{1}H NMR (700 MHz, $CDCl_3$) δ 5.66-5.71 (m, 1H), 5.25-5.26 (d, 1H, *J* = 10.3), 5.22-5.25 (d, 1H, *J* = 17.2), 4.91-4.93 (m, 1H), 4.33-4.34 (d, 1H, *J* = 6.5), 3.75 (s, 3H), 3.55-3.56 (m, 1H), 3.46-3.48 (m, 1H), 2.55-2.56 (m, 1H), 1.87-1.89 (m, 2H), 1.46 (s, 9H); ^{13}C{^{1}H} NMR (175 MHz, $CDCl_3$) δ 173.4, 155.4, 137.0, 119.0, 80.1, 52.5, 51.6, 48.5, 42.7, 35.1, 28.4; FT-IR (neat) ν_{max} 3392, 2979, 1735, 1712, 1516, 1438, 1392, 1366, 1304, 1285, 1223 cm^{-1}; HRMS (ESI-TOF) m/z [M+Na]$^+$ calcd for $C_{13}H_{22}ClNO_4Na$ 314.1130 found 314.1140.

(2*S*,4*S*)-*N*-Boc-4-Vinylproline [(2*S*,4*S*)-2.2]

A solution of (2*S*,4*S*)-methyl 2-(Boc)amino-4-(chloromethyl)hex-5-enoate [(2*S*,4*S*)-**1.63**, 2.0 g, 6.87 mmol] in DCM (20 mL) was treated with HCl gas bubbles for 3 h, when TLC showed complete conversion of starting material (R_f = 0.45 (100% EtOAc visualized with $KMnO_4$). Argon was bubbled into the mixture to purge excess HCl for 15 min. The reaction mixture was treated with K_2CO_3 (4.74 g, 34.3 mmol, 5 equiv) and $AgNO_3$ (0.93 g, 5.5 mmol, 0.8 equiv), stirred for 36

h, treated with $(Boc)_2O$ (1.8 g, 8.2 mmol, 1.2 equiv), and stirred for 2 h. The reaction mixture was filtered through a pad of silica gel (0.5 cm height x 7 cm diameter), which was washed with DCM. Evaporation of the filtrate and washings under reduced pressure gave a residue that was purified by chromatography using 5-7% EtOAc in hexane as eluent. Evaporation of the collected fractions afforded (2*S*,4*S*)-Boc-Vyp-OMe [(2*S*,4*S*)-**2.2**, 1.4 g, 80%] as pale-yellow liquid: R_f = 0.25 (1:9 EtOAc/hexanes, visualized with $KMnO_4$); $[\alpha]_D^{25}$ –34.8 (*c* 0.54, $CHCl_3$); ^1H NMR (700 MHz, $CDCl_3$): (1:2 mixture of carbamate isomers) δ 5.69-5.75 (m, 1H), 5.05-5.14 (m, 2H), [4.39-4.40 (m, 1H)], 4.28-4.30 (m, 1H), 3.77-3.79 (m, 1H) [3.75 (s, 3H,)], 3.74 (s, 3H), [3.70-3.72 (m, 1H)], 3.17-3.20 (t, 1H, *J* = 8.9) [3.10-3.13 (t, 1H, *J* = 9.3)], 2.93-3.01 (m, 1H), 2.07-2.13 (m, 2H), [2.00-2.05 (m, 1H)], [1.47 (s, 9H)], 1.42 (s, 9H); $^{13}C\{^1H\}$ NMR (175 MHz, $CDCl_3$): δ 173.5/(173.3), (154.3)/153.6, 137.5, 116.1, 80.5, 58.9/(58.6), (52.2)/52.0, (51.3)/50.9, (41.3)/40.3, 36.5/(35.7), (28.4)/28.3; FT-IR (neat) ν_{max} 2976, 1747, 1697, 1390, 1198, 1178, 1160 cm^{-1}; HRMS (ESI-TOF) m/z $[M+Na]^+$ calcd for $C_{13}H_{21}NO_4Na$ 278.1363, found 278.1356.

(2*S*,4*R*)-*N*-Boc-4-Vinylproline [(2*S*,4*R*)-2.2]

(2*S*,4*R*)-Boc-Vyp-OMe [(2*S*,4*R*)-**2.2**] was synthesized as described for (2*S*,4*S*)-**2.2** using (2*S*,4*R*)-**1.63** (4.0 g, 13.7 mmol), and purified by chromatography on silica gel (5–7% EtOAc in hexane), which gave a pale-yellow liquid (2.9 g, 82%). R_f = 0.25 (1:9 EtOAc/hexanes, visualized with $KMnO_4$); $[\alpha]_D^{25}$ –104.0 (*c* 0.54, $CHCl_3$); ^1H NMR (500 MHz, $CDCl_3$): (1:2 mixture of carbamate isomers) δ 5.70-5.79 (m, 1H), 5.12-5.15 (d, 1H, *J* = 16.9), 5.06-5.09 (dd, 1H, *J* = 4.6, 10.3), [4.29-4.32 (t, 1H, *J* = 8.5)], 4.22-4.25 (m, 1H), 3.78-3.84 (m, 1H), [3.75 (s, 3H)], 3.74 (s, 3H), [3.69-3.73 (m, 1H)], 3.17-3.22 (m, 1H), 2.74-2.88 (m, 1H), 2.40-2.46 (m,1H), 1.74-1.83 (m, 1H), [1.47 (s, 9H)], 1.42 (s, 9H); $^{13}C\{^1H\}$ NMR (125 MHz, $CDCl_3$): δ 173.5/(173.3), (154.1)/153.4, (137.2)/137.0, 116.3 /(116.2), 80.1/(80.0), 59.3/(58.8), (52.1)/51.9, (51.6)/51.1, (42.5)/41.7, 36.9

/(36.0), (28.4)/28.2; FT-IR (neat) ν_{max} 2977, 1750, 1697, 1393, 1157, 1113 $cm^{-1.}$ HRMS (ESI-TOF) m/z $[M+Na]^+$ calcd for $C_{13}H_{21}NO_4Na$ 278.1363, found 278.1356.

(2*S*,4*S*)-4-Vinylproline [(2*S*,4*S*)-2.1]

A solution of (2*S*,4*S*)-Boc-Vyp-OMe [(2*S*,4*S*)-**2.1**, 250 mg, 0.98 mmol] in 1,4-dioxane was treated with 6N HCl, heated to 80 °C for 2 h, cooled, and washed with ethyl acetate. The aqueous layer was lyophilized to provide hydrochloride salt (170 mg, 98%) as a pale-yellow gum. $[\alpha]_D^{25}$ – 4.4 (*c* 0.5, $CHCl_3$); ^1H NMR (400 MHz, CD_3OD) δ 5.79-5.88 (m, 1H), 5.22-5.29 (d,1H, *J* = 17.2), 5.19-5.22 (d, 1H, *J* = 10.4), 4.50-4.53 (m, 1H), 3.57-3.62 (m, 1H), 3.11-3.16 (t, 1H, *J* = 9.7), 3.02-3.16 (m, 1H), 2.40-2.46 (m, 1H), 2.24-2.32 (m, 1H); $^{13}C\{^1H\}$ NMR (125 MHz, CD_3OD) δ 171.7, 136.7, 118.1, 60.2, 51.1, 42.0, 35.3; FT-IR (neat) ν_{max} 3377, 2938, 1727, 1644, 1216, 1143 cm^{-1}; HRMS (ESI-TOF) m/z $[M+H]^+$ calcd for $C_7H_{12}NO_2$ 142.0863, found 142.0856. The hydrochloride salt was purified by ion-exchange chromatography on Dowex-50WX8 resin hydrogen form (prewashed with 2M HCl, followed by water until neutral effluent), eluting with ammonia. Freeze-drying of the collected fractions gave 126 mg (91% yield) as off white solid: mp = 228-230 °C, R_f = 0.64 (3:1:1 *tert*-BuOH/AcOH/H_2O, visualized with $KMnO_4$); $[\alpha]_D^{25}$ – 54.2 (*c* 0.7, MeOH); ^1H NMR (500 MHz, CD_3OD) δ 5.74-5.81 (m, 1H), 5.20-5.24 (dt, 1H, *J* = 1.2, *J* = 17.2), 5.13-5.16 (dt, 1H, *J* = 1, *J* = 10.4), 4.04-4.07 (dd, 1H, *J* = 4.1, *J* = 9.3), 3.52-3.55 (m, 1H), 2.88-3.01 (m, 2H), 2.32-2.36 (m, 1H), 2.09-2.15 (m, 1H); $^{13}C\{^1H\}$ NMR (125 MHz, CD_3OD) δ 173.9, 137.0, 117.6, 62.2, 51.0, 42.4, 36.4.

(2*S*,4*R*)-4-Vinylproline [(2*S*,4*R*)-2.1]

Synthesized as described for (2*S*,4*S*)-**2.1**, which gave hydrochloride salt (165 mg, 95% yield) as gum: $[\alpha]_D^{25}$ –6.1 (*c* 0.5, $CHCl_3$); ^1H NMR (400 MHz, CD_3OD) δ 5.77-5.86 (m, 1H), 5.25-5.30 (d, 1H, *J* = 17.1), 5.18-5.20 (d, 1H, *J* = 10.4), 4.45-4.49 (m, 1H), 3.51-3.59 (m, 1H), 3.11-3.18 (m,

2H), 2.62-2.69 (m, 1H), 1.94-2.02 (m, 1H); $^{13}C\{^{1}H\}$ NMR (125 MHz, CD_3OD) δ 169.9, 135.2, 116.9, 59.4, 49.6, 41.9, 34.4; FT-IR (neat) ν_{max} 3388, 2922, 1731, 1645, 1453, 1420, 1223 cm^{-1}; HRMS (ESI-TOF) m/z $[M+H]^+$ calcd for $C_7H_{12}NO_2$ 142.0863, found 142.0862. Purified by Ion-exchange chromatography as described for (2*S*,4*S*)-**2.1** above gave (2*S*,4*R*)-**2.1** (125 mg , 91% yield) as off white solid: mp = 218-220 °C, R_f = 0.64 (3:1:1 *tert*-BuOH/AcOH/H_2O, visualized with $KMnO_4$); $[\alpha]_D^{25}$ – 12.4 (*c* 0.5, MeOH); ^1H NMR (500 MHz, CD_3OD) δ 5.75-5.82 (m, 1H), 5.17-5.21 (dt, 1H, *J* = 1.1, *J* = 17.1), 5.08-5.10 (dt, 1H, *J* = 1.0, *J* = 10.4), 3.93-3.96 (m, 1H), 3.33-3.36 (m, 1H), 3.01-3.10 (m, 1H), 2.91-2.99 (m, 1H), 2.47-2.53 (m, 1H), 1.77-1.83 (m, 1H); $^{13}C\{^{1}H\}$ NMR (125 MHz, CD_3OD) δ 174.9, 137.8, 117.2, 62.8, 51.2, 44.3, 37.1

(2*S*,4*S*-Methyl 2-amino-4-(chloromethyl)hex-5-enoate hydrochloride [(2*S*,4*S*)-2.3]

A solution of carbamate (2*S*,4*S*)-**1.63** (200 mg, 0.69 mmol) in DCM (5 mL) was treated with HCl gas bubbles for 3 h, and concentrated under reduced pressure to afford hydrochloride (2*S*,4*R*)-**2.3** (156 mg, 100%) as off-white solid: mp 146-148 °C; $[\alpha]_D^{25}$ –15.2 (*c* 0.5, $CHCl_3$); ^1H NMR (500 MHz, $CDCl_3$) δ 8.87 (br, s, 3H), 5.70-5.77 (m, 1H), 5.34-5.37 (d, 1H, *J* = 17.1), 5.24-5.26 (d, 1H, *J* = 11.0), 4.18-4.21 (m, 1H), 3.83 (s, 3H), 3.65-3.69 (m, 1H), 3.56-3.59 (m, 1H), 2.89-2.95 (m, 1H), 2.38-2.43 (m, 1H), 2.15-2.23 (m, 1H); $^{13}C\{^{1}H\}$ NMR (125 MHz, $CDCl_3$) δ 169.7, 136.7, 119.5, 53.3, 51.3, 48.3, 41.5, 32.4. FT-IR (neat) ν_{max} 2847, 1743, 1644, 1583, 1504, 1437, 1222 cm^{-1}; HRMS (ESI-TOF) m/z $[M+H]^+$ calcd for $C_8H_{15}ClNO_2$ 192.0786, found 192.0794.

(2*S*,4*R*)-Methyl 2-amino-4-(chloromethyl)hex-5-enoate hydrochloride [(2*S*,4*R*)-**2.3**] was prepared from carbamate (2*S*,4*R*)-**1.63** (200 mg, 0.687 mmol) as described for hydrochloride (2*S*,4*S*)-**2.3** to afford hydrochloride (2*S*,4*R*)-**2.3** as off-white solid (156 mg, 100%): mp 150-152 °C; $[\alpha]_D^{25}$ –24 (*c* 0.5, $CHCl_3$); ^1H NMR (500 MHz, $CDCl_3$) δ 8.98 (br, s, 3H), 5.71-5.77 (m, 1H), 5.57-5.60 (dd, 1H, *J* = 1.0, 17.1), 5.33-5.35 (dd, 1H, *J* = 1.3, 10.3), 4.06-4.07 (m, 1H), 3.85 (s, 3H), 3.62-3.70 (m,

2H), 3.07-3.12 (m, 1H), 2.31-2.37 (m, 1H), 2.19-2.20 (m, 1H); $^{13}C\{^{1}H\}$ NMR (125 MHz, $CDCl_3$) δ 170.0, 136.1, 120.8, 53.5, 51.6, 48.9, 41.4, 33.1; FT-IR (neat) ν_{max} 2860, 1747, 1581, 1505, 1438, 1283, 1214 cm^{-1}; HRMS (ESI-TOF) m/z $[M+H]^+$ calcd for $C_8H_{15}ClNO_2$ 192.0786, found 192.0793.

(2'*S*,2*S*,4*S*)-Methyl *N*-(Boc)alaninyl-2-amino-4-(chloromethyl)hex-5-enoate [(2'*S*,2*S*,4*S*)-2.4]

A stirred solution of *N*-Boc-L-alanine (83 mg, 0.44 mmol, 1 equiv) in DCM (5 mL) was treated with TBTU (141 mg, 0.44 mmol, 1 equiv) and HOBt (60 mg, 0.44 mmol, 1 equiv), stirred for 10-15 min, treated with *N*-ethylmorpholine (76 mg, 0.66 mmol, 1.5 equiv) and hydrochloride (2*S*,4*S*)-**2.3** (100 mg, 0.44 mmol), and stirred overnight. The reaction mixture was partitioned between water and DCM. The organic layer was separated, dried over Na_2SO_4 and concentrated under reduced pressure to a residue which was examined for diastereomeric purity by evaluation of the methyl ester singlet (3.208 ppm) with that of the (2'*R*)-diastereomer (3.222 ppm). Incremental additions of the (2'*R*)- into the (2'*S*)-isomer established the limits of detection at 1%. Subsequent purification by column chromatography using 14-16% EtoAc in hexane eluent to afforded peptide **2.4** (125 mg, 78%) as colourless liquid. R_f = 0.50 (3:7 EtOAc/hexanes, 3 times eluted, visualized with $KMnO_4$); $[\alpha]_D^{25}$ –11.8 (*c* 1, $CHCl_3$); ^1H NMR (400 MHz, C_6D_6) δ 6.54-6.56 (d, 1H, *J* = 7.84), 5.49-5.58 (m, 1H), 5.04-5.08 (d, 1H, *J* = 17.2), 4.97-4.99 (d, 1H, *J* = 10.4), 4.91 (br, s, 1H), 4.71-4.77 (m, 1H), 4.03-4.10 (m, 1H), 3.35-3.40 (m, 1H), 3.21-3.22 (d, 1H, *J* = 5.16), 3.20 (s, 3H), 2.41-2.49 (m, 1H), 2.07-2.04 (m, 1H), 1.52-1.59 (m, 1H), 1.40 (s, 9H), 1.06-1.08 (d, 3H); $^{13}C\{^{1}H\}$ NMR (100 MHz, C_6D_6) δ 172.0, 171.9, 155.0, 137.4, 116.6, 79.2, 51.4, 49.8, 47.7, 41.5, 34.2, 29.8, 28.0, 17.5; FT-IR (neat) ν_{max} 3307, 2979, 1742, 1659, 1163 cm^{-1}; HRMS (ESI-TOF) m/z $[M+Na]^+$ calcd for $C_{16}H_{27}ClN_2O_5Na$ 385.1501, found 385.1504

(2'*R*,2*S*,4*S*)-Methyl *N*-(Boc)alaninyl-2-amino-4-(chloromethyl)hex-5-enoate [(2'*R*,2*S*,4*S*)-2.4]

(2'*R*,2*S*,4*S*)- **2.4** was synthesized, analyzed and later purified as described for (2'*S*,2*S*,4*S*)-**2.4** from hydrochloride (2*S*,4*R*)-**2.3** (100 mg, 0.44 mmol): off-white solid (122 mg, 76%); R_f = 0.50 (3:7 EtOAc/hexanes, 3 times eluted, visualized with $KMnO_4$); $[\alpha]_D^{25}$ –41.4 (*c* 1, $CHCl_3$); ^{1}H NMR (400 MHz, C_6D_6) δ 7.07-7.09 (br d, 1H, *J* = 5.2), 5.49-5.58 (m, 1H), 5.17-5.18 (brd, 1H, *J* = 3.2), 5.02-5.07 (d, 1H, *J* = 17.1), 4.97-5.00 (d, 1H, *J* = 10.3), 4.74-4.80 (m, 1H), 4.27-4.30 (br, t, 1H, *J* = 7.1), 3.34-3.38 (m, 1H), 3.25 (s, 3H), 3.15-3.23 (m, 1H), 2.42-2.50 (m, 1H), 2.09-2.18 (m, 1H), 1.57-1.66 (m, 1H), 1.42 (s, 9H), 1.16-1.18 (d, 3H, *J* = 6.9); $^{13}C\{^1H\}$ NMR (100 MHz, C_6D_6) δ 172.7, 172.6, 155.9, 138.2, 117.4, 79.6, 51.8, 50.4, 48.1, 42.1, 34.5, 30.2, 28.4, 18.1; FT-IR (neat) ν_{max} 3380, 2980, 1748, 1703, 1663, 1570, 1527, 1207, 1161 cm^{-1}; HRMS (ESI-TOF) m/z $[M+Na]^+$ calcd for $C_{16}H_{27}ClN_2O_5Na$ 385.1506, found 385.1501.

Methyl (2*S*,4*S*)-4-(azidomethyl)-2-((tert-butoxycarbonyl)amino)hex-5-enoate [(2*S*,4*S*)-1.64]

A solution of methyl (2*S*,4*S*)-2-((tert-butoxycarbonyl)amino)-4-(chloromethyl)hex-5-enoate **1.63** (50 mg, 0.171 mmol) in *N*,*N*-dimethylformamide (2.5 mL) was treated with sodium azide (33 mg, 0.515 mmol, 3 equiv), heated at 80 ºC overnight, cooled, and poured into water. The mixture was extracted with ethyl acetate. The combined organic layer was washed with water (4 X 5 mL), dried with sodium sulfate, and evaporated to a residue that was purified by column chromatography using 6-8% EtOAc in hexane as eluent to provide azide (2*S*,4*R*)-**1.64** (41 mg, 80%) as a colourless liquid. R_f = 0.44 (1:9 EtOAc/hexanes, 3 times eluted, visualized with $KMnO_4$); $[\alpha]_D^{25}$ –1.39 (*c* 0.6, $CHCl_3$); ^{1}H NMR (500 MHz, $CDCl_3$) δ 5.64-5.71 (m, 1H), 5.18-5.22 (m, 2H), 5.10-5.11 (d, 1H, *J* = 7.4), 4.35-4.39 (m, 1H), 3.75 (s, 3H), 3.30-3.47 (m, 2H), 2.44-2.51 (m, 1H), 1.96-2.01 (m, 1H), 1.68-1.73 (m, 1H), 1.46 (s, 9H); $^{13}C\{^1H\}$ NMR (125 MHz, $CDCl_3$) δ 173.0, 155.3, 138.0,

117.9, 80.2, 55.1, 52.5, 51.6, 40.3, 34.9, 28.1; FT-IR (neat) ν_{max} 3358, 2978, 2095, 1742, 1708, 1503, 1365, 1159 cm^{-1}; HRMS (ESI-TOF) m/z $[M+Na]^+$ calcd for $C_{13}H_{22}N_4O_4Na$ 321.1533, found 321.1537.

Methyl (2*S*,4*R*)-4-(azidomethyl)-2-((tert-butoxycarbonyl)amino)hex-5-enoate [(2*S*,4*R*)-1.64]

Azide (2*S*,4*R*)-**1.64** was synthesized from (2*S*,4*R*)-**1.63** (50 mg, 0.171 mmol) using the protocol for (2*S*,4*S*)-**1.64** to provide colourless liquid (41 mg, 80%): R_f = 0.34 (1:9 EtOAc/hexanes, 3 times eluted, visualized with $KMnO_4$); $[\alpha]_D^{25}$ –13.09 (*c* 0.8, $CHCl_3$); ^1H NMR (500 MHz, $CDCl_3$) δ 5.63-5.68 (m, 1H), 5.23-5.27 (m, 2H), 4.92-4.94 (m, 1H), 4.26-4.34 (m, 1H), 3.76 (s, 3H), 3.31-3.35 (m, 1H), 3.24-3.28 (m, 1H), 2.43-2.50 (m, 1H), 1.81-1.90 (m, 1H), 1.72-1.77 (m, 1H), 1.46 (s, 9H); $^{13}C\{^1H\}$ NMR (125 MHz, $CDCl_3$) δ 173.3, 155.3, 137.2, 118.9, 80.1, 55.5, 52.4, 51.5, 40.7, 35.0, 28.3; FT-IR (neat) ν_{max} 3357, 2978, 2096, 1707, 1510, 1437, 1391, 1365, 1159 cm^{-1}; HRMS (ESI-TOF) m/z $[M+Na]^+$ calcd for $C_{13}H_{22}N_4O_4Na$ 321.1533, found 321.1536.

(2*S*,4*S*)-Methyl 4-vinylprolinate hydrochloride [(2*S*,4*S*)-2.5]

A solution of (2*S*,4*S*)-methyl *N*-Boc-4-vinylprolinate **2.2** (50 mg, 0.196 mmol) in DCM (20 mL) was treated with HCl gas bubbles for 2h and concentrated under reduced pressure to afford hydrochloride (2*S*,4*S*)-**2.5** as off-white solid (38 mg, 100%). $[\alpha]_D^{25}$ –1.53 (*c* 0.8, $CHCl_3$); ^1H NMR (500 MHz, $CDCl_3$) δ 10.99 (br, s, 1H), 9.31 (br, s, 1H), 5.71-5.78 (m, 1H), 5.20-5.23 (d, 1H, *J* = 17.0), 5.16-5.18 (d, 1H, *J* = 10.3), 4.59-4.60 (m, 1H), 3.83 (s, 3H), 3.81-3.82 (m, 1H), 3.18-3.22 (m, 1H), 3.01-3.09 (m, 1H), 2.39-2.44 (m, 1H), 2.18-2.27 (m, 1H); $^{13}C\{^1H\}$ NMR (125 MHz, $CDCl_3$) δ 169.2, 134.8, 118.1, 58.9, 53.6, 49.6, 40.7, 34.6; FT-IR (neat) ν_{max} 2954, 2825, 2673, 2541, 2446, 1744, 1644, 1595, 1443, 1388, 1353, 1330, 1289, cm^{-1}; HRMS (ESI-TOF) m/z $[M+H]^+$ calcd for $C_8H_{14}NO_2$ 156.1019, found 156.1023.

(2*S*,4*R*)-Methyl 4-vinylprolinate hydrochloride [(2*S*,4*R*)-2.5]

Hydrochloride (2*S*,4*R*)-**2.5** was synthesized from (2*S*,4*R*)-**2.2** (50mg, 0.196 mmol) using the protocol for (2*S*,4*S*)-**2.5** to afford off-white solid (38 mg, 100%): $[\alpha]_D^{25}$ –16.5 (*c* 0.8, $CHCl_3$); ^1H NMR (500 MHz, $CDCl_3$) δ 5.68-5.75 (m, 1H), 5.20-5.23 (d, 1H, *J* = 17.1), 5.15-5.17 (d, 1H, *J* = 10.3), 4.53-4.56 (t, 1H, *J* = 8.7), 3.85 (s, 3H), 3.68-3.72 (m, 1H), 3.28-3.30 (t, 1H, *J* = 10.9), 3.12-3.22 (m, 1H), 2.58-2.64 (m, 1H), 1.93-2.00 (m, 1H); $^{13}C\{^1H\}$ NMR (125 MHz, $CDCl_3$) δ 169.0, 134.5, 118.2, 58.8, 53.5, 50.0, 41.9, 34.8; FT-IR (neat) ν_{max} 3388, 2920, 2852, 2695, 2527, 2418, 1745, 1647, 1583, 1483, 1411, 1381, 1356, 1265 cm^{-1}; HRMS (ESI-TOF) m/z $[M+H]^+$ calcd for $C_8H_{14}NO_2$ 156.1019, found 156.1021.

2.6. Acknowledgment

This work was supported by NSERC Canada. For aid in analyses, we thank Dr. A. Fürtös, K. Venne, M-C. Tang (mass spectrometry); S. Bilodeau, C. Malveau (NMR spectroscopy) from the U. de Montréal Regional Laboratories. Shastri Indo-Canadian Institute, India is thanked for a Quebec Tuition Fee Exemption grant to N.D.P.A.

2.7. References

1. Koskinen, A. M.; Rapoport, H., Synthesis of 4-substituted prolines as conformationally constrained amino acid analogs. *J. Org. Chem.* **1989**, *54*, 1859-1866.

2. Mothes, C.; Caumes, C.; Guez, A.; Boullet, H.; Gendrineau, T.; Darses, S.; Delsuc, N.; Moumné, R.; Oswald, B.; Lequin, O., 3-Substituted prolines: from synthesis to structural applications, from peptides to foldamers. *Molecules* **2013**, *18*, 2307-2327.

3. Nevalainen, M.; Kauppinen, P. M.; Koskinen, A. M., Synthesis of Fmoc-Protected trans-4-Methylproline. *J. Org. Chem.* **2001**, *66*, 2061-2066.

4. Koivisto, J. J.; Kumpulainen, E. T.; Koskinen, A. M., Conformational ensembles of flexible β-turn mimetics in DMSO-d6. *Org. Biomol. Chem.* **2010**, *8*, 2103-2116.

5. Zwick III, C. R.; Renata, H., Remote C–H Hydroxylation by an α-Ketoglutarate-Dependent Dioxygenase Enables Efficient Chemoenzymatic Synthesis of Manzacidin C and Proline Analogs. *J. Am. Chem. Soc.* **2018**, *140*, 1165-1169.

6. Johnston, H. J.; McWhinnie, F. S.; Landi, F.; Hulme, A. N., Flexible, phase-transfer catalyzed approaches to 4-substituted prolines. *Org. Lett.* **2014**, *16*, 4778-4781.

7. Mauger, A. B., Naturally occurring proline analogues. *J. Nat. Prod.* **1996**, *59*, 1205-1211.

8. Bulleid, N.; John, D.; Kadler, K., Recombinant expression systems for the production of collagen. Portland Press Limited: **2000**.

9. Myllyharju, J., Prolyl 4-hydroxylases, key enzymes in the synthesis of collagens and regulation of the response to hypoxia, and their roles as treatment targets. *Ann. Med.* **2008**, *40*, 402-417.

10. Kang, Y. K.; Shin, K. J.; Yoo, K. H.; Seo, K. J.; Hong, C. Y.; Lee, C.-S.; Park, S. Y.; Kim, D. J.; Park, S. W., Synthesis and antibacterial activity of new carbapenems containing isoxazole moiety. *Bioorg. Med. Chem. Lett.* **2000**, *10*, 95-99.

11. Jiraskova, P.; Gazak, R.; Kamenik, Z.; Steiningerova, L.; Najmanova, L.; Kadlcik, S.; Novotna, J.; Kuzma, M.; Janata, J., New concept of the biosynthesis of 4-alkyl-L-proline precursors of lincomycin, hormaomycin, and pyrrolobenzodiazepines: Could a γ-glutamyltransferase cleave the C–C Bond? *Front. Microbiol.* **2016**, *7*, 276.

12. Höfer, I.; Crüsemann, M.; Radzom, M.; Geers, B.; Flachshaar, D.; Cai, X.; Zeeck, A.; Piel, J., Insights into the biosynthesis of hormaomycin, an exceptionally complex bacterial signaling metabolite. *Chem. Biol.* **2011**, *18*, 381-391.

13. Krapcho, J.; Turk, C.; Cushman, D. W.; Powell, J. R.; DeForrest, J. M.; Spitzmiller, E. R.; Karanewsky, D. S.; Duggan, M.; Rovnyak, G., Angiotensin-converting enzyme inhibitors. Mercaptan, carboxyalkyl dipeptide, and phosphinic acid inhibitors incorporating 4-substituted prolines. *J. Med. Chem.* **1988**, *31*, 1148-1160.

14. Mollica, A.; Pinnen, F.; Stefanucci, A.; Feliciani, F.; Campestre, C.; Mannina, L.; Sobolev, A. P.; Lucente, G.; Davis, P.; Lai, J., The cis-4-amino-L-proline residue as a scaffold for the synthesis of cyclic and linear endomorphin-2 analogues. *J. Med. Chem.* **2012**, *55*, 3027-3035.

15. Enomoto, H.; Morikawa, Y.; Miyake, Y.; Tsuji, F.; Mizuchi, M.; Suhara, H.; Fujimura, K.-i.; Horiuchi, M.; Ban, M., Synthesis and biological evaluation of N-mercaptoacylproline and N-mercaptoacylthiazolidine-4-carboxylic acid derivatives as leukotriene A 4 hydrolase inhibitors. *Bioorg. Med. Chem. Lett.* **2008**, *18*, 4529-4532.

16. Krogsgaard-Larsen, N.; Delgar, C. G.; Koch, K.; Brown, P. M.; Møller, C.; Han, L.; Huynh, T. H.; Hansen, S. W.; Nielsen, B.; Bowie, D., Design and Synthesis of a Series of l-trans-4-Substituted Prolines as Selective Antagonists for the Ionotropic Glutamate Receptors Including Functional and X-ray Crystallographic Studies of New Subtype Selective Kainic Acid Receptor Subtype 1 (GluK1) Antagonist (2 S, 4 R)-4-(2-Carboxyphenoxy) pyrrolidine-2-carboxylic Acid. *J. Med. Chem.* **2016**, *60*, 441-457.

17. Yamashita, H.; Kato, T.; Oba, M.; Misawa, T.; Hattori, T.; Ohoka, N.; Tanaka, M.; Naito, M.; Kurihara, M.; Demizu, Y., Development of a cell-penetrating peptide that exhibits responsive changes in its secondary structure in the cellular environment. *Sci Rep.* **2016**, *6*, 33003.

18. Fillon, Y. A.; Anderson, J. P.; Chmielewski, J., Cell penetrating agents based on a polyproline helix scaffold. *J. Am. Chem. Soc.* **2005**, *127*, 11798-11803.

19. Crespo, L.; Sanclimens, G.; Montaner, B.; Pérez-Tomás, R.; Royo, M.; Pons, M.; Albericio, F.; Giralt, E., Peptide dendrimers based on polyproline helices. *J. Am. Chem. Soc.* **2002**, *124*, 8876-8883.

20. Newberry, R. W.; Raines, R. T., 4-Fluoroprolines: Conformational analysis and effects on the stability and folding of peptides and proteins. In *Peptidomimetics I*; Springer: **2016**; pp 1-25.

21. Bhagwat, S. S.; Fink, C. A.; Gude, C.; Chan, K.; Qiao, Y.; Sakane, Y.; Berry, C.; Ghai, R. D., 4-Substituted proline derivatives that inhibit angiotensin converting enzyme and neutral endopeptidase 24.11. *Bioorg. Med. Chem. Lett.* **1994**, *4*, 2673-2676.

22. Arasappan, A.; Chen, K. X.; Njoroge, F. G.; Parekh, T. N.; Girijavallabhan, V., Novel Dipeptide macrocycles from 4-oxo,-thio, and-amino-substituted proline derivatives. *J. Org. Chem.* **2002**, *67*, 3923-3926.

23. Pandey, A. K.; Naduthambi, D.; Thomas, K. M.; Zondlo, N. J., Proline editing: a general and practical approach to the synthesis of functionally and structurally diverse peptides. Analysis of steric versus stereoelectronic effects of 4-substituted prolines on conformation within peptides. *J. Am. Chem. Soc.* **2013**, *135*, 4333-4363.

24. Del Valle, J. R.; Goodman, M., Asymmetric hydrogenations for the synthesis of Boc-protected 4-alkylprolinols and prolines. *J. Org. Chem.* **2003**, *68*, 3923-3931.

25. Murphy, A. C.; Mitova, M. I.; Blunt, J. W.; Munro, M. H., Concise, stereoselective route to the four diastereoisomers of 4-methylproline. *J. Nat. Prod.* **2008**, *71*, 806-809.

26. Hack, V.; Reuter, C.; Opitz, R.; Schmieder, P.; Beyermann, M.; Neudörfl, J. M.; Kühne, R.; Schmalz, H. G., Efficient α-Helix Induction in a Linear Peptide Chain by N-Capping with a Bridged-tricyclic Diproline Analogue. *Angew. Chem. Int. Ed.* **2013**, *52*, 9539-9543.

27. Dunn, M. J.; Jackson, R. F.; Pietruszka, J.; Turner, D., Synthesis of Enantiomerically Pure Unsaturated. alpha.-Amino Acids Using Serine-Derived Zinc/Copper Reagents. *J. Org. Chem.* **1995**, *60*, 2210-2215.

28. Surprenant, S.; Lubell, W. D., From macrocycle dipeptide lactams to azabicyclo [XY 0] alkanone amino acids: A transannular cyclization route for peptide mimic synthesis. *Org. Lett.* **2006**, *8*, 2851-2854.

29. Atmuri, N. P.; Lubell, W. D., Insight into Transannular Cyclization Reactions To Synthesize Azabicyclo [XY Z] alkanone Amino Acid Derivatives from 8-, 9-, and 10-Membered Macrocyclic Dipeptide Lactams. *J. Org. Chem.* **2015**, *80*, 4904-4918.

30. Atmuri, N. P.; Reilley, D. J.; Lubell, W. D., Peptidomimetic Synthesis by Way of Diastereoselective Iodoacetoxylation and Transannular Amidation of 7–9-Membered Lactams. *Org. Lett.* **2017**, *19*, 5066-5069.

31. Atmuri, N. P.; Lubell*, W. D., Preparation of N-(Boc)-Allylglycine Methyl Ester Using a Zinc-Mediated, Palladium-Catalyzed Cross-Coupling Reaction. *Org. Synth.* **2003**, *92*, 103-116.

32. Trost, B. M.; Rudd, M. T., Chemoselectivity of the ruthenium-catalyzed hydrative diyne cyclization: total synthesis of (+)-cylindricine C, D, and E. *Org. Lett.* **2003**, *5*, 4599-4602.

33. Falciola, C. A.; Alexakis, A., 1, 4-Dichloro-and 1, 4-Dibromo-2-butenes as Substrates for Cu-Catalyzed Asymmetric Allylic Substitution. *Angew. Chem. Int. Ed.* **2007**, *119*, 2673-2676.

34. Börner, C.; Gimeno, J.; Gladiali, S.; Goldsmith, P. J.; Ramazzotti, D.; Woodward, S., Asymmetric chemo-and regiospecific addition of organozinc reagents to Baylis–Hillman derived allylic electrophiles. *Chem. Commun.* **2000**, 2433-2434.

35. Belelie, J. L.; Chong, J. M., Stereoselective reactions of acyclic allylic phosphates with organocopper reagents. *J. Org. Chem.* **2001**, *66*, 5552-5555.

36. Godina, T. A.; Lubell, W. D., Mimics of peptide turn backbone and side-chain geometry by a general approach for modifying azabicyclo [5.3. 0] alkanone amino acids. *J. Org. Chem.* **2011**, *76*, 5846-5849.

37. Diness, F.; Schoffelen, S.; Meldal, M., Advances in merging triazoles with peptides and proteins. In *Peptidomimetics I*, Springer: **2015**; pp 267-304.

38. Brik, A., Metathesis in peptides and peptidomimetics. *Adv. Synth. Catal.* **2008**, *350*, 1661-1675.

39. Zhang, X.; Hsung, R. P.; Li, H., A triazole-templated ring-closing metathesis for constructing novel fused and bridged triazoles. *Chem. Commun.* **2007**, 2420-2422.

40. Kanemitsu, T.; Seeberger, P. H., Use of olefin cross-metathesis to release azide-containing sugars from solid support. *Org. Lett.* **2003**, *5*, 4541-4544.

41. Rai, A. N.; Basu, A., Sphingolipid Synthesis via Olefin Cross Metathesis: Preparation of a Differentially Protected Building Block and Application to the Synthesis of d-erythro-Ceramide. *Org. Lett.* **2004**, *6*, 2861-2863.

42. Still, W. C.; Kahn, M.; Mitra, A., Rapid chromatographic technique for preparative separations with moderate resolution. *J. Org. Chem.* **1978**, *43*, 2923-2925.

Chapter 3: Constrained Glu-Gly and Gln-Gly dipeptide surrogates from γ-substituted α-amino-δ-lactam synthesis

3.0. Context

3.01. Lactams

α-amino-lactams are conformationally constrained building blocks, which are commonly used in the synthesis of biologically active peptide analogs to enhance potency and selectivity. For example, the incorporation of α-amino-γ-lactam (Agl, **3.01**), so called "Freidinger-Veber lactam", into Luteinizing Hormone-Releasing Hormone (LH-RH) analog **3.03** gave 8.9 times enhanced potency relative to the parent system.[1] α-Amino-δ-lactams (Adl, **3.02**), the six-membered ring counterparts of Freidinger-Veber lactams, have been used less commonly. Notably, introduction of a six-membered lactam into methionine-enkephalin analog **3.04** gave higher activity than the related 5- and 7-membered γ- and ε-lactam analogs (Figure 3.01).[2]

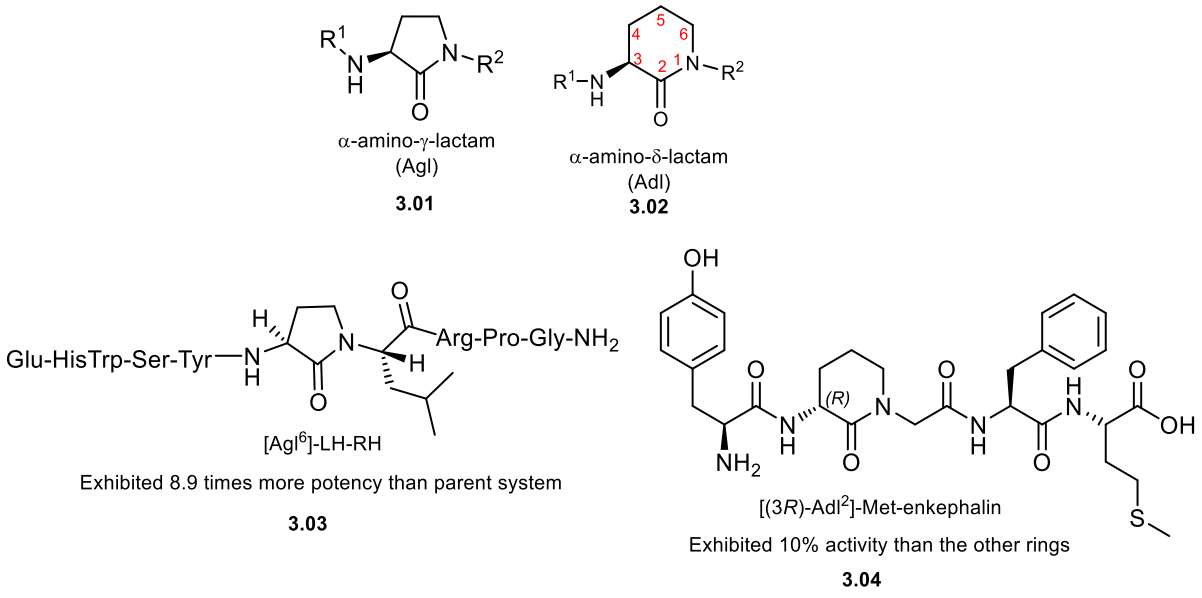

Figure 3.01. γ- and δ-Lactams and their analogs

Unsubstituted Adl residues (**3.02**) can be readily obtained from cyclization of ornithine and employed in conformationally constrained peptidomimetics. More challenging to synthesize, substituted Adl analogs have exhibited biological activity and received attention in drug discovery

(Figure 3.02). For example, glorin (**3.013**) and glorinamide (**3.014**) are natural chemoattractant peptide derivatives containing Adl residues.[3] Insect kinin analogs were synthesized using 3,6-disubstituted Adl residue **3.05**.[4] 3-Methyl [(3*R*)-Adl], 4-silyloxy and 5-hydroxy Adl residues **3.06-3.08** have been used as building blocks in the synthesis of thalidomide metabolites exhibiting antiangiogenic and teratogenic properties.[5, 6, 7]

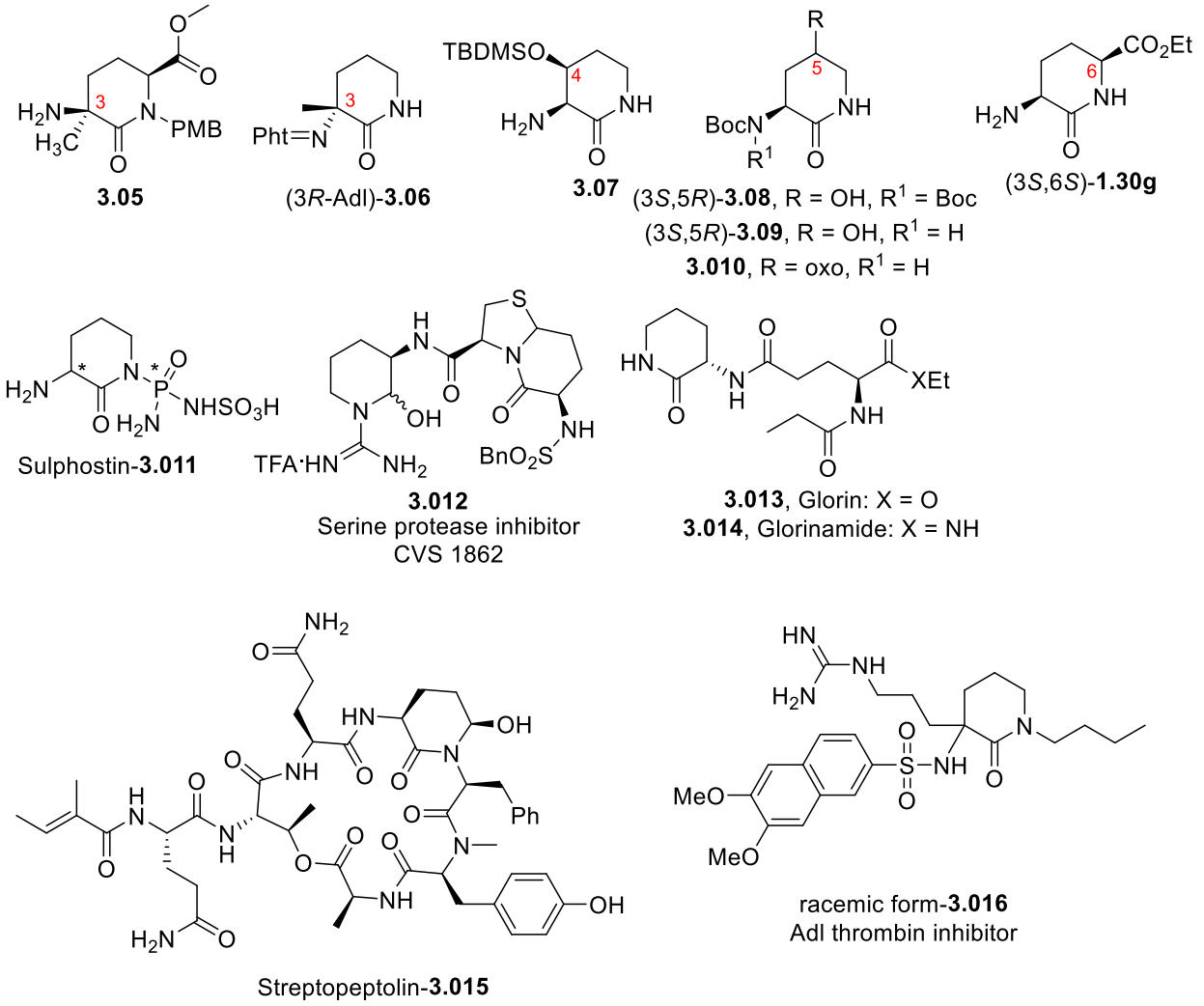

Figure 3.02. α-Amino-δ-lactam (Adl) residues in small molecule and peptide analogs

Constrained Ala-Gly dipeptide analogs were synthesized using (3*S*,5*R*)-Adl **3.09** and 5-oxo-Adl **3.010** analogs.[8] Similarly, 6-substituted ethyl-3-amino-2-piperidone-6-carboxylate

(3*S*,6*S*)-**1.30g** was incorporated into peptides as a constrained dipeptide analog.[9] Fused bicyclic systems featuring Adl components, such as thiaindolizidin-2-one **3.012**, have also been prepared for use as rigid dipeptide residues in structure-activity relationship (SAR) studies.[10]

Enzyme inhibitors have also featured substituted Adl residues. For example, Sulphostin **3.011** is naturally occurring dipeptidyl peptidase IV inhibitor isolated from *Streptomyces sp*.[11] A 6-hydroxy Adl **3.015** residue is present in the peptide Streptopeptolin, which was isolated from the extract of *Streptomyces olivochromogenes* and shown to exhibit inhibitory activity against Chymotrypsin.[12] Substituted Adl **3.016** inhibited thrombin and blood coagulation .[13]

3.02. Application of lactams in conformational analysis

The introduction of Adl residues into peptides has been used to study relationships between conformation and biological activity. For example, Adl residues have been substituted for the central leucine in tripeptide **3.017** (L-Pro-L-Leu-Gly-NH_2, PLG, Figure 3.03), which is a modulator of dopamine receptors derived from the *C*-terminal fragment of oxytocin.[14,15] Application of (*R*)-Adl gave tripeptide **3.018**, which adapt a type II β-turn possessing a ψ^2 torsion angle of 108° and exhibited enhanced binding affinity towards the dopamine receptors compared to the linear tripeptide PLG. On the other hand, (*S*)-Adl tripeptide **3.019** adopted a type II' β-turn conformation which possessed a ψ^2 torsion angle of −156° and exhibited no detectable dopamine receptor affinity.[15]

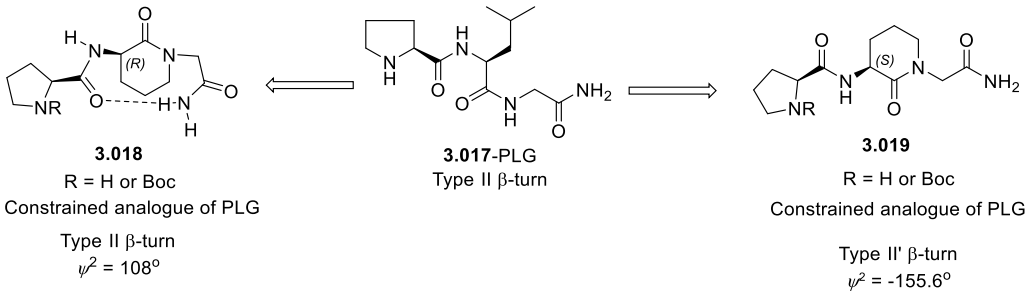

Figure 3.03. Conformational analysis of PLG using α-amino-δ-lactams

3.03. Synthesis of α-amino-δ-lactam analogs

The conformational constraint induced by α-amino-δ-lactam (Adl) residues offers interesting potential for studying structure-activity relationships of biologically active peptides. Since the pioneering synthesis of Adl-Gly dipeptide **3.022** from ornithine **3.020** by Freidinger and Veber (Scheme 3.01-A),[16] a number of methods have been developed to prepare functionalized analogs of the parent structure featuring various substitution patterns.[4,5,6,7,9] Among strategies for the addition of substituents onto Adl residues, modification at the 5-position offers potential to prepare constrained variants of certain amino acids known to occupy the *i* + 1 position of β-turns: e.g., Glu, Gln, Lys, Arg and Met.[17]

Towards the synthesis of 5-substituted Adl derivatives, 5-hydroxy and 5-oxo Adl residues **3.028** and **3.026** were respectively prepared by a route featuring the coupling of the zincate **1.62**, which is derived from β-iodo alanine **1.61**, and *N*-(Cbz)glycine phenylthioester **3.023** to provide a common γ-keto ester intermediate **3.024** in 49% yield (Scheme 3.01). Diastereoselective reduction of ketone **3.026** with *L*-selectride followed by lactam formation gave 5-hydroxy Adl **3.028**.[8] Alternatively, γ-keto ester **3.024** was converted to 5-oxo-α-amino-δ-lactam **3.026** by a route featuring methyl ester hydrolysis and carboxylate activation as pentafluorophenyl ester **3.025**, followed by hydrogenolysis of the Cbz protecting group and lactam cyclization.[8] Although alcohol

3.028 and ketone **3.026** may respectively serve as accesses to other 5-substitued Adl residues, the low overall yields to make these precursors motivated the development of an alternative approach to 5-substituted Adl derivatives.

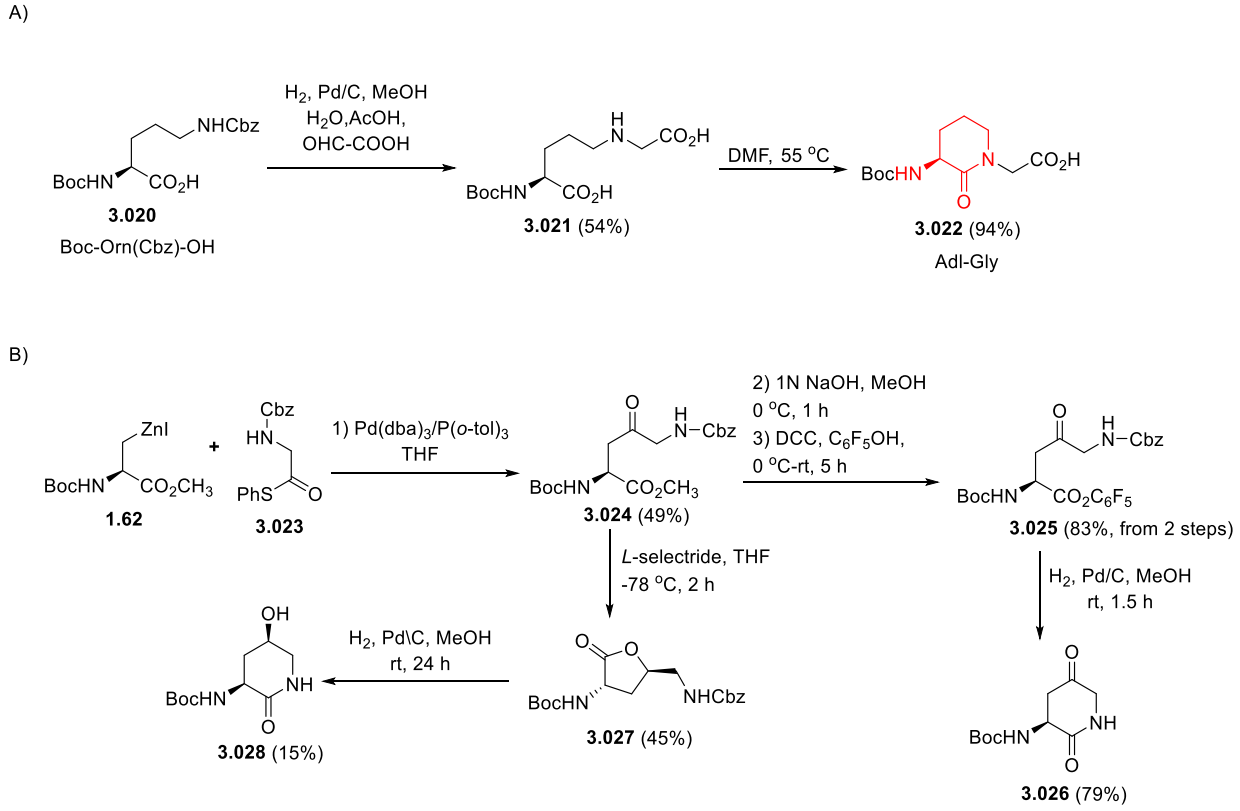

Scheme 3.01. Synthesis of Adl and substituted Adl derivatives

Chapter 3 relates our publication "Constrained Glu-Gly and Gln-Gly dipeptide surrogates from γ-substituted α-amino-δ-lactam synthesis". This publication was included in a Special Issue: Tribute to Professor Louis A. Carpino. A pioneer of peptide science, Professor Carpino developed several amine protecting groups and coupling reagents for solution and solid phase peptide synthesis including the *tert*-butyloxycarbonyl (Boc) and 9-fluorenylmethoxycarbonyl (Fmoc) groups, and well as the reagents 7-aza-1-hydroxybenzotriazole (HOAt), tetramethylfluoroformamidinium hexafluorophosphate (TFFH) and [(7-azabenzotriazol-1-yl)oxy]

tris(pyrrolidino) phosphonium hexafluorophosphate (PyAOP).[18,19,20,21] For protection of the guanidine side chain of arginine residues, Professor Carpino invented the 2,2,4,6,7-pentamethyldihydrobenzofuran-5-sulfonyl group (Pbf) group.[22] Moreover, Professor Carpino introduced protecting groups that could be removed using Michael addition approaches, such as the 1,1-dioxobenzo[b]thiophene-2-ylmethyloxycarbonyl (Bsmoc).[23] In our contribution to this tribute, the Boc group invented by Professor Carpino serves in the synthesis of constrained dipeptide analogs for the mimicry of the central residues of β-turn conformations.

As mentioned, the Adl-Gly dipeptide adopted type II and II' conformations contingent on lactam stereochemistry.[24] Moreover, 5-position substituents on the Adl lactam could mimic the side chains of amino acids that commonly situate in such turn conformers, among which Gln-Gly and Glu-Gly are very common in protein structures.[17] A plan to synthesize such dipeptide turn mimics was considered based on oxidation of a 5-vinyl Adl precursor.

Employing 4-vinylornithine **1.64** which was described in Chapter 2, a route to 5-vinyl Adl analog **3.10** was developed featuring azide reduction, cyclization, and *N*-alkylation of the resulting lactam. The utility of the olefin moiety for introducing side chain diversity was demonstrated in the synthesis of constrained glutamate and glutamine analogs by oxidation to the corresponding carboxylic acid and subsequent coupling to prepare the amide. Considering the abundance of Glu-Gly and Gln-Gly residues in nature, this method offers an effective entry into these constrained mimics of backbone and side chain topology for conformational analysis of various biologically active peptides.

3.04. References

1. Freidinger, R. M.; Veber, D. F.; Perlow, D. S.; Saperstein, R., Bioactive conformation of luteinizing hormone-releasing hormone: evidence from a conformationally constrained analog. *Science* **1980**, *210*, 656-658.

2. Shuman, R.; Smithwick, E.; Frederickson, R.; Gesellchen, P.; Rich, D.; Gross), E., Peptides: Proceedings of the 7th American Peptide Symposium. *Pierce Chemical Co., Rockford, IL, USA* **1981**, 617-618.

3. Barnett, R.; Raszkowski, D.; Winckler, T.; Stallforth, P., Versatile synthesis of the signaling peptide glorin. *Beilstein J. Org. Chem.* **2017**, *13*, 247-250.

4. Kamoune, L.; De Borggraeve, W. M.; Verbist, B. M.; Broeck, J. V.; Coast, G. M.; Compernolle, F.; Hoornaert, G., Structure based design of simplified analogues of insect kinins. *Tetrahedron* **2005**, *61*, 9555-9562.

5. Luzzio, F. A.; Thomas, E. M.; Figg, W. D., Thalidomide metabolites and analogs. Part 2: Cyclic derivatives of 2-N-phthalimido-2S, 3S (3-hydroxy) ornithine. *Tetrahedron Lett.* **2000**, *41*, 7151-7155.

6. Yadav, S. R.; Tiwari, V. S.; Haq, W., Stereoselective Synthesis of (R)-3-Methylthalidomide by Piperidin-2-one Ring Assembly Approach. *Chirality* **2015**, *27*, 619-624.

7. Luzzio, F. A.; Duveau, D. Y.; Figg, W. D., A chiral pool approach toward the synthesis of thalidomide metabolites. *Heterocycles* **2006**, *70*, 321-334.

8. Estiarte, M. A.; Diez, A.; Rubiralta, M.; Jackson, R. F., Synthesis of a 3-aminopiperidin-2, 5-dione as a conformationally constrained surrogate of the Ala-Gly dipeptide. *Tetrahedron* **2001**, *57*, 157-161.

9. Kemp, D.; McNamara, P. E., An efficient synthesis of ethyl LL-3-amino-2-piperidone-6-carboxylate. *J. Org. Chem.* **1984**, *49*, 2286-2288.

10. Tamura, S. Y.; Goldman, E. A.; Brunck, T. K.; Ripka, W. C.; Semple, J. E., Rational design, synthesis, and serine protease inhibitory activity of a novel P1-argininal derivative featuring a conformationally constrained P2–P3 bicyclic lactam moiety. *Bioorg. Med. Chem. Lett.* **1997**, *7*, 331-336.

11. Abe, M.; Akiyama, T.; Nakamura, H.; Kojima, F.; Harada, S.; Muraoka, Y., First synthesis and determination of the absolute configuration of sulphostin, a novel inhibitor of dipeptidyl peptidase IV. *J. Nat. Prod.* **2004**, *67*, 999-1004.

12. Kodani, S.; Komaki, H.; Hemmi, H.; Miyake, Y.; Kaweewan, I.; Dohra, H., Streptopeptolin, a cyanopeptolin-type peptide from Streptomyces olivochromogenes. *ACS Omega* **2018**, *3*, 8104-8110.

13. Okayama, T.; Seki, S.; Ito, H.; Takeshima, T.; Hagiwara, M.; Morikawa, T., Lactam-Cohformationally Restricted Analogs of Nα-Arylsulfonyl Arginine Amide: Design, Synthesis and Inhibitory Activity toward Thrombin and Related Enzymes. *Chem. Pharm. Bull.* **1995**, *43*, 1683-1691.

14. Valle, G.; Crisma, M.; Toniolo, C.; Yu, K.-L.; Johnson, R. L., Crystal-state structures of Boc-Pro-Leu-Gly-NH 2, hemihydrate and two lactam-restricted analogues. *J. Chem. Soc., Perkin Trans. 2* **1989**, 83-87.

15. Sreenivasan, U.; Mishra, R. K.; Johnson, R. L., Synthesis and dopamine receptor modulating activity of lactam conformationally constrained analogs of Pro-Leu-Gly-NH2. *J. Med. Chem.* **1993**, *36*, 256-263.

16. Freidinger, R. M.; Perlow, D. S.; Veber, D. F., Protected lactam-bridged dipeptides for use as conformational constraints in peptides. *J. Org. Chem.* **1982**, *47*, 104-109.

17. Wilmot, C.; Thornton, J., Analysis and prediction of the different types of β-turn in proteins. *J. Mol. Biol.* **1988**, *203*, 221-232.

18. Carpino, L. A.; Han, G. Y., 9-Fluorenylmethoxycarbonyl function, a new base-sensitive amino-protecting group. *J. Am. Chem. Soc.* **1970**, *92*, 5748-5749.

19. Carpino, L. A.; El-Faham, A., Tetramethylfluoroformamidinium hexafluorophosphate: a rapid-acting peptide coupling reagent for solution and solid phase peptide synthesis. *J. Am. Chem. Soc.* **1995**, *117*, 5401-5402.

20. Carpino, L. A., 1-Hydroxy-7-azabenzotriazole. An efficient peptide coupling additive. *J. Am. Chem. Soc.* **1993**, *115*, 4397-4398.

21. Carpino, L. A., New Methods of Introducing the Carbo-t-butoxy Protective Group. Preparation of t-Butyl Cyanoformate[1]. *J. Am. Chem. Soc.* **1960**, *82*, 2725-2727.

22. Carpino, L. A.; Shroff, H.; Triolo, S. A.; Mansour, E.-S. M.; Wenschuh, H.; Albericio, F., The 2,2,4,6,7-pentamethyldihydrobenzofuran-5-sulfonyl group (Pbf) as arginine side chain protectant. *Tetrahedron Lett.* **1993**, *34*, 7829-7832.

23. Carpino, L. A.; Philbin, M.; Ismail, M.; Truran, G. A.; Mansour, E.; Iguchi, S.; Ionescu, D.; El-Faham, A.; Riemer, C.; Warrass, R., New family of base-and nucleophile-sensitive amino-protecting groups. A Michael-acceptor-based deblocking process. Practical utilization of the 1,1-dioxobenzo[b]thiophene-2-ylmethyloxycarbonyl (Bsmoc) group. *J. Am. Chem. Soc.* **1997**, *119*, 9915-9916.

24. Bhagwanth, S.; Mishra, R. K.; Johnson, R. L., Development of peptidomimetic ligands of Pro-Leu-Gly-NH2 as allosteric modulators of the dopamine D2 receptor. *Beilstein J. Org. Chem.* **2013**, *9*, 204-214.

Article 2: Constrained Glu-Gly and Gln-Gly dipeptide surrogates from γ-substituted α-amino-δ-lactam synthesis

Ramakotaiah Mulamreddy, William D. Lubell*

Département de Chimie, Université de Montréal, C.P. 6128 Succursale Centre-Ville, Montréal H3C 3J7 QC, Canada.

Peptide Sci. **2020**, *112*, e24149.

3.1. Abstract

Conformationally rigid α-amino-δ-lactam surrogates of Glu-Gly and Gln-Gly dipeptides have been synthesized from α-amino-γ-vinyl-δ-lactam precursors. A reductive cyclization protocol from the respective (4*R*)- and (4*S*)-2-*N*-(Boc)amino-4-(azidomethyl)hexenoates gave δ-lactams, which were converted to the corresponding dipeptide surrogates by *N*-alkylation with methyl bromoacetate. The utility of these α-amino-γ-vinyl-δ-lactam building blocks was demonstrated by olefin oxidation and peptide coupling to prepare constrained Glu and Gln residues.

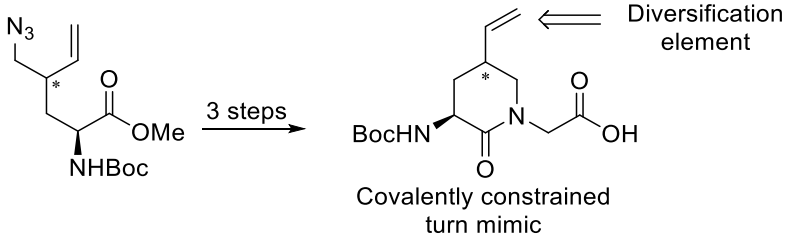

3.2. Introduction

In peptide science, α-amino-δ-lactams (Adl) residues (e.g., **3.1-3.8**, Figure 3.1) have received less attention than their γ-lactam Agl counterparts.[1] Specifically, the Adl-Gly dipeptide has exhibited interesting effects on conformation[2] and biology.[3] For example, cyclo-[(*S*)-Adl-Gly]$_3$ exhibited equal ability as cyclo-(Ala-Sar)$_3$ to inhibit methane production in the fermentation of rumen stomach fluid.[4] Replacement of the Gly^2-Gly^2 dipeptide in methionine-enkephalin with (*R*)-Adl-Gly gave analog **3.8** with 2–10% activity and greater potency than the corresponding γ- and ε-lactam counterparts and their configurational isomers.[5] In the development of inhibitors of angiotensin converting enzyme, Adl-Gly served to explore the structural requirements for binding of Enalapril.[6] In studies of dopamine receptor allosteric modulators, Pro-(*R*)-Adl-Gly-NH$_2$ enhanced agonist binding and supported an active type II β-turn conformation, but the corresponding (*S*)-Adl analog was inactive.[7,8] Replacement of the D-Phe-Pro residue by (*S*)-Adl-

Gly in thrombin inhibitors (e.g., **3.7**) enhanced selectivity and oral bioavailability.[9] In a design of potential dimerization inhibitors of HIV1-protease, attachment of adipic acid to the *N*-terminal of Adl-Gly-Asn-Phe-OH provided access to analogs with activity against wild type HIV1 in the μM range.[10]

The utility of Adl residues has also led to the synthesis of ring substituted analogs to mimic both the backbone and side chain geometry of β-turns and other peptide structures.[11,12,13,14,15,16,17,18,19,20,21] For example, 3-benzyl substituted Adl residues were synthesized and shown to mitigate chymotrypsin-catalyzed proteolysis in peptide analogs.[11,17] In the study of the hematopoiesis regulating tetrapeptide Ac-Ser-Asp-Lys-Pro-OH, 4-carboxy-Adl was employed as a constrained Asp surrogate.[18] Aliphatic and aromatic 4-position substituents have been installed on Adl-Xaa analogs to mimic Trp-Gly, Ile-Gly, Phe-Gly and Phe-Leu residues,[19,20,21] which have been respectively employed in renin inhibitors,[21] and shown by NMR experiments and molecular modeling calculations to adopt γ-turn and distorted type II β-turn geometry contingent on stereochemistry and structure.[21] 5-Amino-, 5-hydroxy-6-carboxy- and 5-methylthio-Adl residues have respectively been prepared as constrained diaminobutyric acid (Dab),[12] Ala-Ser,[13] and Met analogs.[14,15] The latter were pursued to develop inhibitors of hepatic glutathione transport.[14,15] In addition, Adl derivatives with fused rings, such as indolizidine-2-one[22] and quinolizidinone[23] amino acid analogs (e.g., **3.4** and 3**.5**), and with spirocyclic[24] systems (e.g., **3.6**), all have been used to mimic β-turns and to study peptide ligands of various receptors.[22,25,26]

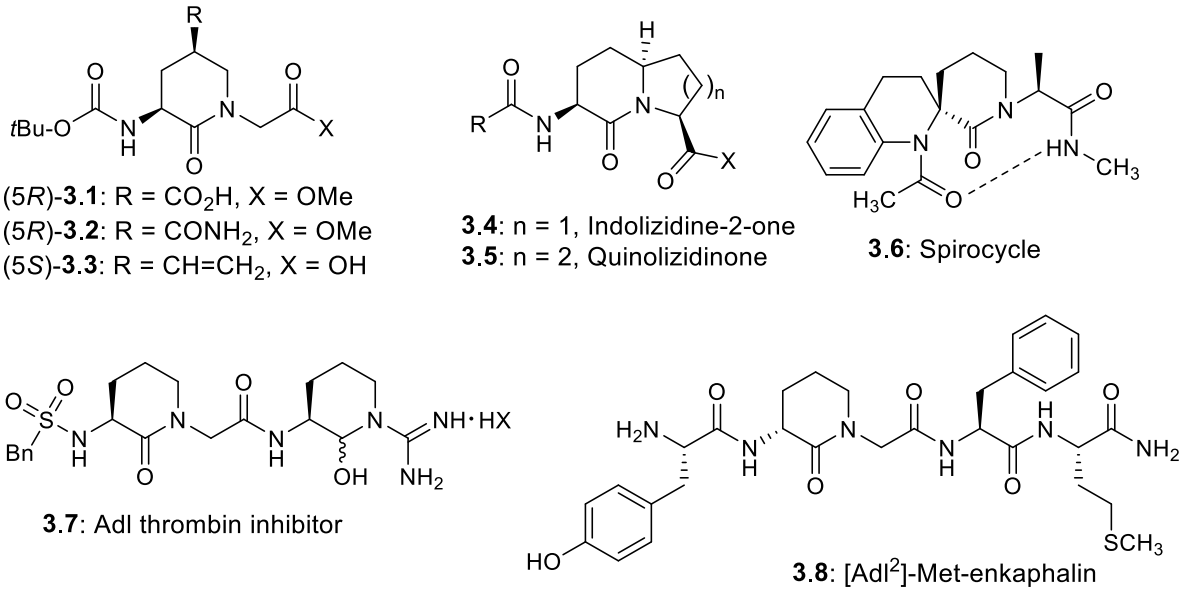

Figure 3.1. α-Amino-δ-lactam (Adl) residue derivatives

In light of the broad utility of such constrained dipeptides and methods for δ-lactam synthesis,[27,28,29,30,31,32] versatile approaches to install ring substituents onto Adl residues merit development for exploring the importance of backbone and side chain function and geometry in peptide recognition. The synthesis of γ-vinyl Adl residues is herein reported and used to synthesize Glu-Gly and Gln-Gly surrogates **3.1** and **3.2** to demonstrate the versatility of the double bond substituent as a handle for installing side chain diversity.

The Gln-Gly and Glu-Gly sequences, both are common in peptides and proteins. For example, Gln-Gly is a frequent component of transglutaminase donor substrates.[33] Four Glu-Gly units are found in the tumor suppressor protein tazarotene-induced gene 1.[34] Two Glu-Gly units are present in the long acting human glucagon-like polypeptide-1 analogue and antidiabetic drug Taspoglutide (Hoffmann-La Roche).[35] The *N*-terminals of several scorpion β-toxins, such as centruroides suffusus suffusus toxin II terminate in the H-Lys-Glu-Gly-Tyr sequence.[36] In addition, the peptide hormones, growth hormone-releasing hormone and secretin, both contain a Gln-Gly unit.[37,38]

Analysis of X-ray data of type II turn conformations has demonstrated the preference for Gly at the *i*+2 position, as well as the statistically significant preferences for Glu and more preferably Gln at the *i*+1 position.[39] Considering that Adl-Gly has been shown to favor type II and II' turn geometry contingent on amino-lactam stereochemistry,[2, 7] the placement of a γ-carboxylate (γ-carboxamide) residue on the δ-lactam residue may furnish building blocks well suited for mimicry of the active conformers of Glu-Gly and Gln-Gly peptides. Effective methods for synthesizing the corresponding suitably protected 5-(HO_2C)-, 5-(H_2NOC)- and 5-(vinyl)Adl-Gly analogs **3.1-3.3** have now been achieved in the interest of using these surrogates to explore various biologically active peptides in the future.

3.3. Experimental section

3.3.1. General Methods: Unless otherwise specified, non-aqueous reactions were performed under an inert argon atmosphere, glassware was flame dried under argon or stored in the oven and cooled under inert atmosphere prior to use. Anhydrous THF was obtained by passage through a solvent filtration system (Glass Contour, Irvine, CA) and transferred by syringe. After aqueous workup, organic reaction mixtures were dried over anhydrous Na_2SO_4, filtered, and rotary-evaporated under reduced pressure. Flash chromatography was performed on 230−400 mesh silica gel.[45] Thin-layer chromatography (TLC) was performed on alumina plates coated with silica gel (Merck 60 F254 plates), and visualized by UV absorbance or staining with potassium permanganate solution and bromo-cresol green solutions. Melting points were obtained on a Buchi melting point B-540 apparatus and are uncorrected. Specific rotations, $[\alpha]_D$ values, were calculated from optical rotation measurements at 25 °C in $CHCl_3$ or MeOH at the specified concentrations (*c* in g/100 ml) using a 0.5-dm cell length (l) on a Anton Paar Polarimeter, MCP 200 at 589 nm, and calculated by the general formula: $[\alpha]_D^{25} = (100 \times \alpha)/(l \times c)$. Accurate mass measurements were

performed on an LC-MSD instrument in electrospray ionization (ESI-TOF) mode at the Université de Montréal Mass Spectrometry facility. Sodium adducts $[M + Na]^+$ were used for empirical formula confirmation. Nuclear magnetic resonance spectra (^1H, ^{13}C) were recorded on a Bruker 500 MHz spectrometer. 1H NMR spectra are referenced to $CDCl_3$ (7.26 ppm). ^{13}C NMR spectra were measured in $CDCl_3$ (77.16 ppm) as specified below. Coupling constant *J* values were measured in Hertz (Hz) and chemical shift values in parts per million (ppm).

3.3.2. Synthetic experimental conditions and characterization data of compounds:

(3*S*,5*R*)-Boc-(5-carboxy)Adl-Gly-OMe [(5*R*)-3.1]

Acid (5*R*)-3.1 was prepared from olefin (5*R*)-**3.11** (250 mg, 0.8 mmol) using the protocol described below for the synthesis of acid (5*S*)-**3.1**. Evaporation of the collected fractions afforded acid (5*R*)-**3.1** as a white solid (172 mg, 65% yield): mp = 145–148 ºC R_f = 0.22 (1:9 MeOH/DCM, visualized with bromo cresol green), $[\alpha]_D^{25}$ –11.6 (*c* 1.3, $CHCl_3$); ^1H NMR (500 MHz, $CDCl_3$) δ 5.7-5.69 (d, 1H, *J* = 5.2), 4.48-4.45 (m, 2H), 3.98-3.82 (m, 2H), 3.77 (s, 3H), 3.53-3.49 (dd, 1H, 12.2, 6.1), 3.15 (s, 1H), 2.87 (s, 1H), 1.93-191 (d, 1H, *J* = 9.8), 1.46 (s, 9H); $^{13}C\{^1H\}$ NMR (125 MHz, $CDCl_3$) δ 177.9, 170.6, 169.3, 156.1, 80.5, 52.3, 48.9, 48.7, 48.0, 36.6, 29.5, 28.3; HRMS (ESI-TOF) m/z $[M+Na]^+$ calcd for $C_{14}H_{22}N_2O_7Na$ 353.1319, found 353.1322.

(3*S*,5*S*)-Boc-(5-carboxy)Adl-Gly-OMe [(5*S*)-3.1]

A 50 mL single-necked round bottom flask was equipped with stir bar, and charged with $NaIO_4$ (856 mg, 4 mmol, 5 equiv.), followed by H_2O (4 mL). After stirring for 10 min, the mixture was treated with $RuCl_3 \cdot 3H_2O$ (18 mg, 0.08 mmol, 0.1 equiv.), followed by CH_3CN (2.5 mL). The reaction mixture color turned red orange. After stirring vigorously for 10 min, the reaction mixture was treated slowly with a solution of olefin (5S)-**3.11** (250 mg, 0.8 mmol) in CH_2Cl_2 (2.5 mL). After stirring 1h, the reaction mixture turned dark brown, a light yellow solid precipitated, and TLC showed complete disappearance of (5S)-**3.11** and formation of a polar product. The reaction

was diluted with CH_2Cl_2 (15 mL) and quenched with saturated NH_4Cl solution (10 mL). The layers were separated. The aqueous layer was extracted with CH_2Cl_2 (10 mL X 2) and EtOAc (10 mL X 2). The organic layers were combined, dried over anhydrous Na_2SO_4, filtered and evaporated under reduced pressure. The residue was purified by flash chromatography using 1% MeOH in dichloromethane. Evaporation of the collected fractions afforded acid (5*S*)-**3.1** (145 mg, 55% yield) as off-white solid: mp = 118–120 ºC, R_f = 0.22 (1:9 MeOH/DCM, visualized with bromo cresol green), $[\alpha]_D^{25}$ –30 (*c* 1.1, $CHCl_3$); ^{1}H NMR (500 MHz, $CDCl_3$) δ 5.62 (br s, 1H), 4.21-4.16 (m, 3H), 3.76 (s, 3H), 3.66-3.63 (m, 2H), 3.07 (s, 1H), 2.81 (s, 1H), 1.88 (s, 1H), 1.46 (s, 9H); ^{13}C{^{1}H} NMR (125 MHz, $CDCl_3$) δ 178.3, 169.9, 169.0, 155.9, 79.8, 52.3, 50.6, 48.9, 41.9, 39.2, 30.3, 28.4; HRMS (ESI-TOF) m/z $[M+Na]^+$ calcd for $C_{14}H_{22}N_2O_7Na$ 353.1319, found 353.1325.

(3*S*,5*R*)-Boc-(5-carboxamide)Adl-Gly-OMe [(5*R*)-3.2]

A solution of carboxylic acid (5*R*)-**3.1** (100 mg, 0.3 mmol) in *N*-methyl-2-pyrrolidone (1 mL) was treated with NH_4Cl (32.4 mg, 0.6 mmol, 2 equiv) followed by *N,N,N′,N′*-tetramethyl-*O*-(benzotriazol-1-yl)uronium tetrafluoroborate (TBTU, 146 mg, 0.45 mmol, 1.5 equiv.) and *N*-methyl morpholine (153 mg, 1.5 mmol, 5 equiv.). After stirring overnight at room temperature, TLC analysis showed complete disappearance of carboxylic acid (5*R*)-**3.1** and formation of a less polar product. The reaction mixture was diluted with H_2O. The mixture was extracted with ethyl acetate (5 mL X 3). The organic layers were combined, dried with anhydrous Na_2SO_4, filtered and evaporated under reduced pressure. The residue was purified by column chromatography using 5% MeOH in DCM as an eluent. Evaporation of the collected fractions gave amide (5*R*)-**3.2** (55 mg, 55% yield) as light yellow solid: mp = 180–182 ºC, R_f = 0.6 (1:9 MeOH/DCM, visualized with $KMnO_4$), $[\alpha]_D^{25}$ –28.4 (*c* 1, $CHCl_3$); ^{1}H NMR (500 MHz, $CDCl_3$) δ 6.82 (s, 1H), 5.65 (s, 1H), 5.49 (s, 1H), 4.28-4.25 (d, 1H, *J* = 16.2), 4.17-4.14 (m, 2H), 3.81-3.76 (m, 4H), 3.59-3.55 (dd, 1H, *J* = 12.7, 5.8), 3.03-2.99 (m, 1H), 2.77-2.72 (dt, 1H, *J* = 12.9, 5), 2.11-2.05 (dt, 1H, *J* = 13.0, 6.4),

1.47 (s, 9H); $^{13}C\{^{1}H\}$ NMR (125 MHz, $CDCl_3$) δ 173.9, 170.1, 169.8, 155.9, 80.0, 52.5, 49.2, 48.8, 48.1, 37.9, 30.2, 28.3; HRMS (ESI-TOF) m/z $[M+Na]^+$ calcd for $C_{14}H_{23}N_3O_6Na$ 352.1479, found 352.1485.

(3*S*,5*R*)-Boc-(5-vinyl)Adl-Gly-OH [(5*R*)-3.3]

Acid (5*R*)-3.3 was prepared from ester (5*R*)-**3.10** (50 mg, 0.16 mmol) using the protocol described below for the synthesis of acid (5*S*)-**3.3**. Evaporation of the collected fractions afforded acid (5*R*)-**3.3** as white solid (42 mg, 87%): mp = 135−138 ºC, R_f = 0.2 (3:7 MeOH/DCM, visualized with $KMnO_4$), $[\alpha]_D^{25}$ –2.4 (*c* 1.4, $CHCl_3$); ^{1}H NMR (500 MHz, $CDCl_3$) δ 5.93-5.86 (m, 1H), 5.53 (br s, 1H), 5.24-5.18 (m, 2H), 4.35-4.27 (m, 2H), 4.07-4.03 (m, 1H), 3.49-3.42 (m, 2H), 2.87-2.83 (m, 1H), 2.37-2.29 (m, 1H), 2.00-1.94 (m, 1H), 1.47 (s, 9H); $^{13}C\{^{1}H\}$ NMR (125 MHz, $CDCl_3$) δ 171.8, 171.0, 155.8, 137.7, 116.3, 79.9, 52.1, 49.0, 48.7, 34.8, 32.7, 28.3; HRMS (ESI-TOF) m/z $[M+Na]^+$ calcd for $C_{14}H_{22}N_2O_5Na$ 321.1420, found 321.1420.

(3*S*,5*S*)-Boc-(5-vinyl)Adl-Gly-OH [(5*S*)-3.3]

A solution of ester (5*S*)-**3.10** (50 mg, 0.16 mmol) in a 1:1 H_2O: dioxane mixture (2 mL) was treated with $LiOH{\cdot}H_2O$ (7 mg, 0.16 mmol), and stirred for 4 h, when TLC analysis showed complete disappearance of (5*S*)-**3.10** and formation of a more polar product. The volatiles were evaporated. The reduced volume was washed with EtOAc (5 mL). The layers were separated. The aqueous layer was acidified with 1M HCl to pH 4 and extracted with EtOAc (10 mL x 3). The organic extractions were combined, washed with brine, dried with anhydrous Na_2SO_4, filtered and evaporated to provide acid (5*S*)-**3.3** (39 mg, 81% yield) as a white solid: mp = 162−165 ºC, R_f = 0.2 (3:7 MeOH/DCM, visualized with $KMnO_4$), $[\alpha]_D^{25}$ –18.8 (*c* 1.2, $CHCl_3$); ^{1}H NMR (500 MHz, $CDCl_3$) δ 5.78-5.71 (ddd, 1H, *J* = 17.2, 10.4, 6.9), 5.53 (br s, 1H), 5.19-5.12 (m, 2H), 4.34-4.30 (d, 1H, *J* = 17.3), 4.20-4.19 (m, 1H), 3.96-3.92 (d, 1H, *J* = 17.7), 3.39-3.36 (m, 1H), 3.34-3.29 (t, 1H, *J* = 11.2) 2.81 (br s, 1H), 2.50 (br s, 1H), 1.75-1.68 (m, 1H), 1.47 (s, 9H); $^{13}C\{^{1}H\}$ NMR (125

MHz, $CDCl_3$) δ 171.7, 170.4, 156.2, 137.2, 116.3, 79.9, 53.9, 51.4, 49.2, 36.5, 33.8, 28.3; HRMS (ESI-TOF) m/z $[M+Na]^+$ calcd for $C_{14}H_{22}N_2O_5Na$ 321.1420, found 321.1424.

(3*S*,5*R*)-α-Amino-γ-vinyl-δ-lactam [(5*R*)-3.9]

Lactam (5*R*)-**3.9** was prepared from 4-vinylornithine (4*R*)-**1.64** (1.0 g, 3.3 mmol) using the protocol described below for the synthesis of lactam (5*S*)-**3.9**. Evaporation of the collected fractions gave an off-white solid (600 mg, 75% yield): mp = 105−107 ºC, R_f = 0.25 (100% EtOAc, visualized with $KMnO_4$), $[\alpha]_D^{25}$ –44.1 (*c* 1, $CHCl_3$); ^1H NMR (500 MHz, $CDCl_3$) δ 6.33 (s, 1H), 5.93-5.86 (ddd, 1H, *J* = 17.1, 10.5, 6.5), 5.43 (s, 1H), 5.23-5.17 (m, 2H), 4.2 (s, 1H), 3.45-3.41 (m, 1H), 3.28-3.24 (m, 1H), 2.75-2.71 (m, 1H), 2.4-2.37 (m, 1H), 1.92-1.86 (m, 1H), 1.47 (s, 9H); $^{13}C\{^1H\}$ NMR (125 MHz, $CDCl_3$) δ 171.8, 155.7, 137.8, 116.0, 79.7, 48.5, 44.9, 35.3, 32.7, 28.3; HRMS (ESI-TOF) m/z $[M+Na]^+$ calcd for $C_{12}H_{20}N_2O_3Na$ 263.1366, found 263.1363.

(3*S*,5*S*)-α-Amino-γ-vinyl-δ-lactam [(5*S*)-3.9]

To a solution of (2*S*,4*S*)-4-(azidomethyl)-2-((*tert*-butoxycarbonyl)amino)-hex-5-enoate [(4*S*)-**1.64**, 1.0 g, 3.3 mmol, prepared according to reference 40] in an ethanol (10 mL) and water (10 mL) mixture, NH_4Cl (0.45 g, 8.3 mmol, 2.5 equiv.) and Zn powder (0.33 g, 5.0 mmol, 1.5 equiv.) were added. After stirring vigorously at room temperature for 6-7 h, TLC of the reaction mixture showed complete disappearance of starting material [(R_f = 0.34 (1:9 EtOAc/hexanes)] and appearance of a more polar product [**3.9**, R_f = 0.25 (EtOAc)]. Ethyl acetate (30 mL) and ammonium hydroxide (13 M, 5 mL) were added to the reaction mixture, which was transferred to a separatory funnel. The organic layer was separated, washed with brine, dried over Na_2SO_4, filtered and evaporated under reduced pressure to a residue, which was purified by flash chromatography using 60-80% EtOAc in hexanes as eluent. Evaporation of the collected fractions gave lactam (5*S*)-**3.9** (600 mg, 75% yield) as off-white solid: mp = 112−114 ºC, R_f = 0.25 (100% EtOAc, visualized

with $KMnO_4$), $[\alpha]_D^{25}$ –62.3 (*c* 1.1, $CHCl_3$); ^1H NMR (500 MHz, $CDCl_3$) δ 6.01 (s, 1H) 5.78-5.72 (ddd, 1H, *J* = 17.2, 10.4, 6.8) 5.43 (s, 1H), 5.17-5.10 (m, 2H), 4.12-4.10 (m, 1H), 3.41-3.37 (m, 1H), 3.1-3.13 (t, 1H, *J* = 11.3), 2.78-2.70 (m, 1H), 2.59-2.57 (m, 1H), 1.63-1.56 (m, 1H), 1.47 (s, 9H); $^{13}C\{^1H\}$ NMR (125 MHz, $CDCl_3$) δ 171.1, 155.9, 137.7, 115.9, 79.8, 51.2, 46.8, 36.7, 33.9, 28.6; HRMS (ESI-TOF) m/z $[M+Na]^+$ calcd for $C_{12}H_{20}N_2O_3Na$ 263.1366, found 263.1371.

(3*S*,5*R*)-Boc-(5-vinyl)Adl-Gly-OMe [(5*R*)-3.10]

Dipeptide ester (5*R*)-**3.10** was prepared from lactam (4*R*)-**3.9** (0.5 g, 2.03 mmol) using the protocol described below for the synthesis of ester (5*S*)-**3.10**. Evaporation of the collected fractions gave dipeptide ester (5*R*)-**3.10** as colorless liquid (460 mg, 71%): R_f = 0.53 (7:3 EtOAc/hexanes, visualized with $KMnO_4$), $[\alpha]_D^{25}$ –19.8 (*c* 3, $CHCl_3$); ^1H NMR (500 MHz, $CDCl_3$) δ 5.95-5.88 (ddd, 1H, *J* = 17.2, 10.5, 6.7), 5.41 (br s, 1H), 5.25-5.18 (m, 2H), 4.28-4.25 (d, 2H, *J* = 17.8), 4.09-4.06 (d, 1H, *J* = 17.8), 3.77 (s, 3H), 3.42-3.41 (d, 2H, *J* = 6.5), 2.88-2.84 (m, 1H), 2.42-2.36 (m, 1H), 1.96-1.89 (ddd, 1H, *J* = 13.3, 10.7, 6.8), 1.47 (s, 9H); $^{13}C\{^1H\}$ NMR (125 MHz, $CDCl_3$) δ 170.5, 169.3, 155.6, 137.9, 116.2, 79.6, 52.2, 51.8, 48.7, 34.9, 32.7, 28.3, 27.8; HRMS (ESI-TOF) m/z $[M+Na]^+$ calcd for $C_{15}H_{24}N_2O_5Na$ 335.1577, found 335.1589.

(3*S*,5*S*)-Boc-(5-vinyl)Adl-Gly-OMe [(5*S*)-3.10]

A solution of lactam (5*S*)-**3.9** (0.5 g, 2.0 mmol) in dry THF (5 mL) was cooled to –78 °C, treated slowly with a solution of LiHMDS in THF (1.0 M, 5.2 mmol, 2.5 equiv.), stirred for 30 minutes, treated dropwise with methyl bromoacetate (0.48 g, 3.1 mmol, 1.5 equiv) and allowed to warm to 0 °C with stirring. After 2 h, TLC analysis showed complete disappearance of (5*S*)-**3.9** and formation of a new less polar product. The reaction mixture was quenched with saturated NH_4Cl solution, stirred for 20-30 min, diluted with ethyl acetate (15 mL), and partitioned. The organic layer was washed with brine, dried over Na_2SO_4, filtered and evaporated under reduced pressure to a residue, which was purified by flash chromatography using 30-40% EtOAc in

hexanes as eluent. Evaporation of the collected fractions gave dipeptide ester (5S)-**3.10** (470 mg, 72% yield) as a colorless liquid. R_f = 0.53 (7:3 EtOAc/hexanes, visualized with $KMnO_4$), $[\alpha]_D^{25}$ – 31.4 (*c* 1.2, $CHCl_3$); ^{1}H NMR (500 MHz, $CDCl_3$) δ 5.78-5.71 (ddd, 1H, *J* = 17.2, 10.4, 6.9), 5.41 (br s, 1H), 5.18-5.11 (m, 2H), 4.29-4.25 (d, 1H, *J* = 17.2), 4.24-4.17 (m, 1H), 3.95-3.92 (d, 1H, *J* = 17.2) 3.77 (s, 3H), 3.39-3.35 (ddd, 1H, *J* = 11.5, 6.0, 1.5), 3.30-3.26 (t, 1H, *J* = 11.2), 2.87-2.77 (m, 1H), 2.6-2.58 (d, 1H, *J* = 10), 1.69-1.64 (t, 1H, *J* = 12.4), 1.47 (s, 9H); ^{13}C{^{1}H} NMR (125 MHz, $CDCl_3$) δ 169.9, 169.1, 155.9, 137.5, 116.1, 79.7, 53.7, 52.2, 51.5, 48.9, 36.5, 34.0, 28.3; HRMS (ESI-TOF) m/z $[M+Na]^+$ calcd for $C_{15}H_{24}N_2O_5Na$ 335.1577, found 335.1572.

3.4. Results and Discussion

Protected 4-vinylornithine (Von) **1.64** was previously synthesized in 5 steps from serine by a route featuring a copper-catalyzed S_N2' reaction onto (*Z*)-1,4-dichloro-2-butene using the zincate derived from *N*-(Boc)iodo-alanine, which yielded 2-(Boc)amino-4-(chloromethyl)hexenoate, followed by chloride displacement with azide ion.[40] Employing (4*R*)- and (4*S*)-Von **1.64**, (5*R*)- and (5*S*)-α-amino-γ-vinyl-δ-lactams **3.9** were respectively synthesized by a reductive cyclization strategy (Scheme 1). Initially, azide **1.64** was reduced using Staudinger reaction conditions employing triphenylphosphine in THF/H_2O.[41] However, removal of residual triphenylphosphine oxide complicated purification of lactam **3.9**. Purer (5*R*)- and (5*S*)-α-amino-γ-vinyl-δ-lactams **3.9** were effectively prepared in 75% yields respectively by reduction of the corresponding azide **1.64** using zinc and ammonium chloride in an EtOH:water solution.[42]

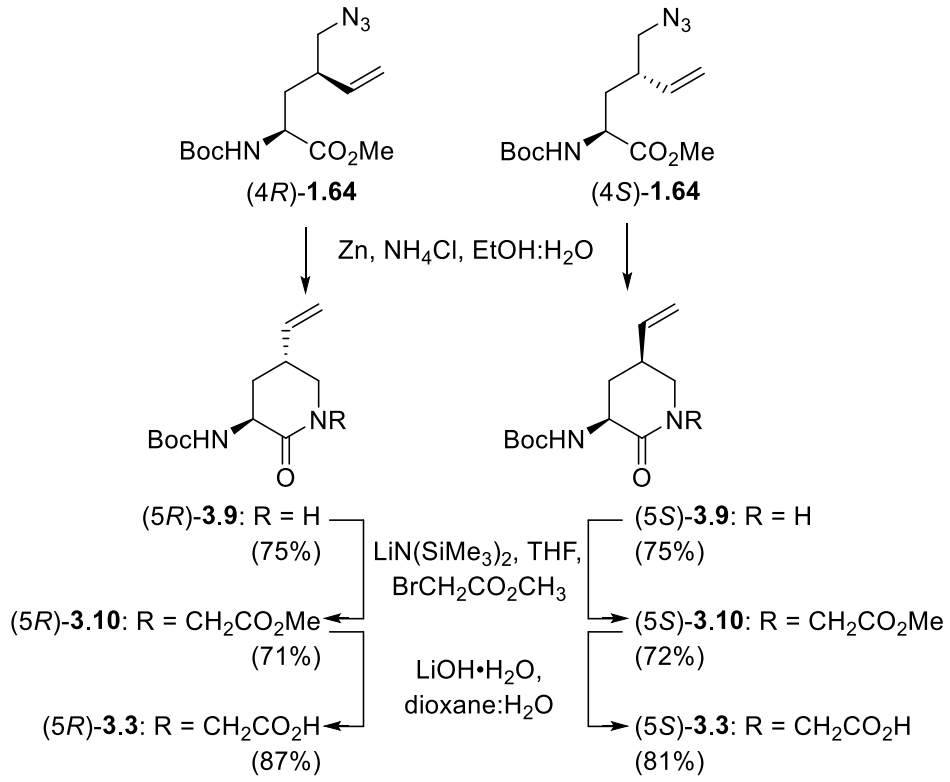

Scheme 3.1. Synthesis of α-amino-γ-substituted-δ-lactams

With δ-lactams **3.9** in hand, the glycine residue was installed by *N*-alkylation using LiHMDS and methyl bromoacetate.[9] Dipeptides (5*R*)- and (5*S*)-**3.10** were obtained in 71% and 72% yields after purification by column chromatography. Saponification of glycinates (5*R*)- and (5*S*)-**3.10** using LiOH in a dioxane:water mixture followed by 1M HCl workup provided acids (5*R*)- and (5*S*)-**3.3** in 87% and 81% yield, respectively.[25]

In principle, acids **3.3** may be introduced into peptides prior to olefin modification. To demonstrate the utility of the double bond on the lactam ring as a handle for the installation of different functional groups, carboxylic acid and amide moieties were prepared to provide constrained Glu-Gly and Gln-Gly dipeptides **3.1** and **3.2**, respectively (Scheme 3.2). Oxidation of olefins (5*R*)- and (5*S*)-**3.10** was performed using $RuCl_3$ and $NaIO_4$ in a mixture of acetonitrile, water and dichloromethane to afford carboxylic acids in constrained Glu-Gly derivatives (5*R*)- and

(5*S*)-**3.1** in 65% and 55% yields after flash column chromatography.[43] Constrained Gln-Gly derivative (5*R*)-**3.2** was subsequently prepared in 55% yield from acid (5*R*)-**3.1** by coupling to NH_4Cl using TBTU and *N*-methyl morpholine in *N*-methyl pyrrolidone followed by chromatographic purification.[44]

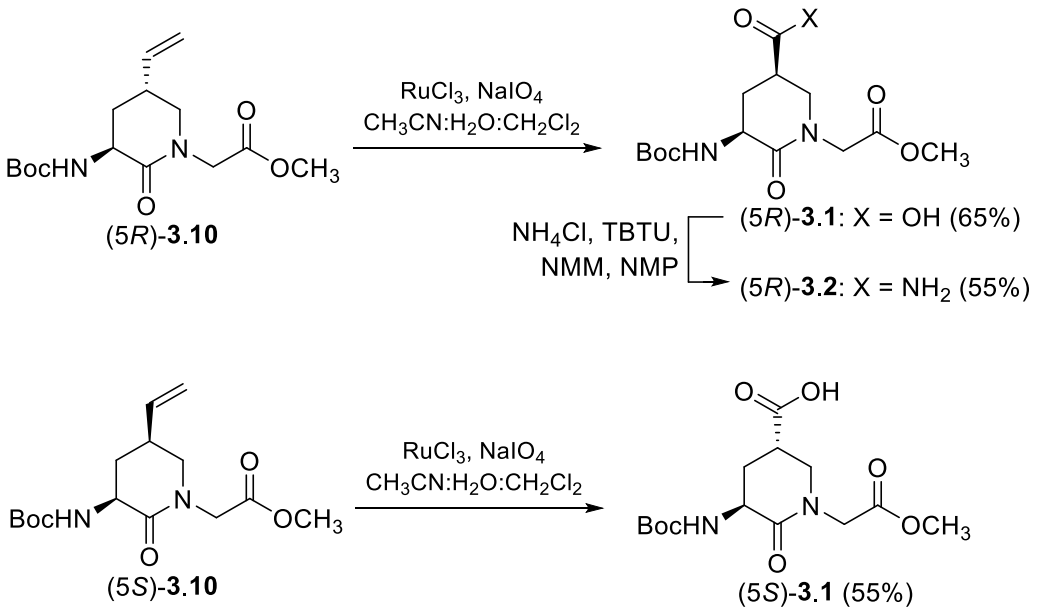

Scheme 3.2. Synthesis of Glu-Gly and Gln-Gly dipeptides

3.5. Conclusion

Commencing with enantiomerically pure 4-vinylornithine diasteromers (4*R*)- and (4*S*)-**1.64**, (5*R*)- and (5*S*)-Boc-(5-vinyl)Adl-Gly-OH dipeptides **3.3** were assembled in three steps and 46% and 44% overall yields. Oxidation of the 5-vinyl substituent and subsequent coupling of ammonium chloride to the resulting carboxylate gave access to constrained Glu-Gly and Gln-Gly mimics **3.1** and **3.2**. In light of the relevance of such dipeptide sequences at the central residues of β-turns, the potential for Adl-Gly analogs to adopt turn conformations, and the abundance of Glu-Gly and Gln-Gly moieties in biologically active peptides, this effective method for accessing these conformationally constrained surrogates should find broad utility for the study of biologically

active peptides. Efforts to study Adl dipeptides **3.1-3.3** in various peptides are ongoing in our laboratory and will be presented in due time.

3.6. Acknowledgement

We thank the Natural Sciences and Engineering Research Council of Canada (NSERC) for funding for a Discovery Research Project #04079, the Fonds de recherche nature et technologie Quebec for the Centre in Green Chemistry and Catalysis (FRQNT-2020-RS4-265155-CCVC), and the Université de Montreál. We thank Dr. Alexandra Furtös, Marie-Christine Tang, Karine Venne (mass spectrometry), S. Bilodeau, Dr. Pedro M. Aguiar, C. Malveau (NMR spectroscopy) from Université de Montreál Regional Facilities for aid in analyses. MR is grateful for support from the Faculty of Arts and Sciences, Université de Montreál for tuition expenses.

3.7. References

1. St-Cyr, D. J.; García-Ramos, Y.; Doan, N.-D.; Lubell, W. D., Aminolactam, N-aminoimidazolone, and N-aminoimdazolidinone peptide mimics. In *Peptidomimetics I*, Springer **2017**; pp 125-175.

2. Gillespie, P.; Cicariello, J.; Olson, G. L. Conformational analysis of dipeptide mimetics. *Pept. Sci.* **1997**, *43*, 191-217.

3. Perdih, A.; Kikelj, D. The application of Freidinger lactams and their analogs in the design of conformationally constrained peptidomimetics. *Curr. Med. Chem.* **2006**, *13*, 1525-1556.

4. Freidinger, R. M.; Veber, D. F.; Hirschmann, R.; Paege, L. M. Lactam restriction of peptide conformation in cyclic hexapeptides which alter rumen fermentation. *Int. J. Pept. Protein Res.* **1980**, *16*, 464-470.

5. Freindineger, R.M.; In *Peptides: Synthesis, Structure, Function*. Proceedings of the 7th American Peptide Symposium (Eds: Rich, D. H.; Gross, E), Pierce Chemical Company: Rockford, **1981**; P 673.

6. Thorsett, E. D.; Harris, E. E.; Aster, S. D.; Peterson, E. R.; Snyder, J. P.; Springer, J. P.; Hirshfield, J.; Tristram, E. W.; Patchett, A. A. Conformationally restricted inhibitors of angiotensin-converting enzyme. Synthesis and computations. *J. Med. Chem.* **1986**, *29*, 251-260.

7. Bhagwanth, S.; Mishra, R. K.; Johnson, R. L. Development of peptidomimetic ligands of Pro-Leu-Gly-NH_2 as allosteric modulators of the dopamine D2 receptor. *Beilstein J. Org. Chem.* **2013**, *9*, 204-214.

8. Sreenivasan, U.; Mishra, R. K.; Johnson, R. L. Synthesis and dopamine receptor modulating activity of lactam conformationally constrained analogs of Pro-Leu-Gly-NH_2. *J. Med. Chem.* **1993**, *36*, 256-263.

9. Semple, J. E.; Rowley, D. C.; Brunck, T. K.; Ha-Uong, T.; Minami, N. K.; Owens, T. D.; Tamura, S. Y.; Goldman, E. A.; Siev, D. V.; Ardecky, R. J.; Carpenter, S. H.; Ge. Y.; Richard. B. M.; Nolan, T. G.; Hakanson, K.; Tulinsky. A.; Nutt, R. F.; Ripka, W. C.; Design, synthesis, and evolution of a novel, selective, and orally bioailable class of thrombin inhibitors: P1-argininal derivatives incorporating P3-P4 lactam sulfonamide moieties. *J. Med. Chem.* **1996**, *39*, 4531-4536.

10. Pinyol, E.; Frutos, S.; Grillo-Bosch, D.; Giralt, E.; Clotet, B.; Esté, J. A.; Diez, A. Applications of 3-aminolactams: design, synthesis, and biological evaluation of a library of potential dimerisation inhibitors of HIV1-protease. *Org. Biomol. Chem.* **2012**, *10*, 4348-4354.

11. Zydowsky, T. M.; Dellaria Jr, J. F.; Nellans, H. N. Efficient and versatile synthesis of dipeptide isosteres containing. gamma.-or. delta.-lactams. *J. Org. Chem.* **1988**, *53*, 5607-5616.

12. Tanaka, K.-i.; Nemoto, H.; Sawanishi, H. Synthesis of (3S, 5S)-3, 5-diaminopiperidin-2-one as a conformationally restricted surrogate of Dab-Gly dipeptide. *Tetrahedron: Asymmetry* **2005**, *16*, 809-815.

13. Koulocheri, S. D.; Magiatis, P.; Haroutounian, S. A. Asymmetric synthesis of γ-keto-δ-lactam derivatives: Application to the synthesis of a conformationally constrained surrogate of ala-ser dipeptide. *J. Org. Chem.* **2001**, *66*, 7915-7918.

14. Rodriguez, R.; Estiarte, M. A.; Diez, A.; Rubiralta, M.; Colell, A.; García-Ruiz, C.; Fernández-Checa, J. Conformationally restricted analogues of methionine: Synthesis of chiral 3-Amino-5-methylthio-2-piperidones. *Tetrahedron* **1996**, *52*, 7727-7736.

15. Estiarte, M. A.; de Souza, M. V.; del Rio, X.; Dodd, R. H.; Rubiralta, M.; Diez, A. Synthesis and synthetic applications of 3-amino-Δ5-piperidein-2-ones: Synthesis of methionine-derived pseudopeptides. *Tetrahedron* **1999**, *55*, 10173-10186.

16. Piró, J.; Forns, P.; Blanchet, J.; Bonin, M.; Micouin, L.; Diez, A. Asymmetric synthesis of β-pseudopeptides from chiral 3, 4-aziridinolactams. *Tetrahedron: Asymmetry* **2002**, *13*, 995-1004.

17. Scott, W. L.; Alsina, J.; Kennedy, J. H.; O'Donnell, M. J. Solid-phase synthesis of constrained terminal and internal lactam peptidomimetics. *Org. Lett.* **2004**, *6*, 1629-1632.

18. Kumar, S.; Flamant-Robin, C.; Wang, Q.; Chiaroni, A.; André Sasaki, N. Synthesis of 4-substituted-3-aminopiperidin-2-ones: application to the synthesis of a conformationally constrained tetrapeptide N-Acetyl-Ser-Asp-Lys-Pro. *J. Org. Chem.* **2005**, *70*, 5946-5953.

19. Ecija, M.; Diez, A.; Rubiralta, M.; Casamitjana, N.; Kogan, M. J.; Giralt, E. Synthesis of 3-aminolactams as X-Gly constrained pseudodipeptides and conformational study of a Trp-Gly surrogate. *J. Org. Chem.* **2003**, *68*, 9541-9553.

20. Han, L.; Li, K.; Xu, H.; Mei, T.; Sun, Y.; Qu, J.; Song, Y. N-TFA-Gly-Bt-Based Stereoselective Synthesis of Substituted 3-Amino Tetrahydro-2 H-pyran-2-ones via an Organocatalyzed Cascade Process. *J. Org. Chem.* **2019**, *84*, 10526-10534.

21. De Laszlo, S.; Bush, B.; Doyle, J.; Greenlee, W.; Hangauer, D.; Halgren, T.; Lynch, R.; Schorn, T.; Siegl, P. Synthesis and use of 3-amino-4-phenyl-2-piperidones and 4-amino-2-benzazepin-3-ones as conformationally restricted phenylalanine isosteres in renin inhibitors. *J. Med. Chem.* **1992**, *35*, 833-846.

22. Khashper, A.; Lubell, W. D. Design, synthesis, conformational analysis and application of indolizidin-2-one dipeptide mimics. *Org. Biomol. Chem.* **2014**, *12*, 5052-5070.

23. Gosselin, F.; Lubell, W. D. Rigid dipeptide surrogates: Syntheses of enantiopure quinolizidinone and pyrroloazepinone amino acids from a common diaminodicarboxylate precursor. *J. Org. Chem.* **2000**, *65*, 2163-2171.

24. Sacchetti, A.; Silvani, A.; Lesma, G.; Pilati, T. Phe-Ala-based diazaspirocyclic lactam as nucleator of type II′ β-turn. *J. Org. Chem.* **2011**, *76*, 833-839.

25. Atmuri, N. D. P.; Lubell, W. D. Insight into Transannular Cyclization Reactions To Synthesize Azabicyclo [XY Z] alkanone Amino Acid Derivatives from 8-, 9-, and 10-Membered Macrocyclic Dipeptide Lactams. *J. Org. Chem.* **2015**, *80*, 4904-4918.

26. Halab, L.; Becker, J. A.; Darula, Z.; Tourwé, D.; Kieffer, B. L.; Simonin, F.; Lubell, W. D. Probing opioid receptor interactions with azacycloalkane amino acids. Synthesis of a potent and selective ORL1 antagonist. *J. Med. Chem.* **2002**, *45*, 5353-5357.

27. Lee, D. L.; Rapoport, H. Synthesis of tabtoxinine-. delta.-lactam. *J. Org. Chem.* **1975**, *40*, 3491-3495.

28. Weber, K.; Ohnmacht, U.; Gmeiner, P. Enantiopure 4-and 5-Aminopiperidin-2-ones: Regiocontrolled Synthesis and Conformational Characterization as Bioactive β-Turn Mimetics. *J. Org. Chem.* **2000**, *65*, 7406-7416.

29. Bowen, E. G.; Wardrop, D. J. Total Synthesis of the α-Glucosidase Inhibitors Schulzeine A, B, and C and a Structural Revision of Schulzeine A. *J. Am. Chem. Soc.* **2009**, *131*, 6062-6063.

30. Suh, Y. G.; Kim, S. A.; Jung, J. K.; Shin, D. Y.; Min, K. H.; Koo, B. A.; Kim, H. S. Asymmetric total synthesis of fluvirucinine A1. *Angew. Chem. Int. Ed.* **1999**, *38*, 3545-3547.

31. Enders, D.; Gröbner, R.; Raabe, G.; Runsink, J. Enantioselective synthesis of 2-substituted 5-, 6-and 7-membered lactams via α-alkylation of their chiral N-dialkylamino derivatives. *Synthesis* **1996**, *1996*, 941-948.

32. Stille, J. R.; Barta, N. S. Aza-Annulation of Enamine Related Substrates with a, b-Unsaturated Carboxylate Derivatives as a Route to the Selective Synthesis of d-Lactams and Pyridones. *Stud. Nat. Prod. Chem. Stereoselect. Synth.* **1996**, *18*, 315.

33. Keillor, J. W.; Chica, R. A.; Chabot, N.; Vinci, V.; Pardin, C.; Fortin, E.; Gillet, S. M.; Nakano, Y.; Kaartinen, M. T.; Pelletier, J. N. The bioorganic chemistry of transglutaminase—from mechanism to inhibition and engineering. *Can. J. Chem.* **2008**, *86*, 271-276.

34. Jing, C.; El-Ghany, M. A.; Beesley, C.; Foster, C. S.; Rudland, P. S.; Smith, P.; Ke, Y. Tazarotene-induced gene 1 (TIG1) expression in prostate carcinomas and its relationship to tumorigenicity. *J. Natl. Cancer Inst.* **2002**, *94*, 482-490.

35. Kueh, C. J.; Fisher, M. Taspoglutide. *Practical Diabetes* **2014**, *31*, 393-394a.

36. Martin, M.; y Perez, L. G.; El Ayeb, M.; Kopeyan, C.; Bechis, G.; Jover, E.; Rochat, H. Purification and chemical and biological characterizations of seven toxins from the Mexican scorpion, Centruroides suffusus suffusus. *J. Biol. Chem.* **1987**, *262*, 4452-4459.

37. Stanley, T. Diagnosis of growth hormone deficiency in childhood. *Curr. Opin. Endocrinol. Diabetes. Obes.* **2012**, *19*, 47.

38. Lieb II, J. G.; Draganov, P. V. Pancreatic function testing: here to stay for the 21st century. *World J. Gastroenterol: WJG* **2008**, *14*, 3149.

39. Wilmot, C.; Thornton, J. Analysis and prediction of the different types of β-turn in proteins. *J. Mol. Biol.* **1988**, *203*, 221-232.

40. Mulamreddy, R.; Atmuri, N. D. P.; Lubell, W. D. 4-Vinylproline. *J. Org. Chem.* **2018**, *83*, 13580-13586.

41. Mattarei, A.; Azzolini, M.; Zoratti, M.; Biasutto, L.; Paradisi, C. N-Monosubstituted methoxy-oligo (ethylene glycol) carbamate ester prodrugs of resveratrol. *Molecules* **2015**, *20*, 16085-16102.

42. Lin, W.; Zhang, X.; He, Z.; Jin, Y.; Gong, L.; Mi, A. Reduction of azides to amines or amides with zinc and ammonium chloride as reducing agent. *Synth. Commun.* **2002**, *32*, 3279-3284.

43. Ghosh, A. K.; Rodriguez, S. An enantioselective synthesis of the C3–C21 segment of the macrolide immunosuppressive agent FR252921. *Tetrahedron Lett.* **2016**, *57*, 2884-2887.

44. Tahoori, F.; Balalaie, S.; Sheikhnejad, R.; Sadjadi, M.; Boloori, P. Design and synthesis of anti-cancer cyclopeptides containing triazole skeleton. *Amino Acids* **2014**, *46*, 1033-1046.

45. Still, W. C.; Kahn, M.; Mitra, A. Rapid chromatographic technique for preparative separations with moderate resolution. *J. Org. Chem.* **1978**, *43*, 2923-2925.

Chapter 4: 6-Hydroxymethyl Indolizidin-2-one Amino Acid Synthesis, Conformational Analysis, and Biomedical Application as Dipeptide Surrogates in Prostaglandin-$F_{2\alpha}$ Modulators

4.0. Context

4.01. Indolizidin-2-one amino acids (I^2aa)

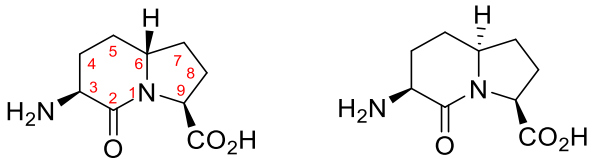

(3*S*,6*R*,9*S*)-**1.8**-I^2aa (3*S*,6*S*,9*S*)-**1.8**-I^2aa

The utility of peptide drugs may be compromised by conformational flexibility leading to rapid metabolism and poor selectivity.[1] Preorganization of a peptide into a single biologically active conformer may ideally enhance receptor selectivity and binding. As previously mentioned, heterocycles such as the pyrrolidine in proline and the lactam in Adl residues can limit conformational flexibility, improve binding affinity, and enhance potency. Combining the attributes of proline and Adl residues, indolizidine-2-one amino acid (I^2aa) analogs restrict multiple dihedral angles in the peptide backbone contained within the azabicyclo[X.Y.0]alkanone ring system.[2] Contingent on backbone stereochemistry, I^2aa residues can mimic type II' β-turn conformations as demonstrated by X-ray diffraction and NMR spectroscopic studies.[3]

In structure-activity relationship (SAR) studies of peptide leads,[2] substituted I^2aa analogs have been used to rigidify peptide conformation to elucidate biologically relevant backbone and side chain geometry.[3] In the context of the present research, I^2aa residues have been used to study the SAR of prostaglandin-$F_{2\alpha}$ ($PGF_{2\alpha}$) receptor (FP) modulators towards the development of tocolytic (labour delaying) agents to inhibit preterm birth (PTB).[4,5]

Worldwide, nearly 3.1 million neonatal deaths are attributed to complications associated with PTB.[6] Moreover, preterm infants may suffer long-term health and developmental problems,

such as respiratory impairment, blindness, deafness, and cognitive challenges. In 2005, hospitalization costs associated with preterm birth in the USA was estimated to be $26.2 billion.[7] There were a half million preterm births in the USA in 2008.[8] Globally, PTB is a major healthcare concern driving development of efficient tocolytic (labour delaying) drugs.[5]

Currently available tocolytics are ineffective and associated with side effects.[9] Efforts to develop novel tocolytics have shifted focus towards new mechanisms of actions.[10] Among such novel points of intervention, interest has focused on prostaglandin, interleukin and somatostatin receptors.[10] Agonists of FP have been used to regulate the estrus cycle and induce labor in pregnant farm animals.[11] Moreover, FP knockout mice fail to go into labour even after uterine contractions are induced with oxytocin.[12] Modulators of FP were pursued as tocolytic agents to prolong labor by suppressing uterine contractions.[5]

4.02. Application of fused bicycles on modulators of FP

The linear all D-amino acid peptide **4.01** was initially shown in a model of $PGF_{2\alpha}$-induced porcine ocular micro vessel contraction to inhibit prostaglandin activity by more than 80% with an IC_{50} of 340 nmol/L (Figure 4.01).[9] Subsequently, peptide **4.01** reduced myometrial contractions induced by $PGF_{2\alpha}$ on mouse uterine tissue *ex vivo*.[9] Conversion of peptide **4.01** to a peptide mimic lead compound was achieved by respectively replacing the *N*-terminal H-D-Ile-D-Leu-Gly-D-His tetrapeptide and the *C*-terminal D-Lys with a phenylacetyl-7-benzyl-I^2aa moiety and a benzylamide. The resulting mimic **4.03** exhibited > 25-fold potency compared to peptide **4.01** on the $PGF_{2\alpha}$-induced porcine ocular micro vessel contraction assay with an IC_{50} of 13.6 nmol/L. Subsequent refinements in which the 7-benzyl-I^2aa was replaced by the parent (3*S*,6*S*,9*S*)-I^2aa, and the *C*-terminal D-citrullinyl-D-aspartyl benzyl amide was exchanged for (2*S*)-3-pyridylalaninyl-(3*S*)-β-homophenylalanine gave the FP modulator **4.06** (PDC113.824), which exhibited 98%

inhibition of porcine vasomotor response induced by $PGF_{2\alpha}$ with an IC_{50} of 1.1 nmol/L.[9] Further examination demonstrated that I^2aa derivative **4.06** delayed labour up to 40 h in a $PGF_{2\alpha}$-induced PTB mouse model.[13]

Subsequent SAR studies demonstrated that analogs possessing the corresponding (3*R*,6*R*,9*R*)-I^2aa residue (e.g., **4.04** and **4.05**) exhibited no activity on $PGF_{2\alpha}$-induced myometrial contractions (Figure 4.01). Modification of the ring fusion stereochemistry gave (3*S*,6*R*,9*S*)-I^2aa diastereomer **4.06** which exhibited significantly reduced activity, which was one-third that the (3*S*,6*R*,9*S*)-isomer **4.06** at 10 μM.[5] Relative to the (3*S*,6*R*,9*S*)-I^2aa diastereomer, the flatter Δ^5-I^2aa analog **4.010** gave improved activity, but exhibited only half the activity of (3*S*,6*S*,9*S*)-I^2aa analog **4.06** at 1 μM. Furthermore, replacement of the (3*S*,6*S*,9*S*)-I^2aa moiety in **4.06** with the corresponding indolizidine-9-one amino acid (I^9aa) and quinolizidine-2-one amino acid (Qaa) residues provided isomer **4.07** and homologue **4.08** which lacked inhibitory activity on $PGF_{2\alpha}$-induced myometrial contractions.[13]

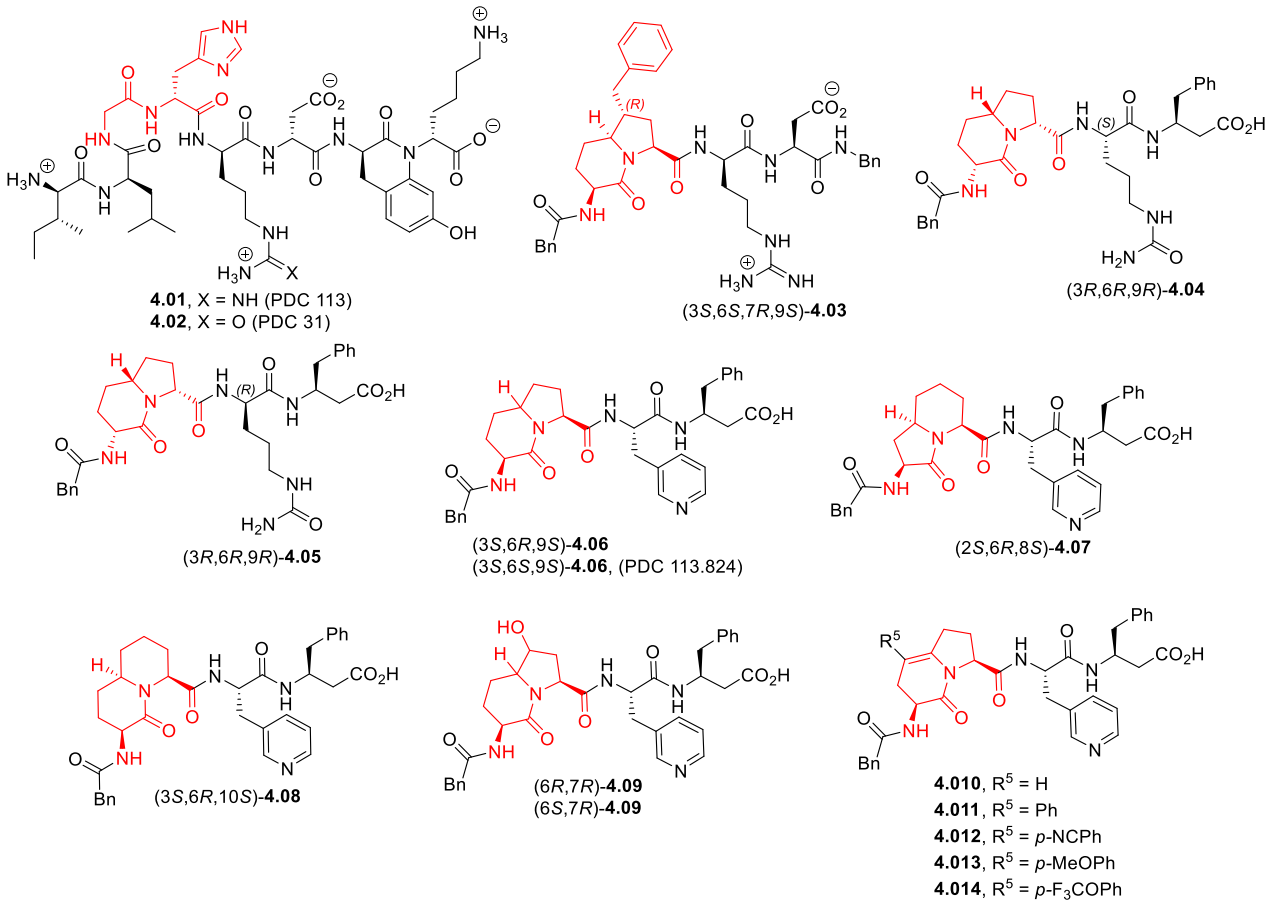

Figure 4.01. Application of various ring systems in the synthesis of tocolytic FP modulators

Efforts were subsequently made to use substituted I^2aa residues to improve labour delaying activity.[5] For example, (6*R*,7*R*)- and (6*S*,7*R*)-7-hydroxy I^2aa derivatives (6*R*,7*R*)- and (6*S*,7*R*)-**4.09** were synthesized and exhibited no effect on $PGF_{2\alpha}$-induced uterine contractions.[5] 5-Substituted Δ^5-I^2aa analogs **4.011-4.014** were synthesized by way of 5-iodo I^2aa derivative.[5] Among the 5-substituted Δ^5-I^2aa analogs, only the phenyl derivative **4.011** exhibited about 30% of the activity of (3*S*,6*S*,9*S*)-I^2aa analog **4.06**, the others exhibited no effect on $PGF_{2\alpha}$-induced myometrial contractions.[5]

4.03. Conformational analysis of fused bicycles

The SAR obtained with various bicycles indicates the importance of stereochemistry, ring puckering and substituents for activity. The backbone dihedral angles within certain fused bicycles, such as I^2aa, I^9aa and Qaa residues, may be inferred from the X-ray analyses of the corresponding *N*-protected esters **4.015-4.020** (Figure 4.02). Note, the synthesis and dihedral angles values of **4.020** are reported in Chapter 4. In contrast to exocyclic torsion angles, the internal ψ and ϕ dihedral angles are presumed to be relatively unaffected by protection and crystal packing forces. The internal dihedral angles fall within a wide range around the values of the central residues of an ideal type II' β-turn conformation ($\psi^{i+1} = -120° \pm 56$, $\phi^{i+2} = -80° \pm 128$).

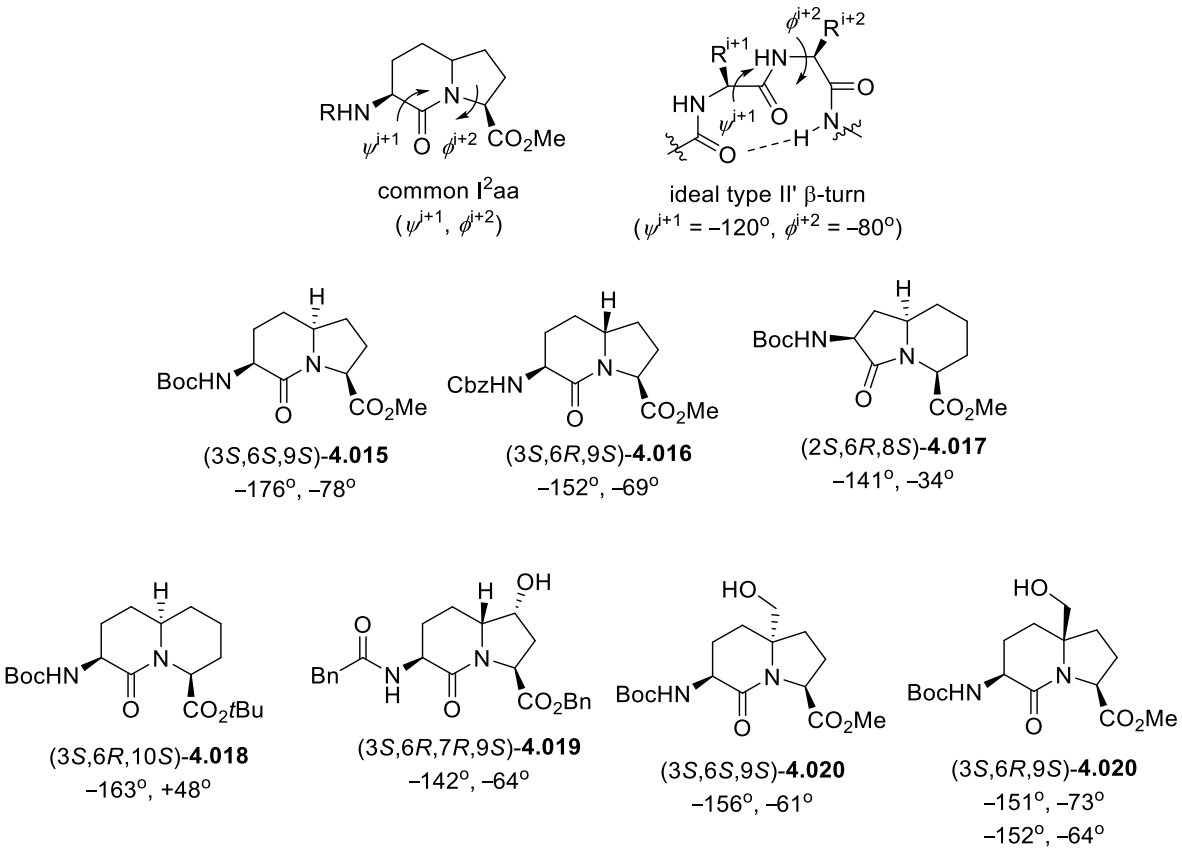

Figure 4.02. Backbone dihedral angles of I^2aa, I^9aa and Qaa residues ascertained by X-ray analyses and ideal type II' β-turn geometry

The active parent FP modulator (3*S*,6*S*,9*S*)-**4.06** is related to (3*S*,6*S*,9*S*)-Boc-I^2aa-OMe (**4.015**), the X-ray structure of which possesses values of $\psi^{i+1} = -176°$ and $\phi^{i+2} = -78°$. Such backbone geometry may be assumed to be important for biological activity. The X-ray structure of the (3*S*,6*R*,9*S*)-diastereomer (3*S*,6*R*,9*S*)-Cbz-I^2aa-OMe [(3*S*,6*R*,9*S*)-**4.016**] has torsion angles ($\psi^{i+1} = -152°$ and $\phi^{i+2} = -69°$), which deviate from those of (3*S*,6*S*,9*S*)-**4.015**. Reduced biological activity of the corresponding peptide mimic **4.06** may likely be due to such subtle changes in backbone orientation. In the case of the X-ray structures of I^9aa and Qaa esters **4.017** and **4.018**, the ψ^{i+1} and ϕ^{i+2} values are significantly different, which may explain the absence of activity on myometrial contractions exhibited by their peptide mimic counterparts **4.07** and **4.08**.

In Chapter 4, the synthesis and X-ray data is described for 6-hydroxymethyl I^2aa analogs **4.020**. Examination of the dihedral angles of the 6-hydroxymethyl analogs illustrates that their geometry is respectively similar to values found in the parent structure (3*S*,6*R*,9*S*)-Cbz-I^2aa-OMe [(3*S*,6*R*,9*S*)-**4.016**].[14] The synthesis and examination of activity of peptide mimic analogs possessing these 6-hydroxymethyl I^2aa residues was pursued to study the influences of backbone topology and substituent on ability to inhibit myometrial contractility.

4.04. Objective of Chapter 4

Continuing the effort towards more potent FP modulators for use as tocolytic agents, we have synthesized 6-substituted I^2aa derivatives.[14] The copper catalyzed S_N2' reaction of two zincates derived from β-iodoalanine **1.61** onto allylic dihalide has provided unsaturated diaminoazelate **1.65**, which was previously discussed in Chapter 1.[14] 6-Hydroxymethyl I^2aa

derivatives were synthesized from symmetrical azelate **1.65** by a route featuring epoxidation, intramolecular oxirane ring opening to provide separable proline derivatives and lactam formation.[14] Subsequently, the 6-hydroxymethyl I^2aa residues were introduced into analogs of FP modulator (3*S*,6*S*,9*S*)-**4.06** and examined for effects on $PGF_{2\alpha}$-induced myometrial contractions. In sum, Chapter 4 presents the synthesis, peptide chemistry and biomedical application of 6-hydroxymethyl I^2aa derivatives in the search of prostaglandin F2α receptor modulators for delaying preterm birth.

4.05. References

1. Abell, A. D. Heterocyclic-based peptidomimetics. *Lett. Pept. Sci.* **2001**, *8*, 267-272.

2. Khashper, A.; Lubell, W. D. Design, synthesis, conformational analysis and application of indolizidin-2-one dipeptide mimics. *Org. Biomol. Chem.* **2014**, *12*, 5052-5070.

3. Cluzeau, J.; Lubell, W. D. Design, synthesis, and application of azabicyclo [X.Y.0] alkanone amino acids as constrained dipeptide surrogates and peptide mimics. *Peptide Sci.* **2005**, *80*, 98-150.

4. Goupil, E.; Tassy, D.; Bourguet, C.; Quiniou, C.; Wisehart, V.; Pétrin, D.; Le Gouill, C.; Devost, D.; Zingg, H. H.; Bouvier, M. A novel biased allosteric compound inhibitor of parturition selectively impedes the prostaglandin F2α-mediated Rho/ROCK signaling pathway. *J. Biol. Chem.* **2010**, *285*, 25624-25636.

5. Mir, F. M.; Atmuri, N. P.; Bourguet, C. B.; Fores, J. R.; Hou, X.; Chemtob, S.; Lubell, W. D. Paired utility of aza-amino acyl proline and indolizidinone amino acid residues for peptide mimicry: Conception of prostaglandin F2α receptor allosteric modulators that delay preterm birth. *J. Med. Chem.* **2019**, *62*, 4500-4525.

6. Blencowe, H.; Cousens, S.; Oestergaard, M. Z.; Chou, D.; Moller, A.-B.; Narwal, R.; Adler, A.; Garcia, C. V.; Rohde, S.; Say, L. National, regional, and worldwide estimates of preterm birth rates in the year 2010 with time trends since 1990 for selected countries: a systematic analysis and implications. *Lancet* **2012**, *379*, 2162-2172.

7. Behrman, R. E.; Butler, A. S. Preterm birth: causes, consequences, and prevention. *Obstet. Gynecol*. **2008**, *10*, 280. 2008.

8. Haas, D. M.; Caldwell, D. M.; Kirkpatrick, P.; McIntosh, J. J.; Welton, N. J. Tocolytic therapy for preterm delivery: systematic review and network meta-analysis. *BMJ* **2012**, *345*.

9. Bourguet, C. B.; Claing, A.; Laporte, S. A.; Hebert, T. E.; Chemtob, S.; Lubell, W. D. Synthesis of azabicycloalkanone amino acid and azapeptide mimics and their application as modulators of the prostaglandin F2α receptor for delaying preterm birth. *Can. J. Chem.* **2014**, *92*, 1031-1040.

10. Coler, B. S.; Shynlova, O.; Boros-Rausch, A.; Lye, S.; McCartney, S.; Leimert, K. B.; Xu, W.; Chemtob, S.; Olson, D.; Li, M. Landscape of preterm birth therapeutics and a path forward. *J. Clin. Med.* **2021**, *10*, 2912.

11. Weems, Y.; Nett, T.; Rispoli, L.; Davis, T.; Johnson, D.; Uchima, T.; Raney, A.; Lennon, E.; Harbert, T.; Bowers, G. Effects of prostaglandin E and F receptor agonists in vivo on luteal function in ewes. *Prostaglandins Other Lipid Mediat.* **2010**, *92*, 67-72.

12. Sugimoto, Y.; Yamasaki, A.; Segi, E.; Tsuboi, K.; Aze, Y.; Nishimura, T.; Oida, H.; Yoshida, N.; Tanaka, T.; Katsuyama, M. Failure of parturition in mice lacking the prostaglandin F receptor. *Science* **1997**, *277*, 681-683.

13. Bourguet, C. B.; Goupil, E.; Tassy, D.; Hou, X.; Thouin, E.; Polyak, F.; Hébert, T. E.; Claing, A.; Laporte, S. A.; Chemtob, S. Targeting the prostaglandin F2α receptor for preventing preterm labor with azapeptide tocolytics. *J. Med. Chem.* **2011**, *54*, 6085-6097.

14. Mulamreddy, R.; Hou, X.; Chemtob, S.; Lubell, W. D. 6-Hydroxymethyl Indolizidin-2-one Amino Acid Synthesis, Conformational Analysis, and Biomedical Application as Dipeptide Surrogates in Prostaglandin-F2α Modulators. *Org. Lett.* **2021**, *23*, 5192-5196.

Article 3: 6-Hydroxymethyl Indolizidin-2-one Amino Acid Synthesis, Conformational Analysis, and Biomedical Application as Dipeptide Surrogates in Prostaglandin-$F_{2\alpha}$ Modulators

Ramakotaiah Mulamreddy, Xin Hou, Sylvain Chemtob and William D. Lubell*

Département de Chimie, Université de Montréal, C.P. 6128 Succursale Centre-Ville, Montréal H3C 3J7 QC, Canada.

Centre Hospitalier Universitaire Sainte-Justine Research Center, Montreal H3T 1C5, QC, Canada.

Org. Lett. **2021**, *23*, 5192-5196.

4.1. Abstract

6-Hydroxymethyl indolizidin-2-one amino acids were synthesized in ten steps from L-serine by intramolecular ring-opening of a symmetrical epoxide and lactam formation. X-ray analyses indicated the bicycles replicated ideal peptide type II' β-turn central dihedral angle geometry. Inside a prostaglandin-$F_{2\alpha}$ receptor modulator, the 6-hydroxymethyl analog retained inhibitory activity on myometrial contractility.

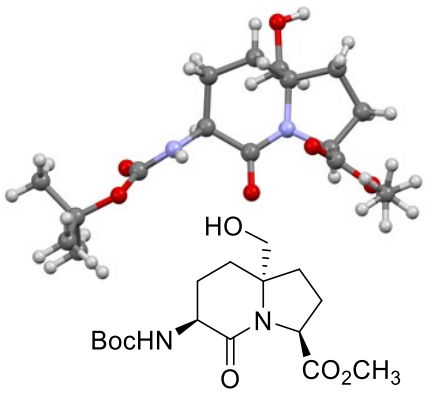

(3*S*,6*S*,9*S*)-**4.020**

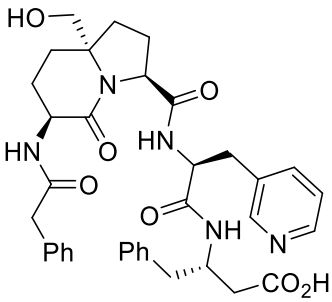

(6*S*,9*S*)-**4.4** : Inhibitory activity on myometrial contractility.

4.2. Introduction

In peptide-based drug discovery, indolizidine-2-one amino acid (I^2aa) isomers (e.g., **4.1**, Figure 4.1) and ring-substituted derivatives (e.g., **4.020** and **4.2**) act as discerning probes and privileged scaffolds in structure-activity relationship (SAR) studies to evolve leads to peptidomimetic prototypes [e.g., (6*S*)-**4.3**].[1,2] A myriad of synthetic methods have been used to introduce substituents at various positions along the I^2aa ring system to develop enzyme inhibitors and receptor ligands.[1-18] For example, thrombin inhibitor potency and selectivity were improved through the synthesis and applications of 3-benzyl and 3,5,7-trisubstituted I^2aa cores.[6,7] 4-Hydroxymethyl, 4-azidomethyl, 7-carboxymethyl and 7-guanidinylethyl I^2aas have been used to develop high binding αvβ3 and αvβ5 integrin receptor ligands.[2,8-10] In addition, 8-phenyl and 8-

carboxy I^{2}aa analogs act as constrained Ala-Phe and Ala-Asp dipeptides, the latter serving in a hybrid cholecystokinin-opioid peptide mimic.[11,12]

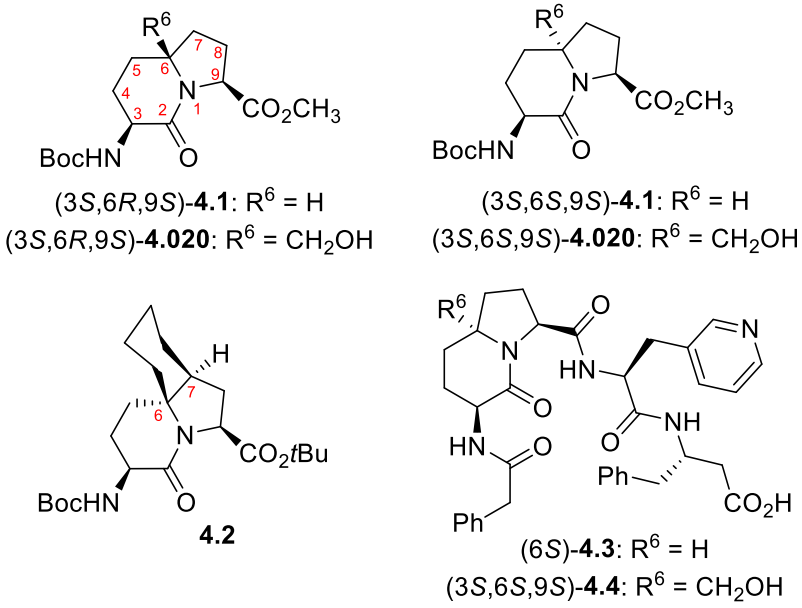

Figure 4.1. Parent and 6-substituted indolizidin-2-one amino acid (I^{2}aa) derivatives with embedded quaternary centers

Among I^{2}aa locations, the ring fusion 6-position has only once been functionalized to the best of our knowledge in 6,7-cyclohexylindolizidinone **4.2**.[13] Although the challenge of preparing quaternary centers may account in part for the absence of such I^{2}aa analogs (e.g. **4.2**), a single 6-position appendage may impose milder effects on conformation, in contrast to groups at other locations which may have significant consequences on ring puckering and alter backbone dihedral angle geometry within the bicycle as shown by X-ray analyses.[2,3,15-18] Ability to introduce a relatively large substituent without influencing backbone orientation has utility for discriminating effects on conformation from those caused on receptor engagement.[19]

The quest for a streamlined synthesis of 6-substituted I^{2}aa analogs has now been fulfilled. 6-Hydroxymethyl I^{2}aa analogs (6*R*)- and (6*S*)-**4.020** have been made, studied by X-ray crystallography, and introduced into a biologically active peptide mimic. Substitution of

hydroxymethyl diastereomers for the central (3*S*,6*S*,9*S*)-I^2aa core of prostaglandin-$F_{2\alpha}$ ($PGF_{2\alpha}$) receptor (FP) modulator PDC113.824 [(6*S*)-**4.3**)][21,22] has revealed SAR for inhibiting $PGF_{2\alpha}$-induced myometrial contractility.

4.3. Results and Discussion

6-Hydroxymethyl Boc-I^2aa-OMe diastereomers (6*R*)- and (6*S*)-**4.020** were pursued with the future intent to modifying the alcohol for introducing other substituents onto the heterocycle skeleton. Inspired by the use of symmetric 2,8-diaminoazelates (e.g., **4.5**) in syntheses of I^2aa systems (e.g., **4.1**),[15-17] 5-methylenyl 2,8-di-*N*-(Boc)aminoazelate (**1.65**) was assembled effectively from L-serine in four steps by the Jackson laboratory route featuring double S_N2' additions of the zincate derived from methyl β-iodo *N*-(Boc)alaninate onto 2-chloromethyl-3-chloroprop-1-ene (Scheme 4.1).[23] Iodoamination of olefin **1.65** with I_2 and $NaHCO_3$ in MeCN at –20°C gave a separable 3:1 mixture of (5*R*)- and (5*S*)-iodomethyl prolines **4.6**,[1,3,24] but spiro-cycles **4.7** resulted from Boc group removal using HCl in dichloromethane (DCM). Spiro-cycles (5*R*)- and (5*S*)-**4.7** are members of the bicyclic diamine class, which has garnered interest due to intriguing properties as conformationally restricted scaffolds.[25-27]

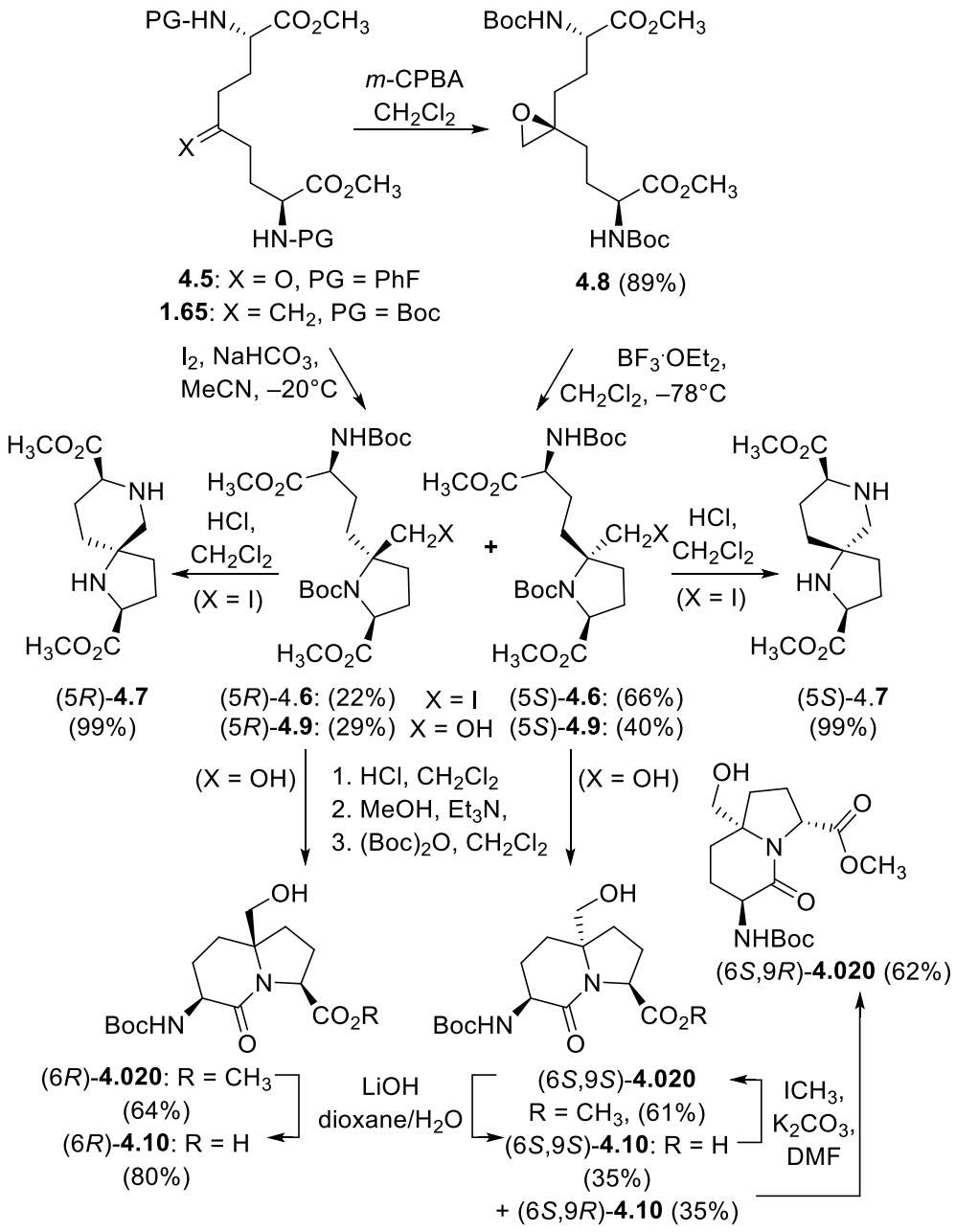

Scheme 4.1. Synthesis of 6-hydroxymethyl Boc-I^{2}aa-OMe **4.020**

Alternatively, epoxidation of olefin **1.65** using *m*-CPBA in CH_2Cl_2 gave C2 symmetric oxirane **4.10** in 89% yield after chromatography. Intramolecular ring opening of epoxide **4.8** and cyclization were accomplished by employing Lewis acid activation using $BF_3{\cdot}Et_2O$ in CH_2Cl_2 at –78 °C to give (5*R*)- and (5*S*)-5-hydroxymethyl prolines **4.9** which were separated and isolated by chromatography in 29% and 40% yields, respectively. 6-Hydroxymethyl I^{2}aa diastereomers (6*R*)-

and (6*S*)-**4.020** were prepared in 64% and 61% overall yields from prolines (5*R*)- and (5*S*)-**4.9**, respectively, using a three-step sequence featuring Boc group removal with HCl gas in CH_2Cl_2, lactam formation on treatment of the hydrochlorides with Et_3N in MeOH at reflux, and amine protection with $(Boc)_2O$ in CH_2Cl_2.

The relative stereochemistry of the ring fusion carbon of I^2aa diastereomers (6*R*)- and (6*S*)-**4.020** was determined by X-ray analyses of crystals grown from mixtures of CH_2Cl_2 and hexanes (Figure 4.2). Stereochemical assignments of prolines **4.6** and **4.9** were inferred from those of **4.020**. X-ray analysis of esters (6*R*)- and (6*S*)-**4.020** indicated that the peptide backbone dihedral angles within the bicyclic scaffolds replicated those of an ideal type II' β-turn ($\psi^{i+1} = -120°$ and $\phi^{i+2} = -80°$, Figure 4.2).[20] Contingent on the relative stereochemistry, the 6-position substituent had inconsequential and considerable effects on the backbone dihedral angles compared to those of the parent I^2aa system.

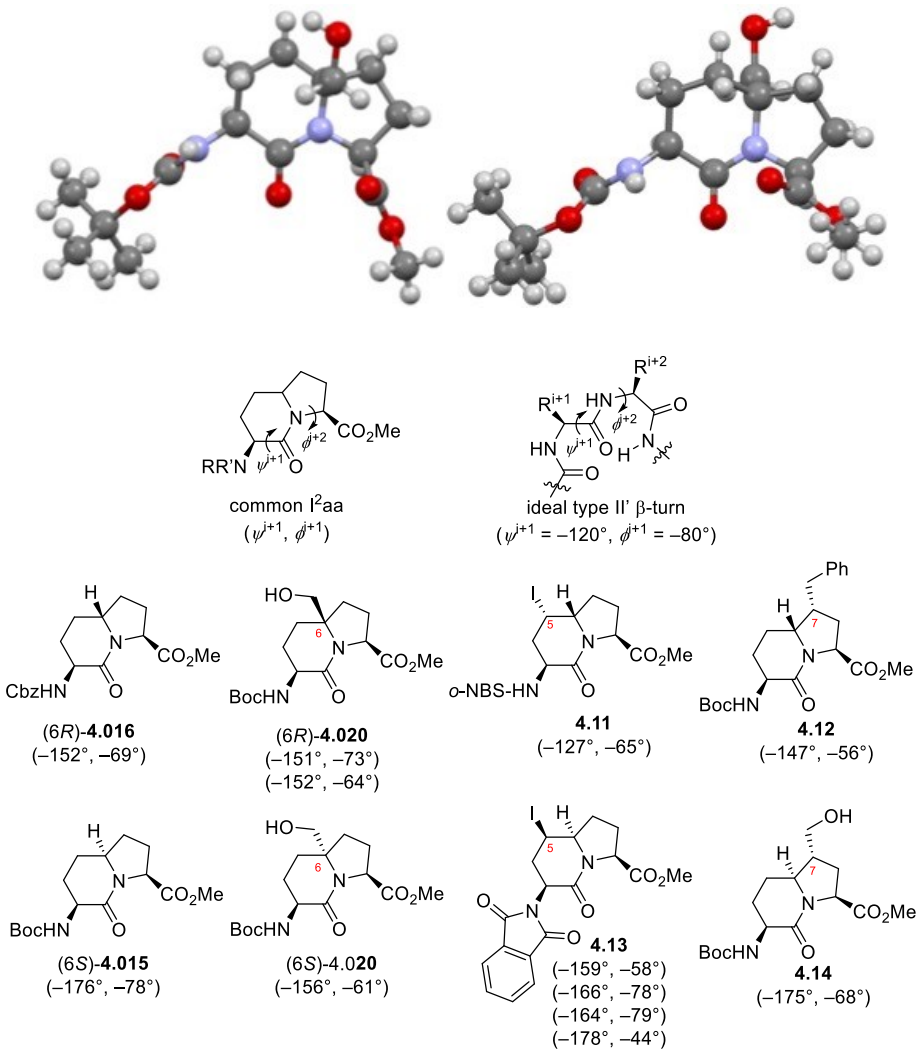

Figure 4.2. Depictions of X-ray structures of (3*S*,6*R*,9*S*)- and (3*S*,6*S*,9*S*)-Boc-(6-HOCH$_2$)I^{2}aa-OMe diastereomers (top left and top right respectively). X-ray determined backbone dihedral angle values of related I^{2}aa systems and ideal type II' β-turn.[3,15-18,20]

X-ray-derived intracyclic dihedral angle [ψ^{i+1} and ϕ^{i+2}] differences were contingent upon configuration and ring substituent location in related I^{2}aa systems possessing consistent L,L (*S*,*S*)-dipeptide backbones. Upon, comparison of I^{2}aa systems, the dihedral angles about exocyclic amine and carbonyl groups were not considered, because they may be more easily perturbed by protection and crystal packing forces. In comparison with the unsubstituted (3*S*,6*R*,9*S*)-Cbz-I^{2}aa-OMe [(6*R*)-**4.016**],[18] 6-hydroxymethyl analog (6*R*)-**4.020** had similar dihedral angles (ψ^{i+1} = –152

± 1° and ϕ^{i+2} = –69 ± 4°). More pronounced changes in $\psi^{i+1}$and ϕ^{i+2} values were respectively observed in 5-iodo and 7-benzyl counterparts **4.11** and **4.12**, respectively, likely due to effects on ring puckering.[3,16] Compared to parent (3*S*,6*S*,9*S*)-**4.1**,[15] (6*S*)-hydroxymethyl substituted I^{2}aa diastereomer (6*S*)-**4.020** had pronounced dihedral angle differences (ψ^{i+1} = –176 ± 20° and ϕ^{i+2} = –78 ± 17°), which were more prominent than those in the lactam and proline rings of 5-iodo and 7-hydroxymethyl I^{2}aa analogues **4.13** and **4.14**, respectively.[3,17]

The conformational preferences of hydroxymethyl I^{2}aa diastereomers (6*R*)- and (6*S*)-**4.020** offer interesting potential for exploring the geometrical requirements for peptide activity. Moreover, the alcohol appendage may engage in molecular recognition events by providing a partner for hydrogen bonding and metal chelation. To validate utility in peptide-based medicinal chemistry, hydroxymethyl I^{2}aa diastereomers (6*R*)- and (6*S*)-**4.020** were employed to replace the indolizidin-2-one amino acid moiety in the prostaglandin-F$_{2\alpha}$ (PGF$_{2\alpha}$) receptor (FP) modulator (6*S*)-**4.3**.[21] An inhibitor of myometrial contractions, I^{2}aa peptide (6*S*)-**4.3** has delayed parturition in a murine model of preterm labor by a mechanism involving allosteric modulation of FP and biased signalling.[21,22] In a program that aims to inhibit preterm birth and improve neonatal outcomes, I^{2}aa peptide (6*S*)-**4.3** is a lead for developing tocolytic (labor-suppressing) agents. Attempts to modify the stereochemistry and to add ring substituents to the I^{2}aa residue of peptide (6*S*)-**4.3** have, however typically produced inactive and less potent analogs.[1,14,21,22] For example, inversion of the I^{2}aa residue ring fusion stereochemistry from 6*S* to 6*R* in **4.3** weakened the ability to diminish the mean tension induced by PGF$_{2\alpha}$ on spontaneous myometrial contractions to approximately one-third at 10 μM.[14] Similarly, replacement of the I^{2}aa residue in (6*S*)-**4.3** with (6*R*,7*R*)- and (6*S*,7*R*)-7-hydroxyl I^{2}aa counterparts abolished activity in the myometrial contraction assay.[14] Peptide (6*S*)-**4.3** is thus a stringent model for examining the utility of 6-

substituted I^{2}aa analogues. 6-Hydroxymethyl analogues **4.4** were prepared for comparison with FP modulator (6*S*)-**4.3**.

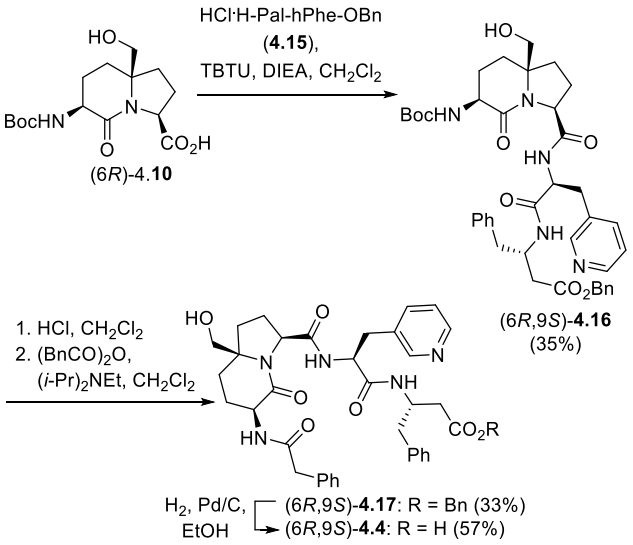

Scheme 4.2. Synthesis of 6-hydroxymethyl I^{2}aa peptide (6*R*,9*S*)-**4.4** synthesis by representative protocol for assembly of diastereomers **4.4**

The syntheses of 6-hydroxymethyl I^{2}aa analogues **4.4** commenced with saponification of esters **4.020** using LiOH in aqueous dioxane (Scheme 4.1). Acid (6*R*)-**4.10** was uneventfully prepared, but epimerization occurred during saponification of ester (6*S*)-**4.020** providing diastereomeric acids (6*S*,9*S*)- and (6*S*,9*R*)-**4.10** which were separated by column chromatography. Although epimerization during saponification of parent ester (3*S*,6*S*,9*S*)-**4.1** was minimized by controlling hydroxide ion stoichiometry,[15] similar conditions, and use of NaOH and $CaCl_2$ in *i*-PrOH/H_2O,[28] all gave significant acid (6*S*,9*R*)-**4.10**, which was assigned by esterification of each diastereomer independently using iodomethane and K_2CO_3 in DMF to obtain (6*S*,9*S*)-**4.020** and (6*S*,9*R*)-**4.020**, the latter eluted more rapidly on HPLC than the (9*S*)-diastereomer.

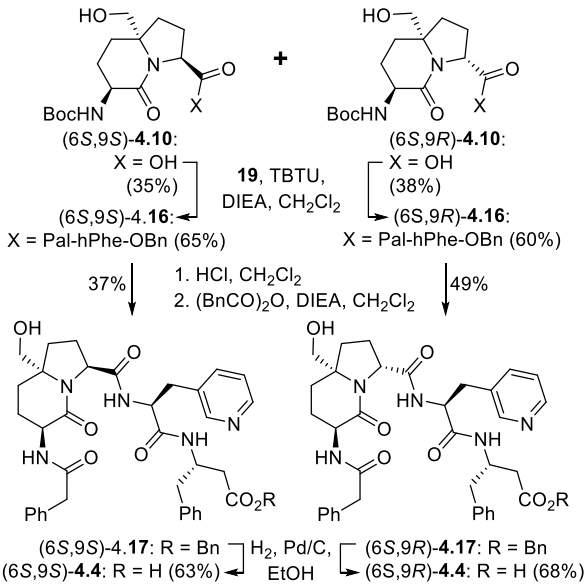

Scheme 4.3. Synthesis of hydroxymethyl I^2aa peptides (6*S*,9*R*)- and (6*S*,9*S*)-**4.4**

Diastereomeric acids (6*R*,9*S*)-, (6*S*,9*S*)- and (6*S*,9*R*)-**4.10** were independently converted to peptides (6*R*,9*S*)-, (6*S*,9*S*)- and (6*S*,9*R*)-**4.4**, respectively, by coupling to (*S*,*S*)-pyridinylalaninyl-β-homophenylalanine benzyl ester (**4.15**)[22] using TBTU and *N*,*N*-diisopropylethylamine (DIEA) to afford peptides **4.16**. After Boc group removal with HCl gas in CH_2Cl_2, amine acylation with phenylacetic anhydride and DIEA in CH_2Cl_2 gave benzyl esters **4.20**. Hydrogenolytic cleavage of ester **4.17** using H_2 and Pd/C in EtOH provided **4.4** as illustrated for the (6*R*,9*S*)-**4.4** isomer in Scheme 4.2 and for (6*S*,9*S*)-, and (6*S*,9*R*)-**4.4** in Scheme 4.3). Purification by preparative HPLC gave peptides (6*R*,9*S*)-, (6*S*,9*R*)- and (6*S*,9*S*)-**4.4**, respectively, in ≥ 95% purity as assessed by LC-MS in two different solvent systems.

The activity of peptides **4.4** was examined in an *ex vivo* contraction assay.[14,21,22] The mean tension of spontaneous contractions of mouse myometrial tissue after treatment with $PGF_{2\alpha}$ was measured using a digital polygraph system in the presence and absence of peptide **4.4** (1 μM and 10 μM). Among the three tested diastereomers, only peptide (6S,9S)-**4.4** exhibited significant

activity at 1 μM and 10 μM (Figure 4.3A). The (6*R*,9*S*)- and (6*S*,9*R*)-diastereomers did not show significant effects on $PGF_{2\alpha}$-induced contraction at both concentrations (Figure 4.4).

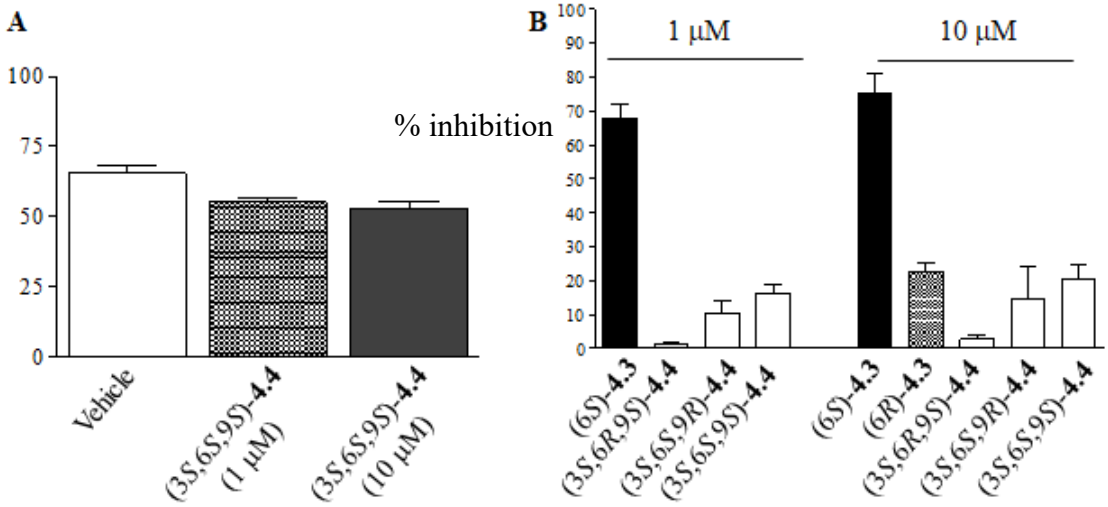

Figure 4.3. A) Effects of (6-$HOCH_2$)I^2aa peptide (6*S*,9*S*)-**4.4** (1 and 10 mM) on the increase in myometrial mean tension induced by $PGF_{2\alpha}$ ((0.1 μM, presented as % of baseline). B) Relative effects of peptide diastereomers **4.4** (1 and 10 mM) vs parent (6*S*)- and (6*R*)-I^2aa peptides **4.3** on $PGF_{2\alpha}$-induced myometrial contraction (presented as % inhibition of $PGF_{2\alpha}$-induced mean tension increase).

The inhibitory action of peptides **4.4** on the increase in mean tension induced by $PGF_{2\alpha}$ was compared with that of parent peptide (6*S*)-**4.3** and ring fusion diastereomer (6*R*)-**4.3** as positive controls (Figure 4.3B). Relative to FP modulator (6*S*)-**4.3**, (6*S*,9*S*)-**4.4** exhibited between 22 and 28% activity at both measured concentrations. Diastereomer (6*R*)-**4.3** was active only at 10 μM and exhibited approximately one-third of the activity of FP modulator (6*S*)-**4.3**. The (6*R*)-6-hydroxymethyl analogue was inactive at both concentrations (Figure 4.4).

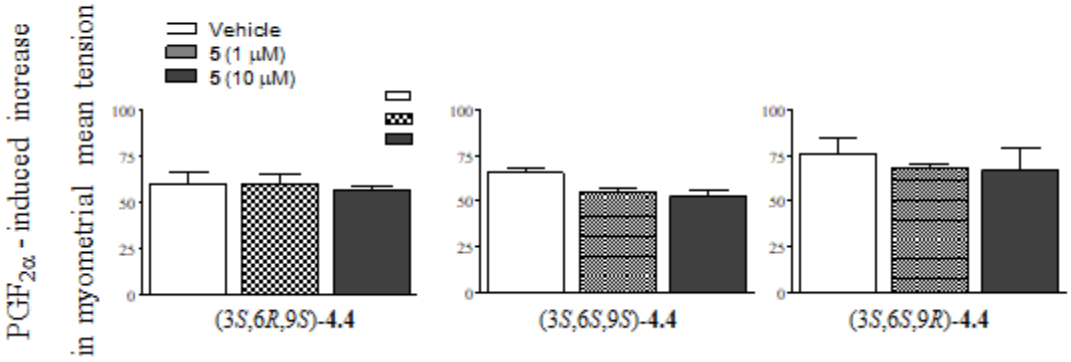

Figure 4.4. Effects of diastereomeric (6-$HOCH_2$)-I^2aa peptides **4.4** (1 and 10 μM) on the increase in mean tension induced by PGF_{2a} (%) in myometrial tissue

Influences on biological activity from ring substituents may arise from a combination of the conformational change in the I^2aa backbone dihedral angle geometry and direct interactions with the receptor. In this light, the modicum of difference of dihedral angle geometry in the X-ray structures of I^2aa esters (6*R*)-**4.020** and (6*R*)-**4.016** may offer potential to separating the influence of substituent on backbone topology from effects on activity due to receptor interaction. The backbone dihedral angles of Boc-I^2aa-OMe (6*R*)-**4.016** are similar to those in 6-hydroxymethyl counterparts (6*R*)- and (6*S*)-**4.020**, but differ from ester (6*S*)-**4.1** (Figure 4.2). The decrease in activity upon addition of a 6-hydroxymethyl substituent onto FP modulator (6*S*)-**4.3** may likely be due to a shift in conformational preference, particularly because of the similar activity between (6*S*,9*S*)-**4.4** and (6*R*)-**4.3**. On the contrary, similar backbone dihedral angles of esters (6*R*)-**4.020** and (6*R*)-**4.015** suggest that the loss of activity in placing a 6-hydroxymethyl substituent on (6*R*)-**4.3** may likely be due to added steric interactions with the receptor.

4.4. Conclusions

Novel 6-substituted indolizidin-2-one amino acid (I^2aa) derivatives have been effectively synthesized to study the impact of the ring fusion substituent on bicycle conformation and biological activity. Enantiomerically pure 6-hydroxymethyl indolizidin-2-one amino esters (3*S*,6*R*,9*S*)- and (3*S*,6*S*,9*S*)-**4.020**, both were synthesized in five steps and 17% and 22% yields, respectively, from azelate **1.65** as a readily obtainable precursor derived in four steps from L-serine. Examination of the X-ray structures of the hydroxymethyl esters demonstrated that (6*R*)- and (6*S*)-**4.020**, both replicated the central dihedral angles of type II' β-turns with backbone geometry similar to that of parent I^2aa ester (6*R*)-**4.015** but significantly different from that of (6*S*)-**4.1**. Installment of a 6-hydroxymethyl group on the (3*S*,6*S*,9*S*)-I^2aa residue in FP modulator (6*S*)-**4.3** gave (3*S*,6*S*,9*S*)-**4.4**, which exhibited approximately one-quarter of the activity of the parent structure likely due to conformational changes on the peptide backbone. Considering their effective synthesis, potential to modify the 6-hydroxymethyl substituent to prepare other side chain functional groups, knowledge gleaned from X-ray crystallographic analyses of the conformers of esters **4.020** and retained activity upon modification of the I^2aa residue 6-position in the relatively stringent biologically active peptide (6*S*)-**4.3**, 6-hydroxymethyl indolizidin-2-one amino acids represent valuable tools for studying peptide chemical biology.

4.5. Acknowledgment

We thank the Natural Sciences and Engineering Research Council of Canada (NSERC) for funding for a Discovery Research Project (No. 04079), the Canadian Institutes of Health Research (CIHR), the NSERC-CIHR for funding the Collaborative Health Research Project ″Treatment of Preterm Birth with ProstaglandinF2alpha Receptor Modulators″ No. 337381. We acknowledge the assistance of members of the Université de Montréal facilities: Dr. A. Fürtös, K. Gilbert, M.-C.

Tang, and L. Mahrouche (mass spectroscopy), C. Malveau, Dr. P. Aguiar, and S. Bilodeau (NMR spectroscopy), and Mr. T. Maris (X-ray).

4.6. References

1. Atmuri, N.D.P.; Surprenant, S.; Diarra, S.; Bourguet, C.; Lubell, W.D. "Ring closing metathesis / transannular cyclization to azabicyclo[X.Y.0]alknanone dipeptide turn mimics for biomedical applications". *Peptide and Peptidomimetic Therapeutics: From Bench to Bedside*; Elsevier (Academic Press), **2021** (in press).

2. Khashper, A.; Lubell, W. D. Design, synthesis, conformational analysis and application of indolizidin-2-one dipeptide mimics. *Org. Biomol. Chem.* **2014**, *12*, 5052-5070.

3. Atmuri, N. D. P.; Lubell, W. D. Stereo-and regiochemical transannular cyclization of a common hexahydro-1H-azonine to afford three different indolizidinone dipeptide mimetics. *J. Org. Chem.* **2020**, *85*, 1340–1351.

4. Hanessian, S.; McNaughton-Smith, G.; Lombart, H.-G.; Lubell, W. D. Design and synthesis of conformationally constrained amino acids as versatile scaffolds and peptide mimetics. *Tetrahedron* **1997**, *53*, 12789-12854.

5. Cluzeau, J.; Lubell, W. D. Design, synthesis, and application of azabicyclo [XY 0] alkanone amino acids as constrained dipeptide surrogates and peptide mimics. *Peptide Sci.* **2005**, *80*, 98-150.

6. Hanessian, S.; Therrien, E.; Granberg, K.; Nilsson, I. Targeting thrombin and factor VIIa: design, synthesis, and inhibitory activity of functionally relevant indolizidinones. *Bioorg. Med. Chem. Lett.* **2002**, *12*, 2907-2911.

7. Boatman, P. D.; Ogbu, C. O.; Eguchi, M.; Kim, H.-O.; Nakanishi, H.; Cao, B.; Shea, J. P.; Kahn, M. Secondary structure peptide mimetics: design, synthesis, and evaluation of β-strand mimetic thrombin inhibitors. *J. Med. Chem.* **1999**, *42*, 1367-1375.

8. Manzoni, L.; Belvisi, L.; Arosio, D.; Civera, M.; Pilkington-Miksa, M.; Potenza, D.; Caprini, A.; Araldi, E. M.; Monferini, E.; Mancino, M. Cyclic RGD-containing functionalized azabicycloalkane peptides as potent integrin antagonists for tumor targeting. *ChemMedChem* **2009**, *4*, 615-632.

9. Manzoni, L.; Arosio, D.; Belvisi, L.; Bracci, A.; Colombo, M.; Invernizzi, D.; Scolastico, C. Functionalized azabicycloalkane amino acids by nitrone 1, 3-dipolar intramolecular cycloaddition. *J. Org. Chem.* **2005**, *70*, 4124-4132.

10. Manzoni, L.; Bassanini, M.; Belvisi, L.; Motto, I.; Scolastico, C.; Castorina, M.; Pisano, C. Nonpeptide integrin antagonists: RGD mimetics incorporating substituted azabicycloalkanes as amino acid replacements. *Eur. J. Org. Chem.* **2007**, *2007*, 1309-1317.

11. Wang, W.; Yang, J.; Ying, J.; Xiong, C.; Zhang, J.; Cai, C.; Hruby, V. J. Stereoselective synthesis of dipeptide β-turn mimetics: 7-benzyl and 8-phenyl substituted azabicyclo [4.3. 0] nonane amino acid esters. *J. Org. Chem.* **2002**, *67*, 6353-6360.

12. Ndungu, J. M.; Cain, J. P.; Davis, P.; Ma, S.-W.; Vanderah, T. W.; Lai, J.; Porreca, F.; Hruby, V. J. Synthesis of constrained analogues of cholecystokinin/opioid chimeric peptides. *Tetrahedron Lett.* **2006**, *47*, 2233-2236.

13. Belvisi, L.; Colombo, L.; Colombo, M.; Di Giacomo, M.; Manzoni, L.; Vodopivec, B.; Scolastico, C. Practical stereoselective synthesis of conformationally constrained unnatural proline-based amino acids and peptidomimetics. *Tetrahedron* **2001**, *57*, 6463-6473.

14. Mir, F. M.; Atmuri, N. P.; Bourguet, C. B.; Fores, J. R.; Hou, X.; Chemtob, S.; Lubell, W. D. Paired utility of aza-amino acyl proline and indolizidinone amino acid residues for peptide mimicry: Conception of prostaglandin F2α receptor allosteric modulators that delay preterm birth. *J. Med. Chem.* **2019**, *62*, 4500-4525.

15. Lombart, H.-G.; Lubell, W. D. Rigid dipeptide mimetics: efficient synthesis of enantiopure indolizidinone amino acids. *J. Org. Chem.* **1996**, *61*, 9437-9446.

16. Polyak, F.; Lubell, W. D. Rigid dipeptide mimics: Synthesis of enantiopure 5-and 7-benzyl and 5, 7-dibenzyl indolizidinone amino acids via enolization and Alkylation of δ-Oxo α, ω-Di-[N-(9-(9-phenylfluorenyl)) amino] azelate Esters. *J. Org. Chem.* **1998**, *63*, 5937-5949.

17. Polyak, F.; Lubell, W. D. Mimicry of peptide backbone geometry and heteroatomic side-chain functionality: synthesis of enantiopure indolizidin-2-one amino acids possessing alcohol, acid, and azide functional groups. *J. Org. Chem.* **2001**, *66*, 1171-1180.

18. Mulzer, J.; Schülzchen, F.; Bats, J.-W. Rigid dipeptide mimetics. Stereocontrolled synthesis of all eight stereoisomers of 2-Oxo-3-(N-Cbz-amino)-1-azabicyclo [4.3.0]nonane-9-carboxylic acid ester. *Tetrahedron* **2000**, *56*, 4289-4298.

19. Jeannotte, G.; Lubell, W. D. Large structural modification with conserved conformation: Analysis of Δ^3-fused aryl prolines in model β-turns. *J. Am. Chem. Soc.* **2004**, *126*, 14334-14335.

20. Ball, J. B.; Alewood, P. F. Conformational constraints: Nonpeptide β-turn mimics *J. Mol. Recogn.* **1990**, *3*, 55-64.

21. Le Gouill, C.; Devost, D.; Zingg, H. H.; Bouvier, M.; Saragovi, H. U. A Novel Biased Allosteric Compound Inhibitor of Parturition Selectively Impedes the Prostaglandin F2-mediated Rho/ROCK Signaling Pathway. *J. Biol. Chem*. **2010**, *2010*, 25624-25636.

22. Bourguet, C. B.; Goupil, E.; Tassy, D.; Hou, X.; Thouin, E.; Polyak, F.; Hébert, T. E.; Claing, A.; Laporte, S. A.; Chemtob, S. Targeting the prostaglandin F2α receptor for preventing preterm labor with azapeptide tocolytics. *J. Med. Chem.* **2011**, *54*, 6085-6097.

23. Reeve, P. A.; Grabowska, U.; Oden, L. S.; Wiktelius, D.; Wångsell, F.; Jackson, R. F. Radical functionalization of unsaturated amino acids: synthesis of side-chain-fluorinated, azido-substituted, and hydroxylated amino acids. *ACS Omega* **2019**, *4*, 10854-10865.

24. Mizar, P.; Wirth, T. Iodoaminations of alkenes. *Synthesis* **2017**, *49*, 981-986.

25. Grygorenko, O. O.; Radchenko, D. S.; Volochnyuk, D. M.; Tolmachev, A. A.; Komarov, I. V. Bicyclic conformationally restricted diamines. *Chem. Rev.* **2011**, *111*, 5506-5568.

26. Keith, J. M.; Jones, W. M.; Pierce, J. M.; Seierstad, M.; Palmer, J. A.; Webb, M.; Karbarz, M. J.; Scott, B. P.; Wilson, S. J.; Luo, L. Heteroarylureas with spirocyclic diamine cores as inhibitors of fatty acid amide hydrolase. *Bioorg. Med. Chem. Lett.* **2014**, *24*, 737-741.

27. Degorce, S. L.; Bodnarchuk, M. S.; Scott, J. S. Lowering lipophilicity by adding carbon: AzaSpiroHeptanes, a log D lowering twist. *ACS Med. Chem. Lett.* **2019**, *10*, 1198-1204.

28. Pascal, R.; Sola, R. Preservation of the protective group under alkaline conditions by using $CaCl_2$. Applications in peptide synthesis *Tetrahedron Lett.* **1998**, *39*, 5031-5034.

Chapter 5: Constrained Dipeptide Surrogates: 5- and 7- Hydroxy Indolizidin-2-one Amino Acid Synthesis from Iodolactonization of Dehydro-2,8-Diaminoazelates

5.0. Context

5.01. Synthesis of substituted indolizidin-2-one amino acids (I^2aa)

In the introduction to Chapter 4, the importance of the indolizidine-2-one core for the synthesis of FP modulators was discussed as a key innovation in the design of novel tocolytic agents to delay preterm birth (PTB). Pursuing research to address this unmet medical need,[1] other substituted I^2aa residues have been synthesized for introduction into the lead FP modulators to explore their activity on $PGF_{2\alpha}$-induced myometrial contractions. Chapter 5 describes our efforts towards the synthesis 5- and 7-hydroxyindolizidine-2-one amino acids.

Previously, 5- and 7-hydroxyindolizidine-2-one derivatives were synthesized from 5-iodo I^2aa derivative **5.01**. Iodide elimination using Et_3N and CH_3CN gave enamine **5.02**. Allylic oxidation of enamine **5.02** using SeO_2 and *tert*-butyl hydroperoxide gave separable mixtures of 7- and 5-hydroxy isomers **5.03** and **5.04** in 22% and 28% yield, respectively.[2] The olefin of 7-hydroxy Δ^5-I^2aa **5.03** was reduced using $NaCNBH_3$ to provide a mixture 7-hydroxy I^2aa diastereomers (3*S*,6*R*,7*R*,9*S*)-**4.019** and (3*S*,6*S*,7*R*,9*S*)-**5.05** in 44% and 26% yield, respectively (Scheme 5.01). Both 7-hydroxy I^2aa diastereomers were incorporated respectively into tetrapeptides (6*R*,7*R*)- and (6*S*,7*R*)-**4.09**, which as discussed in Chapter 4 proved inactive in inhibiting $PGF_{2\alpha}$-induced myometrial contractions.[2]

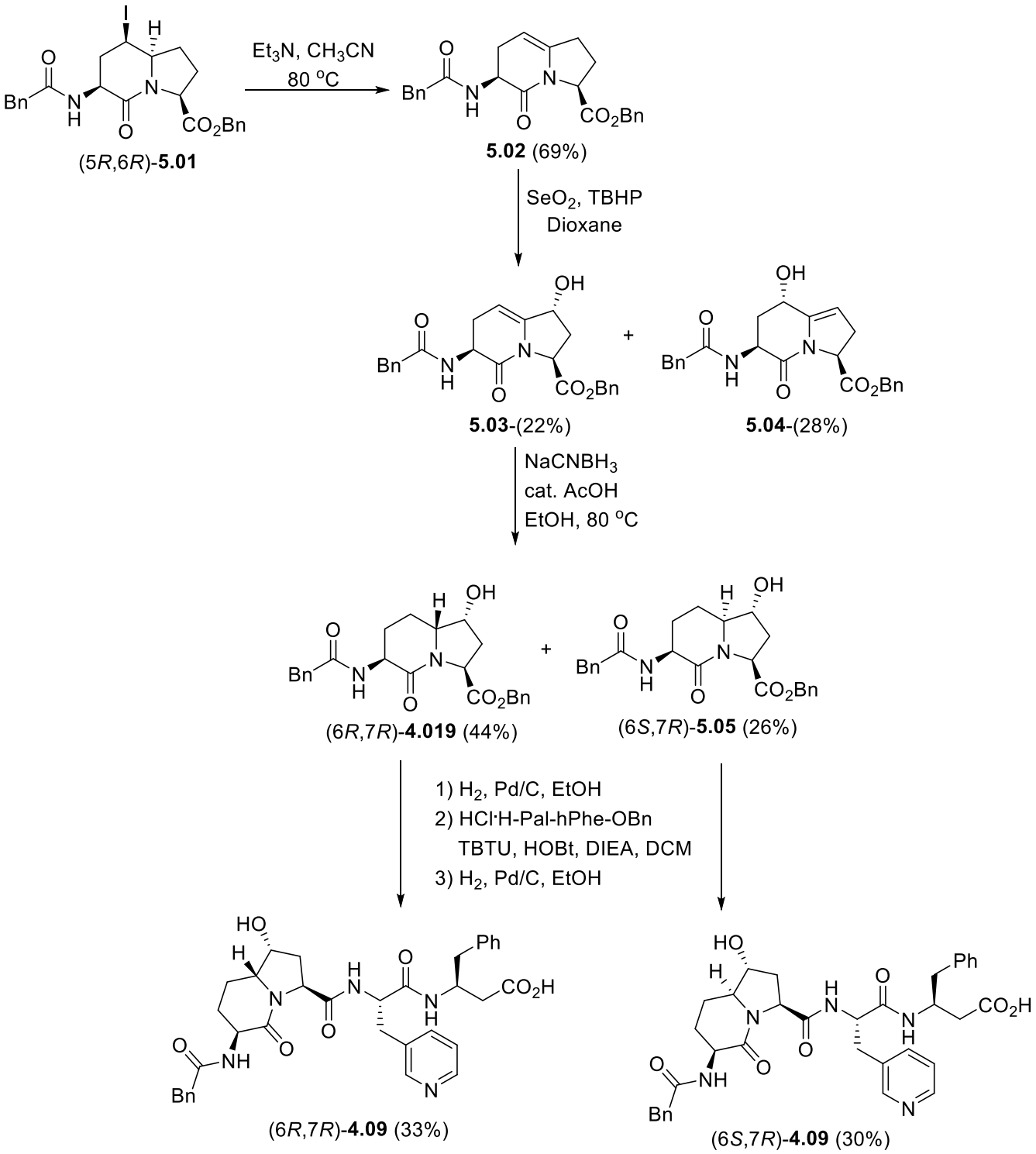

Scheme 5.01. Synthesis of (6*R*,7*R*)- and (6*S*,7*R*)-7-hydroxy I^2aa derivatives

5.02. Conformational analysis of fused ring systems

The SAR studies of FP modulators was discussed in Chapter 4. Briefly, various bicycles such as I^2aa, I^9aa and Qaa residues **4.015**-**4.018** were synthesized, but few exhibited significant activity. The dihedral angle values inside model bicycles have been used to predict conformations responsible for activity as discussed in Chapter 4.[3,4] For example, the absence of activity exhibited by 7-hydroxy I^2aa analog (6*R*,7*R*)-**4.09** may be due to a combination of backbone geometry and the effect of the alcohol substituent. The X-ray structure of (3*S*,6*R*,7*R*,9*S*)-**4.019** had dihedral angle values (ψ^{i+1} = –142° and ϕ^{i+2} = –64°) which deviated more significantly than those of the unsubstituted (3*S*,6*R*,9*S*)-diastereomer (3*S*,6*R*,9*S*)-**4.016** from those of the parent (3*S*,6*S*,9*S*)-isomer (3*S*,6*S*,9*S*)-**4.015** found in the most active FP modulator (3*S*,6*S*,9*S*)-**4.06** (Figure 402).[2,4]

In Chapter 5, the synthesis and X-ray data are described for 7-hydroxy I^2aa analog (3*S*,6*S*,7*S*,9*S*)-**5.06**. Examination of the dihedral angles of the 7-hydroxy I^2aa analogs indicated similar to values as those found in the parent system (3*S*,6*S*,9*S*)-Boc-I^2aa-OMe [(3*S*,6*S*,9*S*)-**4.015**].[5] The synthesis and examination of activity of peptide mimic analogs possessing 5- and 7-hydroxy I^2aa residues merits pursuit to study the influences of backbone topology and substituent on ability to inhibit myometrial contractility.

5.03. Objective of Chapter 5

Continuing the effort towards more potent FP modulators for use as tocolytic agents, we have synthesized of 5- and 7-substituted I^2aa derivatives.[5] The copper catalyzed S_N2' reaction of two zincates derived from β-iodoalanine **1.61** onto allylic dihalide has provided unsaturated diaminoazelate **1.66**, which was previously discussed in Chapter 1.[5] Diaminoazelate **1.66** was converted into 5- and 7-hydroxy I^2aa derivatives by routes featuring iodolactonization,

intramolecular S_N2 displacement and lactam formation.[5] Applications of 5- and 7-hydroxy I^2aa residues in the study of FP modulators are currently in progress and will be report in due time. In sum, Chapter 5 presents effective methods for synthesizing substituted indolizidine-2-one amino acid derivatives which have potential utility for biomedical applications.

5.04. References

1) Blencowe, H.; Cousens, S.; Oestergaard, M. Z.; Chou, D.; Moller, A.-B.; Narwal, R.; Adler, A.; Garcia, C. V.; Rohde, S.; Say, L. National, regional, and worldwide estimates of preterm birth rates in the year 2010 with time trends since 1990 for selected countries: a systematic analysis and implications. *Lancet*. **2012,** *379*, 2162-2172.

2) Mir, F. M.; Atmuri, N. P.; Bourguet, C. B.; Fores, J. R.; Hou, X.; Chemtob, S.; Lubell, W. D. Paired utility of aza-amino acyl proline and indolizidinone amino acid residues for peptide mimicry: Conception of prostaglandin F2α receptor allosteric modulators that delay preterm birth. *J. Med. Chem.* **2019**, *62*, 4500-4525.

3) Bourguet, C. B.; Goupil, E.; Tassy, D.; Hou, X.; Thouin, E.; Polyak, F.; Hébert, T. E.; Claing, A.; Laporte, S. A.; Chemtob, S. Targeting the prostaglandin F2α receptor for preventing preterm labor with azapeptide tocolytics. *J. Med. Chem.* **2011**, *54*, 6085-6097.

4) Goupil, E.; Tassy, D.; Bourguet, C.; Quiniou, C.; Wisehart, V.; Pétrin, D.; Le Gouill, C.; Devost, D.; Zingg, H. H.; Bouvier, M. A novel biased allosteric compound inhibitor of parturition selectively impedes the prostaglandin F2α-mediated Rho/ROCK signaling pathway. *J. Biol. Chem.* **2010**, *285*, 25624-25636.

5) Mulamreddy, R.; Lubell, W. D. Constrained Dipeptide Surrogates: 5-and 7-Hydroxy Indolizidin-2-one Amino Acid Synthesis from Iodolactonization of Dehydro-2, 8-diamino Azelates. *Molecules* **2022**, *27*, 67.

Article 4: Constrained Dipeptide Surrogates: 5- and 7- HydroxyIndolizidin-2-one Amino Acid Synthesis from Iodolactonization of Dehydro-2,8-DiaminoAzelates

Ramakotaiah Mulamreddy, William D. Lubell*

Département de Chimie, Université de Montréal, C.P. 6128 Succursale Centre-Ville, Montréal H3C 3J7 QC, Canada.

Molecules **2022**, *27*, 67.

5.1. Abstract

The constrained dipeptide surrogates 5- and 7-hydroxy indolizidin-2-one *N*-(Boc)amino acids have been synthesized from L-serine as a chiral educt. A linear precursor Δ^4-unsaturated (2*S*,8*S*)-2,8-bis[*N*-(Boc)amino]azelicacid was prepared in five steps from L-serine. Although epoxidation and dihydroxylation pathways gave mixtures of hydroxy indolizidin-2-one diastereomers, iodolactonization of the Δ^4-azelate stereoselectively delivered a lactone iodide from which separable (5*S*)- and (7*S*)-hydroxy indolizidin-2-one *N*-(Boc)amino esters were synthesized by sequences featuring intramolecular iodide displacement and lactam formation. X-ray analysis of the (7*S*)-hydroxy indolizidin-2-one *N*-(Boc)amino ester indicated that the backbone dihedral angles embedded in the bicyclic ring system resembled those of the central residues of an ideal type II' β-turn indicating potential for peptide mimicry.

5.2. Introduction

In peptide science, conformationally constrained dipeptides serve effectively as tools for structure–activity relationship studies to identify biologically active conformers.[1–20] Among approaches for creating constrained dipeptides that employ steric,[2,3] stereoelectronic,[4,5] and covalent constraints,[1,5–21] the use of azabicyclo[X.Y.0]alkanone amino acids offers unique potential for locking the polyamide backbone into specific orientations that may mimic natural secondary structures such as β-turns. Among such bicyclic systems, the azabicyclo[4.3.0]alkanone amino acids, so-called indolizidine-2-one amino acid (I^2aa) analogs and their ring-substituted derivatives (e.g., **5.1–5.3**, Figure 5.1), are among the most studied for utility in dissecting the backbone geometry and side chain alignment responsible for peptide activity towards the development of receptor ligands (e.g., **5.4**) and enzyme inhibitors (e.g., **5.5–5.7**).[9–21]

Several synthetic methods have been developed to introduce substituents at the 5- and 7-positions along the I^2aa ring system (Figure 5.1).[9–19] For example, 5-hydroxy-5-phenyl I^2aa analogs were synthesized by diastereoselective photochemical cyclization of carbamate-protected β-benzoylalaninyl prolinates.[13] A 5-chloro methyl I^2aa derivative was synthesized by the treatment of phthalimido allylglycinyl 5-methoxyprolinate with $TiCl_4$ in 64% yield.[14] Furthermore, 5-hydroxymethyl, 5-azidomethyl, 5-formyl, 5-carboxy, 5-benzyl, 7-hydroxymethyl, 7-hydroxypropyl, 7-azidopropyl and 7-benzyl, as well as 5,7-dibenzyl I^2aa derivatives were all synthesized diastereoselectively by routes featuring, respectively, intramolecular displacements and reductive aminations of 4-substituted 5-methanesulfonyl and 5-keto 2,8-diaminoazelates to form 5-substituted prolines, which reacted in lactam cyclization.[10–12] Furthermore, 5-iodo I^2aa diastereomers were respectively prepared by transannular iodolactamization of hexahydro-1H-azonines.[15] Iodide elimination afforded the corresponding Δ^5-indolizidine-2-one, which was subsequently arylated at the 5-position by oxidative Heck chemistry.[16] In addition, 7-hydroxyethyl, 7-azidoethyl, 7-carboxymethyl, and 7-guanidinylethyl I^2aas have been synthesized from routes commencing with allylation of glutamic acid,[17,22] and utilized in a program towards the development of $\alpha_v\beta_3$ and $\alpha_v\beta_5$ integrin receptor ligands.[18]

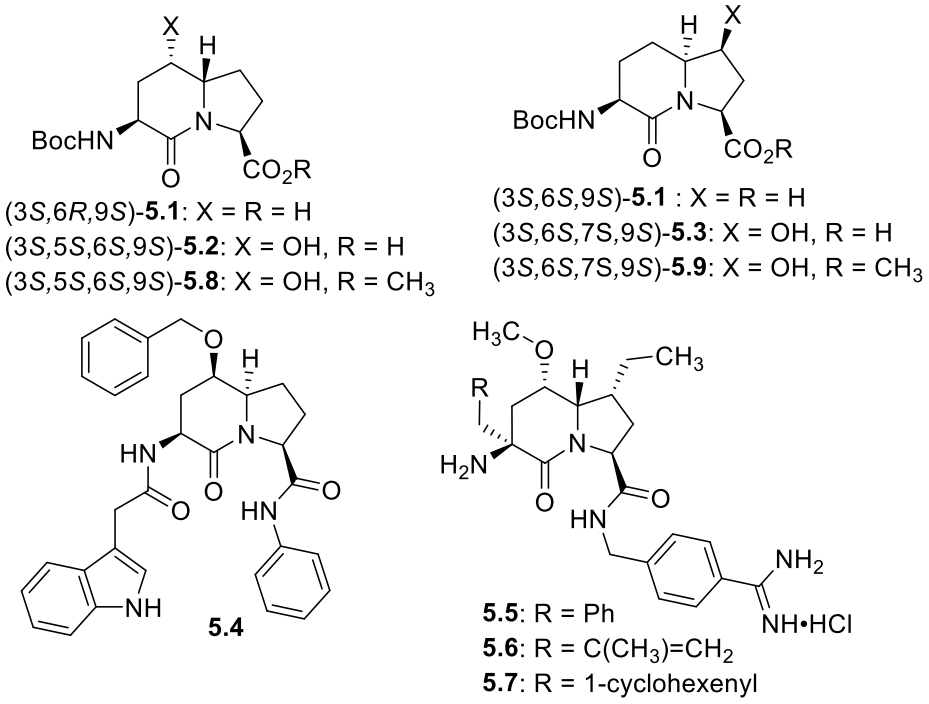

Figure 5.1. Indolizidine-2-one amino acid (Boc-I^{2}aa-OH) isomers **5.1**, 5- and 7-hydroxy I^{2}aas **5.2** and **5.3**, methyl ester counterparts **5.8** and **5.9**, and biologically active 5- and 7-substituted I^{2}aa NK-2 ligand 5.4 and thrombin inhibitors **5.5–5.7**.

The Hanessian laboratory has played an instrumental role in demonstrating the value of 5- and 7-substituted I^{2}aa residues in the study of biologically active peptide receptors.[19–21] For example, 5-benzyloxy I^{2}aa **5.4** was designed by Hanessian and shown to be a weak but selective antagonist of the tachykinin NK-2 (neurokinin-2) receptor.[19] Furthermore, 3,5,7-trisubstituted I^{2}aas **5.5–5.7** were designed, synthesized, and shown to act as potent thrombin [Factor IIa] and Factor VIIa inhibitors exhibiting selectivity over plasmin and Factor XIa.[20] Substituted I^{2}aa peptides **5.4–5.7** were respectively synthesized from pyroglutamate by routes featuring the addition of 2-trimethylsilyloxy furan onto an iminium ion intermediate, followed by lactone to lactam ring expansion to obtain the corresponding 5-hydroxy 9-silyloxymethyl indolizidine-2-one.[19–21] Subsequent installation of the amine and alkyl substituents at the 3-position and

hydroxymethyl group oxidation at the 9-position gave the 3-azido indolizidine-2-one 9-carboxylate counterparts, which were introduced into the peptide mimic structures.[19–21] Validating their utility for peptide-based medicinal chemistry, the herculean research of the Hanessian laboratory has illustrated the necessity for effective synthetic routes to access 5- and 7-substituted I^2aa residues.

Streamlined syntheses of 5- and 7-hydroxy indolizidine-2-one *N*-(Boc)amino acids **5.2** and **5.3** are now reported by methods employing L-serine as a chiral educt. Motivated by the research of the Jackson laboratory in which (2*S*,8*S*)-1,9-dibenzyl Δ^4-2,8-bis[*N*-(Boc)amino]azelate was prepared by the copper-catalyzed S_N2' reaction of the zincate derived from *N*-(Boc)-β-iodo alanine benzyl ester onto (*E*)-1,3-dichloroprop-1-ene,[23] a series of related Δ^4-2,8-diaminoazelates were synthesized and studied in different olefin oxidation chemistries to prepare intermediates towards the hydroxy indolizidine-2-one structures. Among different oxidation approaches yielding access to 5-hydroxy and 7-hydroxy I^2aa derivatives, useful routes to (3*S*,5*S*,6*S*,9*S*)-**5.2** and (3*S*,6*S*,7*S*,9*S*)-**5.3** were conceived by way of diastereoselective iodolactonization chemistry inspired by the seminal research of the Bartlett laboratory.[24]

5.3. Results and Discussion

Initially, 5- and 7-hydroxy indolizidine-2-one *N*-(Boc)amino esters **5.8** and **5.9** were pursued by pathways featuring a ring opening of 4-oxiranyl-2,8-diaminoazelates. Oxiranes **5.10a-c** were synthesized by epoxidation of Δ^4-2,8-diaminoazelates **1.66-1.68**, which were respectively prepared from (*E*)-1,3-dichloroprop-1-ene by copper catalyzed S_N2' additions of zincates derived from methyl β-iodo alaninates **1.61a–c** protected with Boc,[25] Cbz,[26] and Fmoc groups[27] (Scheme 5.1). Although the 15 Hz coupling constant suggested the formation of the *E-trans* olefins **1.66** and **1.67**, without the corresponding *Z-cis* isomer, NOESY experiments were performed to confirm

the double-bond geometry. The *E*-geometry of olefins **1.66** and **1.67** was ascertained by NOESY experiments in which the long-range through-space transfer of magnetization was observed, respectively, between the vinyl C4 (5.38 and 5.35 ppm) and allylic C6 protons (2.09 and 2.07 ppm) and between the vinyl C5 (5.51 and 5.48 ppm) and allylic C3 protons (2.47 and 2.50 ppm) (Scheme 5.1). No nuclear Overhauser effect was observed between the two vinyl protons nor between the two sets of allylic protons.

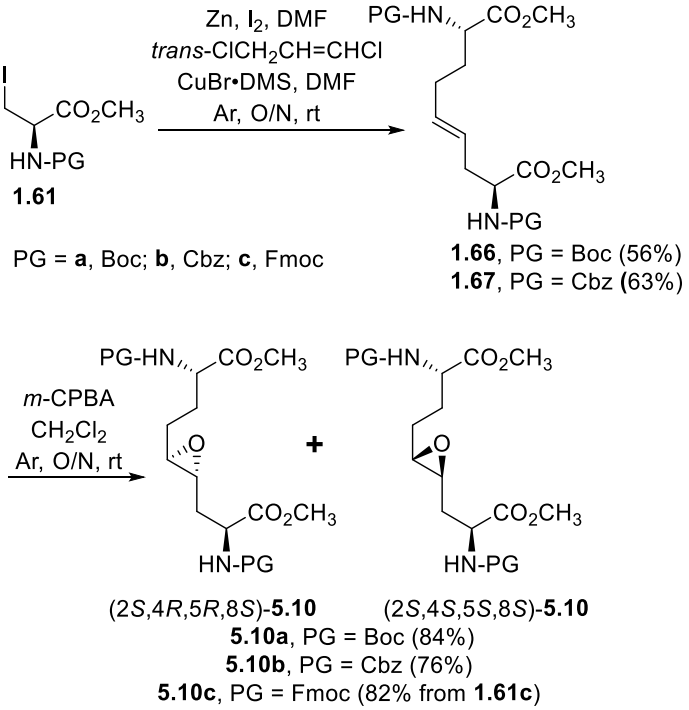

Scheme 5.1. Synthesis of protected epoxides **5.10**

Previously, epoxidations of *N*-Boc and *N*-Cbz allyl- and homoallyl-glycine esters with *m*-chloroperbenzoic acid (*m*-CPBA) in dichloromethane had given 1:1 diastereomeric mixtures of the corresponding oxiranes, which were inseparable by chromatography.[28–30] The C3-protons of benzyl (2*S*,4*RS*)-2-(Boc)amino-3-(2-oxiranyl)propionate was reported to exhibit a doubling of signals in the ^{1}H NMR spectrum.[28] The appearance of multiple sets of signals for the two possible isomers was similarly observed in the spectra of inseparable epoxide diastereomers **5.10a–c** and

validated by COSY spectra of the Cbz and Fmoc analogs **5.10b** and **5.10c** in which through-bond couplings between two sets of C3-protons with two overlapping downfield α-(C2)-proton signals were observed. Oxiranes **5.10a–c** were thus obtained as 1:1 diastereomeric mixtures, which were used in the subsequent chemistry.

Based on the successful synthesis of 6-hydroxymethyl I^2aa diastereomers in which 5-hydroxymethyl prolines were prepared from a related C2 symmetric oxirane using Lewis-acid activation with $BF_3{\cdot}Et_2O$ in DCM at −78 °C,[31] similar conditions were employed for the intramolecular ring-opening of epoxide **5.10a** (Scheme 5.2). Multiple isomers of the material with a molecular ion corresponding to proline **5.11** and hydroxyproline **5.12** were obtained from oxirane **5.10a** likely by *endo* and *exo* ring openings by the attack of the two different carbamate-protected nitrogen.[28,32,33] Considering that the isomeric mix could be due, in part, to carbocation intermediates formed under the Lewis acid conditions, a method to remove the Boc group without the ring opening of the epoxide was attempted featuring heating oxirane **5.10a** in water at reflux.[34] Deprotection of the Boc group, intramolecular epoxide ring opening, and lactam formation all occurred upon treating **5.10a** with boiling water. Amine protection with di-*tert*-butyl dicarbonate and triethyl amine in dichloromethane, however, afforded four isomers of 5- and 7-hydroxy I^2aa esters **5.8** and **5.9**, which were observed by LCMS in a 1:1:1:1 ratio. Employing Cbz-protected epoxide **5.10b**, hydrogenolytic cleavage of the carbamate using hydrogen and palladium-on-carbon in ethanol commenced an epoxide ring opening and lactam formation sequence, which was followed by Boc protection as described above to afford four isomers of **5.8** and **5.9**, which were observed in a 1:5:5:1 ratio by HPLC. The improvement in selectivity may be due to a favored *exo-tet*-like ring opening of the epoxide diastereomers by the free amine, which when generated at a lower temperature reacted to favor the proline instead of the hydroxyproline counterparts.[32,33] In

spite the possibility of improved regioselectivity in the oxirane ring opening, the route (Scheme 5.2) was, however, deemed inefficient due to the complications engendered from the lack of diastereomeric selectivity in the epoxidation of olefins **1.66-1.67**.

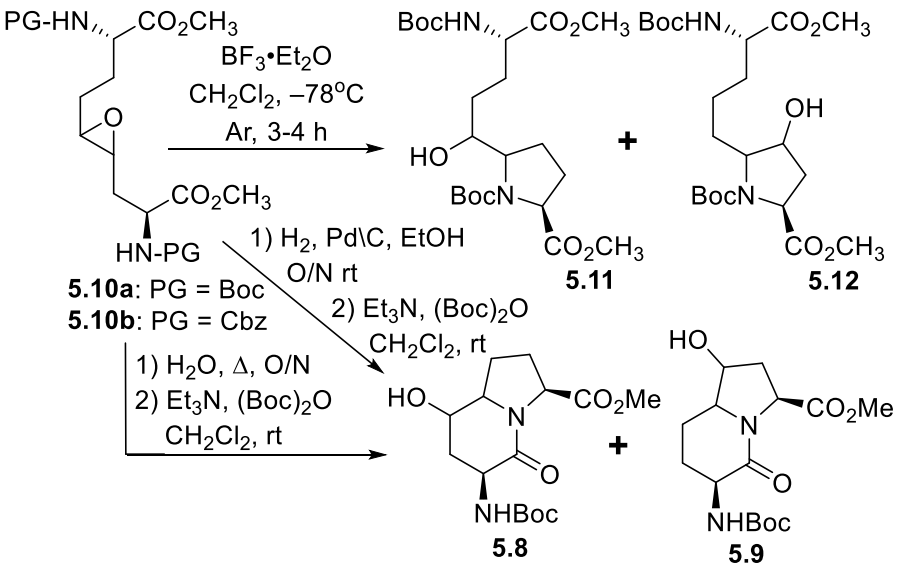

Scheme 5.2. Syntheses of 5- and 7-hydroxy Boc-I[2]aa-OMe **5.8** and **5.9** from epoxide **5.10**

Prompted by earlier success using transannular iodolactamization to prepare azabicyclo[X.Y.0]alkan-2-one ring systems,[15,35] and related iodoamination protocols for preparing iodomethyl pyrrolidines and piperidines,[36–38] Δ^4-diaminoazelate **1.66** was subjected to iodine and $NaHCO_3$ at −20 °C (Scheme 5.3). The ring opening of the iodonium intermediate by one of the two carbamate-protected nitrogen appeared to be a method for selectively obtaining proline **5.13** instead of the azetidine counterpart; however, a mixture of diastereomeric iodolactones **5.14** was also produced as a competing side product. Considering the lactone as a potential means for differentiating between the two carboxylates, dihydroxylation of Δ^4-diaminoazelate **1.66** was performed using osmium tetroxide and *N*-methylmorpholine *N*-oxide (NMO) in aqueous acetone to provide hydroxylactone **5.15** as a mixture of diasteromers.[39] Mesylate **5.16** was obtained by methanesulfonation of hydroxylactone **5.15** using methanesulfonyl chloride and triethylamine in

dichloromethane. Mesylate **5.16** was converted to hydroxy I^{2}aa analogs **5.8** and **5.9** by a three-step sequence featuring proline formation after Boc group removal with HCl gas bubbles in dichloromethane, lactam cyclization upon treatment of the hydrochloride salt with triethylamine in methanol at reflux, and amine protection with di-*tert*-butyl dicarbonate in dichloromethane. The HPLC chromatogram of the products from this sequence exhibited four peaks with molecular ions corresponding to 5- and 7-hydroxy Boc-I^{2}aa-OMe isomers **5.8** and **5.9** (Scheme 5.3) in a 1:1:1:1 ratio.

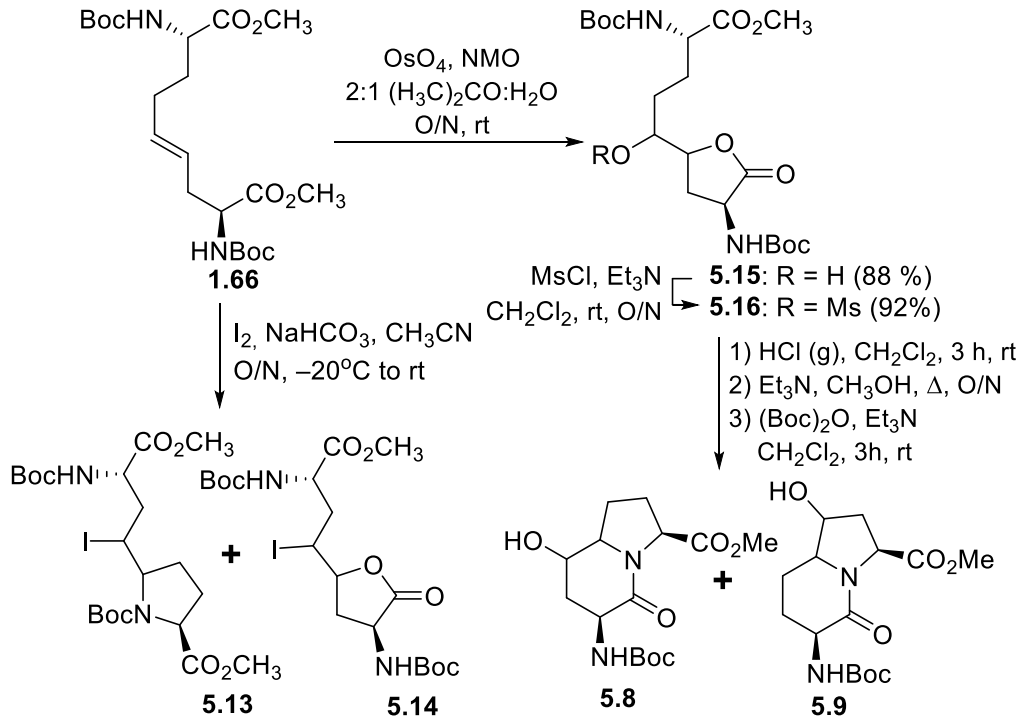

Scheme 5.3. Strategies featuring iodoamination and dihydroxylation of Δ^4-diaminoazelate

Different mixtures of 5- and 7-hydroxy Boc-I^{2}aa-OMe diastereomers **5.8** and **5.9** likely arose from a combination of a lack of facial selectivity in the epoxidation and the dihydroxylation of olefin **1.66** and competing nucleophilic attack from both nitrogen of diamino azelate epoxide **5.10** and methanesulfonate **5.16**. The loss of stereochemical integrity may also arise from competing S_N1 processes due to the epoxide ring opening prior to pyrrolidine formation. Intrigued

by the production of iodolactone **5.14** as a side product from the iodoamination strategy, an iodolactonization approach was considered because of the high facial selectivity achieved on simpler γ,δ-unsaturated carboxylic acids.[24,40,41]

After saponification of diester **1.66** with lithium hydroxide in aqueous dioxane, dicarboxylic acid **5.17** was treated with cesium carbonate and iodine in an ice-cold acetonitrile solution (Scheme 5.4). Analysis by LCMS demonstrated a major peak with a molecular ion corresponding to lactone **5.18**. Subsequent treatment with iodomethane and potassium carbonate in DMF furnished the corresponding methyl ester tetrahydrofuran-2-one (1′*R*,5*S*)-**5.14** after chromatography in 55% yield from diacid acid **5.18**. Attempts to perform the iodolactonization without a base gave a product mostly from the loss of Boc protection. Employing the same three-step sequence described above to convert methane sulfonate **5.16** into esters **5.8** and **5.9**, iodide (1′*R*,5*S*)-**5.14** was transformed into separable 5- and 7-hydroxy I^2aa esters (5*S*,6*S*)-**5.8** and (6*S*,7*S*)-**5.9** in 42% and 34% overall yields, respectively. Subsequent saponification of esters (5*S*,6*S*)-**5.8** and (6*S*,7*S*)-**5.9** gave, respectively, the acids (5*S*,6*S*)-**5.2** and (6*S*,7*S*)-**5.3** in 64% and 78% yields.

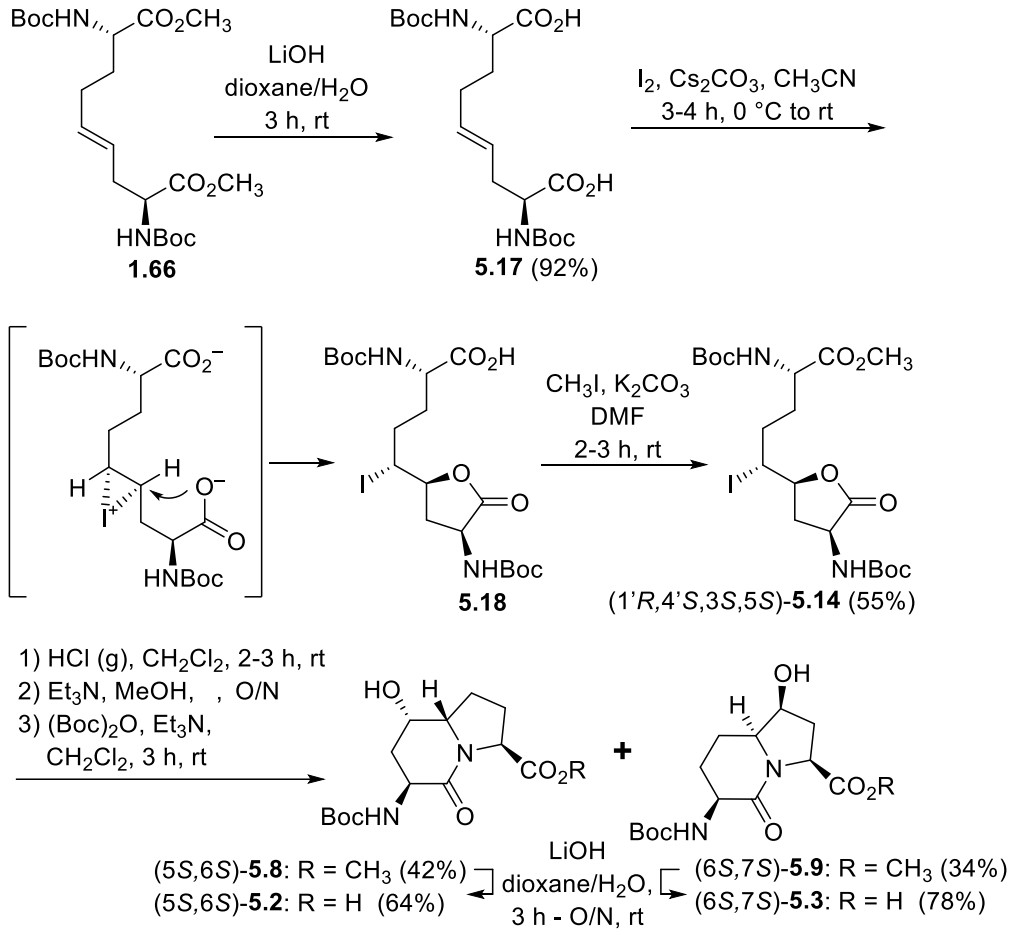

Scheme 5.4. Synthesis of 5- and 7- hydroxy I^{2}aa derivatives **5.2** and **5.3**

5.4. Assignment of regiochemistry and stereochemistry of 5- and 7-hydroxy I^{2}aa esters

The configuration of the ring fusion and hydroxyl group carbons of the 5- and 7-hydroxy I^{2}aa esters **5.8** and **5.9**, as well as the alcohol position on the ring system, were all assigned based on two-dimensional NMR spectroscopic experiments. The locations of the indolizidine-2-one ring protons were initially assigned by COSY experiments in which through-bond couplings were used to trace the sequence from the downfield shifted carbamate NH to the C9 hydrogen. Subsequently, heteronuclear single quantum coherence (HSQC) spectroscopy was used to correlate the protons linked to similar carbons. The β-protons on the same face as the C3 carbamate and C9 carboxylate appeared generally upfield of their α-counterparts due to anisotropic effects caused by the latter functional groups.[42] Finally, relative configurations were ascertained (Figure 5.2) based on

NOESY experiments in which the observed through-space transfers of magnetization were used to correlate the stereochemical assignments.

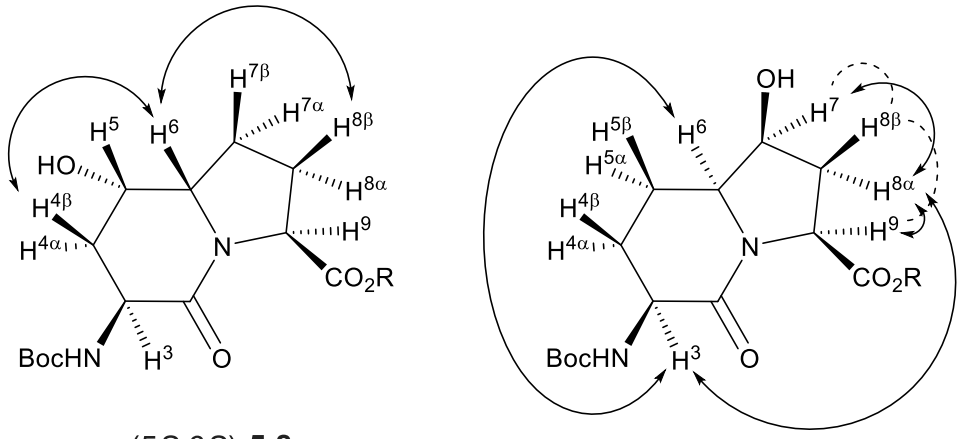

Figure 5.2. Strong (solid double-tipped arrows) and weak (dotted lines) through-space transfer of magnetization used to assign relative stereochemistry of (5*S*,6*S*)-**5.8** and (6*S*,7*S*)-**5.9**

The ring fusion protons (3.88 and 3.74 ppm) of 5- and 7-hydroxy Boc-I[2]aa-OMe (5*S*,6*S*)-**5.8** and (6*S*,7*S*)-**5.9** were respectively assigned the *S* stereochemistry based on nuclear Overhauser effects (nOe) with the C4β and C8β protons (1.99 and 1.84 ppm) and with the C3 proton (4.13 ppm, Figure 5.2). No long-range through-space transfer of magnetization was observed for the protons on the alcohol-bearing carbons. In the case of (6*S*,7*S*)-**5.9**, the relative nOe between the C7 proton was stronger for the C8α proton (2.35 ppm) compared to that of the C8β proton (2.15 ppm). The stereochemical assignments for Boc-(7-OH)I[2]aa-OMe (6*S*,7*S*)-**5.9** were confirmed by X-ray analysis as discussed below.

The configurations of the hydroxyl group in Boc-(5-OH)I[2]aa-OMe (5*S*,6*S*)-**5.8** and the iodolactone of tetrahydrofuran-2-one (1′*R*,5*S*)-**5.14** were based on the latter serving as a common intermediate for both the former and Boc-(7-OH)I[2]aa-OMe (6*S*,7*S*)-**5.9**. The stereochemistry of the ring-fusion and alcohol carbons are respectively derived from the inversion on nitrogen attack

of the iodide and retention on the lactone opening during synthesis of the bicycle. Although the order of attack of the iodine and carboxylate may proceed by a traditional iodonium intermediate (Scheme 5.4),[24] and by a more concerted nucleophile-assisted alkene activation mechanism,[43] the stereochemical outcome of iodolactone (1′*R*,5*S*)-**5.14** arises from the attack of iodine by the face of the olefin on the opposite side of the proximal carboxylate of Δ^4-azelate **5.17** (Scheme 5.4).

The relative configurational assignments for 7-hydroxy Boc-I^2aa-OMe (6*S*,7*S*)-**5.9** were confirmed by X-ray analysis of crystals grown from a dichloromethane-in-hexanes mixture (Figure 5.3). Two conformers differing primarily by the carbamate orientation were present in the unit cell and connected by an intermolecular hydrogen bond from the 7-hydroxyl group donor to the lactam carbonyl oxygen acceptor. Examination of the backbone dihedral angles embedded in the I^2aa ring system (ψ^{i+1} −172° and ϕ^{i+2} −78°; ψ^{i+1} −175° and ϕ^{i+2} −71°) of the conformers in the X-ray structure of the 7-hydroxy analog (6*S*,7*S*)-**5.9** indicated a close relation to those of the central residues of an ideal type II' β-turn (ψ^{i+1} −120° and ϕ^{i+2} −80°),[44] and to that of the methyl ester of the parent I^2aa counterpart (6*S*)-**5.18** (ψ^{i+1} −176° and ϕ^{i+2} −78°, Figure 5.4).[45] Relative to the values in the crystal structure of Boc-I^2aa-OMe (6*S*)-**5.18**, the ϕ^{i+2} dihedral angle was apparently less influenced by the smaller 7β-hydroxy substituent than the 7α-hydroxymethyl substituent in Boc-(7-$HOCH_2$)I^2aa-OMe (**5.19**, ψ^{i+1} −175° and ϕ^{i+2} −68°).[11]

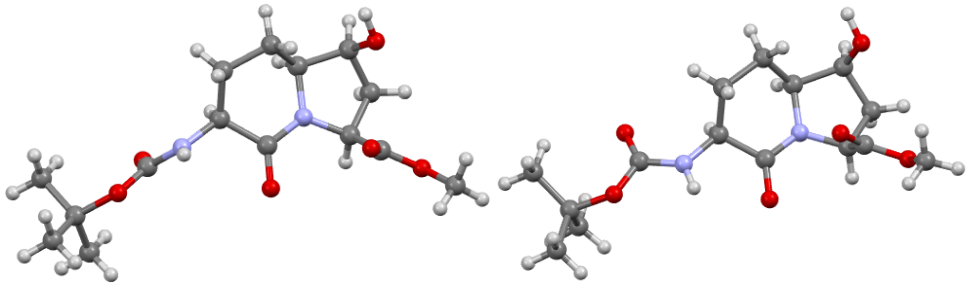

Figure 5.3. Depictions of conformers in the X-ray structure of (6*S*,7*S*)-**5.9**

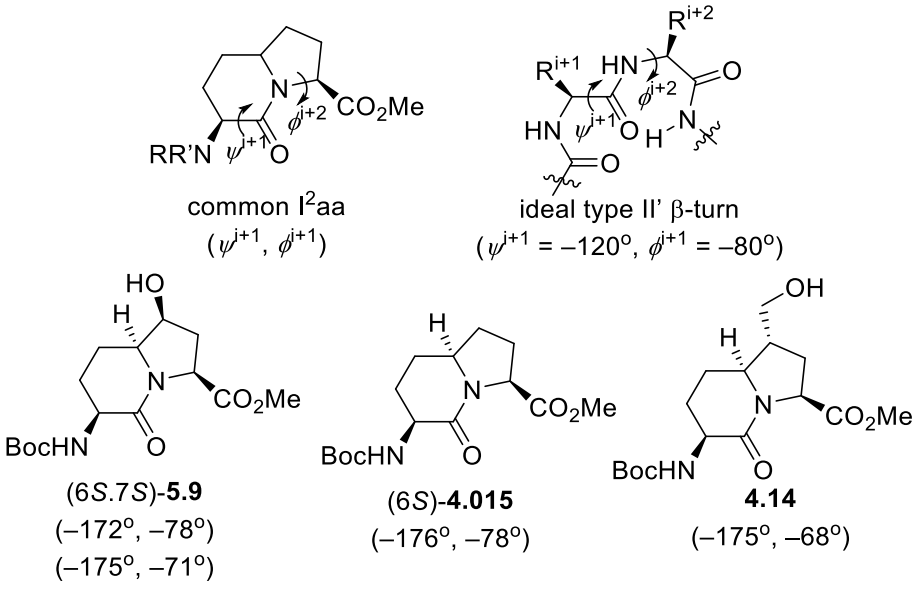

Figure 5.4. X-ray-determined backbone dihedral angles of related I^2aa systems and an ideal type II′ β-turn[11,44,45]

5.5. Experimental section

5.5.1 General Methods:

Anhydrous solvents (CH_3CN, DMF, $(CH_3)_2CO$, CH_2Cl_2, and CH_3OH) were obtained by passage through solvent filtration systems (GlassContour, Irvine, CA, USA). All reagents from commercial sources were used as received: Iodine was purchased from Aldrich (USA) and solvents were obtained from Fisher Chemical. The *N*-(Boc)-, (Cbz)-, and (Fmoc)-3-iodo-L-alanine methyl esters 5.10a–c were respectively prepared according to the literature methods reported in references [25–27]. Purification by silica gel chromatography was performed on 230−400 mesh silica gel; analytical thin-layer chromatography (TLC) was performed on silica gel 60 F254 (aluminum sheet) and visualized by UV absorbance or staining with $KMnO_4$. Melting points are reported in degree Celsius (°C), uncorrected and obtained using a Mel-Temp melting point apparatus equipped with a thermometer on the sample that was placed in a capillary tube.

Spectroscopic ^{1}H and ^{13}C NMR experiments were recorded at room temperature (298 K) in $CDCl_3$ (7.26/77.16 ppm), DMSO-d_6 (2.5/39.56), and CD_3OD (3.31/ 49.0 ppm) on Bruker AV (500/125, and 700/175 MHz) instruments using an internal solvent as the reference. Spectra are presented in the Supporting Information. Chemical shifts are reported in parts per million (ppm), and coupling constant (*J*) values in Hertz (Hz). Abbreviations for peak multiplicities are s (singlet), d (doublet), t (triplet), q (quadruplet), q (quintuplet), m (multiplet), and br (broad). Certain ^{13}C NMR chemical shift values were extracted from HSQC spectra. High-resolution mass spectrometry (HRMS) data were obtained on an LC-MSD instrument in electrospray ionization (ESI-TOF) mode by the Centre Régional de Spectrométrie de Masse de l'Université de Montréal. Either protonated molecular ions $[M + H]^+$ or sodium adducts $[M + Na]^+$ were used for empirical formula confirmation. Infrared spectra were recorded in the neat on a Perkin Elmer Spectrometer FT-IR instrument, and are reported in reciprocal centimeters (cm^{-1}). The X-ray structure was solved using a Bruker Venture Metaljet diffractometer by the Laboratoire de diffraction des rayons X de l'Université de Montréal. Specific rotations $[\alpha]_D$ were measured at 25 °C at the specified concentrations (*c* in g/100 mL) using a 0.5 dm cell on a PerkinElmer Polarimeter 589 instrument and expressed using the general formula $[\alpha]_D^{25} = (100 \times \alpha)/(d \times c)$.

5.5.2 Synthetic experimental conditions and characterization data of compounds:

(3S,5S,6S,9S)-3-*N*-(Boc)amino-5-hydroxy indolizin-2-one-9-carboxylic acid [(3*S*,5*S*,6*S*,9*S*)-5.2]

A 0 °C solution of ester (3*S*,5*S*,6*S*,9*S*)-**5.8** (15 mg, 0.046 mmol) in 1,4-dioxane (0.5 mL) was treated with a 1N solution of LiOH (1.9 mg, 0.046 mmol, 1 equiv.). The cooling bath was removed. The reaction mixture was warmed to room temperature with stirring overnight, at which time TLC indicated the consumption of the starting material. The volatiles were evaporated under

reduced pressure. The residue was partitioned between H_2O (5 mL) and ethyl acetate (5 mL). The aqueous phase was acidified with 1N HCl to pH 3 and extracted with ethyl acetate (3 × 10 mL). The organic extractions were combined, dried with Na_2SO_4, filtered, and concentrated under vacuum to afford (3*S*,5*S*,6*S*,9*S*)-**5.2** (9 mg, 64%) as a white foam; $[\alpha]_D^{25}$ –10.2 (*c* 0.32, $CHCl_3$); ^{1}H NMR (500 MHz, $CDCl_3$): δ 5.39 (s, br, 1H), 4.71 (s, 1H), 4.39 (s, br, 1H), 4.29–4.28 (m, 1H), 3.84–3.80 (m, 1H), 2.6–2.52 (m, 1H), 2.39-2.33 (m, 2H), 2.26-2.20 (m, 1H), 2.05-2.02 (m, 1H), 2.0-1.95 (m, 1H), 1.67-1.63 (m, 1H), 1.47 (s, 9H); ^{13}C{^{1}H} NMR (125 MHz, $CDCl_3$) δ 172.0, 167.3, 147.3, 80.5, 64.0, 60.0, 35.2, 32.0, 30.0, 28.3, 26.1, 23.0; FT-IR (neat) ν_{max} 3328, 2919, 1702, 1521, 1449, 1362, 1208, 1166, 1050, 1031cm^{-1}; HRMS (ESI-TOF) *m*/*z* $[M + Na]^+$ calcd for $C_{14}H_{22}N_2O_6Na$ 337.1370, found 337.1374.

(3S,6S,7S,9S)-3-*N*-(Boc)amino-7-hydroxy indolizin-2-one-9-carboxylic acid [(3*S*,6*S*,7*S*,9*S*)-5.3]

A 0 °C solution of ester (3*S*,6*S*,7*S*,9*S*)-**5.9** (150 mg, 0.46 mmol) in 1,4-dioxane (5 mL) was treated with a 1N solution of LiOH (19.2 mg, 0.46 mmol, 1 equiv.). The cooling bath was removed. The reaction mixture was warmed to room temperature with stirring for 3 h, at which time TLC indicated the consumption of the starting material. The volatiles were evaporated under reduced pressure. The residue was partitioned between H_2O (10 mL) and ethyl acetate (5 mL). The aqueous phase was acidified with 1N HCl to pH 3 and extracted with ethyl acetate (3 × 10 mL). The organic extractions were combined, dried with Na_2SO_4, filtered, and concentrated under vacuum to afford (3*S*,6*S*,7*S*,9*S*)-**5.3** (112 mg, 78%) as a white solid: mp 105–106 °C; $[\alpha]_D^{25}$ –19.13 (*c* 0.23, $CHCl_3$); ^{1}H NMR (500 MHz, CD_3OD): δ 4.460–4.43 (dd, *J* = 9.3, 4.3 Hz, 1H), 4.26–4.24 (m, 1H), 4.22–4.17 (m, 1H), 3.76–3.72 (m, 1H), 2.47–2.41 (m, 1H), 2.21–2.18 (d, *J* = 14.2 Hz, 1H), 2.15–2.07 (m, 2H), 1.87–1.82 (m, 2H), 1.48 (s, 9H); ^{13}C{^{1}H} NMR (125 MHz, CD_3OD) δ 174.0, 170.0,

156.6, 79.1, 71.2, 62.3, 57.2, 50.0, 37.0, 27.3, 27.0, 19.0; FT-IR (neat) ν_{max} 3325, 2922, 1697, 1523, 1451, 1365, 1211, 1162, 1055, 1032cm^{-1}; HRMS (ESI-TOF) *m*/*z* [M + Na]$^+$ calcd for $C_{14}H_{22}N_2O_6Na$ 337.1370, found 337.1374.

Methyl (3*S*,5*S*,6*S*,9*S*)-3-*N*-(Boc)amino)-5-hydroxy-indolizin-2-one-9-carboxylate and (3*S*,6*S*,7*S*,9*S*)-3-*N*-(Boc)amino)-7-hydroxy-indolizin-2-one-9-carboxylate [(3*S*,5*S*,6*S*,9*S*)-5.8 and (3*S*,6*S*,7*S*,9*S*)-5.9]

A solution of (1′*R*,5*S*)-1′-iodo-tetrahydrofuran-2-one (1′*R*,5*S*)-**5.14** (1.0 g, 1.8 mmol) in dichloromethane (20 mL) was treated with HCl gas bubbles for 2-3 h, when TLC indicted complete consumption of the starting carbamate and LCMS analysis indicated a new peak RT = 0.7 min (C18 column, 10:90 CH_3CN:H_2O) with a molecular ion of [M + H]$^+$ *m*/*z* 357. The reaction mixture was evaporated to a residue, which was dissolved in MeOH (5 mL), treated with triethylamine (545 mg, 5.4 mmol, 3 equiv.), and heated at reflux using an oil bath overnight, when LCMS indicated a new peak RT = 0.68 min (eluent C18 column, 10:90 CH_3CN:H_2O) with the molecular ion [M + H]$^+$ *m*/*z*. The volatiles were evaporated under reduced pressure. The residue was dissolved in dichloromethane (10 mL), treated with $(Boc)_2O$ (0.14 g, 0.63 mmol, 1.2 equiv.), and stirred for 3 h, when TLC indicated two new spots and LCMS indicated a new peak RT = 5.0 min (C18 column, 10:90 CH_3CN:H_2O). The volatiles were removed under reduced pressure. The residue was purified by flash column chromatography using 60–80% EtOAc in hexanes as eluent. The first to elute was Boc-(7-HO)I^{2}aa-OMe (3*S*,6*S*,7*S*,9*S*)-**5.9** (200 mg, 34%) as a white solid: mp 138–140 °C; R_f = 0.47, (100% EtOAc twice eluted, visualized with $KMnO_4$); $[\alpha]_D^{25}$ –28.2 (*c* 0.85, $CHCl_3$); ^{1}H NMR (500 MHz, $CDCl_3$) δ 5.14 (s, br, NH), 4.46–4.44 (dd, *J* = 10 Hz, 1H), 4.22–4.18 (m, 1H), 4.15–4.12 (m, 1H), 3.84 (s, 3H), 3.76–3.71 (m, 1H), 3.61–3.58 (d, *J* = 15 Hz, OH), 2.4–2.33 (m, 2H), 2.29–2.22 (m, 1H), 2.15–2.12 (dt, *J* = 14.5, 0.9 Hz, 1H), 2.0–1.93 (m, 1H), 1.77–

1.69 (m, 1H), 1.47 (s, 9H); $^{13}C\{^{1}H\}$ NMR (125 MHz, $CDCl_3$) δ 175.5, 170.1, 156.0, 80.0, 73.0, 61.5, 57.1, 53.2, 51.0, 36.3, 28.3, 27.1, 19.2; FT-IR (neat) ν_{max} 3357, 2979, 1693, 1636, 1518, 1437, 1392, 1365, 1249, 1165, 1099, 1063, 1005 cm^{-1} HRMS (ESI-TOF) m/z $[M + Na]^+$ calcd for $C_{15}H_{24}N_2O_6Na$ 351.1526 found 351.1522.

Next to elute was Boc-(5-HO)I^{2}aa-OMe (3*S*,5*S*,6*S*,9*S*)-**5.8** (250 mg, 42%) as a white solid: mp 75-77 °C; R_f = 0.3 (100% EtOAc, twice eluted, visualized with $KMnO_4$); $[\alpha]_D^{25}$ –12.6 (*c* 0.75, $CHCl_3$). ^1H NMR (500 MHz, $CDCl_3$) δ 5.25 (s, br, NH), 4.50–4.44 (m, 2H), 4.27 (s, 1H), 3.89-3.86 (m, 1H), 3.77 (s, 3H), 2.74–2.68 (m, 1H), 2.44–2.40 (m, 1H), 2.11–2.04 (m, 2H), 2.00–1.97 (m, 1H), 1.95–1.92 (m, 1H), 1.88–1.83 (m, 1H), 1.45 (s, 9H); $^{13}C\{^{1}H\}$ NMR (125 MHz, $CDCl_3$) δ 173.0, 168.0, 156.2, 80.0, 64.0, 63.3, 58.2, 52.3, 47.4, 36.0, 28.3, 28.0, 27.0; FT-IR (neat) ν_{max} 3360, 2983, 1702, 1633, 1518, 1438, 1395, 1250, 1162, 1102, 1002 cm^{-1}; HRMS (ESI-TOF) m/z $[M + Na]^+$ calcd for $C_{15}H_{24}N_2O_6Na$ 351.1526 found 351.1522.

Dimethyl (2*S*,4*E*,8*S*)-Δ^4-2,8-(di-*N*-(Boc)amino)azelate (1.66)

In a 250-mL round bottom flask, fitted with a three-way stopcock, CuBr•DMS (1.22 g, 0.006 mol, 0.13 equiv.) was weighed, dried gently with a heat gun under vacuum until the powder changed color from white to light green, placed under argon, treated with dry DMF (30 mL), followed by (*E*)-1,3-dichloroprop-1-ene (2.5 g, 0.023 mol, 0.5 equiv.). In a Schlenk tube, zinc (8.9 g, 0.14 mol, 3 equiv.) and iodine (0.35 g, 0.0014 mol, 0.03 equiv.) were mixed under an argon atmosphere, and thrice heated under vacuum with a heat gun for 10 min and cooled under a flush of argon. A solution of *N*-(Boc)-3-iodo-L-alanine methyl ester **1.61** (15 g, 0.046 mol) in dry DMF (30 mL) was added to the Schlenk tube and stirred for 1h, when TLC analysis confirmed the consumption of the iodide (R_f = 0.7, 30% EtOAc in hexanes) and formation of the organozinc reagent (R_f = 0.2, 30% EtOAc in hexanes). Stirring was stopped, the excess zinc powder was

allowed to settle, and the supernatant was transferred dropwise via a syringe with care to minimize the transfer of zinc into the flask containing the copper catalyst. After stirring at rt overnight, TLC indicated a new spot (R_f = 0.48, 40% EtOAc in hexanes) and the reaction mixture was diluted with ethyl acetate (150 mL), stirred for 15 min, and filtered through a silica gel pad. The filtrate was treated with water (100 mL), transferred into a separatory funnel, and diluted with ethyl acetate (50 mL). The organic phase was washed successively with 1 M $Na_2S_2O_3$ (2 × 100 mL), water (4 × 100 mL), and brine (2 × 100 mL), dried over Na_2SO_4, filtered, and evaporated. The volatiles were removed under reduced pressure to afford a residue that was purified by chromatography using 25–30% EtOAc in hexanes as the eluent. Evaporation of the collected fractions gave azelate **1.66** (11.4 g, 56%) as a colorless liquid: R_f = 0.48 (2:3 EtOAc/Hexanes, visualized with $KMnO_4$); $[\alpha]_D^{25}$ +25.2 (*c* 1.04, $CHCl_3$); ^{1}H NMR (500 MHz, $CDCl_3$) δ 5.54–5.48 (dt, *J* = 15, 5 Hz, 1H), 5.39–5.34 (dt, *J* = 15, 5 Hz, 1H), 5.25–5.24 (d, *J* = 5.0 Hz, 1H), 5.03–5.01 (d, *J* = 10 Hz, 1H), 4.40–4.37 (m, 1H), 4.34–4.30 (m, 1H), 3.76 (s, 3H), 3.75 (s, 3H), 2.52–2.43 (m, 2H), 2.12–2.07 (m, 2H), 1.90–1.84 (m, 1H), 1.71–1.67 (m, 1H), 1.47 (s, 9H), 1.46 (s, 9H); ^{13}C{^{1}H} (125 MHz, $CDCl_3$) δ 173.3, 173.0, 155.3, 155.2, 133.1, 125.5, 79.95, 79.84, 53.2, 53.0, 52.3, 52.2, 35.6, 32.4, 28.4, 28.3, 23.2; FT-IR (neat) ν_{max} 3363, 2977, 1698, 1508, 1437, 1391, 1365, 1247, 1211, 1157, 1103, 1050, 1021 cm^{-1} ; HRMS (ESI-TOF) *m*/*z* $[M + Na]^+$ calcd for $C_{21}H_{36}N_2O_8Na$ 467.2363 found 467.2359.

Dimethyl (2*S*,4*E*,8*S*)-Δ^4-2,8-(di-*N*-(Cbz)amino)azelate (1.67)

Diaminoazelate **1.67** with Cbz protection was synthesized according to the protocol described for the synthesis of Boc counterpart **1.66** using N-(Cbz)-3-iodo-L-alanine methyl ester **1.67** (8.0 g, 0.02 mmol) and isolated as a colorless liquid (3.5 g, 63%): R_f = 0.30 (2:3 E.A/Hexanes, visualized by UV); $[\alpha]_D^{25}$ +15.9 (c 1.09, $CHCl_3$); ^{1}H NMR (500 MHz, CD_3OD): δ 7.40–7.31(m,

10H), 5.57–5.55 (d, J = 10 Hz, 1H), 5.52–5.45 (dt, J = 15, 5 Hz, 1H), 5.38–5.33 (dt, J = 15, 5 Hz, 1H), 5.29–5.27 (d, J = 10Hz, 1H), 5.16–5.11(m, 4H), 4.48–4.44 (m, 1H), 4.42–4.37 (m, 1H), 3.76 (s, 3H), 3.75 (s, 3H) 2.58–2.46 (m, 2H), 2.13–2.01 (m 2H), 1.94–1.82 (m, 1H), 1.74–1.67 (m, 1H); $^{13}C\{^{1}H\}$ NMR (125 MHz, $CDCl_3$) δ 172.2, 156.0, 136.2, 132.3, 128.57, 128.54, 128.52, 128.46, 128.25, 128.22, 128.16, 128.13, 125.32, 67.1, 67.0, 54.0, 53.0, 52.4, 52.3, 35.4, 32.4, 32.2, 28.2; FT-IR (neat) ν_{max} 3332, 2953, 1699, 1521, 1437, 1341, 1207, 1050 cm^{-1}; HRMS (ESI-TOF) m/z $[M + H]^+$ calcd for $C_{27}H_{33}N_2O_8$ 513.2231, found 513.2234.

Dimethyl (2*S*,4*RS*,5*RS*,8*S*)-2,8-di-*N*-(Boc)amino-4-oxiranyl azelate (5.10a)

A solution of Δ^4-di-*N*-(Boc)aminoazelate **1.66** (2.0 g, 4.5 mmol) in dichloromethane (DCM, 30 mL) was cooled to 0 °C and treated with *m*-chloroperoxybenzoic acid (2.0 g, 9.0 mmol, 2.0 equiv.). The ice bath was removed. The suspension was warmed to room temperature with stirring overnight, when TLC showed the complete consumption of olefin 1.66 (R_f = 0.48, 40% EtOAc in hexanes) and a new polar spot for epoxide **5.10a** (R_f = 0.2, 40% EtOAc in hexanes). The reaction mixture was diluted with DCM (30 mL), transferred to a separatory funnel, and washed sequentially with 1N NaOH (2 × 20 mL), water (20 mL), and brine (20 mL), dried over Na_2SO_4, filtered, and concentrated under vacuum to a residue that was purified by flash column chromatography using 20% EtOAc in hexanes as the eluent. Evaporation of the collected fractions afforded epoxide **5.10a** (1.75 g, 84%) as colorless oil: R_f = 0.2 (2:3 EtOAc/hexanes, visualized with $KMnO_4$); $[\alpha]_D^{25}$ +2.5 (*c* 0.81, $CHCl_3$); ^1H NMR (500 MHz, CD_3OD): δ 4.32-4.26 (m, 1H), 4.18-4.13 (m, 1H), 3.75 (s, 3H), 3.74 (s, 3H), 2.87-2.75 (m, 2H), 1.97-1.90 (m, 2H), 1.80-1.72 (m, 1H), 1.64-1.59 (m, 1H), 1.47 (s, 20H); $^{13}C\{^{1}H\}$ NMR (125 MHz, CD_3OD) δ 173.2, 173.0, 156.7, 156.6, 79.4, 79.2, 58.0, 57.5, 55.4, 55.3, 53.5, 53.1, 51.51, 51.4, 51.3, 34.0, 27.3; FT-IR (neat) ν_{max}

3326, 2955, 1699, 1523, 1437, 1210, 1045, 912 cm^{-1}; HRMS (ESI-TOF) m/z $[M + Na]^+$ calcd for $C_{21}H_{36}N_2O_9Na$ 483.2313, found 483.2321.

Dimethyl (2*S*,4*RS*,5*RS*,8*S*)-2,8-di-*N*-(Cbz)amino-4-oxiranyl azelate (5.10b)

Epoxide **5.10b** with Cbz protection was synthesized using the protocol described for the preparation of Boc counterpart **5.10a** using dimethyl Δ^4-di-(Cbz)aminoazelate **1.67** (3.2 g, 6.2 mmol) and isolated as a colorless liquid (2.5g, 76%): R_f = 0.21 (2:3 EtOAc/hexanes, visualized by UV); $[\alpha]_D^{25}$ +7.95 (*c* 0.88, $CHCl_3$); ^{1}H NMR (500 MHz, $CDCl_3$): δ 7.40–7.33 (m, 10H), 5.68–5.62 (d, *J* = 10Hz, 1H), 5.44–5.32 (d, *J* = 5Hz, 1H), 5.16–5.11 (m, 4H), 4.58–4.11 (m, 1H), 4.45–4.39 (s, 1H), 3.79–3.76 (s, 6H), 2.81–2.70 (m, 2H), 2.25–2.07 (m, 1H), 2.04–1.92 (m, 2H), 1.83–1.75 (m, 1H), 1.71–1.65 (m, 1H), 1.54–1.44 (m, 1H); $^{13}C\{^1H\}$ NMR (125 MHz, $CDCl_3$) δ 172.5, 172.1, 156.0, 136.2, 128.6, 128.3, 128.2, 67.1, 57.5, 55.3, 55.1, 53.5, 53.2, 53.0, 52.65, 52.57, 52.51, 52.2, 35.0, 30.0, 29.0, 28.0, 27.5; FT-IR (neat) ν_{max} 3332, 2953, 1700, 1521, 1437, 1344, 1208, 1049 cm^{-1}; HRMS (ESI-TOF) *m*/*z* $[M + H]^+$ calcd for $C_{27}H_{33}N_2O_9$ 529.2180, found 529.2190.

Dimethyl (2*S*,4*RS*,5*RS*,8*S*)-2,8-di-*N*-(Fmoc)amino-4-oxiranyl azelate (5.10c)

Dimethyl (2*S*,4*E*,8*S*)-Δ^4-2,8-(di-*N*-(Fmoc)amino)azelate (**1.68**) was synthesized using the protocol described for the synthesis of Δ^4-di-(Boc)aminoazelate **1.66** from *N*-(Fmoc)-3-iodo-L-alanine methyl ester (**1.61c**, 1.5 g, 0.0022 mol) and isolated as a colorless liquid (0.7 g, 63%): R_f = 0.21 (4:6 ethyl acetate/hexanes, visualized by UV). Epoxidation was performed as described for Boc counterpart **5.10a** using dimethyl (2*S*,4*E*,8*S*)-Δ^4-2,8-(di-*N*-(Fmoc)amino)azelate (**5.10c**, 600 mg, 0.87 mmol), which gave a colorless solid (500 mg, 82%): mp 89-92 °C; R_f = 0.30 (4:6 EtOAc/hexanes, visualized by UV); $[\alpha]_D^{25}$ +5.5 (*c* 0.51, $CHCl_3$); ^{1}H NMR (500 MHz, $CDCl_3$): δ 7.79–7.77 (d, *J* = 10 Hz, 4H) 7.63–7.57 (m, 4H), 7.43–7,40 (m, 4H), 7.34–7.31 (m, 4H), 5.74–5.67 (dd, *J* = 10, 5 Hz, 1H), 5.48–5.34 (dd, *J* = 12, 10 Hz, 1H), 4.60–4.51 (m, 2H), 4.46–4.40 (m, 4H),

4.26–4.22 (m, 2H), 3.81 (s, 3H), 3.78 (s, 3H), 2.85–2.73 (m, 2H), 2.16–1.74 (m, 6H); $^{13}C\{^{1}H\}$ NMR (125 MHz, $CDCl_3$) δ 172.6, 172.1, 156.0, 143.8, 143.7, 141.3, 130.0, 128.0, 127.1, 125.1, 120.0, 67.2, 67.1, 67.0, 57.4, 55.3, 55.1, 53.2, 52.73, 52.7, 52.6, 52.5, 47.1, 35.0, 30.0, 28.97, 28.9, 27.6, 27.5; FT-IR (neat) ν_{max} 3290, 2952, 1690, 1531, 1448, 1260, 1215, 1085, 1045 cm^{-1}; HRMS (ESI-TOF) *m*/*z* $[M + H]^+$ calcd for $C_{41}H_{41}N_2O_9$ 705.2806, found 705.2819.

(2*S*,4*E*,8*S*)-Δ^4-2,8-(di-*N*-(Boc)amino)azelic acid (5.17)

A 0 °C solution of dimethyl (2*S*,4*E*,8*S*)-Δ^4-2,8-(di-*N*-(Boc)amino)azelate (**1.66**, 500 mg, 1.12 mmol) in 1,4-dioxane (5 mL) was treated with a 1N solution of LiOH (94.4 mg, 2.25 mmol, 2 equiv.). The cooling bath was removed. The reaction mixture was warmed to room temperature with stirring for 3 h, at which time TLC indicated the consumption of the starting material. The volatiles were evaporated under reduced pressure. The residue was partitioned between H_2O (10 mL) and EtOAc (5 mL). The aqueous phase was acidified with 1N HCl to pH 3 and extracted with ethyl acetate (3 × 10 mL). The organic extractions were combined, dried with Na_2SO_4, filtered, and concentrated under vacuum to afford diacid **5.17** (430 mg, 92%) as a white solid: mp 71–73 °C; $[\alpha]_D^{25}$ +39.0 (*c* 0.82, $CHCl_3$); ^1H NMR (500 MHz, DMSO-d_6): δ 12.42 (s, 2H), 7.08–7.07 (d, *J* = 5.0 Hz, 1H), 6.97–6.96 (d, *J* = 5 Hz, 1H), 5.50–5.44 (m, 1H), 5.40–5.35 (m, 1H), 3.90–3.84 (m, 2H), 2.37–2.32 (m, 1H), 2.29–2.23 (m, 1H), 1.71–1.50 (m, 4H), 1.39 (s, 9H), 1.38 (s, 9H); $^{13}C\{^{1}H\}$ NMR (125 MHz, DMSO-D6) δ 175.0, 174.0, 156.03, 155.88, 132.2, 127.0, 78.47, 78.41, 60.2, 54.1, 53.3, 34.5, 31.1, 28.68, 28.66; FT-IR (neat) ν_{max} 3697, 2980, 1694, 1507, 1393, 1367, 1245, 1157, 1053, 1033, 1018 cm^{-1}; HRMS (ESI-TOF) m/z $[M + Na]^+$ calcd for $C_{19}H_{32}N_2O_8Na$ 439.2050, found 439.2070.

(1′*R*,5*S*)-3-*N*-(Boc)amino-5-[1′-iodo-4′-*N*-(Boc)amino-4′-methoxcarbonylbutyl]-tetrahydrofuran-2-one [(1′*R*,5*S*)-5.14]

A 0 °C mixture of carboxylic acid (1′*R*,5*S*)-**5.17** (2.1 g, 3.87 mmol) and K_2CO_3 (800 mg, 5.8 mmol, 1.5 equiv.) in DMF (20 mL) was treated with methyl iodide (820 mg, 5.8 mmol, 1.5 equiv.). The ice bath was removed. After stirring for 2-3 h, the room temperature mixture exhibited a nonpolar spot (2:3 EtOAc/hexanes) by TLC and indicated a new peak at RT = 9.0 min (C18 column, 10:90 CH_3CN:H_2O) by LCMS analysis, with a molecular ion of $[M + Na]^+$ m/z 579. The reaction mixture was diluted with water and extracted with ethyl acetate (4 × 50 mL). The ethyl acetate layer was washed with water (4 × 50 mL) and brine (2 × 30 mL), dried over Na_2SO_4, filtered, and concentrated under reduced pressure. The residue was purified by flash column chromatography using 20-30% EtOAc in hexanes as the eluent. Evaporation of the collected fractions gave tetrahydrofuran-2-one (1′*R*,5*S*)-**5.14** (1.1g, 55% from diacid 5.16) as a colorless solid: mp 58-60 °C; R_f = 0.56 (2:3 EtOAc/hexanes, visualized by $KMnO_4$), $[\alpha]_D^{25}$ +13.4 (*c* 0.68, $CHCl_3$); ^{1}H NMR (500 MHz, $CDCl_3$): δ 5.10-5.08 (d, *J* = 10Hz, 2H), 4.45-4.41 (m, 1H), 4.37-4.33 (m, 2H), 4.08-4.04 (t, *J* = 10 Hz, 1H), 3.79 (s, 3H), 3.14-3.09 (m, 1H), 2.23-2.17 (m, 1H), 2.11-2.05 (m, 1H), 1.95-1.87 (m, 2H), 1.78-1.73 (m, 1H), 1.48 (s, 9H), 1,47 (s, 9H); $^{13}C\{^1H\}$ NMR (125 MHz, $CDCl_3$) δ 174.0, 173.0, 155.3, 130.0, 81.0, 80.2, 79.2, 53.0, 52.5, 52.0, 38.0, 36.0, 32.3, 32.0, 28.31, 28.27; FT-IR (neat) ν_{max} 3281, 2921, 2853, 1801, 1747, 1697, 1674, 1537, 1451, 1368, 1294, 1252, 1213, 1154, 1060, 1029, 1005 cm^{-1}; HRMS (ESI-TOF) m/z $[M + Na]^+$ calcd for $C_{20}H_{33}IN_2O_8Na$ 579.1173, found 579.1195.

(1′*R*,5*S*)-3-*N*-(Boc)amino-5-[1′-iodo-4′-*N*-(Boc)amino-4′-hydroxcarbonylbutyl]-tetrahydrofuran-2-one [(1′*R*,5*S*)-5.18]

A solution of diacid **5.17** (1.6 g, 3.8 mmol) in acetonitrile (20 mL) was treated with Cs_2CO_3 (3.7 g, 11.5 mmol, 3 equiv.), stirred for 15 min, cooled to 0°C with an ice bath, and treated with iodine (2.93 g, 11.5 mmol, 3 equiv.). The ice bath was removed. After stirring for 3–4 h, the

reaction mixture had warmed to room temperature and was observed by LCMS to contain a new peak at RT = 8.1 min (C18 column, 10:90 CH_3CN:H_2O) with a molecular ion $[M + Na]^+$ *m*/*z* 565. The reaction mixture was filtered through a pad of Celite™ and the filter cake was washed with acetonitrile (3 × 30 mL). The filtrate and washings were combined and evaporated under reduced pressure. The residue was partitioned between H_2O (50 mL) and EtOAc (25 mL). The aqueous phase was acidified with 1N HCl to pH 3 and extracted with ethyl acetate (3 × 50 mL). The organic extractions were combined, dried with Na_2SO_4, filtered, and concentrated under vacuum to afford tetrahydrofuran-2-one (1′*R*,5*S*)-**5.18** (2.1 g) as a pale-yellow solid, which was used without further purification.

5.6. Conclusions

The copper catalyzed S_N2' addition of zincate derived from methyl β-iodoalaninate onto (*E*)-1,3-dichloroprop-1-ene has given useful entry into a set of protected Δ^4-2,8-diaminoazelates (e.g., **1.66-1.68**). Attempts to fold the latter linear precursors into bicyclic 5- and 7-substituted indolizidin-2-one amino acid (I^2aa) derivatives have, however, demonstrated the challenges of achieving diastereomeric and regioisomeric selectivity in the facial differentiation of the olefin. Epoxidation and dihydroxylation were unselective and gave oxiranes **5.10** and hydroxylactone **5.15** as inseparable mixtures of diastereomers, which were shown by LCMS analyses to be convertible into mixtures of up to four hydroxy indolizidine-2-one isomers due in part to the inability to control the intramolecular cyclization of the respective nitrogen. Moreover, diastereomeric stereochemical integrity may have also been lost due to cyclization by way of planar S_N1 intermediates.

Iodolactonization of Δ^4-2,8-diaminoazelic diacid **5.17** occurred with high facial selectivity to provide tetrahydrofuran-2-one (1′*R*,5*S*)-**5.14** as a single isomer. Both nitrogen of iodide **5.14**

reacted in intramolecular S_N2 displacements to respectively provide hydroxyproline and proline intermediates. Lactam formation provided 5- and 7-hydroxy indolizidin-2-one amino esters (3*S*,5*S*,6*S*,9*S*)-**5.8** and (3*S*,6*S*,7*S*,9*S*)-**5.9** in six steps and 21% and 17% respective overall yields from Δ^4-2,8-diaminoazelate **1.66**. Saponification of the esters (3*S*,5*S*,6*S*,9*S*)-**5.8** and (3*S*,6*S*,7*S*,9*S*)-**5.9** delivered the corresponding carboxylic acids, which are suitable for peptide synthesis.

The configuration of 5- and 7-hydroxy indolizidin-2-one amino esters (3*S*,5*S*,6*S*,9*S*)-**5.8** and (3*S*,6*S*,7*S*,9*S*)-**5.9** was assigned using a series of NMR experiments. Furthermore, X-ray analysis of ester (3*S*,6*S*,7*S*,9*S*)-**5.3** demonstrated that the backbone geometry within the 7-hydroxy indolizidine-2-one framework replicated that of the parent I^2aa ester (6*S*)-**4.14** and mimicked the dihedral angles of the central dipeptide in a type II' β-turn. The utility of 5- and 7-hydroxy indolizidin-2-one amino acids (3*S*,5*S*,6*S*,9*S*)-**5.2** and (3*S*,6*S*,7*S*,9*S*)-**5.3** is currently being investigated inside biologically relevant peptides and will be reported in due time.

5.7. Acknowledgement

The Natural Sciences and Engineering Research Council of Canada (NSERC) for Discovery Research Project (No. 04079), the Canadian Institutes of Health Research (CIHR), and the NSERC-CIHR for the Collaborative Health Research Project ″Treatment of Preterm Birth with ProstaglandinF2alpha Receptor Modulators″ No. 337381.

5.8. References

1. Hanessian, S.; McNaughton-Smith, G.; Lombart, H.G.; Lubell, W.D. Design and synthesis of conformationally constrained amino acids as versatile scaffolds and peptide mimetics. *Tetrahedron* **1997**, *53*, 12789–12854, doi:10.1016/S0040-4020(97)00476-6.

2. Sanchez, C.A.; Gadais, C.; Chaume, G.; Girard, S.; Chelain, E,; Brigaud, T. Enantiopure 5-CF3–Proline: Synthesis, Incorporation in Peptides, and Tuning of the Peptide Bond Geometry. *Org. Lett.* **2021**, *23*, 382–387, doi:10.1021/acs.orglett.0c03880.
3. Beausoleil, E.; Lubell, W.D. Steric Effects on the Amide Isomer Equilibrium of Prolyl Peptides. Synthesis and Conformational Analysis of *N*-Acetyl-5-tert-butylproline *N*′-Methylamides. *J. Am. Chem. Soc.* **1996**, *118*, 12902–12908, doi:10.1021/ja962013b.
4. Bowles, M.; Proulx, C. Solid phase submonomer azapeptide synthesis. In Synthetic and Enzymatic Modifications of the Peptide Backbone; Chapter 6; James Petersson, E., Ed.; Methods in Enzymology; Elsevier Inc.: Amsterdam, The Netherlands **2021**; Volume 656, pp. 169–190, doi:10.1016/bs.mie.2021.04.020.
5. Hamdane, Y.; Chauhan, P.S.; Vutla, S.; Mulumba, M.; Ong, H.; Lubell, W.D. 5-Substituted *N*-Aminoimidazolone Peptide Mimic Synthesis by Organocatalyzed Reactions of Azopeptides and Use in the Analysis of Biologically Active Backbone and Side-Chain Topology. *Org. Lett.* **2021**, *23*, 3491–3495, doi:10.1021/acs.orglett.1c00936.
6. Freidinger, R.M.; Veber, D.F.; Perlow, D.S.; Brooks, J.R.; Saperstein, R. Bioactive conformation of luteinizing hormone-releasing hormone: Evidence from a conformationally constrained analog. *Science* **1980**, *210*, 656–658, doi:10.1126/science.7001627.
7. St-Cyr, D.J.; García-Ramos, Y.; Doan, N.D.; Lubell, W.D. Aminolactam, *N*-Aminoimidazolone, and *N*-Aminoimdazolidinone Peptide Mimics. In *Peptidomimetics I. Topics in Heterocyclic Chemistry*; Lubell, W.D., Ed.; Springer: Cham, Switzerland, **2017**, vol 48., pp 125–175, doi:10.1007/7081_2017_204.

8. Cluzeau, J.; Lubell, W.D. Design, synthesis, and application of azabicyclo [X.Y.0] alkanone amino acids as constrained dipeptide surrogates and peptide mimics. *Pept. Sci.* **2005**, *80*, 98–150, doi:10.1002/bip.20213.
9. Khashper, A.; Lubell, W.D. Design, synthesis, conformational analysis and application of indolizidin-2-one dipeptide mimics. *Org. Biomol. Chem.* **2014**, *12*, 5052–5070, doi:10.1039/c4ob00777h.
10. Polyak, F.; Lubell, W.D. Rigid dipeptide mimics: Synthesis of enantiopure 5-and 7-benzyl and 5, 7-dibenzyl Indolizidinone amino acids via enolization and alkylation of δ-Oxo α, ω-Di-[N-(9-(9-phenylfluorenyl))amino] azelate esters. *J. Org. Chem.* **1998**, *63*, 5937–5949, doi:10.1021/jo980596x.
11. Polyak, F.; Lubell, W.D. Mimicry of peptide backbone geometry and heteroatomic side-chain functionality: Synthesis of enantiopure indolizidin-2-one amino acids possessing alcohol, acid, and azide functional groups. *J. Org. Chem.* **2001**, *66*, 1171–1180, doi:10.1021/jo001251t.
12. Feng, Z.; Lubell, W.D. Synthesis of Enantiopure 7-[3-Azidopropyl]indolizidin-2-one Amino Acid. A Constrained Mimic of the Peptide Backbone Geometry and Heteroatomic Side-Chain Functionality of the Ala-Lys Dipeptide *J. Org. Chem.* **2001**, *66*, 1181–1185, doi:10.1021/jo001252l.
13. Wessig, P. An efficient synthesis of bicyclic β-turn dipeptides via a photochemical key step. *Tetrahedron Lett.* **1999**, *40*, 5987–5988, doi:10.1016/S0040-4039(99)01249-6.
14. Sun, H.; Moeller, K.D. Silyl-substituted amino acids: New routes to the construction of selectively functionalized peptidomimetics. *Org. Lett.* **2002**, *4*, 1547–1550, doi:10.1021/ol025776e.

15. Atmuri, N.P.; Lubell, W.D. Stereo-and Regiochemical Transannular Cyclization of a Common Hexahydro-1H-azonine to Afford Three Different Indolizidinone Dipeptide Mimetics. *J. Org. Chem.* **2019**, *85*, 1340–1351, doi:10.1021/acs.joc.9b01861.
16. Mir, F.M.; Atmuri, N.P.; Bourguet, C.B.; Fores, J.R.; Hou, X.; Chemtob, S.; Lubell, W.D. Paired utility of aza-amino acyl proline and indolizidinone amino ac-id residues for peptide mimicry: Conception of prostaglandin F2α receptor allosteric modulators that delay preterm birth. *J. Med. Chem.* **2019**, *62*, 4500–4525, doi:10.1021/acs.jmedchem.9b00056.
17. Artale, E.; Banfi, G.; Belvisi, L.; Colombo, L.; Colombo, M.; Manzoni, L.; Scolastico, C. Synthesis of substituted conformationally constrained 6, 5-and 7, 5-fused bicyclic lactams as dipeptide mimics. *Tetrahedron* **2003**, *59*, 6241–6250, doi:10.1016/S0040-4020(03)01018-4.
18. Manzoni, L.; Belvisi, L.; Arosio, D.; Civera, M.; Pilkington-Miksa, M.; Potenza, D.; Caprini, A.; Araldi, E.M.; Monferini, E.; Mancino, M. Cyclic RGD-containing functionalized azabicycloalkane peptides as potent integrin antagonists for tumor targeting. *ChemMedChem* **2009**, *4*, 615–632, doi:10.1002/cmdc.200800422.
19. Hanessian, S.; McNaughton-Smith, G. A versatile synthesis of a β-turn peptidomimetic scaffold: An approach towards a designed model antagonist of the tachykinin NK-2 receptor. *Bioorg. Med. Chem. Lett.* **1996**, *6*, 1567–1572, doi:10.1016/S0960-894X(96)00275-2.
20. Hanessian, S.; Therrien, E.; Granberg, K.; Nilsson, I. Targeting thrombin and factor VIIa: Design, synthesis, and inhibitory activity of functionally relevant indolizidinones. *Bioorg. Med. Chem. Lett.* **2002**, *12*, 2907–2911, doi:10.1016/s0960-894x(02)00612-1.
21. Hanessian, S.; Sailes, H.; Munro, A.; Therrien, E. Synthesis of Diversely Functionalized Indolizidinones and Related Bicyclic Lactams Using Intramolecular Grubbs Olefin

Metathesis and Dieckmann Condensation. *J. Org. Chem.* **2003**, *68*, 7219–7233, doi:10.1021/jo030145z.

22. Hanessian, S.; Margarita, R. l,3-Asymmetric Induction in Dianionic Allylation Reactions of Amino Acid Derivatives-Synthesis of Functionally Useful Enantiopure Glutamates, Pipecolates and Pyroglutamates. *Tetrahedron Lett.* **1998**, *39*, 5887–5890, doi:10.1016/S0040-4039(98)00900-9.
23. Dunn, M.J.; Jackson, R.F.; Pietruszka, J.; Turner, D. Synthesis of Enantiomerically Pure Unsaturated. alpha.-Amino Acids Using Serine-Derived Zinc/Copper Reagents. *J. Org. Chem.* **1995**, *60*, 2210–2215, doi:10.1021/jo00112a048.
24. Bartlett, P.A.; Myerson, J. Stereoselective epoxidation of acyclic olefinic carboxylic acids via iodolactonization. *J. Am. Chem. Soc.* **1978**, *100*, 3950–3952, doi:10.1021/ja00480a061.
25. Trost, B.M.; Rudd, M.T. Chemoselectivity of the ruthenium-catalyzed hydrative diyne cyclization: Total synthesis of (+)-cylindricine C., D, and E. *Org. Lett.* **2003**, *5*, 4599–4602, doi:10.1021/ol035752n.
26. Hattori, Y.; Asano, T.; Kirihata, M.; Yamaguchi, Y.; Wakamiya, T. Development of the first and practical method for enantioselective synthesis of 10B-enriched p-borono-L-phenylalanine. *Tetrahedron Lett.* **2008**, *49*, 4977–4980, doi:10.1016/j.tetlet.2008.05.108.
27. Ozturk, S.; Forneris, C.C.; Nguy, A.K.; Sorensen, E.J.; Seyedsayamdost, M.R. Modulating OxyB-catalyzed cross-coupling reactions in vancomycin biosynthesis by incorporation of diverse D-Tyr analogues. *J. Org. Chem.* **2018**, *83*, 7309–7317, doi:10.1021/acs.joc.8b00916.
28. Krishnamurthy, S.; Arai, T.; Nakanishi, K.; Nishino, N. Epoxy amino acids produced from allylglycines intramolecularly cyclised to yield four stereoisomers of 4-hydroxyproline derivatives *RSC Adv.* **2014**, *4*, 2482–2490, doi:10.1039/C3RA45184D.

29. Krishnamurthy, S., Venkataprasad, J., Vagvala, T.C., Moriguchi, T., Tsuge, A. α-Chymotrypsin and l-acylase aided synthesis of 5-hydroxypipecolic acid via Jacobsen's hydrolytic kinetic resolution of epoxy amino acids *RSC Adv.* **2015**, *5*, 52154–52160, doi:10.1039/C5RA09207H.
30. Hoarau, S.; Fauchere, J.L.; Pappalardo, L.; Roumestant, M.L.; Viallefont, P. Synthesis of enantiomerically pure (2*R*, 5*S*)- and (2*R*, 5*R*)-5-hydroxypipecolic acid from glycinate Schiff bases. *Tetrahedron Asymmetry* **1996**, *7*, 2585–2593, doi:10.1016/0957-4166(96)00332-1.
31. Mulamreddy, R.; Hou, X.; Chemtob, S.; Lubell, W.D. 6-Hydroxymethyl Indolizidin-2-one Amino Acid Synthesis, Conformational Analysis, and Biomedical Application as Dipeptide Surrogates in Prostaglandin-F2α Modulators *Org. Lett.* **2021**, *23*, 5192–5196 doi:10.1021/acs.orglett.1c01733.
32. Gilmore, K.; Mohamed, R.K.; Alabugin, I.V. The Baldwin rules: Revisedand extended WIREs Comput. *Mol. Sci.* **2016**, *6*, 487–514 doi:10.1002/wcms.1261.
33. Vilotijevic, I.; Jamison, T.F. Synthesis of marine polycy-clic polyethers via endo-selective epoxide-opening cas-cades. *Mar. Drugs* **2010**, *8*, 763–809, doi:10.3390/md8030763.
34. Wang, J.; Liang, Y.-L.; Qu, J. Boiling water-catalyzed neutral and selective N-Boc deprotection. *Chem. Commun.* **2009**, *2009*, 5144–5146, doi:10.1039/B910239F.
35. Atmuri, A.N.D.; Surprenant, S.; Diarra, S.; Bourguet, C.; Lubell, W.D. *"Ring closing metathesis / transannular cyclization to azabicyclo[X.Y.0]alknanone dipeptide turn mimics for biomedical applications" N. Qvit. Peptide and Peptidomimetic Therapeutics: From Bench to Bedside*; Academic Press: Cambridge, MA, USA, **2022**, ISBN: 012820141X, accepted.

36. Marcotullio, M.C.; Campagna, V.; Sternativo, S.; Costantino, F.; Curini, M. A New, Simple Synthesis of N-Tosyl Pyrrolidines and Piperidines. *Synthesis* **2006**, *2006*, 2760, doi:10.1055/s-2006-942488.

37. Davies, S.G.; Nicholson, R.L.; Price, P.D.; Roberts, P.M.; Russell, A.J.; Savory, E.D.; Smith, A.D.; Thomson, J.E. Iodine-mediated ring-closing iodoamination with concomitant N-debenzylation for the asymmetric synthesis of polyhydroxylated pyrrolidines. *Tetrahedron Asymmetry* **2009**, *20*, 758–772, doi:10.1016/j.tetasy.2009.02.014.

38. Liu, G.-Q.; Li, Y.-M. Regioselective (diacetoxyiodo)benzene-promoted halocyclization of unfunctionalized olefins. *J. Org. Chem.* **2014**, *79*, 10094–10109, doi:10.1021/jo501739j.

39. Reddy Vakiti, J.; Hanessian, S. Total Synthesis and Stereochemical Confirmation of (−)-Olivil, (+)-Cycloolivil, (−)-Alashinols F and G, (+)-Cephafortin A, and Their Congeners: Filling in Biosynthetic Gaps. *Org. Lett.* **2020**, *22*, 3345–3350, doi:10.1021/acs.orglett.0c00773.

40. Nolsøe, J.M.; Hansen, T.V. Asymmetric iodolactonization: An evolutionary account. *Eur. J. Org. Chem.* **2014**, *2014*, 3051–3065, doi:10.1002/ejoc.201301400.

41. Kurth, M.J.; Brown, E.G. Double diastereoselection in the iodolactonization of 1,6-heptadiene-4-carboxylic acids *J. Am. Chem. Soc.* **1987**, *109*, 6844−6845, doi:10.1021/ja00256a045.

42. Mauger, A.; Irreverre, F.; Witkop, B. The stereochemistry of 3-methylproline. *J. Am. Chem. Soc.* **1966**, *88*, 2019–2024, doi:10.1021/ja00961a031.

43. Ashtekar, K.D.; Vetticatt, M.; Yousefi, R.; Jackson, J.E.; Borhan, B. Nucleophile-Assisted Alkene Activation: Olefins Alone Are Often Incompetent. *J. Am. Chem. Soc.* **2016**, *138*, 8114–9, doi:10.1021/jacs.6b02877.

44. Ball, J.B.; Alewood, P.F. Conformational constraints: Nonpeptide β-turn mimics. *J. Mol. Recognit.* **1990**, *3*, 55−64, doi:10.1002/jmr.300030202.

45. Lombart, H.-G.; Lubell, W.D. Rigid dipeptide mimetics: Efficient synthesis of enantiopure indolizidinone amino acids. *J. Org. Chem.* **1996**, *61*, 9437−9446, doi:10.1021/jo961872f.

Chapter 6: Perspectives and Conclusions

6.1 Perspectives

The copper catalyzed S_N2' reaction has served to provide three useful olefins for the synthesis of heterocyclic amino acid and dipeptide mimics. Alternative methods for olefin synthesis may enlarge the gateway to peptide mimic ring systems. For example, nickel catalyzed additions of zincates onto allylic halides proceed regioselectively by way of an S_N2 reaction.[1,2] Employing nickel catalysis in the reaction of the zincate of β-iodoalaninate **1.62** with 1,4-dihalobut-2-enes may provide the corresponding Δ^5-2,9-diaminosebacic acid derivatives **6.1**. Further, sebacic acid derivative **6.1** may undergoe an olefin oxidation with mCPBA to provide a symmetric epoxide **6.2**. Oxirane ring opening using Lewis acid catalysis may give isomeric hydroxyproline **6.3** and hydroxypipecolate **6.4** derivatives, which by way of lactam formation would offer a hydroxypyrroloazepinone and hydroxyquinolizidinone amino acid derivatives **6.5** and **6.6** (Figure 6.1).

Pyrroloazepinone and quinolizidinone amino acids have been less well studied in peptides compared to the indolizidin-2-one amino acid counterparts. However, the 7,5- and 6,6-fused bicycles have been employed in successful SAR studies of biologically active peptides to enhance potency and selectivity.[3] For example, pyrroloazepinone mimics of the second mitochondria-derived activators of caspases (Smac) peptide are apoptosis inhibitors.[4] Pyrroloazepinones have also been employed in the development of ACE inhibitors for the treatment of cardiovascular diseases.[5] Few quinolizidinone amino acid analogs have been synthesized; however, the parent system has been used to prepare an anatagonist of opioid receptor-like receptor (ORL1R).[6] Considering that the nickel catalyzed S_N2 reaction could give access to olefins for the synthesis of substituted 7,5- and 6,6-fused bicycles, a new set of tools may be created for examination of the backbone conformation and side geometry of biologically active peptides.

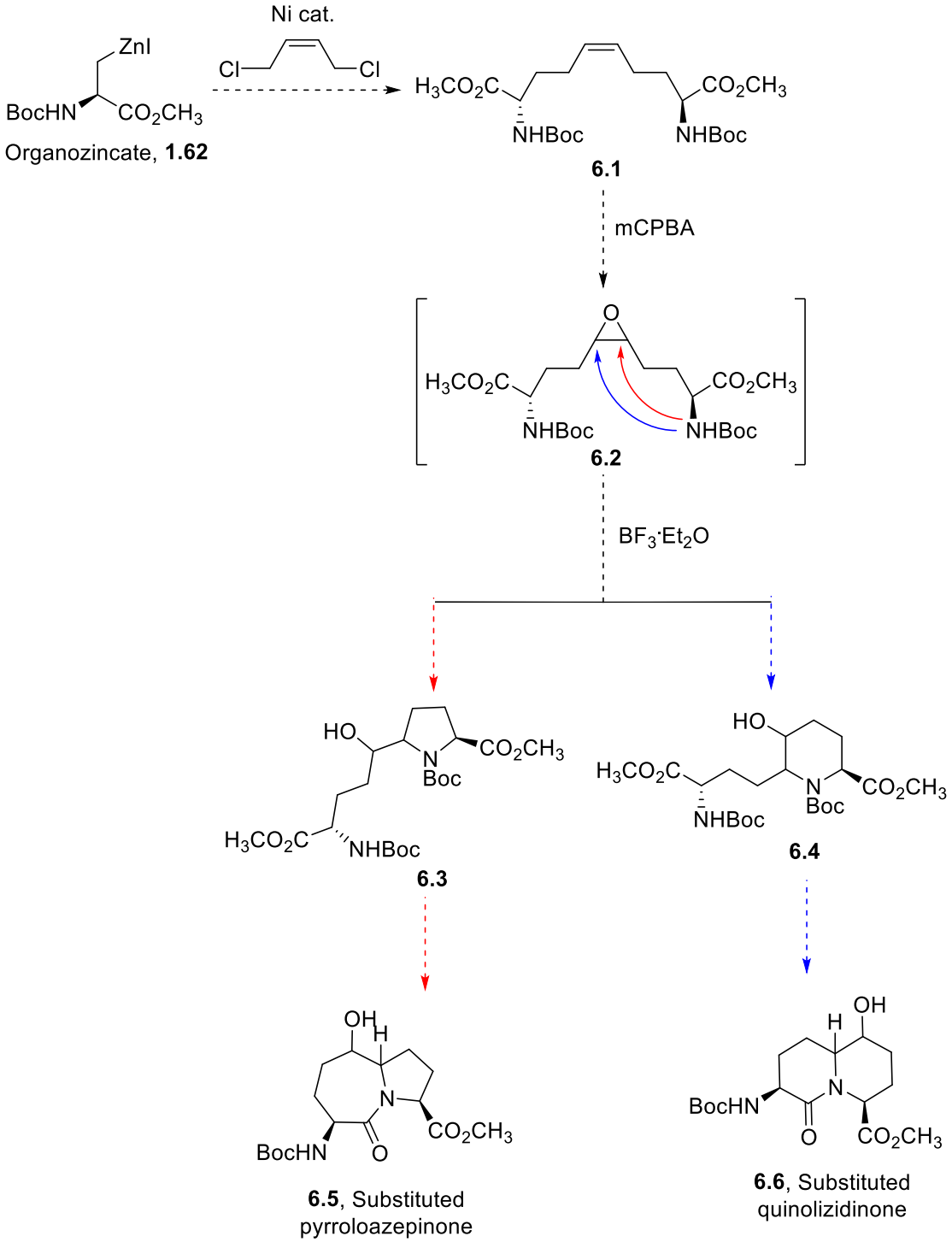

Figure 6.1. Potential synthesis of pyrroloazepinone and quinolizidinone amino acid derivatives

6.2 Conclusions

An olefin entry has been developed for the synthesis of different peptide mimic ring systems. Employing serine **1.60** as inexpensive chiral educt, unsaturated amino acid precursors (**1.63-1.66**), were prepared by copper catalyzed S_N2' reactions on the corresponding zincate derived from β-iodoalanine **1.61**. Novel enantiomerically pure 4-substituted prolines (**2.2**), γ-substituted α-amino-δ-lactams (**3.10**) and 5-, 6- and 7-substituted indolizidine-2-one amino acids (**4.020**, **5.8**, and **5.9**), all were synthesized using approaches to modify the three different unsaturated amnio acid precursors (Figure 6.1). 4-Vinylproline **2.2** and γ-vinyl α-amino-δ-lactams **3.10** were respectively synthesized from 4-halomethyl-2-aminohex-5-enoates **1.63** by routes featuring intra- and intermolecular halide displacements (Chapters 2 and 3).[7,8] The vinyl group offers potential for conversion into various functional groups to mimic side chains, as demonstrated by oxidation and coupling chemistry to provide constrained glutamate and glutamine mimics.

Double S_N2' reactions on allylic dihalides provided respectively 5-methylenyl 2,8-di-*N*-(Boc)aminoazelate **1.65** and (4*E*)-2,8-bis[*N*-(Boc)amino]azelate **1.66**, which upon oxidative cyclization approaches gave respectively 6-hydroxymethyl **4.020** and 5- and 7-hydroxy indolizidine-2-one amino acids (**5.8** and **5.9**, Chapters 4 and 5).[9,10] X-ray crystallographic studies indicated that the substituent and configuration of the I^2aa ring systems altered the embedded peptide backbone dihedral angles, which adopted a range of conformers that mimicked with subtle differences the central residues of an ideal type II' β-turn conformation.

The utility of the substituted I^2aa building blocks was next examined in a biomedical application. Analogs of the prostaglandin-F_{2a} receptor modulator PDC-113.824 were studied

towards the development of tocolytic agents for the treatment of preterm birth.[11] The presence of the alcohol side chains and the configuration of the substituted I^{2}aa units influenced activity on myometrium contractions. 6-Hydroxymethyl I^{2}aa (6S,9S)-**4.020** retained some inhibitory activity on myometrial contractions; however, the (6*R*)-counterpart **4.016** was inactive. As discussed in the chapters 4 and 5, the backbone geometry and side chain conformation of the substituted I^{2}aa both may influence receptor affinity and biological activity.

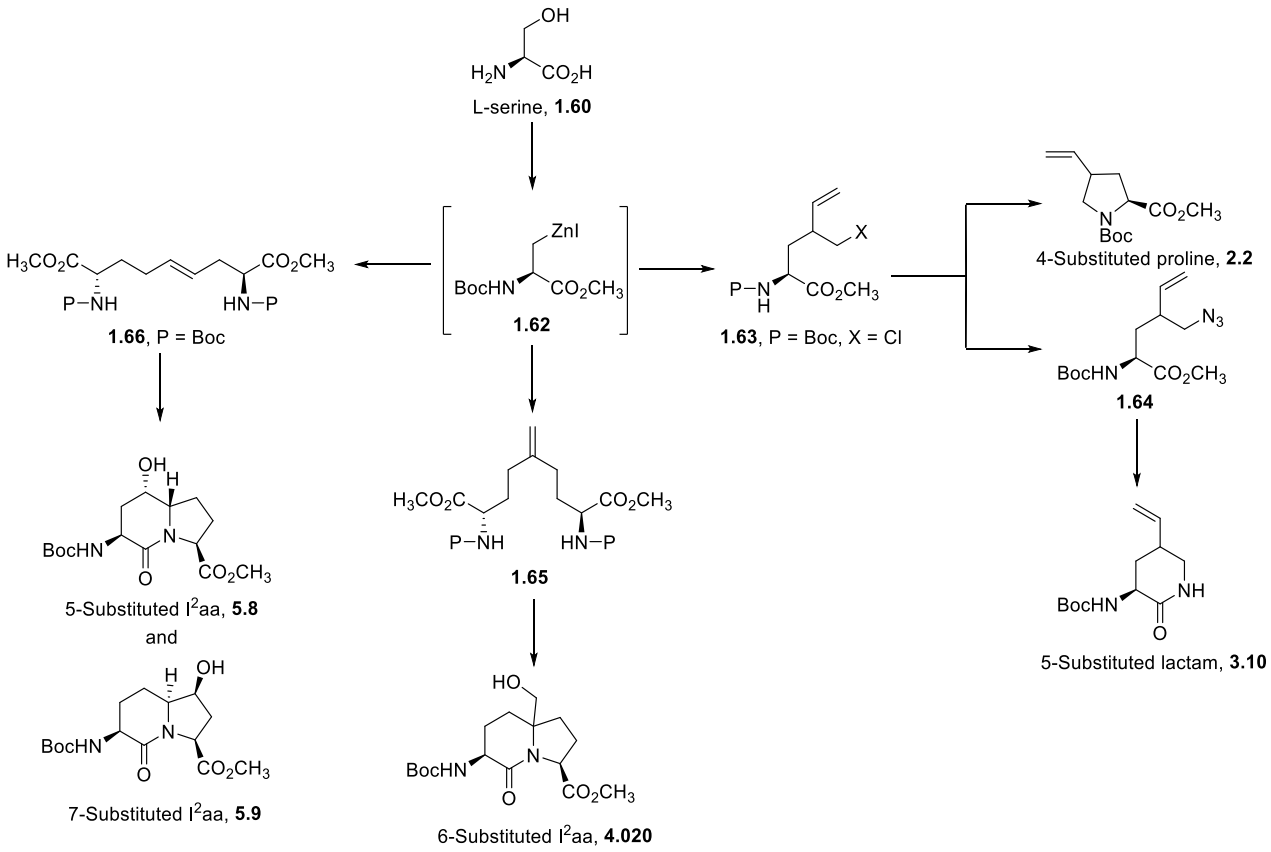

Figure 6.2. Syntheses of different ring systems from unsaturated amino acids

Enantiomerically pure unsaturated amino acid derivatives have served as useful building blocks for the syntheses of various substituted ring systems. The ring systems could serve as secondary structure initiators such as turn motifs in peptidomimetics. Moreover, the olefin ring substituents can function as a handle for introducing side chain diversity, which may enhance

molecular recognition by interactions with the receptor surface. Considering that related ring systems have exhibited imporatnt utility in medicinal chemistry, the described olefin gateways may lead to various applications for exploring the peptide world.

6.3 References

1. Sekiya, K.; Nakamura, E. Copper-and nickel-catalysis in SN2′-and SN2-regioselective allylation of organozinc reagents. *Tetrahedron Lett.* **1988**, *29*, 5155-5156.

2. Son, S.; Fu, G. C. Nickel-catalyzed asymmetric Negishi cross-couplings of secondary allylic chlorides with alkylzincs. *J. Am. Chem. Soc.* **2008**, *130*, 2756-2757.

3. Gosselin, F.; Lubell, W. D. Rigid dipeptide surrogates: Syntheses of enantiopure quinolizidinone and pyrroloazepinone amino acids from a common diaminodicarboxylate precursor. *J. Org. Chem.* **2000**, *65*, 2163-2171.

4. Zhang, B.; Nikolovska-Coleska, Z.; Zhang, Y.; Bai, L.; Qiu, S.; Yang, C.-Y.; Sun, H.; Wang, S.; Wu, Y. Design, synthesis, and evaluation of tricyclic, conformationally constrained small-molecule mimetics of second mitochondria-derived activator of caspases. *J. Med. Chem.* **2008**, *51*, 7352-7355.

5. Robl, J. A.; Cimarusti, M. P.; Simpkins, L. M.; Brown, B.; Ryono, D. E.; Bird, J. E.; Asaad, M. M.; Schaeffer, T. R.; Trippodo, N. C. Dual metalloprotease inhibitors. 6. Incorporation of bicyclic and substituted monocyclic azepinones as dipeptide surrogates in angiotensin-converting enzyme/neutral endopeptidase inhibitors. *J. Med. Chem.* **1996**, *39*, 494-502.

6. Van Cauwenberghe, S.; Simonin, F.; Cluzeau, J.; Becker, J. A.; Lubell, W. D.; Tourwé, D. Structure− Activity Study of the ORL1 Antagonist Ac-Arg-d-Cha-Qaa-d-Arg-d-p-ClPhe-NH2. *J. Med. Chem.* **2004**, *47*, 1864-1867.

7. Mulamreddy, R.; Atmuri, N. P.; Lubell, W. D. 4-Vinylproline. *J. Org. Chem.* **2018**, *83*, 13580-13586.

8. Mulamreddy, R.; Lubell, W. D. Constrained Glu-Gly and Gln-Gly dipeptide surrogates from γ-substituted α-amino-δ-lactam synthesis. *Peptide Sci.* **2020**, *112*, e24149.

9. Mulamreddy, R.; Hou, X.; Chemtob, S.; Lubell, W. D. 6-Hydroxymethyl Indolizidin-2-one Amino Acid Synthesis, Conformational Analysis, and Biomedical Application as Dipeptide Surrogates in Prostaglandin-F2α Modulators. *Org. Lett.* **2021**, *23*, 5192-5196.

10. Mulamreddy, R.; Lubell, W. D. Constrained Dipeptide Surrogates: 5-and 7-Hydroxy Indolizidin-2-one Amino Acid Synthesis from Iodolactonization of Dehydro-2,8-diamino Azelates. *Molecules* **2022**, *27*, 67.

11. Mir, F. M.; Atmuri, N. P.; Bourguet, C. B.; Fores, J. R.; Hou, X.; Chemtob, S.; Lubell, W. D. Paired utility of aza-amino acyl proline and indolizidinone amino acid residues for peptide mimicry: Conception of prostaglandin F2α receptor allosteric modulators that delay preterm birth. *J. Med. Chem.* **2019**, *62*, 4500-4525.

Appendix

Spectral data for Article 1

^{1}H NMR 700 MHz
Solvent: $CDCl_3$

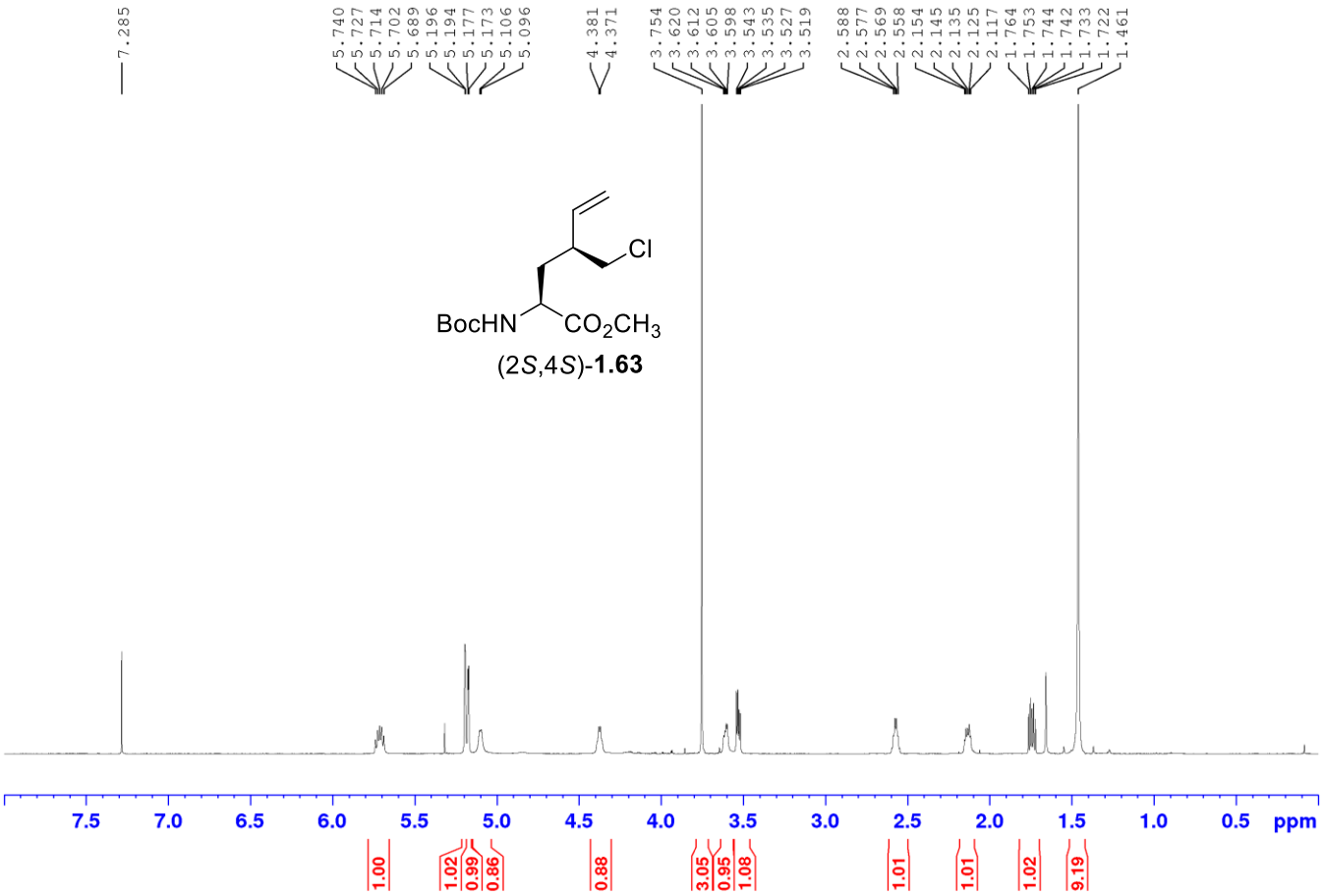

^{13}C NMR 175 MHz
Solvent: $CDCl_3$

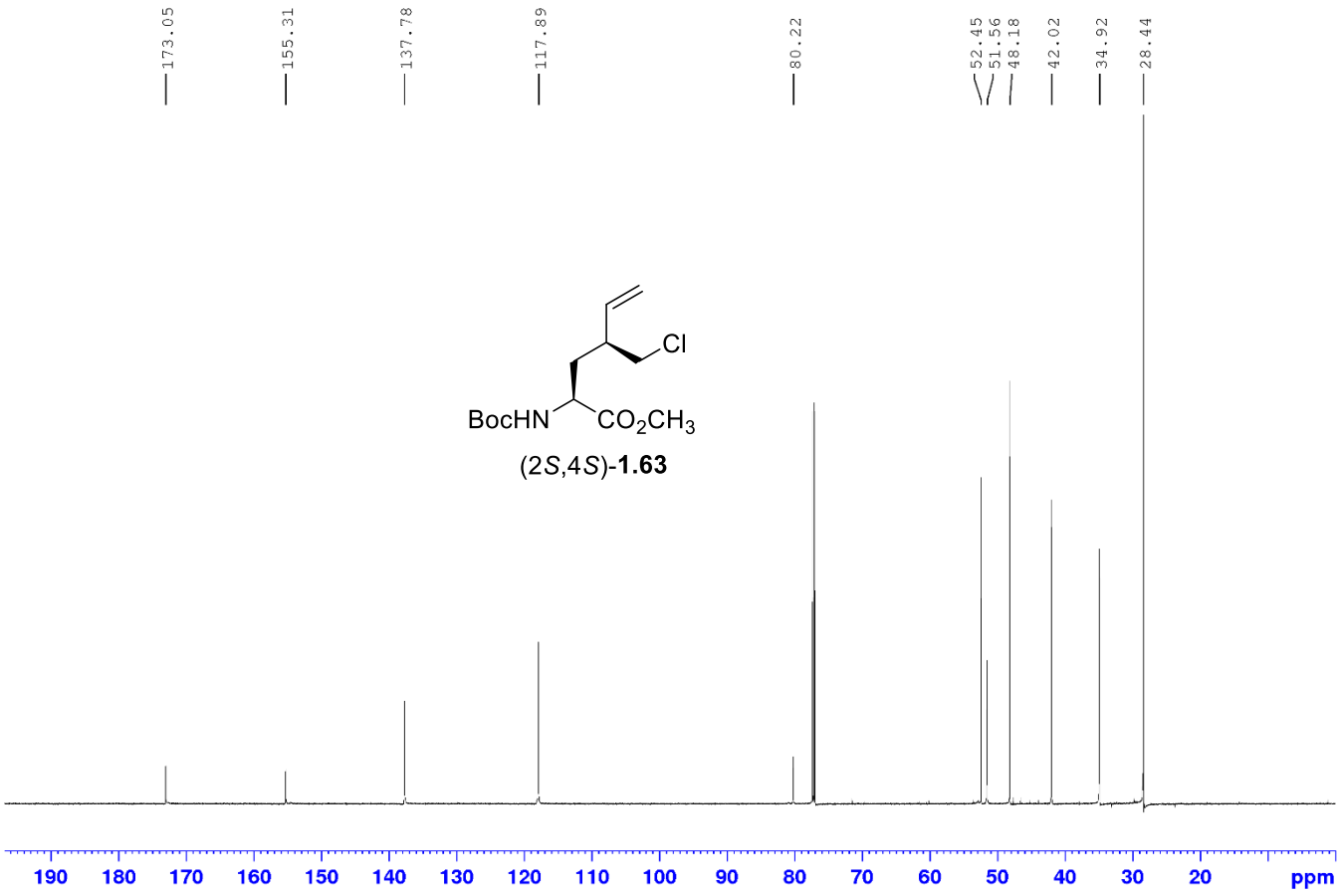

COSY 700 MHz
Solvent: $CDCl_3$

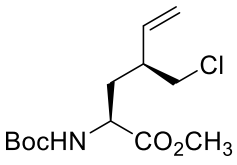

(2*S*,4*S*)-**1.63**

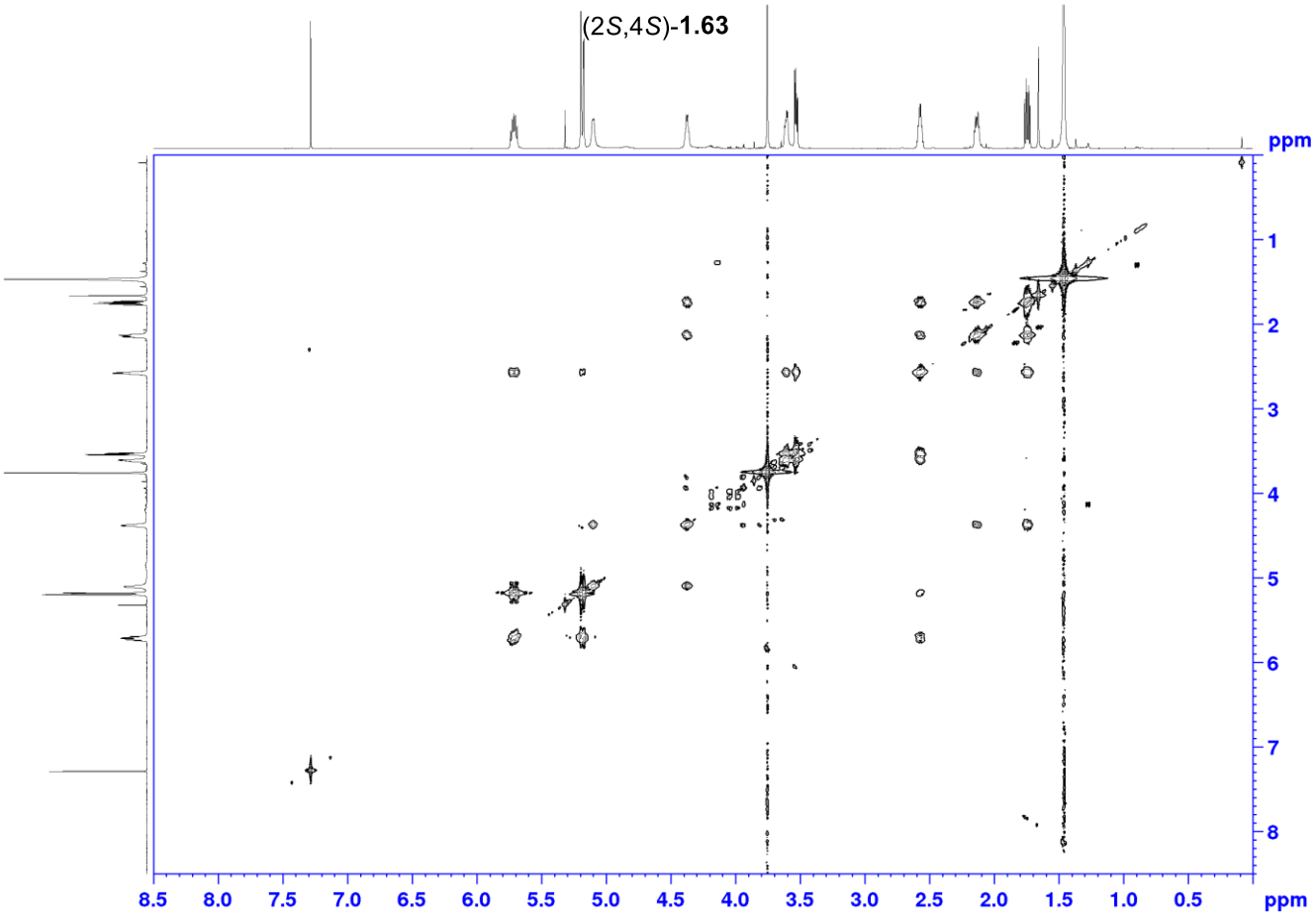

HSQC 700 MHz
Solvent: $CDCl_3$

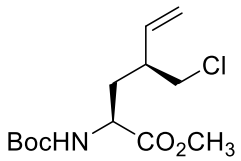

(2*S*,4*S*)-**1.63**

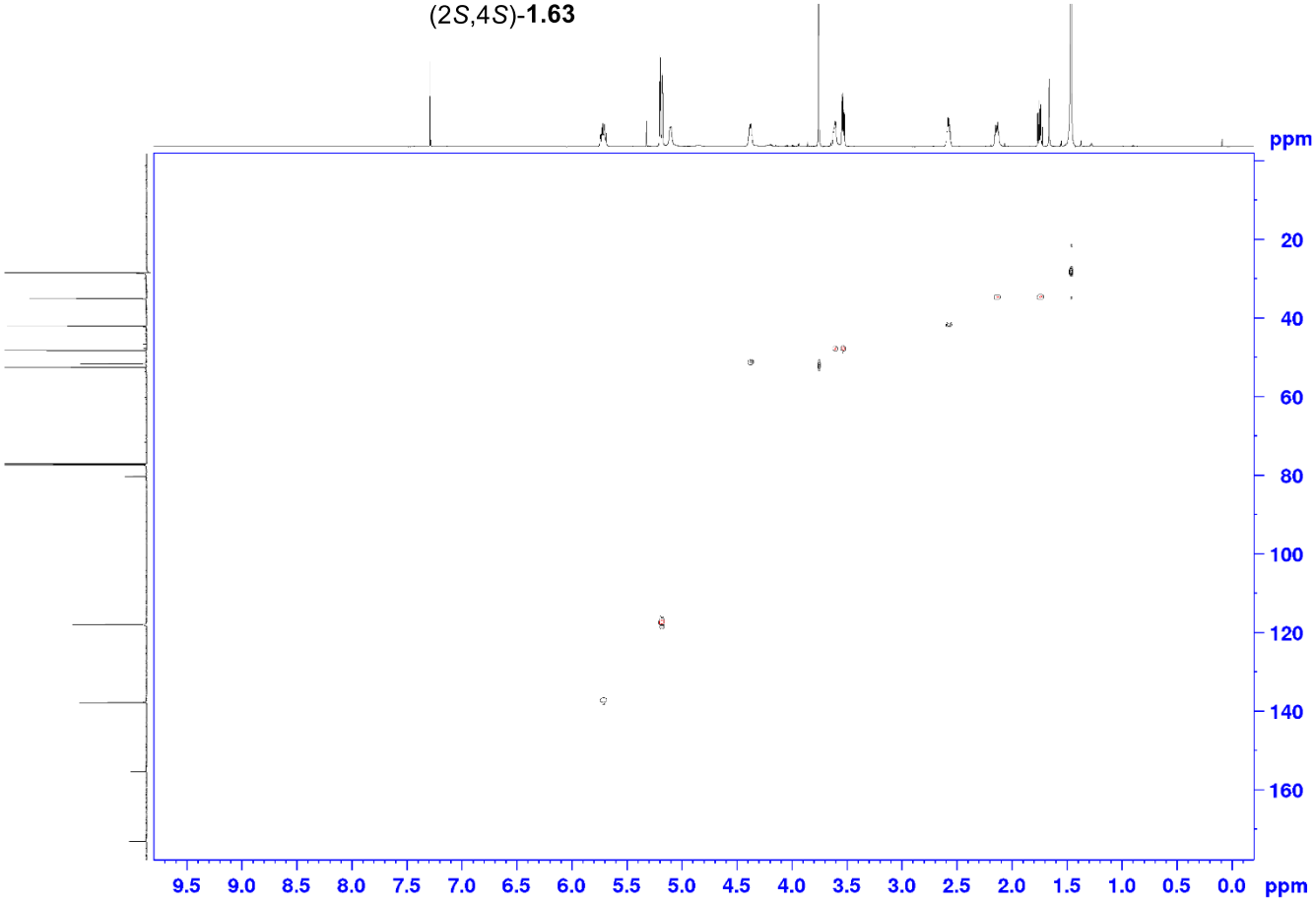

^{1}H NMR 700 MHz
Solvent: $CDCl_3$

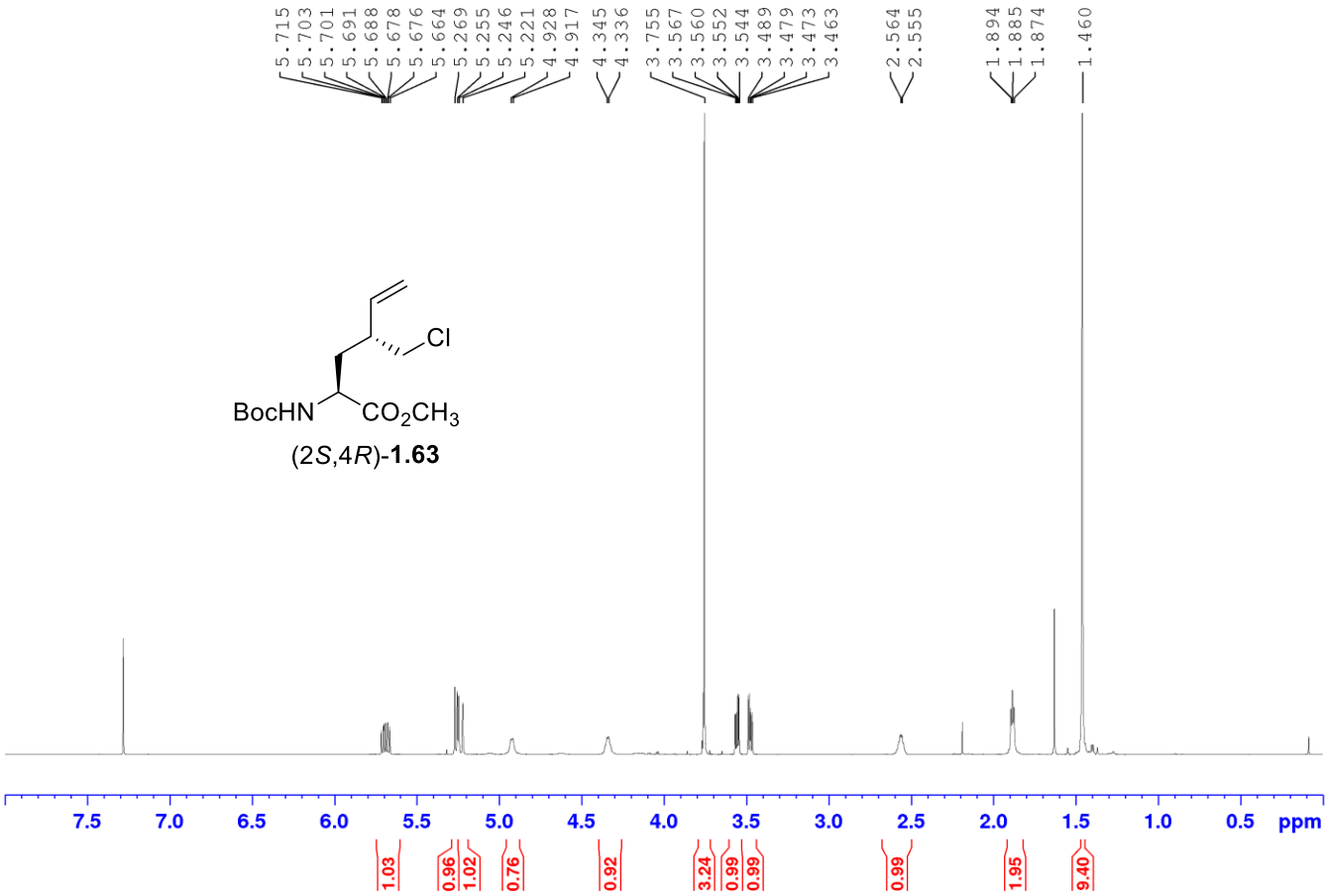

^{13}C NMR 175 MHz
Solvent: $CDCl_3$

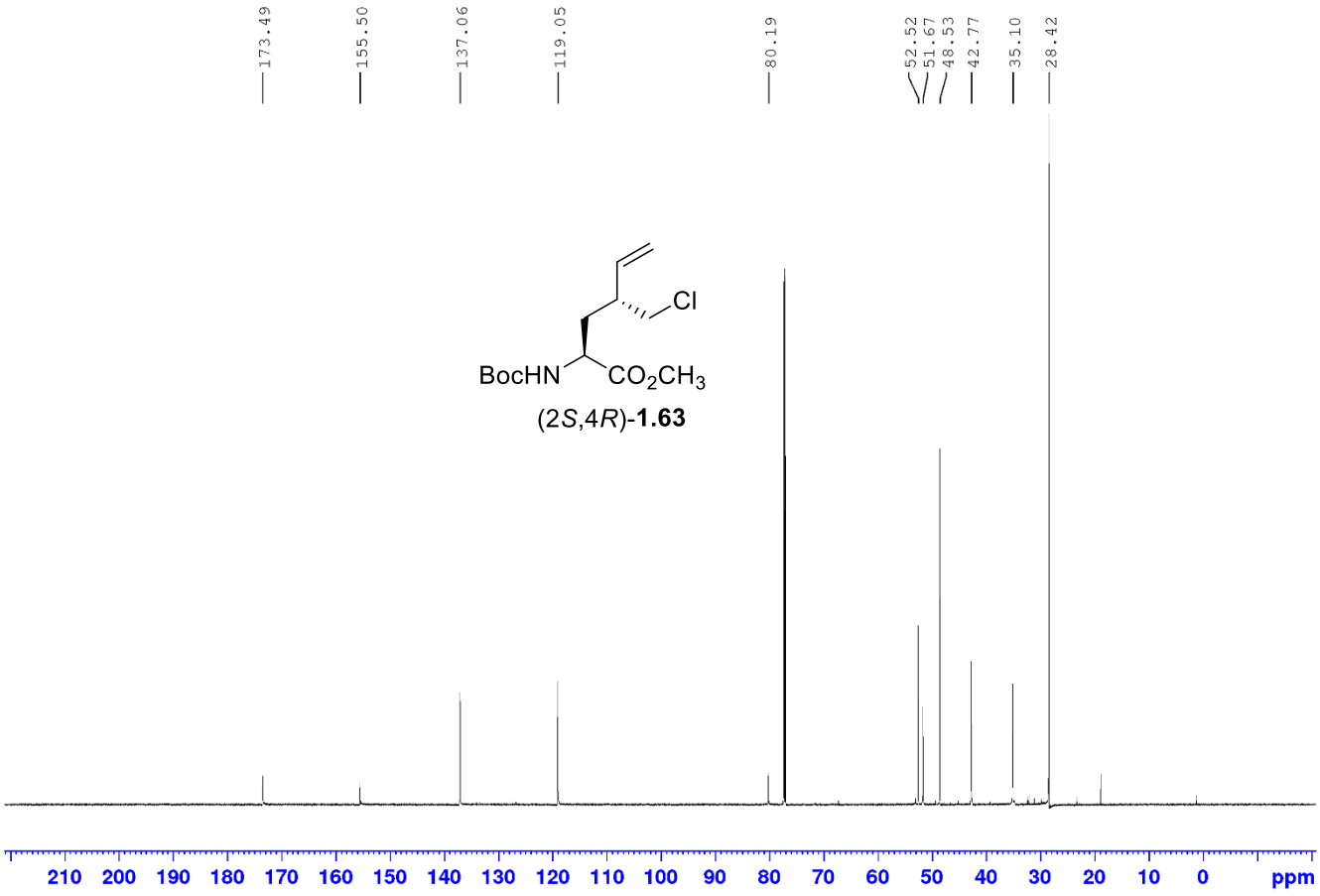

COSY NMR 700 MHz
Solvent: $CDCl_3$

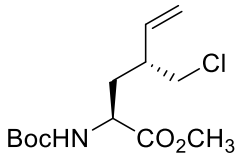

(2*S*,4*R*)-**1.63**

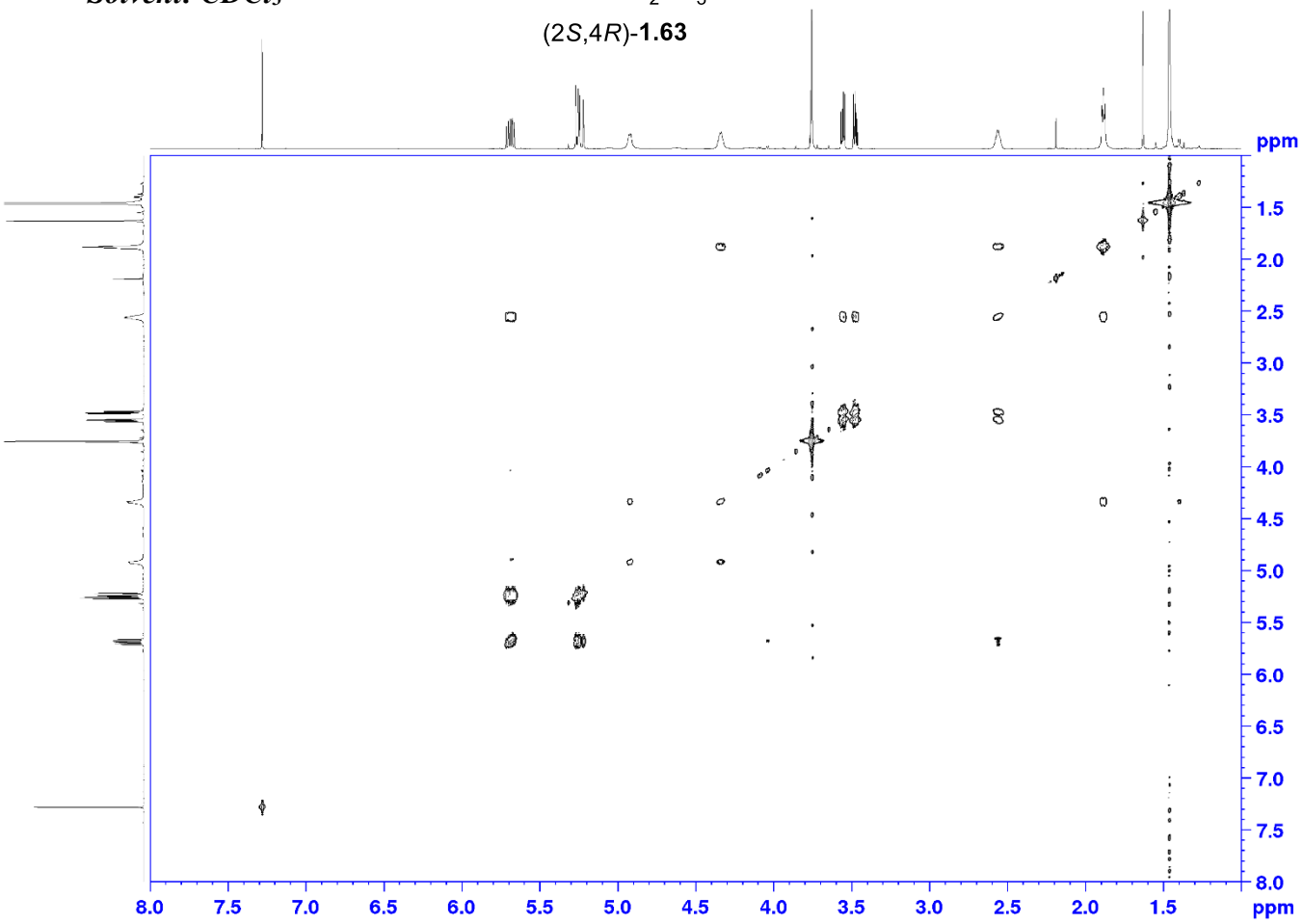

HSQC NMR 700 MHz
Solvent: $CDCl_3$

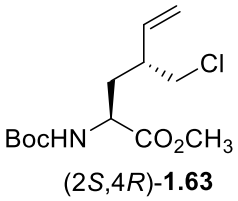

(2*S*,4*R*)-**1.63**

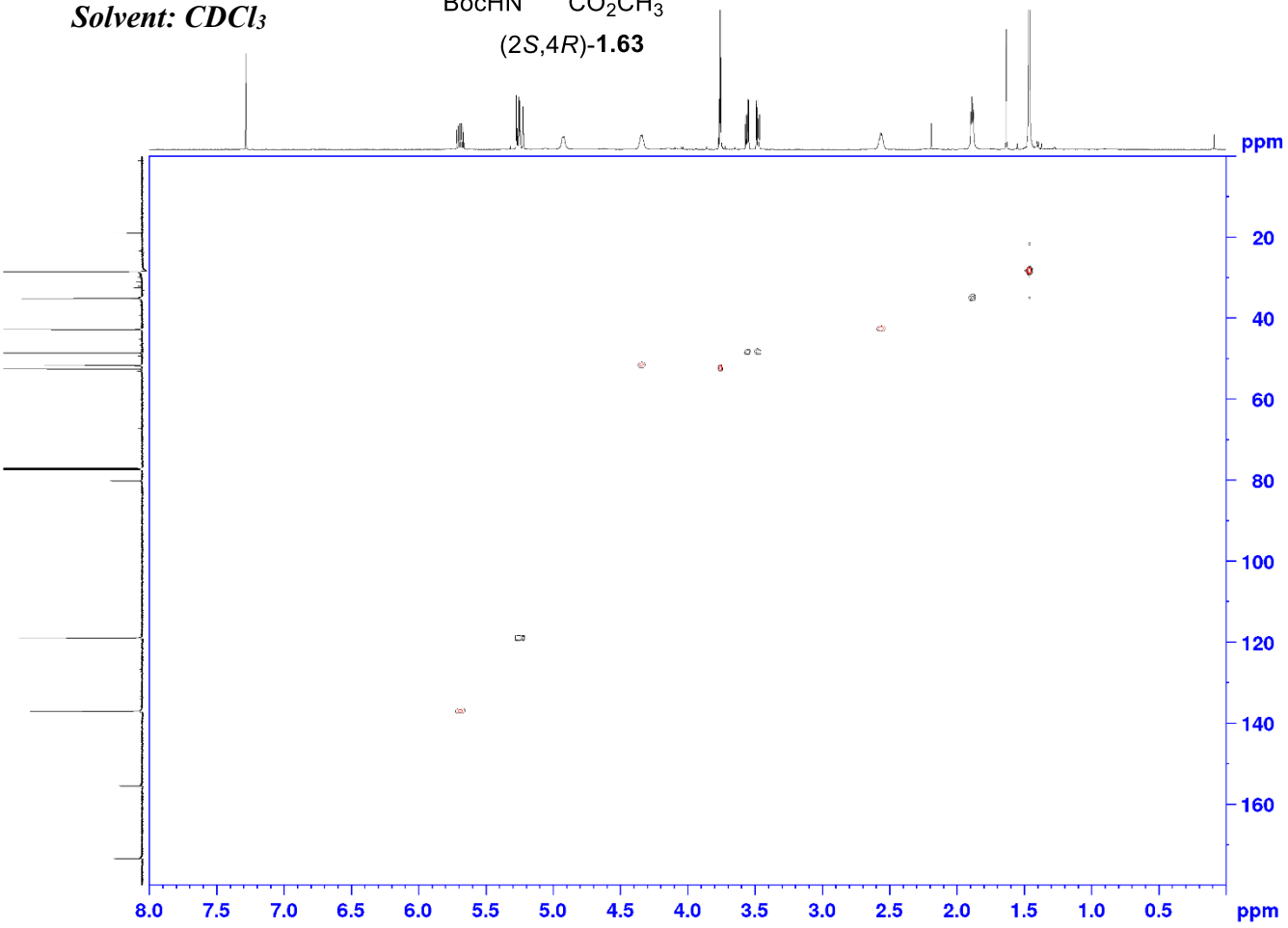

^{1}H NMR 700 MHz
Solvent: $CDCl_3$

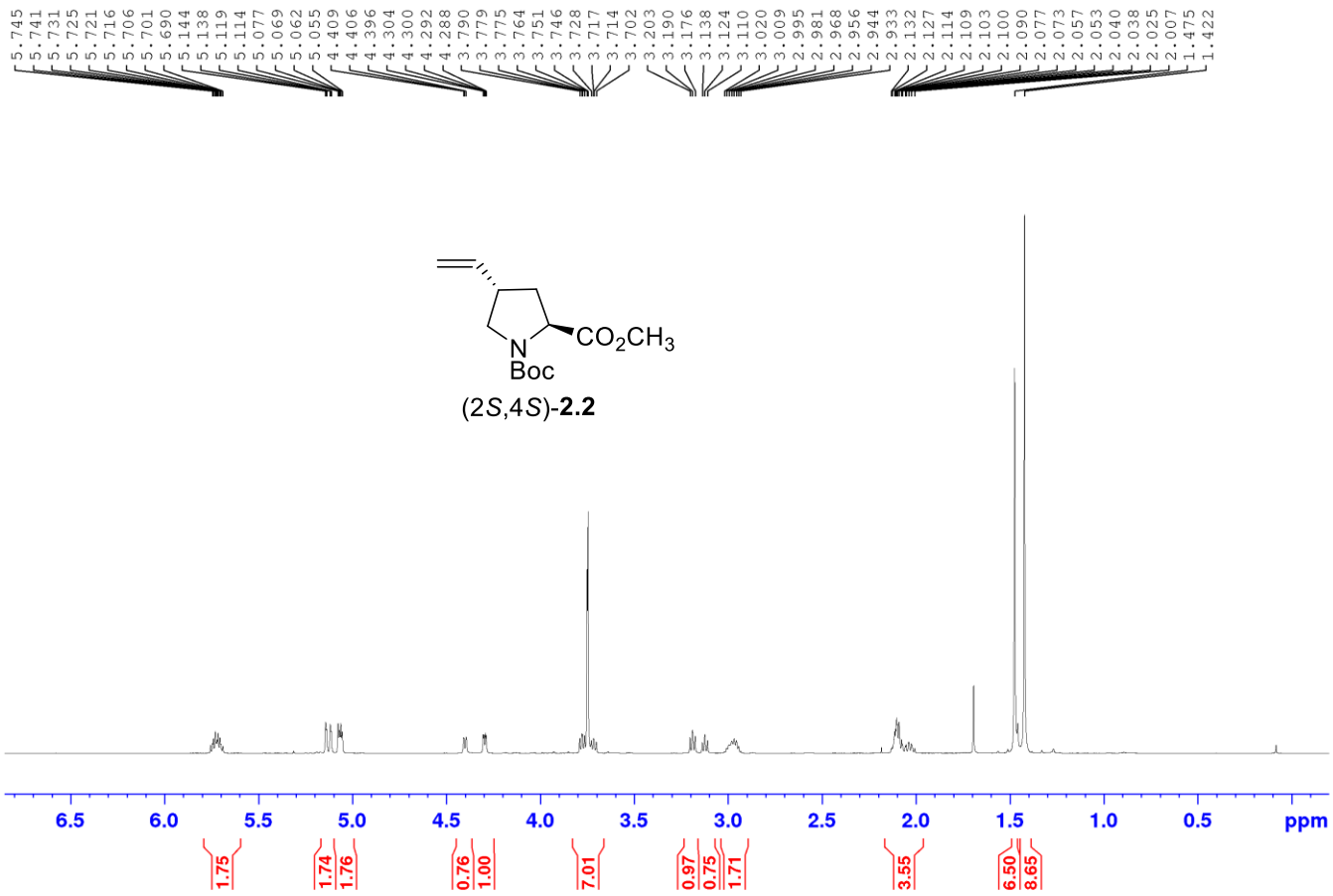

^{13}C NMR 175 MHz
Solvent: $CDCl_3$

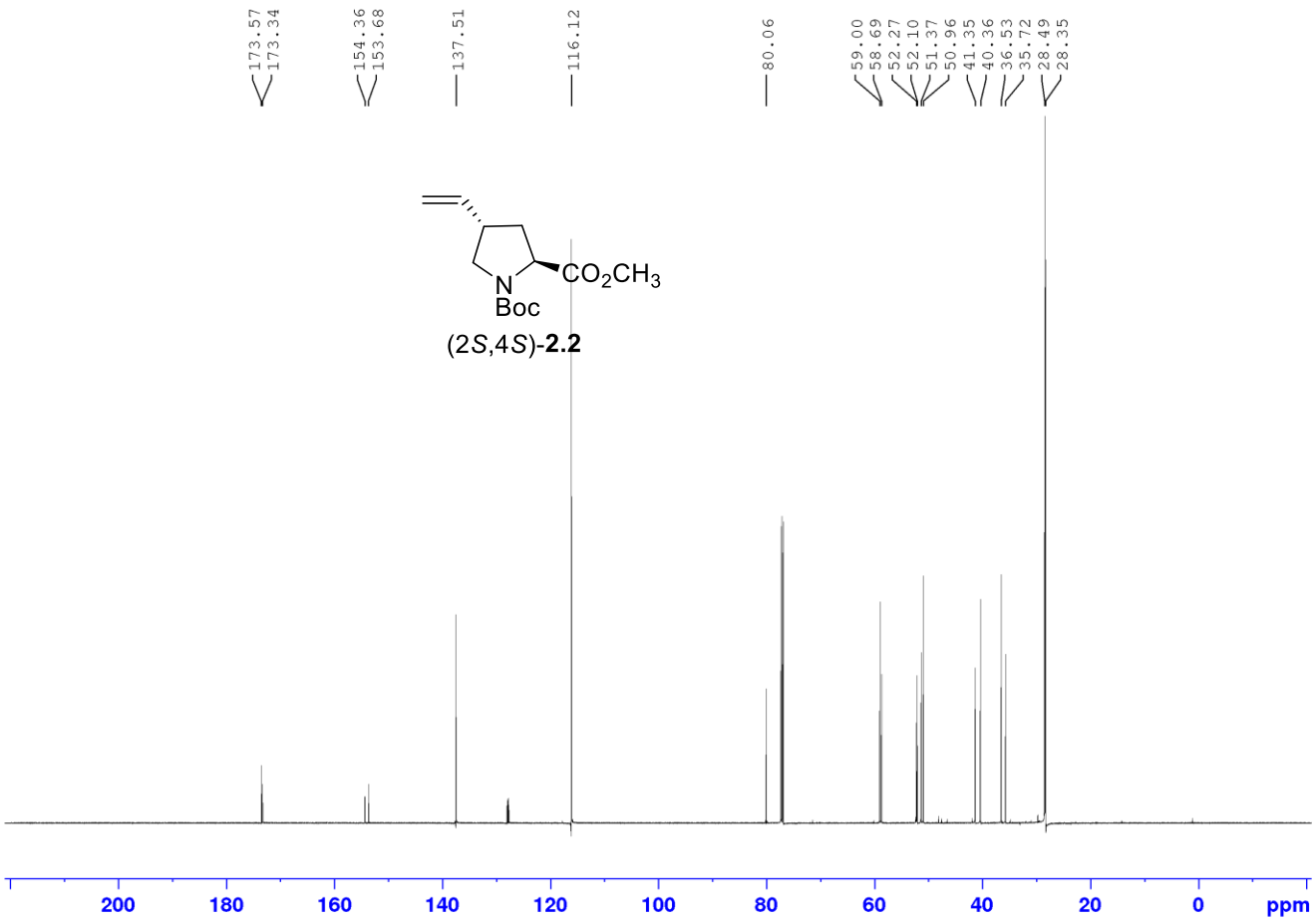

^{1}H NMR 500 MHz
Solvent: $CDCl_3$

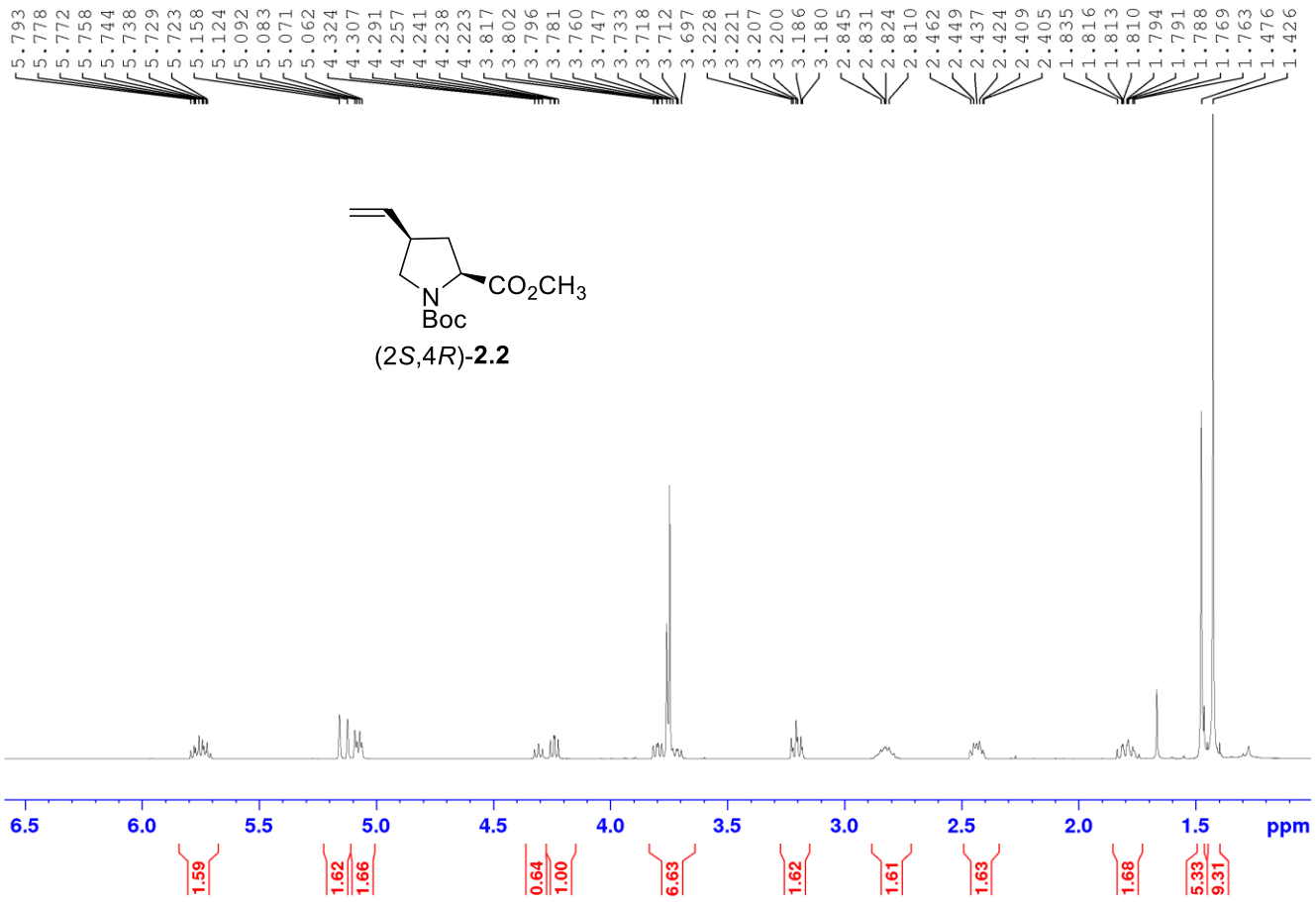

(2*S*,4*R*)-**2.2**

^{13}C NMR 125 MHz
Solvent: $CDCl_3$

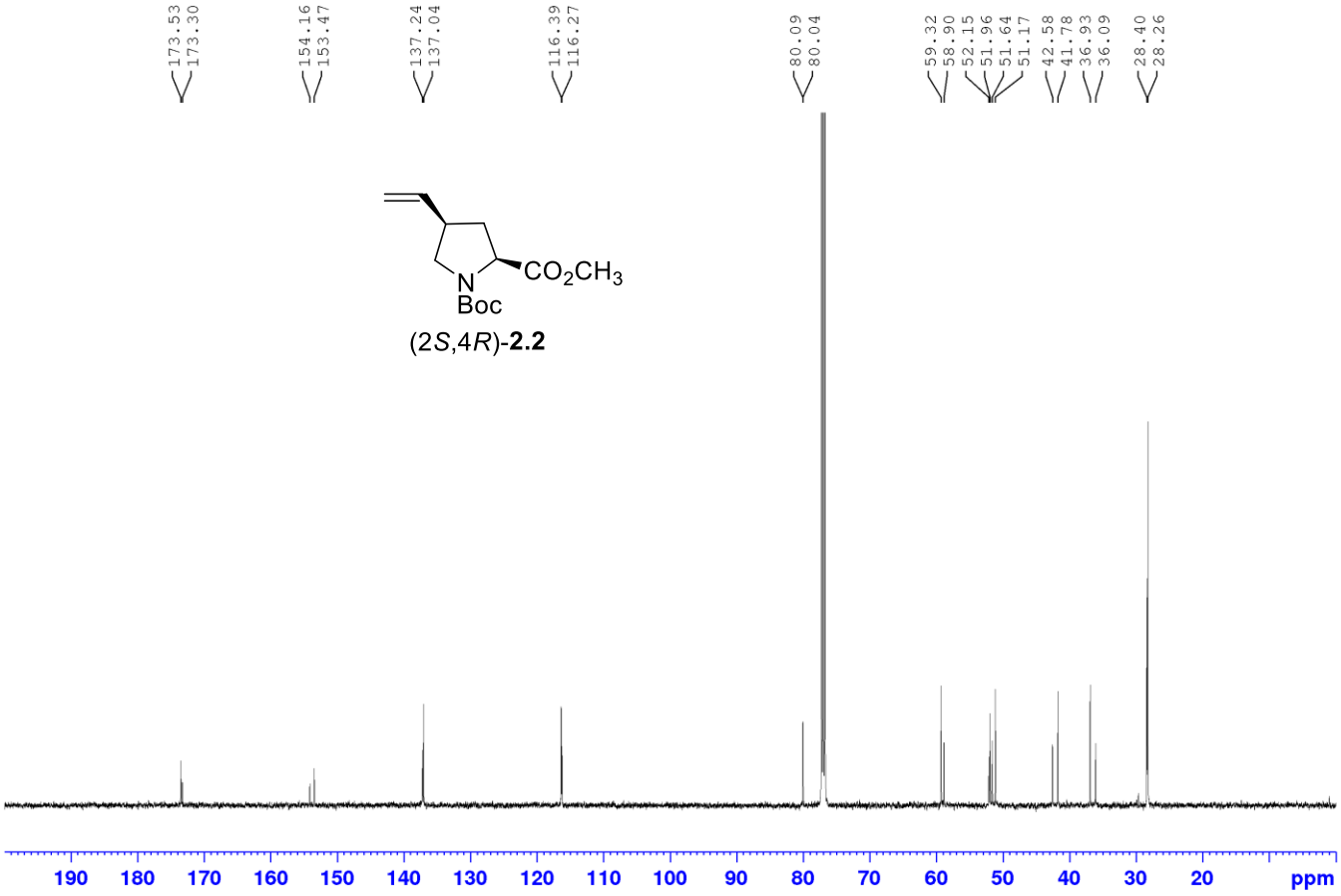

(2*S*,4*R*)-**2.2**

^{1}H NMR 400 MHz
Solvent: CD_3OD

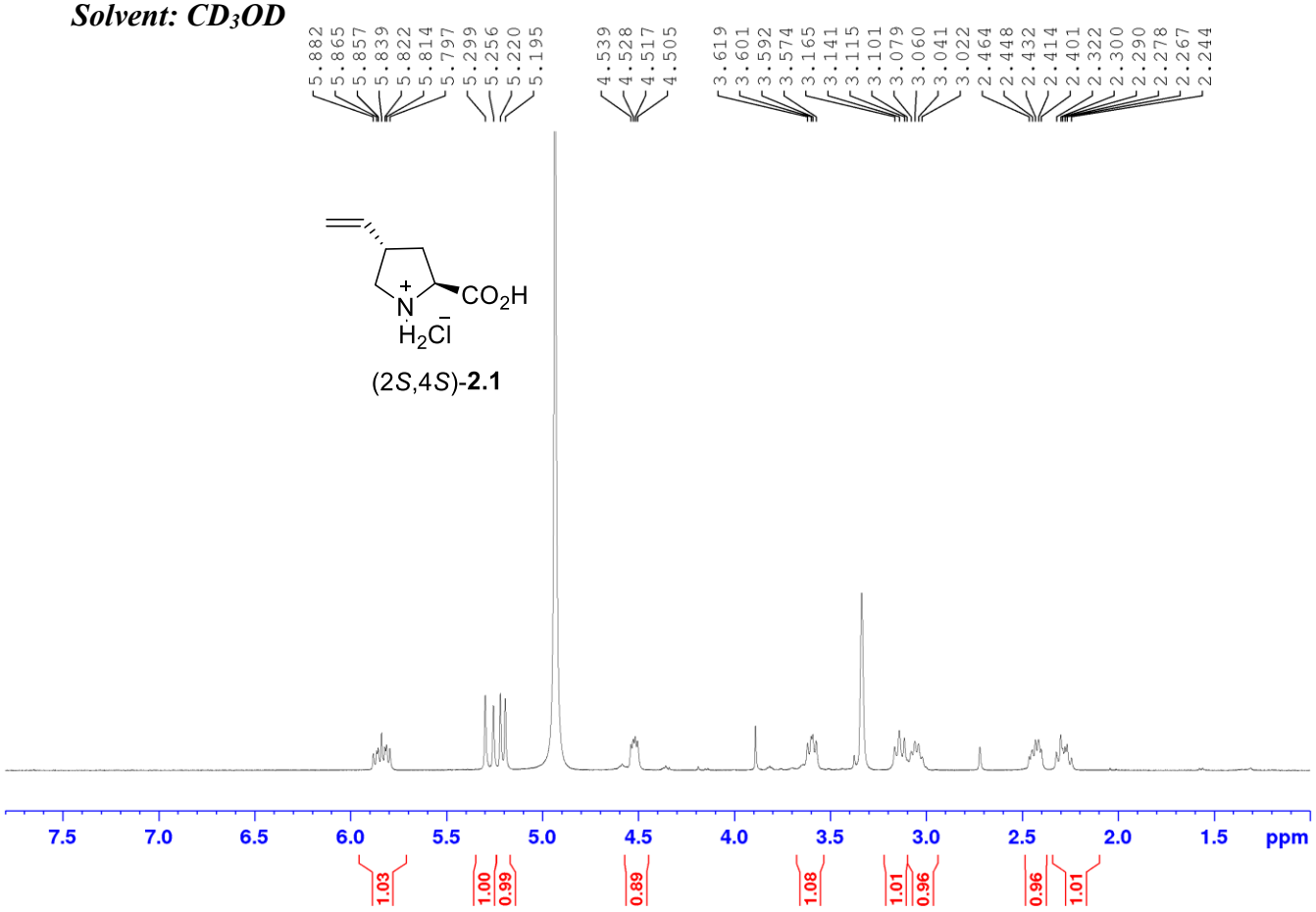

(2*S*,4*S*)-**2.1**

^{13}C NMR 125 MHz
Solvent: CD_3OD

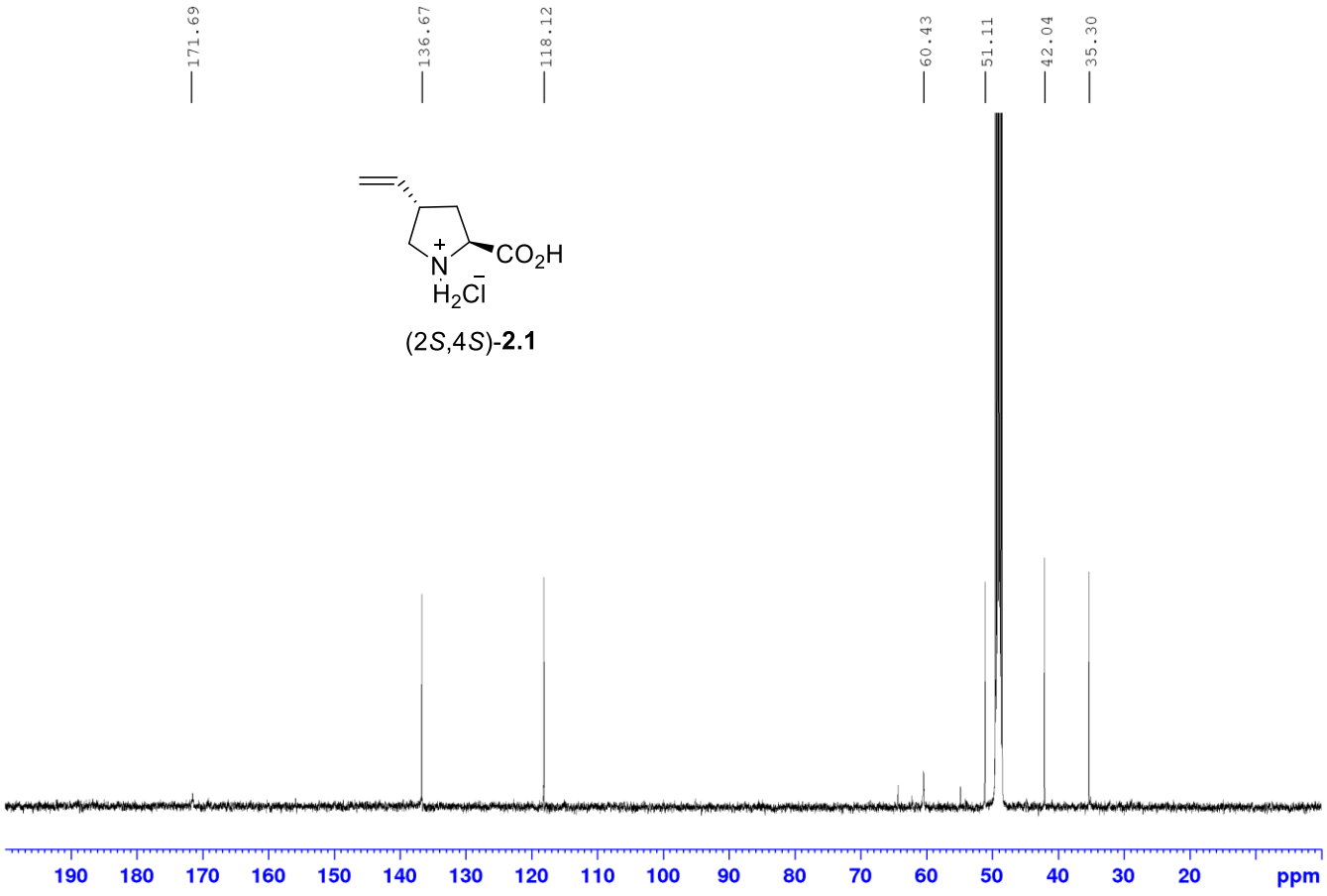

(2*S*,4*S*)-**2.1**

^{1}H NMR 400 MHz
Solvent: CD_3OD

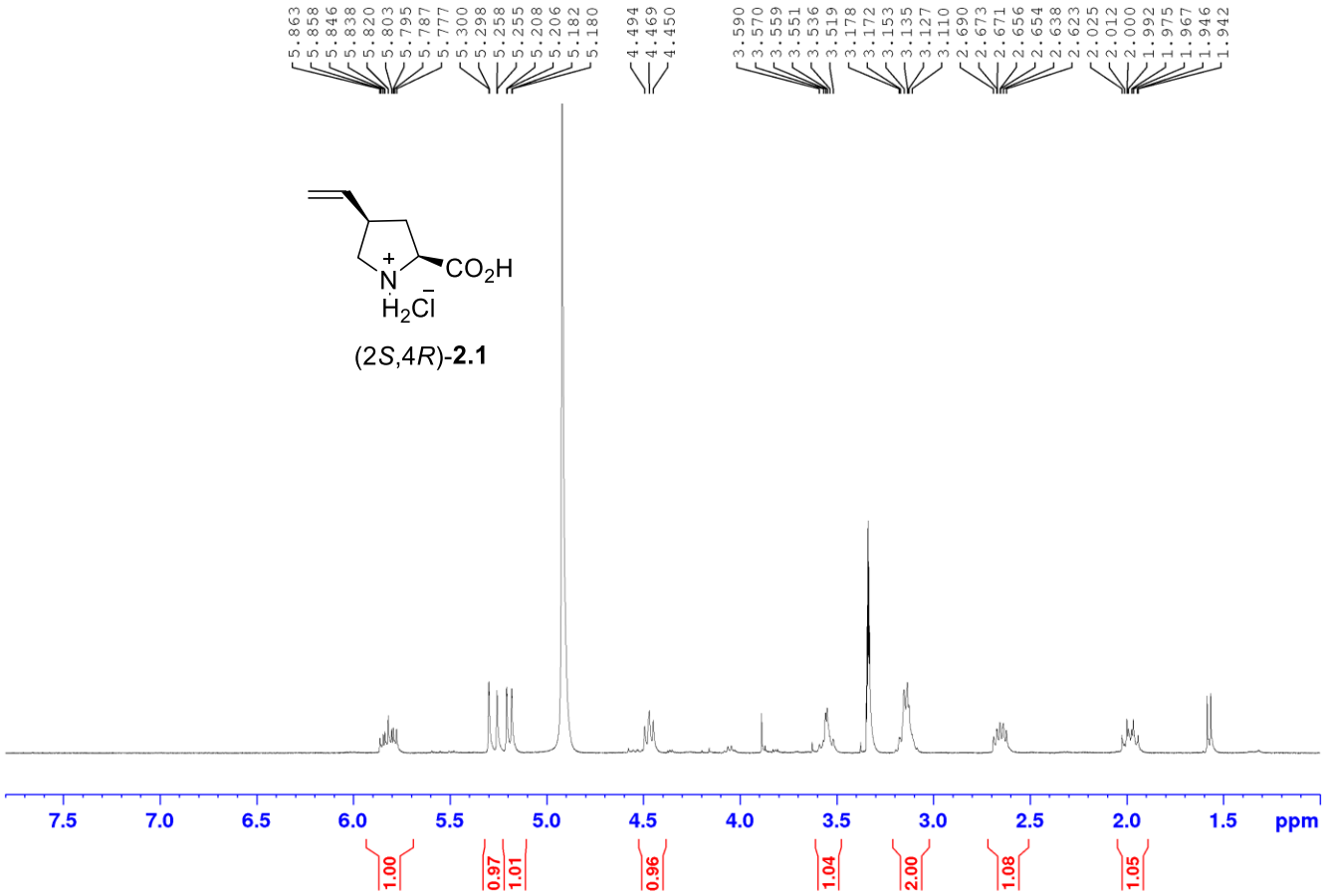

^{13}C NMR 125 MHz
Solvent: CD_3OD

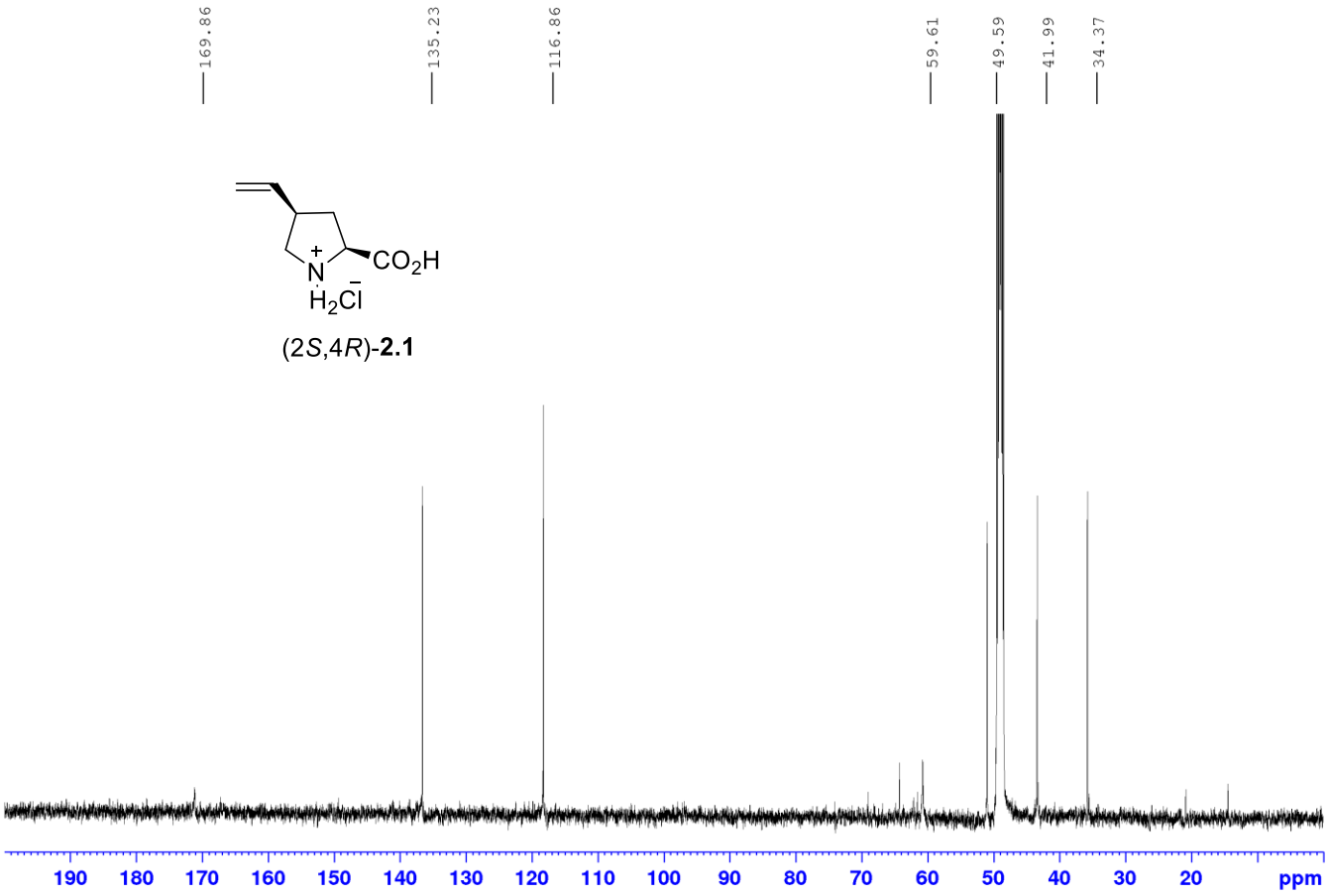

(2*S*,4*R*)-**2.1**

^{1}H NMR 500 MHz
Solvent: CD_3OD

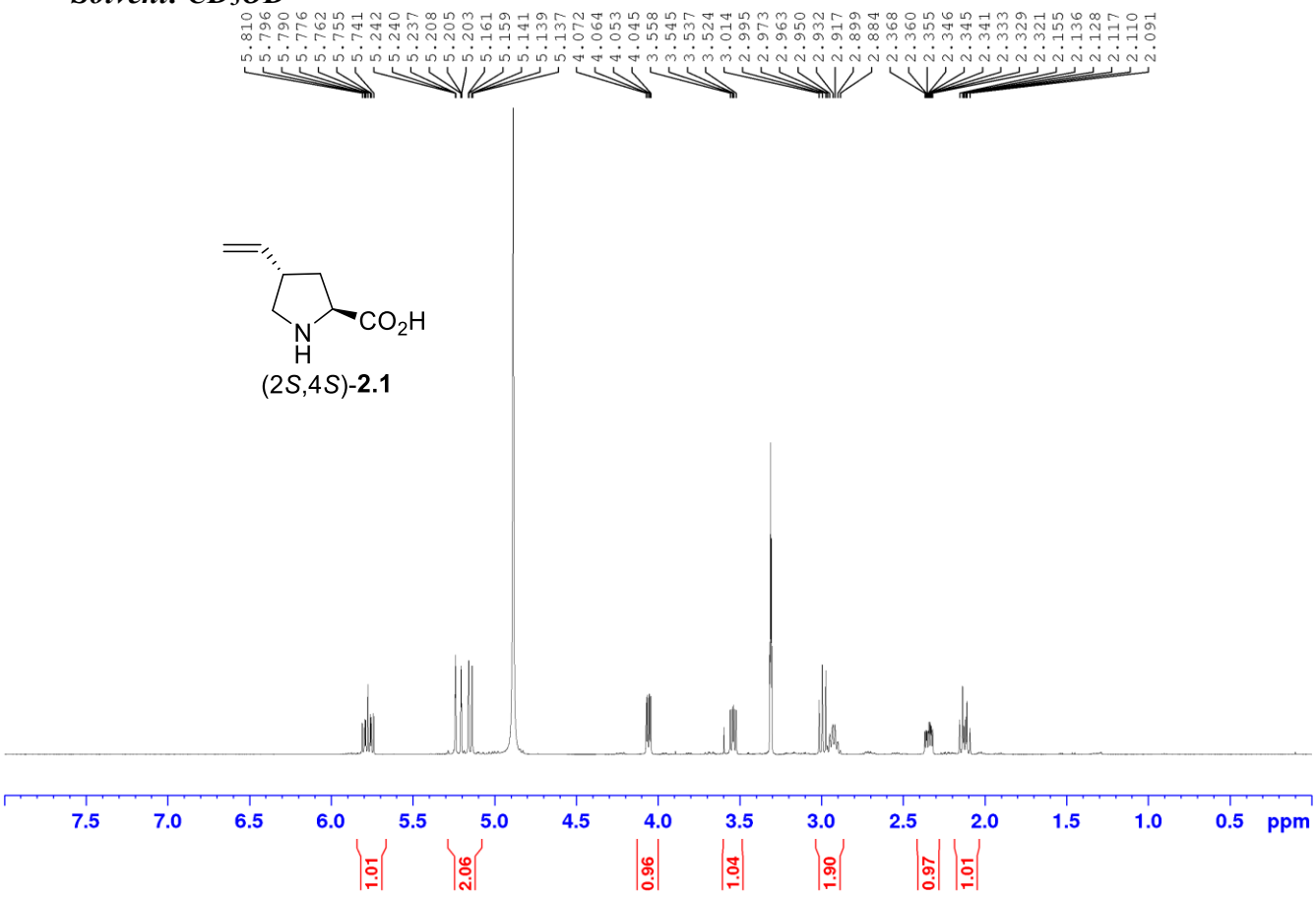

^{13}C NMR 125 MHz
Solvent: CD_3OD

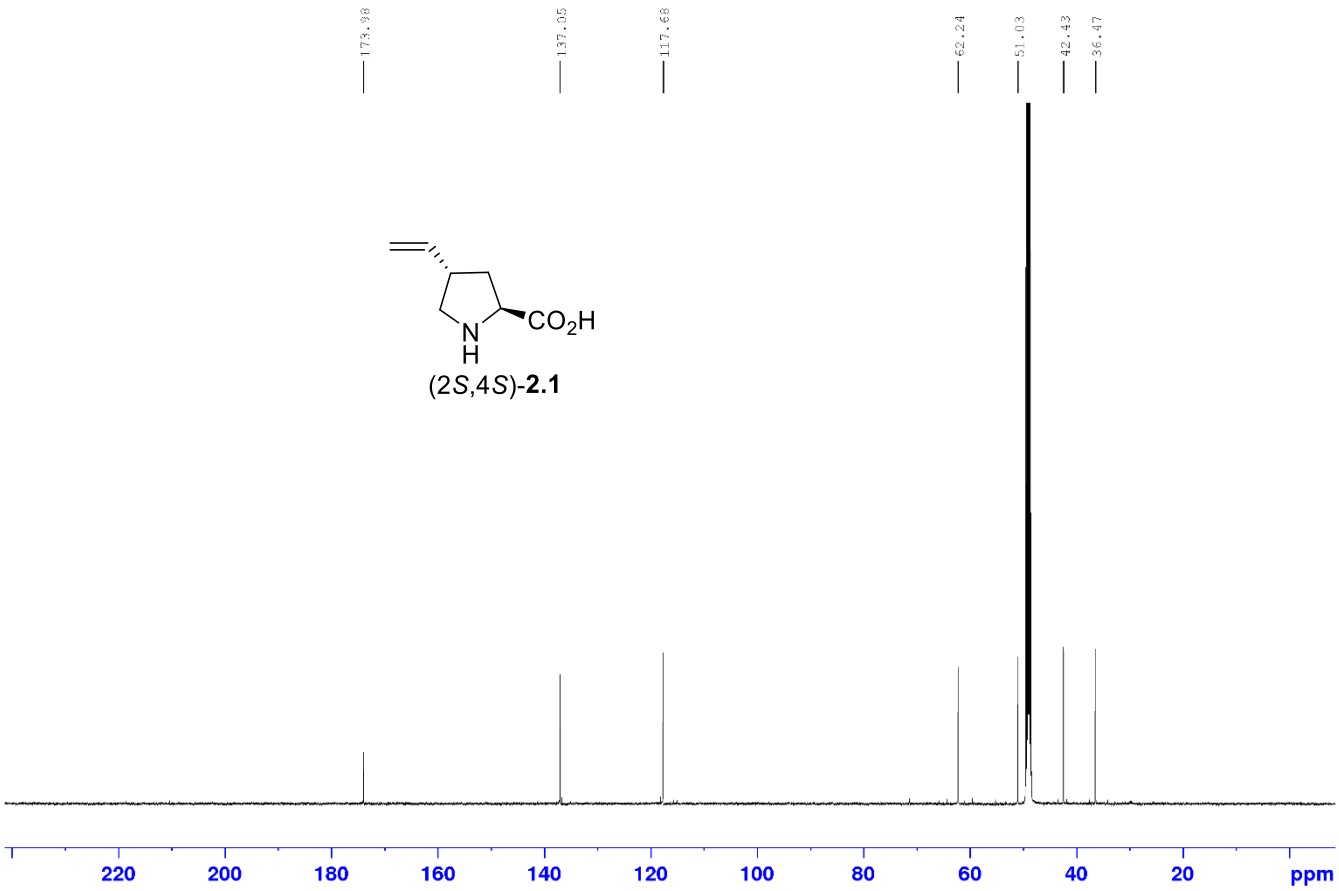

(2*S*,4*S*)-**2.1**

^{1}H NMR 500 MHz
Solvent: CD_3OD

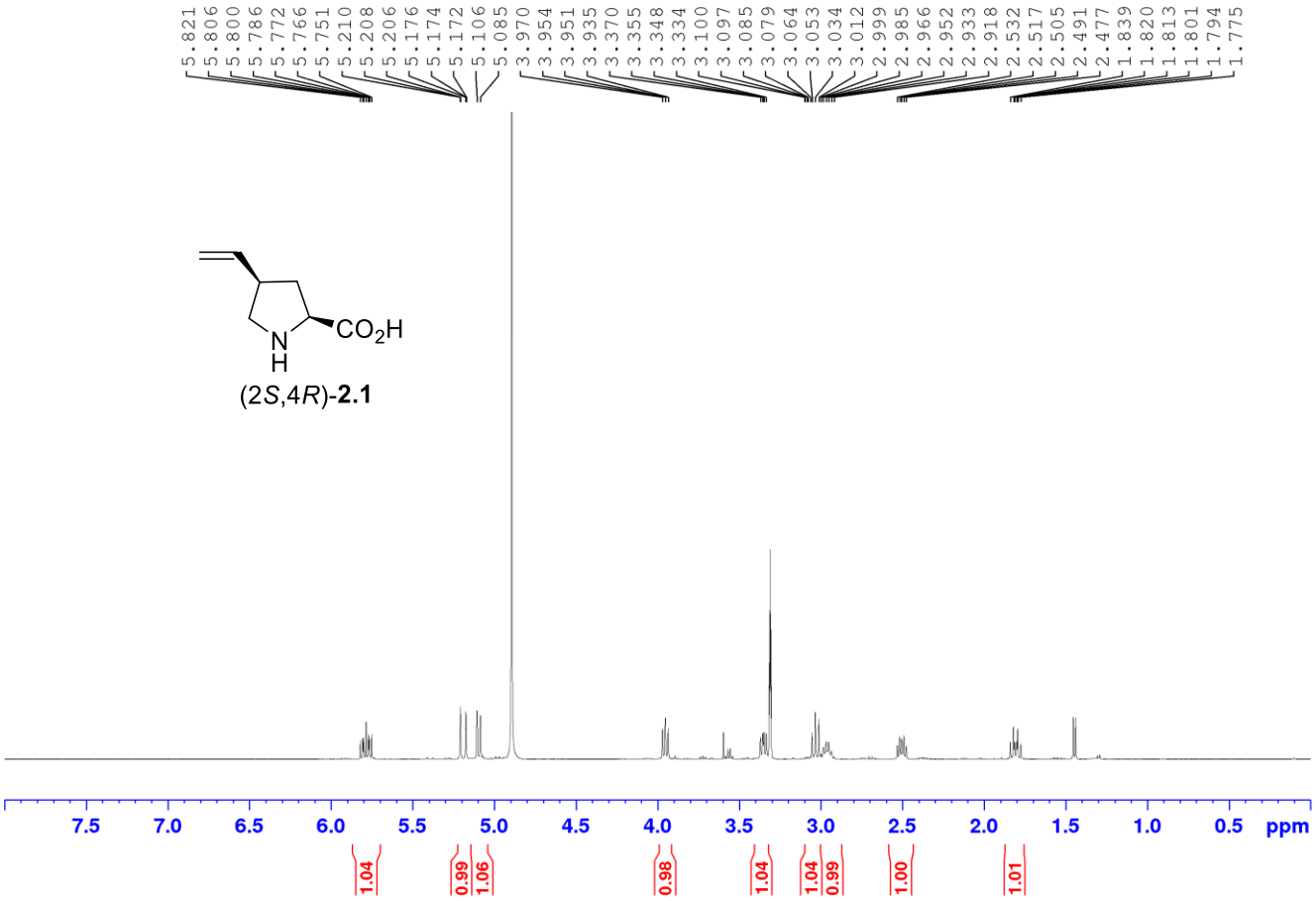

(2*S*,4*R*)-**2.1**

^{13}C NMR 125 MHz
Solvent: CD_3OD

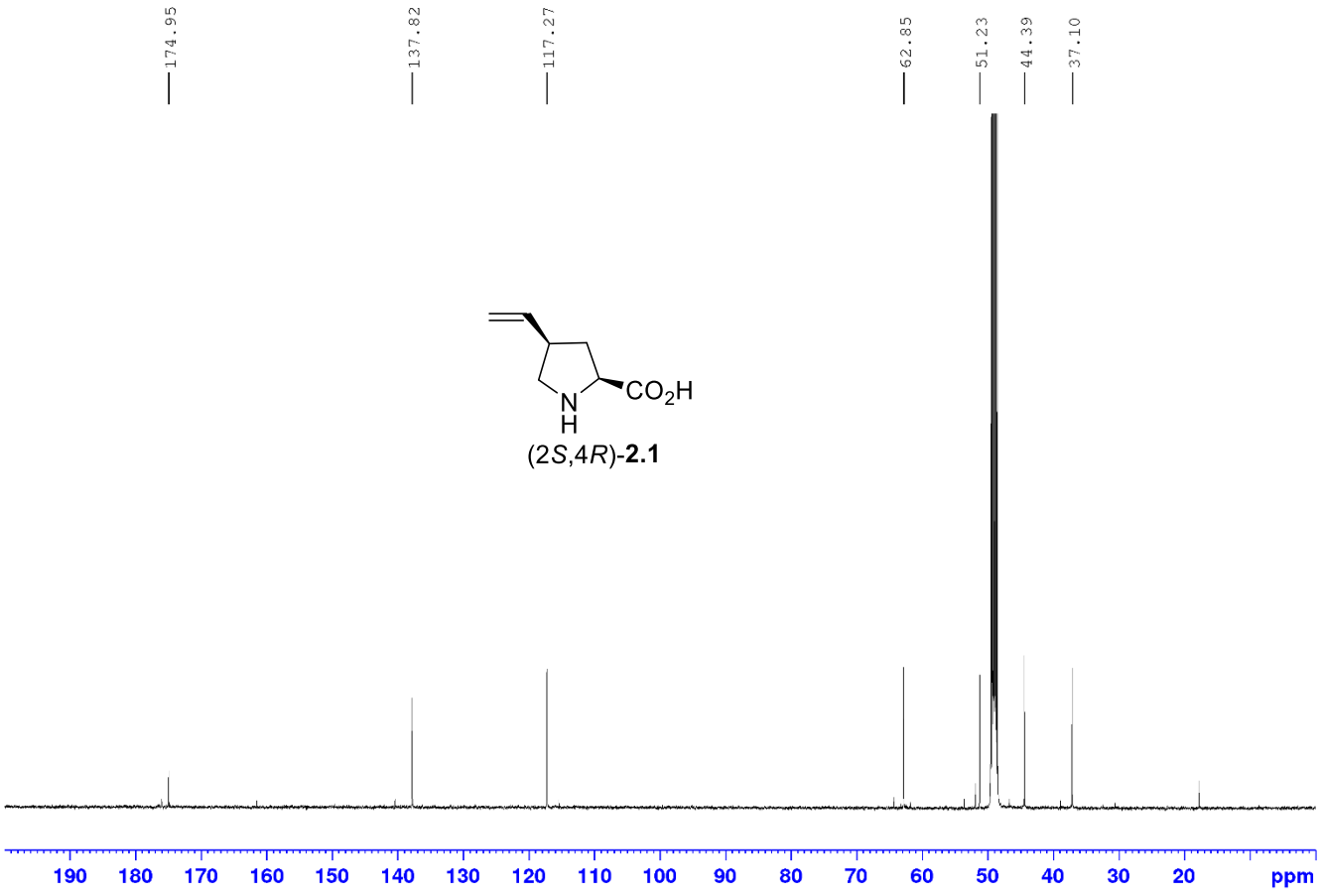

(2*S*,4*R*)-**2.1**

^{1}H NMR 500 MHz
Solvent: $CDCl_3$

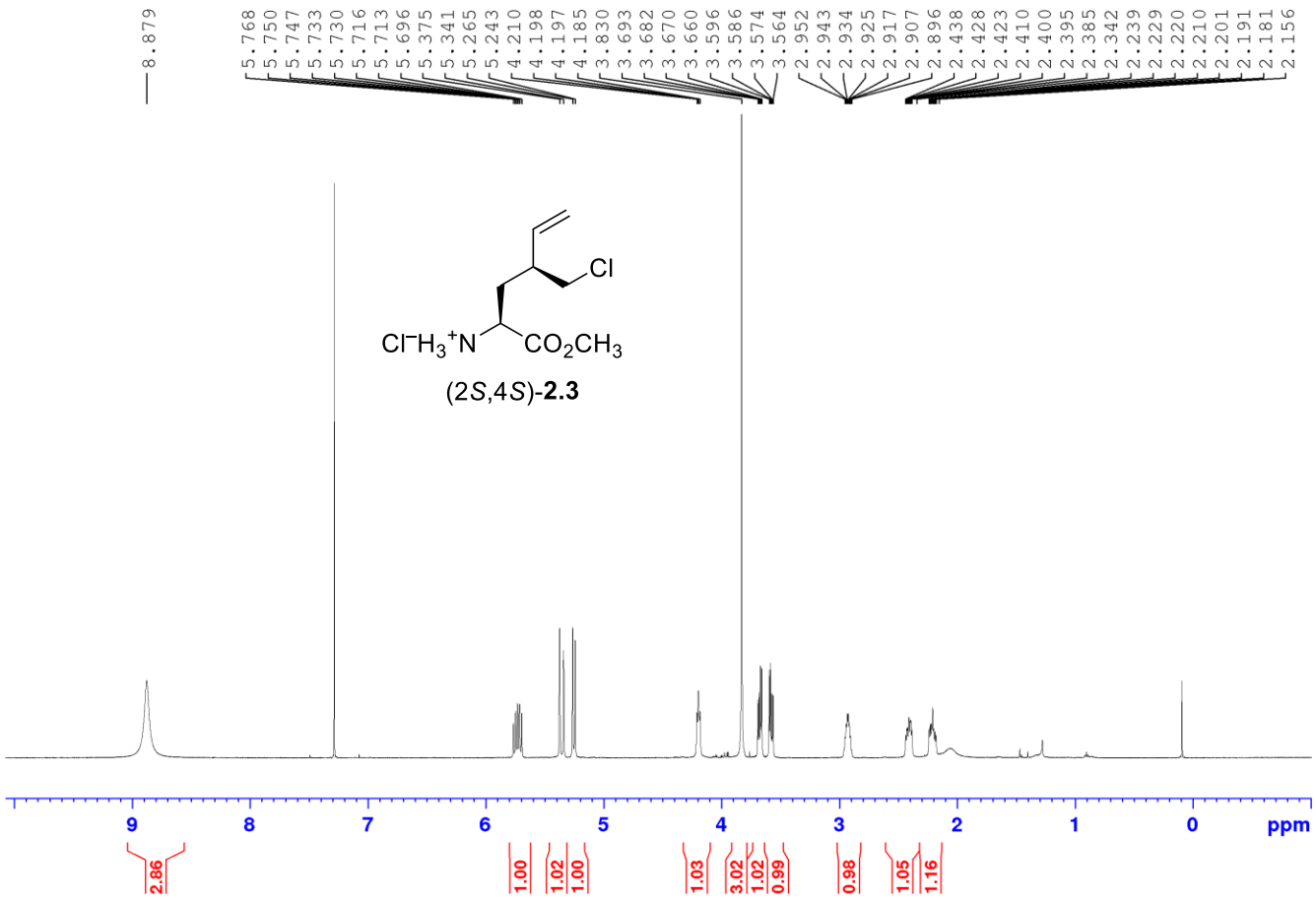

^{13}C NMR 125 MHz
Solvent: $CDCl_3$

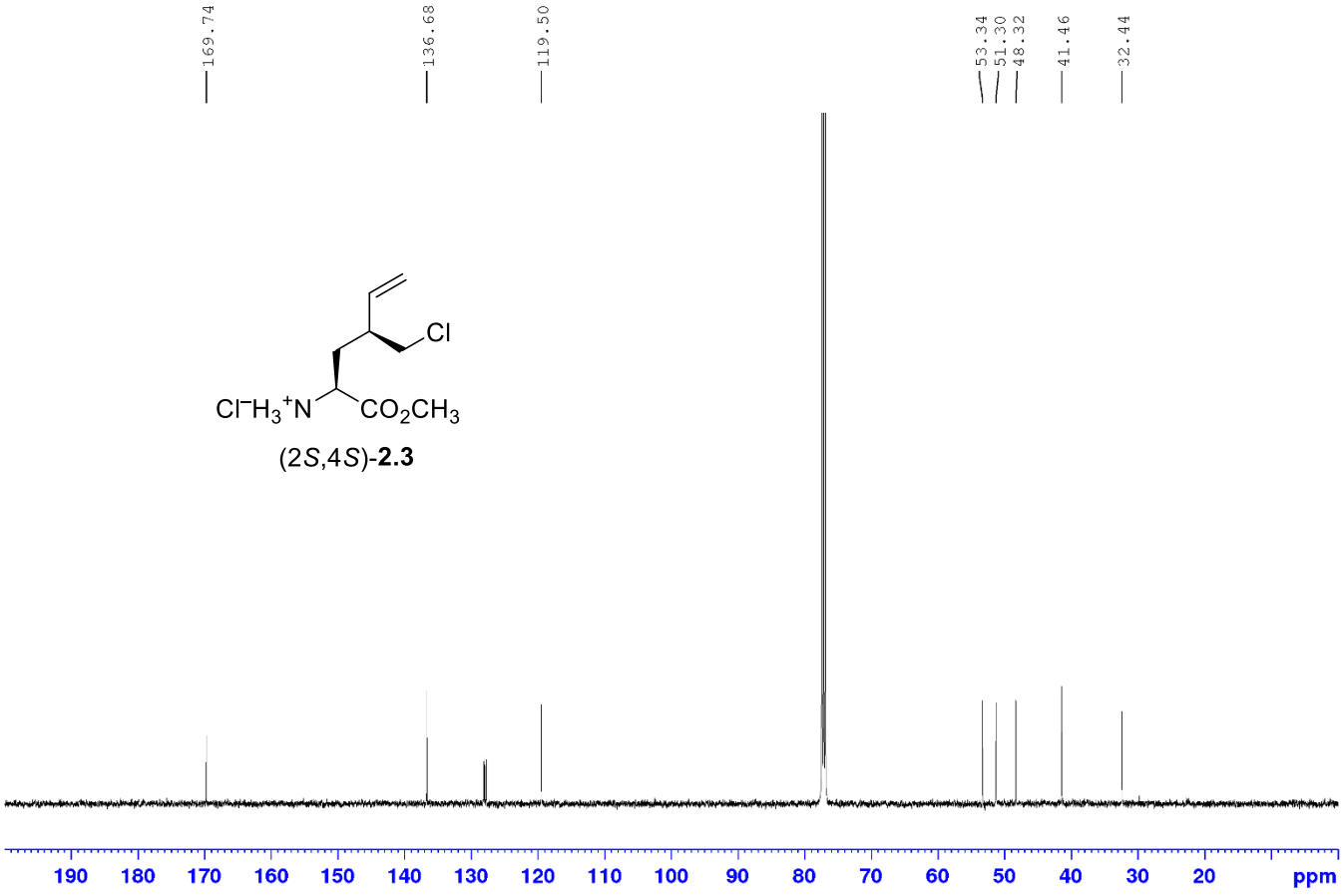

^{1}H NMR 500 MHz
Solvent: $CDCl_3$

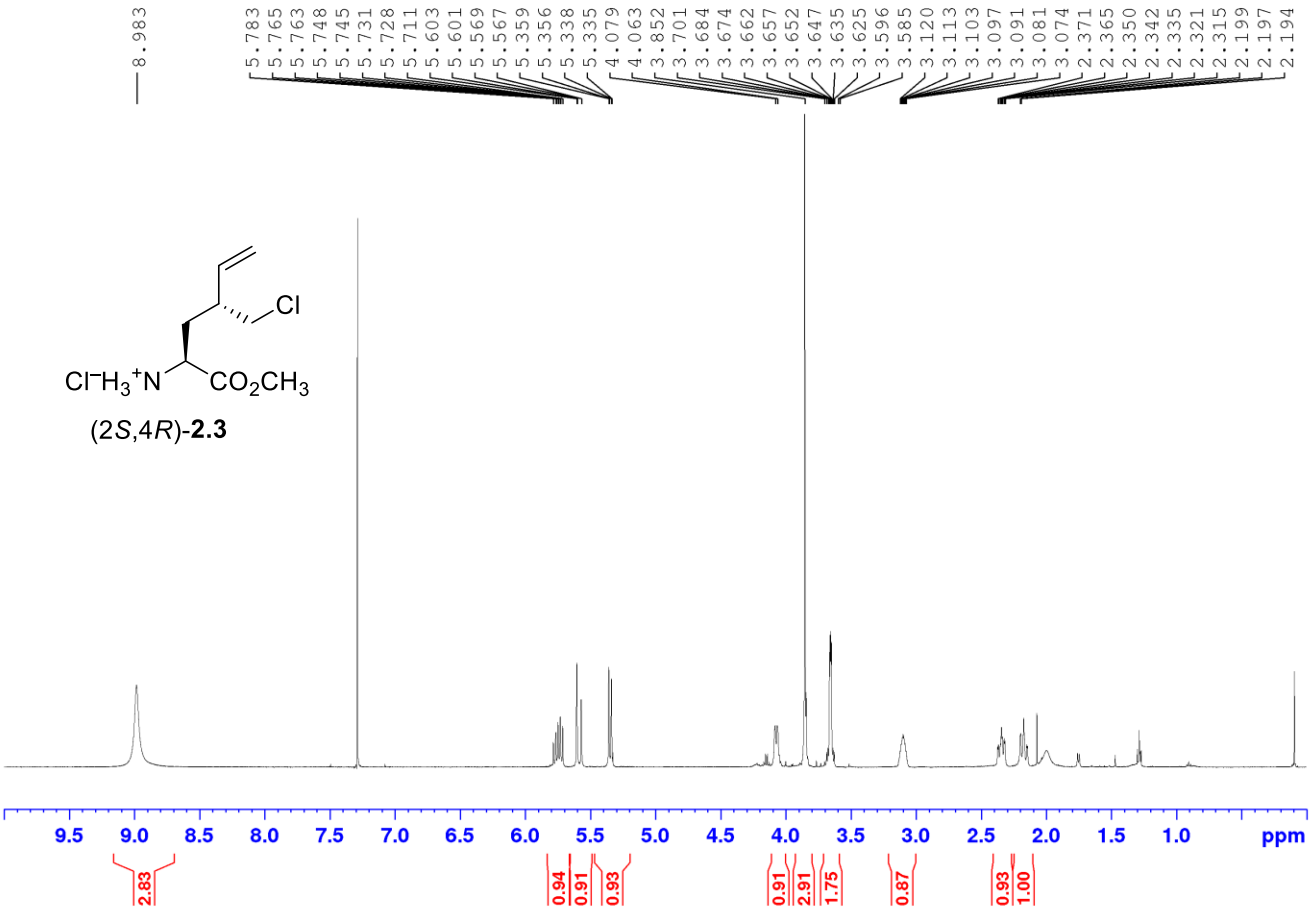

^{13}C NMR 125 MHz
Solvent: $CDCl_3$

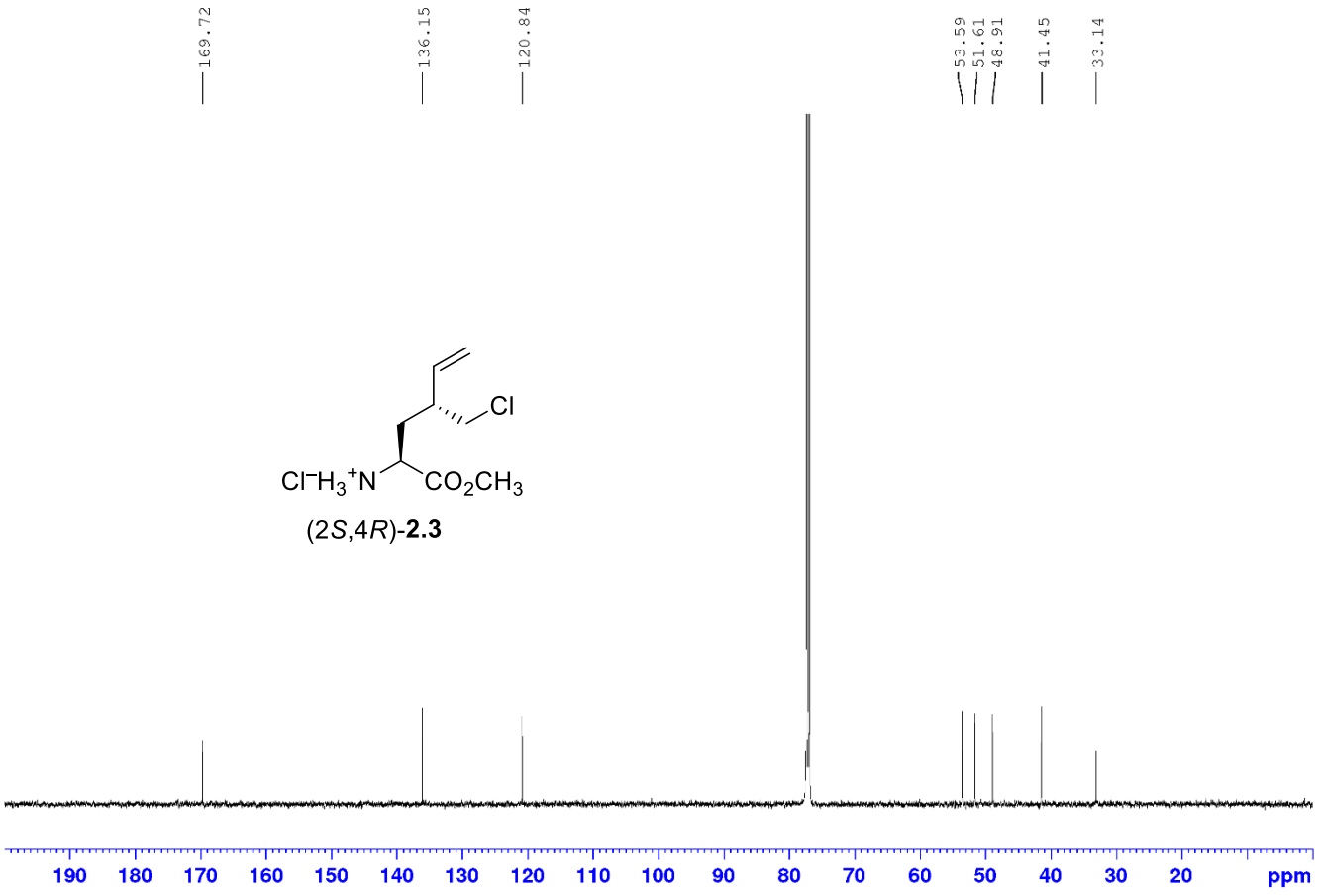

^{1}H NMR 500 MHz
Solvent: C_6D_6

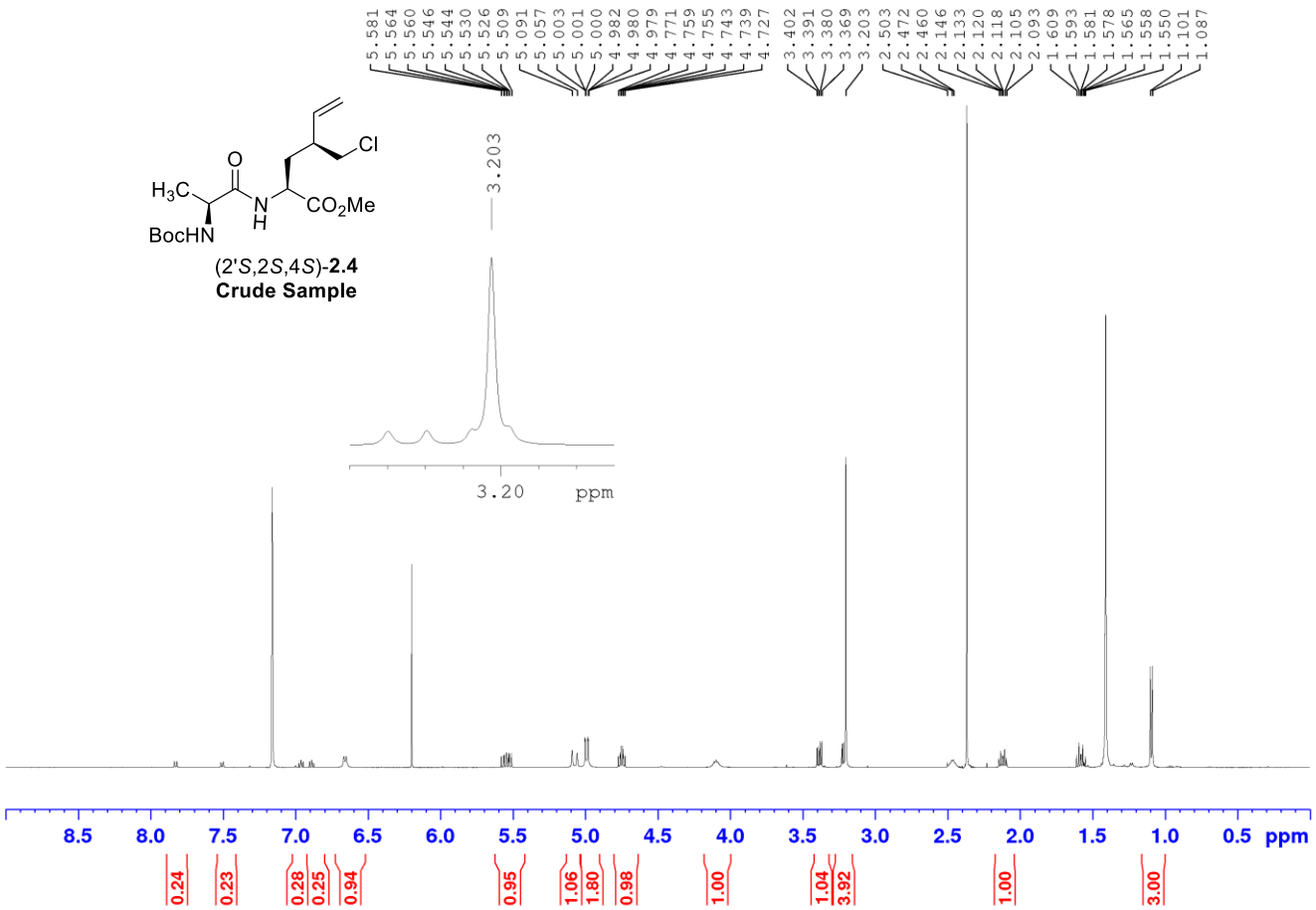

^{1}H NMR 500 MHz
Solvent: C_6D_6

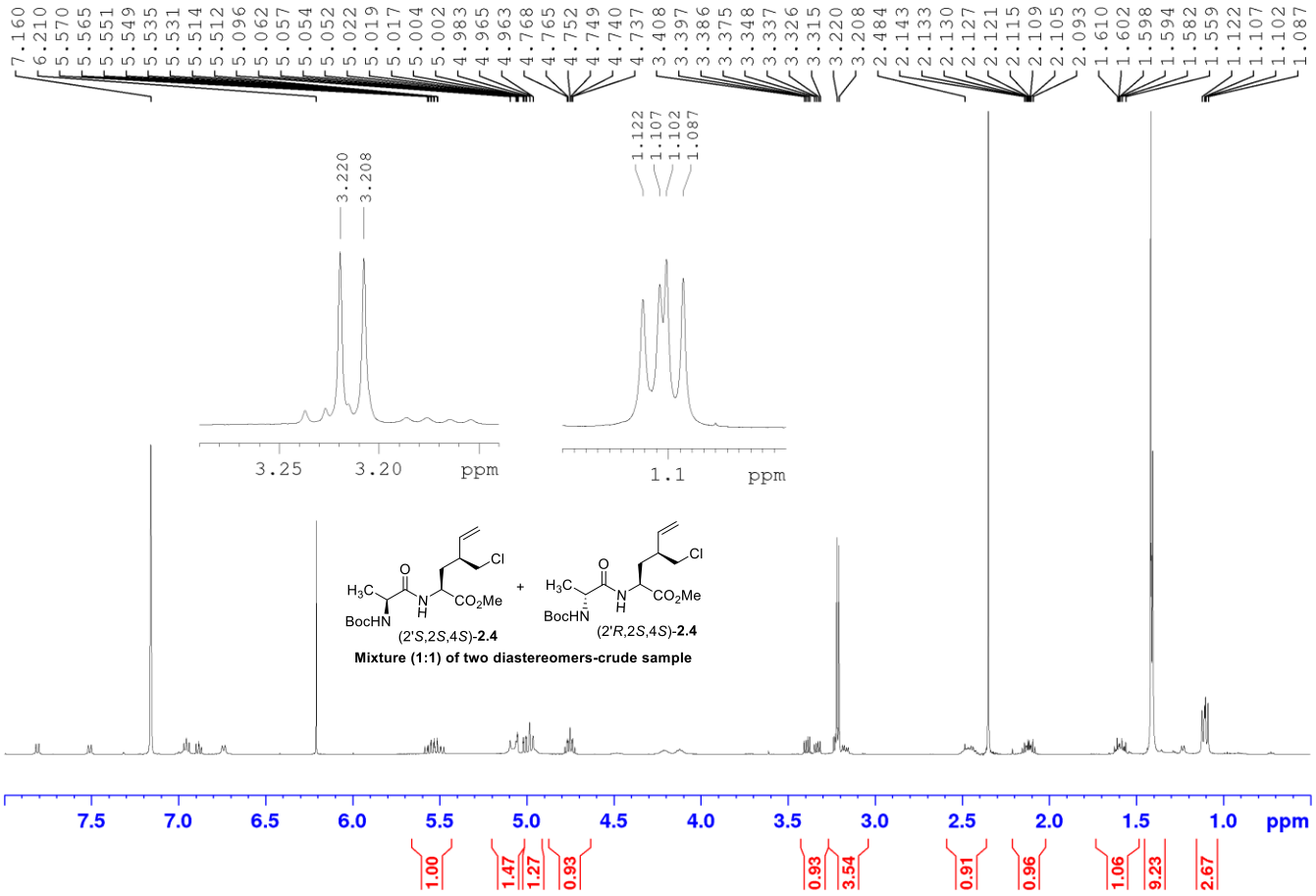

^{1}H NMR 500 MHz
Solvent: C_6D_6

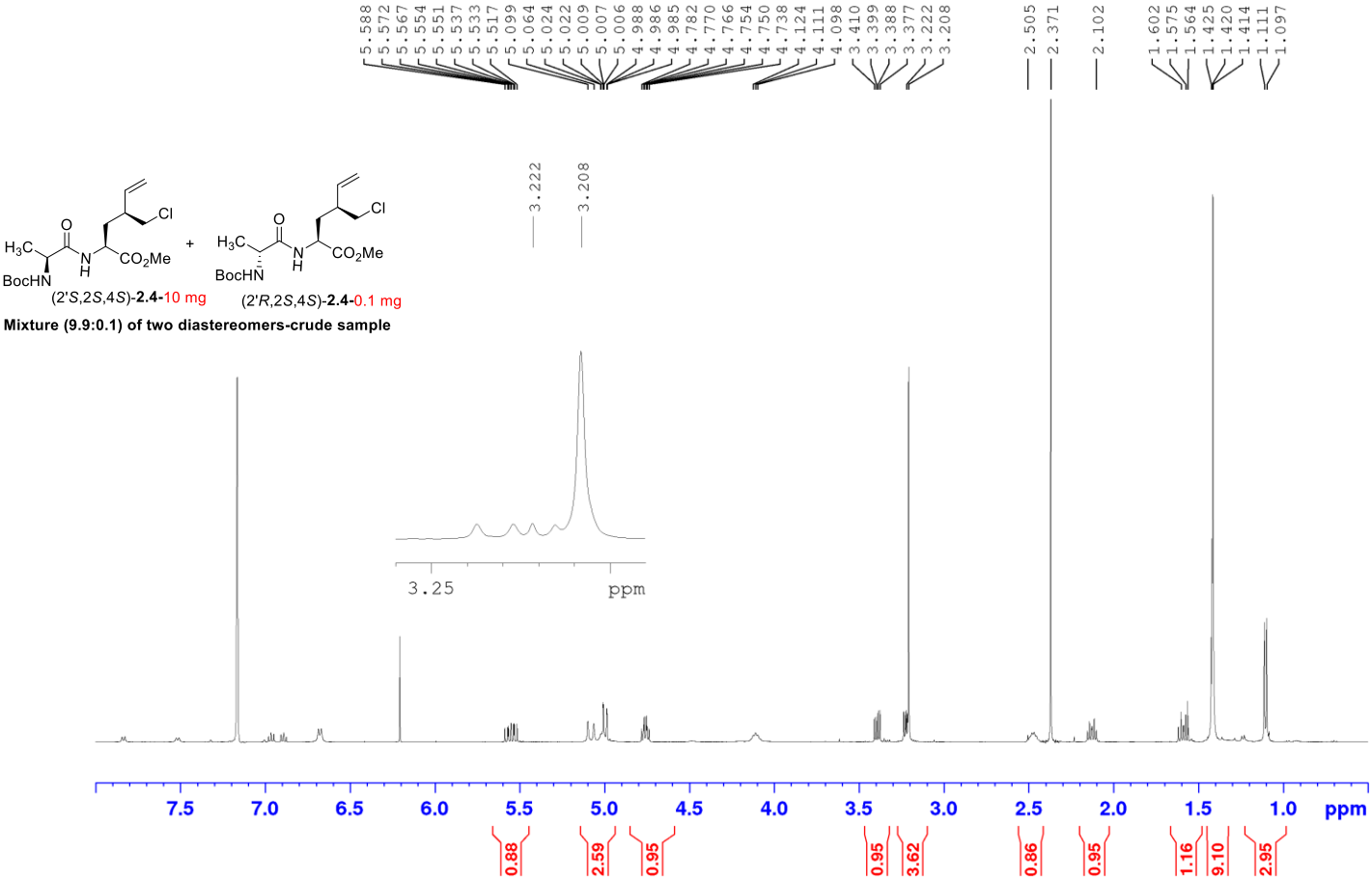

^{1}H NMR 500 MHz
Solvent: C_6D_6

Examination of the diastereotopic methyl ester at 3.208 and 3.222 ppm

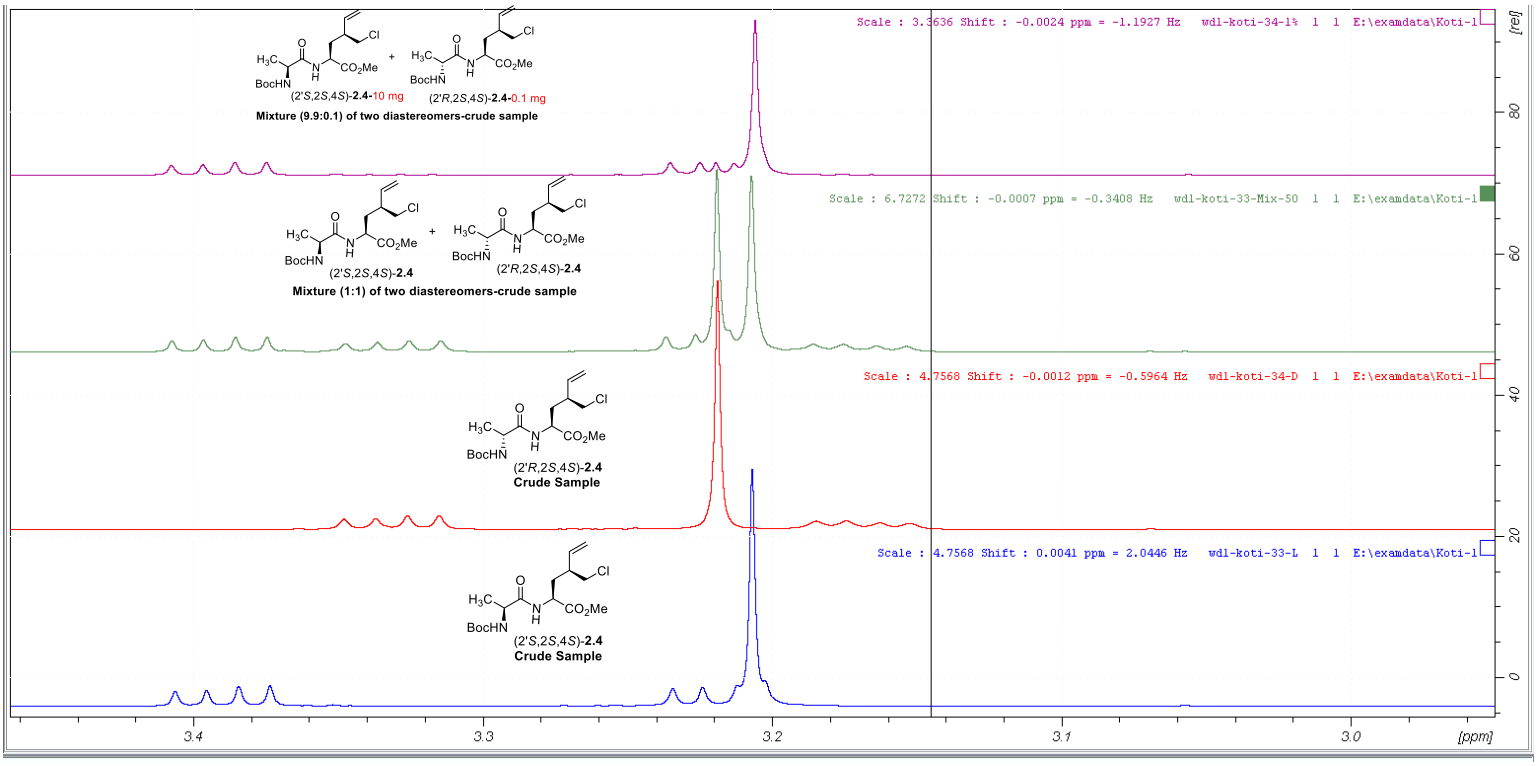

^{1}H NMR 400 MHz
Solvent: C_6D_6

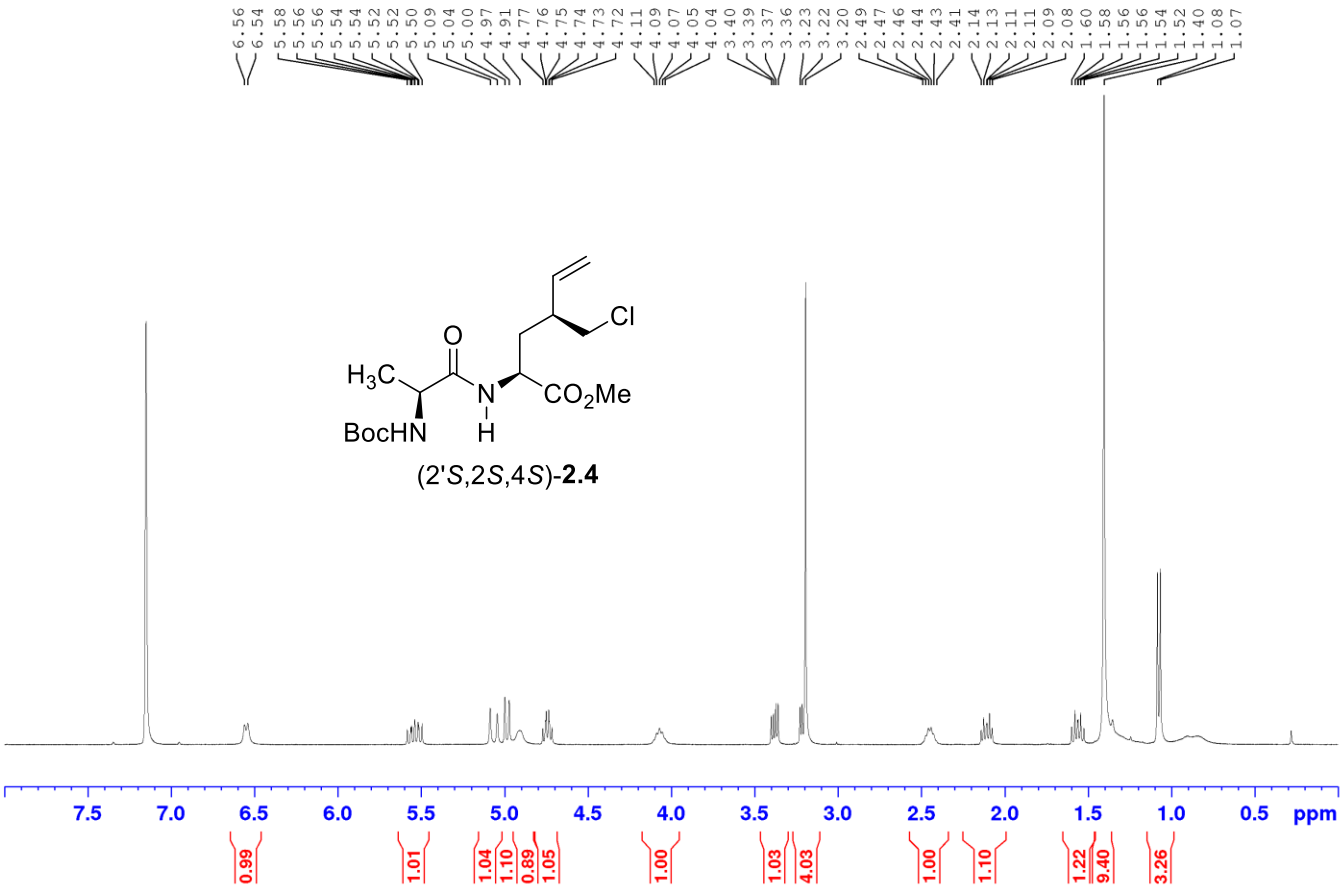

^{13}C NMR 100 MHz
Solvent: C_6D_6

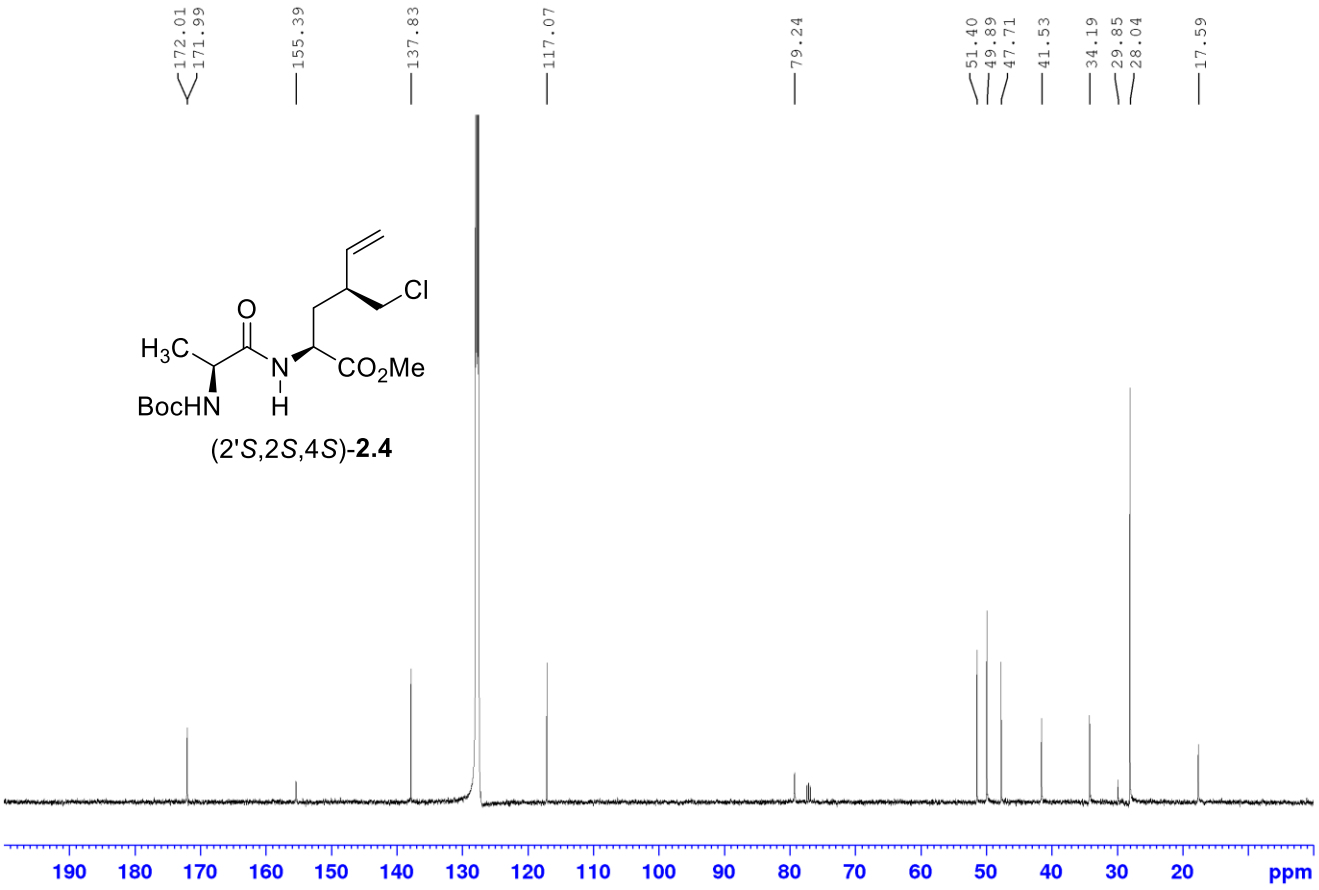

^{1}H NMR 400 MHz
Solvent: C_6D_6

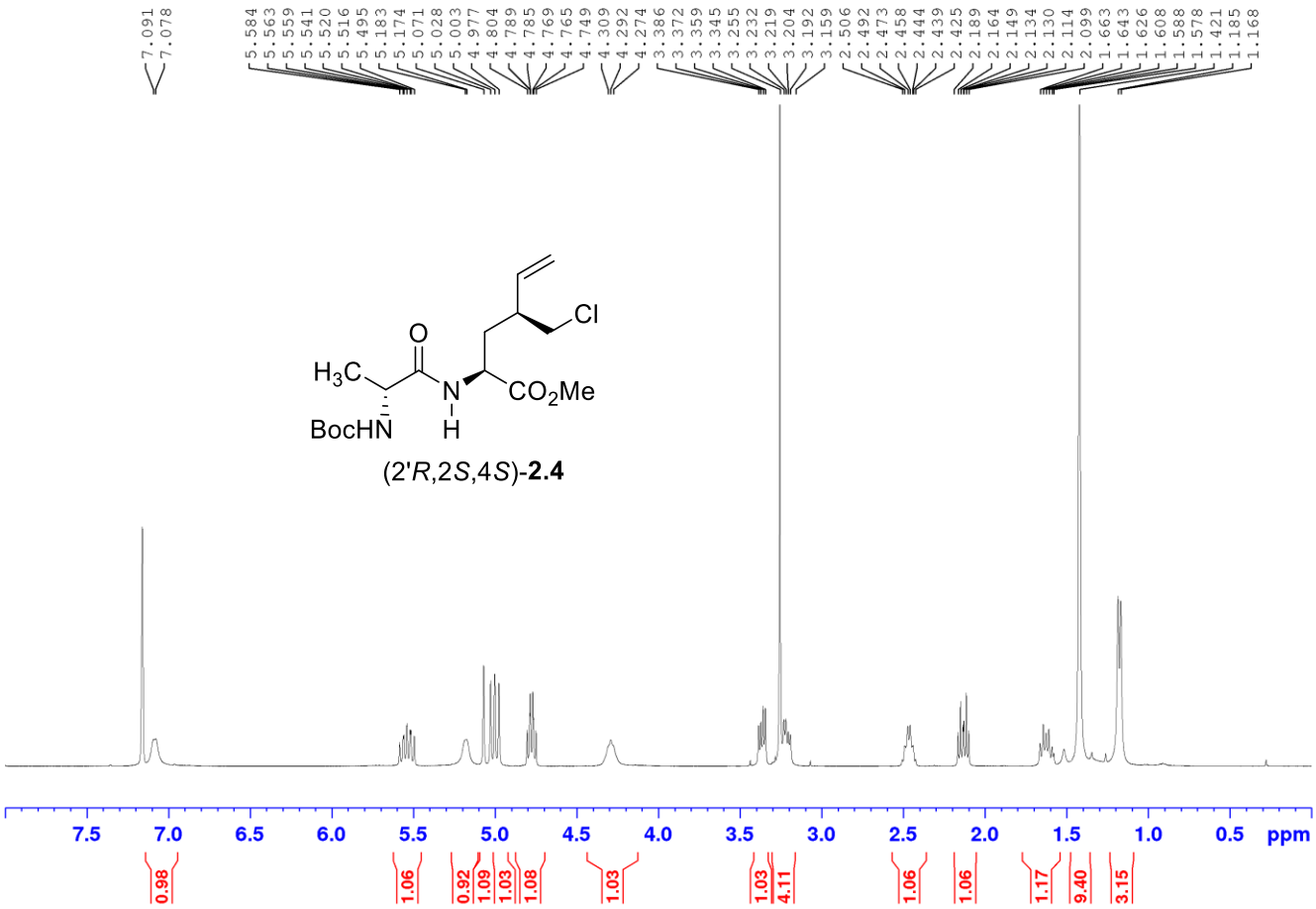

^{13}C NMR 100 MHz
Solvent: C_6D_6

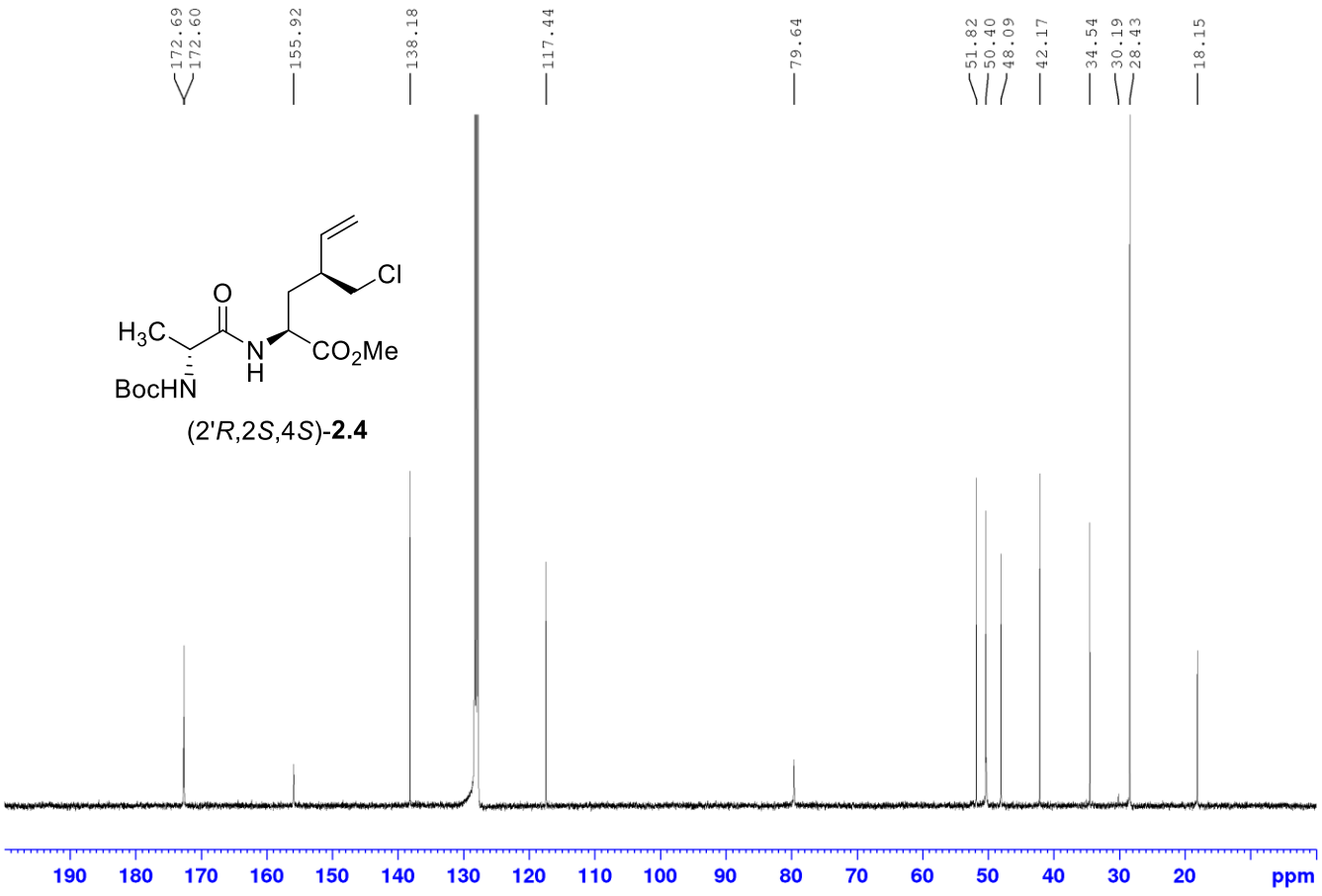

^{1}H NMR 500 MHz
Solvent: $CDCl_3$

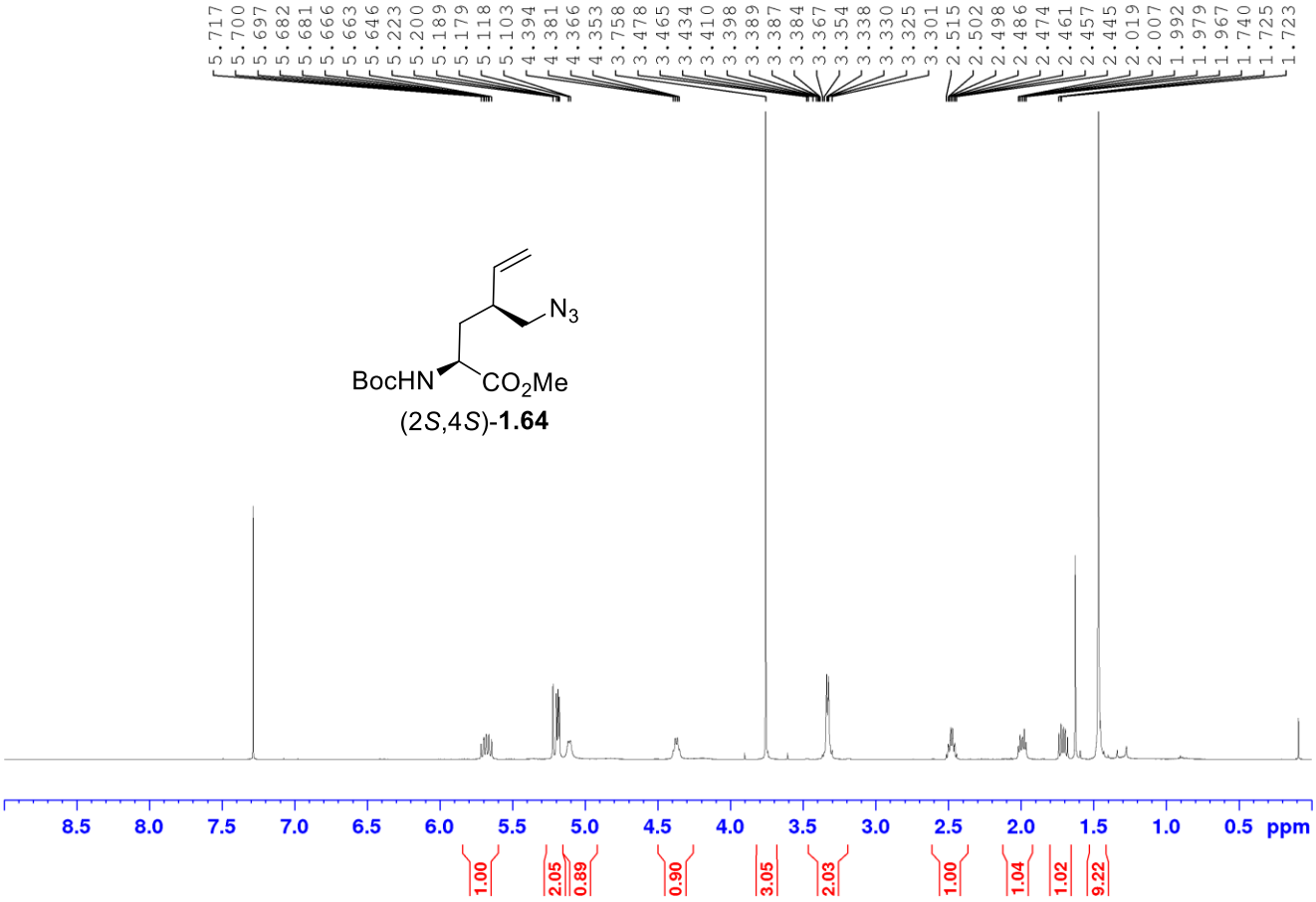

^{13}C NMR 125 MHz
Solvent: $CDCl_3$

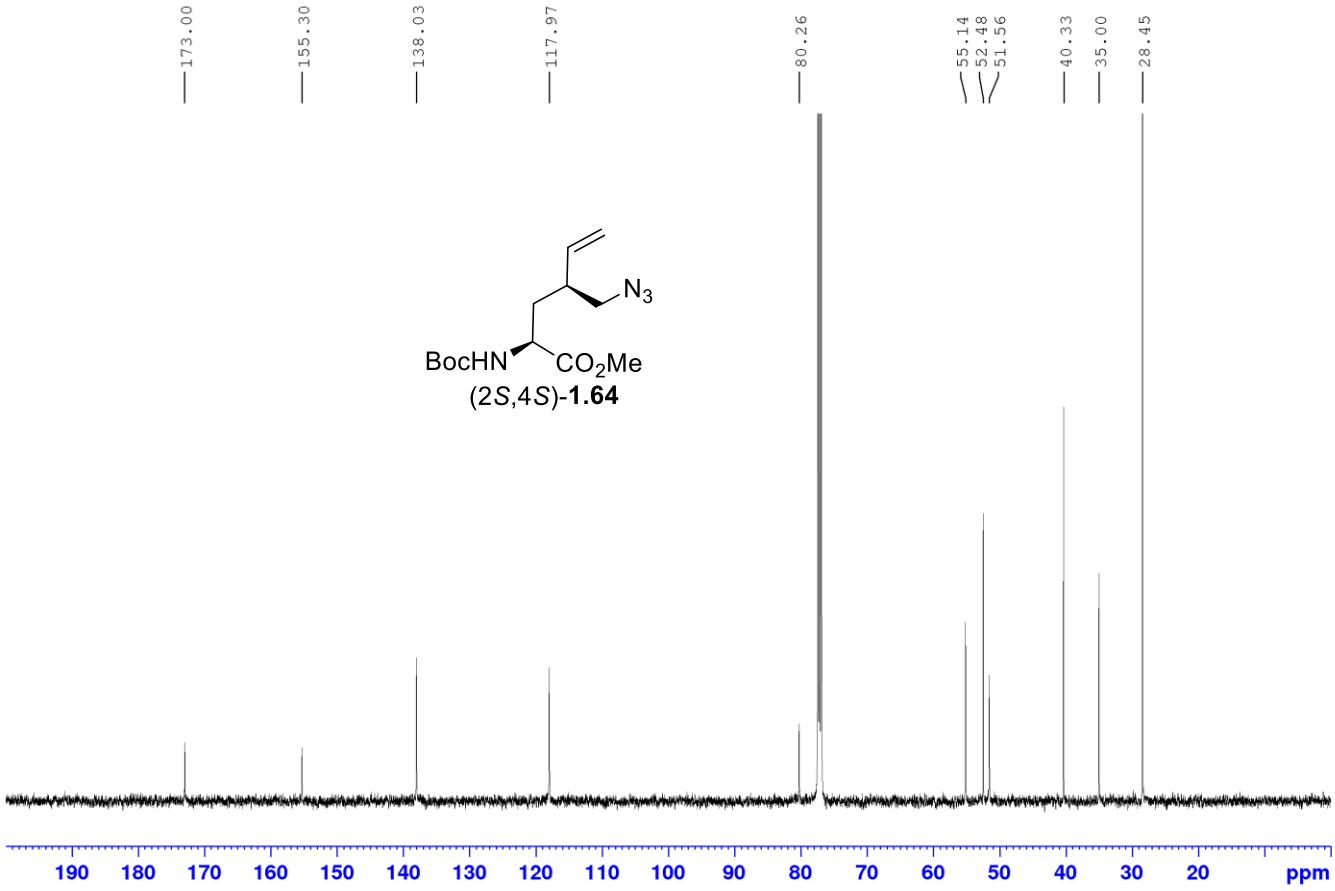

^{1}H NMR 500 MHz
Solvent: $CDCl_3$

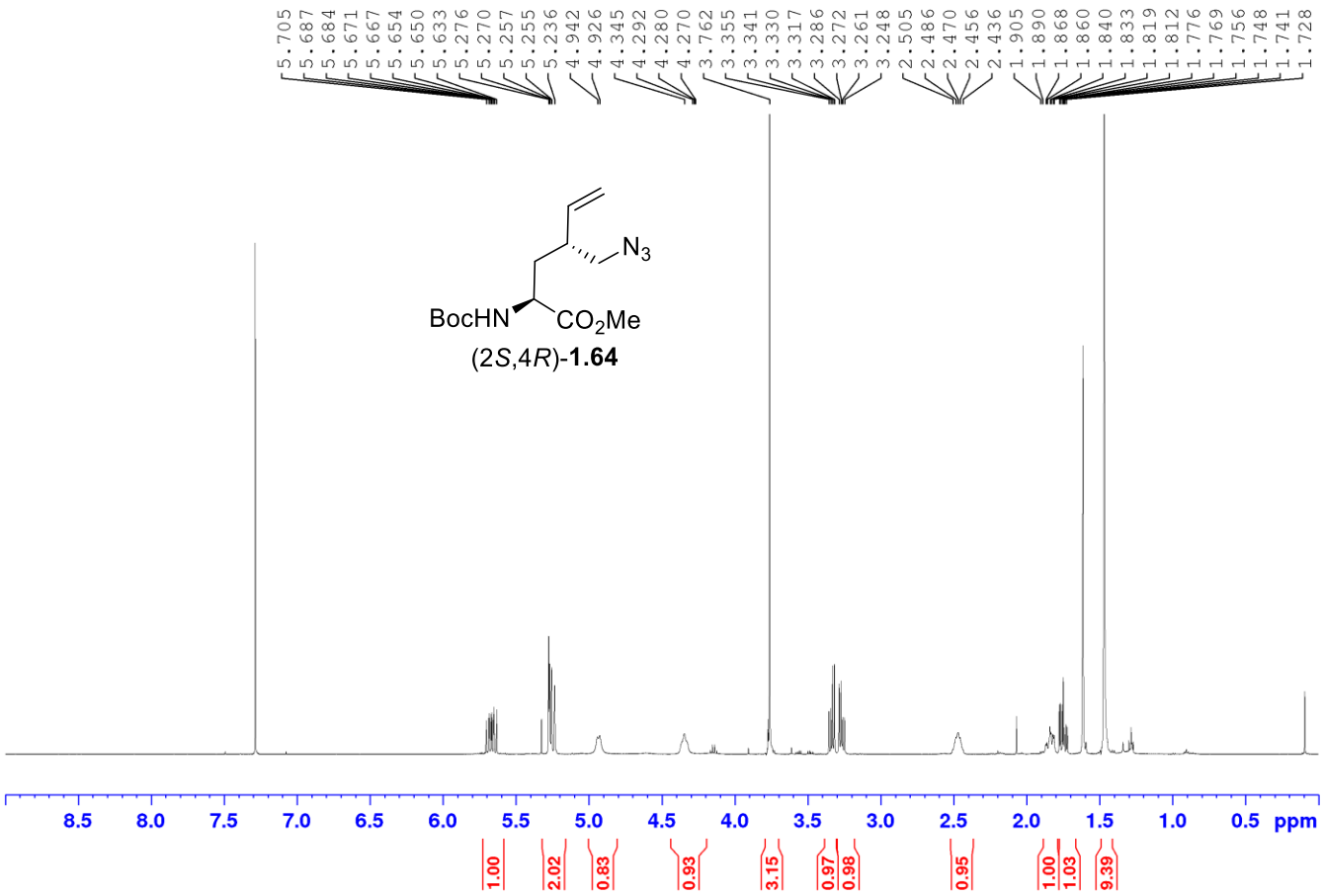

^{13}C NMR 125 MHz
Solvent: $CDCl_3$

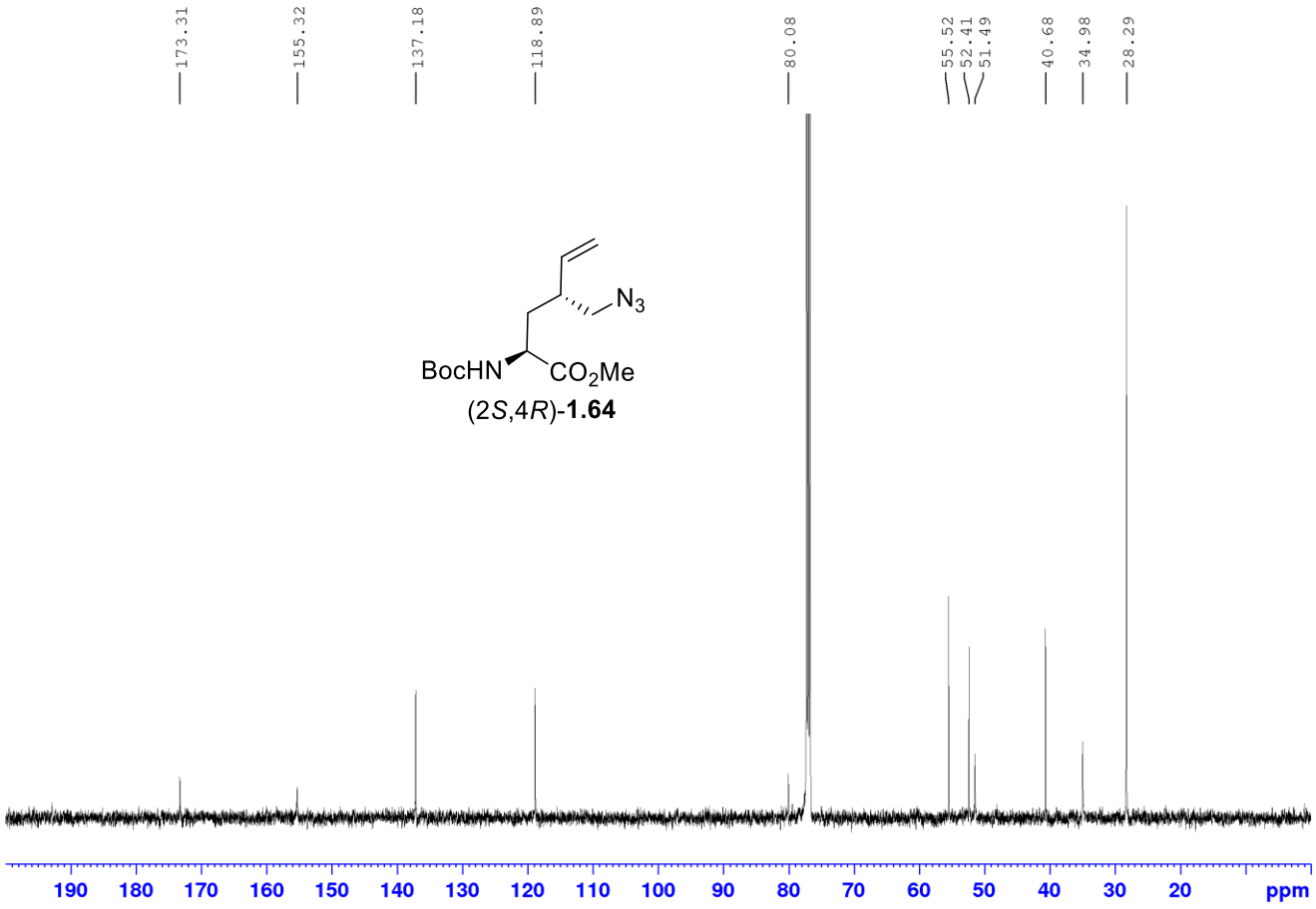

^{1}H NMR 500 MHz
Solvent: $CDCl_3$

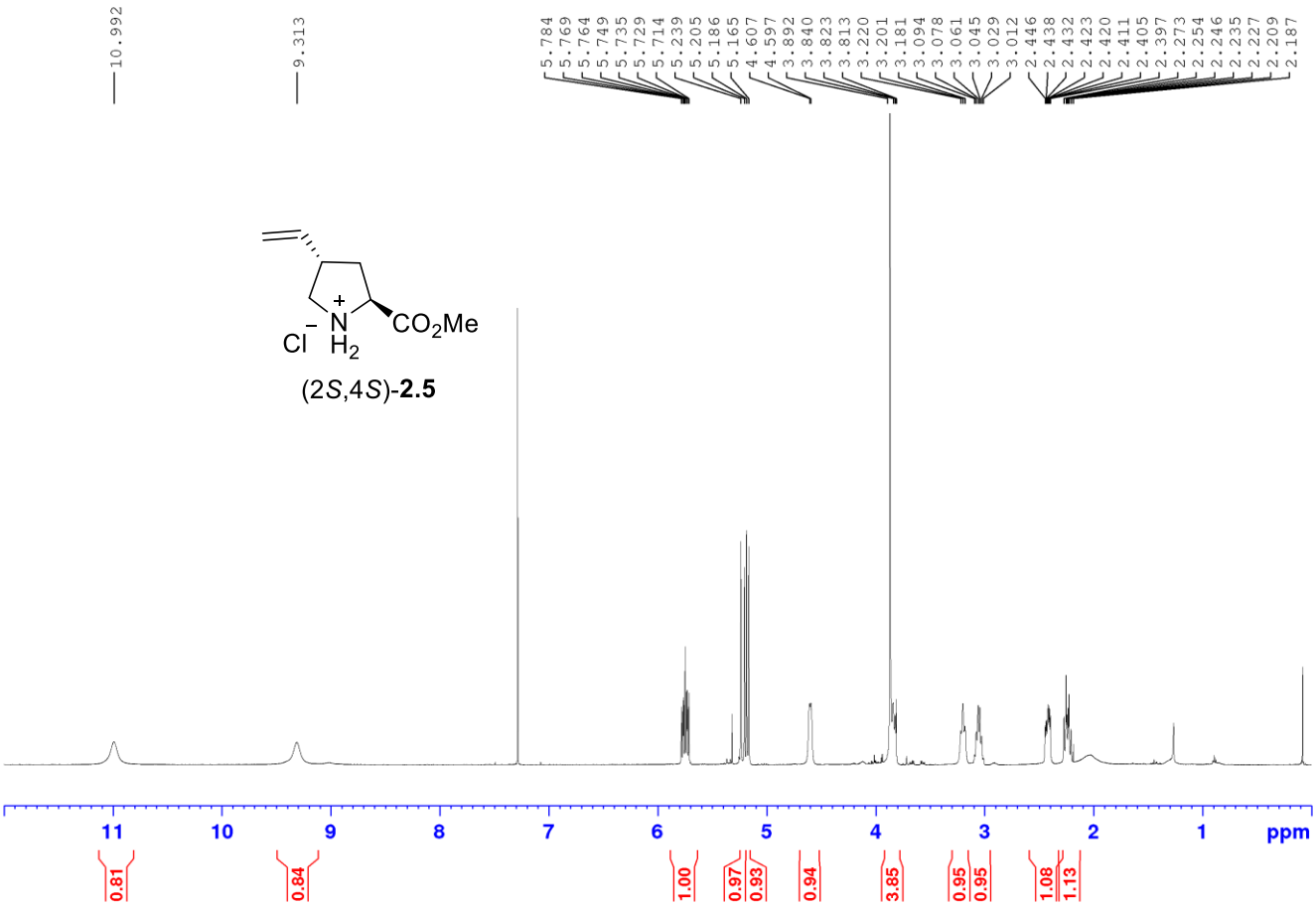

^{13}C NMR 125 MHz
Solvent: $CDCl_3$

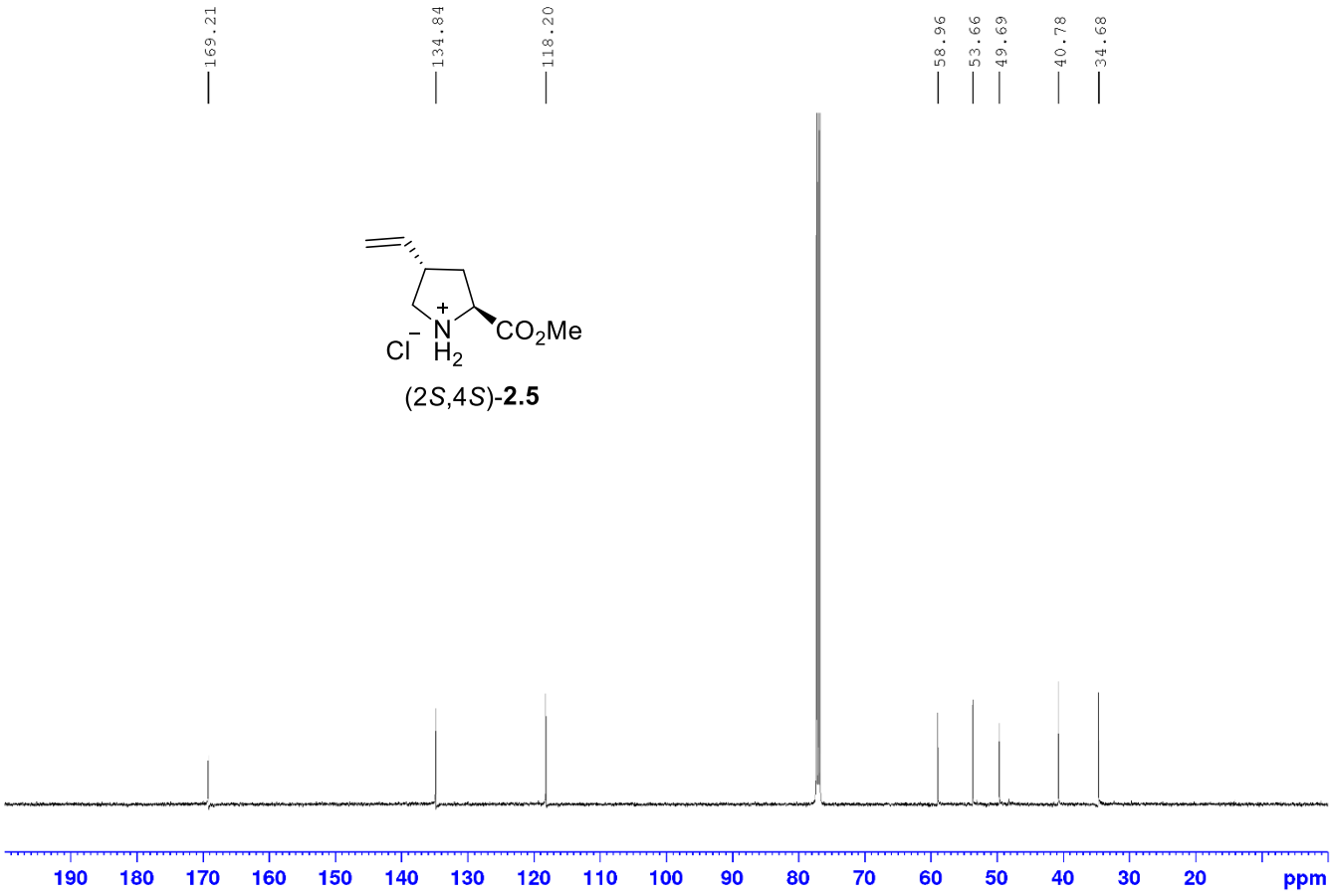

(2*S*,4*S*)-**2.5**

COSY NMR 500 MHz
Solvent: $CDCl_3$

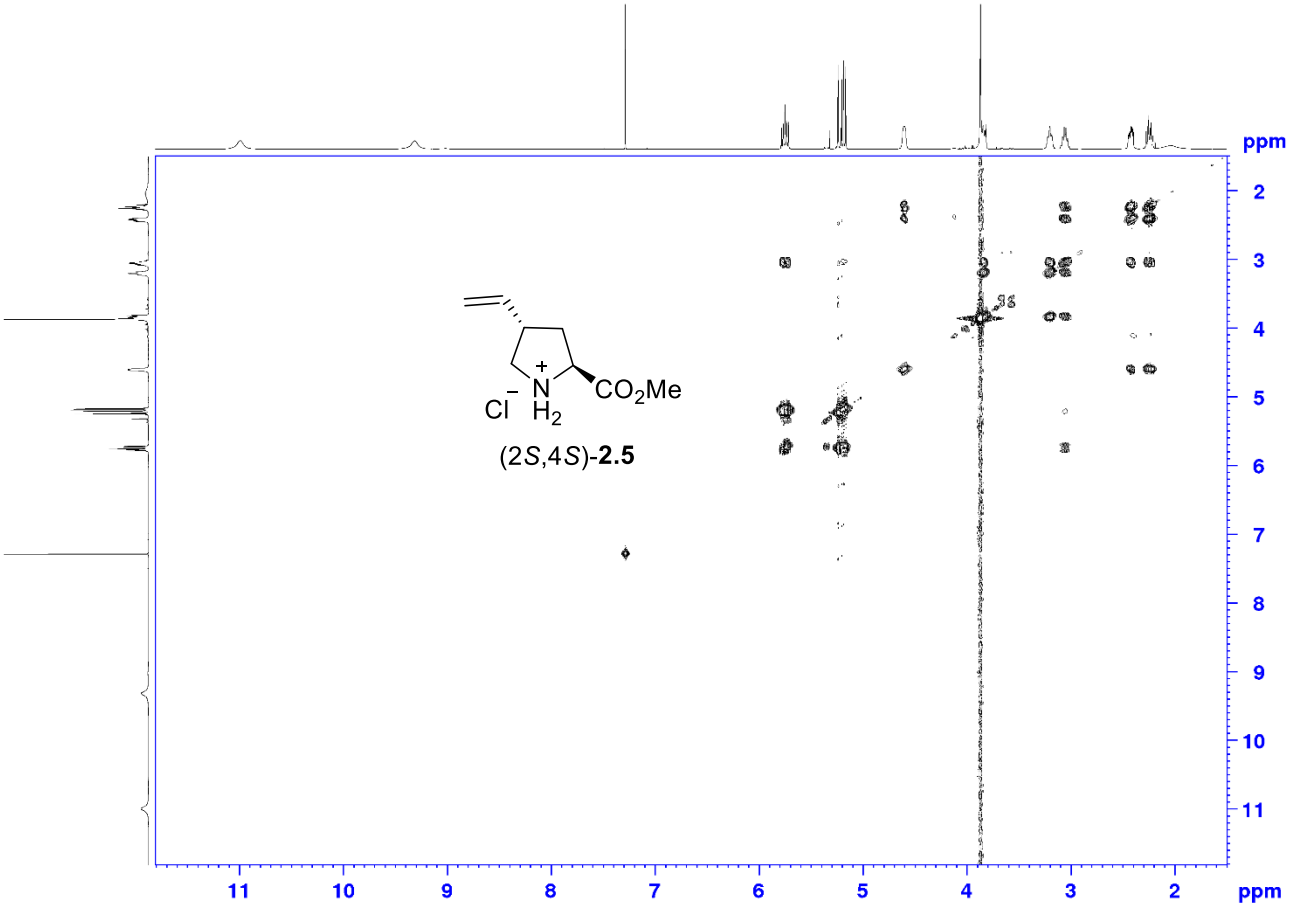

HSQC NMR 500 MHz
Solvent: $CDCl_3$

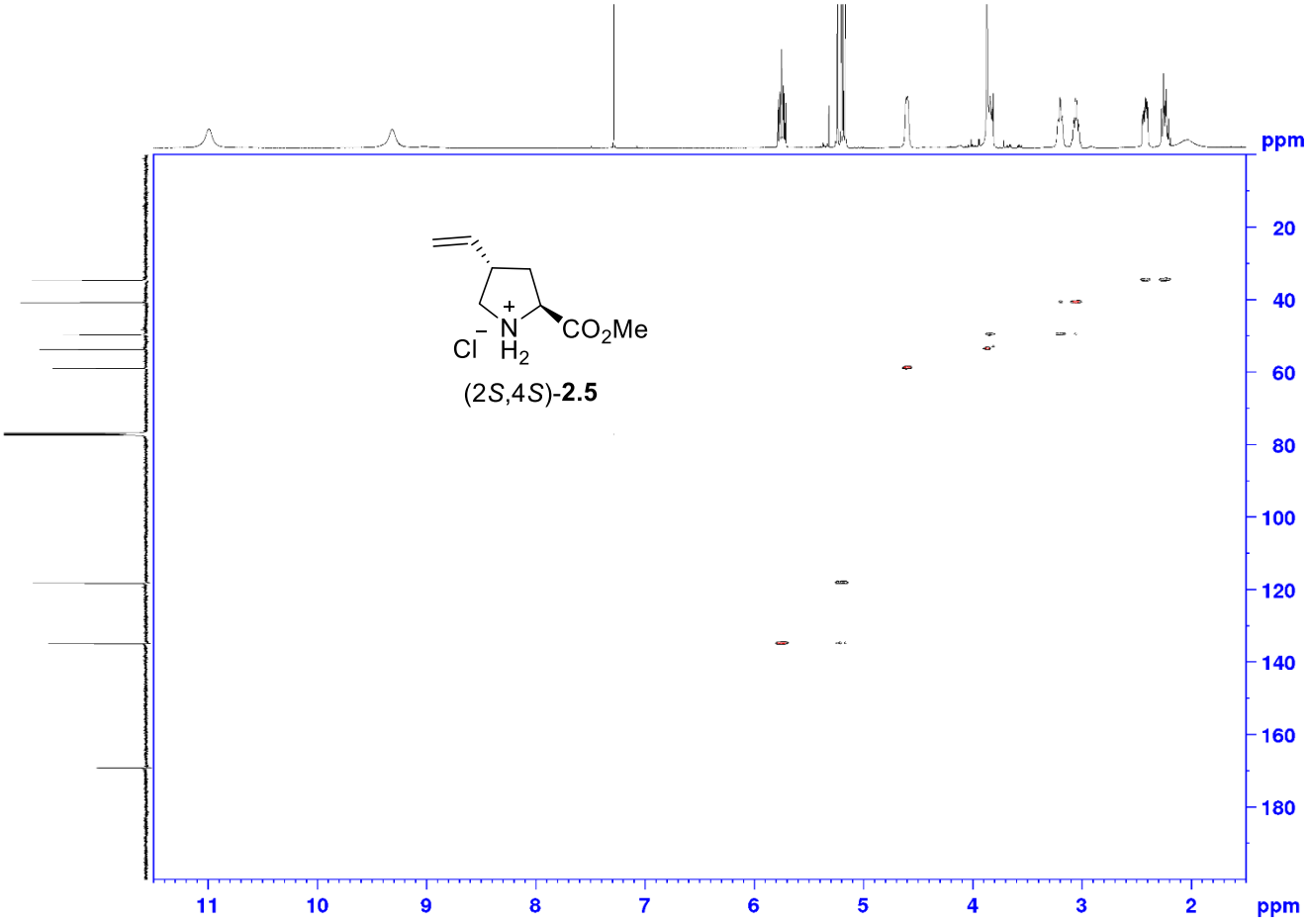

NOESY NMR 500 MHz
Solvent: $CDCl_3$

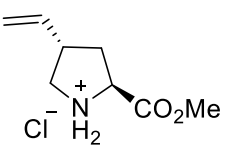

(2*S*,4*S*)-**2.5**

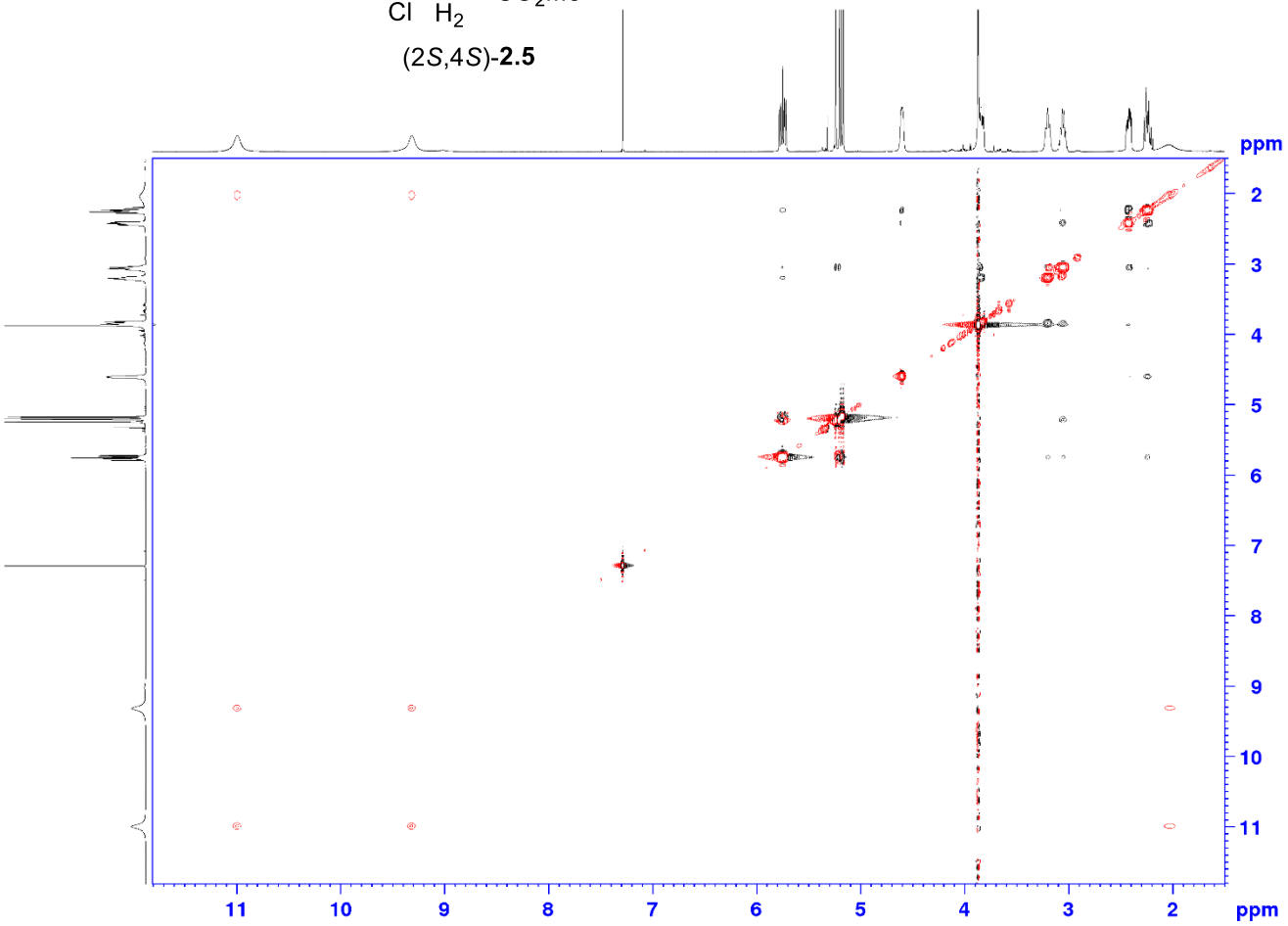

^{1}H NMR 500 MHz
Solvent: $CDCl_3$

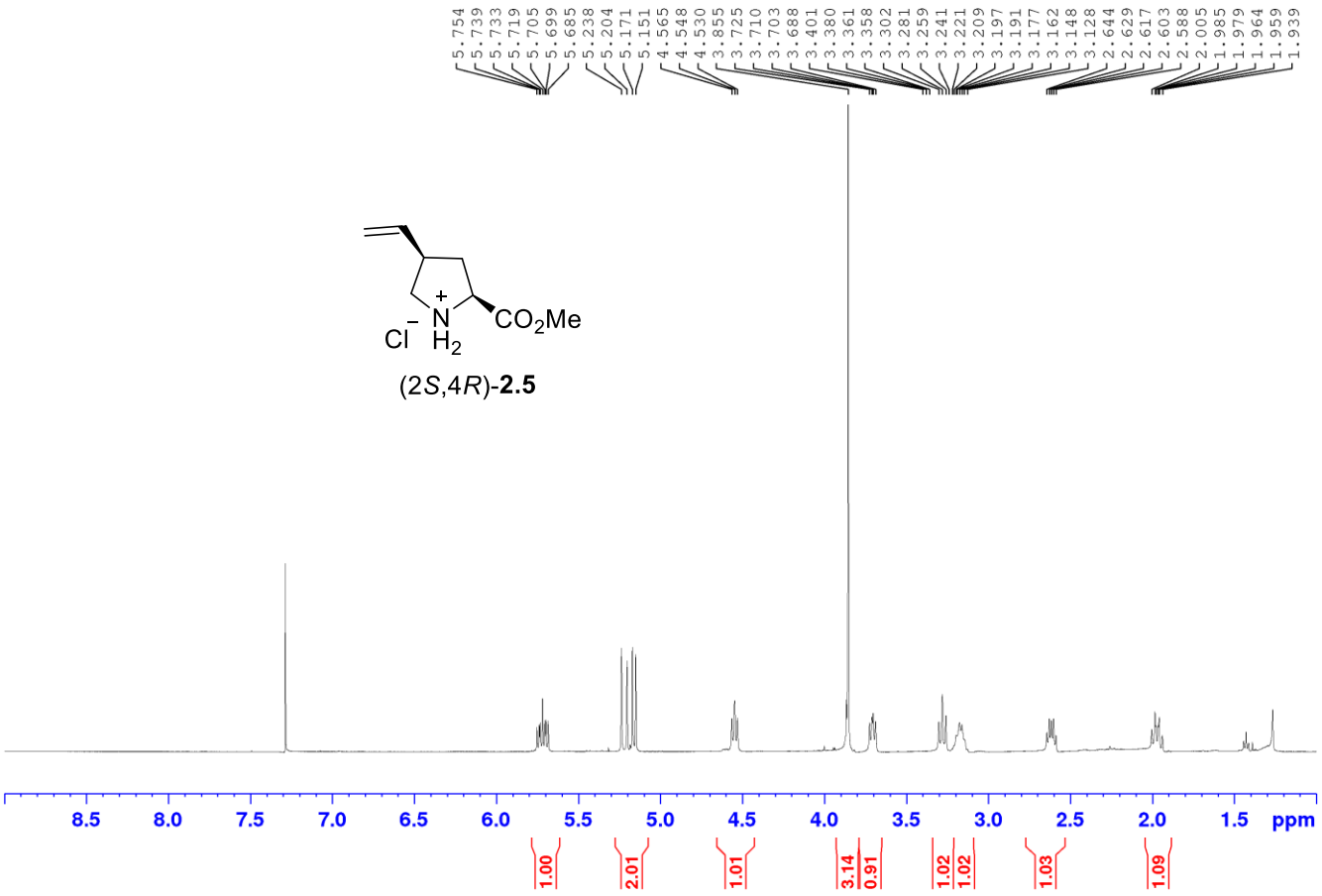

(2*S*,4*R*)-**2.5**

^{13}C NMR 125 MHz
Solvent: $CDCl_3$

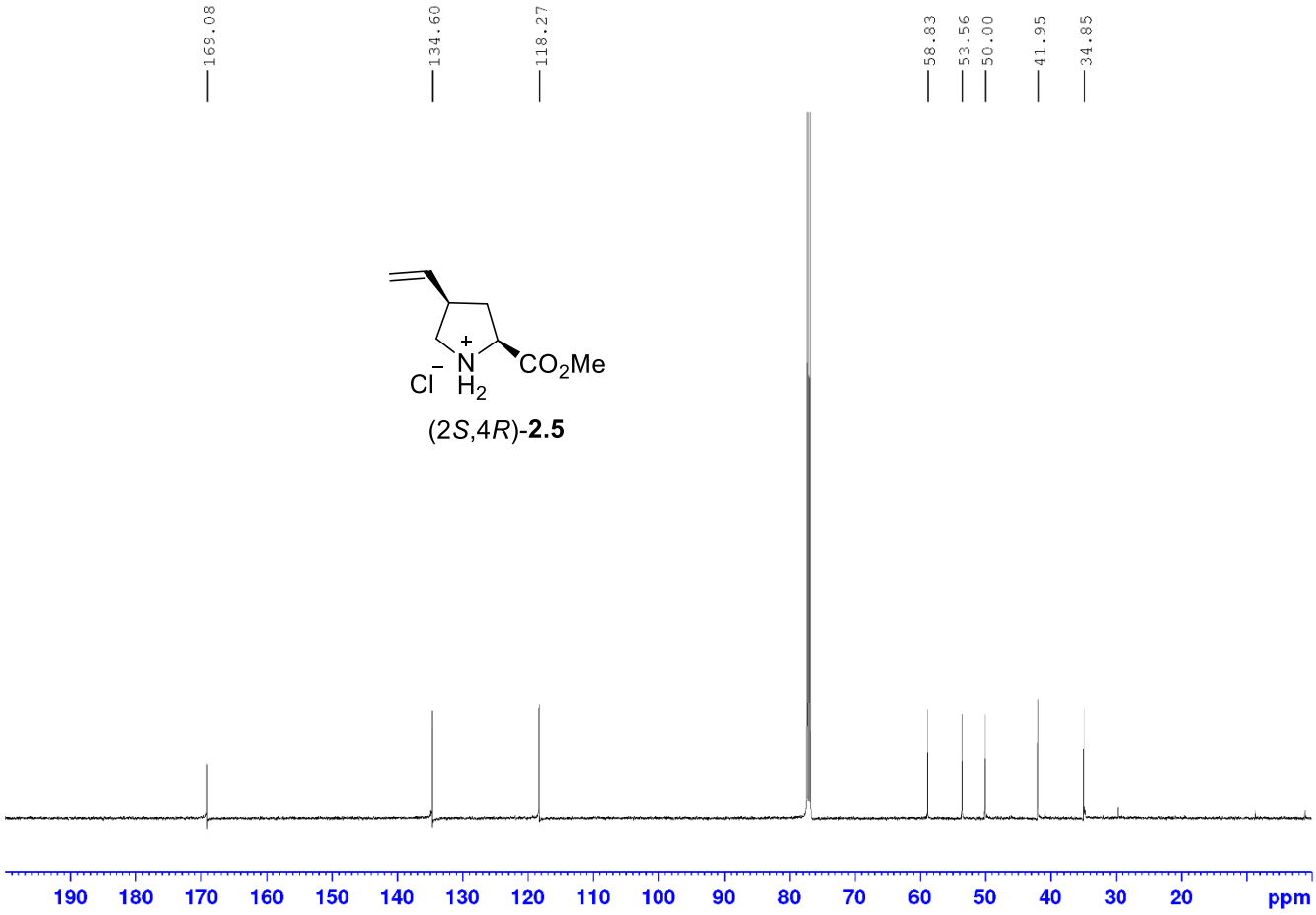

(2*S*,4*R*)-**2.5**

COSY NMR 500 MHz
Solvent: $CDCl_3$

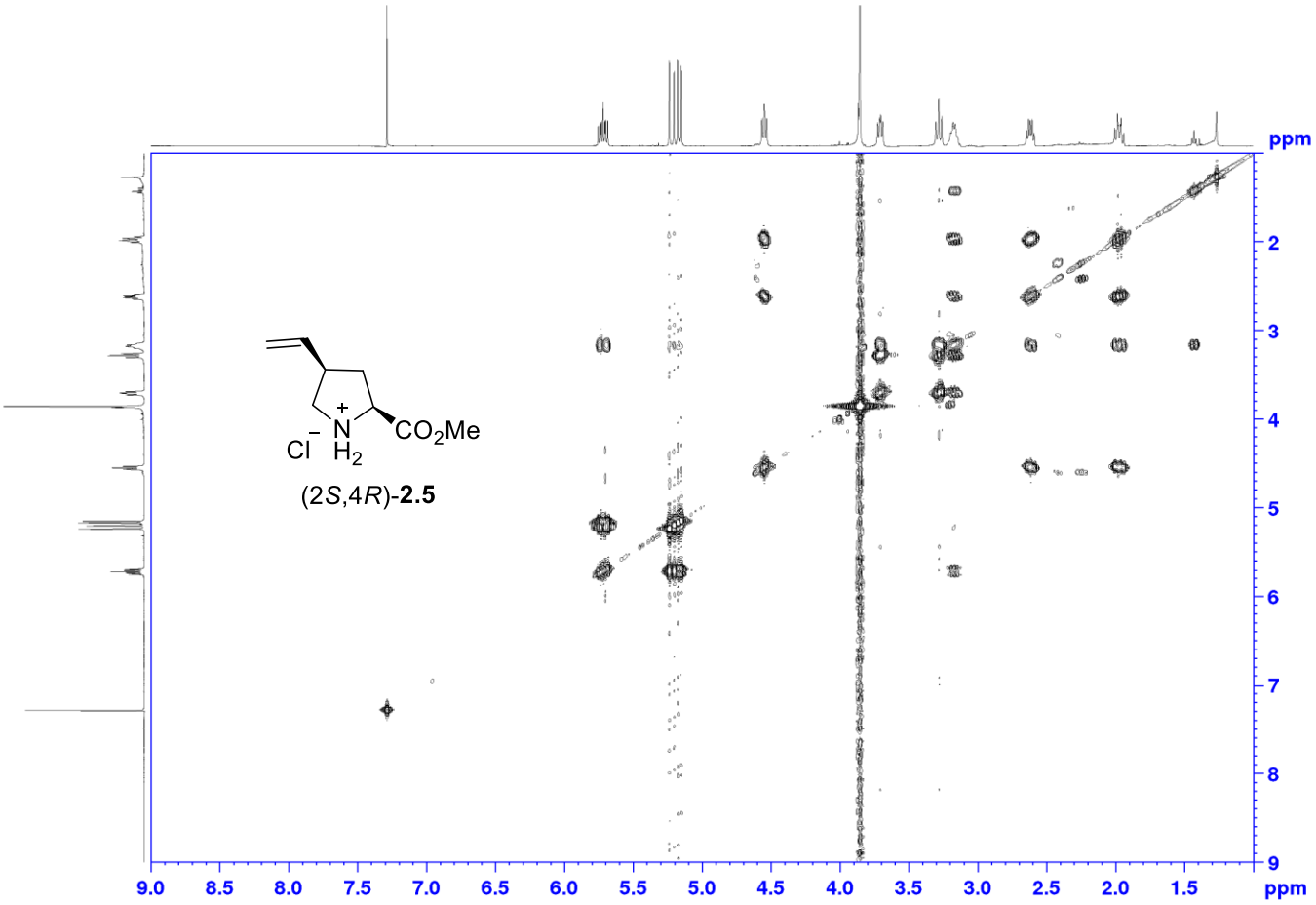

HSQC NMR 500 MHz
Solvent: $CDCl_3$

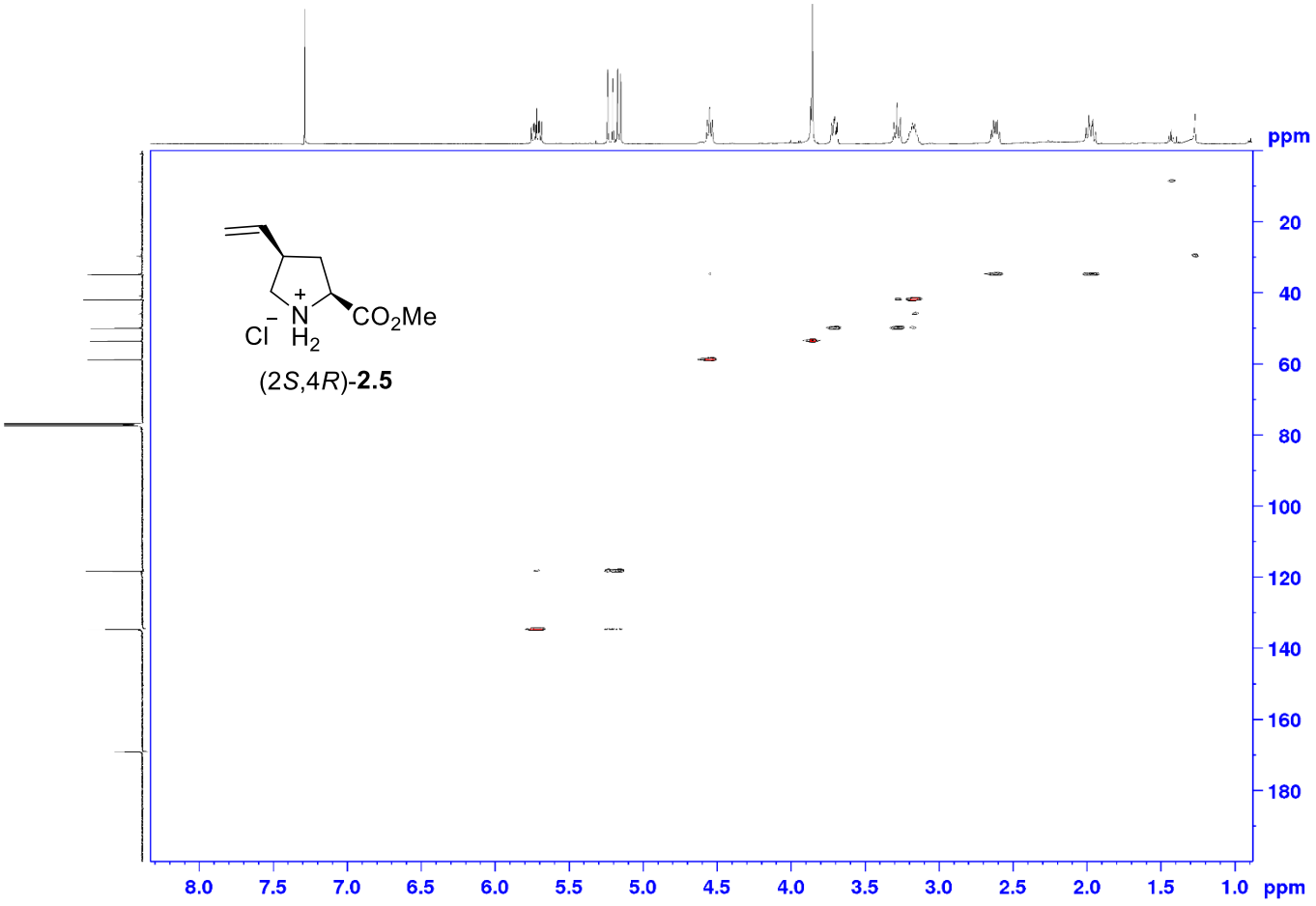

NOESY NMR 500 MHz
Solvent: $CDCl_3$

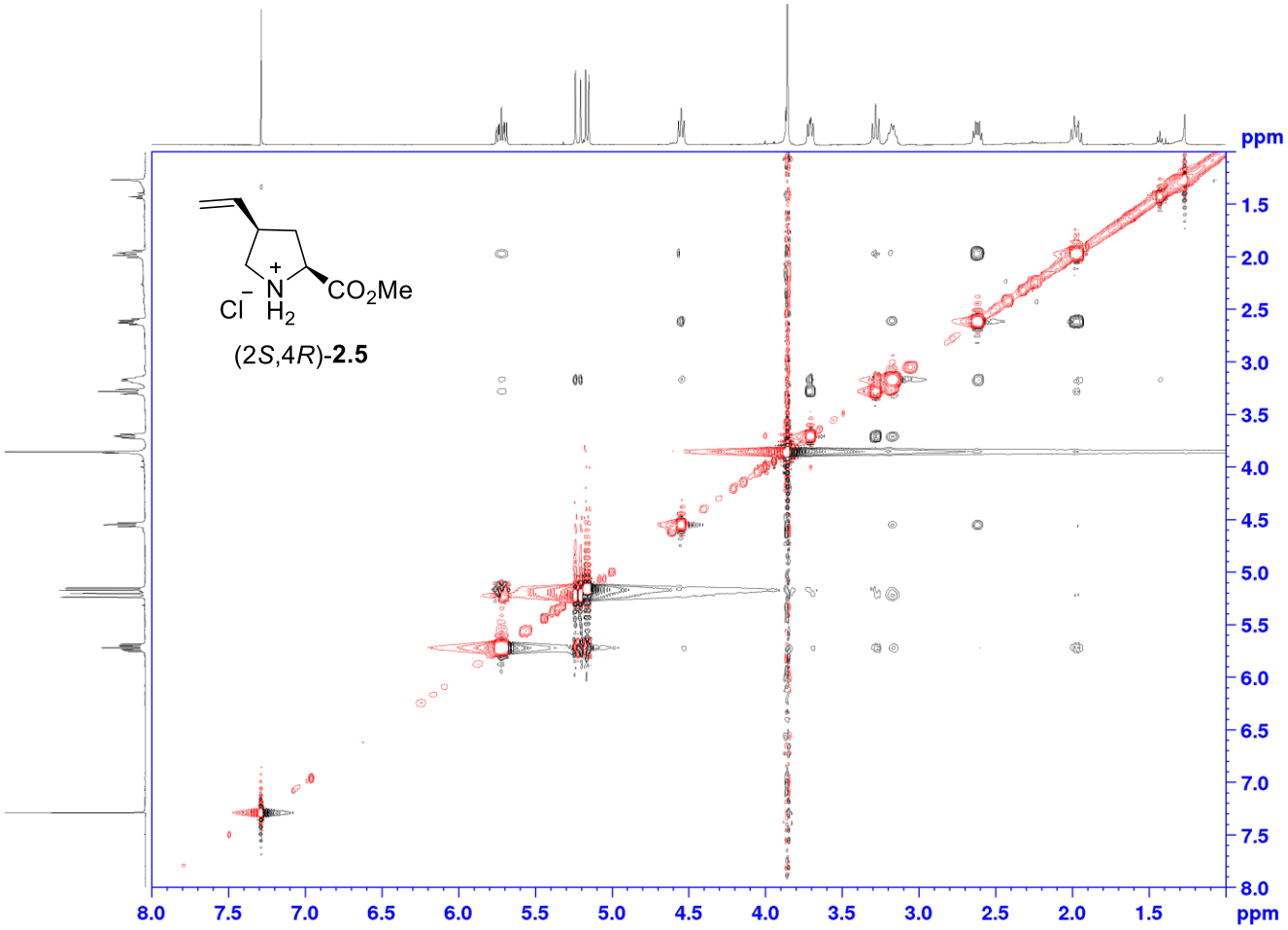

Spectral data for Article 2

^{1}H *NMR 500 MHz*

Solvent: $CDCl_3$

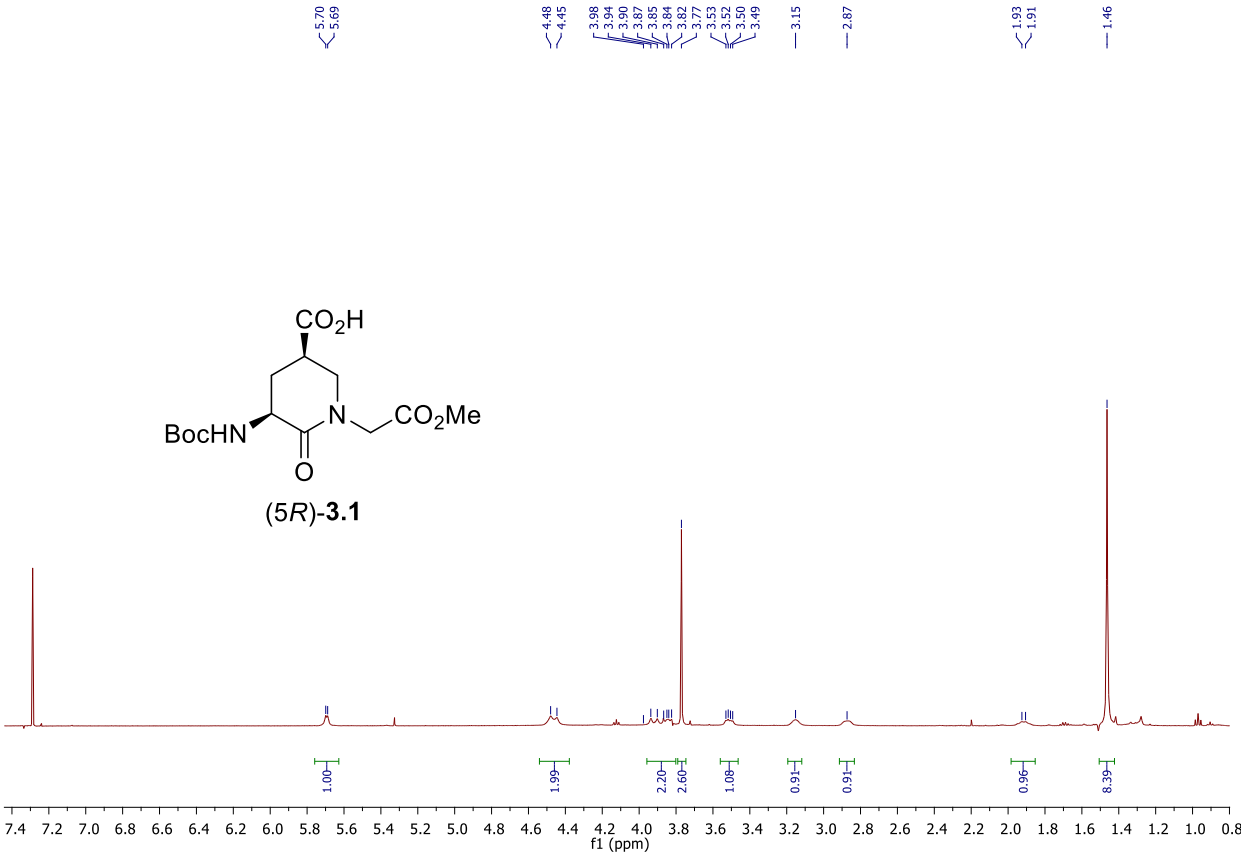

^{13}C *NMR 125 MHz*

Solvent: $CDCl_3$

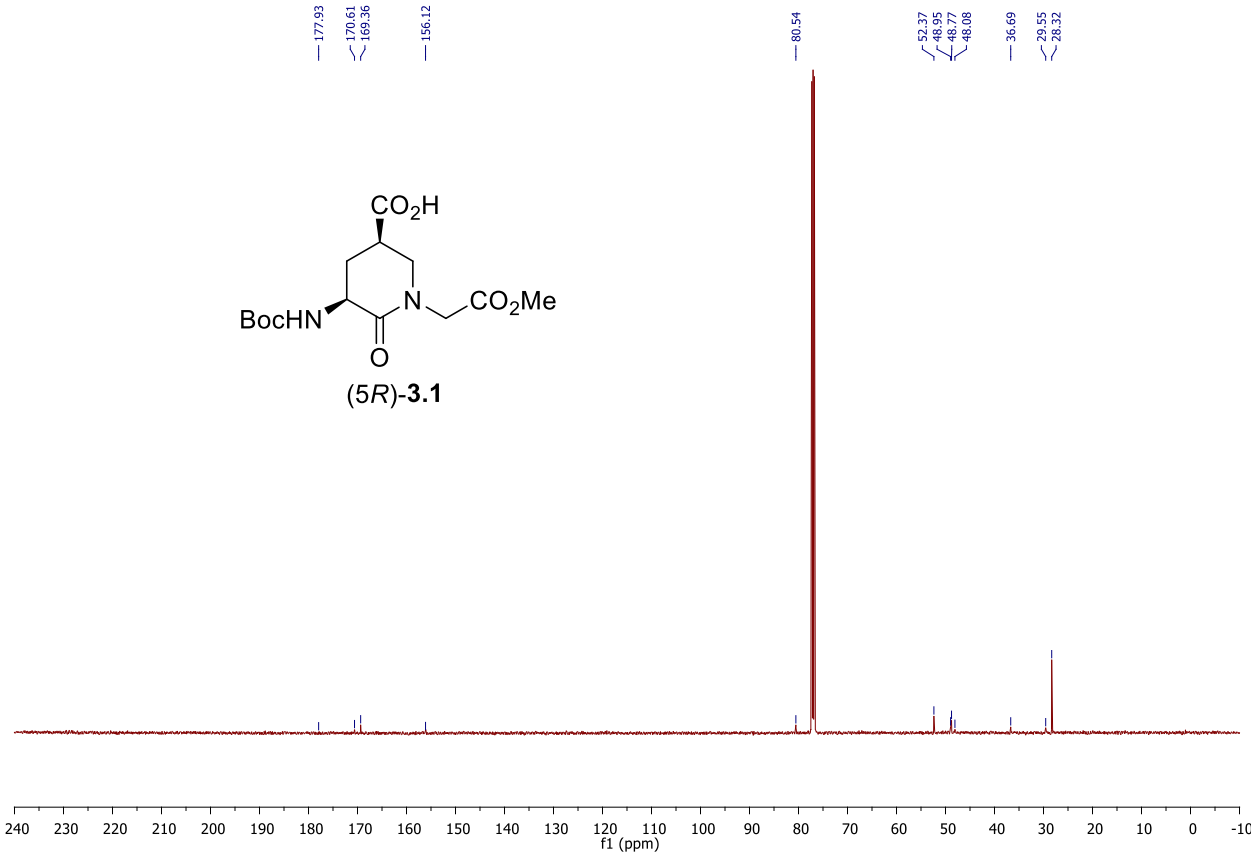

^{1}H *NMR 500 MHz*

Solvent: $CDCl_3$

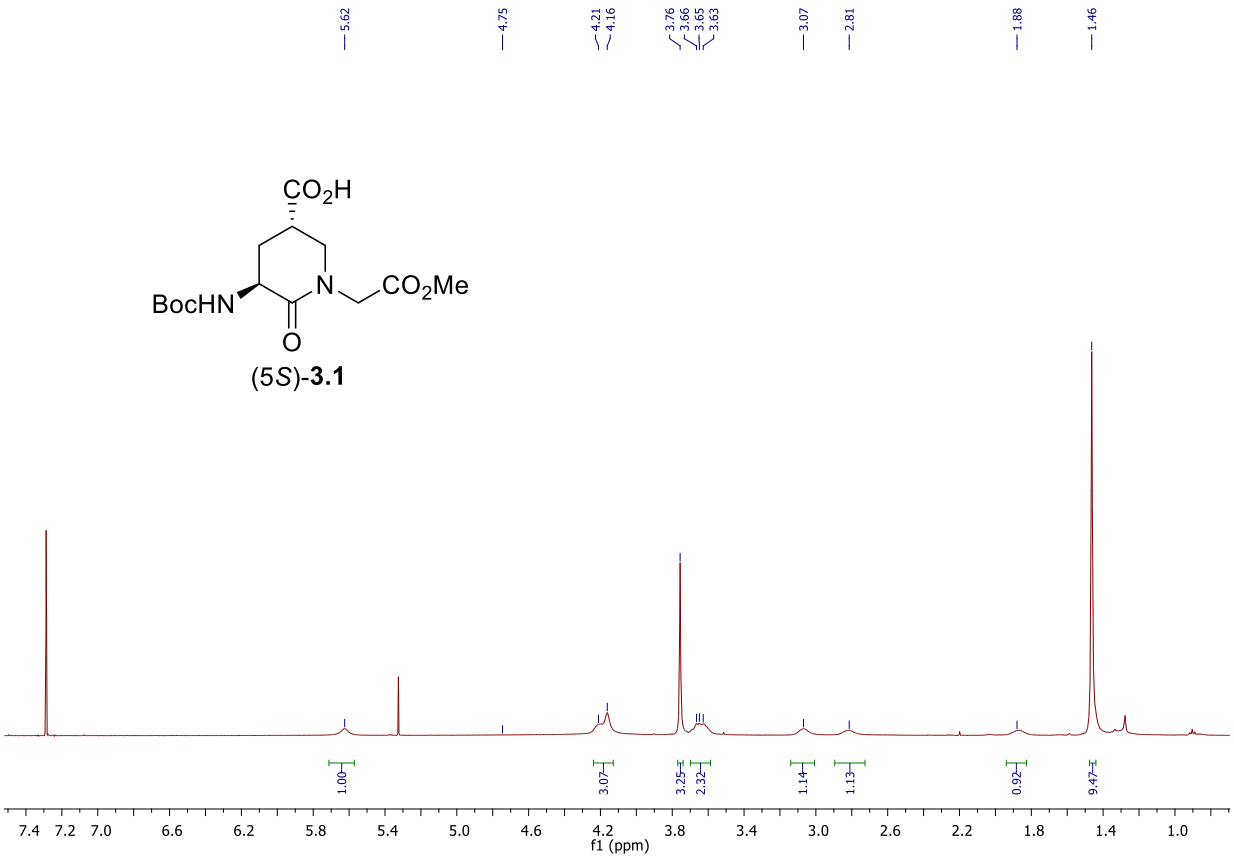

^{13}C *NMR 125 MHz*

Solvent: $CDCl_3$

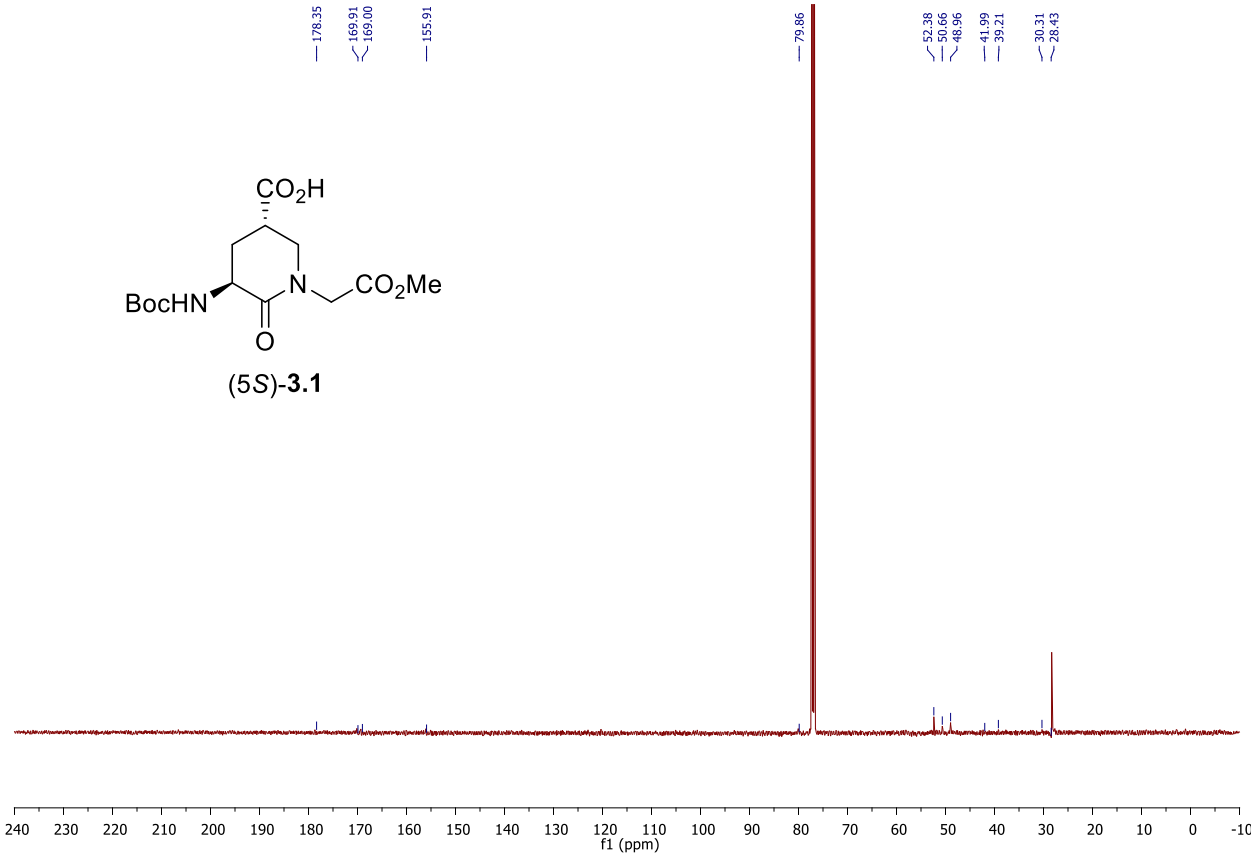

(5*S*)-**3.1**

^{1}H *NMR 500 MHz*

Solvent: $CDCl_3$

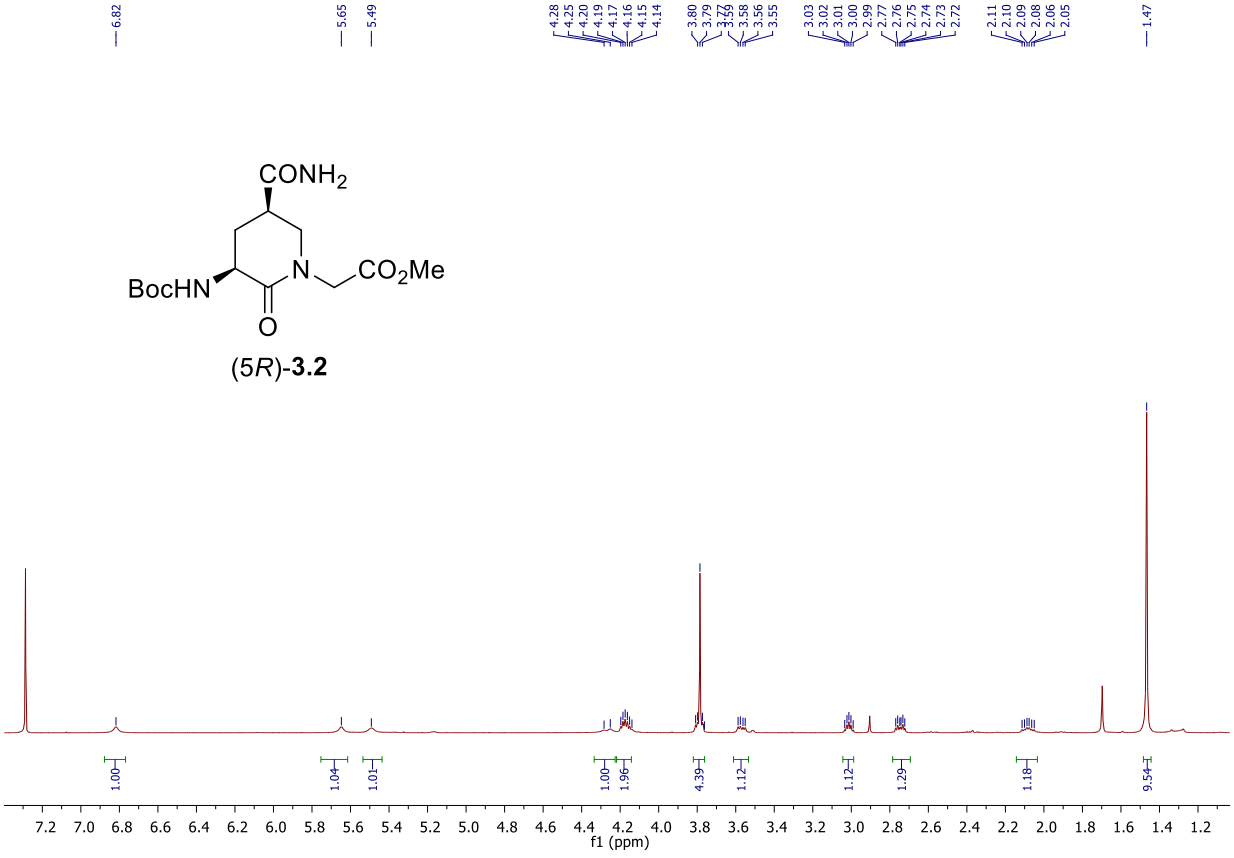

(5*R*)-**3.2**

^{13}C *NMR 125 MHz*

Solvent: $CDCl_3$

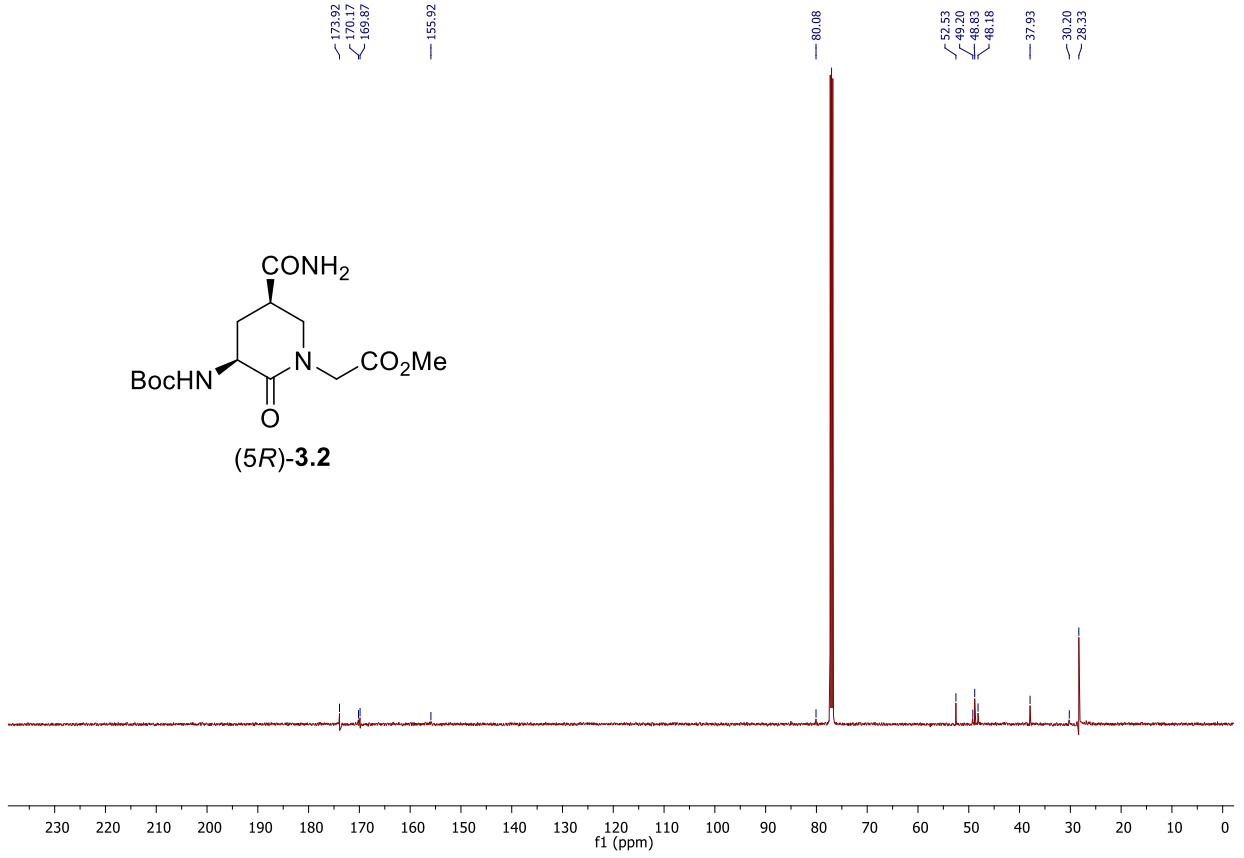

^{1}H *NMR 500 MHz*

Solvent: $CDCl_3$

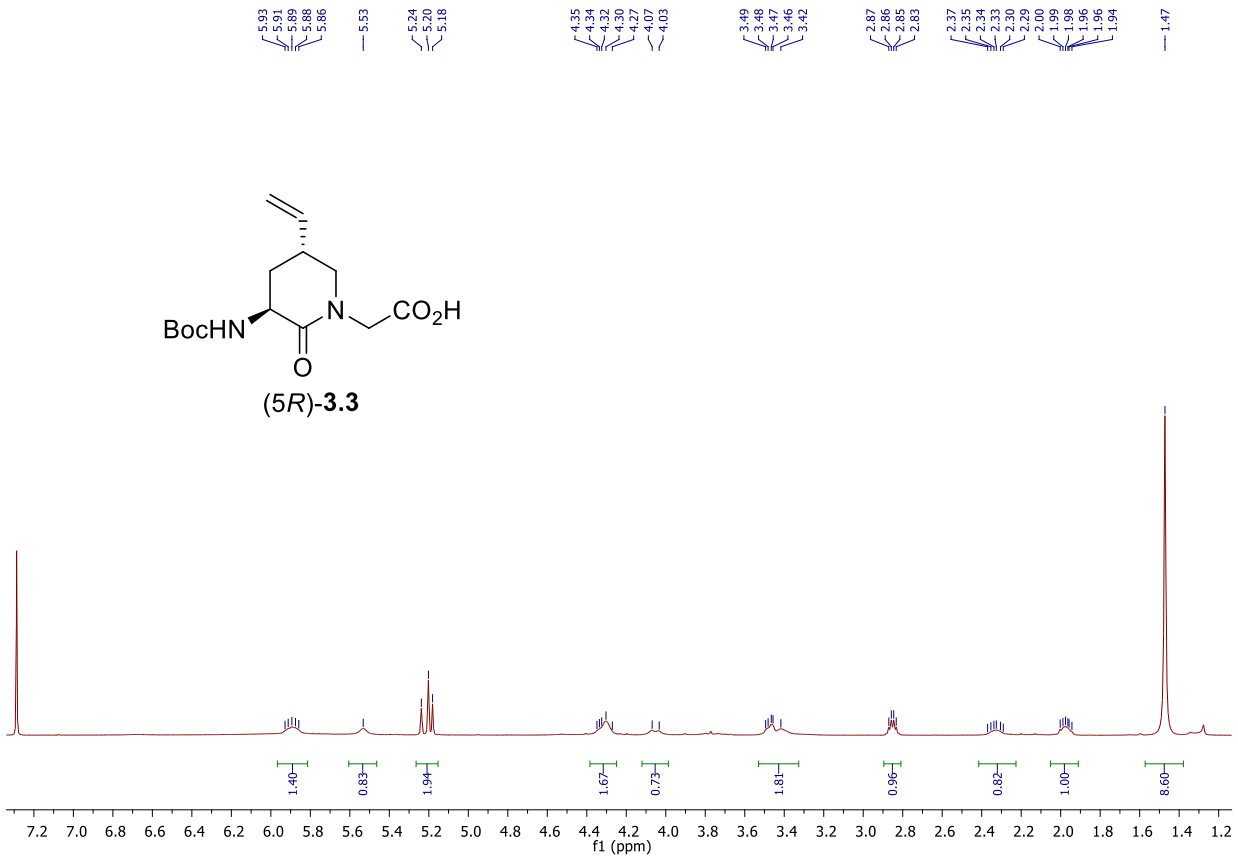

^{13}C *NMR 125 MHz*

Solvent: $CDCl_3$

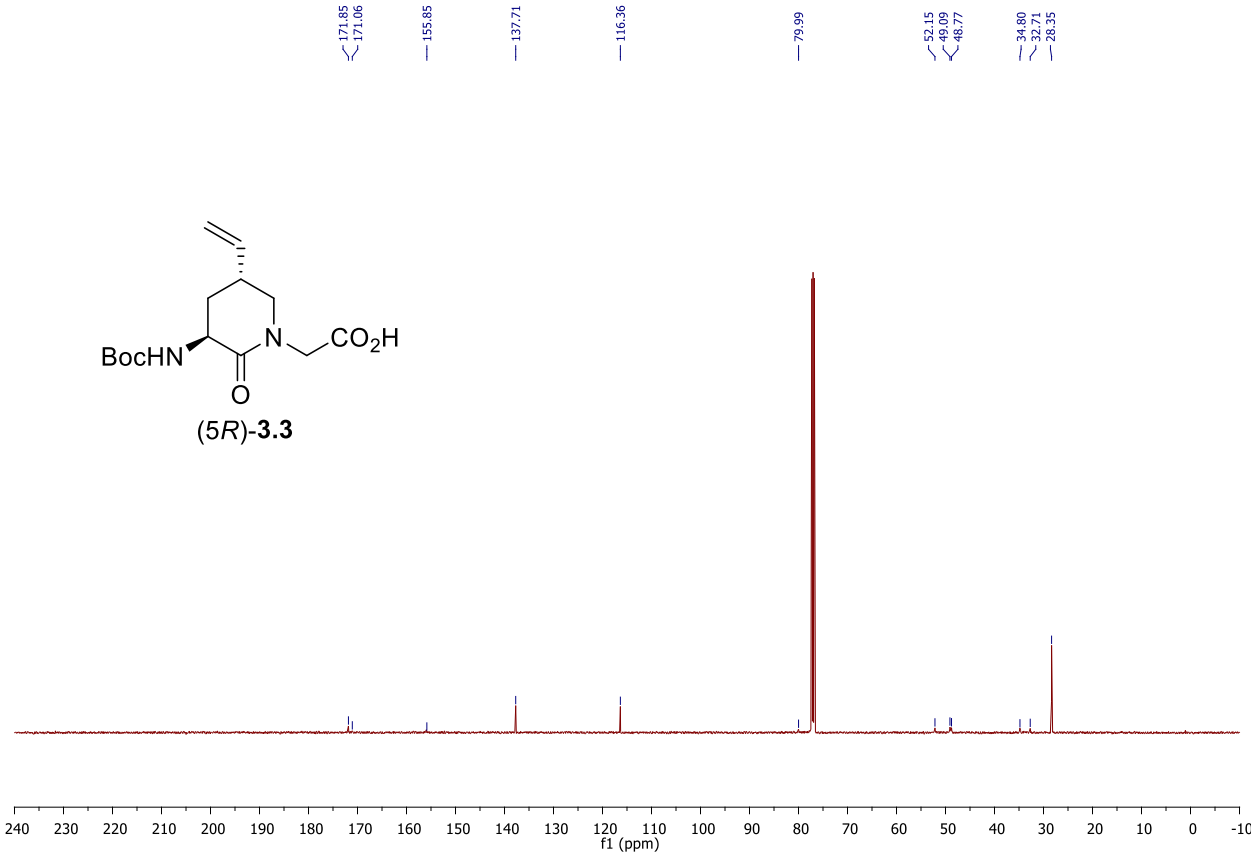

^{1}H *NMR 500 MHz*

Solvent: $CDCl_3$

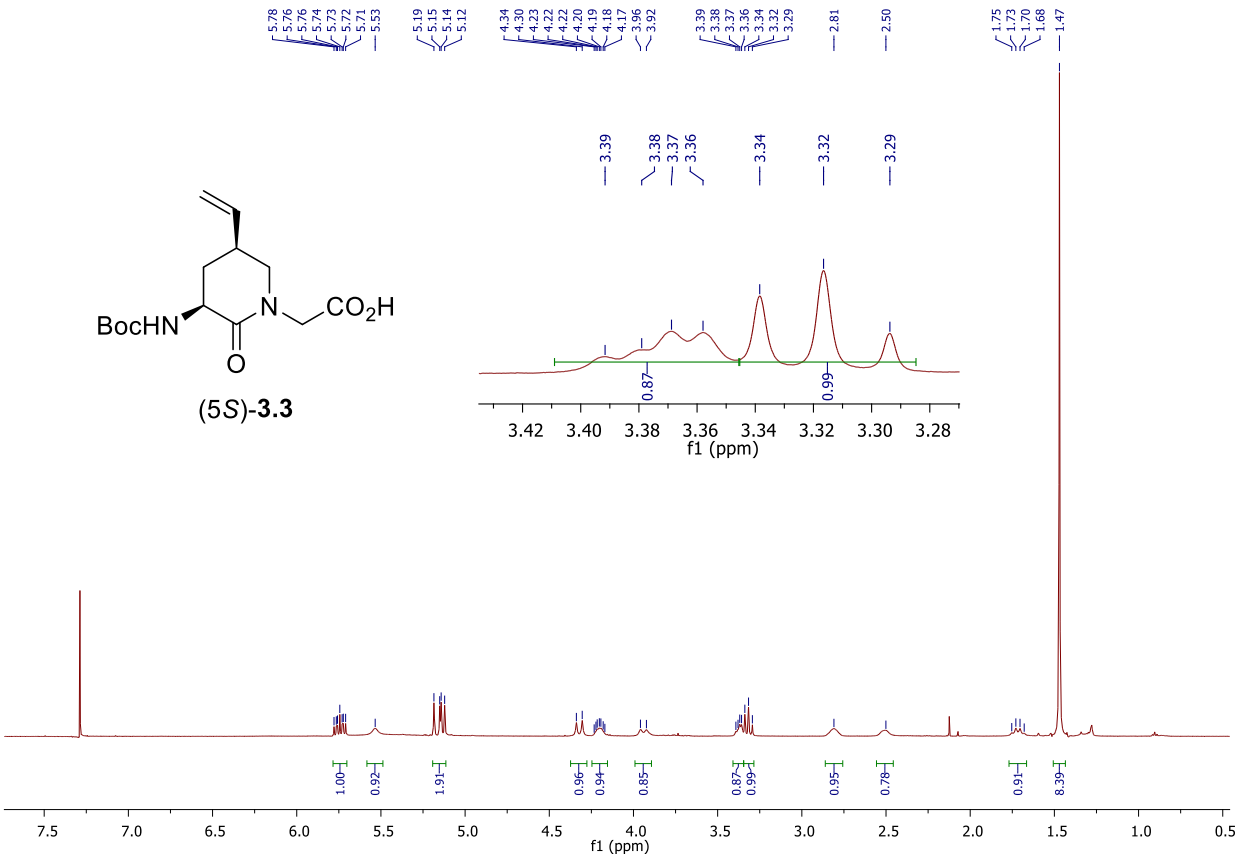

^{13}C *NMR 125 MHz*

Solvent: $CDCl_3$

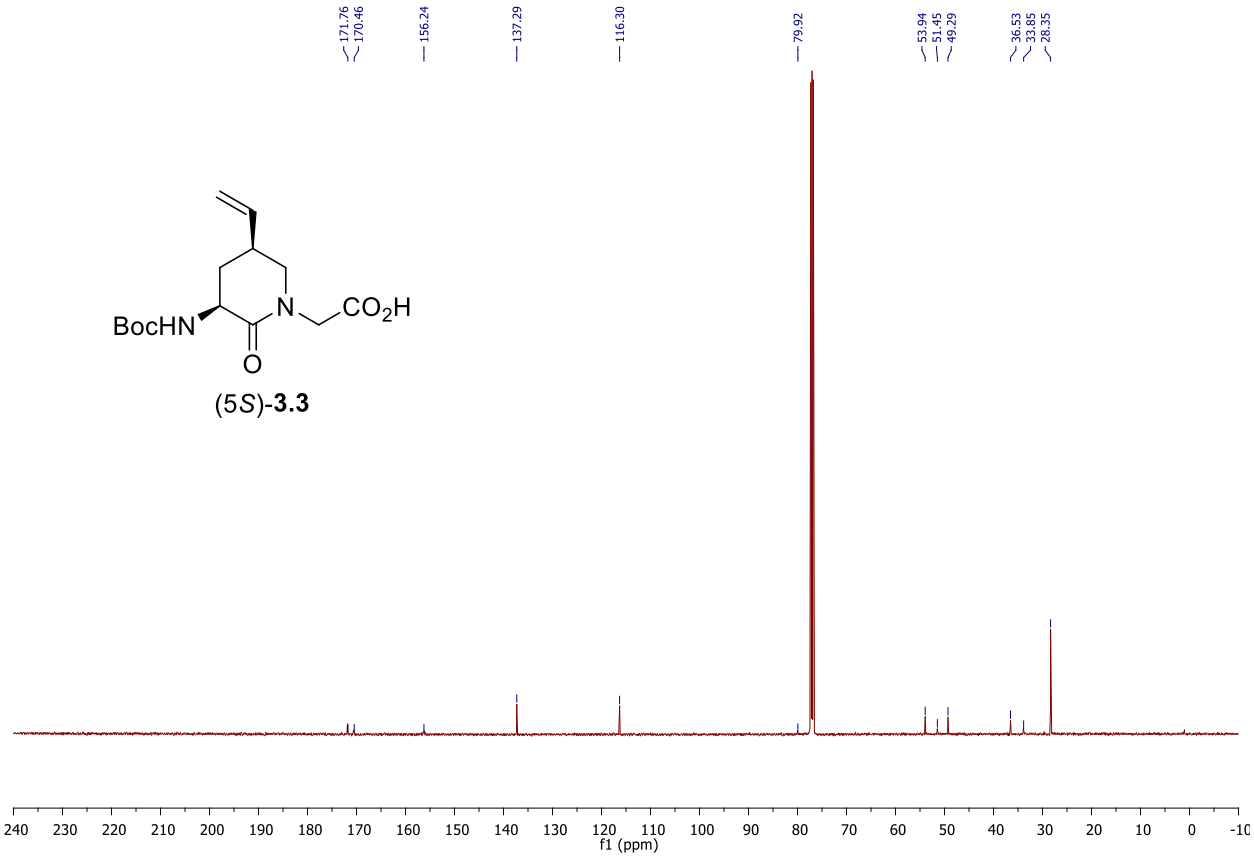

^{1}H *NMR 500 MHz*

Solvent: $CDCl_3$

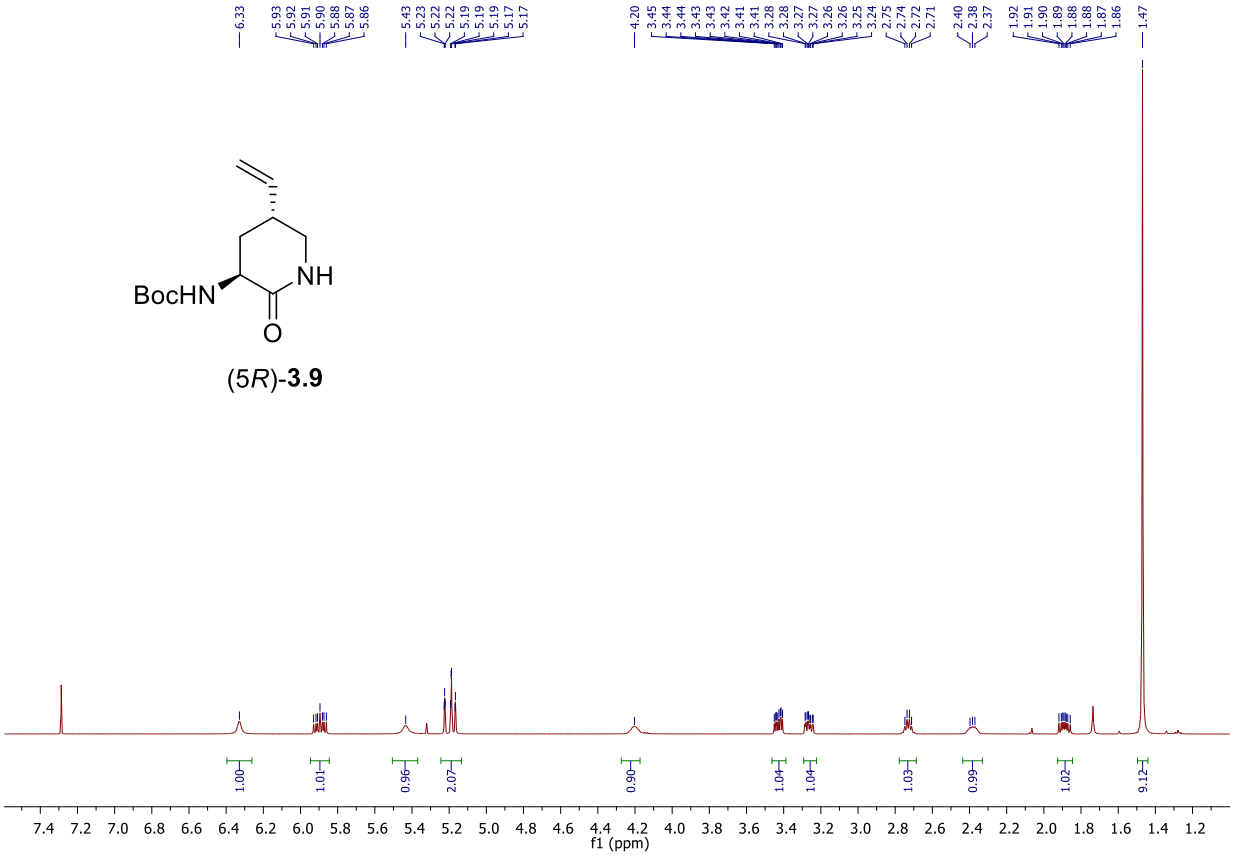

(5*R*)-**3.9**

^{13}C *NMR 125 MHz*

Solvent: $CDCl_3$

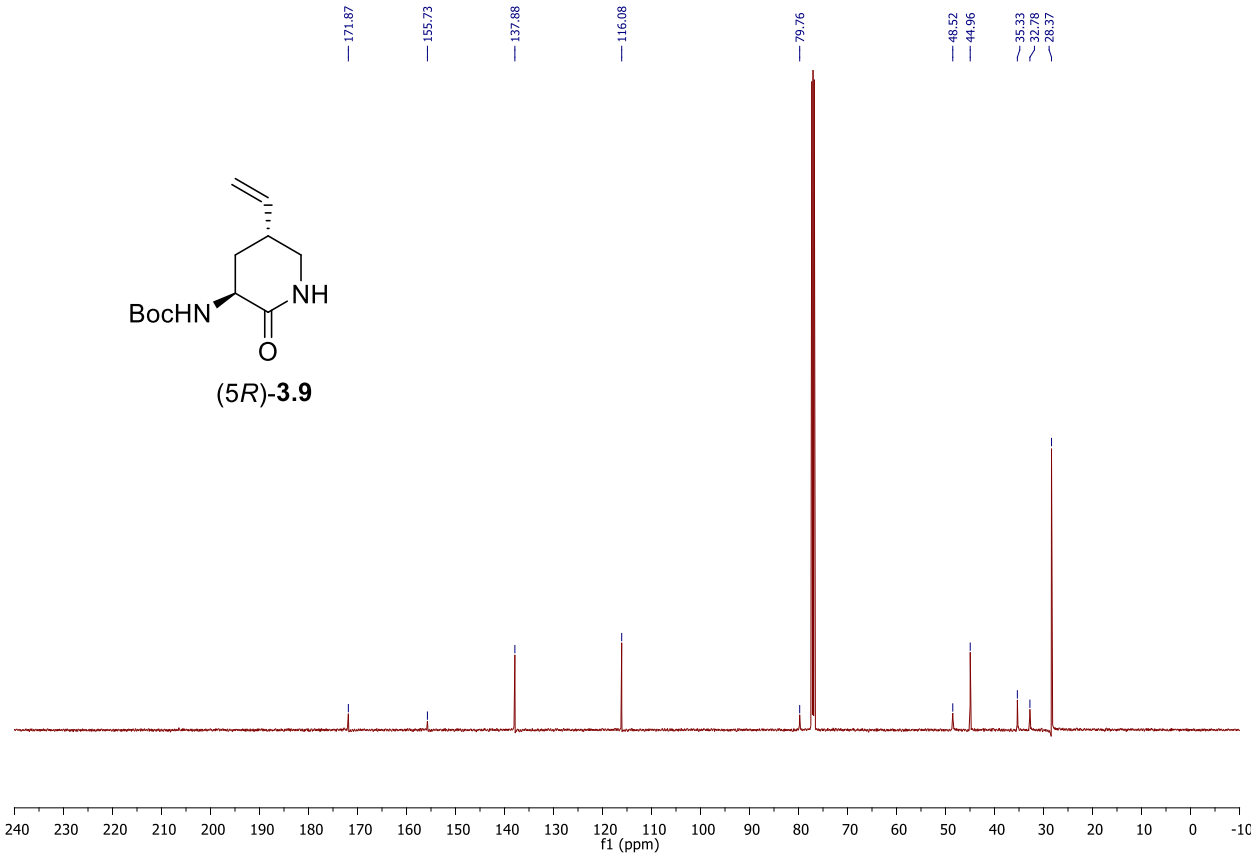

^{1}H *NMR 500 MHz*

Solvent: $CDCl_3$

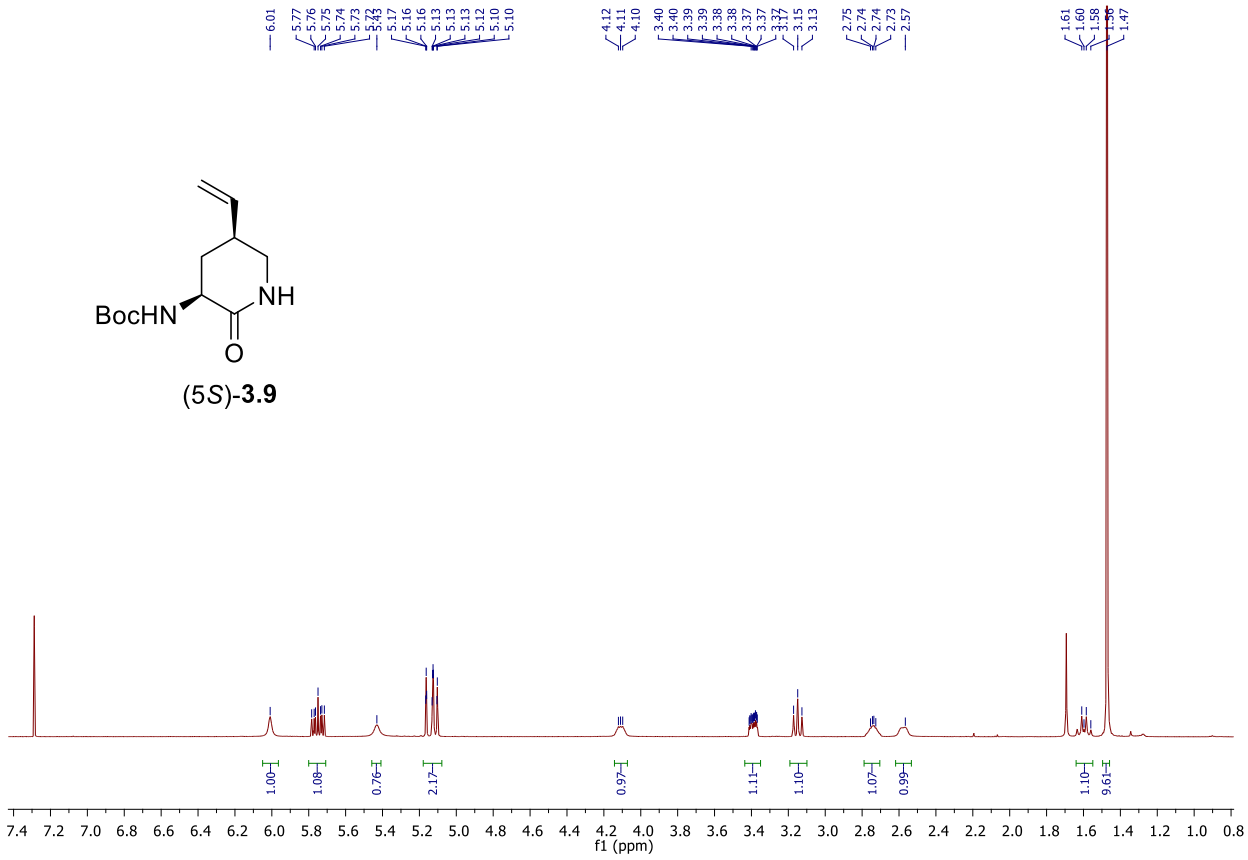

^{13}C *NMR 125 MHz*

Solvent: $CDCl_3$

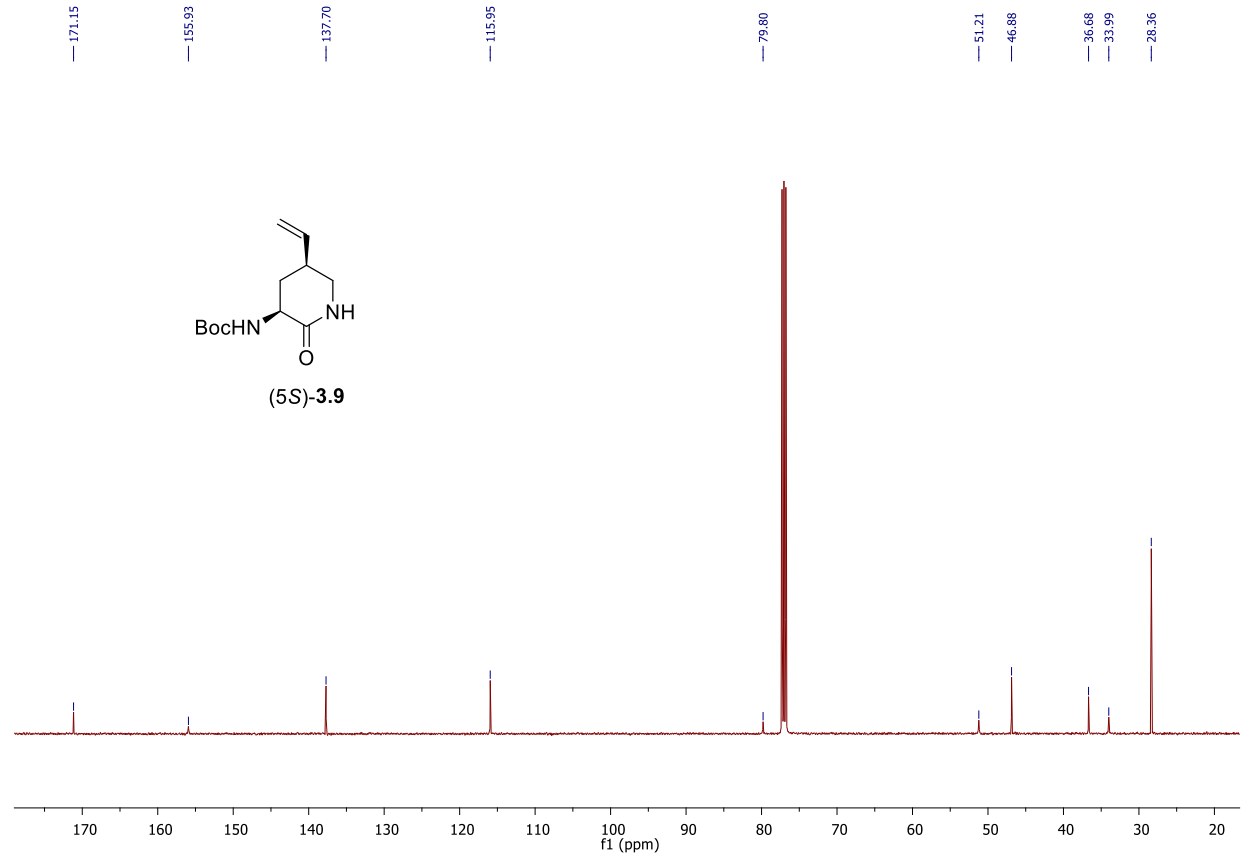

(5*S*)-**3.9**

^{1}H *NMR 500 MHz*

Solvent: $CDCl_3$

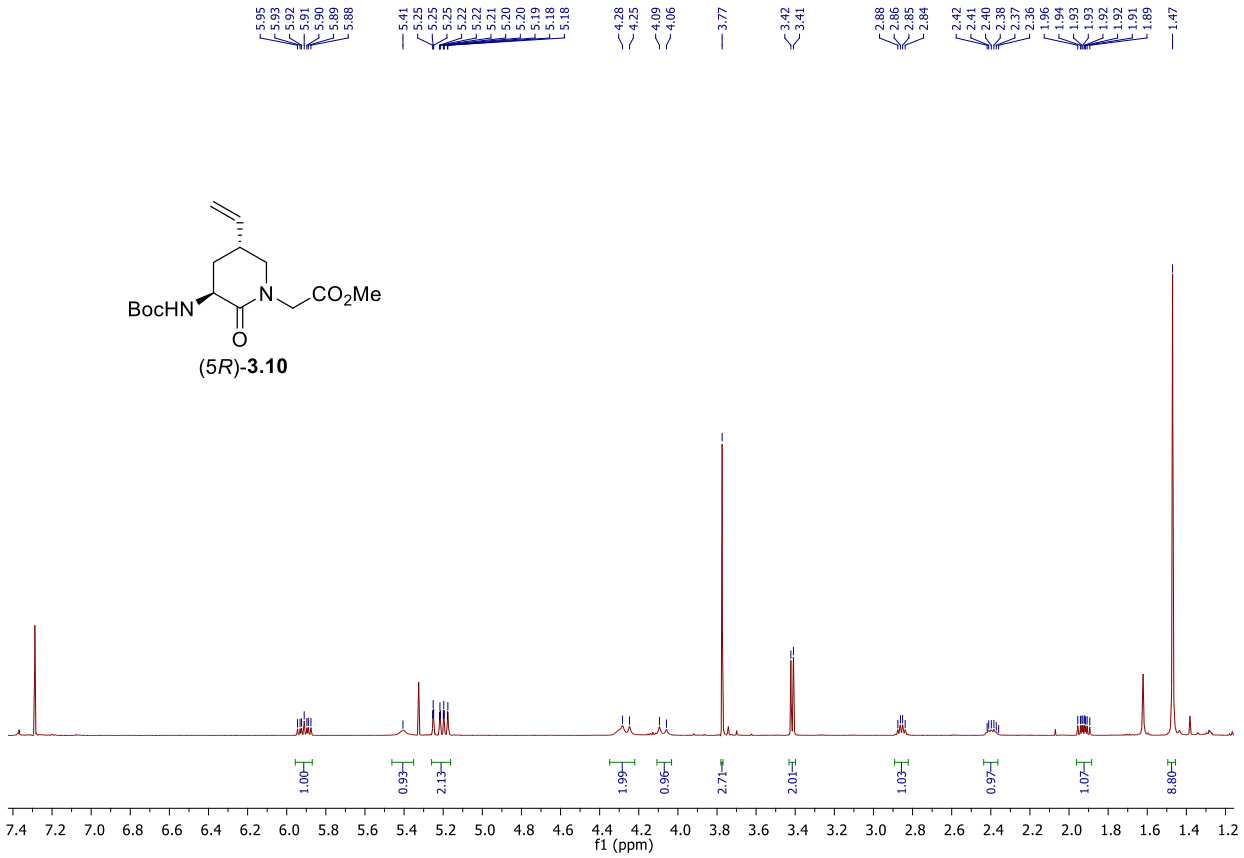

^{13}C *NMR 125 MHz*

Solvent: $CDCl_3$

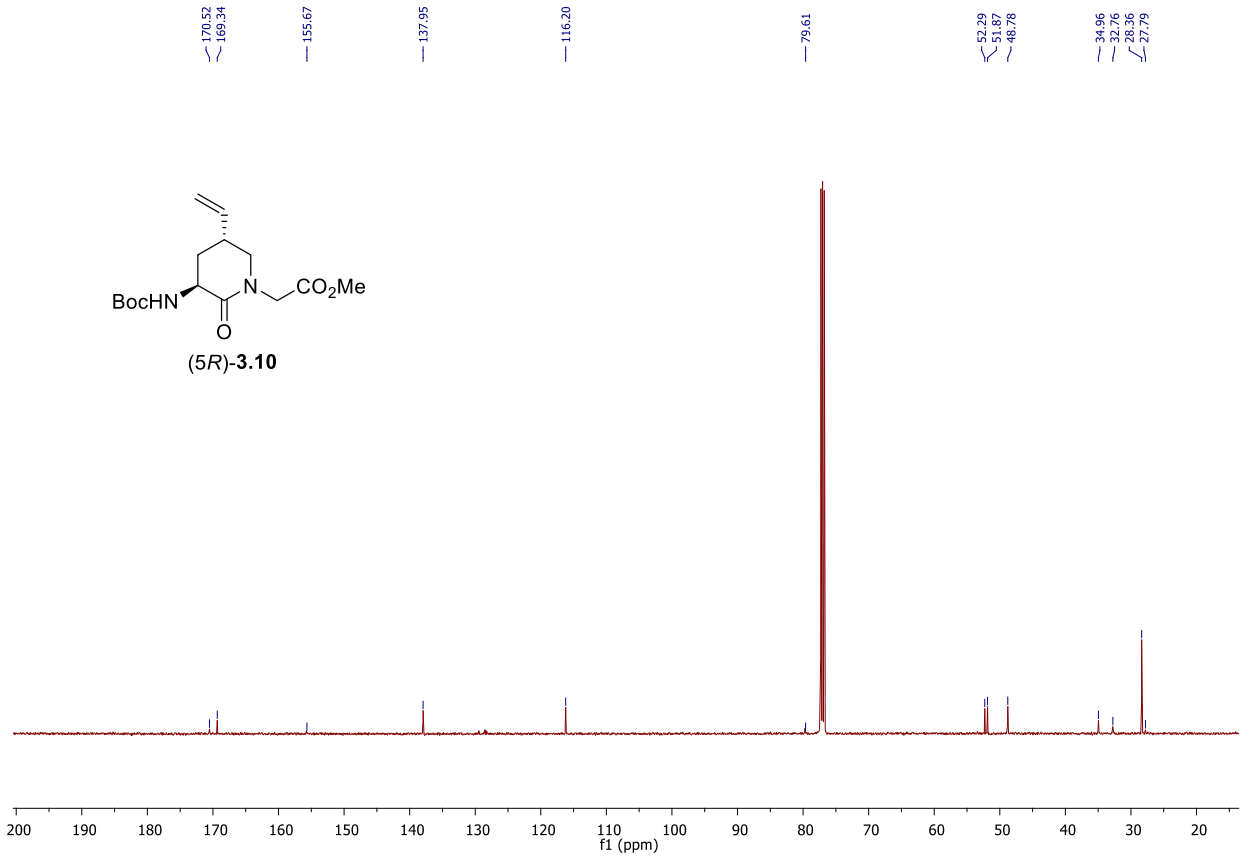

^{1}H *NMR 500 MHz*

Solvent: $CDCl_3$

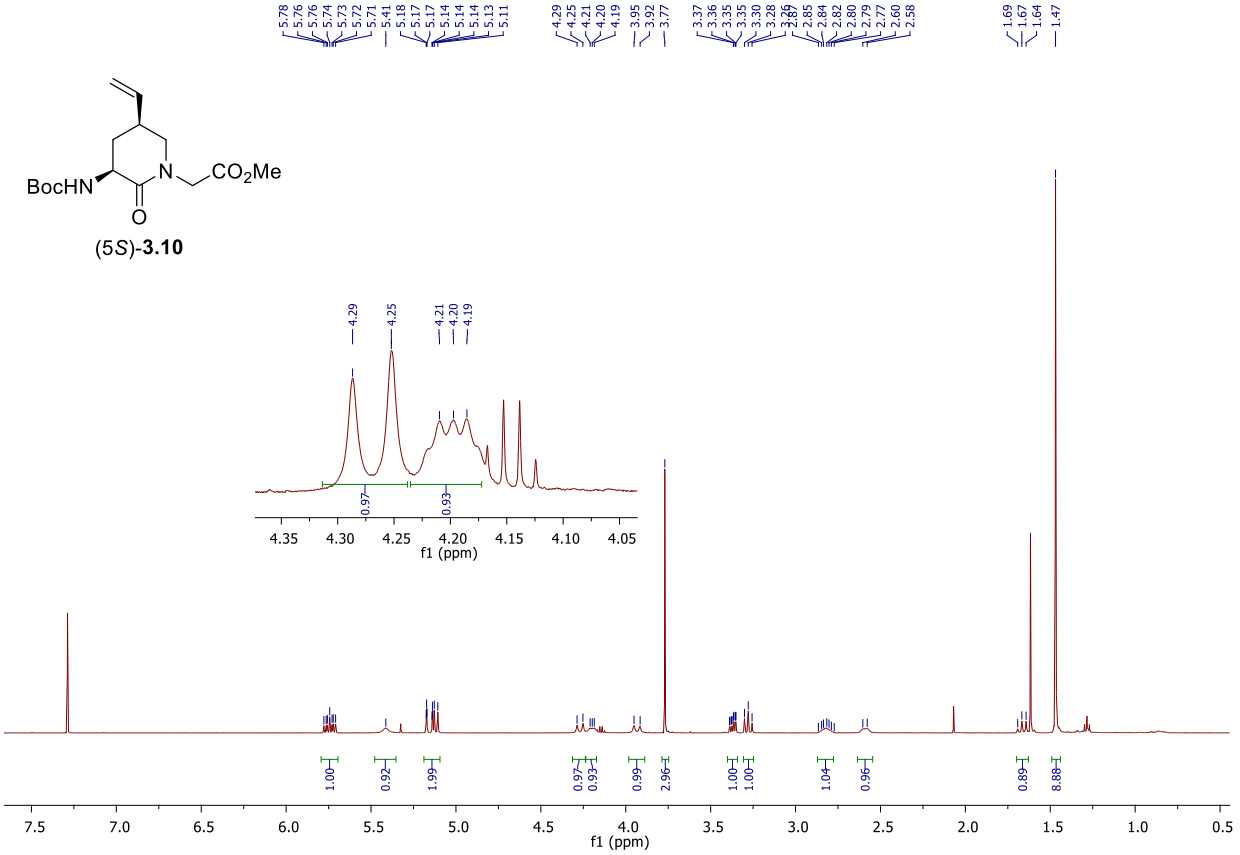

^{13}C *NMR 125 MHz*

Solvent: $CDCl_3$

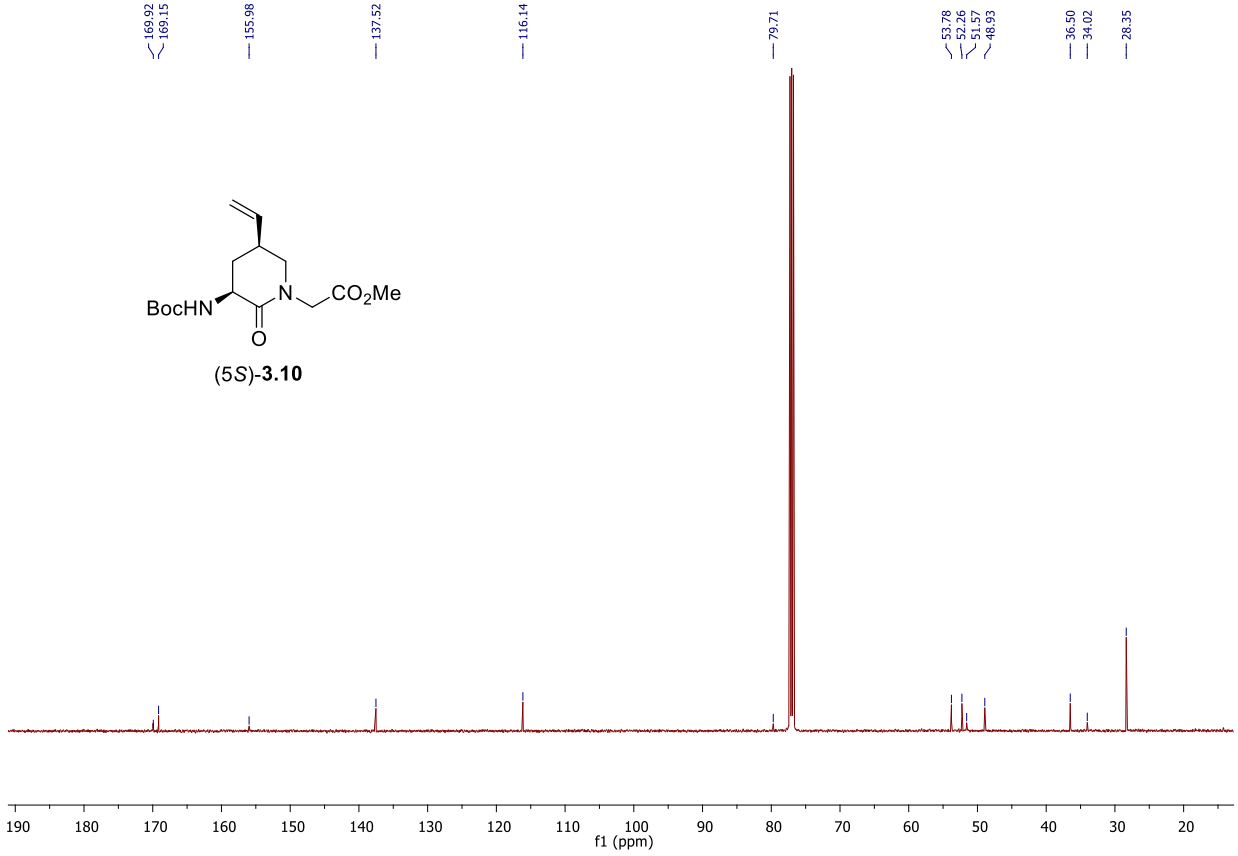

(5*S*)-**3.10**

Spectral data for Article 3

4.7. Experimental Section

4.7.1. Myometrial contraction preparations:

Pregnant CD-1 mice (16-17 days gestation, term 19 days) were obtained from Charles River Inc. Animals were used according to a protocol of the Animal Care Committee of CHU Sainte-Justine along the principles of the Guide for the Care and Use of Experimental Animals of the Canadian Council on Animal Care. The animals were maintained on standard laboratory chow under a 12h:12h light: dark cycle and given free access to chow and water.

Uterus from CD-1 mice were obtained from animals immediately after term delivery under anesthesia (2.5% isoflurane). Briefly, a midline abdominal incision was made. The uterine horns were rapidly excised, carefully cleansed of surrounding connective tissues and removed. Longitudinal myometrial strips (2 to 3 mm wide and 1 cm long) were dissected free from the uterus and mounted isometrically in an organ tissue baths (*Kent* Scientific Corp. *Litchfield*, *CT, USA*). Initial tension was set at 2 g. The tissue baths contain 20 mL of Krebs buffer of the following composition (in mM): 118 NaCl, 4.7 KCl, 2.5 $CaCl_2$, 0.9 $MgSO_4$, 1 KH_2PO_4, 11.1 glucose, and 23 $NaHCO_3$ (pH 7.4). The buffer was equilibrated with 95% oxygen/5% carbon dioxide at 37°C. Isometric tension was measured by a force transducer and recorded by BIOPAC data acquisition system (BIOPAC MP150, BIOPAC systems Inc, Goleta, CA, USA). Experiments were begun after 1hour equilibration. Mean tension of spontaneous contractions was measured using a BIOPAC digital polygraph system (AcqKnowledge 4.2); parameters were determined after addition of $PGF_{2\alpha}$ (0.1 μM, Cayman Chemical Company) in the presence or absence of a 20 min pretreatment with different FP inhibitors.

4.7.2. Data analysis:

At the start of each experiment, mean tension of spontaneous myometrial contractions was considered as a reference response. Increase in mean tension (%) was expressed as percentages of (X/Y) x 100, in which X is the change in mean tension (g) induced by (0.1 μM) $PGF_{2\alpha}$ and Y is the initial reference response (g). The inhibition (%) was calculated as (A-B)/A x 100%, in which A is the increase in mean tension that was induced by (0.1 μM) $PGF_{2\alpha}$ in the absence of a 20 min pretreatment with FP inhibitor and B is the increase in mean tension induced by (0.1 μM) $PGF_{2\alpha}$ in the presence of a 20 min pretreatment with FP inhibitor.

4.7.3. General Methods:

Anhydrous solvents (THF, DMF, CH_2Cl_2, and CH_3OH) were obtained by passage through solvent filtration systems (GlassContour, Irvine, CA). All reagents from commercial sources were used as received: $BF_3{\cdot}Et_2O$ was purchased from Aldrich and coupling reagent such as TBTU and HOBt were purchased from GL Biochem; solvents were obtained from Fisher Chemical. (2*S*)-(3-Pyridyl)alaninyl-(3*S*)-β-homophenylalanine benzyl ester hydrochloride (**4.15**) was prepared according to the literature procedure and exhibited ^{1}H NMR spectral data and R_f value identical to that reported in reference 22. Purification by silica gel chromatography was performed on 230−400 mesh silica gel; analytical thin-layer chromatography (TLC) was performed on silica gel 60 F254 (aluminum sheet) and visualized by UV absorbance or staining with iodine. Melting points are uncorrected and were obtained on a sample that was placed in a capillary tube using a Mel-Temp melting point apparatus equipped with a thermometer and reported in degree Celsius (°C). ^{1}H and ^{13}C NMR spectra were recorded at room temperature (298 K) in $CDCl_3$ (7.26/77.16 ppm) and CD_3OD (3.31/ 49.0 ppm) on Bruker AV (300/75, 500/125, and 700/ 175 MHz) instruments and referenced to an internal solvent. Chemical shifts are reported in parts per million (ppm); coupling

constant (J) values in Hertz (Hz). Abbreviations for peak multiplicities are s (singlet), d (doublet), t (triplet), q (quadruplet), q (quintuplet), m (multiplet), and br (broad). Certain ^{13}C NMR chemical shift values were extracted from HSQC spectra. High resolution mass spectrometry (HRMS) data were obtained on an LC-MSD instrument in electrospray ionization (ESI-TOF) mode by the Centre Régional de Spectrommétrie de Masse de l'Université de Montréal. Either protonated molecular ions $[M + H]^+$, or sodium adducts $[M + Na]^+$ were used for empirical formula confirmation. X-ray structures were solved using a Bruker Venture Metaljet diffractometer by the Laboratoire de diffraction des rayons X de l'Université de Montréal. Specific rotations $[\alpha]_D$ were measured at 25 °C at the specified concentrations (*c* in g/100 mL) using a 0.5 dm cell on a PerkinElmer Polarimeter 589 instrument and expressed using the general formula $[\alpha]_D^{25} = (100 \times \alpha)/(d \times c)$.

4.7.4. Peptide Purifications and Analysis:

Final peptides were purified on a preparative column (C18 Gemini column) using a gradient from pure water [0.1% formic acid (FA)] to mixtures with MeOH (0.1% FA) at a flow rate of 10 mL/min. Purity of peptides (>95%) was evaluated using analytical LC−MS on a 5 μM 50 × 4.6 mm C18 Phenomenex Gemini column in two different solvent systems: water (0.1% FA) with CH_3CN (0.1% FA) and water (0.1% FA) with MeOH (0.1% FA) at a flow rate of 0.5 mL/min using the appropriate linear gradient.

4.7.5. Synthetic experimental conditions and characterization data of compounds:

Methyl (3*S*,6*R*,9*S*)-3-*N*-(Boc)amino-6-hydroxymethyl-indolizidin-2-one-9-carboxylate [(3*S*,6*R*,9*S*)-4.020]

A solution of (2*S*,5*R*,8*S*)-proline (2*S*,5*R*,8*S*)-**4.9** (250 mg, 0.53 mmol) in DCM (20 mL) was treated with HCl gas bubbles for 2-3 h, when TLC indicted complete consumption of the starting carbamate and LCMS indicated a new peak RT = 1.54 min (C18 column, 5:50

MeOH:H_2O) having a molecular ion $[M+H]^+$ m/z 275. The reaction mixture was evaporated to a residue, that was dissolved in MeOH (5 mL), treated with triethylamine (0.16 g, 1.5 mmol, 3 equiv.), and heated at reflux using an oil bath for 24 h, when LCMS indicated a new peak RT = 2.1 min (eluent C18 column, 5:50 MeOH:H_2O) having a molecular ion $[M+H]^+$ m/z 243. The volatiles were evaporated under reduced pressure. The residue was dissolved in DCM (10 mL), treated with $(Boc)_2O$ (0.14 g, 0.63 mmol, 1.2 equiv.), and stirred for 3 h, when TLC indicated a new spot (R_f = 0.3, 100% EtOAc). The volatiles were removed under reduced pressure. The residue was purified by flash column chromatography using 80% EtOAc in hexanes as eluent. Evaporation of the collected fractions gave indolizidin-2-one (3*S*,6*R*,9*S*)-**4.020** (115 mg, 64%) as a solid: mp 105-107 °C; R_f = 0.3 (100% EtOAc, visualized with $KMnO_4$); $[\alpha]_D^{25}$ –75 (*c* 0.56, $CHCl_3$); ^1H NMR (500 MHz, $CDCl_3$) δ 5.14 (s, 1H), 4.62-4.59 (dd, *J* = 9.8, 7.6 Hz, 1H), 4.23-4.18 (dd, *J* = 15.9, 7.6 Hz, 1H), 3.81 (s, 3H), 3.80-3.79 (d, *J* = 5.3 Hz, 1H), 3.65-3.60 (dd, *J* = 12.1, 9.7 Hz, 1H), 3.53-3.50 (ddd, *J* = 12.1, 5.2, 1.5 Hz, 1H), 2.43-2.39 (m, 1H), 2.31-2.28 (m, 2H), 2.21-2.17 (dt, *J* = 13.6, 3.8 Hz, 1H), 1.99-1.95 (m, 2H), 1.75-1.71 (m, 2H), 1.46 (s, 9H); $^{13}C\{^1H\}$ NMR (125 MHz, $CDCl_3$) δ 175.1, 169.8, 156.1, 79.6, 67.1, 66.0, 58.4, 52.8, 51.5, 36.7, 33.5, 28.3, 26.3, 26.1; FT-IR (neat) ν_{max} 3371, 2955, 1694, 1633, 1518, 1432, 1392, 1365, 1247, 1162, 1103, 1044, 1005 cm^{-1}. HRMS (ESI-TOF) m/z $[M+Na]^+$ calcd for $C_{16}H_{26}N_2O_6Na$ 365.1683 found 365.1676 and $[M+H]^+$ calcd for $C_{16}H_{27}N_2O_6$ 343.1863 found 343.1857.

Methyl (3*S*,6*S*,9*R*)-3-*N*-(Boc)amino-6-hydroxymethyl-indolizidin-2-one-9-carboxylate [(3*S*,6*S*,9*R*)-4.020]

Ester (3*S*,6*S*,9*R*)-**4.020** was synthesized from acid (3*S*,6*S*,9*R*)-**4.10** (20 mg, 0.06 mmol) by using the protocol described for the synthesis of ester (3*S*,6*S*,9*S*)-**4.020** and isolated as a solid (13 mg, 62%): mp 65-67 °C; R_f = 0.32 (100% EtOAc, visualized with $KMnO_4$); $[\alpha]_D^{25}$ –59.5 (*c* 0.83,

$CHCl_3$); ^1H NMR (500 MHz, $CDCl_3$) δ 4.52-4.50 (dd, *J* = 9.9, 1.1 Hz, 1H), 3.90-3.86 (m, 1H), 3.74 (s, 3H), 3.71-3.69 (d, *J* = 11.3 Hz, 1H), 3.58-3.56 (d, *J* = 11.3 Hz, 1H), 2.43-2.37 (m, 1H), 2.31-2.27 (m, 2H), 2.16-2.12 (dd, *J* = 12.4, 7.0 Hz, 1H), 1.96-1.91 (m, 2H), 1.86-1.78 (m, 2H), 1.45 (s, 9H); $^{13}C\{^1H\}$ NMR (125 MHz, $CDCl_3$) δ 172.5, 170.0, 156.0, 80.0, 66.0, 65.2, 59.0, 52.3, 52.0, 35.1, 30.1, 28.4, 26.7, 25.4; FT-IR (neat) ν_{max} 3416, 2990, 1747, 1711, 1648, 1452, 1434, 1386, 1254, 1196, 1158, 1102, 1052, 1023 cm^{-1}. HRMS (ESI-TOF) m/z $[M+Na]^+$ calcd for $C_{16}H_{26}N_2O_6Na$ 365.1683 found 365.1682 and $[M+H]^+$ calcd for $C_{16}H_{27}N_2O_6$ 343.1863 found 343.1865.

Methyl (3*S*,6*S*,9*S*)-3-*N*-(Boc)amino-6-hydroxymethyl-indolizidin-2-one-9-carboxylate [(3*S*,6*S*,9*S*)-4.020]

Methyl 3-*N*-(Boc)amino-6-hydroxymethyl-indolizidin-2-one-9-carboxylate (3*S*,6*S*,9*S*)-**4.020** was synthesized from (2*S*,5*S*,8*S*)-proline (2*S*,5*S*,8*S*)-**4.9** (250 mg, 0.53 mmol) using the protocol described for the preparation of (3*S*,6*R*,9*S*)-**4.020**, and isolated as a solid (110 g, 61%): mp 90-93 °C; R_f = 0.35 (100% EtOAc, visualized with $KMnO_4$); $[\alpha]_D^{25}$ –6.4 (*c* 1.0, $CHCl_3$); ^1H NMR (500 MHz, $CDCl_3$) δ 5.62-5.61 (d, *J* = 4.8 Hz, 1H), 4.50-4.48 (d, *J* = 9.5 Hz, 1H), 4.28-4.24 (m, 1H), 3.75 (s, 3H), 3.54-3.53 (d, *J* = 3.6 Hz, 2H), 2.48-2.33 (m, 4H), 2.21-2.15 (m, 2H), 1.94-1.88 (m, 3H), 1.45 (s, 9H); $^{13}C\{^1H\}$ NMR (125 MHz, $CDCl_3$) δ 172.6, 171.0, 156.0, 79.6, 67.1, 66.2, 59.5, 52.3, 50.0, 36.0, 29.0, 28.4, 27.3, 27.1; FT-IR (neat) ν_{max} 3409, 2979, 1744, 1710, 1643, 1495, 1432, 1392, 1365, 1247, 1200, 1163, 1109, 1060, 1021 cm^{-1}. HRMS (ESI-TOF) m/z $[M+Na]^+$ calcd for $C_{16}H_{26}N_2O_6Na$ 365.1683 found 365.1682 and $[M+H]^+$ calcd for $C_{16}H_{27}N_2O_6$ 343.1863 found 343.1865.

Methyl (3*S*,6*S*,9*S*)-3-*N*-(Boc)amino-6-hydroxymethyl-indolizidin-2-one-9-carboxylate [(3*S*,6*S*,9*S*)-4.020]

A 0 °C solution of acid (3*S*,6*S*,9*S*)-**4.10** (20 mg, 0.061 mmol) in DMF (2 mL) was treated with and K_2CO_3 (13 mg, 0.09 mmol, 1.5 equiv.) and dropwise with iodomethane (10.4 mg, 0.07 mmol, 1.2 equiv.). The cooling bath was removed. The reaction mixture warmed to room temperature and stirred for 2-3 h, when TLC indicated a new nonpolar spot (R_f = 0.35, 100% ethyl acetate). The reaction mixture was diluted with H_2O and extracted with ethyl acetate (3 x 10 mL). The organic layers were combined and washed with H_2O (5 x 10 mL) and brine (10 mL), dried over Na_2SO_4, filtered, and concentrated under vacuum. The residue was purified by column chromatography using 60-80% of ethyl acetate in hexanes as eluent. Evaporation of the collected fractions gave indolizidin-2-one (3*S*,6*S*,9*S*)-**4.020** (13 mg, 62%) as a solid exhibiting identical physical and spectroscopic properties as described above.

Phenylacetyl-(3*S*,6*R*,9*S*)-I^{2}aa-(2*S*)-(3-pyridyl)alaninyl-(3*S*)-β-homophenylalanine [(6*R*,9*S*)-4.4]

A solution of benzyl ester (6*R*,9*S*)-**4.17** (10 mg) in EtOH (5 mL) was treated with palladium-on-carbon (10% by wt, 10 mg), placed under a hydrogen atmosphere and stirred under a balloon of H_2 gas for 3-4 h. The catalyst was filtered onto Celite™. The filter cake was washed with MeOH. The filtrate and washings were combined and evaporated to a residue, which was purified by preparative HPLC (Phenomenex Gemini 5 µm, C18, 250 × 21.2 mm) using a gradient from 10 to 90% MeOH (containing 0.1% FA) in water (containing 0.1% FA). Free-drying of the collected fractions afforded peptide (6*R*,9*S*)-**4.4** (5 mg, 57%) as a white foam: $[\alpha]_D^{25}$ +20 (*c* 0.35, MeOH); ^{1}H NMR (700 MHz, CD_3OD): δ 8.39-8.38 (d, *J* = 5.9 Hz, 3H), 7.75-7.74 (d, *J* = 7.8 Hz, 1H), 7.36-7.32 (m, 5H), 7.26-7.22 (m, 3H), 7.20-7.18 (m, 3H), 4.55-4.52 (t, *J* = 9.3 Hz, 1H), 4.50-4.46 (m, 1H), 4.42-4.40 (dd, *J* = 11.2, 4.3 Hz, 1H), 3.94-3.91 (dd, *J* = 10.5, 8.0 Hz, 1H), 3.68-3.67 (d, *J* = 11.2 Hz, 1H), 3.59-3.57 (d, *J* = 15.1 Hz, 1H), 3.03-3.00 (dd, *J* = 14.3, 4.2 Hz, 1H), 2.96-

2.93 (dd, *J* = 13.8, 7.0 Hz, 1H), 2.89-2.84 (m, 2H), 2.71-2.68 (dd, *J* = 14.2, 11.3 Hz, 1H), 2.52-2.49 (dd, *J* = 16.0, 7.3 Hz, 1H), 2.46-2.43 (dd, *J* = 16.0, 5.9 Hz, 1H), 2.37-2.34 (m, 1H), 2.32-2.28 (m, 1H), 2.24-2.21 (dd, *J* = 12.4, 7.4 Hz, 1H), 2.13-2.04 (m, 2H), 1.77-1.71 (m, 1H), 1.52-1.47 (m, 2H); $^{13}C\{^{1}H\}$ NMR (175 MHz, CD_3OD) δ 173.2, 172.4, 171.3, 170.6, 149.5, 147.0, 138.2, 137.7, 135.2, 134.4, 129.1, 129.0, 128.2, 128.1, 126.5, 126.2, 123.7, 67.0, 60.4, 59.5, 55.4, 51.0, 48.3, 42.0, 40.0, 38.0, 34.3, 33.0, 29.4, 28.0, 25.0, 24.6; FT-IR (neat) ν_{max} 3349, 2973, 1721, 1658, 1622, 1521, 1422, 1359, 1338, 1257, 1151, 1119, 1055, 1033, 1014 cm^{-1}. HRMS (ESI-TOF) m/z $[M+H]^+$ calcd for $C_{36}H_{41}N_5O_7$ 656.3078, found 656.3090.

Phenylacetyl-(3*S*,6*S*,9*R*)-I^{2}aa-(2*S*)-(3-pyridyl)alaninyl-(3*S*)-β-homophenylalanine [(6*S*,9*R*)-4.4]

Acid (6*S*,9*R*)-**4.4** was synthesized from ester (6*S*,9*R*)-**4.17** (10 mg) using the protocol described for the synthesis of acid (6*R*,9*S*)-**4.4** and isolated as white foam (6.0 mg, 68%): $[\alpha]_D^{25}$ +9.6 (*c* 0.46, MeOH); ^1H NMR (500 MHz, $CDCl_3$): δ 8.45-8.35 (m, 5H), 7.86-7.84 (d, *J* = 8.9 Hz, 1H), 7.43 (s, 1H), 7.32-7.31 (m, 4H), 7.28-7.25 (m, 3H), 7.23-7.21 (m, 3H), 4.49 (s, 1H), 4.41-4.39 (t, *J* = 6.8 Hz, 1H), 4.34-4.33 (d, *J* = 9.8 Hz, 1H), 4.10-4.07 (m, 1H), 3.82-3.80 (d, *J* = 11.6 Hz, 1H), 3.57-3.53 (m, 2H), 3.39-3.37 (d, *J* = 11.5 Hz, 1H), 3.17-3.14 (dd, *J* = 13.6, 6.6 Hz, 1H), 3.07-3.04 (dd, *J* = 13.6, 7.1 Hz, 1H), 2.83-2.80 (m, 1H), 2.76-2.73 (dd, *J* = 14.0, 6.5 Hz, 1H), 2.42-2.37 (m, 1H), 2.35-2.28 (m, 3H), 2.23-2.16 (m, 2H), 2.03-1.99 (m, 1H) 1.78-1.69 (m, 3H); $^{13}C\{^{1}H\}$ NMR (175 MHz, $CDCl_3$) δ 172.4, 172.3, 170.2, 169.4, 138.0, 135.3, 129.1, 129.0, 128.1, 128.0, 126.4, 126.1, 66.4, 61.2, 60.0, 55.0, 51.0, 49.0, 42.3, 40.2, 34.3, 33.6, 32.0, 29.4, 29.2, 29.0, 28.8, 28.0, 26.4, 25.0, 24.2, 22.3; FT-IR (neat) ν_{max} 3355, 2975, 1726, 1661, 1612, 1521, 1421, 1363, 1342, 1256, 1150, 1120, 1058, 1037, 1016 cm^{-1}. HRMS (ESI-TOF) m/z $[M+H]^+$ calcd for $C_{36}H_{41}N_5O_7$ 656.3078, found 656.3083.

Phenylacetyl-(3*S*,6*S*,9*S*)-I^{2}aa-(2*S*)-(3-pyridyl)alaninyl-(3*S*)-β-homophenylalanine [(6*S*,9*S*)-4.4]

Acid (6*S*,9*S*)-**4.4** was synthesized from ester (6*S*,9*S*)-**4.17** (10 mg) using the protocol described for the synthesis of acid (6*R*,9*S*)-**4.4** and isolated as white foam (5.5 mg, 63%): $[\alpha]_D^{25}$ +52.4 (*c* 0.12, MeOH); ^{1}H NMR (700 MHz, $CDCl_3$): δ 8.44 (s, 1H), 8.42-8.40 (m, 4H), 7.81-7.80 (d, *J* = 7.4 Hz, 1H), 7.40-7.38 (m, 1H), 7.30-7.26 (m, 8H), 7.24-7.20 (m, 2H), 4.47-4.42 (m, 3H), 4.38-4.37 (d, *J* = 9.6 Hz, 1H), 3.58-3.51 (m, 2H), 3.47-3.43 (q, *J* = 11.6 Hz, 2H), 3.13-3.10 (dd, *J* = 14.1, 6.0 Hz, 1H), 3.02-2.99 (dd, *J* = 14.0, 8.2 Hz, 1H), 2.90-2.84 (m, 2H), 2.42-2.35 (m, 3H), 2.33-2.27 (m, 1H), 2.22-2.17 (m, 1H), 2.11-2.09 (dd, 12.2, 7.1 Hz, 1H), 1.88-1.84 (dt, *J* = 13.5, 8.0 Hz, 1H), 1.78-1.64 (m, 3H); $^{13}C\{^1H\}$ NMR (175 MHz, $CDCl_3$) δ 173.0, 172.4, 171.0, 170.1, 149.4, 147.0, 138.0, 135.3, 129.1, 129.1, 129.0, 128.2, 128.1, 126.5, 126.1, 124.0, 70.0, 67.0, 64.1, 60.4, 55.0, 42.2, 40.0, 38.0, 35.0, 34.0, 33.5, 32.0, 29.4, 29.0, 28.3, 27.0, 26.5, 25.0; FT-IR (neat) ν_{max} 3351, 2949, 1726, 1671, 1609, 1520, 1431, 1361, 1341, 1253, 1150, 1122, 1054, 1035, 1014 cm^{-1}. HRMS (ESI-TOF) m/z $[M+H]^+$ calcd for $C_{36}H_{41}N_5O_7$ 656.3078, found 656.3054.

Dimethyl (2*S*,8*S*)-2,8-di-*N*-(Boc)amino-5-methylene-azelate (1.65)

In a 250-mL round bottom flask, fitted with three-way tap, CuBr•DMS (1.2 g, 0.006 mol, 0.13 equiv.) was weighed, dried gently with a heat gun under vacuum until the powder changed color from white to light green, placed under argon, treated with dry DMF (30 mL), followed by 3-chloro-2-chloromethyl-1-propene (2.8 g, 0.03 mol, 0.5 equiv.). In a Schlenk tube, zinc (8.9 g, 0.14 mol, 3 equiv.) and iodine (0.35 g, 0.0014 mol, 0.03 equiv.) were mixed under argon atmosphere, heated under vacuum with a heat gun for 10 min and cooled under a flush of argon three times. A solution of *N*-(Boc)-3-iodo-L-alanine methyl ester **1.61** (15 g, 0.046 mol) in dry DMF (30 mL) was added to Schlenk tube and stirred for 1h, when TLC analysis confirmed that

consumption of the iodide (R_f = 0.7, 30% EtOAc in hexanes) and formation of the organozinc reagent (R_f = 0.2, 30% EtOAc in hexanes). Stirring was stopped, the excess zinc powder was allowed to settle, and the supernatant was transferred dropwise via syringe with care to minimize the transfer of zinc into the flask containing the copper catalyst. After stirring at rt overnight, TLC indicated a new spot (R_f = 0.40, 30% EtOAc in hexanes) and the reaction mixture was diluted with ethyl acetate (150 mL), stirred for 15 min, and filtered through a silica gel pad. The filtrate was treated with water (100 mL), transferred into a separating funnel and diluted with ethyl acetate (50 mL). The organic phase was washed successively with 1 M $Na_2S_2O_3$ (2 x100 mL), water (4 x 100 mL) and brine (2 x 100 mL), dried over Na_2SO_4, filtered and evaporated. The volatiles were removed under reduced pressure to afford a residue that was purified by chromatography using 25-30% EtOAc in hexanes as eluent. Evaporation of the collected fractions gave azelate **1.66** (6.3 g, 64%) which solidified on standing in the fridge: R_f = 0.4 (30% EtOAc/hexanes, visualized with $KMnO_4$). The physical and spectroscopic properties were identical to those reported in ref. 23.

Dimethyl-(2*S*,5*R*) and (2*S*,5*S*)-5-(iodomethyl)pyrrolidine-1,2-dicarboxylate [(2*S*,5*R*)- and (2*S*,5*S*)-4.6]

In a 100 mL round bottom flask, azelate **1.65** (0.5 g, 1.1 mmol) was dissolved in acetonitrile (10 mL), cooled to –20° C, treated simultaneously with $NaHCO_3$ (0.27 g, 3.3 mmol, 3 equiv.) and iodine (0.83 g, 3.3 mmol, 3 equiv.) and stirred for 30 min, when TLC indicated that consumption of starting material (R_f = 0.4 (30% EtOAc/hexanes, visualized with $KMnO_4$) and formation two new non-polar spots (R_f = 0.3 and 0.2 (20% EtOAc in hexanes, twice eluted). The reaction mixture was diluted with diethyl ether (20 mL), washed with saturated aq. $Na_2S_2O_3$ (2 x 10 mL), water (10 mL) and brine (10 mL), dried over Na_2SO_4, and concentrated in vacuo to residue. The residue was purified by flash column chromatography using 8-12% EtOAc in hexanes as eluent.

First to elute was (2*S*,5*R*)-**4.6** (140 mg, 22%) as a gum: R_f = 0.3 (20% EtOAc in hexanes, twice eluted): $[\alpha]_D^{25}$ –61.5 (*c* 1.3, $CHCl_3$); ^1H NMR (500 MHz, $CDCl_3$) (2:3 mixture of carbamate isomers) δ 5.25-5.23 (d, *J* = 7.1 Hz, 1H), [5.00-4.99 (d, *J* = 5.0 Hz, 1H], [4.53-4.50 (dd, *J* = 10.0, 5.0 Hz, 1H)], 4.37-4.35 (dd, *J* = 8.2, 5.9 Hz, 1H), 4.29-4.27 (m, 1H), 3.97-3.95 (d, *J* = 9.9 Hz, 1H), [3.79 (s, 3H)], 3.76 (s, 3H), 3.75 (s, 3H), [3.69-3.67 (d, *J* = 10 Hz, 1H)], 3.6-3.58 (d, *J* = 9.9 Hz, 1H), 2.21-2.11 (m, 3H), 2.06-2.03 (m, 2H), 1.91-1.87 (m, 3H), [1.51 (s, 9H)], 1.47 (s, 9H), 1.41 (s, 9H); $^{13}C\{^1H\}$ NMR (125 MHz, $CDCl_3$) δ 173.5, 173.1, 155.5, 153.0, 81.0, 80.0, 66.0, 62.4, 62.2, 53.3, (52.3), 52.1, (38.0), 35.6, 31.0, (30.0), 28.3, 28.2, 27.1, 26.7, (26.4), (15.6), 15.0; FT-IR (neat) ν_{max} 2985, 1744, 16945, 1364, 1201, 1161 cm^{-1}. HRMS (ESI-TOF) m/z $[M+Na]^+$ calcd for $C_{22}H_{37}IN_2O_8Na$ 607.1486 found 607.1488.

Next to elute was (2*S*,5*S*)-**4.6** (420 mg, 66%) as a gum: R_f = 0.2 (20% EtOAc in hexanes, twice eluted): $[\alpha]_D^{25}$ –13.3 (*c* 1.2, $CHCl_3$); ^1H NMR (500 MHz, $CDCl_3$) (2:3 mixture of carbamate isomers) δ 5.32-5.30 (d, *J* = 7.8 Hz, 1H), [5.13-5.11 (d, *J* = 10.0 Hz, 1H)], [4.45-4.32 (dd, *J* = 8.8, 6.1 Hz, 2H)], 4.36-4.33 (dd, *J* = 8.8, 6.1 Hz, 2H), 4.31-4.29 (m, 1H), 3.97-3.95 (d, *J* = 10.0 Hz, 1H), [3.80, (s, 3H)], 3.77 (s, 3H), 3.75 (s, 3H), 3.48 (d, *J* = 10 Hz, 1H), 3.46 (d, *J* = 10 Hz, 1H), 2.33-2.28 (m, 2H), 2.22-2.17 (m, 1H), 2.11-2.08 (m, 1H), 1.98-1.92 (m, 2H), [1.52 (s, 9H)], [1.47 (s, 9H)], 1.46 (s, 9H), 1.42 (s, 9H); $^{13}C\{^1H\}$ NMR (125 MHz, $CDCl_3$) δ 173.3, 173.0, 155.5/(153.3), 153.0, (81.3)/81.0, 80.0, 66.3, (62.0)/61.5, 53.4, (52.2)/52.0, 36.1, 35.0, 31.3, (28.4)/28.3, 28.2, 27.4, 26.6/(26.0), 16.3 ; FT-IR (neat) ν_{max} 2980, 1748, 1698, 1360, 1205, 1156 cm^{-1}. HRMS (ESI-TOF) m/z $[M+Na]^+$ calcd for $C_{22}H_{37}IN_2O_8Na$ 607.1486 found 607.1485.

Dimethyl (2*S*,5*R*,8*S*)-1,7-diazaspiro[4.5]decane-2,8-dicarboxylate bis hydrochloride [(2*S*,5*R*,8*S*)-4.7]

In a 100 mL round bottom flask, as solution of iodide (2*S*,5*R*)-**4.6** (100 mg, 0.17 mmol) in dichloromethane was treated with HCl gas bubbles for 2 h, when TLC showed consumption of starting iodide [R_f = 0.3 (20% EtOAc in hexanes)]. The volatiles were evaporated under vacuum and the residue was dissolved in DCM and evaporated three times before drying to a constant weight under vacuum to give hydrochloride (2*S*,5*S*,8*S*)-**4.7** (56 mg, 100% yield) as a yellow solid: $[\alpha]_D^{25}$ –46.5(*c* 0.42, MeOH); ^{1}H NMR (400 MHz, CD_3OD) δ 4.78-4.73 (q, *J* = 8.3 Hz, 1H), 4.21-4.18 (t, *J* = 6.4 Hz, 1H), 4.05-3.97 (m, 1H), 3.93 (s, 3H), 3.91 (s, 3H), 3.73-3.65 (m, 1H), 2.69-2.60 (m, 1H), 2.42-2.20 (m, 4H), 2.10-2.03 (m, 2H), 1.96-1.90 (m, 1H); $^{13}C\{^1H\}$ NMR (100 MHz, CD_3OD) δ 169.0, 168.4, 71.0, 69.6, 59.2, 53.0, 32.1, 32.0, 27.0, 26.6, 24.6, 24.3; FT-IR (neat) ν_{max} 2931, 1740, 1442, 1226, 1037 cm^{-1}. HRMS (ESI-TOF) m/z $[M+H]^+$ calcd for $C_{12}H_{20}N_2O_4$ 257.1495 found 257.1496.

Dimethyl (2*S*,5*S*,8*S*)-1,7-diazaspiro[4.5]decane-2,8-dicarboxylate bis hydrochloride [(2*S*,5*S*,8*S*)-4.7]

Iodide (2*S*,5*S*)-**4.6** (45 mg, 0.07 mmol) in dichloromethane was treated with HCl and isolated as described for the diastereomer to afford hydrochloride (2*S*,5*S*,8*S*)-**4.7** (25 mg, 100% yield) as a yellow solid: $[\alpha]_D^{25}$ –3.7 (*c* 1.75, MeOH); ^{1}H NMR (400 MHz, CD_3OD) δ 4.72-4.66 (dt, *J* = 15.4, 7.3 Hz, 1H), 4.24-4.21 (t, *J* = 6.0 Hz, 1H), 4.05-3.97 (q, *J* = 12.0 Hz, 1H), 3.93 (s, 3H), 3.91 (s, 3H), 3.75-3.63 (q, *J* = 12.5 Hz, 1H) 2.63-2.52 (m, 1H), 2.46-2.37 (m, 1H), 2.31-2.15 (m, 4H), 2.10-1.97 (m, 2H); $^{13}C\{^1H\}$ NMR (100 MHz, CD_3OD) δ 169.0, 168.6, 71.5, 70.2, 60.0, 53.0, 34.0, 32.2, 29.3, 27.2, 25.0, 24.5; FT-IR (neat) ν_{max} 2926, 1736, 1438, 1230, 1042 cm^{-1}. HRMS (ESI-TOF) m/z $[M+H]^+$ calcd for $C_{12}H_{20}N_2O_4$ 257.1495 found 257.1491.

Dimethyl (2*S*,8*S*)-2,8-di-*N*-(Boc)amino-5-oxyranyl-azelate (4.8)

A solution of azelate **1.65** (4.5 g, 9.8 mmol) in DCM (45 mL) was cooled to 0°C and treated with *m*-chloroperbenzoic acid (2.5 g, 14.7 mmol, 1.5 equiv.). The ice bath was removed. The suspension warmed to room temperature with stirring for 2 h, when TLC showed complete consumption of olefin 7 (R_f = 0.40, 30% EtOAc in hexanes) and a more polar spot for epoxide 4.8 (R_f = 0.18, 30% EtOAc in hexanes). The reaction mixture was diluted with DCM (45 mL), transferred to a separating funnel, and washed sequentially with 1N NaOH (2 x 15 mL), water (15 mL) and brine (15 mL), dried over Na_2SO_4, filtered and concentrated in vacuo to a residue, that was purified by flash column chromatography using 20% EtOAc in hexanes as eluent. Evaporation of the collected fractions afforded epoxide **4.8** (4.1 g, 89%) as colorless oil: R_f = 0.18 (3:7 EtOAc/hexanes, visualized with $KMnO_4$); $[\alpha]_D^{25}$ +11.1 (*c* 0.72, $CHCl_3$); ^1H NMR (500 MHz, $CDCl_3$): δ 5.12-5.10 (d, *J* = 5, 8.9 Hz, 1H), 5.07-5.06 (d, *J* = 8.9 Hz, 1H), 4.31-4.29 (m, 2H), 3,77 (s, 3H), 3.77 (s, 3H), 2.64-2.61 (m, 2H), 1.94-1.84 (m, 2H), 1.68-1.64 (m, 6H), 1.47 (s, 9H), 1.46 (s, 9H); $^{13}C\{^1H\}$ NMR (125 MHz, $CDCl_3$) δ 173.0 (2C), 155.4 (2C), 80.1 (2C), 58.1, 53.2, 53.1, 52.4, 52.4, 52.0, 30.0, 29.7, 28.3 (6C), 28.0, 27.7; FT-IR (neat) ν_{max} 3352, 2929, 1699, 1513, 1452, 1391, 1365, 1247, 1212, 1158, 1049, 1025 cm^{-1}. HRMS (ESI-TOF) m/z $[M+Na]^+$ calcd for $C_{22}H_{38}N_2O_9Na$ 497.2469, found 497.2466.

(2*S*,5*R*,3'*S*)- and (2*S*,5*S*,8*S*)-Methyl *N*-(Boc)-5-(3'-*N*-(Boc)amino)-4-methoxy-4-oxobutyl)-5-(hydroxymethyl)prolinate [(2*S*,5*R*,8*S*)- and (2*S*,5*S*,8*S*)-4.9]

A solution of epoxide **4.8** (2.5 g, 5.3 mmol) in DCM (100 mL) was cooled to –70°C, treated with a solution of $BF_3{\cdot}Et_2O$ (1.4 mL, 10.5 mmol, 2 equiv.), and stirred for 4 h, when TLC indicated two new spots (R_f = 0.36 and 0.24, 40% EtOAc in hexanes, twice eluted). The reaction mixture was quenched with saturated NH_4Cl (15 mL), diluted with DCM (50 mL), washed with saturated NH_4Cl (4 x 30 mL), dried over Na_2SO_4, filtered and concentrated in vacuo. The residue was

purified by flash column chromatography using 40% EtOAc in hexanes as eluant. First to elute was (2*S*,5*R*,8*S*)-proline (2*S*,5*R*,8*S*)-**4.9** (720 mg, 29%) as a gummy liquid: R_f = 0.36 (2:3 EtOAc/hexanes, twice eluted and visualized with $KMnO_4$); $[\alpha]_D^{25}$ –27.4 (*c* 0.65, $CHCl_3$); ^{1}H NMR (500 MHz, $CDCl_3$) δ 5.21-5.19 (d, *J* = 8.4 Hz, 1H), 4.62-4.59 (t, *J* = 6.7 Hz, 1H), 4.36-4.34 (dd, *J* = 9.4, 3.0 Hz, 1H), 4.32-4.30 (m, 1H), 3.92-3.88 (dd, *J* = 12.5, 6.3 Hz, 1H), 3.80-3.78 (d, *J* = 7.8 Hz, 2H), 3.76 (s, 3H), 3.76 (s, 3H), 3.66-3.63 (dd, *J* = 11.9, 6.0 Hz, 1H), 2.17-2.13 (m, 1H), 1.97-1.93 (m, 2H), 1.84-1.78 (m, 3H), 1.46 (s, 9H), 1.42 (s, 9H); $^{13}C\{^1H\}$ NMR (125 MHz, $CDCl_3$) δ 173.4, 173.3, 155.7, 155.1, 81.3, 80.0, 69.0, 68.0, 61.6, 54.0, 52.2, 52.0, 33.0, 28.3, 28.2, 28.1, 27.0, 26.6; FT-IR (neat) ν_{max} 3371, 2980, 1704, 1513, 1454, 1390, 1365, 1209, 1158, 1047, 1021 cm^{-1}.HRMS (ESI-TOF) m/z $[M+Na]^+$ calcd for $C_{22}H_{38}N_2O_9Na$ 497.2469 found 497.2465.

Next to elute was (2*S*,5*S*,8*S*)-proline (2*S*,5*S*,8*S*)-**4.9** (1.0 g, 40%) as a gummy liquid: R_f = 0.24 (2:3 EtOAc/hexanes, twice eluted and visualized with $KMnO_4$); $[\alpha]_D^{25}$ –28.3 (*c* 0.6, $CHCl_3$); ^{1}H NMR (500 MHz, $CDCl_3$) δ 5.34-5.32 (d, *J* = 8.2 Hz, 1H), 4.72-4.70 (dd, *J* = 9.0, 2.8 Hz, 1H), 4.32-4.29 (dd, *J* = 8.5, 6.4 Hz, 1H), 4.27-4.24 (m, 1H), 3.76 (s, 3H), 3.75 (s, 3H), 3.69-3.66 (dd, *J* = 10.7, 6.3 Hz, 2H), 2.21-2.15 (m, 2H), 1.90-1.82 (m, 6H), 1.47 (s, 9H), 1.42 (s, 9H); $^{13}C\{^1H\}$ NMR (125 MHz, $CDCl_3$) δ 174.6, 173.0, 155.5, 154.2, 81.0, 80.0, 68.9, 67.4, 61.4, 53.4, 52.3, 33.0, 32.0, 31.0, 28.3, 28.2, 27.2, 26.7; FT-IR (neat) ν_{max} 3367, 2979, 1743, 1684, 1517, 1454, 1365, 1253, 1160, 1046, 1022 cm^{-1}. HRMS (ESI-TOF) m/z $[M+Na]^+$ calcd for $C_{22}H_{38}N_2O_9Na$ 497.2469 found 497.2472.

(3*S*,6*R*,9*S*)-3-*N*-(Boc)amino-6-hydroxymethyl-indolizidin-2-one-9-carboxylic acid [(3*S*,6*R*,9*S*)-4.10]

A 0 °C solution of ester (3*S*,6*R*,9*S*)-**4.020** (250 mg, 0.73 mmol) in 1,4-dioxane (2.5 mL) was treated with a 1N solution of LiOH (37 mg, 0.87 mmol, 1.2 equiv.). The cooling bath was

removed. The reaction mixture warmed to room temperature with stirring for 3 h, at which time, TLC indicated a new polar spot (R_f = 0.20, 15% acetic acid in ethyl acetate, visualized with bromocresol green). The volatiles were evaporated under reduced pressure. The residue was partitioned between H_2O (10 mL) and EtOAc (5 mL). The aqueous phase was acidified with 1N HCl to pH 3 and extracted twice with ethyl acetate (2 × 10 mL). The organic extractions were combined, dried with Na_2SO_4, filtered, and concentrated under vacuum to afford acid (3*S*,6*R*,9*S*)-**4.10** (193 mg, 80%) as a white solid: mp 58-60 ºC; $[\alpha]_D^{25}$ –117.8 (*c* 0.46, $CHCl_3$); ^{1}H NMR (400 MHz, DMSO-D_6): δ 12.3 (s, 1H), 7.06-7.04 (d, *J* = 9.0 Hz, 1H), 4.23-4.18 (t, *J* = 9.1 Hz, 1H), 3.95-3.88 (m, 1H), 3.48-3.45 (d, *J* = 11.8 Hz, 1H), 3.31 (s, 1H), 2.29-2.18 (m, 4H), 1.86-1.73 (m, 3H), 1.39 (overlapping m, 2H and s, 9H); ^{13}C{^{1}H} NMR (100 MHz, DMSO-D6) δ 174.2, 169.0, 156.0, 78.1, 66.3, 61.1, 59.5, 51.0, 35.0, 29.0, 28.7, 26.3, 25.0; FT-IR (neat) ν_{max} 3352, 2922, 1692, 1630, 1519, 14301, 1393, 1366, 1314, 1247, 1160, 1102, 1042 cm^{-1}. HRMS (ESI-TOF) m/z [M-H]$^-$ calcd for $C_{15}H_{23}N_2O_6$ 327.1561, found 327.1549.

(3*S*,6*S*,9*S*)- and (3*S*,6*S*,9*R*)-3-*N*-(Boc)amino-6-hydroxymethyl-indolizidin-2-one-9-carboxylic acid [(3*S*,6*S*,9*R*)- and (3*S*,6*S*,9*S*)-4.10]

As described for the (3*S*,6*R*,9*S*)-diastereomer above, ester (3*S*,6*S*,9*S*)-**4.020** (100 mg, 0.29 mmol) in 1,4-dioxane (2.5 mL) was treated with a 1N solution of LiOH (15 mg, 0.35 mmol, 1.2 equiv.) and stirred overnight, when TLC indicated consumption of starting material. After aqueous work up as above, the residue was purified by column chromatography using 1-2% of acetic acid in ethyl acetate. First to elute was (3*S*,6*S*,9*S*)-**4.10** (34 mg, 35%) as a solid: mp 86-88 ºC; R_f = 0.18 (15% of CH_3CO_2H in EtOAc, visualized with $KMnO_4$); $[\alpha]_D^{25}$ –96.3 (*c* 1.1, $CHCl_3$); ^{1}H NMR (500 MHz, $CDCl_3$): δ 4.54-4.53 (d, *J* = 9.5Hz, 1H), 4.39-4.34 (m, 1H), 3.59-3.52 (m, 2H), 2.43-2.37 (m, 2H), 2.20-2.15 (m, 2H), 2.06-1.95 (m, 2H), 1.92-1.87 (m, 1H), 1.78-1.71 (m, 1H), 1.47 (s, 9H);

$^{13}C\{^{1}H\}$ NMR (125 MHz, $CDCl_3$) δ 174.4, 171.6, 156.4, 80.0, 67.1, 66.5, 60.4, 59.7, 49.7, 36.1, 28.7, 28.4, 27.1; FT-IR (neat) ν_{max} 3345, 2947, 1634, 1434, 1163, 1057, 1033, 1018 cm^{-1}. HRMS (ESI-TOF) m/z $[M–H]^-$ calcd for $C_{15}H_{23}N_2O_6$ 327.1561, found 327.1549.

Second to elute was (3*S*,6*S*,9*R*)-**4.10** (36.5 mg, 38%) as a solid: mp 92-94 ºC; R_f = 0.10 (15% of CH_3CO_2H in EtOAc, visualized with $KMnO_4$); $[\alpha]_D^{25}$ –123.8 (*c* 0.63, $CHCl_3$); ^1H NMR (500 MHz, $CDCl_3$): δ 4.51-4.49 (d, *J* = 10.3 Hz, 1H), 4.06-4.01 (m, 1H), 3.68-3.57 (dd, *J* = 15.5, 11.6 Hz, 2H), 2.48-2.40 (m, 1H), 2.26-2.24 (m, 1H), 2.14-2.10 (m, 2H), 2.05-2.01 (m, 1H), 1.87 – 1.79 (m, 2H), 1.48-1.45 (m, 10H); $^{13}C\{^{1}H\}$ NMR (125 MHz, $CDCl_3$) δ 175.2, 174.4, 156.2, 80.1, 66.4, 59.4, 53.4, 51.3, 35.1, 34.5, 28.4, 26.6, 20.5; FT-IR (neat) ν_{max} 3356, 2936, 1631, 1439, 1167, 1063, 1041, 1022 cm^{-1}. HRMS (ESI-TOF) m/z $[M–H]^-$ calcd for $C_{15}H_{23}N_2O_6$ 327.1561, found 327.1549.

Benzyl 3-*N*-(Boc)amino-6-hydroxymethyl-(3*S*,6*R*,9*S*)-I^{2}aa-(2*S*)-(3-pyridyl)alaninyl-(3*S*)-β-homophenylalaninate [(6*R*,9*S*)-4.16]

A solution of acid (3*S*,6*S*,9*S*)-**4.10** (150 mg, 0.45 mmol) in DCM (10 mL) was treated with HOBt (62 mg, 0.45 mmol, 1 equiv.) and TBTU (147 mg, 0.45 mmol, 1 equiv.), stirred for 15 min, treated with dipeptide hydrochloride 4.15 (207.4 mg, 0.45 mmol, 1 equiv.), followed by DIEA (118 mg, 0.91 mmol, 2 equiv.), and stirred at room temperature for 5-6 h, when TLC indicated a new nonpolar spot (R_f = 0.58, 1:9 MeOH/$CHCl_3$). The reaction mixture was diluted with DCM (10 mL) and washed with water (10 mL) and brine (10 mL), dried over Na_2SO_4, filtered and evaporated to a residue, which was purified by flash column chromatography using 3-4 % MeOH in $CHCl_3$ as eluant. Evaporation of the collected fractions afforded peptide (3*S*,6*R*,9*S*)-**4.16** (115 mg, 35%) as a white foam: R_f = 0.58 (1:9 MeOH/$CHCl_3$, visualized by UV); $[\alpha]_D^{25}$ –27.6 (*c* 0.50, $CHCl_3$); ^1H NMR (400 MHz, $CDCl_3$): δ 8.49-8.46 (m, 2H), 7.74-7.72 (d, *J* = 7.6 Hz, 1H), 7.44-

7.42 (d, *J* = 7.6 Hz, 1H), 7.37-7.34 (m, 6H), 7.28-7.22 (m, 4H), 5.81-5.79 (d, *J* = 7.6 Hz, 1H), 5.13-5.04 (q, *J* = 12.3 Hz, 2H), 4.66-4.60 (m, 1H), 4.57-4.53 (t, *J* = 9.0 Hz, 1H), 4.50-4.45 (m, 1H), 3.89-3.82 (m, 1H), 3.60-3.57 (d, *J* = 10.4 Hz, 1H), 3.48-3.43 (dd, *J* = 14.3, 2.7 Hz, 1H), 3.07-3.01 (dd, *J* = 15.4, 8.1 Hz, 1H), 2.99-2.96 (m, 1H), 2.93-2.83 (m, 2H), 2.57-2.54 (t, *J* = 5.5 Hz, 2H), 2.43-2.40 (m, 1H), 2.26-2.19 (m, 6H), 1.97-1.89 (m, 1H), 1.48 (s, 9H), 1.28 (s, 3H); $^{13}C\{^{1}H\}$ NMR (100 MHz, $CDCl_3$) δ 172.0, 171.1, 170.5, 170.0, 156.2, 150.1, 147.5, 138.0, 137.2, 136.0, 129.4, 128.54, 128.47, 128..4, 128.1, 126.6, 80.3, 71.0, 67.0, 66.4, 62.2, 60.5, 55.0, 52.0, 48.2, 40.2, 37.3, 35.4, 34.0, 30.0, 28.5, 25.6, 25.0; FT-IR (neat) ν_{max} 3359, 2946, 1695, 1621, 1510, 1436, 1387, 1356, 1250, 1156, 1109, 1040, 1010 cm^{-1}. HRMS (ESI-TOF) m/z $[M+H]^+$ calcd for $C_{40}H_{49}N_5O_8$ 728.3653, found 728.3653 and $[M+Na]^+$ calcd for $C_{40}H_{49}N_5O_8$ 750.3473, found 750.3476.

Benzyl 3-*N*-(Boc)amino-6-hydroxymethyl-(3*S*,6*S*,9*R*)-I^{2}aa-(2*S*)-(3-pyridyl)alaninyl-(3*S*)-β-homophenylalaninate [(6*S*,9*R*)-4.16]

Peptide (6*S*,9*R*)-**4.16** was synthesized by using the protocol described for the synthesis of indolizidinone (6*R*,9*S*)-**4.16** using acid (3*S*,6*S*,9*R*)-**4.10** (24 mg, 0.073 mmol) and isolated as a white foam (32 mg, 60%): R_f = 0.30 (1:9 MeOH/$CHCl_3$, visualized by UV); $[\alpha]_D^{25}$ +27.6 (*c* 0.58, $CHCl_3$); ^{1}H NMR (400 MHz, $CDCl_3$): δ 8.44 (s, 2H), 7.59-7.57 (d, *J* = 6.5 Hz, 1H), 7.37-7.36 (m, 4H), 7.27-7.15 (m, 7H), 6.99-6.96 (d, *J* = 9.9 Hz, 1H), 5.47-5.45 (d, *J* = 7.8 Hz, 1H), 5.13-5.05 (m, 2H), 4.50-4.39 (m, 2H), 4.34-4.32 (d, *J* = 9.5 Hz, 1H), 3.8 (s, 1H), 3.63-3.54 (m, 2H), 3.16-3.15 (d, *J* = 6.6 Hz, 2H), 2.93-2.88 (dd, *J* = 13.6, 6.3 Hz, 1H), 2.79-2.73 (dd, *J* = 13.6, 8.3 Hz, 1H), 2.50-2.45 (dd, *J* = 15.0, 5.7 Hz, 6H), 2.24-2.22 (m, 1H), 1.79-73 (m, 3H), 1.43 (s, 9H), 1.28 (s, 2H); $^{13}C\{^{1}H\}$ NMR (100 MHz, $CDCl_3$) δ 172.0, 171.4, 171.0 169.4, 156.0, 150.1, 148.0, 139.1, 137.6, 135.7, 129.4, 128.6, 128.5, 128.4, 126.6, 124.0, 80.0, 66.4, 66.3, 65.5, 60.3, 55.0, 51.5, 48.0, 40.0, 37.0, 36.0, 34.4, 31.0, 30.0, 29.4, 28.4, 27.0, 26.0; FT-IR (neat) ν_{max} 3366, 2955, 1686, 1617,

1515, 1423, 1369, 1339, 1245, 1167, 1118, 1035, 1004 cm^{-1}. HRMS (ESI-TOF) m/z $[M+H]^+$ calcd for $C_{40}H_{49}N_5O_8$ 728.3653, found 728.3657 and $[M+Na]^+$ calcd for $C_{40}H_{49}N_5O_8$ 750.3473, found 750.3481.

Benzyl 3-*N*-(Boc)amino-6-hydroxymethyl-(3*S*,6*S*,9*S*)-I^{2}aa-(2*S*)-(3-pyridyl)alaninyl-(3*S*)-β-homophenylalaninate [(6*S*,9*S*)-4.16]

Peptide (6*S*,9*S*)-**4.16** was synthesized by using the protocol described for the synthesis of indolizidinone (6*R*,9*S*)-**4.16** using acid (3*S*,6*S*,9*S*)-**4.10** (21 mg, 0.064 mmol) and isolated (30 mg, 65%) as a white foam: R_f = 0.37 (1:9 MeOH/$CHCl_3$, visualized by UV); $[\alpha]_D^{25}$ –8.6 (*c* 0.42, $CHCl_3$); ^{1}H NMR (400 MHz, $CDCl_3$): δ 8.48-8.45 (m, 2H), 7.65-7.63 (d, *J* = 7.9 Hz, 1H), 7.38-7.35 (m, 4H), 7.28-7.17 (m, 6H), 7.02-7.00 (d, *J* = 7.7 Hz, 1H), 5.70-5.68 (d, *J* = 7.1 Hz, 1H), 5.14-5.04 (q, *J* = 12.2 Hz, 2H), 4.51-4.43 (m, 2H), 4.34-4.32 (d, *J* = 9.3 Hz, 1H), 4.17-4.12 (dd, *J* = 15.2, 7.7 Hz, 1H), 3.52-3.46 (q, *J* = 11.3 Hz, 2H), 3.32-3.27 (13.2, 4.9 Hz, 1H), 3.17-3.12 (dd, *J* = 14.1, 8.7 Hz, 1H), 2.99-2.95 (dd, *J* = 13.6, 6.1 Hz, 1H), 2.85-2.79 (dd, *J* = 13.5, 8.9 Hz, 1H), 2.52-2.51 (d, *J* = 5.7 Hz, 2H), 2.45-2.38 (m, 4H), 2.05-2.01 (dd, *J* = 12.0, 7.0 Hz, 1H), 1.90-1.83 (m, 1H), 1.79-1.72 (m, 2H), 1.46 (s, 9H), 1.38 (s, 1H), 1.28 (s, 2H); $^{13}C\{^1H\}$ NMR (100 MHz, $CDCl_3$) δ 172.0, 171.3, 171.2, 170.0, 156.3, 150.2, 148.0, 137.6, 137.2, 136.0, 130.0, 129.4, 128.5, 128.4, 128.3, 127.0, 80.0, 66.6, 66.5, 61.0, 55.3, 55.0, 49.4, 48.0, 40.0, 37.0, 36.0, 34.0, 30.0, 29.5, 28.5, 28.3, 27.4, 24.5; FT-IR (neat) ν_{max} 3366, 2955, 1686, 1616, 1515, 1423, 1369, 1339, 1245, 1167, 1118, 1035, 1004 cm^{-1}. HRMS (ESI-TOF) m/z $[M+H]^+$ calcd for $C_{40}H_{49}N_5O_8$ 728.3653, found 728.3657 and $[M+Na]^+$ calcd for $C_{40}H_{49}N_5O_8$ 750.3473, found 750.3481.

Benzyl phenylacetyl-(3*S*,6*R*,9*S*)-I^{2}aa-(2*S*)-(3-pyridyl)alaninyl-(3*S*)-β-homophenylalaninate [6*R*,9*S*)-4.17]

Carbamate (6*R*,9*S*)-**4.16** (35 mg, 0.053 mmol) in DCM (15 mL) was treated with HCl gas bubbles for 1-2 h, when TLC showed complete conversion of starting material [R*f* = 0.58 (1:9 MeOH/$CHCl_3$, visualized by UV)]. The volatiles were evaporated. The residue was dissolved and evaporated from DCM (20 mL) three times. Without further purification, amine HCl salt was dissolved 20 mL of dichloromethane, treated with DIEA (14 mg, 0.10mmol) and incrementally with phenylacetic anhydride (7 mg, 0.026 mmol, 0.5 equiv.) to avoid bis-acylation, and stirred for 5-6 h, when TLC showed remaining starting material and 0.25 equiv. of phenylacetic anhydride was added to the reaction mixture which was stirred for 10 h, when TLC and LCMS indicated consumption of amine starting material and formation of amide (6*R*,9*S*)-**4.17** contaminated with minor amounts of *N*,*O*-bis-phenyl acetylation product. The reaction mixture was washed with 50 mL of brine, dried over Na_2SO_4, filtered and evaporated. The residue was purified by column chromatography using 3-4% MeOH in $CHCl_3$ as an eluent. Evaporation of the collected fractions gave phenyl acetamide (6*R*,9*S*)-**4.17** (12 mg, 33%) as white foam: R_f = 0.5 (10% MeOH in $CHCl_3$, visualized by UV); $[\alpha]_D^{25}$ –32.5 (*c* 0.8, $CHCl_3$); ^{1}H NMR (400 MHz, $CDCl_3$): δ 8.45-8.40 (m, 2H), 7.70-7.68 (d, *J* = 7.8 Hz, 1H), 7.53-7.51 (d, *J* = 8.8 Hz, 1H), 7.37-7.36 (m, 5H), 7.33-7.30 (m, 4H), 7.28-7.24 (m, 7H), 7.09-7.07 (d, *J* = 7.4 Hz, 1H), 5.13-5.05 (q, *J* = 12.3 Hz, 2H), 4.58-4.51 (m, 3H), 4.01-3.95 (dt, *J* = 10.7, 7.5 Hz, 1H), 3.61 (s, 2H), 3.55-3.52 (d, *J* = 10.7 Hz, 1H), 3.31-3.27 (dd, *J* = 14.3, 3.5 Hz, 1H), 3.05-2.98 (m, 2H), 2.90-2.75 (m, 2H), 2.60-2.59 (d, *J* = 6.1 Hz, 2H), 2.42-2.37 (m, 2H), 2.24-2.18 (m, 4H), 2.06-1.93 (m, 4H); ^{13}C{^{1}H} NMR (100 MHz, $CDCl_3$) δ 171.85, 171.83 171.1, 170.1, 169.9, 137.7, 137.1, 136.0, 134.3, 129.5, 129.3, 129.0, 128.6, 128.5, 128.4, 128.1, 127.4, 127.0, 67.0, 66.4, 62.0, 60.3, 55.4, 51.3, 50.1, 48.0, 43.3, 40.5, 37.6, 35.3, 33.6, 33.0, 32.0, 30.0, 29.4, 25.1, 24.5; FT-IR (neat) ν_{max} 3372, 2949, 1695, 1661, 1610, 1513, 1421, 1366, 1348, 1254, 1145, 1109, 1015, 1004 cm^{-1}. HRMS (ESI-TOF) m/z $[M+H]^+$ calcd for

$C_{43}H_{47}N_5O_7$ 746.3548, found 746.3551 and $[M+Na]^+$ calcd for $C_{43}H_{47}N_5O_7$ 768.3367, found 768.3368.

Benzyl phenylacetyl-(3*S*,6*S*,9*R*)-I^{2}aa-(2*S*)-(3-pyridyl)alaninyl-(3*S*)-β-homophenylalaninate [6*S*,9*R*)-4.17]

Phenylacetamide (6*S*,9*R*)-**4.17** was synthesized from carbamate (6*S*,9*R*)-**4.16** (26 mg, 0.04 mmol) using the protocol described for the synthesis of (6*R*,9*S*)-**4.17** and isolated as white foam (10 mg, 49%): R_f = 0.25 (1:9 MeOH/$CHCl_3$, visualized by UV); $[\alpha]_D^{25}$ –29.7 (*c* 0.8, $CHCl_3$); ^{1}H NMR (400 MHz, $CDCl_3$): δ 8.44-8.40 (m, 2H), 7.55-7.52 (dt, *J* = 7.7, 1.6 Hz, 1H), 7.37-7.34 (m, 5H), 7.28-7.27 (m, 4H), 7.21-7.16 (m, 4H), 7.09-7.07 (dd, *J* = 7.4, 1.7 Hz, 2H), 6.95-6.90 (dd, *J* = 13.4, 8.1 Hz, 2H), 6.68-6.66 (d, *J* = 7.4 Hz, 1H), 5.11-5.0 (m, 2H), 4.45-4.39 (m, 3H), 3.72-3.66 (m, 1H), 3.62-3.59 (m, 2H), 3.56-3.48 (m, 2H), 3.17-3.15 (d, *J* = 6.9 Hz, 2H), 2.87-2.72 (m, 2H), 2.54-2.39 (m, 2H), 2.26-2.22 (m, 1H), 2.18-2.14 (m, 2H), 2.03-1.98 (m, 2H), 1.77-1.61 (m, 5H); $^{13}C\{^1H\}$ NMR (100 MHz, $CDCl_3$) δ 172.1, 171.6, 171.4, 170.0, 169.4, 150.4, 148.0, 137.7, 137.0, 135.7, 134.7, 133.1, 129.6, 129.5, 128.8, 128.6, 128.4, 128.3, 127.2, 126.5, 123.6, 66.6, 66.4, 65.6, 60.3, 54.6, 51.1, 48.0, 43.2, 40.0, 37.1, 36.0, 34.2, 31.0, 29.7, 27.0, 25.1; FT-IR (neat) ν_{max} 3360, 2953, 1689, 1668, 1617, 1526, 1426, 1369, 1346, 1257, 1151, 1119, 1020, 1010, 917 cm^{-1}. HRMS (ESI-TOF) m/z $[M+H]^+$ calcd for $C_{43}H_{47}N_5O_7$ 746.3548, found 746.3552 and $[M+Na]^+$ calcd for $C_{43}H_{47}N_5O_7$ 768.3367, found 768.3375.

Benzyl phenylacetyl-(3*S*,6*S*,9*S*)-I^{2}aa-(2*S*)-(3-pyridyl)alaninyl-(3*S*)-β-homophenylalaninate [6*S*,9*S*)-4.17]

Phenylacetamide (6*S*,9*S*)-**4.17** was synthesized from carbamate (6*S*,9*S*)-**4.16** (26 mg, 0.04 mmol) using the protocol described for the synthesis of (6*R*,9*S*)-**4.17** which provided 10 mg (37%) of a white foam: R_f = 0.35 (1:9 MeOH/$CHCl_3$, visualized by UV); $[\alpha]_D^{25}$ –16.3 (*c* 0.8, $CHCl_3$); ^{1}H

NMR (400 MHz, $CDCl_3$): δ 8.49 (s, 1H), 8.42-8.41 (d, *J* = 3.7 Hz, 1H), 7.62-7.60 (d, *J* = 7.8 Hz, 1H), 7.36-7.34 (m, 5H), 7.28-7.25 (m, 6H), 7.22-7.15 (m, 6H), 7.10-7.08 (d, *J* = 8.3 Hz, 1H), 5.13-5.04 (q, *J* = 12.2 Hz, 2H), 4.49-4.43 (m, 2H), 4.34-4.25 (m, 2H), 3.56 (s, 2H), 3.47-3.44 (m, 1H), 3.41-3.38 (d, *J* = 11.3 Hz, 1H), 3.25-3.20 (dd, *J* = 14.2, 4.9 Hz, 1H), 3.11-3.04 (dd, *J* = 14.1, 10.0 Hz, 1H), 3.02-2.95 (m, 1H), 2.87-2.82 (dd, *J* = 13.6, 8.6 Hz, 1H), 2.57-2.52 (dd, *J* = 14.0, 5.9 Hz, 2H), 2.39-2.30 (m, 2H), 2.11-2.04 (m, 2H), 1.97-1.93 (dd, *J* = 12.4, 6.7 Hz, 2H), 1.84-1.73 (m, 4H); $^{13}C\{^1H\}$ NMR (100 MHz, $CDCl_3$) δ 172.0, 171.4, 171.1, 170.0, 137.6, 137.0, 136.0, 135.0, 129.4, 129.3, 129.1, 128.8, 128.6, 128.58, 128.56, 128.44, 128.38, 128.3, 127.2, 126.7, 66.7, 66.5, 61.0, 48.6, 48.0, 43.5, 43.2, 41.6, 40.1, 37.2, 36.0, 34.0, 32.0, 30.0, 27.4, 27.2; FT-IR (neat) ν_{max} 3360, 2953, 1689, 1668, 1617, 1526, 1426, 1369, 1346, 1257, 1151, 1119, 1020, 1010, 917 cm^{-1}. HRMS (ESI-TOF) m/z $[M+H]^+$ calcd for $C_{43}H_{47}N_5O_7$ 746.3548, found 746.3550 and $[M+Na]^+$ calcd for $C_{43}H_{47}N_5O_7$ 768.3367, found 768.3374.

^{1}H *NMR 500 MHz*

Solvent: $CDCl_3$

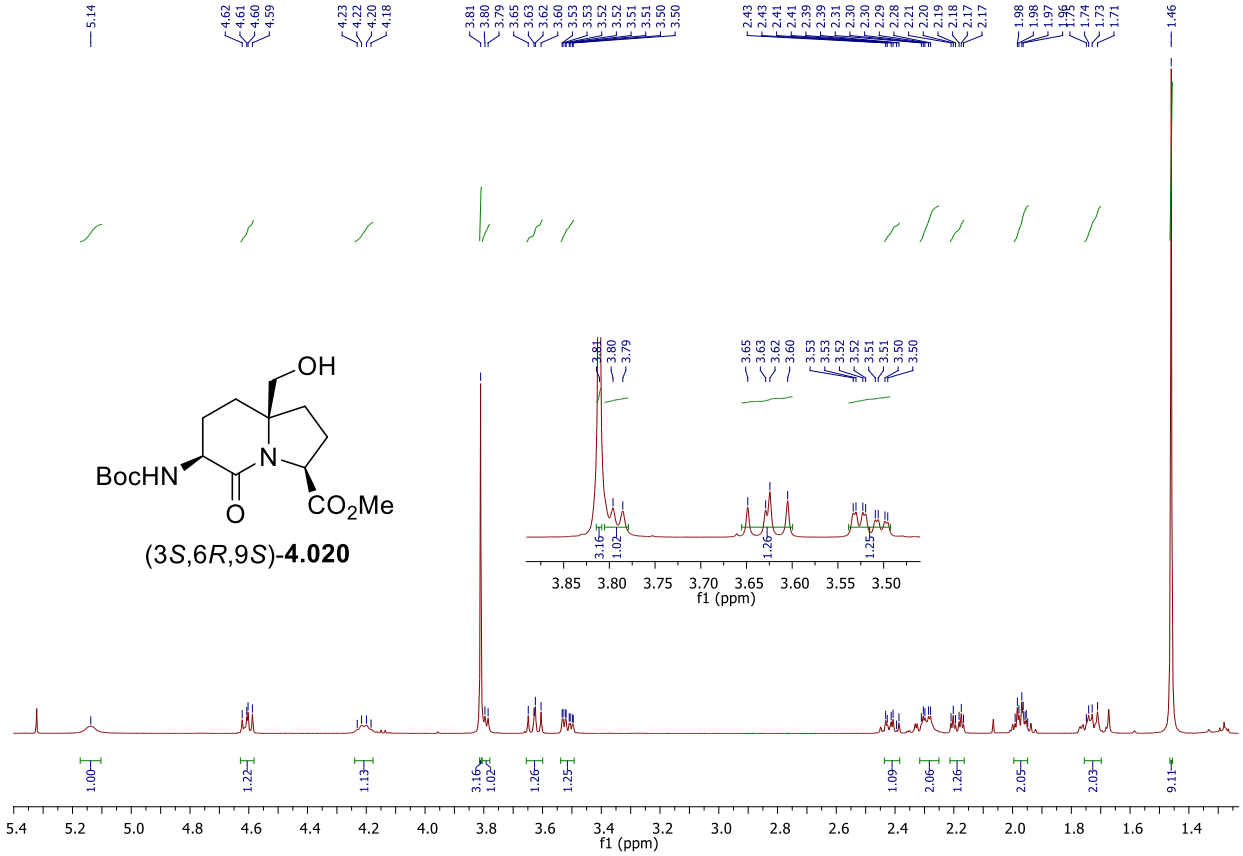

^{13}C *NMR 125 MHz*

Solvent: $CDCl_3$

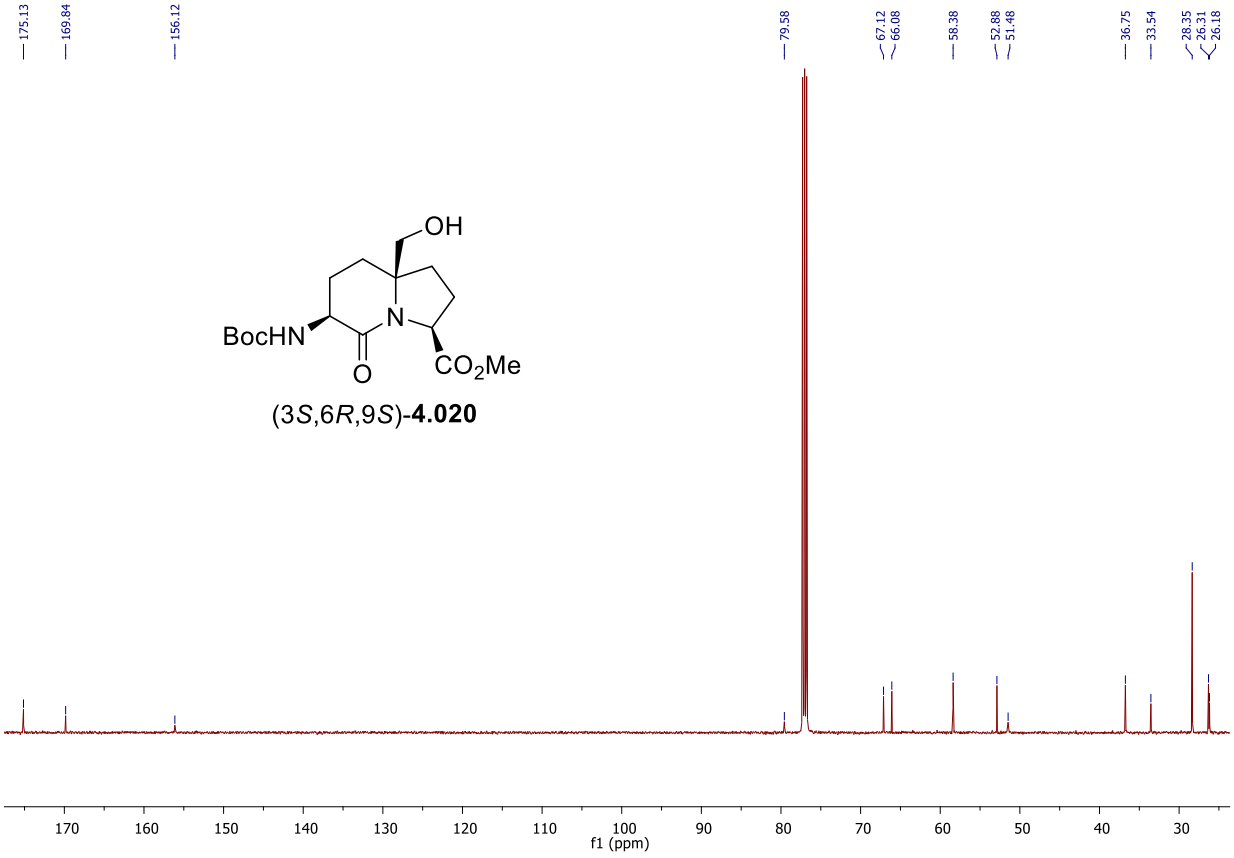

(3*S*,6*R*,9*S*)-**4.020**

^{13}C DEPT *NMR 125 MHz*

Solvent: $CDCl_3$

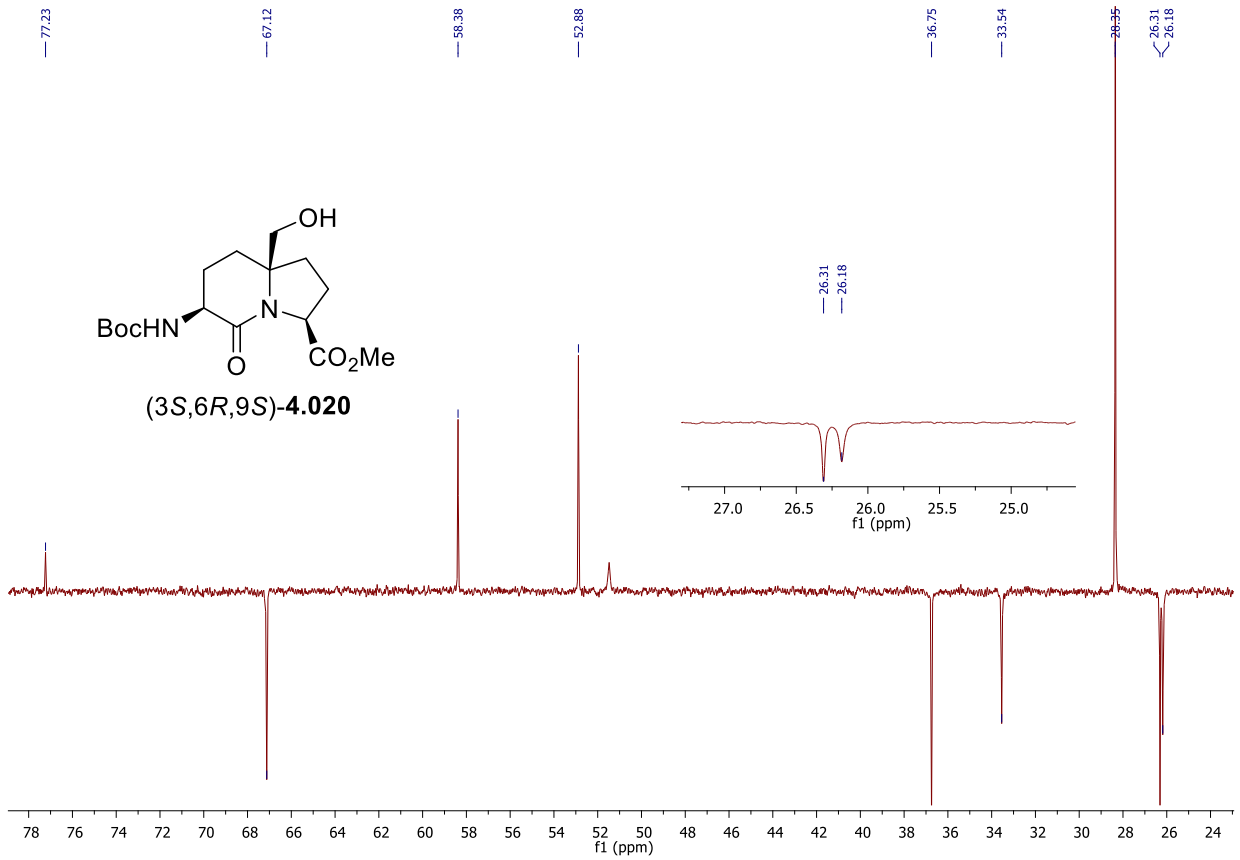

^{1}H NMR, 500 MHz

Solvent: $CDCl_3$

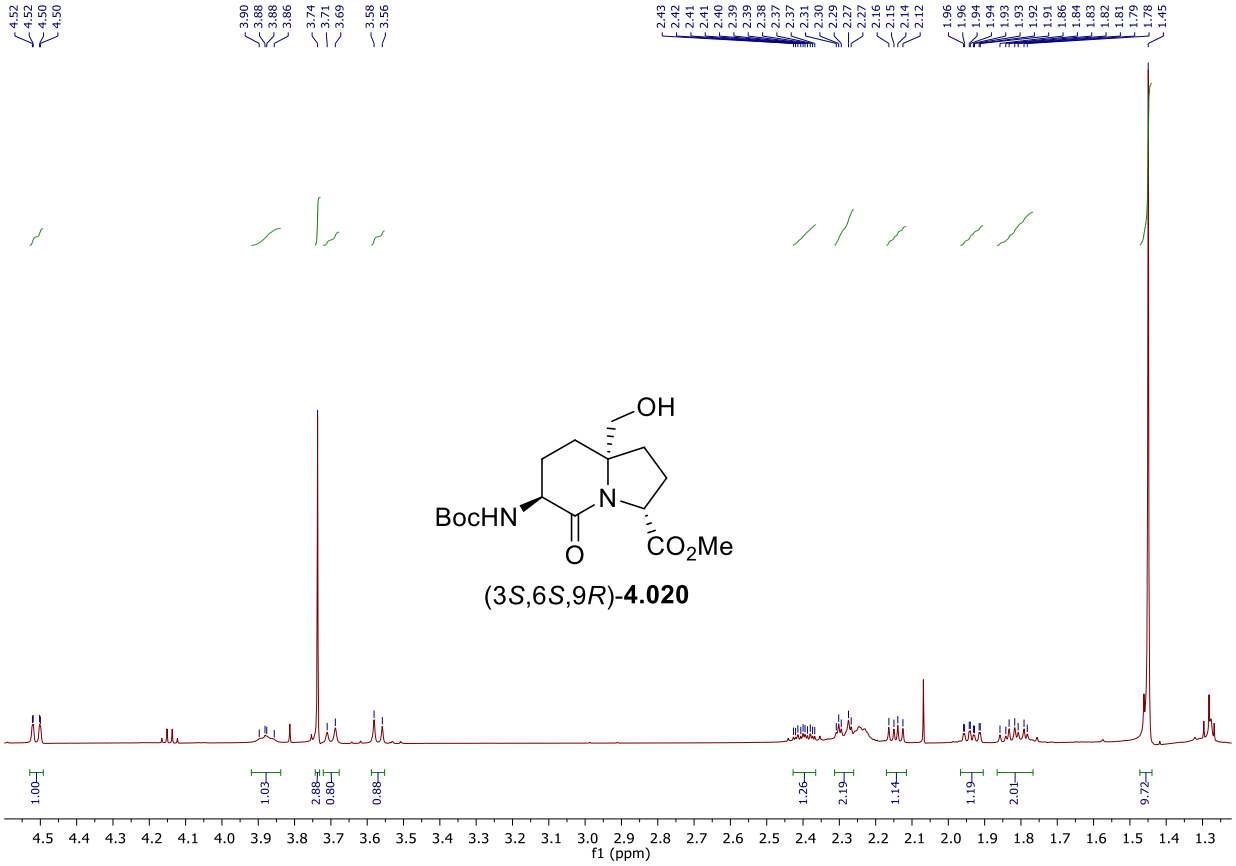

^{13}C NMR, 125 MHz

Solvent: $CDCl_3$

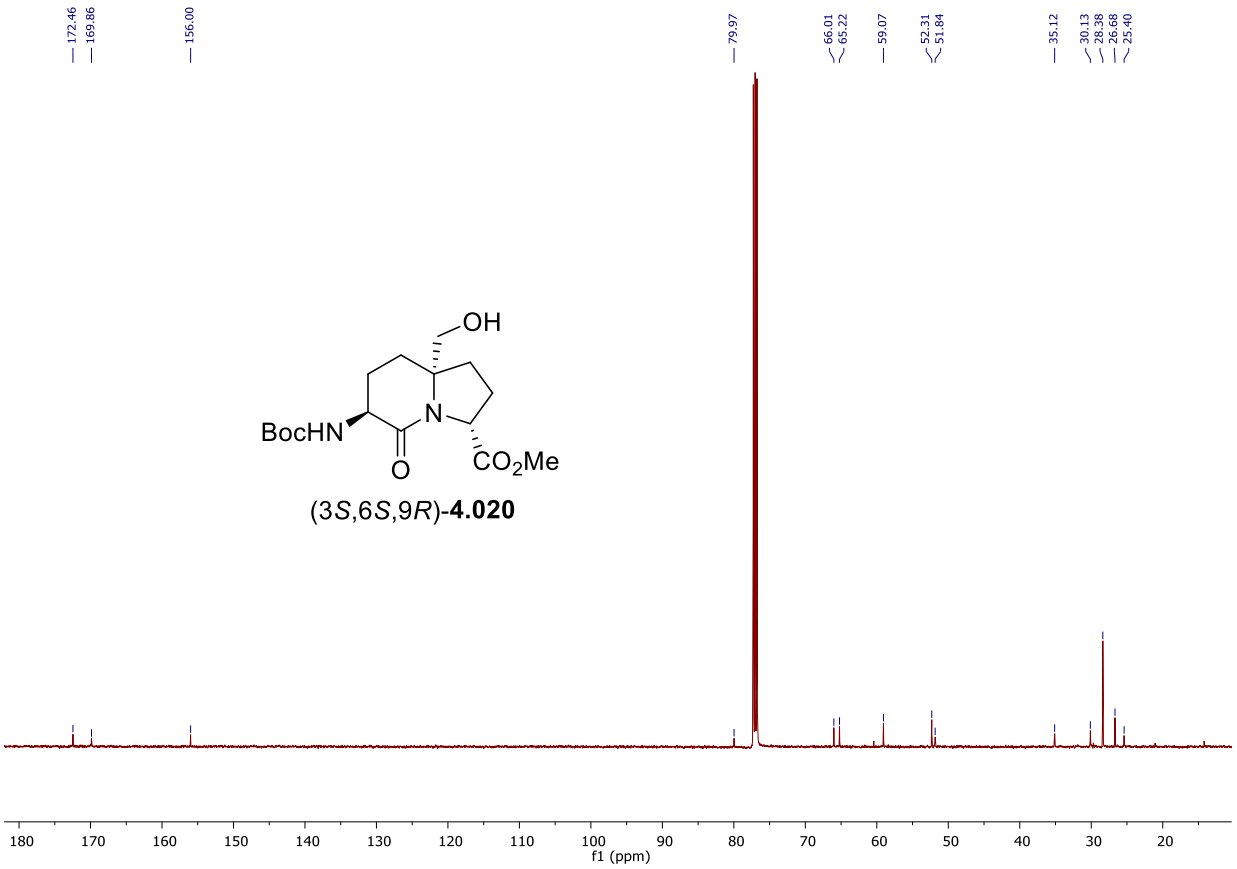

(3*S*,6*S*,9*R*)-**4.020**

^{1}H *NMR 500 MHz*

Solvent: $CDCl_3$

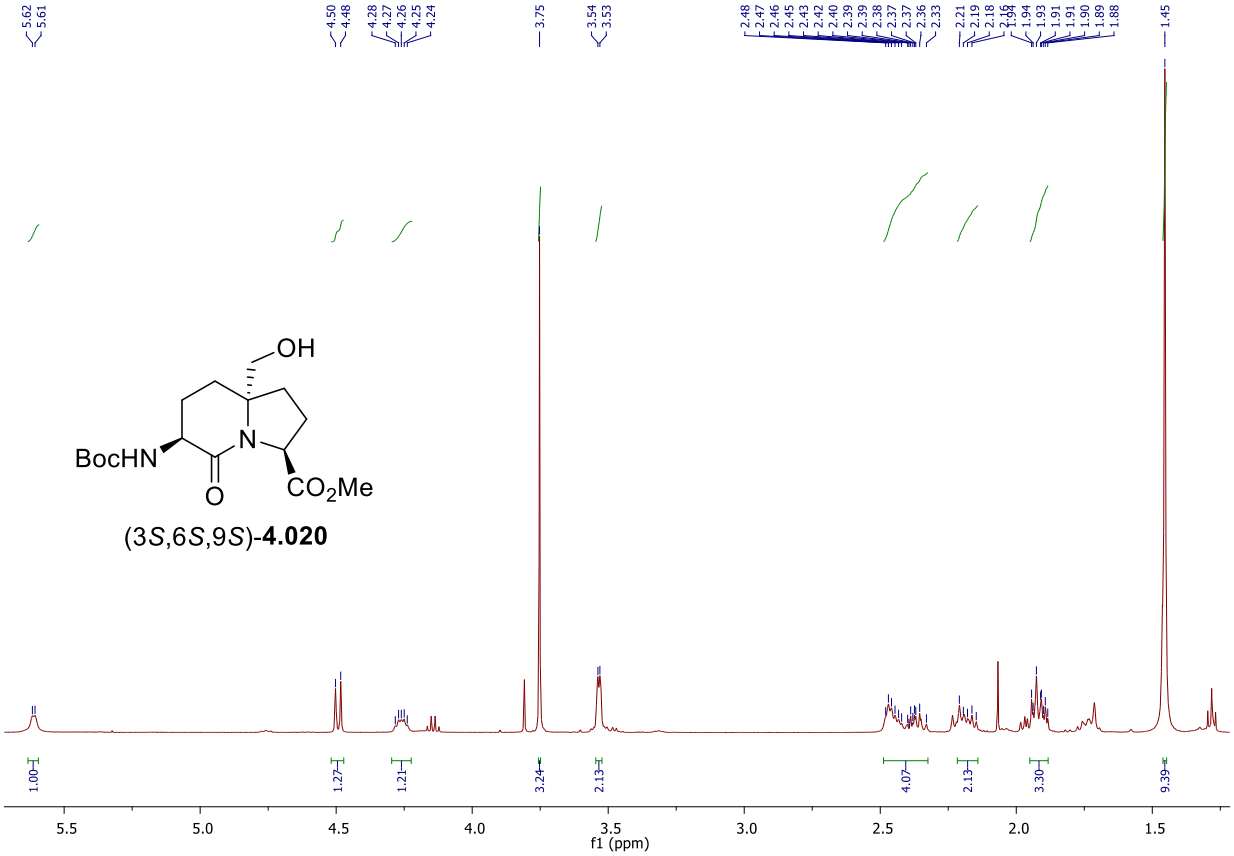

(3*S*,6*S*,9*S*)-**4.020**

^{13}C *NMR 125 MHz*

Solvent: $CDCl_3$

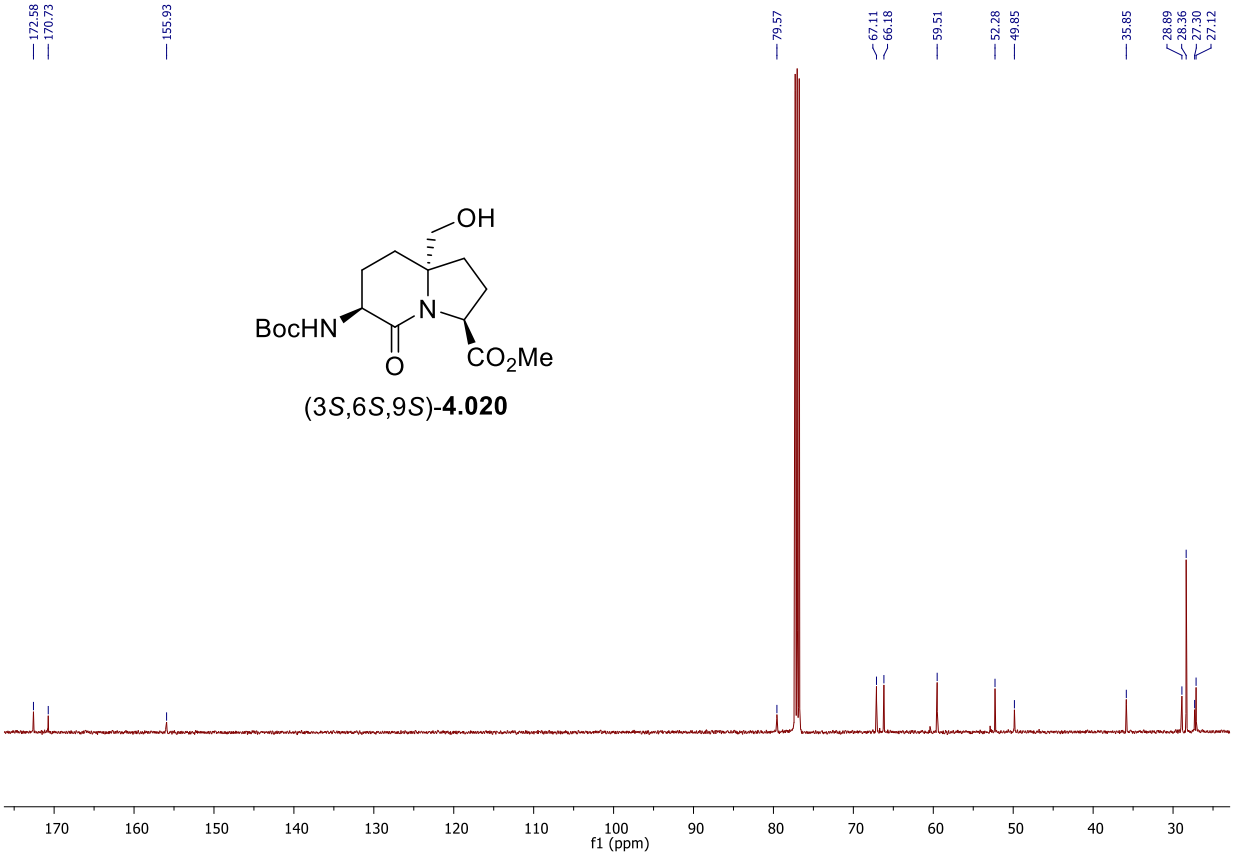

(3*S*,6*S*,9*S*)-**4.020**

^{13}C *NMR 125 MHz*

Solvent: $CDCl_3$

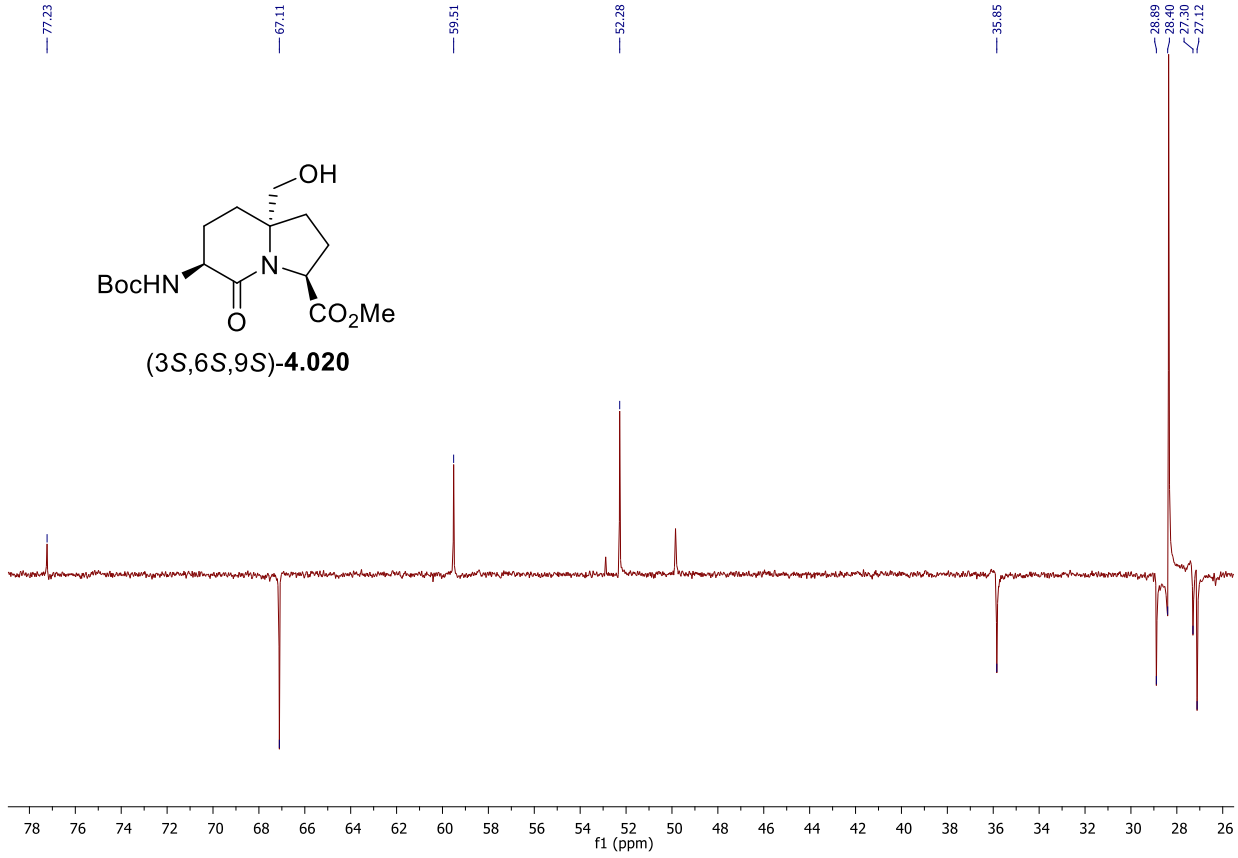

(3*S*,6*S*,9*S*)-**4.020**

^{1}H *NMR 700 MHz*

Solvent: CD_3OD

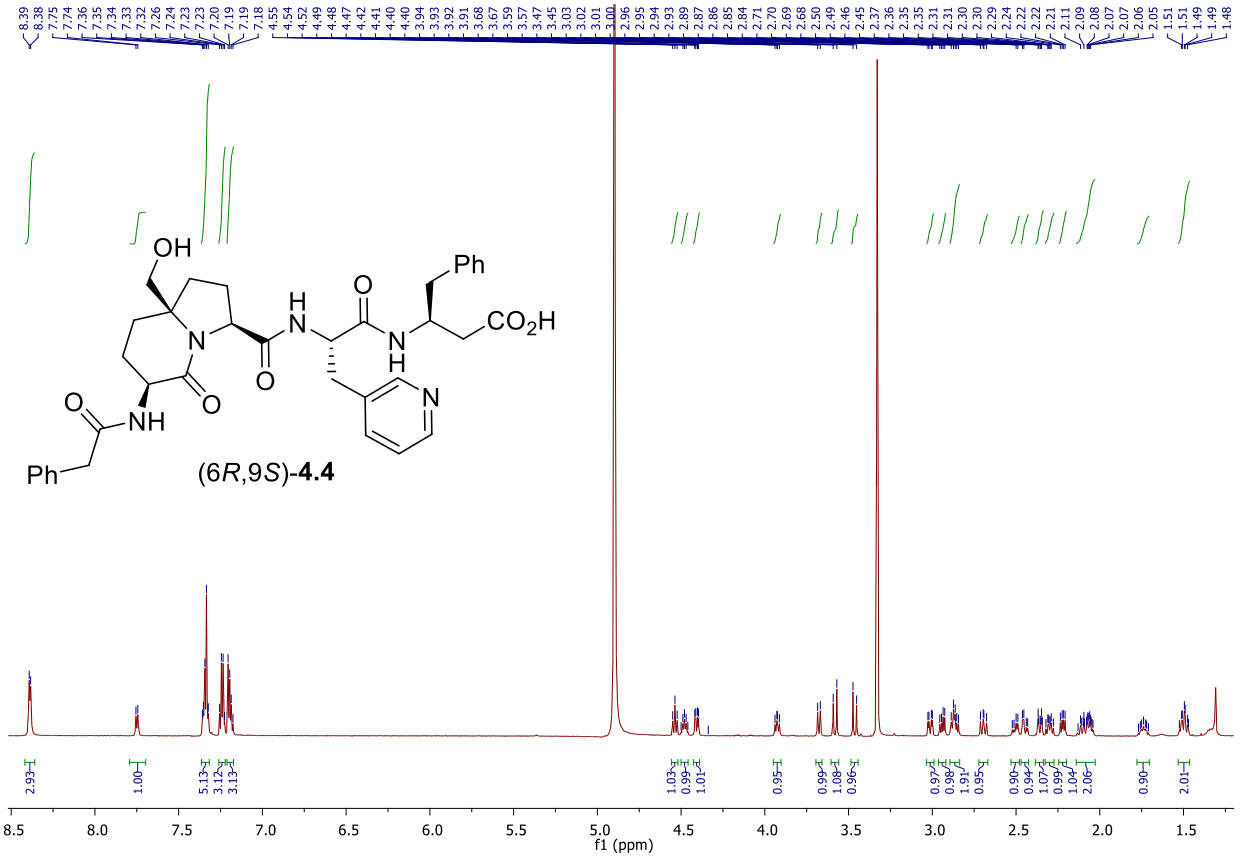

^{13}C *NMR 175 MHz*

Solvent: CD_3OD

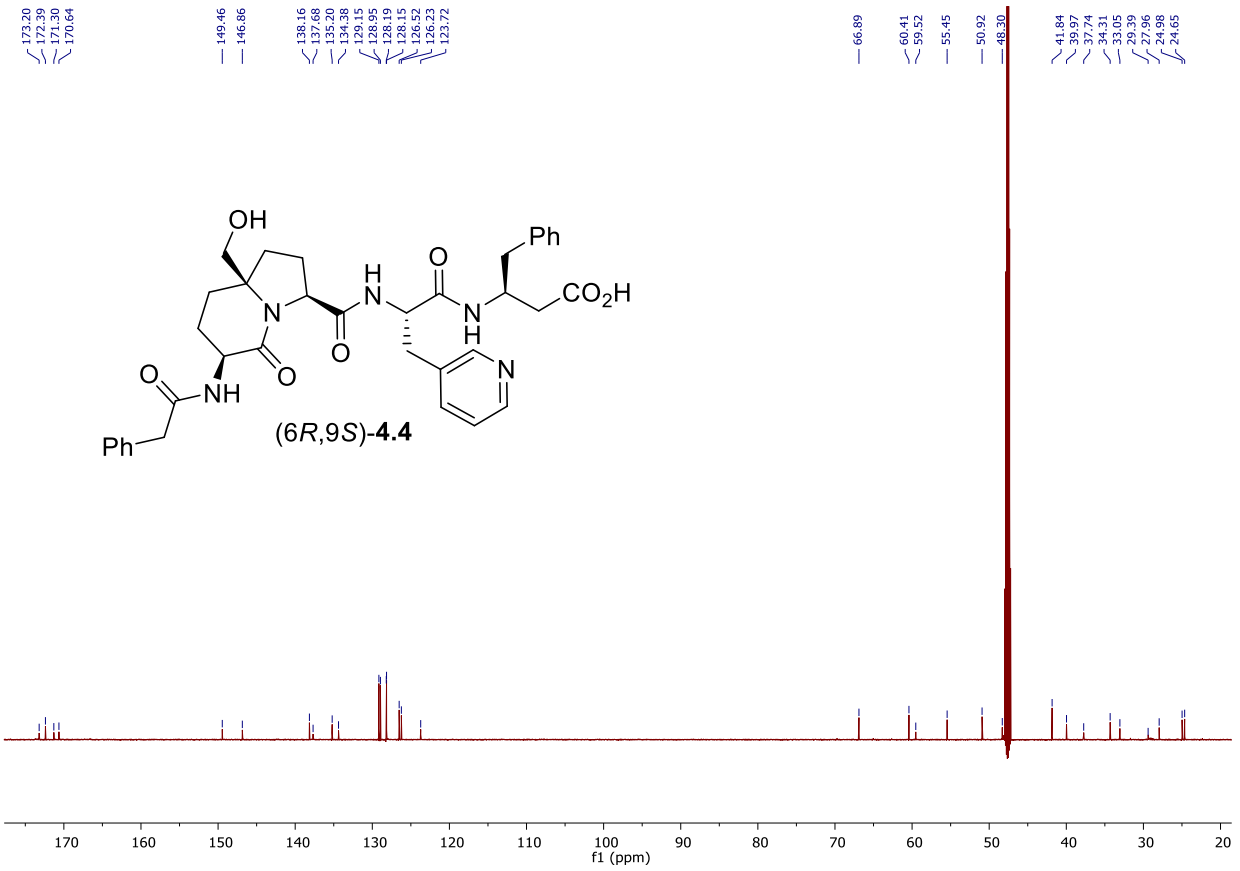

^{1}H *NMR 700 MHz*

Solvent: CD_3OD

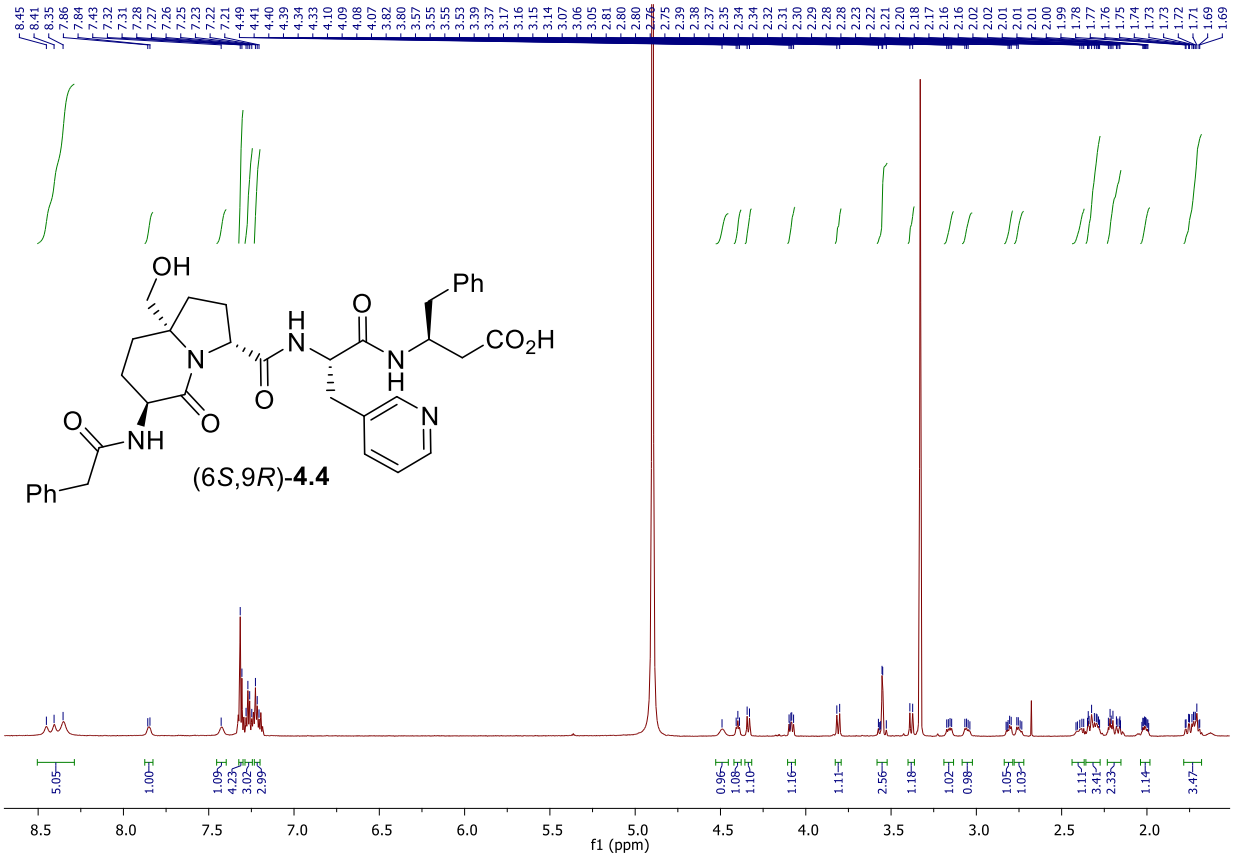

^{13}C *NMR 175 MHz*

Solvent: CD_3OD

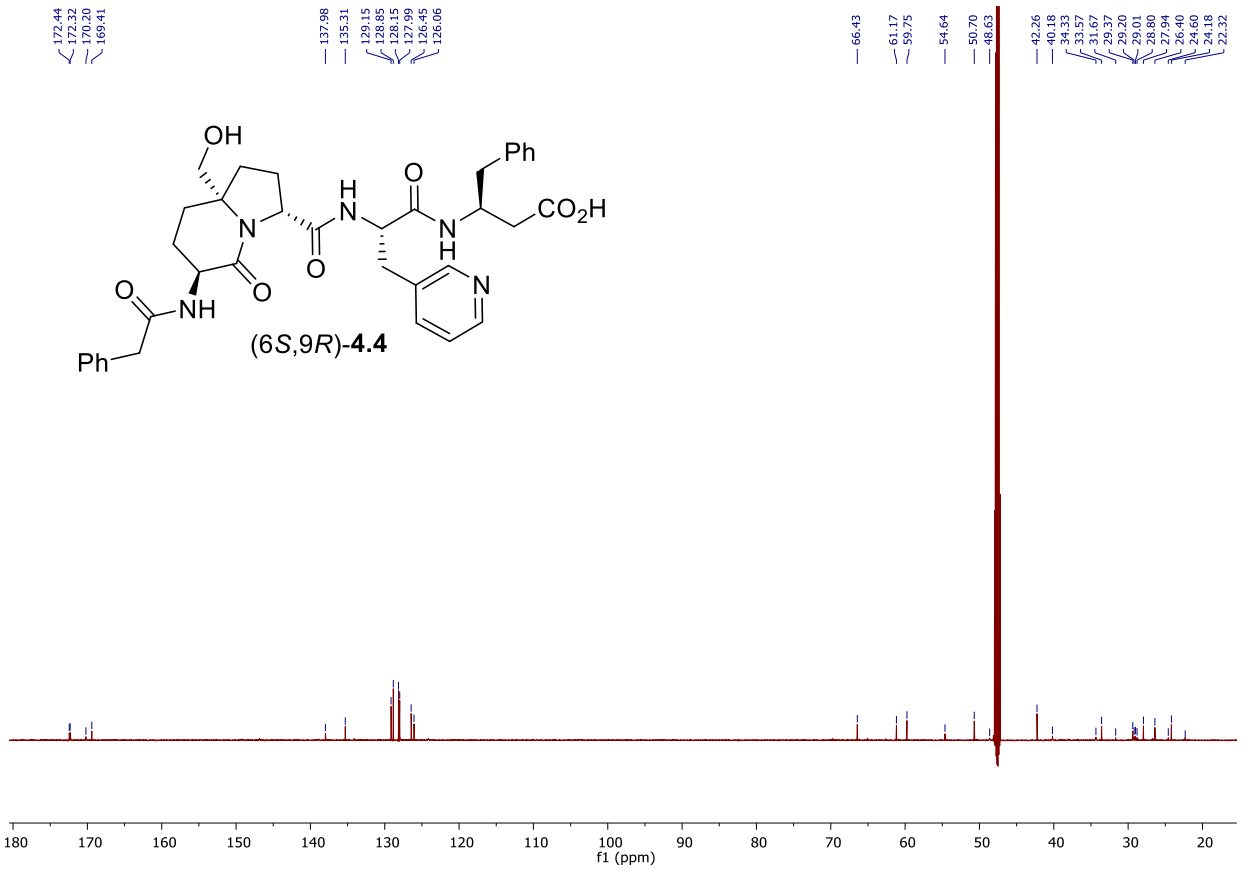

^{1}H *NMR 700 MHz*

Solvent: CD_3OD

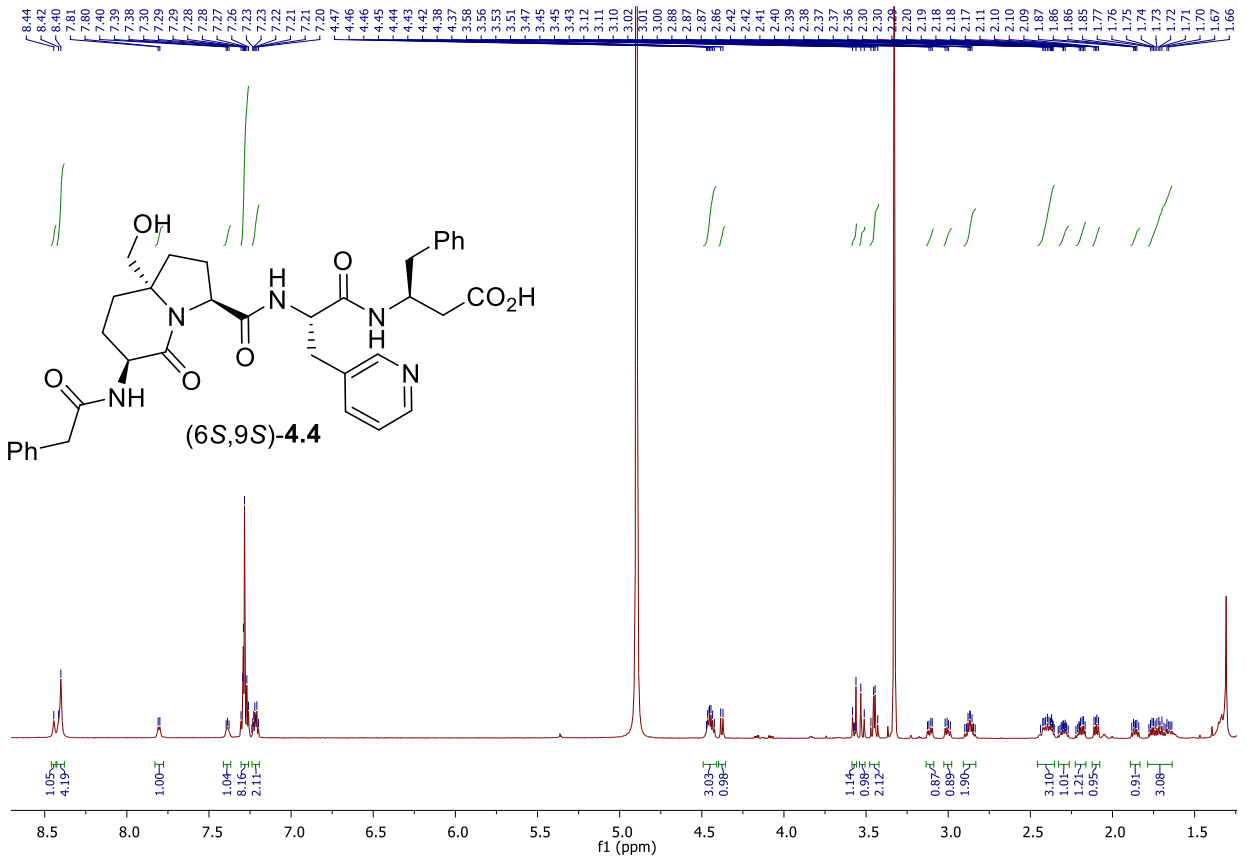

^{13}C *NMR 175 MHz*

Solvent: CD_3OD

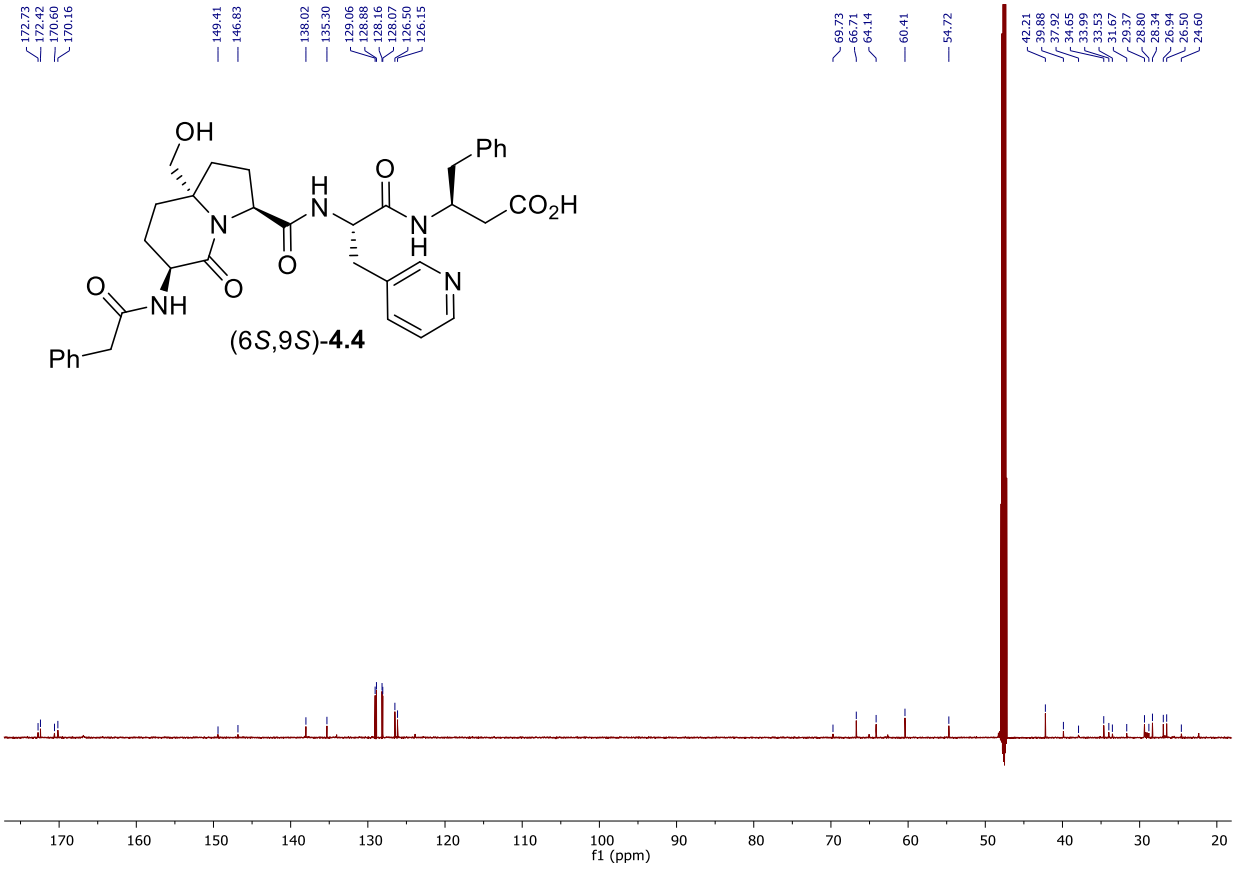

^{1}H *NMR 500 MHz*

Solvent: $CDCl_3$

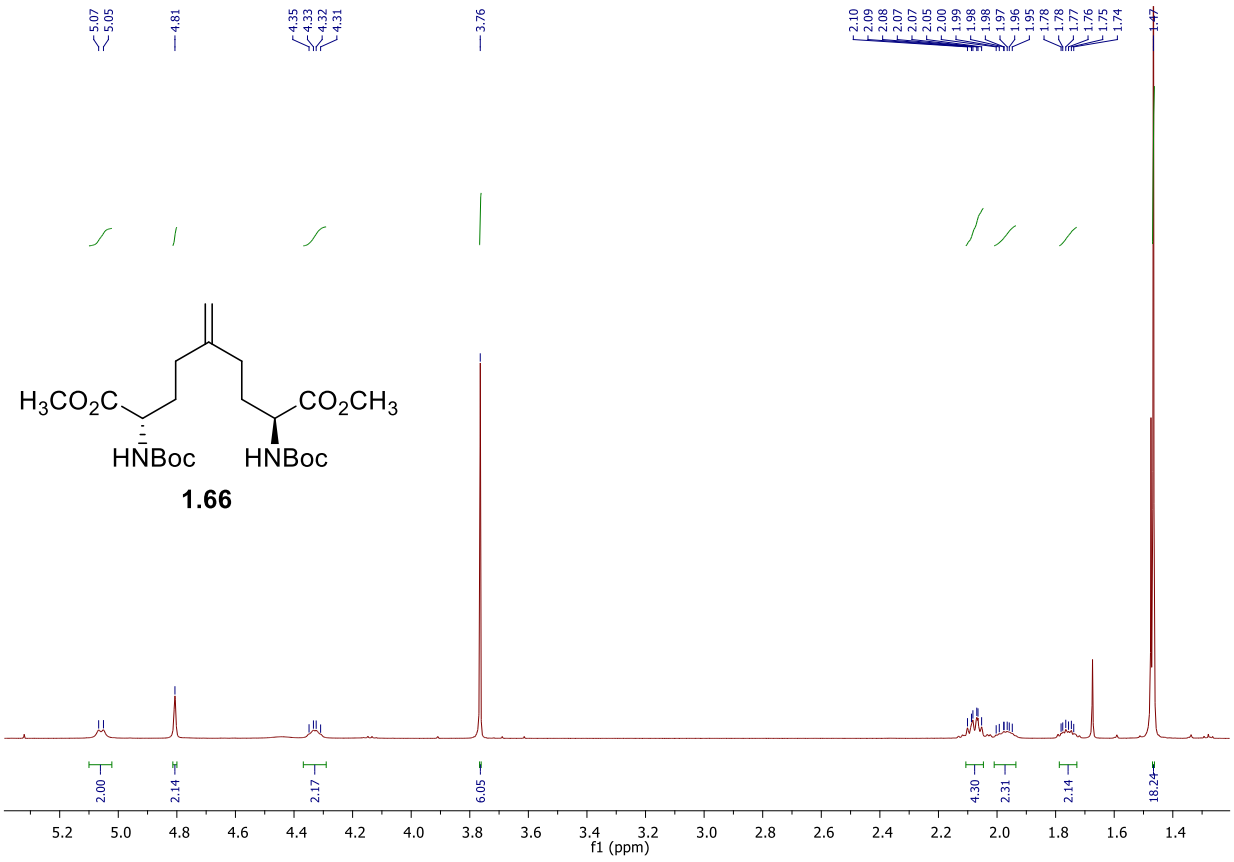

^{13}C *NMR 125 MHz*

Solvent: $CDCl_3$

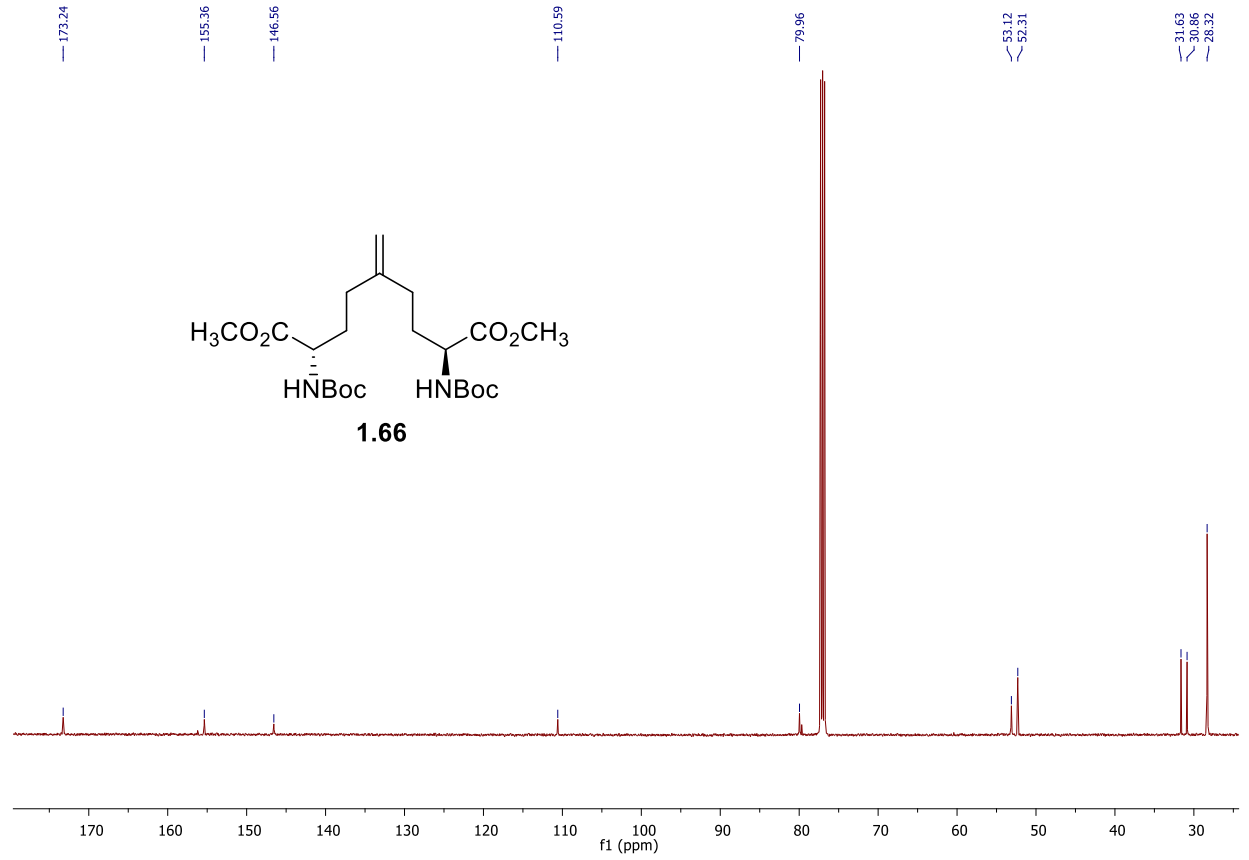

^{1}H *NMR 500 MHz*

Solvent: $CDCl_3$

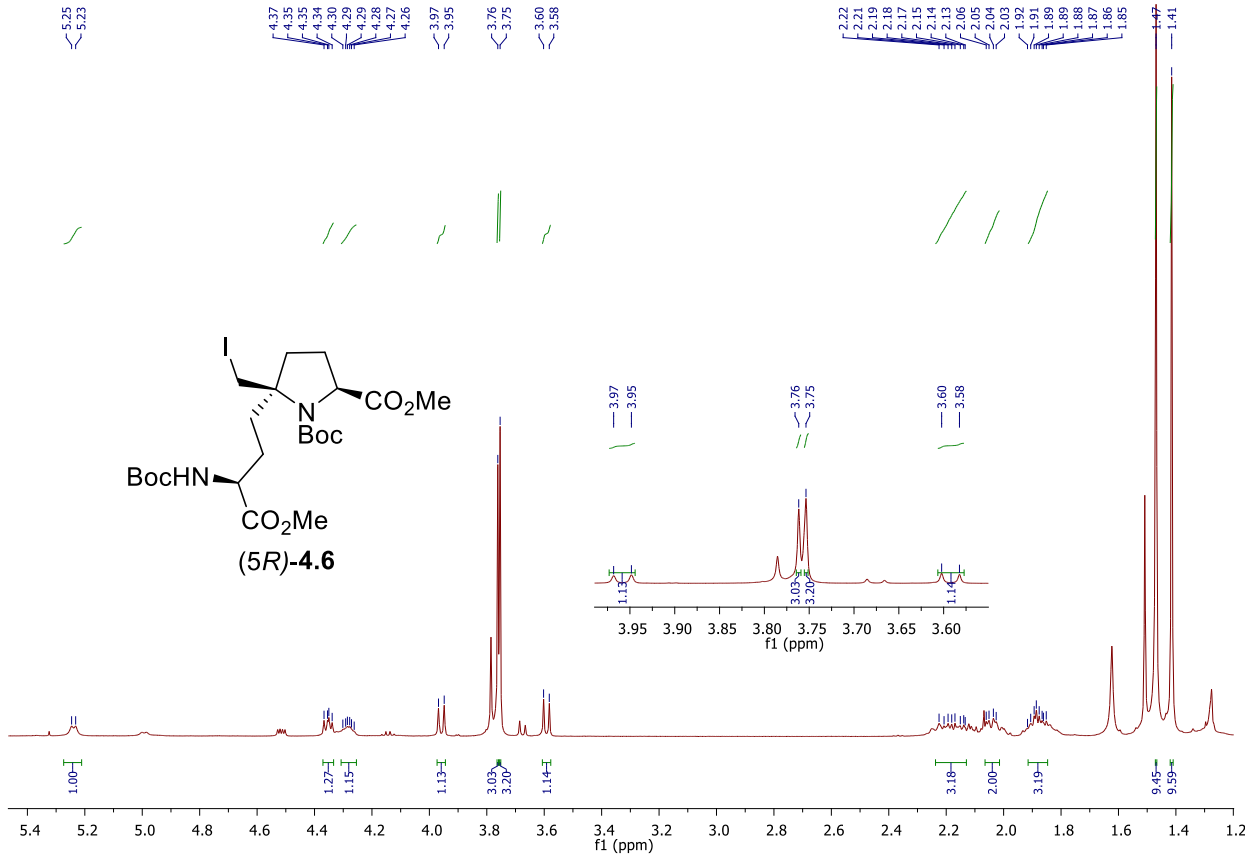

^{13}C *NMR 125 MHz*

Solvent: $CDCl_3$

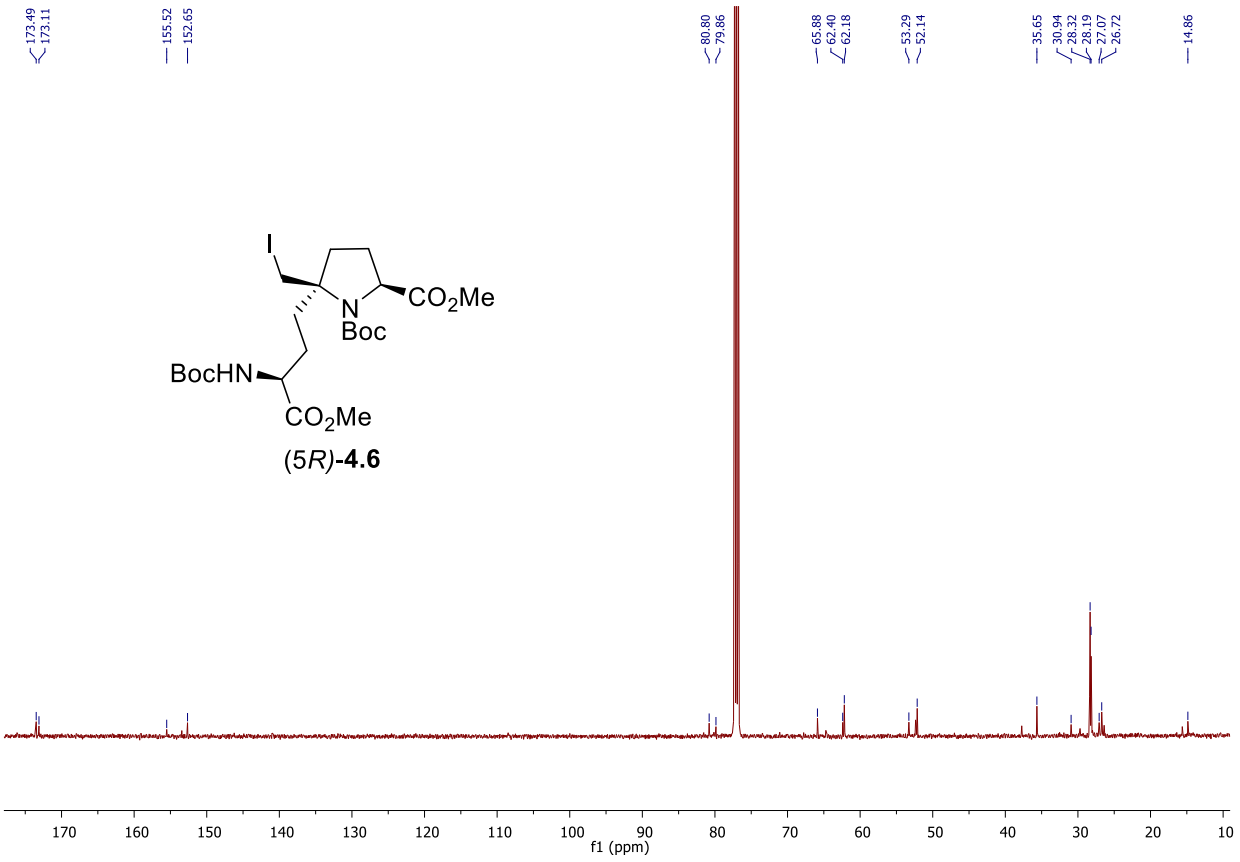

(5*R*)-**4.6**

^{1}H *NMR 500 MHz*

Solvent: $CDCl_3$

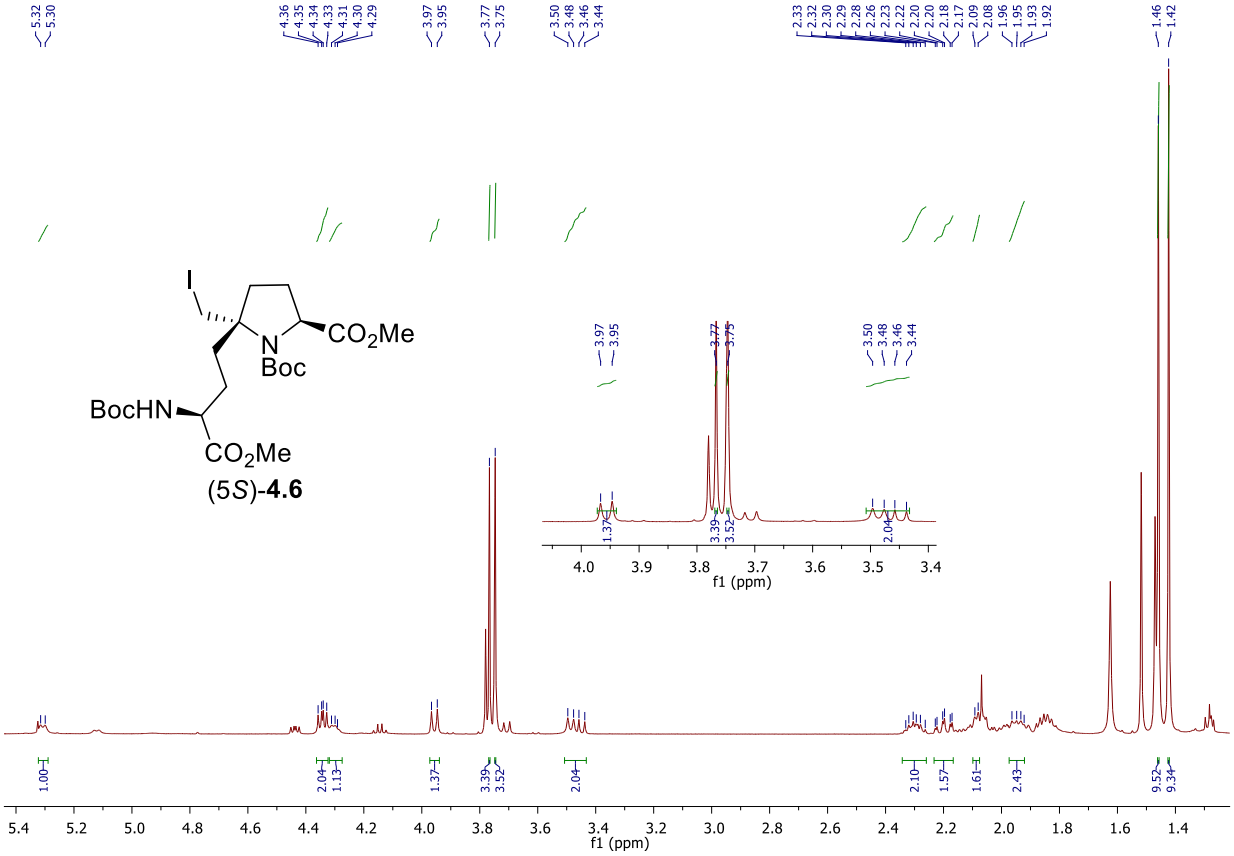

^{13}C *NMR 125 MHz*

Solvent: $CDCl_3$

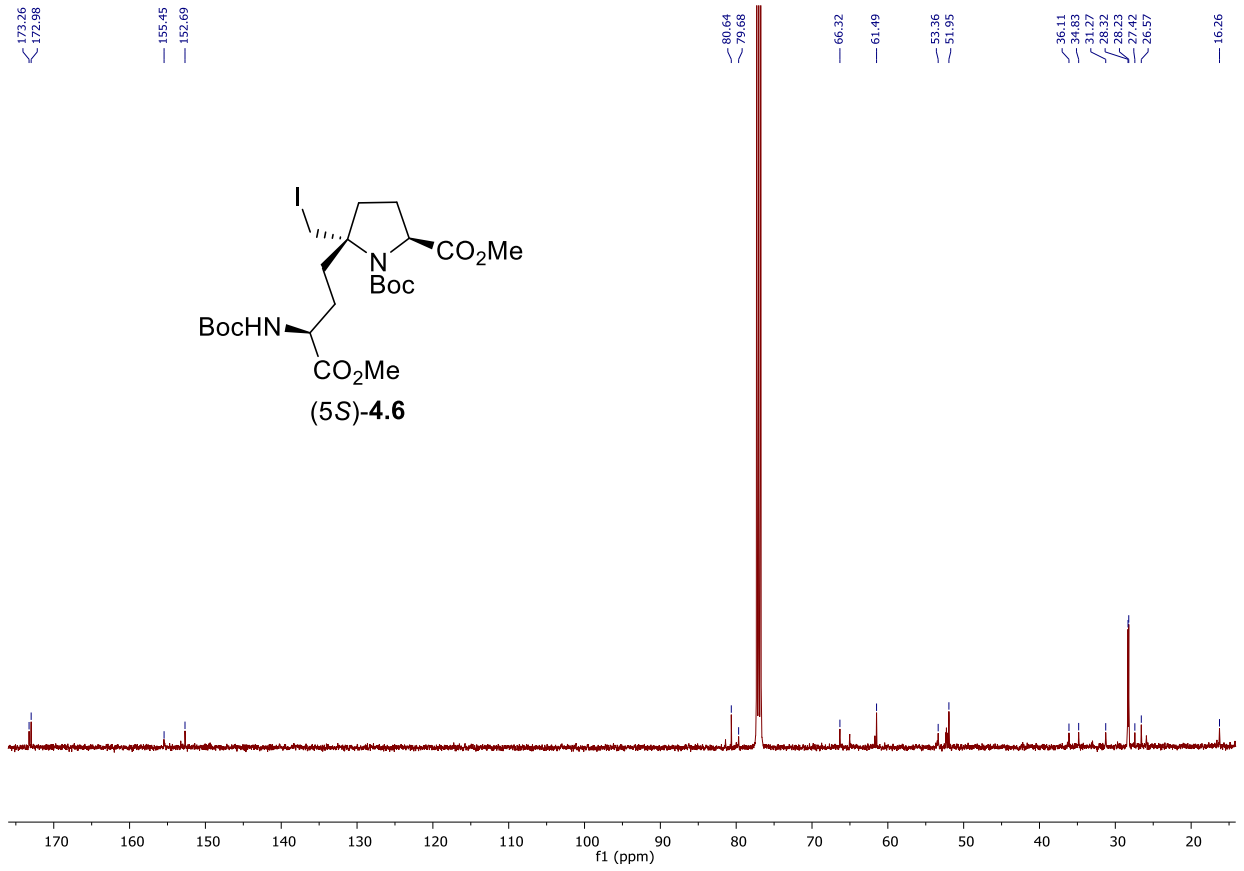

(5*S*)-**4.6**

^{1}H *NMR 400 MHz*

Solvent: CD_3OD

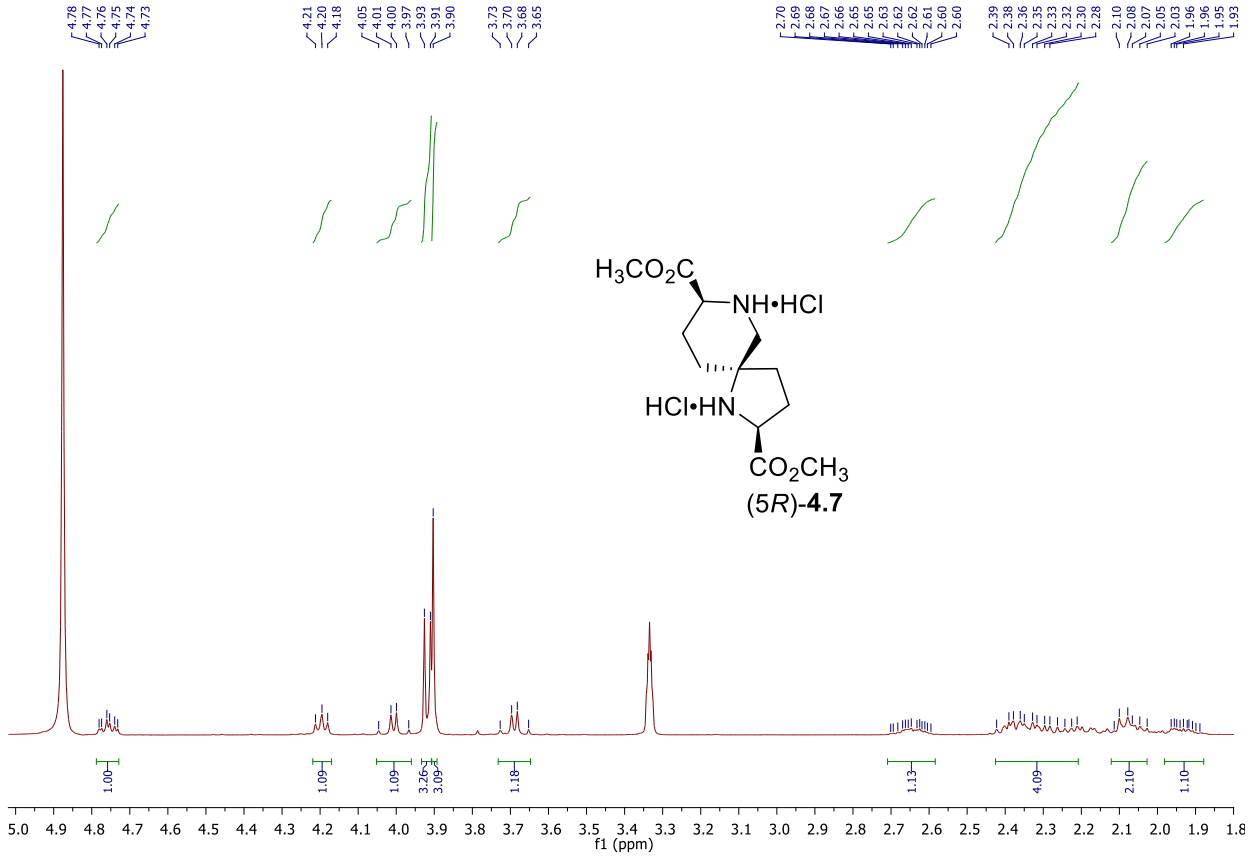

^{13}C *NMR 100 MHz*

Solvent: CD_3OD

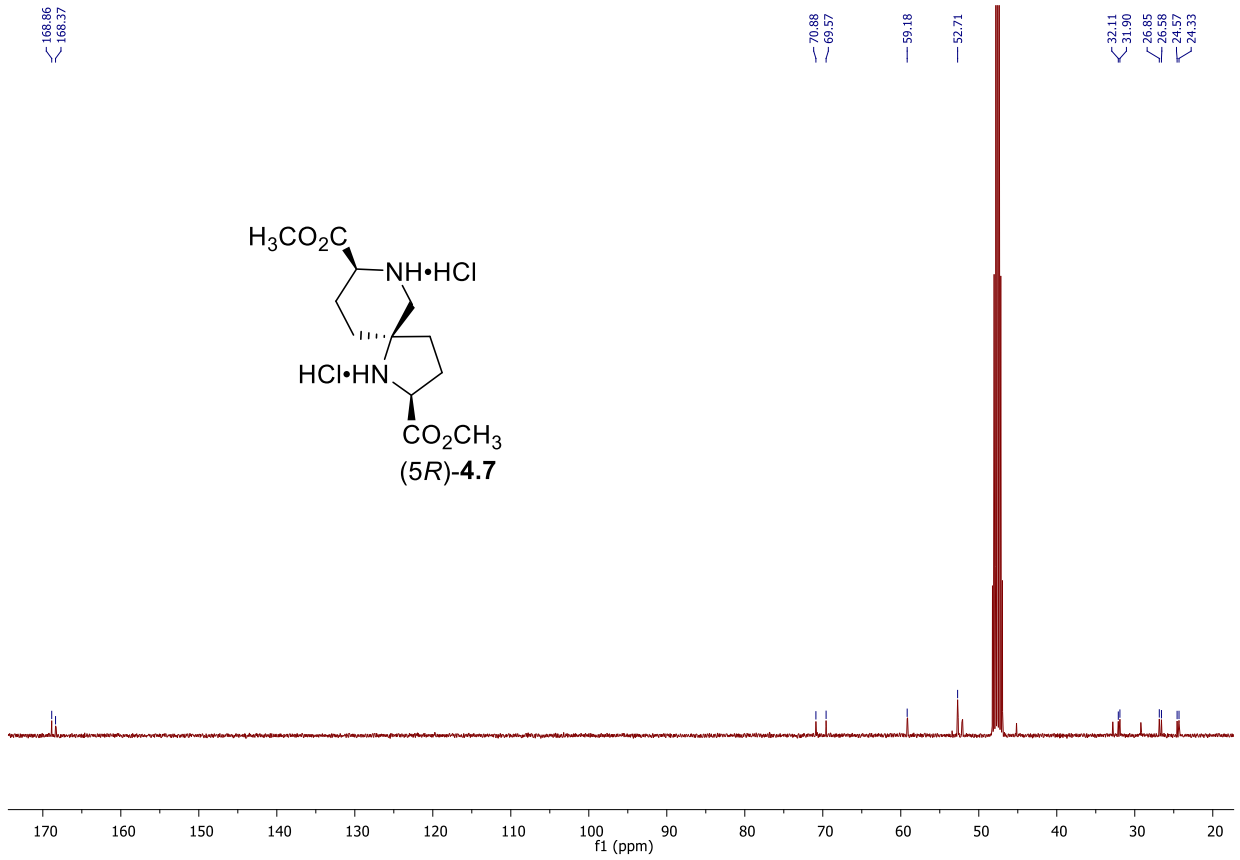

^{1}H *NMR 400 MHz*

Solvent: CD_3OD

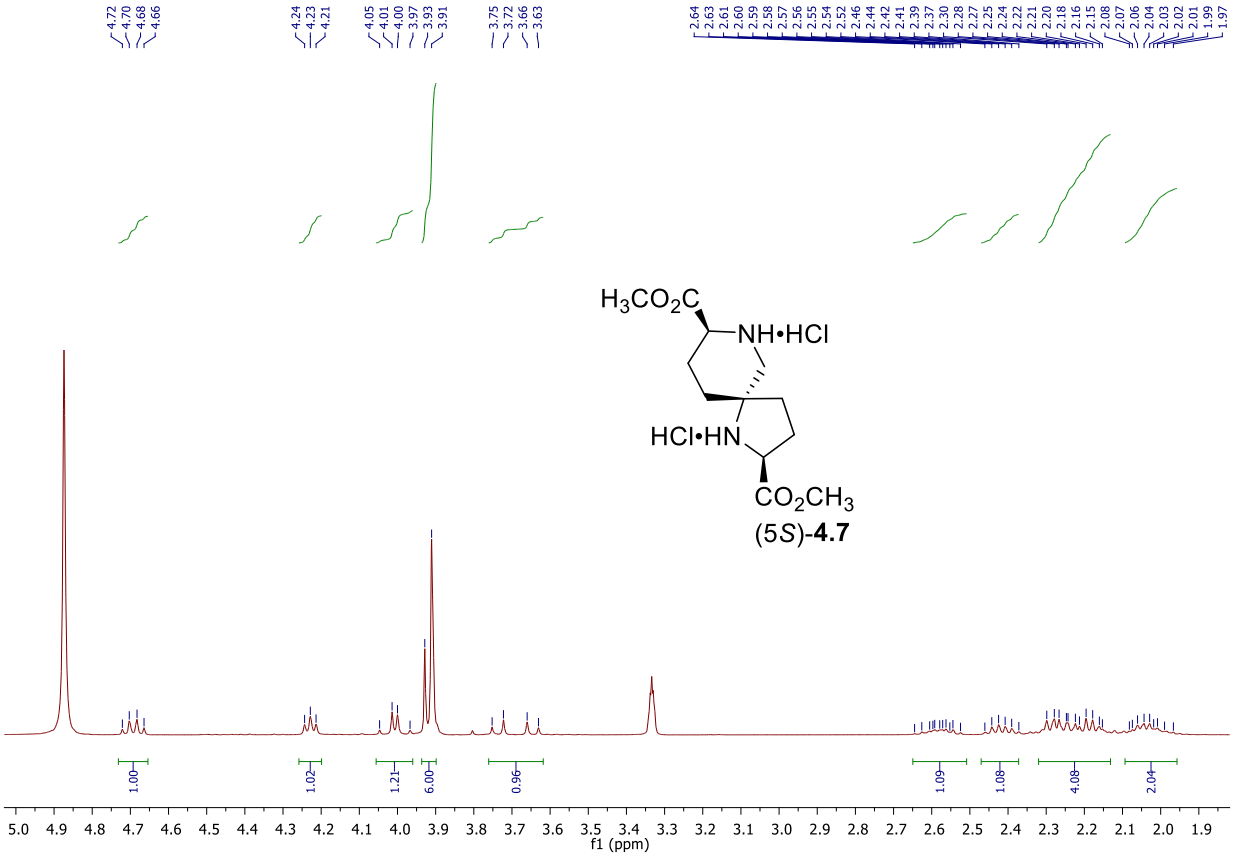

^{13}C *NMR 100 MHz*

Solvent: CD_3OD

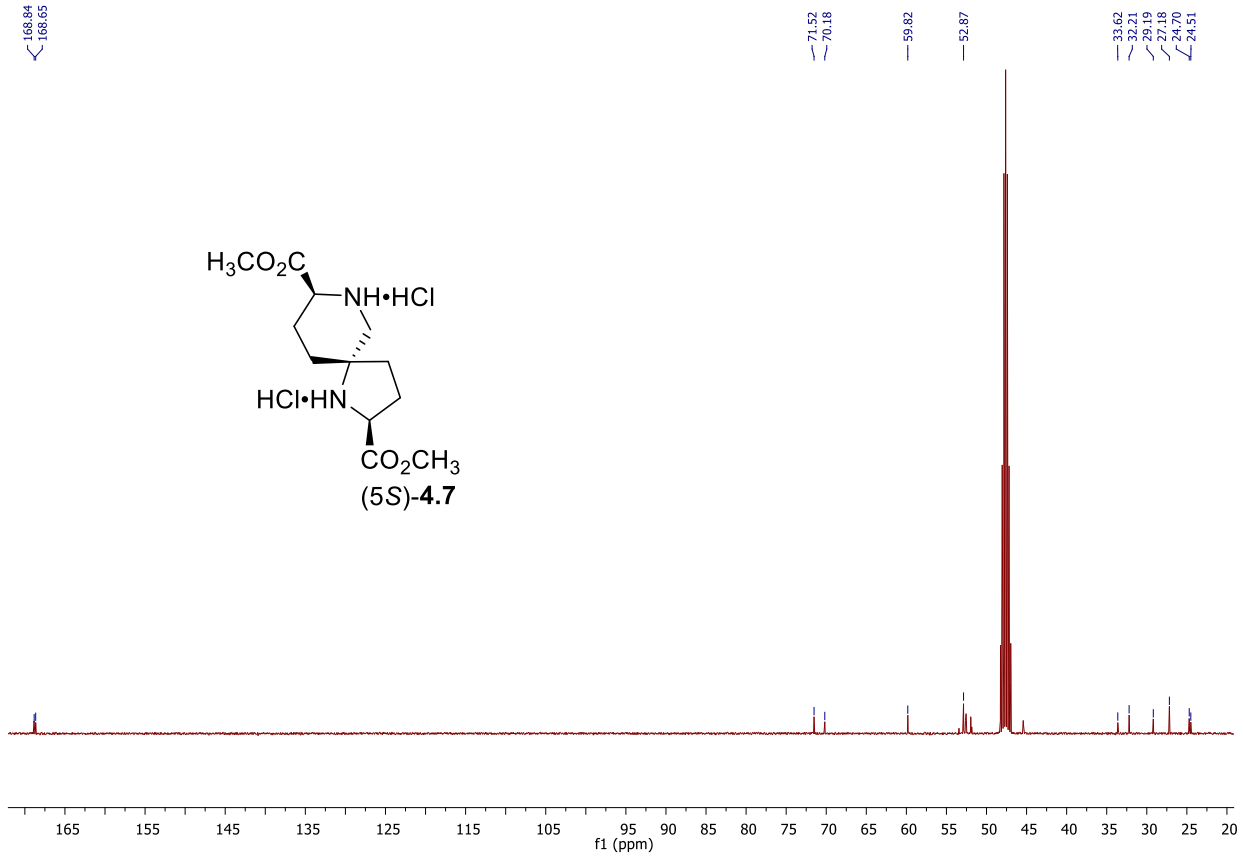

^{1}H *NMR 500 MHz*

Solvent: $CDCl_3$

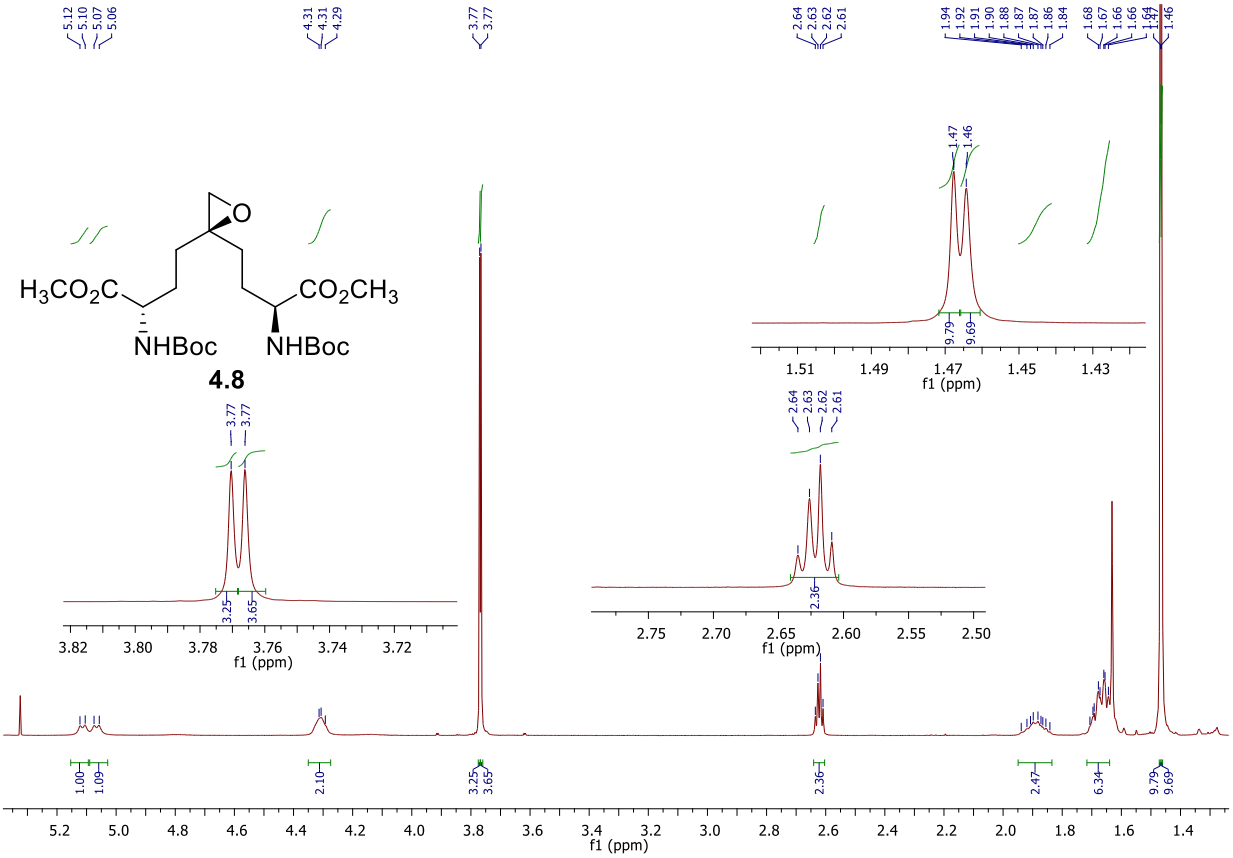

^{13}C *NMR 125 MHz*

Solvent: $CDCl_3$

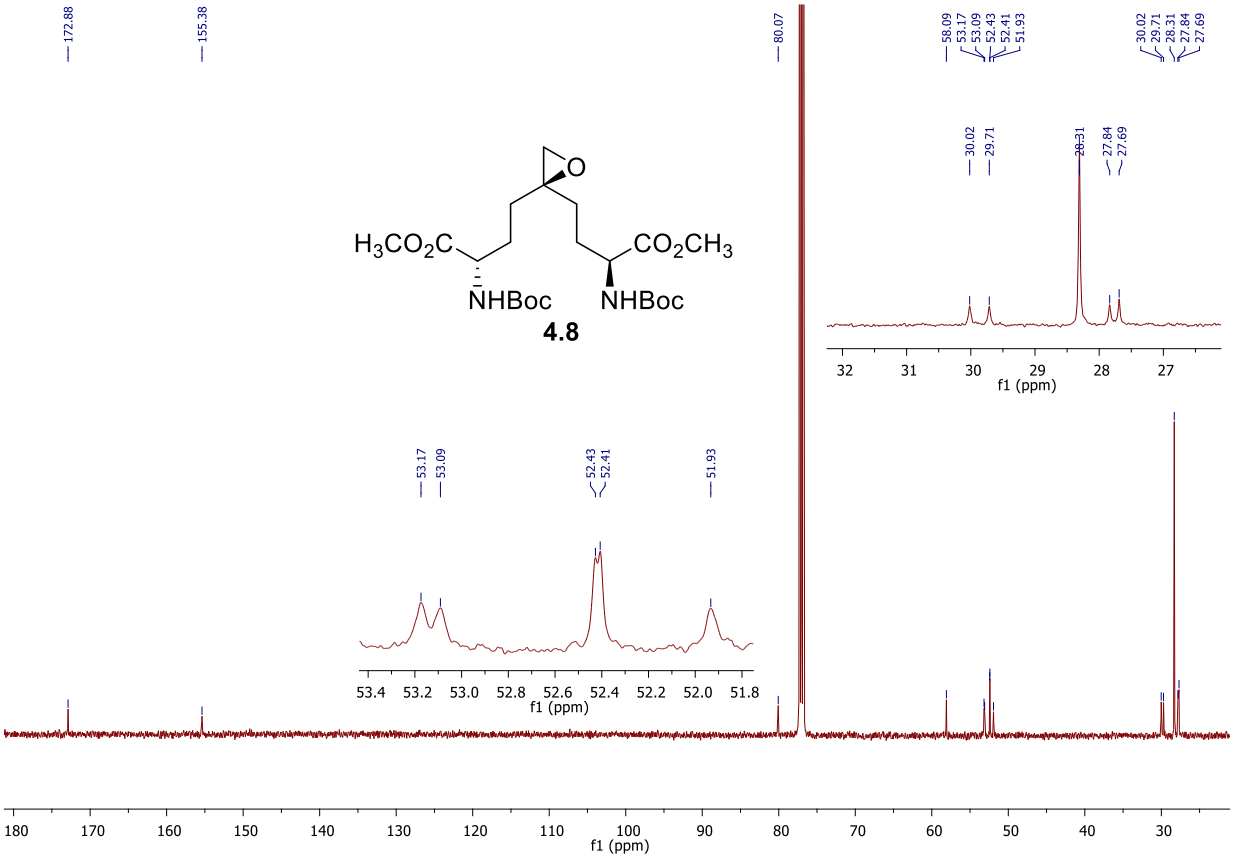

^{1}H *NMR 500 MHz*

Solvent: $CDCl_3$

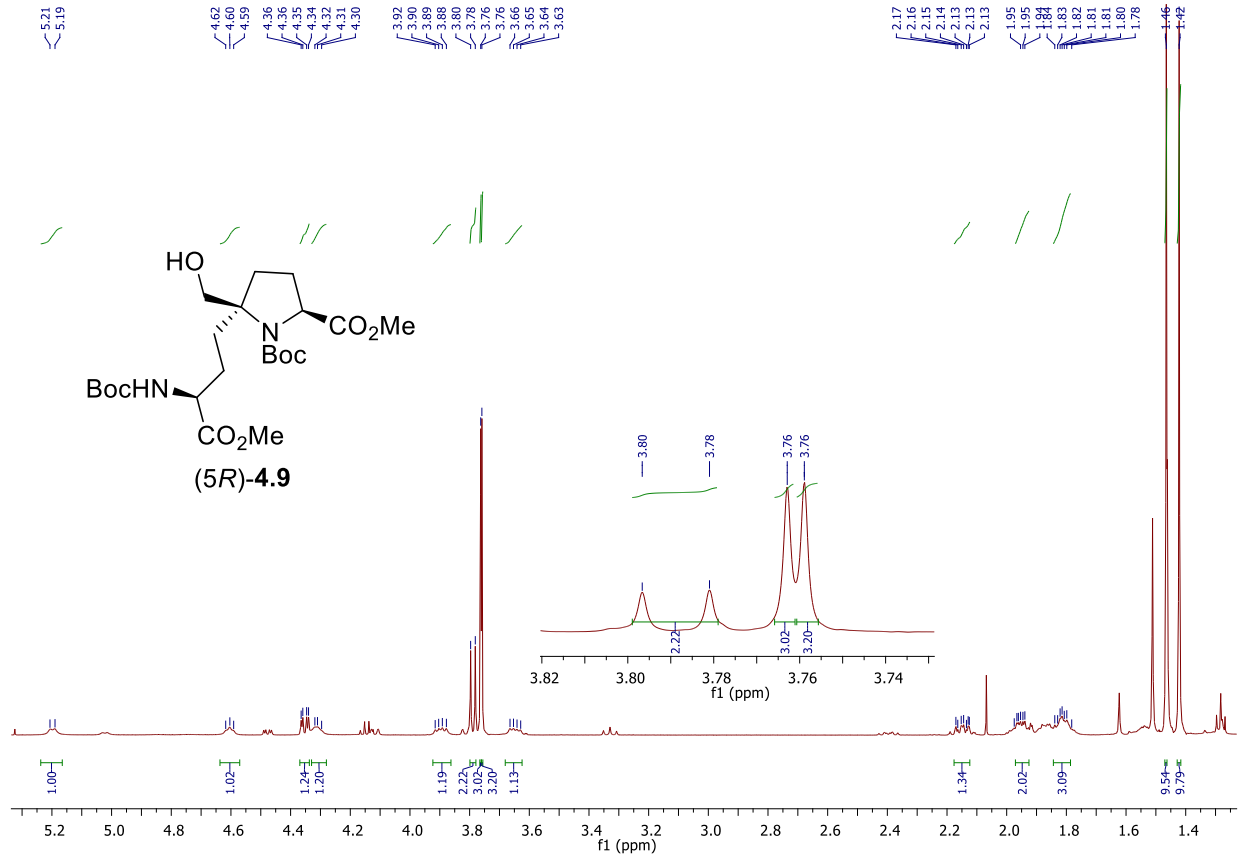

^{13}C *NMR 125 MHz*

Solvent: $CDCl_3$

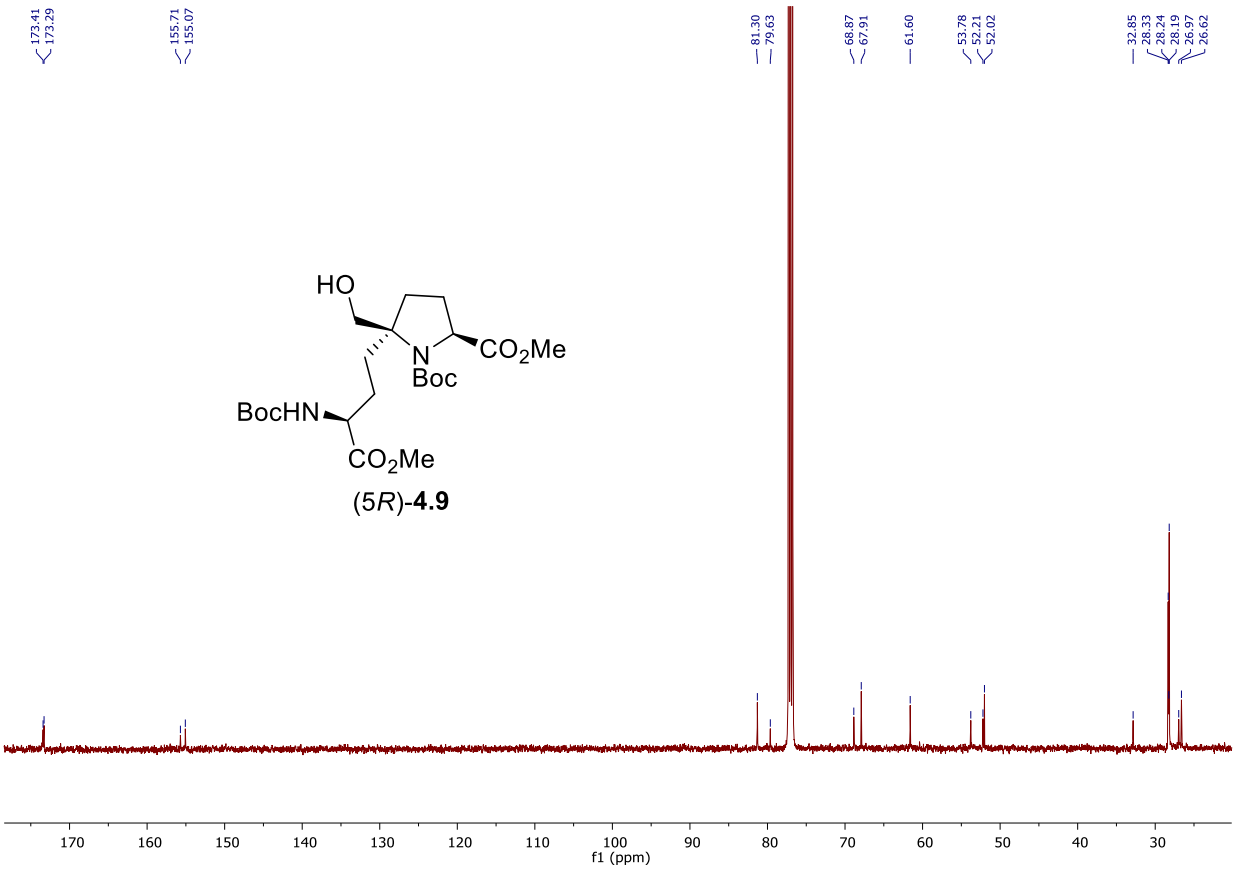

^{1}H *NMR 500 MHz*

Solvent: $CDCl_3$

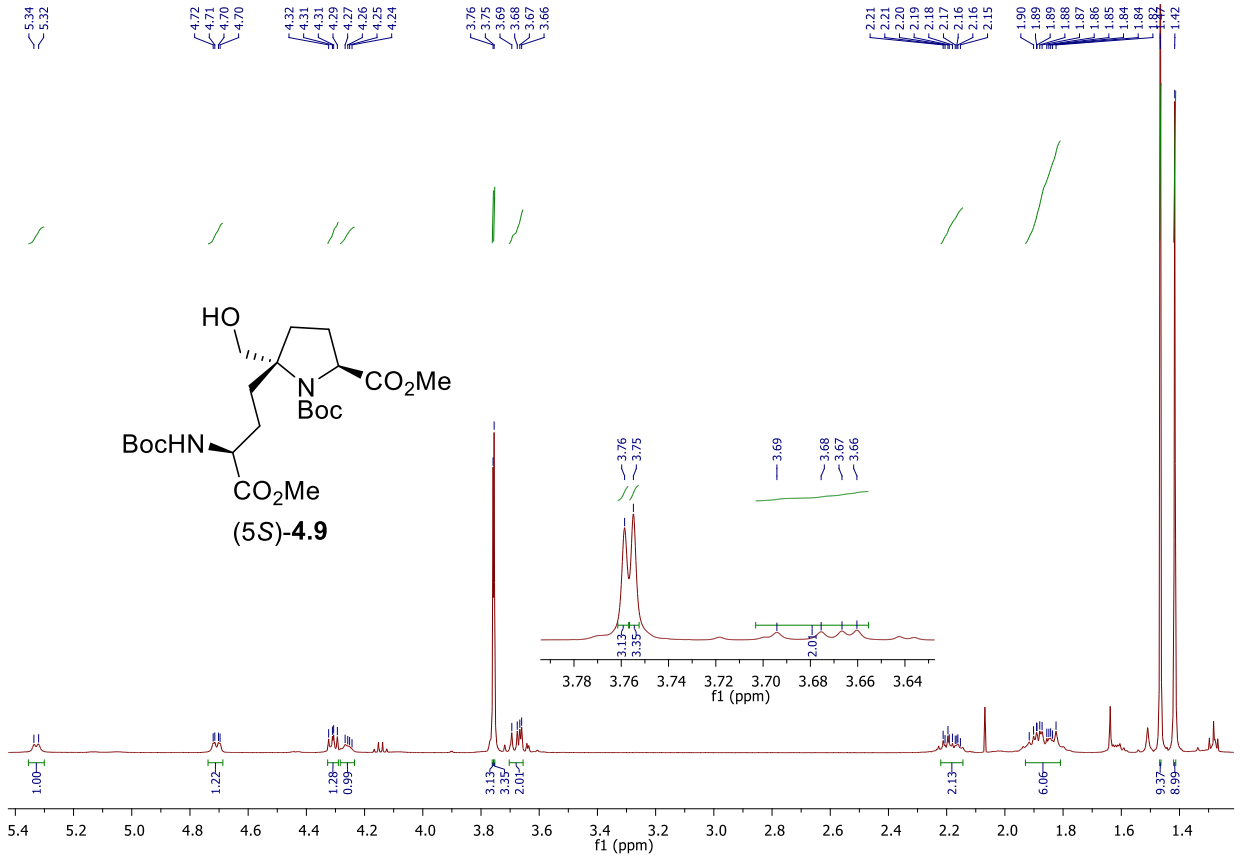

^{13}C *NMR 125 MHz*

Solvent: $CDCl_3$

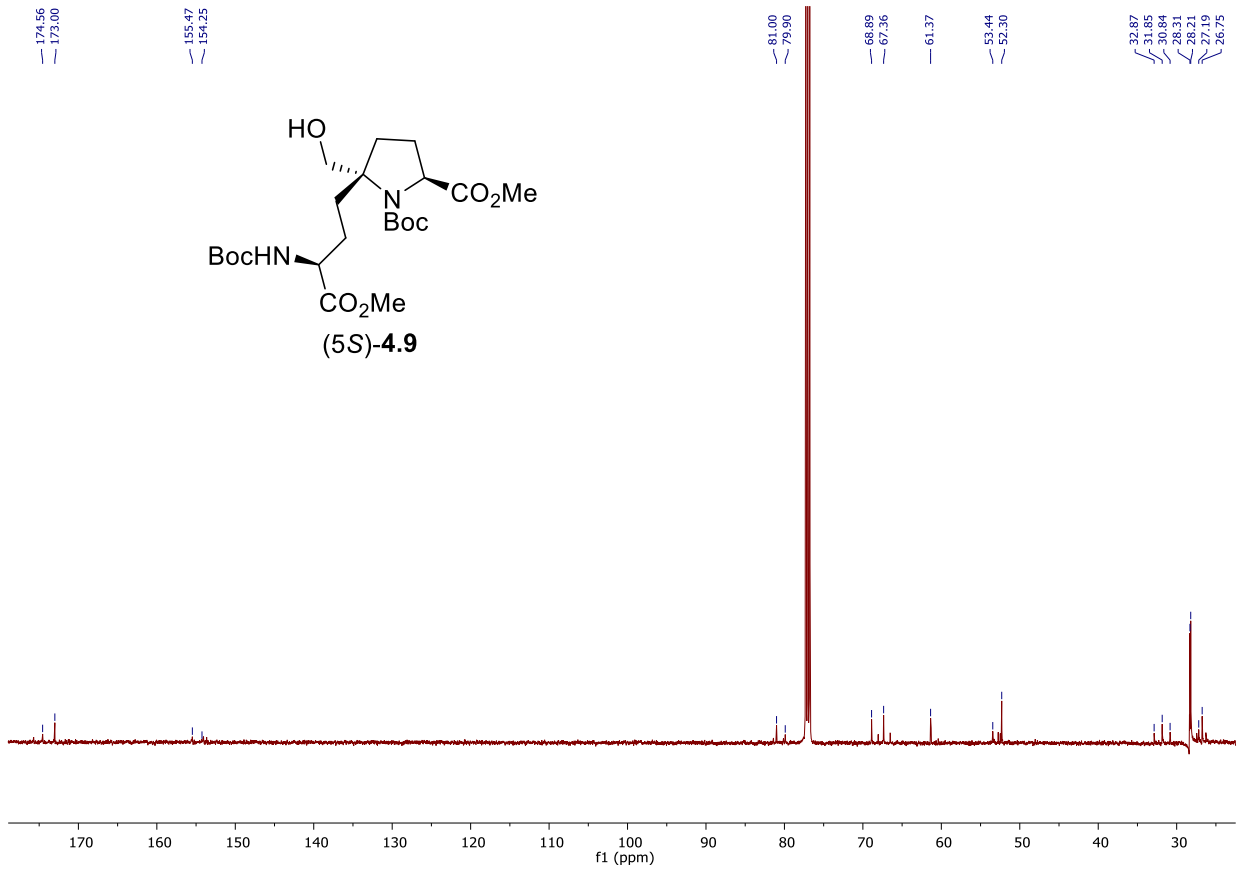

^{1}H *NMR 400 MHz*

Solvent: DMSO-D_6

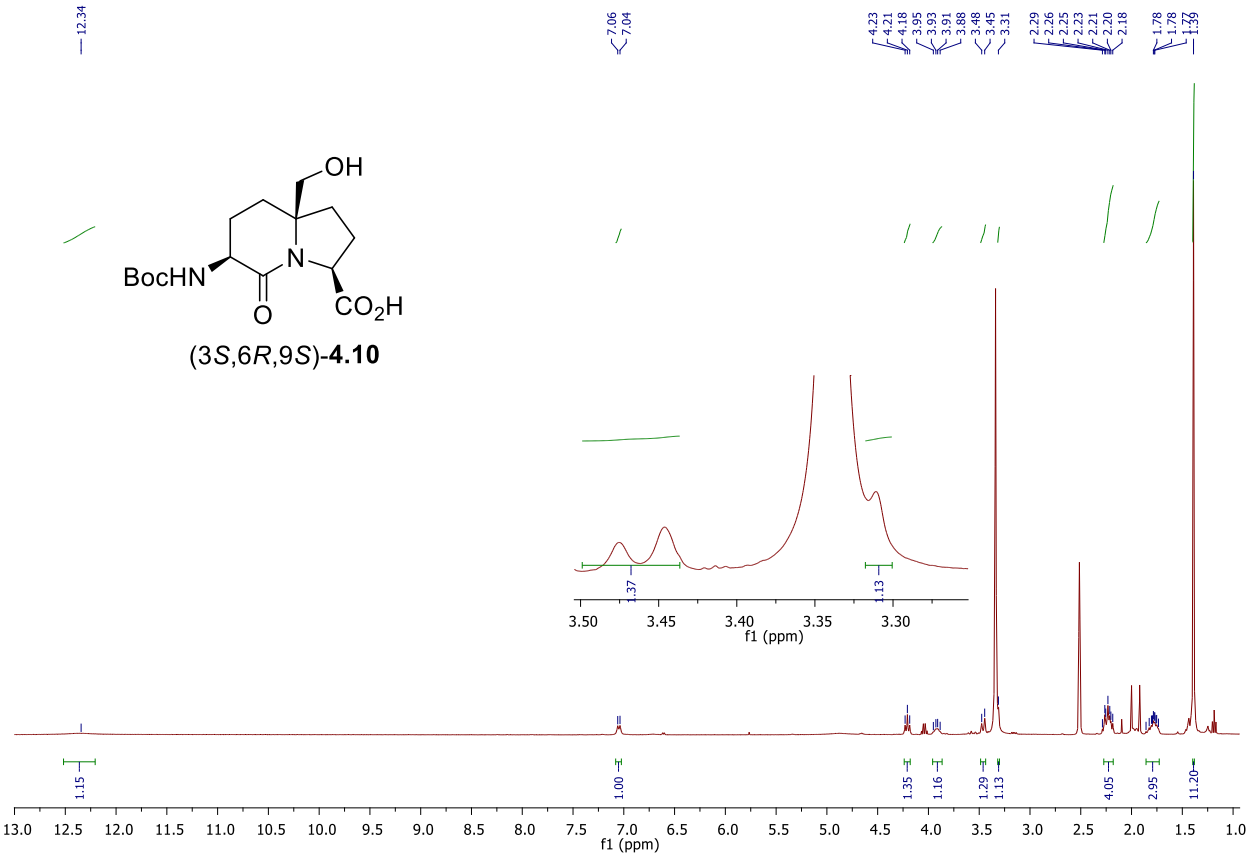

^{13}C *NMR 100 MHz*

Solvent: DMSO-D_6

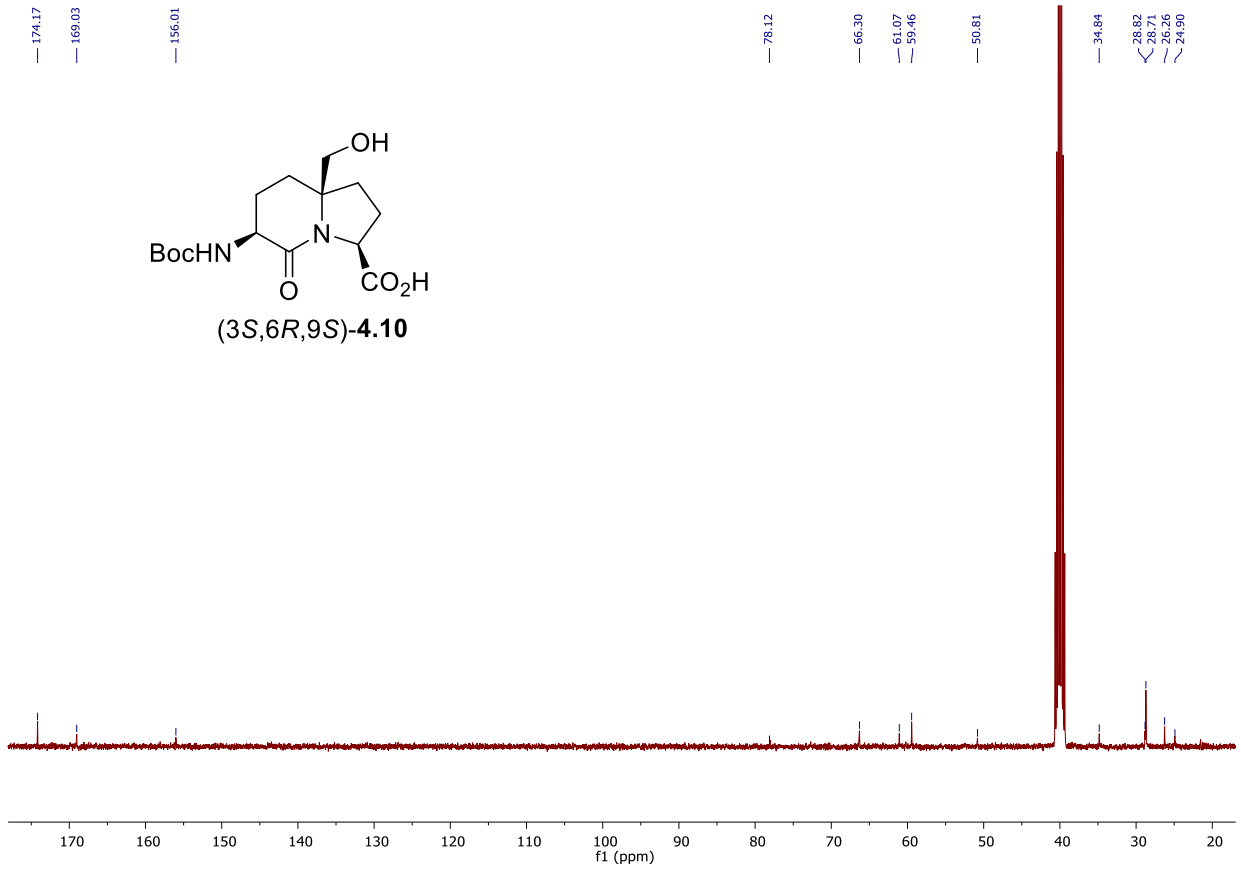

(3*S*,6*R*,9*S*)-**4.10**

^{1}H NMR, 500 MHz

Solvent: $CDCl_3$

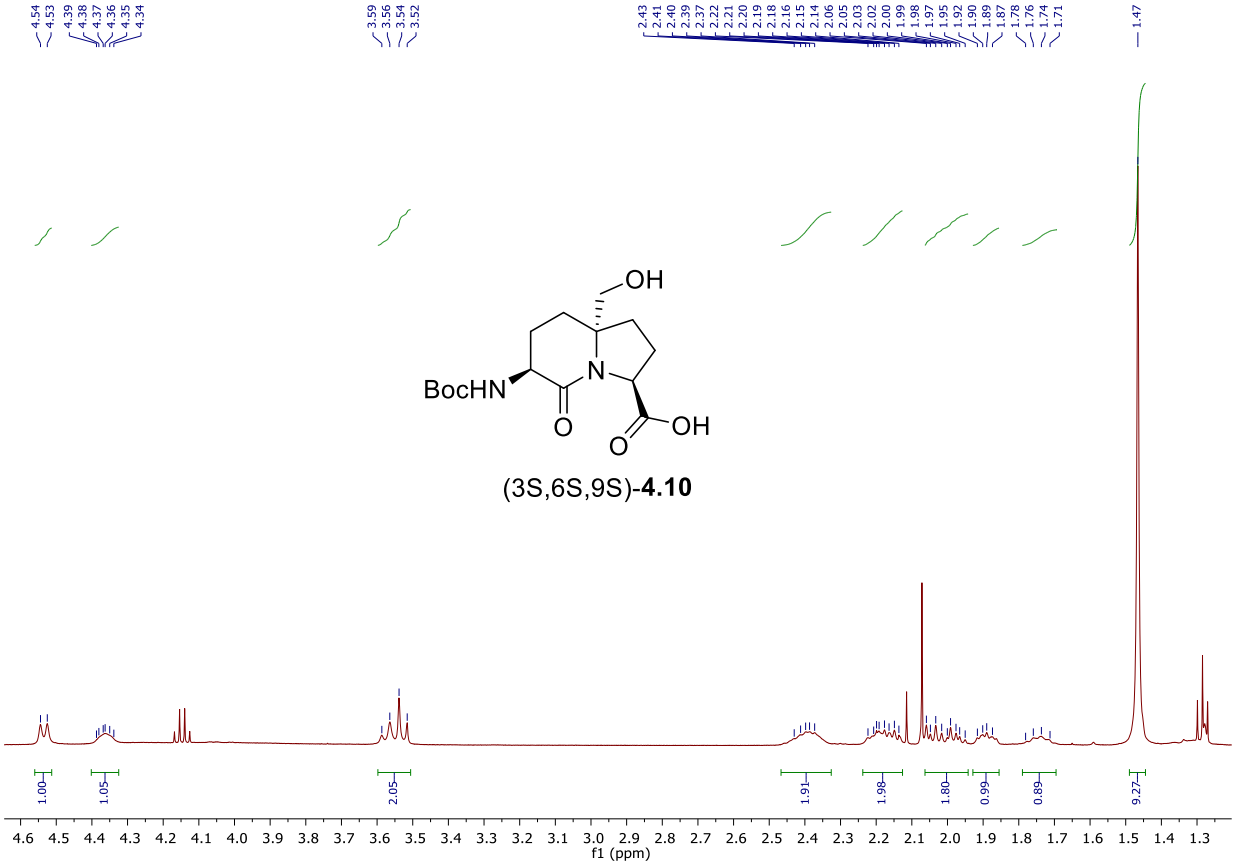

(3S,6S,9S)-**4.10**

^{13}C NMR, 125 MHz

Solvent: $CDCl_3$

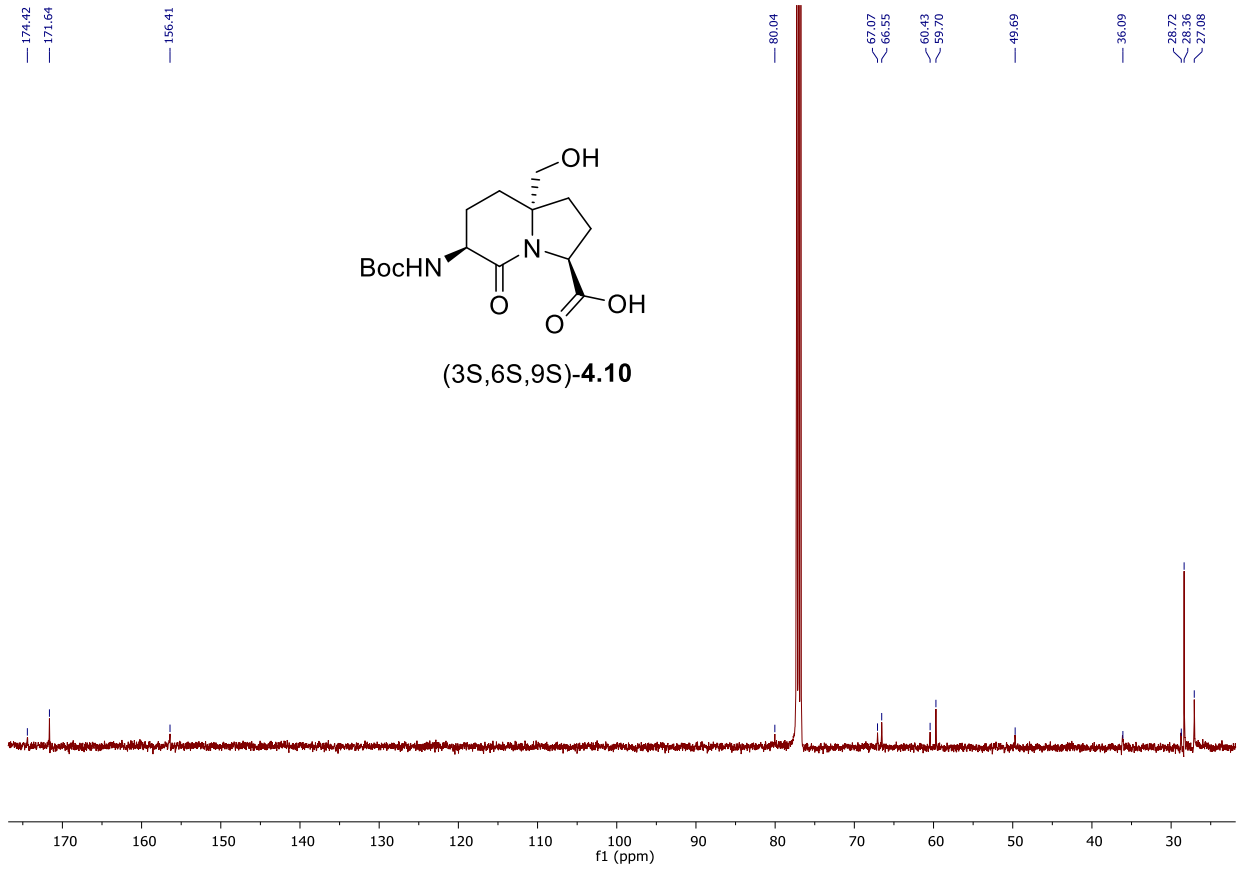

(3S,6S,9S)-**4.10**

^{1}H NMR, 500 MHz

Solvent: $CDCl_3$

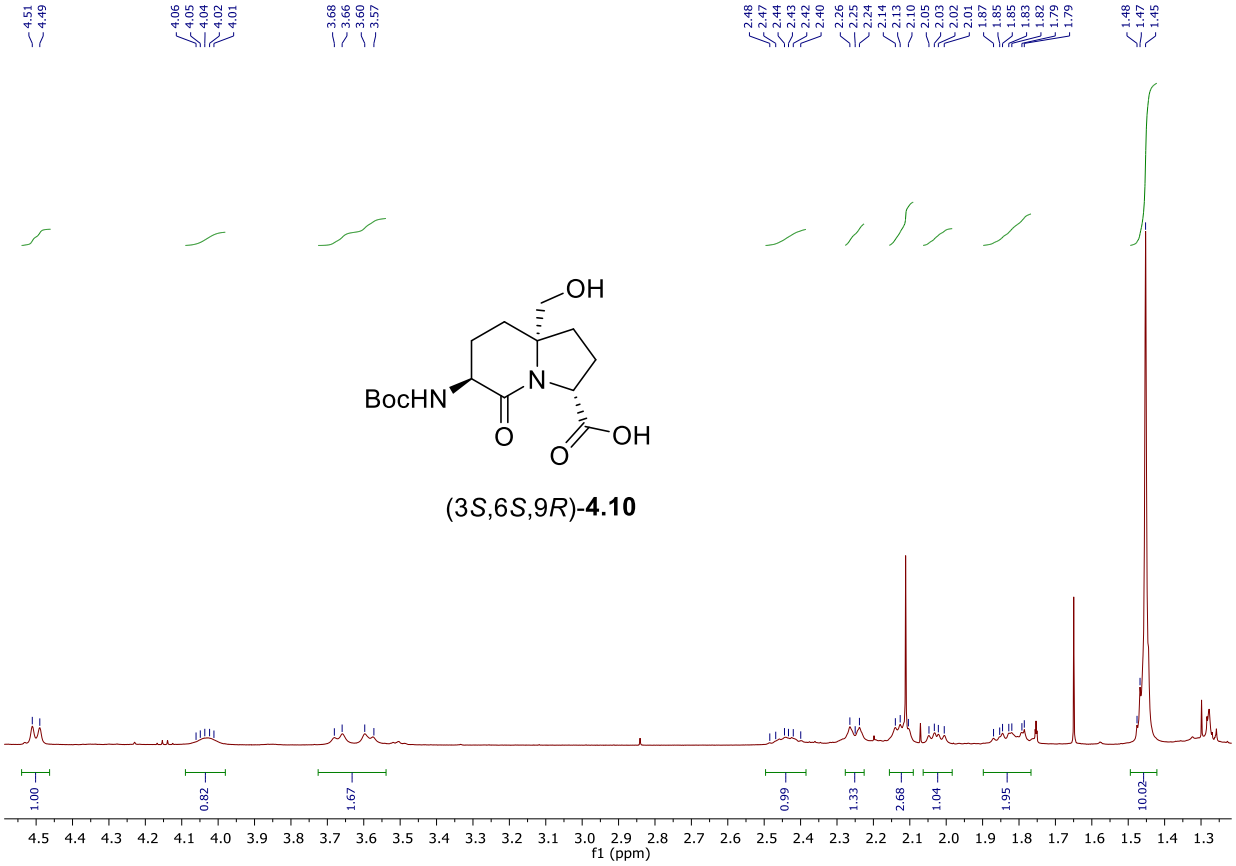

(3*S*,6*S*,9*R*)-**4.10**

^{13}C NMR, 125 MHz

Solvent: $CDCl_3$

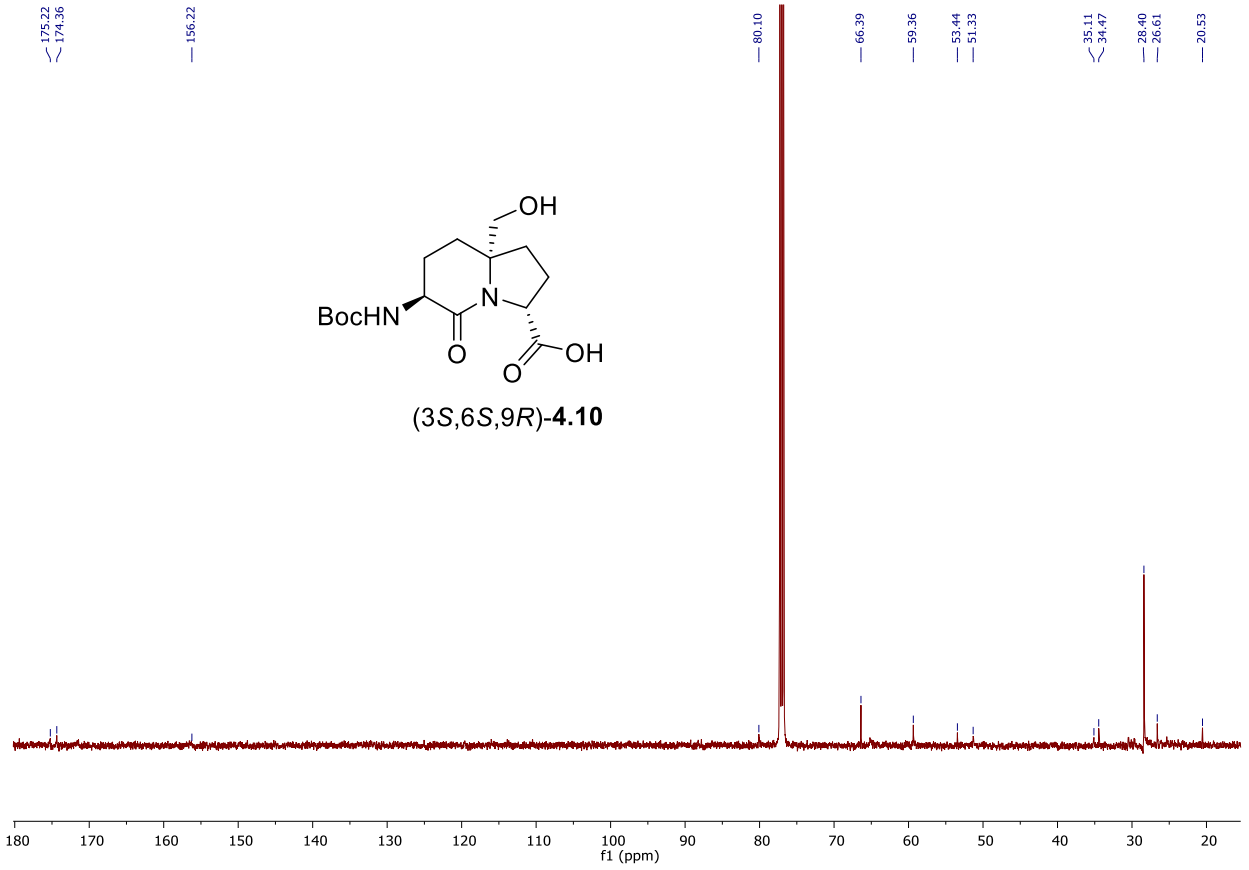

(3*S*,6*S*,9*R*)-**4.10**

^{1}H *NMR 400 MHz*

Solvent: $CDCl_3$

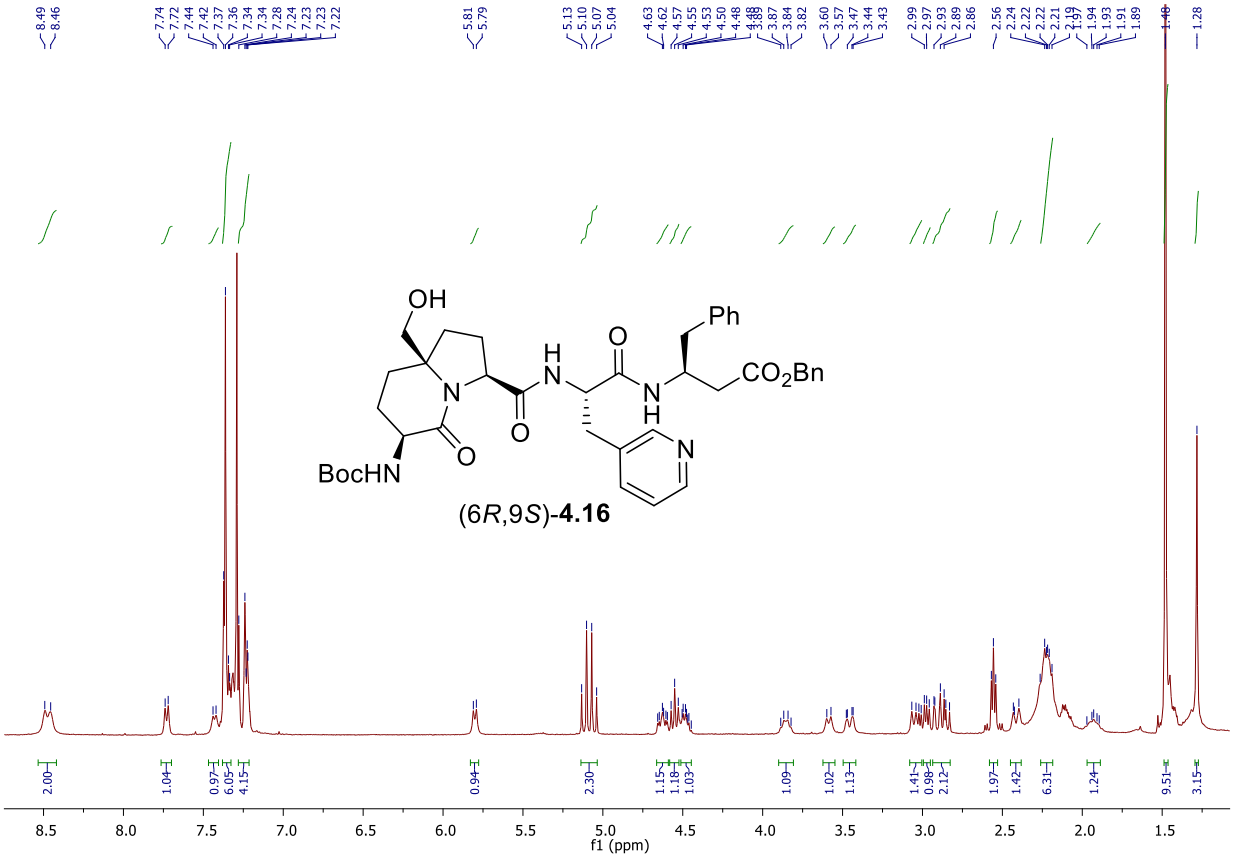

^{13}C *NMR 100 MHz*

Solvent: $CDCl_3$

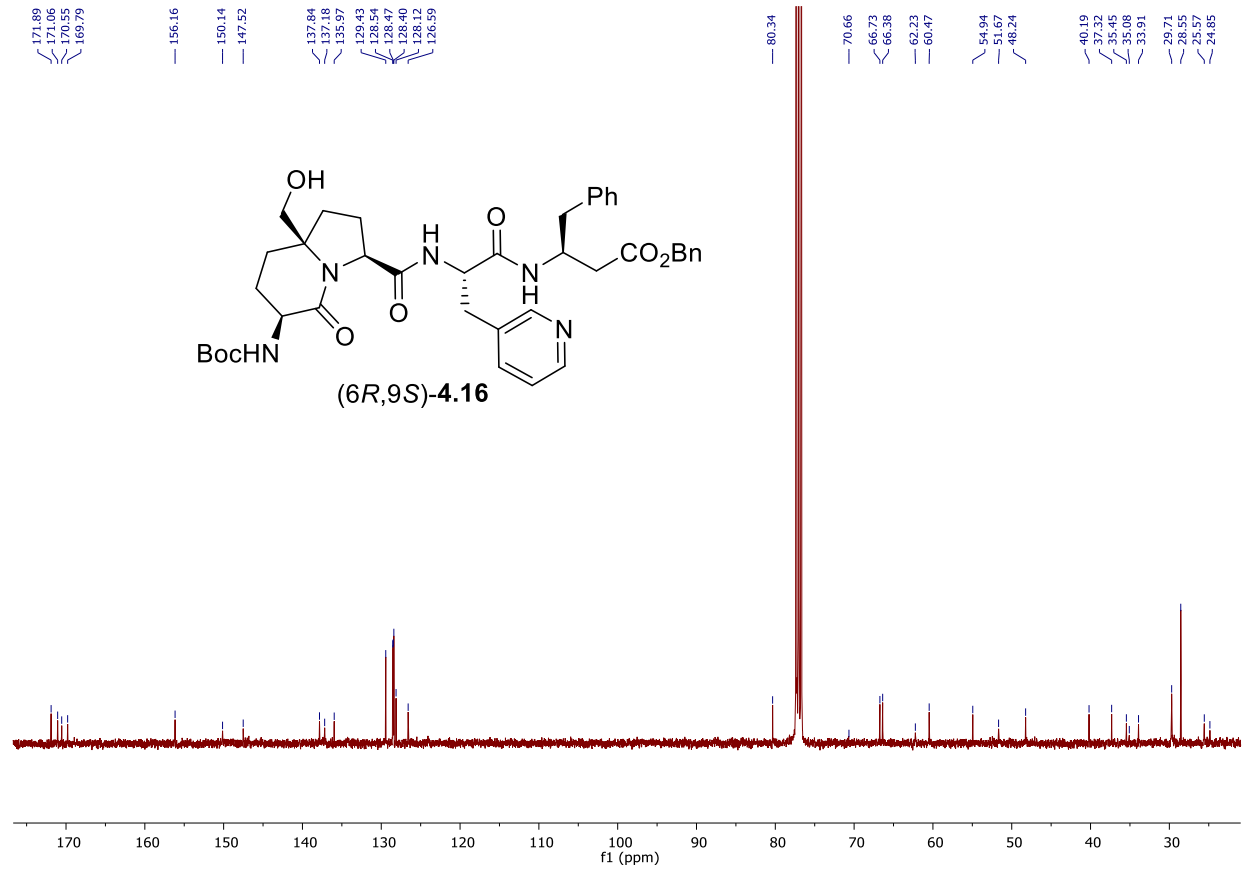

^{1}H *NMR 400 MHz*

Solvent: $CDCl_3$

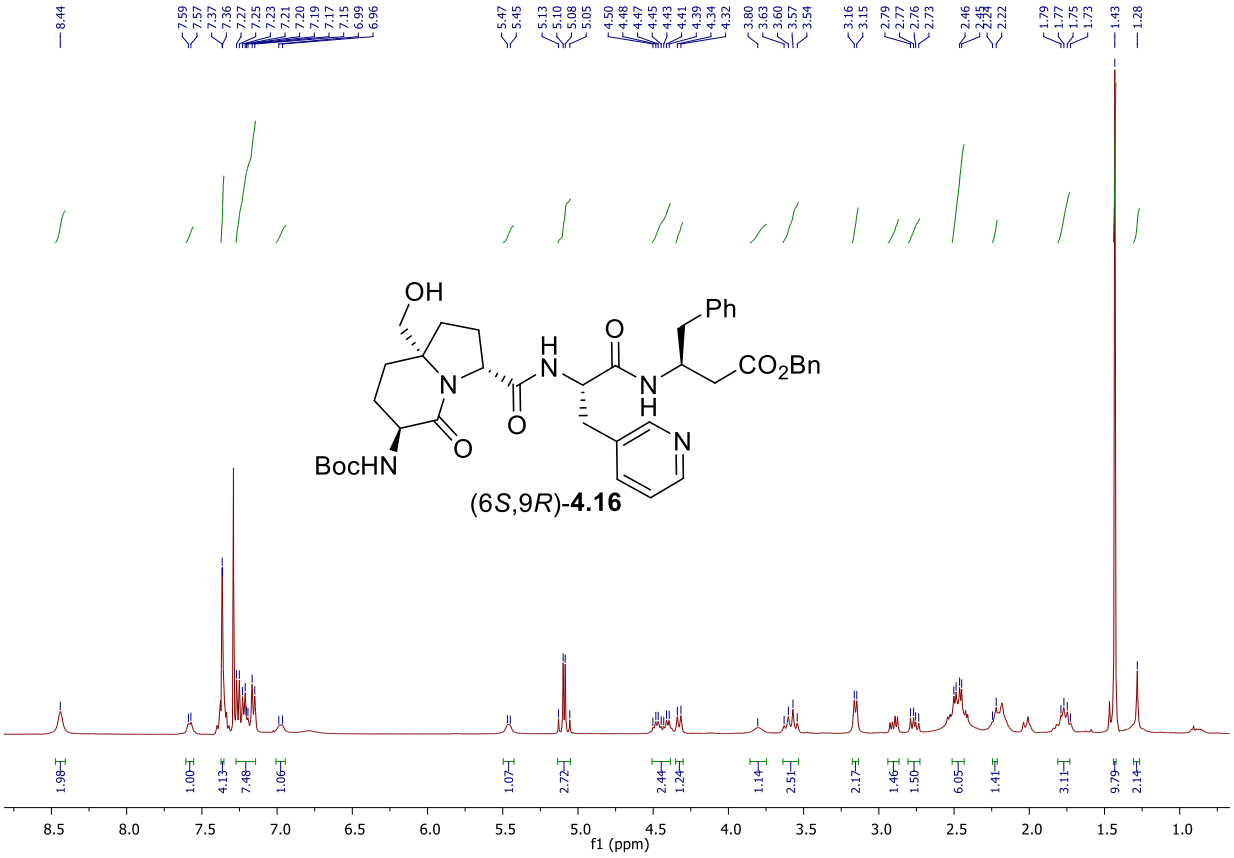

^{13}C *NMR 100 MHz*

Solvent: $CDCl_3$

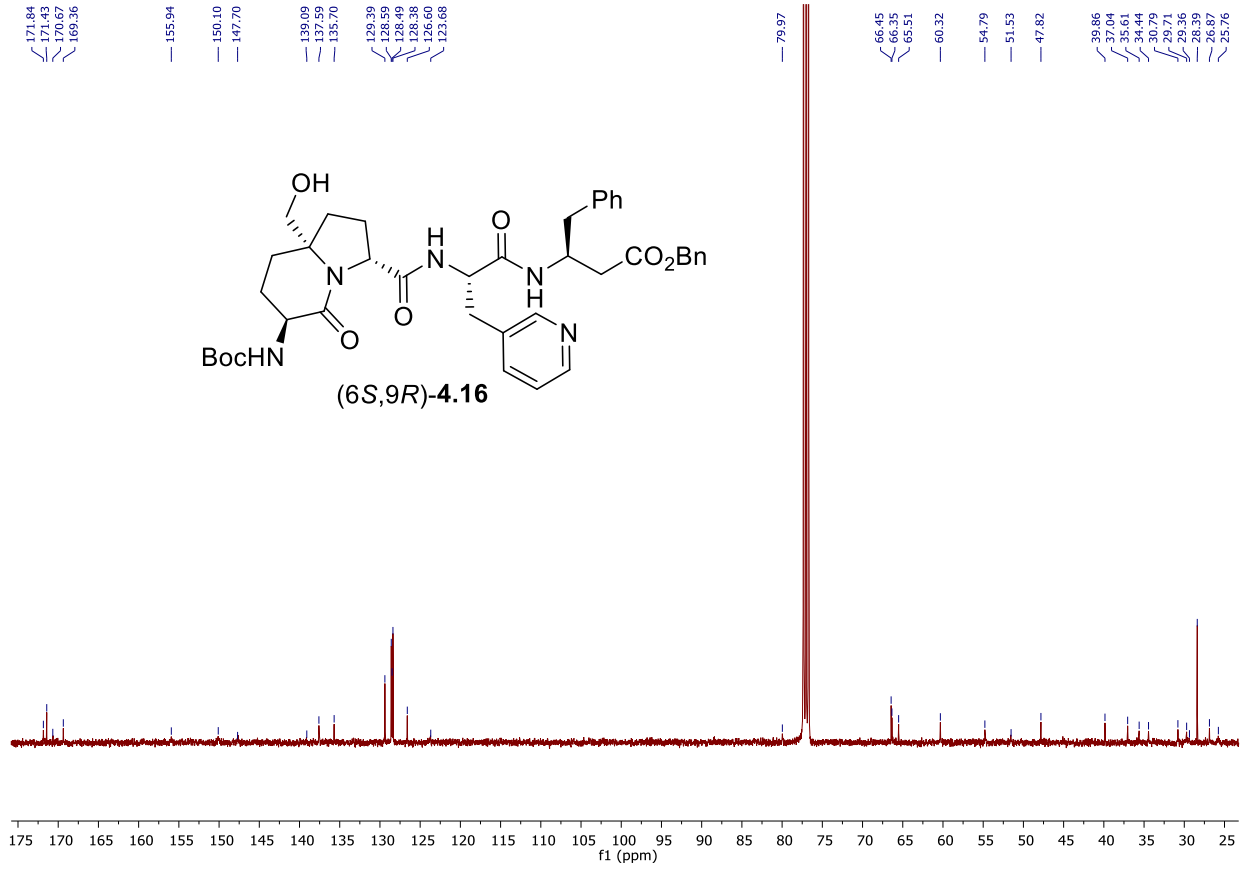

^{1}H *NMR 400 MHz*

Solvent: $CDCl_3$

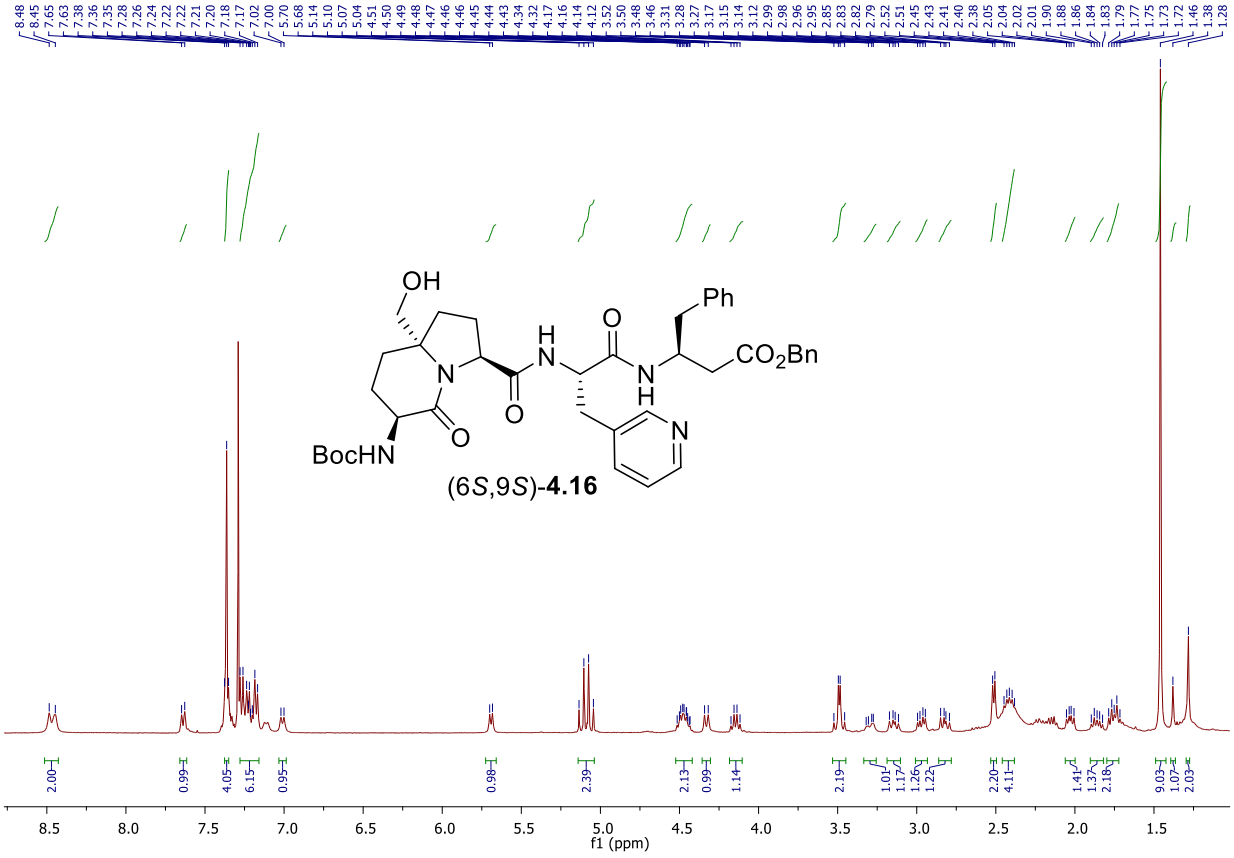

^{13}C *NMR 100 MHz*

Solvent: $CDCl_3$

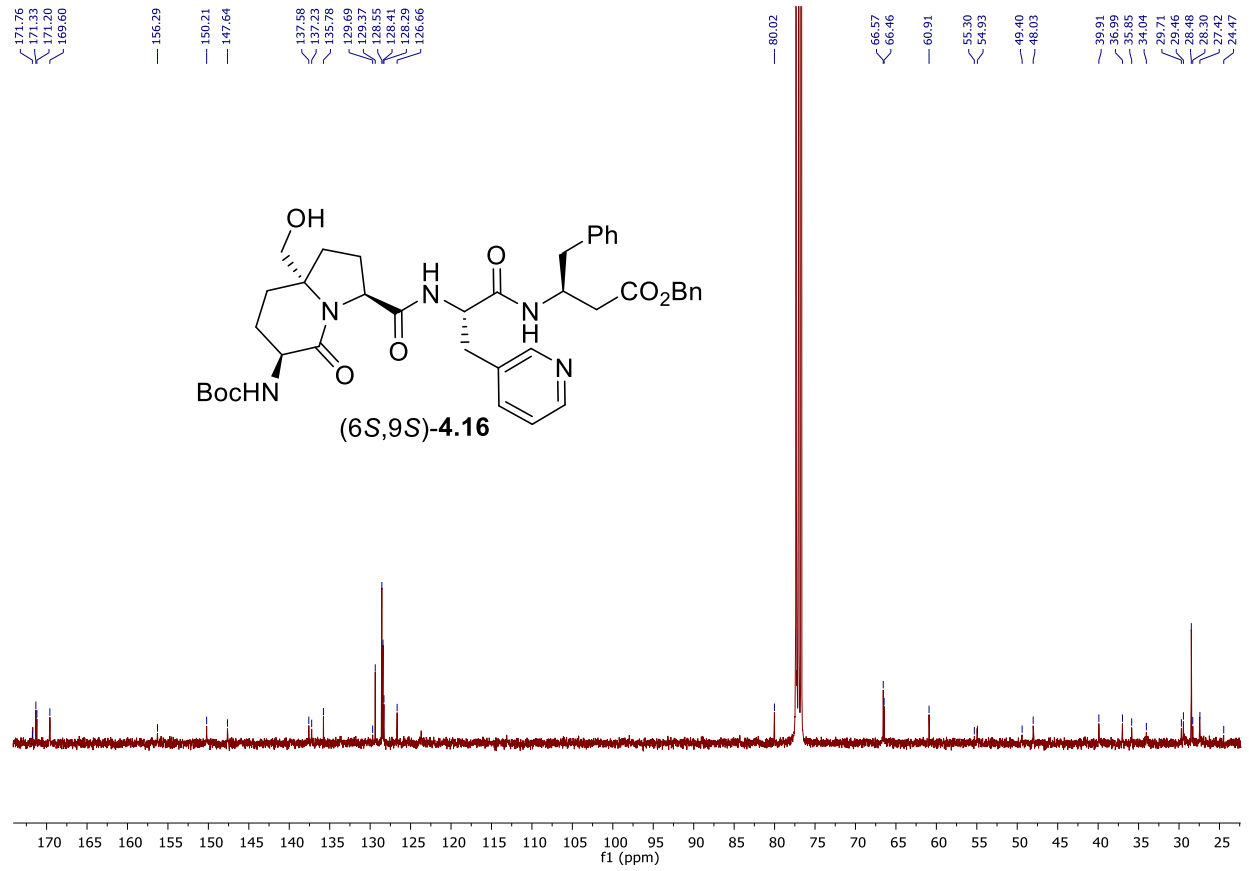

^{1}H *NMR 400 MHz*

Solvent: $CDCl_3$

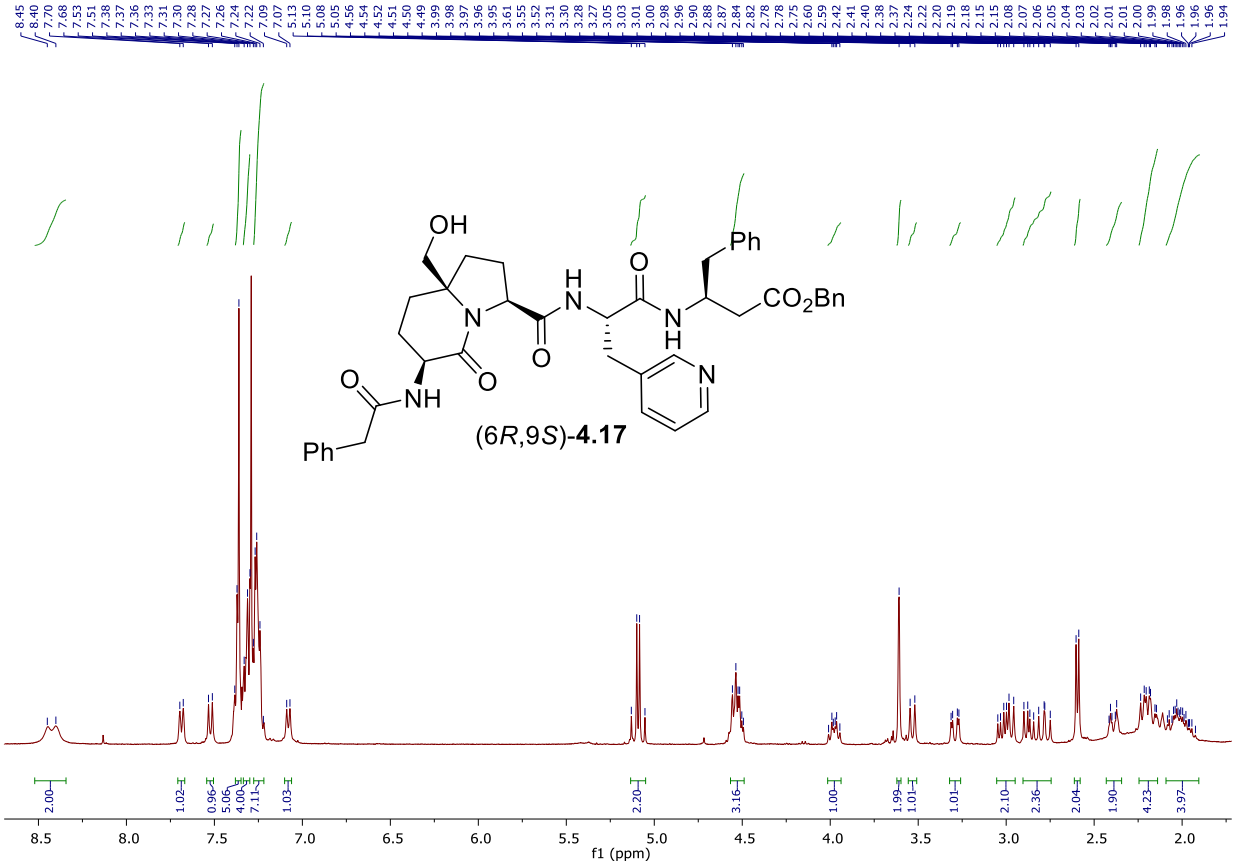

^{13}C *NMR 100 MHz*

Solvent: $CDCl_3$

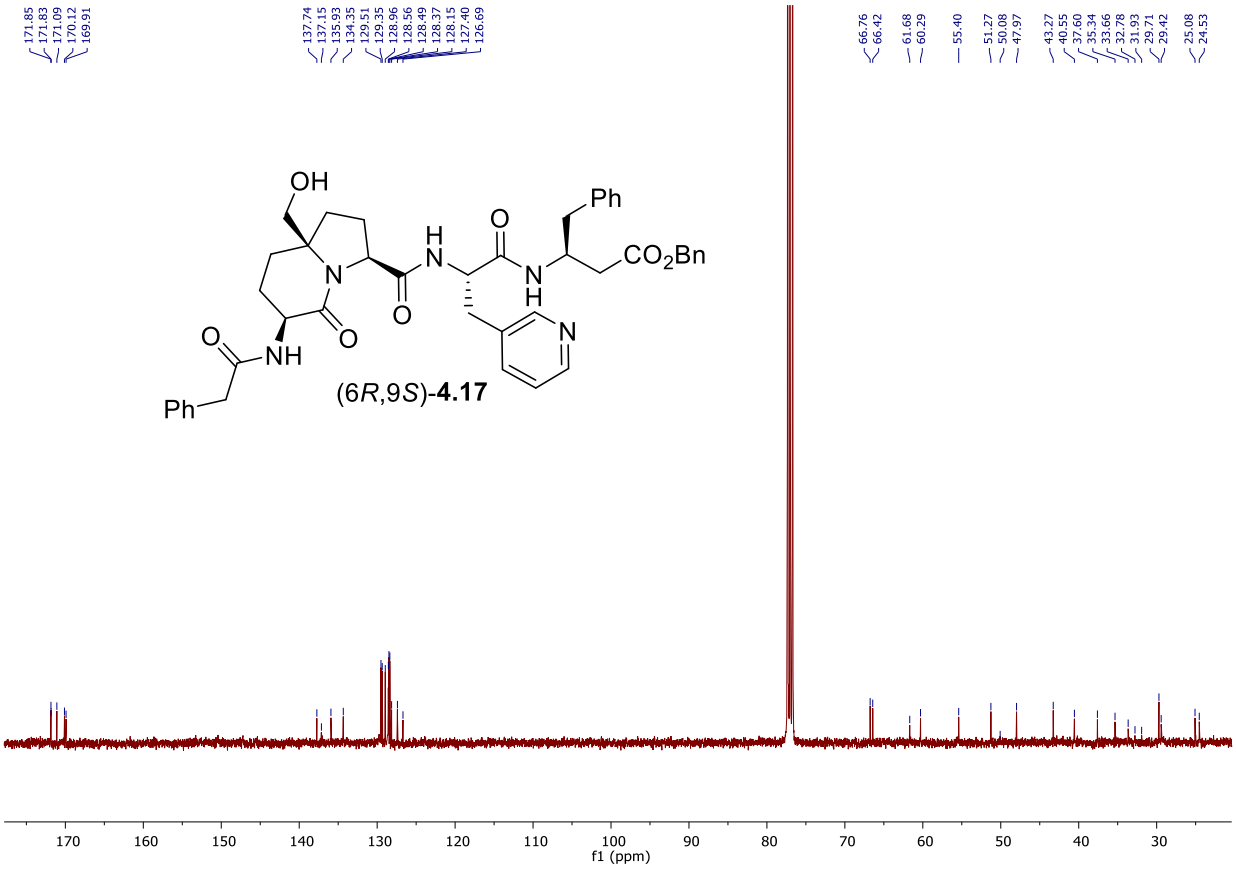

^{1}H *NMR 400 MHz*

Solvent: $CDCl_3$

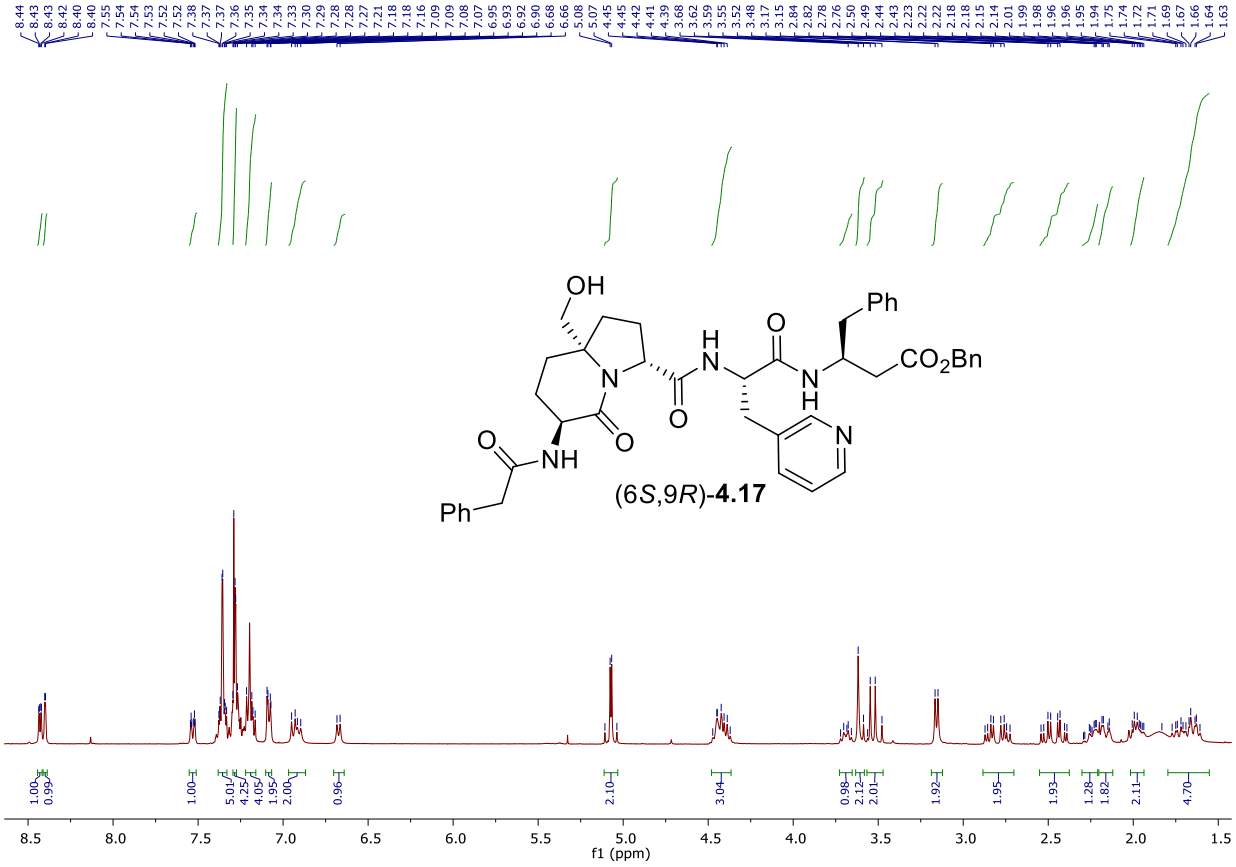

^{13}C *NMR 100 MHz*

Solvent: $CDCl_3$

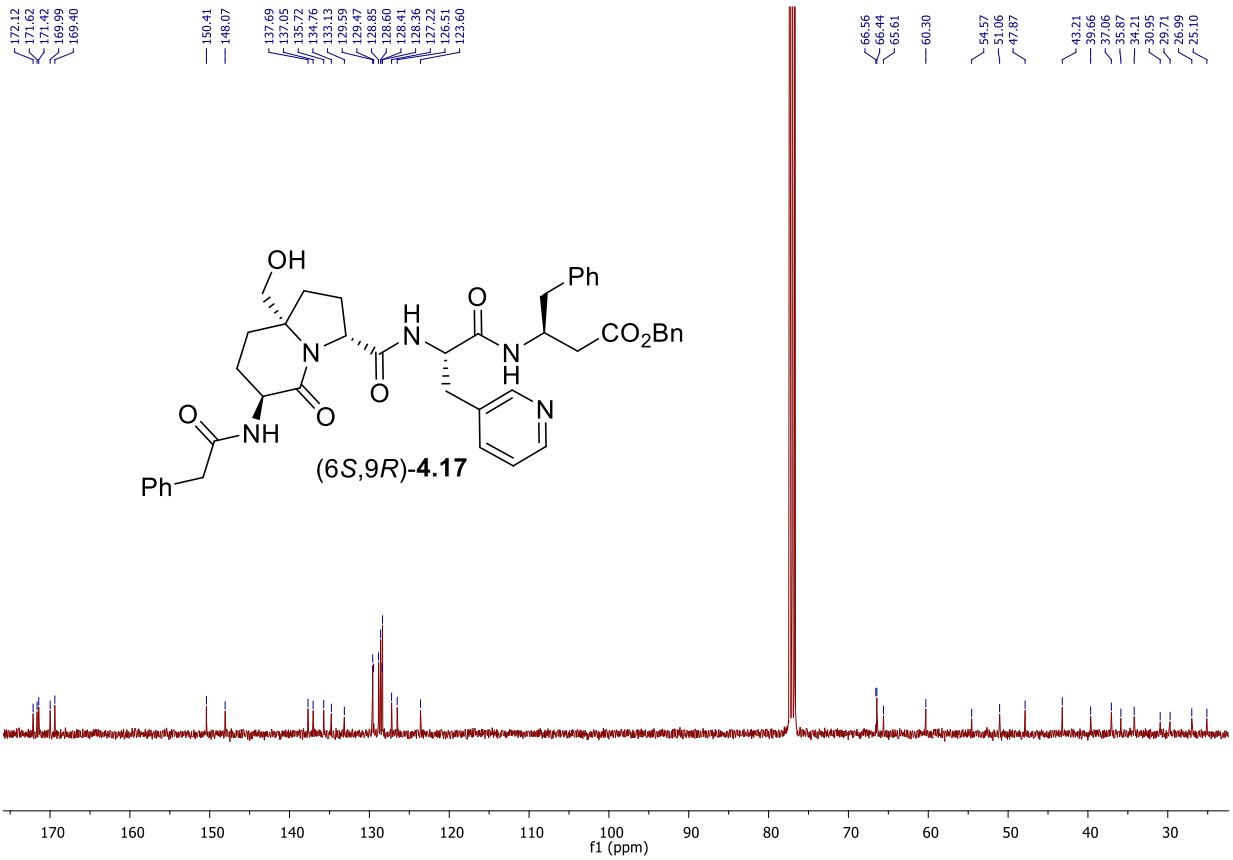

^{1}H *NMR 400 MHz*

Solvent: $CDCl_3$

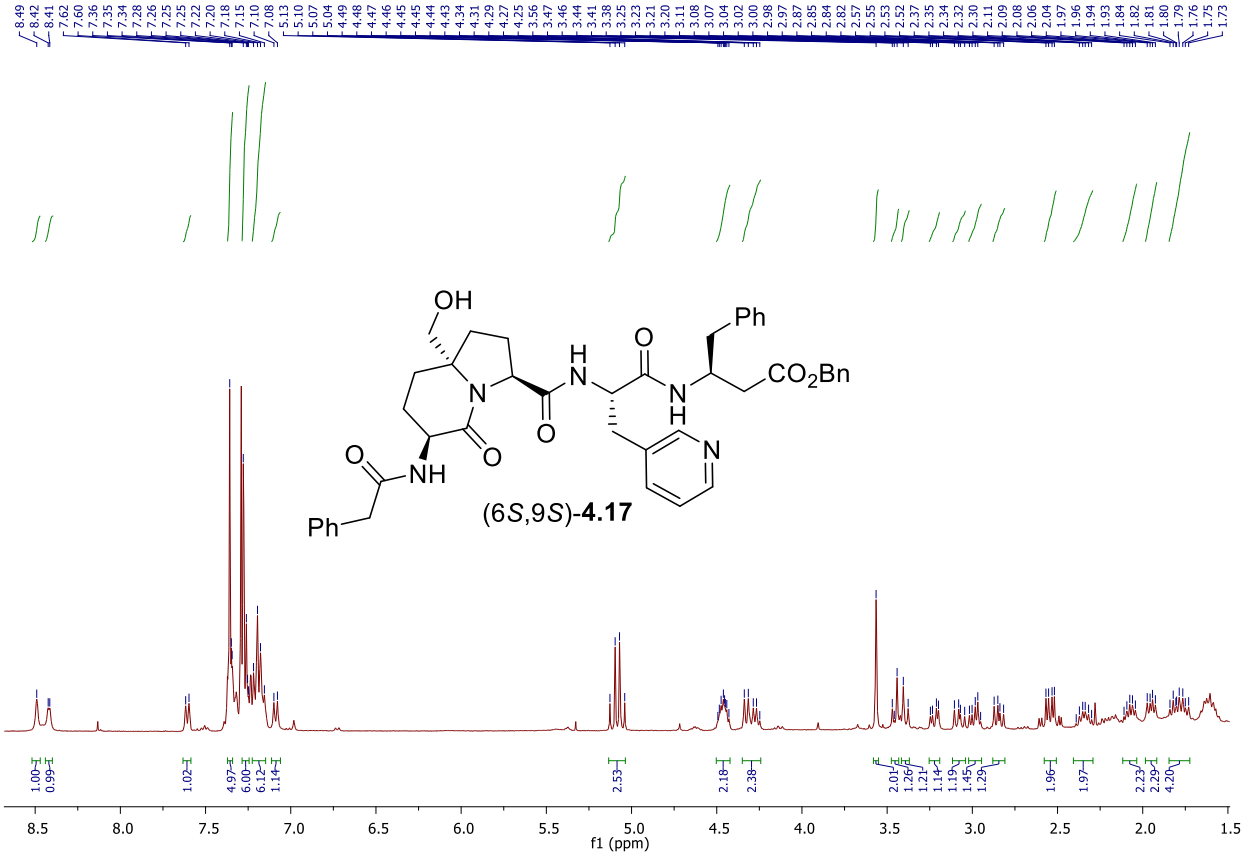

^{13}C *NMR 100 MHz*

Solvent: $CDCl_3$

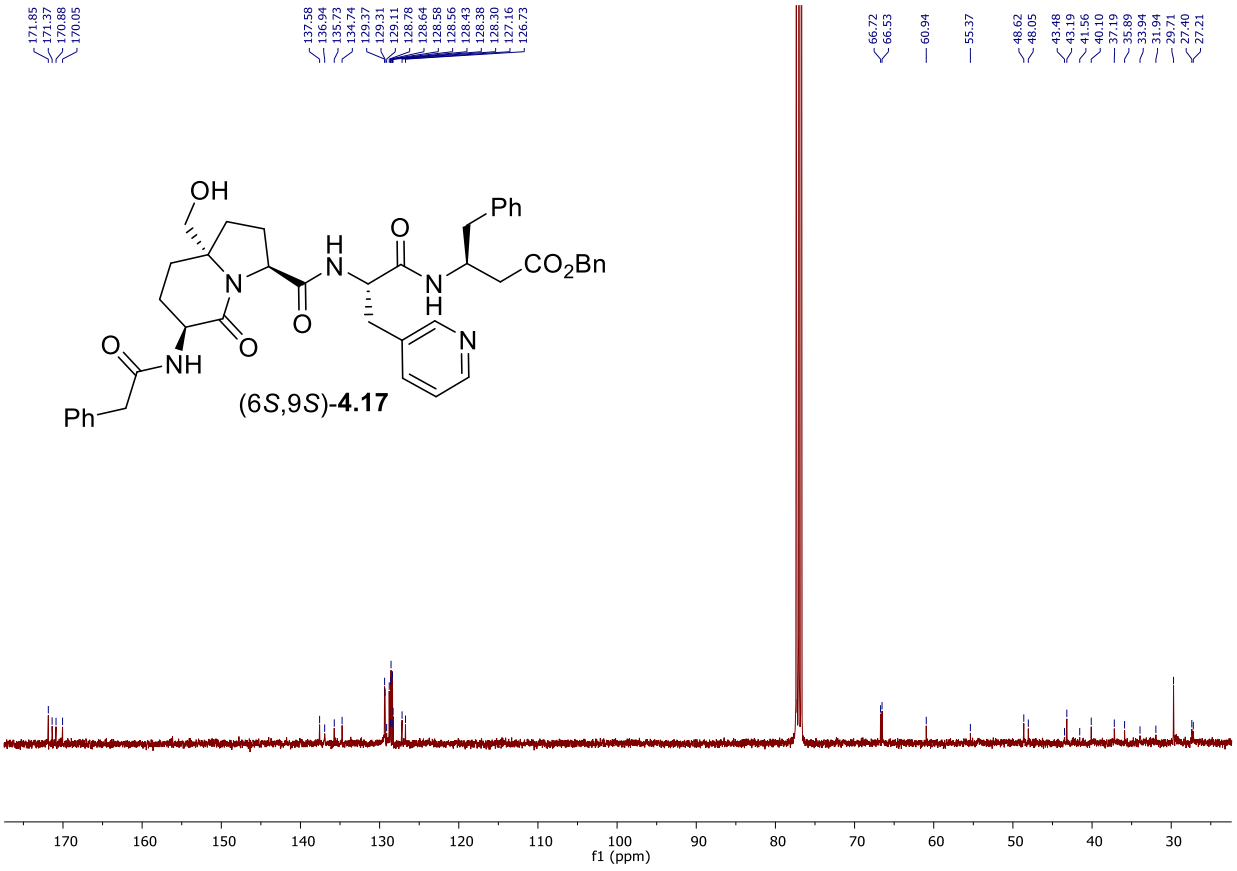

4.8. Ascertainment of purity by HPLC

Method A: Analytical HPLC, 10 to 90% MeOH [0.1% formic acid (FA)] in water (0.1% FA) over 14 min, flow rate of 0.5 mL/min on a on a Sunfire C18 analytical column (3.5 µm, 4.6 mm X 100 mm).

Method B: Analytical HPLC, 10 to 90% MeCN [0.1% formic acid (FA)] in water (0.1% FA) over 14 min, flow rate of 0.5 mL/min on a on a Sunfire C18 analytical column (3.5 µm, 4.6 mm X 100 mm).

Method A, (6*R*,9*S*)-4.4, Purity≥ 96% (MeOH)

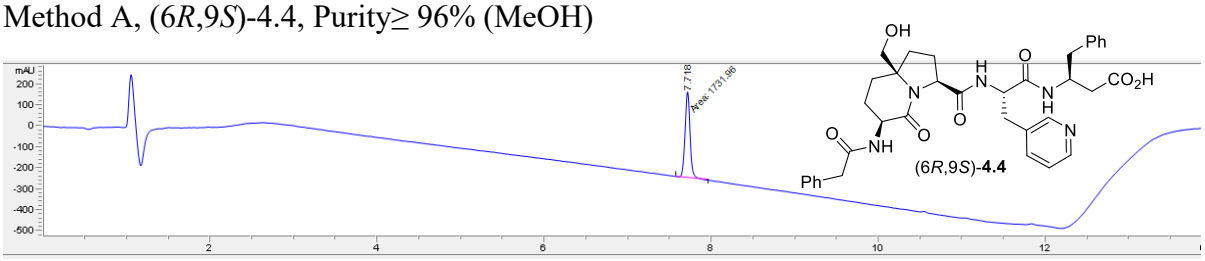

Method B, (6*R*,9*S*)-4.4, Purity≥ 96% (ACN)

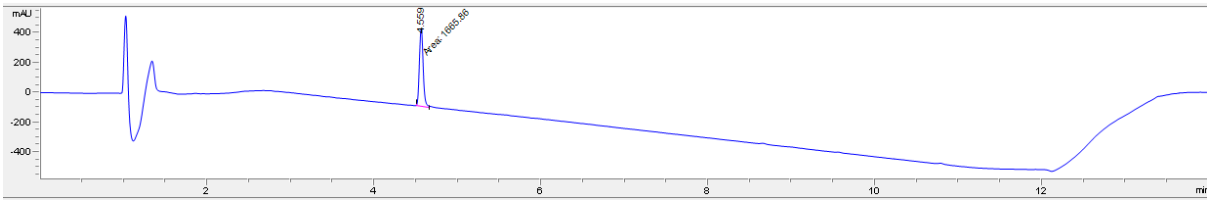

Method A, (6*S*,9*S*)-4.4, Purity≥ 96% (MeOH)

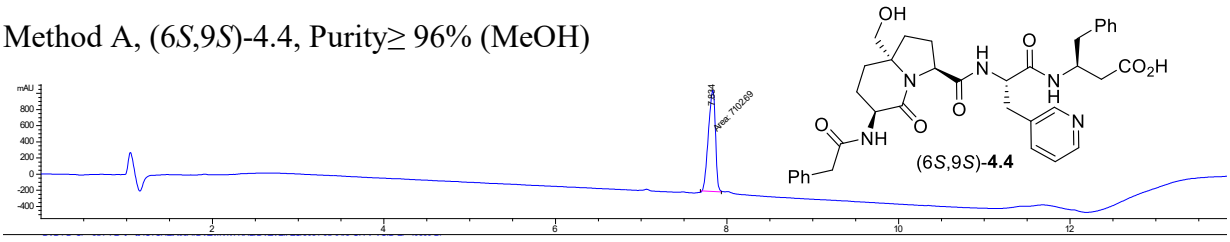

Method B, (6*S*,9*S*)-4.4, Purity≥ 96% (ACN)

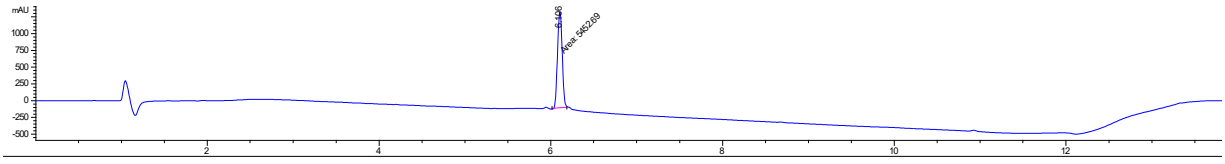

Method A, (6*S*,9*R*)-4.4, Purity≥ 96% (MeOH)

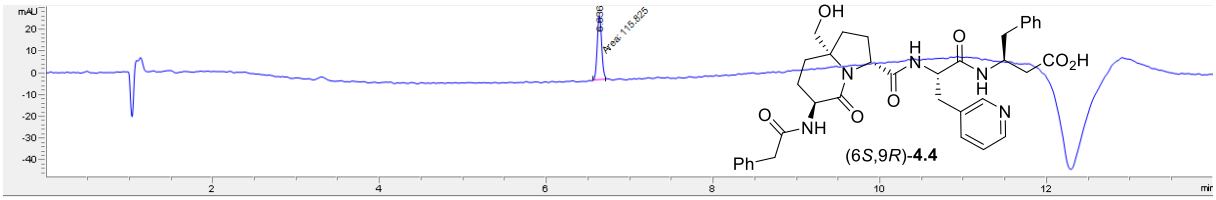

Method B, (6*S*,9*R*)-4.4, Purity≥ 96% (ACN

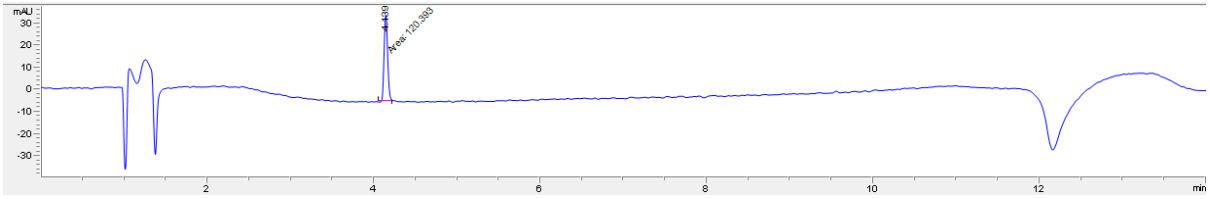

4.9. Crystallography data and Molecular structure for compounds

4.9.1. General methods for making crystals:

Crystals of azabicyclo[X.Y.Z]alkanones (3*S*,6*R*,9*S*)-**4.020** (LUB 140) and (3*S*,6*S*,9*S*)-**4.020** (LUB 139) were grown respectively from dichloromethane-hexane using the liquid-vapour saturation method.

Methyl 3-*N*-(Boc)amino-6-hydroxymethyl-indolizidin-2-one-9-carboxylate [(3*S*,6*R*,9*S*)-4.020, LUB 140]

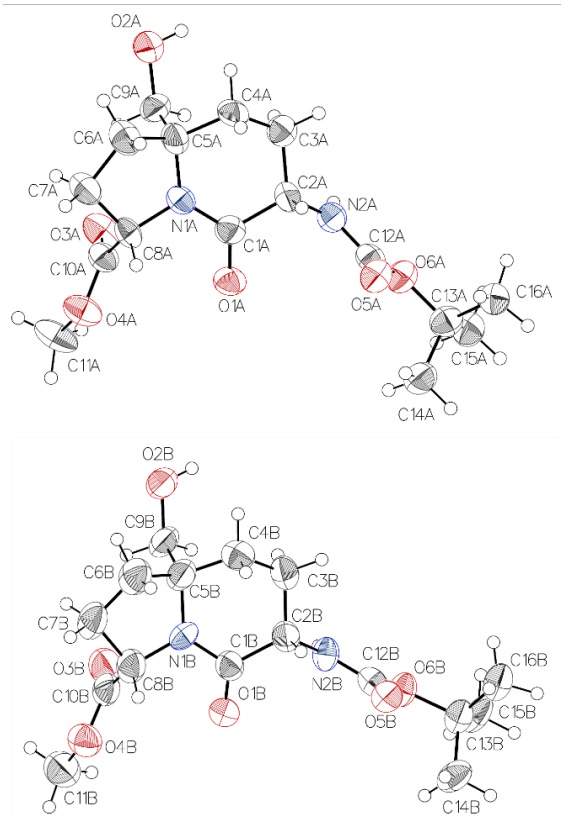

Table 1 Crystal data and structure refinement for LUB140.

Identification code	lub140
Empirical formula	$C_{16}H_{26}N_2O_6$
Formula weight	342.39

Temperature/K	100
Crystal system	orthorhombic
Space group	$P2_12_12_1$
a/Å	11.179(2)
b/Å	15.389(3)
c/Å	23.845(4)
α/°	90
β/°	90
γ/°	90
Volume/Å^3	4101.9(14)
Z	8
ρ_{calc}g/cm^3	1.109
μ/mm^{-1}	0.707
F(000)	1472.0
Crystal size/mm^3	0.3 × 0.04 × 0.03
Radiation	CuKα (λ = 1.54178)
2Θ range for data collection/°	6.836 to 140.582
Index ranges	$-13 \leq h \leq 13$, $-17 \leq k \leq 18$, $-29 \leq l \leq 28$
Reflections collected	24171
Independent reflections	7667 [R_{int} = 0.0999, R_{sigma} = 0.0752]
Data/restraints/parameters	7667/0/444
Goodness-of-fit on F^2	1.064
Final R indexes [I>=2σ (I)]	R_1 = 0.0862, wR_2 = 0.2340
Final R indexes [all data]	R_1 = 0.1203, wR_2 = 0.2641
Largest diff. peak/hole / e Å^{-3}	0.33/-0.31

Flack parameter 0.5(6)

Table 2 Fractional Atomic Coordinates ($\times 10^4$) and Equivalent Isotropic Displacement Parameters ($Å^2 \times 10^3$) for lub140. U_{eq} is defined as 1/3 of of the trace of the orthogonalised U_{IJ} tensor.

Atom	*x*	*y*	*z*	U(eq)
O1A	5669(5)	8596(4)	7355(2)	53.1(13)
O2A	5043(7)	10009(4)	9550(3)	68.7(18)
O3A	3044(6)	8606(4)	8154(3)	64.1(16)
O4A	3310(6)	7296(4)	7773(3)	62.4(15)
O5A	8458(5)	9357(4)	6854(2)	53.9(13)
O6A	7439(6)	10453(4)	6442(2)	54.9(13)
N1A	5598(6)	8634(4)	8303(3)	44.8(14)
N2A	7048(6)	10114(4)	7326(3)	49.4(15)
C1A	6021(8)	8903(5)	7798(3)	51.3(18)
C2A	7054(7)	9558(5)	7814(3)	45.7(16)
C3A	7174(8)	10060(5)	8364(3)	51.6(18)
C4A	7102(8)	9447(5)	8851(3)	53.4(19)
C5A	5870(9)	8987(5)	8853(3)	54(2)
C6A	5799(10)	8181(6)	9223(4)	64(2)
C7A	4821(9)	7613(5)	8951(4)	59(2)
C8A	4903(7)	7846(5)	8321(3)	45.4(16)
C9A	4862(9)	9618(5)	9016(3)	55(2)
C10A	3656(7)	7976(5)	8074(3)	48.5(17)
C11A	2123(10)	7352(6)	7544(5)	76(3)
C12A	7698(7)	9937(5)	6871(3)	45.6(16)

C13A	8040(9)	10372(6)	5902(3)	56(2)
C14A	7820(9)	9486(6)	5639(4)	63(2)
C15A	7433(9)	11066(6)	5548(4)	65(2)
C16A	9363(8)	10569(6)	5972(4)	58(2)
O1B	5197(5)	5911(3)	7208(2)	54.0(13)
O2B	9453(6)	7882(4)	7352(3)	73.8(19)
O3B	6659(7)	6170(4)	8389(3)	73.0(19)
O4B	6302(6)	4738(4)	8287(3)	66.9(17)
O5B	4091(6)	6688(4)	5697(2)	55.9(14)
O6B	3073(5)	7746(3)	6154(2)	53.1(13)
N1B	7159(7)	6143(4)	7205(3)	55.3(17)
N2B	4797(6)	7328(4)	6481(3)	50.3(15)
C1B	6006(9)	6294(5)	7015(3)	52.6(19)
C2B	5947(8)	6856(5)	6490(3)	53.3(19)
C3B	6997(9)	7461(5)	6380(3)	57(2)
C4B	8189(8)	6969(5)	6453(4)	58(2)
C5B	8284(9)	6621(6)	7045(4)	61(2)
C6B	9202(10)	5904(6)	7124(5)	74(3)
C7B	8760(9)	5387(7)	7642(5)	72(3)
C8B	7370(9)	5406(6)	7579(4)	63(2)
C9B	8432(8)	7366(6)	7470(4)	60(2)
C10B	6742(8)	5502(5)	8125(4)	58(2)
C11B	5597(12)	4766(7)	8808(5)	84(3)
C12B	3990(7)	7203(5)	6083(3)	47.1(17)
C13B	2089(9)	7780(6)	5741(4)	60(2)

C14B	1426(8)	6929(7)	5725(5)	69(2)
C15B	1297(8)	8496(6)	5979(5)	68(3)
C16B	2558(10)	8036(6)	5173(4)	69(2)

Table 3 Anisotropic Displacement Parameters ($Å^2 \times 10^3$) for lub140. The Anisotropic displacement factor exponent takes the form: $-2\pi^2[h^2a^{*2}U_{11}+2hka^*b^*U_{12}+\ldots]$.

Atom	U_{11}	U_{22}	U_{33}	U_{23}	U_{13}	U_{12}
O1A	45(3)	64(3)	50(3)	-7(2)	-9(2)	-2(3)
O2A	87(5)	63(3)	56(3)	-1(3)	6(3)	-24(3)
O3A	50(4)	52(3)	90(4)	-6(3)	-14(3)	5(3)
O4A	55(4)	57(3)	75(4)	-12(3)	-21(3)	2(3)
O5A	47(3)	63(3)	52(3)	5(2)	0(2)	8(3)
O6A	55(4)	62(3)	48(3)	5(2)	2(2)	3(3)
N1A	38(3)	47(3)	49(3)	-1(3)	-8(3)	-4(3)
N2A	44(4)	55(3)	50(3)	-1(3)	-2(3)	-3(3)
C1A	59(5)	45(4)	50(4)	-4(3)	1(4)	-1(3)
C2A	41(4)	44(3)	51(4)	4(3)	-1(3)	-8(3)
C3A	45(5)	53(4)	57(4)	-2(3)	3(4)	3(3)
C4A	55(5)	60(4)	45(4)	-2(3)	-15(3)	-14(4)
C5A	63(6)	45(4)	54(4)	6(3)	-1(4)	-15(4)
C6A	66(6)	58(5)	66(5)	12(4)	-15(5)	-13(4)
C7A	64(6)	50(4)	64(5)	3(4)	-13(4)	-13(4)
C8A	32(4)	43(3)	61(4)	-1(3)	-5(3)	-5(3)
C9A	73(6)	51(4)	40(4)	0(3)	5(4)	-5(4)

C10A	42(4)	50(4)	53(4)	-1(3)	-10(3)	-3(3)
C11A	70(7)	61(5)	97(7)	-16(5)	-40(6)	-5(5)
C12A	41(4)	47(4)	49(4)	0(3)	-11(3)	-4(3)
C13A	57(5)	62(5)	48(4)	1(3)	-4(4)	4(4)
C14A	60(6)	73(5)	55(5)	-5(4)	6(4)	-1(5)
C15A	63(6)	68(5)	63(5)	-1(4)	10(4)	-2(5)
C16A	56(5)	60(5)	59(5)	-5(4)	8(4)	-7(4)
O1B	53(3)	55(3)	54(3)	5(2)	1(3)	-4(3)
O2B	64(4)	54(3)	103(5)	9(3)	-30(4)	-6(3)
O3B	94(6)	61(4)	64(4)	0(3)	-13(4)	-3(3)
O4B	62(4)	58(3)	81(4)	8(3)	5(3)	6(3)
O5B	54(4)	54(3)	59(3)	-5(3)	-1(3)	3(3)
O6B	53(3)	55(3)	52(3)	-8(2)	-8(3)	13(3)
N1B	54(4)	59(4)	54(4)	-6(3)	-18(3)	-14(3)
N2B	52(4)	53(3)	46(3)	-4(3)	-4(3)	15(3)
C1B	64(6)	47(4)	47(4)	1(3)	-6(4)	-4(4)
C2B	62(5)	49(4)	49(4)	2(3)	-7(4)	2(4)
C3B	77(6)	48(4)	47(4)	0(3)	-7(4)	5(4)
C4B	46(5)	56(4)	71(5)	4(4)	12(4)	6(4)
C5B	54(5)	57(4)	73(6)	-1(4)	-18(4)	0(4)
C6B	63(6)	70(5)	88(7)	1(5)	-11(5)	12(5)
C7B	59(6)	74(6)	82(6)	2(5)	-19(5)	15(5)
C8B	68(6)	52(4)	69(5)	1(4)	-15(4)	7(4)
C9B	49(5)	63(5)	68(5)	-6(4)	-20(4)	-5(4)
C10B	54(5)	53(4)	67(5)	4(4)	-15(4)	8(4)

C11B	78(8)	80(7)	94(8)	18(6)	4(6)	2(6)
C12B	50(5)	40(3)	52(4)	4(3)	13(3)	10(3)
C13B	57(6)	63(5)	60(5)	-4(4)	-14(4)	7(4)
C14B	38(5)	75(6)	93(7)	-4(5)	-7(5)	2(4)
C15B	44(5)	67(5)	94(7)	-13(5)	-28(5)	17(4)
C16B	63(6)	75(6)	67(6)	-3(4)	-17(5)	12(5)

Table 4 Bond Lengths for lub140.

Atom	Atom	Length/Å	Atom	Atom	Length/Å
O1A	C1A	1.223(10)	O1B	C1B	1.173(10)
O2A	C9A	1.424(10)	O2B	C9B	1.418(11)
O3A	C10A	1.203(10)	O3B	C10B	1.208(11)
O4A	C10A	1.326(9)	O4B	C10B	1.331(11)
O4A	C11A	1.438(11)	O4B	C11B	1.471(13)
O5A	C12A	1.232(9)	O5B	C12B	1.220(9)
O6A	C12A	1.326(9)	O6B	C12B	1.333(9)
O6A	C13A	1.458(10)	O6B	C13B	1.476(10)
N1A	C1A	1.359(10)	N1B	C1B	1.386(12)
N1A	C5A	1.451(10)	N1B	C5B	1.507(12)
N1A	C8A	1.441(9)	N1B	C8B	1.463(11)
N2A	C2A	1.446(9)	N2B	C2B	1.477(11)
N2A	C12A	1.334(10)	N2B	C12B	1.324(11)
C1A	C2A	1.534(10)	C1B	C2B	1.523(11)
C2A	C3A	1.528(10)	C2B	C3B	1.522(12)

C3A	C4A	1.498(11)	C3B	C4B	1.543(12)		
C4A	C5A	1.548(12)	C4B	C5B	1.514(12)		
C5A	C6A	1.524(11)	C5B	C6B	1.519(13)		
C5A	C9A	1.537(13)	C5B	C9B	1.539(12)		
C6A	C7A	1.543(12)	C6B	C7B	1.550(15)		
C7A	C8A	1.547(12)	C7B	C8B	1.562(14)		
C8A	C10A	1.527(10)	C8B	C10B	1.486(13)		
C13A	C14A	1.520(12)	C13B	C14B	1.506(13)		
C13A	C15A	1.522(12)	C13B	C15B	1.522(12)		
C13A	C16A	1.519(13)	C13B	C16B	1.505(13)		

Table 5 Bond Angles for lub140.

Atom	Atom	Atom	Angle/°	Atom	Atom	Atom	Angle/°
C10A	O4A	C11A	115.3(7)	C10B	O4B	C11B	114.7(8)
C12A	O6A	C13A	121.9(6)	C12B	O6B	C13B	120.7(6)
C1A	N1A	C5A	127.9(6)	C1B	N1B	C5B	127.7(7)
C1A	N1A	C8A	118.0(6)	C1B	N1B	C8B	118.7(7)
C8A	N1A	C5A	113.7(6)	C8B	N1B	C5B	113.5(7)
C12A	N2A	C2A	122.1(7)	C12B	N2B	C2B	122.2(6)
O1A	C1A	N1A	122.5(7)	O1B	C1B	N1B	120.2(7)
O1A	C1A	C2A	121.2(7)	O1B	C1B	C2B	125.1(8)
N1A	C1A	C2A	116.1(7)	N1B	C1B	C2B	113.8(8)
N2A	C2A	C1A	111.4(6)	N2B	C2B	C1B	109.2(7)
N2A	C2A	C3A	113.1(6)	N2B	C2B	C3B	111.6(6)

C3A	C2A	C1A	114.8(7)	C3B	C2B	C1B	117.2(7)
C4A	C3A	C2A	110.0(6)	C2B	C3B	C4B	110.3(6)
C3A	C4A	C5A	109.8(7)	C5B	C4B	C3B	109.9(7)
N1A	C5A	C4A	110.8(7)	N1B	C5B	C4B	110.5(7)
N1A	C5A	C6A	101.9(6)	N1B	C5B	C6B	100.2(7)
N1A	C5A	C9A	108.1(7)	N1B	C5B	C9B	106.7(8)
C6A	C5A	C4A	114.8(8)	C4B	C5B	C6B	114.9(9)
C6A	C5A	C9A	109.3(8)	C4B	C5B	C9B	111.0(7)
C9A	C5A	C4A	111.4(7)	C6B	C5B	C9B	112.8(8)
C5A	C6A	C7A	104.8(7)	C5B	C6B	C7B	104.9(9)
C6A	C7A	C8A	103.5(7)	C6B	C7B	C8B	103.4(8)
N1A	C8A	C7A	104.8(6)	N1B	C8B	C7B	103.5(8)
N1A	C8A	C10A	111.8(6)	N1B	C8B	C10B	112.5(7)
C10A	C8A	C7A	110.6(7)	C10B	C8B	C7B	112.8(8)
O2A	C9A	C5A	112.9(8)	O2B	C9B	C5B	111.9(8)
O3A	C10A	O4A	123.8(7)	O3B	C10B	O4B	124.9(9)
O3A	C10A	C8A	124.3(7)	O3B	C10B	C8B	125.1(9)
O4A	C10A	C8A	111.8(7)	O4B	C10B	C8B	109.9(8)
O5A	C12A	O6A	124.0(7)	O5B	C12B	O6B	125.1(8)
O5A	C12A	N2A	123.4(7)	O5B	C12B	N2B	124.9(7)
O6A	C12A	N2A	112.6(7)	N2B	C12B	O6B	110.0(6)
O6A	C13A	C14A	111.4(7)	O6B	C13B	C14B	110.7(7)
O6A	C13A	C15A	103.0(7)	O6B	C13B	C15B	102.2(7)
O6A	C13A	C16A	109.5(7)	O6B	C13B	C16B	110.5(8)
C14A	C13A	C15A	109.3(7)	C14B	C13B	C15B	110.6(8)

C16A	C13A	C14A	112.5(8)	C16B	C13B	C14B	112.1(8)
C16A	C13A	C15A	110.8(8)	C16B	C13B	C15B	110.4(8)

Table 6 Hydrogen Bonds for lub140.

D	H	A	d(D-H)/Å	d(H-A)/Å	d(D-A)/Å	D-H-A/°
O2A	H2A	O5B[1]	0.84	2.07	2.821(8)	148.5
N2A	H2AA	O4A[1]	0.88	2.65	3.389(9)	142.8
N2A	H2AA	O1B[1]	0.88	2.35	3.006(9)	131.7
C3A	H3AB	O1B[1]	0.99	2.48	3.256(10)	134.6
C8A	H8A	O3B	1.00	2.46	3.246(10)	134.6
C9A	H9AA	O1B[1]	0.99	2.57	3.532(10)	163.4
C9A	H9AB	O3A	0.99	2.60	3.283(11)	126.0
C14A	H14A	O5A	0.98	2.41	2.989(10)	116.9
C16A	H16B	O2A[2]	0.98	2.70	3.567(11)	147.5
C16A	H16C	O5A	0.98	2.44	2.987(10)	114.9
O2B	H2B	O5A	0.84	1.97	2.794(8)	168.6
N2B	H2BA	O1A	0.88	2.30	3.016(8)	138.7
C3B	H3BA	O1A	0.99	2.44	3.266(10)	140.6
C8B	H8B	O3A[3]	1.00	2.33	3.308(11)	164.9
C9B	H9BA	O1A	0.99	2.65	3.634(11)	173.2
C14B	H14D	O5B	0.98	2.47	3.003(11)	114.2

[1]1-X,1/2+Y,3/2-Z; [2]3/2-X,2-Y,-1/2+Z; [3]1-X,-1/2+Y,3/2-Z

Table 7 Torsion Angles for lub140.

A	B	C	D	Angle/°	A	B	C	D	Angle/°
O1A	C1A	C2A	N2A	34.2(10)	O1B	C1B	C2B	N2B	38.3(11)
O1A	C1A	C2A	C3A	164.5(7)	O1B	C1B	C2B	C3B	166.4(8)
N1A	C1A	C2A	N2A	-151.2(7)	N1B	C1B	C2B	N2B	-152.2(7)
N1A	C1A	C2A	C3A	-20.9(10)	N1B	C1B	C2B	C3B	-24.1(10)
N1A	C5A	C6A	C7A	-33.1(10)	N1B	C5B	C6B	C7B	-36.6(9)
N1A	C5A	C9A	O2A	-179.7(6)	N1B	C5B	C9B	O2B	-178.4(7)
N1A	C8A	C10A	O3A	-41.2(11)	N1B	C8B	C10B	O3B	-40.5(13)
N1A	C8A	C10A	O4A	140.7(7)	N1B	C8B	C10B	O4B	140.6(8)
N2A	C2A	C3A	C4A	176.7(7)	N2B	C2B	C3B	C4B	174.1(7)
C1A	N1A	C5A	C4A	-25.0(11)	C1B	N1B	C5B	C4B	-29.7(12)
C1A	N1A	C5A	C6A	-147.6(8)	C1B	N1B	C5B	C6B	-151.3(8)
C1A	N1A	C5A	C9A	97.3(9)	C1B	N1B	C5B	C9B	91.0(9)
C1A	N1A	C8A	C7A	167.1(7)	C1B	N1B	C8B	C7B	173.8(7)
C1A	N1A	C8A	C10A	-73.0(9)	C1B	N1B	C8B	C10B	-64.2(10)
C1A	C2A	C3A	C4A	47.2(9)	C1B	C2B	C3B	C4B	47.1(10)
C2A	N2A	C12A	O5A	-9.3(11)	C2B	N2B	C12B	O5B	1.6(12)
C2A	N2A	C12A	O6A	170.9(6)	C2B	N2B	C12B	O6B	-176.2(7)
C2A	C3A	C4A	C5A	-61.5(9)	C2B	C3B	C4B	C5B	-60.0(9)
C3A	C4A	C5A	N1A	49.4(9)	C3B	C4B	C5B	N1B	49.6(9)
C3A	C4A	C5A	C6A	164.2(7)	C3B	C4B	C5B	C6B	162.0(8)
C3A	C4A	C5A	C9A	-71.0(9)	C3B	C4B	C5B	C9B	-68.6(10)
C4A	C5A	C6A	C7A	-152.9(8)	C4B	C5B	C6B	C7B	-155.0(8)

C4A	C5A	C9A	O2A	-57.7(9)	C4B	C5B	C9B	O2B	-58.0(10)
C5A	N1A	C1A	O1A	-174.8(8)	C5B	N1B	C1B	O1B	-174.2(8)
C5A	N1A	C1A	C2A	10.6(12)	C5B	N1B	C1B	C2B	15.7(11)
C5A	N1A	C8A	C7A	-6.1(9)	C5B	N1B	C8B	C7B	-2.8(10)
C5A	N1A	C8A	C10A	113.7(8)	C5B	N1B	C8B	C10B	119.3(9)
C5A	C6A	C7A	C8A	30.1(10)	C5B	C6B	C7B	C8B	36.4(10)
C6A	C5A	C9A	O2A	70.2(9)	C6B	C5B	C9B	O2B	72.5(10)
C6A	C7A	C8A	N1A	-15.2(9)	C6B	C7B	C8B	N1B	-20.3(10)
C6A	C7A	C8A	C10A	-135.8(7)	C6B	C7B	C8B	C10B	-142.2(8)
C7A	C8A	C10A	O3A	75.1(10)	C7B	C8B	C10B	O3B	76.1(11)
C7A	C8A	C10A	O4A	-102.9(8)	C7B	C8B	C10B	O4B	-102.8(9)
C8A	N1A	C1A	O1A	13.0(12)	C8B	N1B	C1B	O1B	9.8(12)
C8A	N1A	C1A	C2A	-161.5(6)	C8B	N1B	C1B	C2B	-160.3(7)
C8A	N1A	C5A	C4A	147.4(6)	C8B	N1B	C5B	C4B	146.4(7)
C8A	N1A	C5A	C6A	24.8(10)	C8B	N1B	C5B	C6B	24.9(9)
C8A	N1A	C5A	C9A	-90.3(7)	C8B	N1B	C5B	C9B	-92.8(8)
C9A	C5A	C6A	C7A	81.2(9)	C9B	C5B	C6B	C7B	76.5(10)
C11A	O4A	C10A	O3A	-0.5(13)	C11B	O4B	C10B	O3B	4.7(13)
C11A	O4A	C10A	C8A	177.6(8)	C11B	O4B	C10B	C8B	-176.4(8)
C12A	O6A	C13A	C14A	61.4(10)	C12B	O6B	C13B	C14B	64.3(10)
C12A	O6A	C13A	C15A	178.4(7)	C12B	O6B	C13B	C15B	-177.9(7)
C12A	O6A	C13A	C16A	-63.7(9)	C12B	O6B	C13B	C16B	-60.4(10)
C12A	N2A	C2A	C1A	-94.5(8)	C12B	N2B	C2B	C1B	-116.9(8)
C12A	N2A	C2A	C3A	134.4(8)	C12B	N2B	C2B	C3B	111.9(8)
C13A	O6A	C12A	O5A	0.4(11)	C13B	O6B	C12B	O5B	-2.0(12)

C13A O6A C12A N2A -179.8(7) C13B O6B C12B N2B 175.7(7)

Table 8 Hydrogen Atom Coordinates (Å×10^4) and Isotropic Displacement Parameters (Å^2×10^3) for lub140.

Atom	*x*	*y*	*z*	U(eq)
H2A	5545.58	10412.48	9521.09	103
H2AA	6600.62	10584.91	7328.3	59
H2AB	7800.37	9203.15	7782.78	55
H3AA	7950.05	10370.34	8372.1	62
H3AB	6526.9	10497.24	8392.14	62
H4AA	7210.48	9771.63	9205.89	64
H4AB	7747.24	9008.63	8822.96	64
H6AA	5577.77	8338.85	9611.58	76
H6AB	6575.76	7871.63	9228.98	76
H7AA	4021.84	7755.46	9104.05	71
H7AB	4983.08	6987.28	9012.91	71
H8A	5329.77	7373.73	8113.74	54
H9AA	4805.48	10080.42	8728.02	65
H9AB	4092.81	9299.64	9018.83	65
H11A	2017.23	6902.39	7257.01	114
H11B	2007.27	7926.39	7374	114
H11C	1535.1	7267.13	7843.48	114
H14A	8196.21	9035.62	5870.25	94
H14B	8164.41	9472.76	5261.45	94

H14C	6957.19	9378.21	5616.98	94
H15A	6576.93	10936.89	5517.73	97
H15B	7790.08	11074.59	5172.67	97
H15C	7540.38	11635.39	5725.62	97
H16A	9458.45	11114.5	6179.19	87
H16B	9736.57	10624.07	5601.9	87
H16C	9746.21	10095.78	6179.99	87
H2B	9243.76	8330.26	7177.37	111
H2BA	4642.27	7704.47	6749.41	60
H2BB	5921.46	6444.48	6165.97	64
H3BA	6967.68	7957.31	6643.69	69
H3BB	6943.77	7693.99	5993.28	69
H4BA	8229.15	6481.85	6182.45	69
H4BB	8866.89	7365.76	6376.19	69
H6BA	10006.15	6150.75	7192.9	88
H6BB	9237.35	5525.08	6788.93	88
H7BA	9014.77	5670.83	7995.17	86
H7BB	9065.69	4783.54	7636.26	86
H8B	7096.9	4859.15	7392.42	75
H9BA	7709.8	7737.99	7461.4	72
H9BB	8505.62	7119.85	7851.88	72
H11D	4941	5183.55	8765.65	126
H11E	6111.72	4944.77	9119.85	126
H11F	5267.13	4188	8885.06	126
H14D	1926.58	6487.17	5544.81	103

H14E	683.6	7000.42	5510.85	103
H14F	1234.58	6745.86	6108.12	103
H15D	1061.37	8345.42	6362.64	103
H15E	581.1	8557.03	5745.31	103
H15F	1740.1	9045.39	5981.69	103
H16D	3128.45	8515.53	5214.45	103
H16E	1891.67	8221.4	4934.79	103
H16F	2960.84	7537.38	5000.52	103

Table 9 Solvent masks information for lub140.

Number	X	Y	Z	Volume	Electron count	Content
1	-0.159	-0.250	0.000	419.9	98.0	2 CH_2Cl_2
2	-0.307	0.250	0.500	419.9	98.0	2 CH_2Cl_2

Experimental

Single crystals of $C_{16}H_{26}N_2O_6$ lub140 were crystallized from DCM. A suitable crystal was selected and mounted on a cryoloop on a Bruker Smart APEX diffractometer. The crystal was kept at 100 K during data collection. Using Olex2 [1], the structure was solved with the SHELXT [2] structure solution program using Intrinsic Phasing and refined with the XL [3] refinement package using Least Squares minimisation.

1. Dolomanov, O.V., Bourhis, L.J., Gildea, R.J, Howard, J.A.K. & Puschmann, H. (2009), J. Appl. Cryst. 42, 339-341.
2. Sheldrick, G.M. (2015). Acta Cryst. A71, 3-8.
3. Sheldrick, G.M. (2015). Acta Cryst. C71, 3-8.

Crystal structure determination of lub140

Crystal Data for $C_{16}H_{26}N_2O_6$ (M =342.39 g/mol): orthorhombic, space group $P2_12_12_1$ (no. 19), a = 11.179(2) Å, b = 15.389(3) Å, c = 23.845(4) Å, V = 4101.9(14) Å^3, Z = 8, T = 100 K, μ(CuKα) = 0.707 mm^{-1}, $Dcalc$ = 1.109 g/cm^3, 24171 reflections measured (6.836° ≤ 2Θ ≤

140.582°), 7667 unique (R_{int} = 0.0999, R_{sigma} = 0.0752) which were used in all calculations. The final R_1 was 0.0862 (I > 2σ(I)) and wR_2 was 0.2641 (all data).

Refinement model description

Number of restraints - 0, number of constraints - unknown.

Details:

1. Twinned data refinement
Scales: 0.5(6)
0.5(6)
2. Fixed Uiso
At 1.2 times of:
All C(H) groups, All C(H,H) groups, All N(H) groups
At 1.5 times of:
All C(H,H,H) groups, All O(H) groups
3.a Ternary CH refined with riding coordinates:
C2A(H2AB), C8A(H8A), C2B(H2BB), C8B(H8B)
3.b Secondary CH2 refined with riding coordinates:
C3A(H3AA,H3AB), C4A(H4AA,H4AB), C6A(H6AA,H6AB), C7A(H7AA,H7AB), C9A(H9AA,
H9AB), C3B(H3BA,H3BB), C4B(H4BA,H4BB), C6B(H6BA,H6BB), C7B(H7BA,H7BB),
C9B(H9BA,H9BB)
3.c Aromatic/amide H refined with riding coordinates:
N2A(H2AA), N2B(H2BA)
3.d Idealised Me refined as rotating group:
C11A(H11A,H11B,H11C), C14A(H14A,H14B,H14C), C15A(H15A,H15B,H15C), C16A(H16A,
H16B,H16C), C11B(H11D,H11E,H11F), C14B(H14D,H14E,H14F), C15B(H15D,H15E,H15F),
C16B(H16D,H16E,H16F)
3.e Idealised tetrahedral OH refined as rotating group:
O2A(H2A), O2B(H2B)

Methyl 3-*N*-(Boc)amino-6-hydroxymethyl-indolizidin-2-one-9-carboxylate [(3*S*,6*S*,9*S*)-4.020, LUB 139]

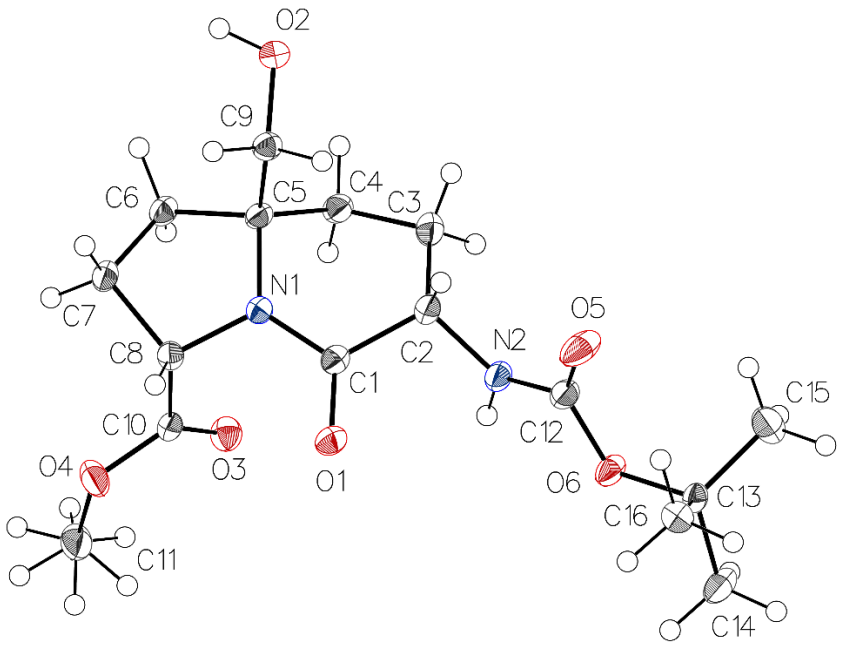

Table 1 Crystal data and structure refinement for LUB 139

Identification code	lub139
Empirical formula	$C_{16}H_{26}N_2O_6$
Formula weight	342.39
Temperature/K	100
Crystal system	orthorhombic
Space group	$P2_12_12_1$
a/Å	7.2138(4)
b/Å	14.8397(8)
c/Å	16.1962(9)
α/°	90
β/°	90
γ/°	90
Volume/Å^3	1733.81(17)

Z	4
ρ_{calc}g/cm^3	1.312
μ/mm^{-1}	0.836
F(000)	736.0
Crystal size/mm^3	0.48 × 0.19 × 0.18
Radiation	CuKα (λ = 1.54178)
2Θ range for data collection/°	8.08 to 140.044
Index ranges	-8 ≤ h ≤ 8, -18 ≤ k ≤ 17, -19 ≤ l ≤ 19
Reflections collected	17974
Independent reflections	3281 [R_{int} = 0.0308, R_{sigma} = 0.0206]
Data/restraints/parameters	3281/0/228
Goodness-of-fit on F^2	1.046
Final R indexes [I>=2σ (I)]	R_1 = 0.0299, wR_2 = 0.0795
Final R indexes [all data]	R_1 = 0.0301, wR_2 = 0.0798
Largest diff. peak/hole / e Å^{-3}	0.23/-0.18
Flack parameter	-0.02(6)

Table 2 Fractional Atomic Coordinates (×10^4) and Equivalent Isotropic Displacement Parameters (Å^2×10^3) for lub139. U_{eq} is defined as 1/3 of of the trace of the orthogonalised U_{IJ} tensor.

Atom	*x*	*y*	*z*	U(eq)
O1	7855.9(17)	2993.6(8)	4479.6(7)	22.8(3)
O2	669.4(17)	3161.2(8)	3016.2(7)	21.4(3)
O3	8265.2(18)	1567.0(8)	3120.9(7)	23.9(3)

O4	7907.9(19)	428.1(9)	4020.4(10)	34.3(3)
O5	7088.7(19)	5701.0(10)	4451.8(10)	37.8(4)
O6	10085.1(17)	5492.2(8)	4033.1(8)	25.2(3)
N1	5304(2)	2490.8(9)	3829.0(8)	17.1(3)
N2	7943(2)	4550.3(10)	3604.4(10)	22.4(3)
C1	6537(2)	3137.6(11)	4017.6(9)	18.1(3)
C2	6196(2)	4074.8(11)	3645.5(11)	21.8(4)
C3	5176(3)	4078.1(13)	2798.9(12)	30.3(4)
C4	4556(2)	3150.0(12)	2496.4(10)	21.2(4)
C5	3813(2)	2577.4(11)	3201.8(10)	17.1(3)
C6	3456(2)	1587.3(11)	2964.7(10)	19.3(3)
C7	3951(2)	1063.9(11)	3749.7(10)	19.2(3)
C8	5655(2)	1562.2(10)	4080.5(9)	17.8(3)
C9	2098(2)	2997.4(11)	3611.1(10)	19.1(3)
C10	7434(2)	1214.3(11)	3680.3(11)	19.2(3)
C11	9433(3)	-61.4(14)	3646.3(16)	38.8(5)
C12	8264(2)	5289.0(11)	4071.4(12)	23.6(4)
C13	10782(2)	6344.1(11)	4381.0(10)	19.2(3)
C14	12848(3)	6266.5(13)	4216.3(12)	28.2(4)
C15	9953(3)	7134.7(12)	3916.5(11)	29.0(4)
C16	10401(3)	6399.7(12)	5304.4(10)	24.3(4)

Table 3 Anisotropic Displacement Parameters ($Å^2 \times 10^3$) for lub139. The Anisotropic displacement factor exponent takes the form: $-2\pi^2[h^2a^{*2}U_{11}+2hka^*b^*U_{12}+\ldots]$.

Atom	U_{11}	U_{22}	U_{33}	U_{23}	U_{13}	U_{12}
O1	20.8(6)	24.1(6)	23.5(6)	-0.9(5)	-5.2(5)	-3.6(5)
O2	17.3(6)	21.6(6)	25.3(6)	1.3(5)	-2.4(5)	-0.2(5)
O3	23.9(7)	23.0(6)	24.9(6)	0.8(5)	4.3(5)	-0.7(5)
O4	24.4(7)	21.3(6)	57.1(9)	14.8(6)	12.9(7)	6.2(5)
O5	17.0(6)	33.3(7)	63.0(10)	-23.8(7)	4.1(7)	-1.3(6)
O6	15.5(6)	18.0(6)	42.2(7)	-11.4(5)	2.5(5)	-1.1(5)
N1	17.4(7)	15.7(7)	18.1(6)	-0.6(5)	-1.8(5)	-1.1(5)
N2	16.3(7)	15.7(7)	35.3(8)	-3.7(6)	1.8(6)	-0.9(6)
C1	17.4(8)	18.4(7)	18.4(7)	-3.0(6)	1.1(6)	-0.7(6)
C2	18.4(8)	16.3(8)	30.6(8)	0.0(6)	-1.3(7)	-2.9(6)
C3	29.7(10)	23.8(9)	37.5(10)	10.9(8)	-9.4(8)	-8.3(8)
C4	18.3(8)	24.1(8)	21.1(7)	3.1(6)	-1.1(6)	-3.0(7)
C5	14.8(8)	17.9(8)	18.6(7)	-1.6(6)	-1.7(6)	-1.7(6)
C6	17.9(8)	18.3(8)	21.5(7)	-3.6(6)	0.0(6)	-2.5(7)
C7	18.7(8)	16.1(7)	22.9(7)	-1.6(6)	1.8(6)	-2.9(6)
C8	18.0(8)	15.7(7)	19.7(7)	0.5(6)	0.4(6)	-0.5(7)
C9	18.0(8)	19.7(8)	19.6(7)	-2.2(6)	-1.6(6)	-0.4(6)
C10	17.5(8)	15.1(8)	25.0(8)	-0.7(6)	-1.9(6)	-3.0(6)
C11	22.5(10)	21.4(9)	72.5(15)	5.9(9)	9.4(10)	3.2(8)
C12	16.7(8)	18.1(8)	35.9(9)	-4.5(7)	-1.0(7)	-0.6(7)
C13	18.9(8)	13.5(7)	25.4(8)	-3.1(6)	-1.9(6)	-1.7(7)
C14	20.0(9)	26.5(9)	38.2(10)	-8.2(8)	3.2(7)	-6.7(7)
C15	37.4(10)	22.3(9)	27.4(9)	1.4(7)	-4.7(8)	3.2(8)

C16	23.8(9)	22.9(8)	26.4(9)	1.7(7)	-1.9(7)	1.0(7)

Table 4 Bond Lengths for lub139.

Atom	Atom	Length/Å	Atom	Atom	Length/Å
O1	C1	1.229(2)	C1	C2	1.536(2)
O2	C9	1.432(2)	C2	C3	1.556(2)
O3	C10	1.206(2)	C3	C4	1.529(2)
O4	C10	1.335(2)	C4	C5	1.521(2)
O4	C11	1.451(2)	C5	C6	1.540(2)
O5	C12	1.213(2)	C5	C9	1.536(2)
O6	C12	1.350(2)	C6	C7	1.532(2)
O6	C13	1.4727(19)	C7	C8	1.531(2)
N1	C1	1.344(2)	C8	C10	1.527(2)
N1	C5	1.485(2)	C13	C14	1.518(2)
N1	C8	1.459(2)	C13	C15	1.517(2)
N2	C2	1.446(2)	C13	C16	1.523(2)
N2	C12	1.352(2)			

Table 5 Bond Angles for lub139.

Atom	Atom	Atom	Angle/°	Atom	Atom	Atom	Angle/°
C10	O4	C11	117.36(15)	C9	C5	C6	111.11(13)
C12	O6	C13	120.45(13)	C7	C6	C5	103.75(12)
C1	N1	C5	124.97(13)	C8	C7	C6	103.46(13)

C1	N1	C8	119.77(14)	N1	C8	C7	102.66(13)
C8	N1	C5	113.47(12)	N1	C8	C10	110.28(13)
C12	N2	C2	121.27(16)	C10	C8	C7	111.26(13)
O1	C1	N1	121.77(15)	O2	C9	C5	110.99(13)
O1	C1	C2	121.35(15)	O3	C10	O4	124.19(16)
N1	C1	C2	116.87(14)	O3	C10	C8	126.14(15)
N2	C2	C1	108.70(14)	O4	C10	C8	109.61(14)
N2	C2	C3	111.72(15)	O5	C12	O6	126.23(16)
C1	C2	C3	115.11(14)	O5	C12	N2	124.99(17)
C4	C3	C2	114.70(14)	O6	C12	N2	108.78(15)
C5	C4	C3	111.45(14)	O6	C13	C14	101.70(13)
N1	C5	C4	107.85(13)	O6	C13	C15	109.85(13)
N1	C5	C6	102.07(12)	O6	C13	C16	111.13(14)
N1	C5	C9	108.87(13)	C14	C13	C16	110.72(15)
C4	C5	C6	113.86(13)	C15	C13	C14	111.03(16)
C4	C5	C9	112.42(14)	C15	C13	C16	111.96(14)

Table 6 Hydrogen Bonds for lub139.

D	H	A	d(D-H)/Å	d(H-A)/Å	d(D-A)/Å	D-H-A/°
O2	H2	O3[1]	0.89(3)	2.05(3)	2.9383(18)	172(2)
N2	H2A	O2[2]	0.80(3)	2.23(3)	3.004(2)	163(2)
C8	H8	O1[3]	1.00	2.57	3.1545(19)	117.1
C15	H15C	O5	0.98	2.51	3.090(3)	117.8
C16	H16A	O5	0.98	2.36	2.948(2)	117.8

C16	H16C	O4[4]	0.98	2.49	3.438(2) 162.9

[1]-1+X,+Y,+Z; [2]1+X,+Y,+Z; [3]-1/2+X,1/2-Y,1-Z; [4]1/2+X,1/2-Y,1-Z

Table 7 Torsion Angles for lub139.

A	B	C	D	Angle/°	A	B	C	D	Angle/°
O1	C1	C2	N2	25.7(2)	C5	N1	C1	C2	9.2(2)
O1	C1	C2	C3	151.91(16)	C5	N1	C8	C7	-14.54(17)
N1	C1	C2	N2	-155.70(14)	C5	N1	C8	C10	104.09(15)
N1	C1	C2	C3	-29.5(2)	C5	C6	C7	C8	-38.68(16)
N1	C5	C6	C7	29.09(16)	C6	C5	C9	O2	-72.97(16)
N1	C5	C9	O2	175.39(13)	C6	C7	C8	N1	32.31(15)
N1	C8	C10	O3	-13.1(2)	C6	C7	C8	C10	-85.62(16)
N1	C8	C10	O4	169.52(14)	C7	C8	C10	O3	100.12(19)
N2	C2	C3	C4	128.49(16)	C7	C8	C10	O4	-77.25(17)
C1	N1	C5	C4	35.2(2)	C8	N1	C1	O1	-8.6(2)
C1	N1	C5	C6	155.46(15)	C8	N1	C1	C2	172.87(14)
C1	N1	C5	C9	-87.01(18)	C8	N1	C5	C4	-129.37(14)
C1	N1	C8	C7	179.98(14)	C8	N1	C5	C6	-9.15(17)
C1	N1	C8	C10	-61.39(18)	C8	N1	C5	C9	108.38(15)
C1	C2	C3	C4	3.9(2)	C9	C5	C6	C7	-86.83(16)
C2	N2	C12	O5	-12.4(3)	C11	O4	C10	O3	-5.1(3)
C2	N2	C12	O6	168.39(15)	C11	O4	C10	C8	172.35(16)
C2	C3	C4	C5	39.8(2)	C12	O6	C13	C14	178.74(17)
C3	C4	C5	N1	-58.33(18)	C12	O6	C13	C15	-63.6(2)

C3	C4	C5	C6	-170.82(14)	C12	O6	C13	C16	60.9(2)
C3	C4	C5	C9	61.70(18)	C12	N2	C2	C1	-113.36(17)
C4	C5	C6	C7	145.02(14)	C12	N2	C2	C3	118.53(18)
C4	C5	C9	O2	55.96(17)	C13	O6	C12	O5	-8.5(3)
C5	N1	C1	O1	-172.28(15)	C13	O6	C12	N2	170.72(14)

Table 8 Hydrogen Atom Coordinates (Å×10^4) and Isotropic Displacement Parameters (Å^2×10^3) for lub139.

Atom	*x*	*y*	*z*	U(eq)
H2	-160(40)	2715(18)	3055(15)	33(6)
H2A	8820(40)	4270(16)	3447(14)	28(6)
H2B	5392.31	4410.87	4043.16	26
H3A	4071.72	4471.28	2843	36
H3B	6009.01	4345.53	2379.43	36
H4A	3578.85	3223.54	2072.64	25
H4B	5619.6	2837.9	2236.52	25
H6A	2141.6	1492.11	2811.92	23
H6B	4253.26	1402.03	2497.06	23
H7A	2920.94	1080.96	4153.1	23
H7B	4249.57	427.98	3621.21	23
H8	5726.7	1513.67	4695.46	21
H9A	1624.66	2585.9	4043.56	23
H9B	2448.93	3572.25	3878.94	23
H11A	9643.24	-623.08	3950.48	58

H11B	9128.84	-200.86	3070.6	58
H11C	10556.69	309.06	3665.24	58
H11D	9909.28	279.83	3173.74	58
H11E	10423.67	-142.39	4053.61	58
H11F	8995.82	-652.31	3458.98	58
H14A	13335.34	5730.06	4494.33	42
H14B	13479.24	6803.75	4427.71	42
H14C	13061.39	6215.74	3620.59	42
H15A	10243.9	7079.46	3327.66	44
H15B	10473.5	7698.19	4130.46	44
H15C	8604.59	7137.37	3991.28	44
H16A	9061.42	6438.23	5398.18	37
H16B	11005.92	6936.31	5532.19	37
H16C	10891	5860.46	5577.17	37

Table 9 Atomic Occupancy for lub139.

Atom	*Occupancy*	Atom	*Occupancy*	Atom	*Occupancy*
H11A	0.5	H11B	0.5	H11C	0.5
H11D	0.5	H11E	0.5	H11F	0.5

Experimental

Single crystals of $C_{16}H_{26}N_2O_6$ lub139 were crystallized from DCM. A suitable crystal was selected and mounted on a cryoloop on a Bruker Smart APEX diffractometer. The crystal was kept at 100 K during data collection. Using Olex2 [1], the structure was solved with the XT [2] structure solution program using Intrinsic Phasing and refined with the XL [3] refinement package using Least Squares minimisation.

1. Dolomanov, O.V., Bourhis, L.J., Gildea, R.J, Howard, J.A.K. & Puschmann, H. (2009), J. Appl. Cryst. 42, 339-341.
2. Sheldrick, G.M. (2015). Acta Cryst. A71, 3-8.
3. Sheldrick, G.M. (2015). Acta Cryst. C71, 3-8.

Crystal structure determination of lub139

Crystal Data for $C_{16}H_{26}N_2O_6$ (M =342.39 g/mol): orthorhombic, space group $P2_12_12_1$ (no. 19), a = 7.2138(4) Å, b = 14.8397(8) Å, c = 16.1962(9) Å, V = 1733.81(17) Å^3, Z = 4, T = 100 K, μ(CuKα) = 0.836 mm^{-1}, *Dcalc* = 1.312 g/cm^3, 17974 reflections measured (8.08° ≤ 2Θ ≤ 140.044°), 3281 unique (R_{int} = 0.0308, R_{sigma} = 0.0206) which were used in all calculations. The final R_1 was 0.0299 (I > 2σ(I)) and wR_2 was 0.0798 (all data).

Refinement model description

Number of restraints - 0, number of constraints - unknown.

Details:

1. Fixed Uiso
 At 1.2 times of:
  All C(H) groups, All C(H,H) groups
 At 1.5 times of:
  All C(H,H,H) groups, All C(H,H,H,H,H,H) groups
2. Others
 Fixed Sof: H11A(0.5) H11B(0.5) H11C(0.5) H11D(0.5) H11E(0.5) H11F(0.5)
3.a Ternary CH refined with riding coordinates:
 C2(H2B), C8(H8)
3.b Secondary CH2 refined with riding coordinates:
 C3(H3A,H3B), C4(H4A,H4B), C6(H6A,H6B), C7(H7A,H7B), C9(H9A,H9B)
3.c Disordered Me refined with riding coordinates:
 C11(H11A,H11B,H11C,H11D,H11E,H11F)
3.d Idealised Me refined as rotating group:
 C14(H14A,H14B,H14C), C15(H15A,H15B,H15C), C16(H16A,H16B,H16

Spectral data for Article 4

^{1}H NMR, 500 MHz

Solvent: $CDCl_3$

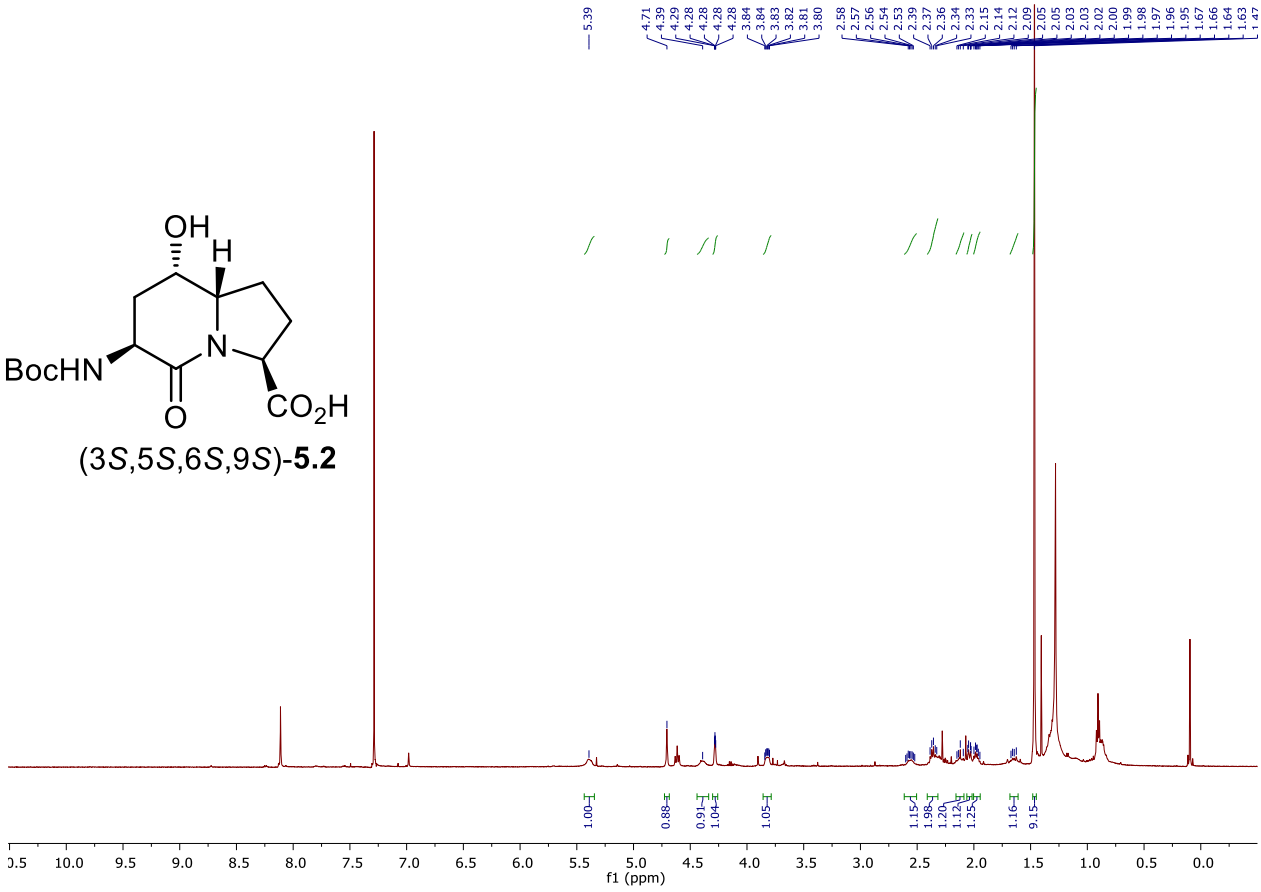

^{13}C NMR, 125 MHz

Solvent: $CDCl_3$

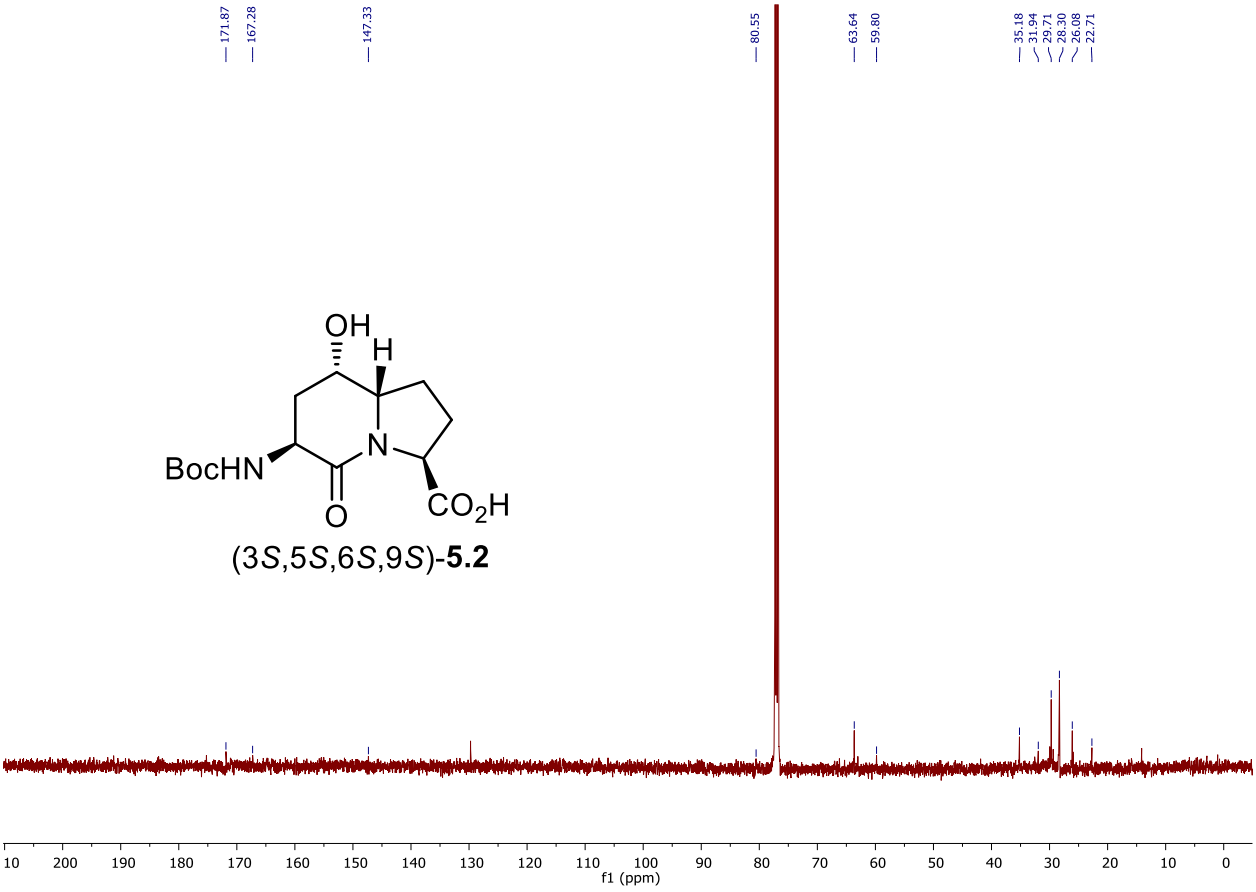

^{1}H NMR, 500 MHz

Solvent: CD_3OD

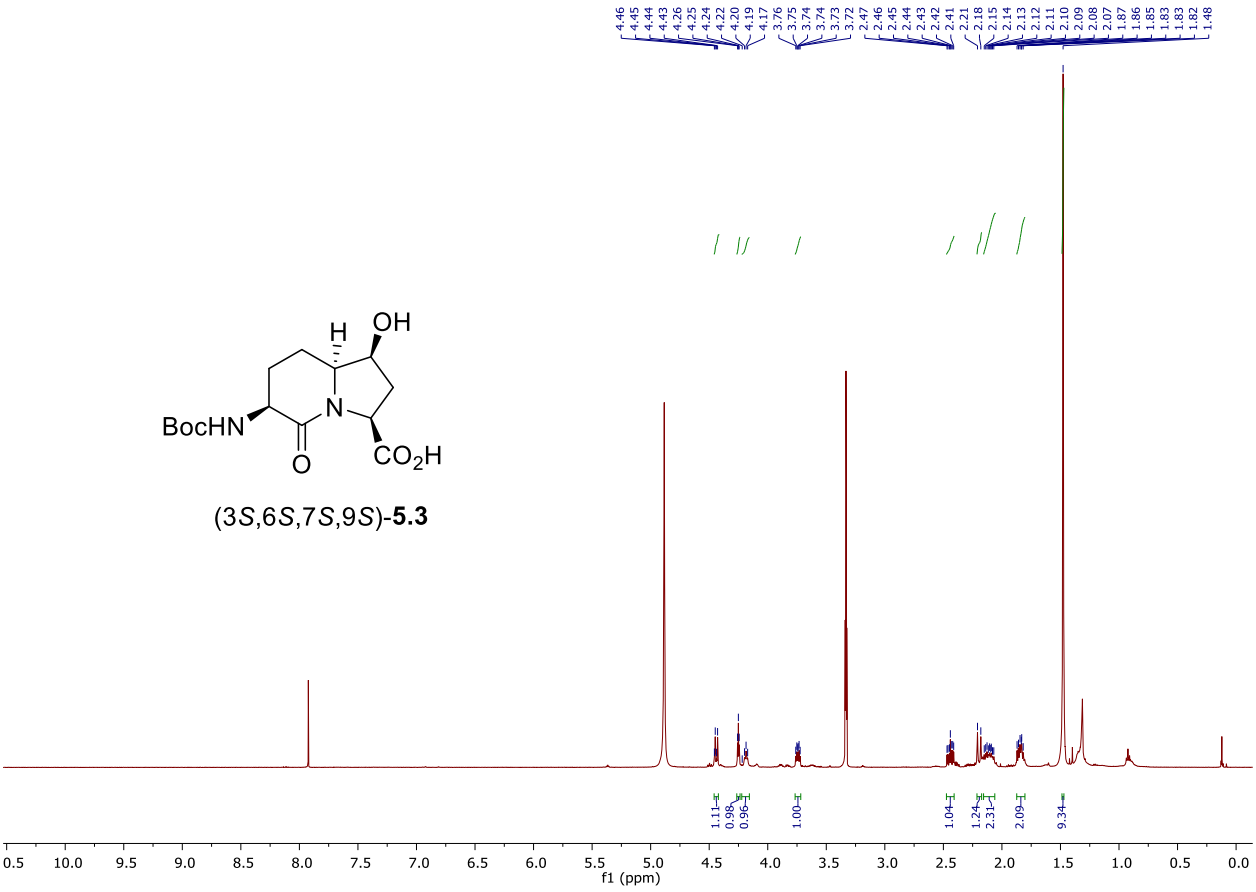

(3*S*,6*S*,7*S*,9*S*)-**5.3**

^{13}C NMR, 125 MHz

Solvent: CD_3OD

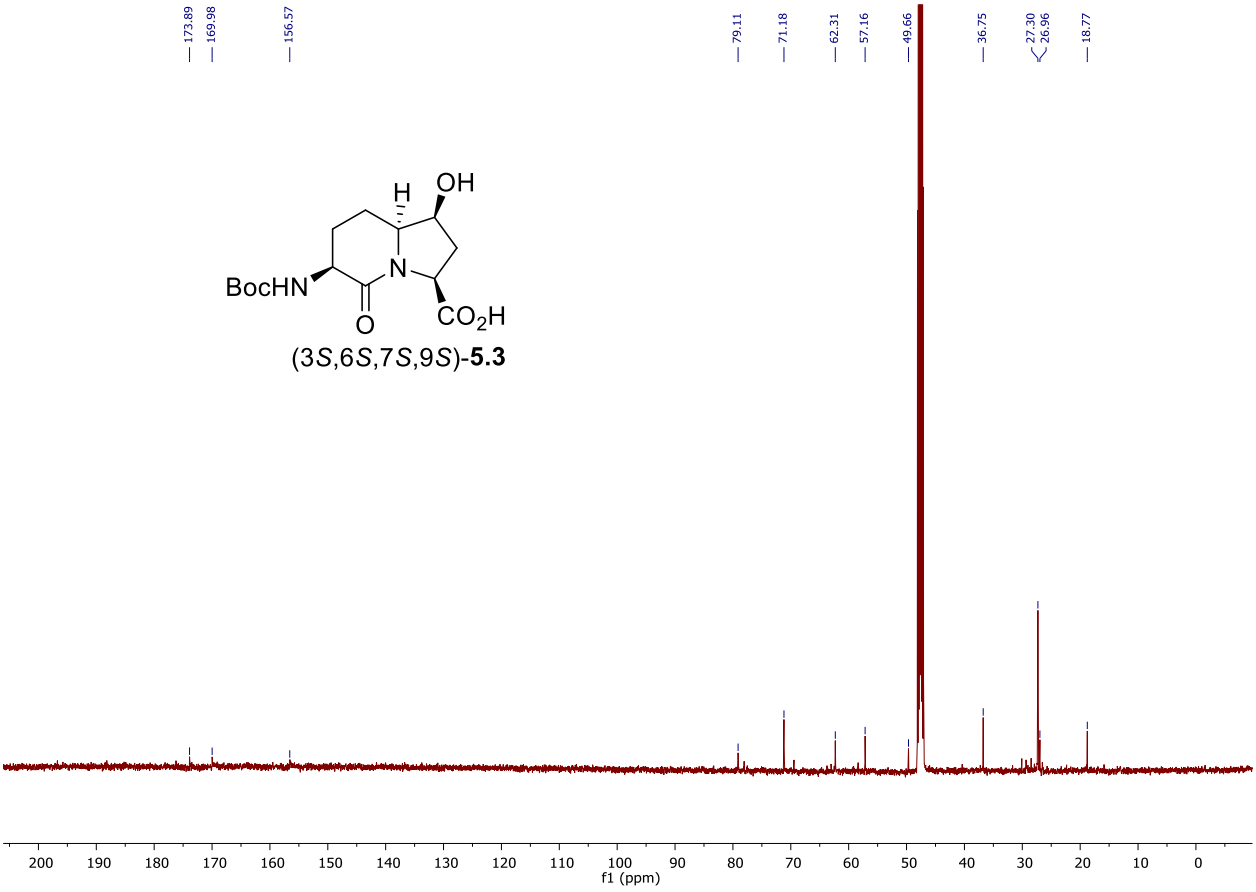

(3*S*,6*S*,7*S*,9*S*)-**5.3**

^{1}H NMR, 500 MHz

Solvent: $CDCl_3$

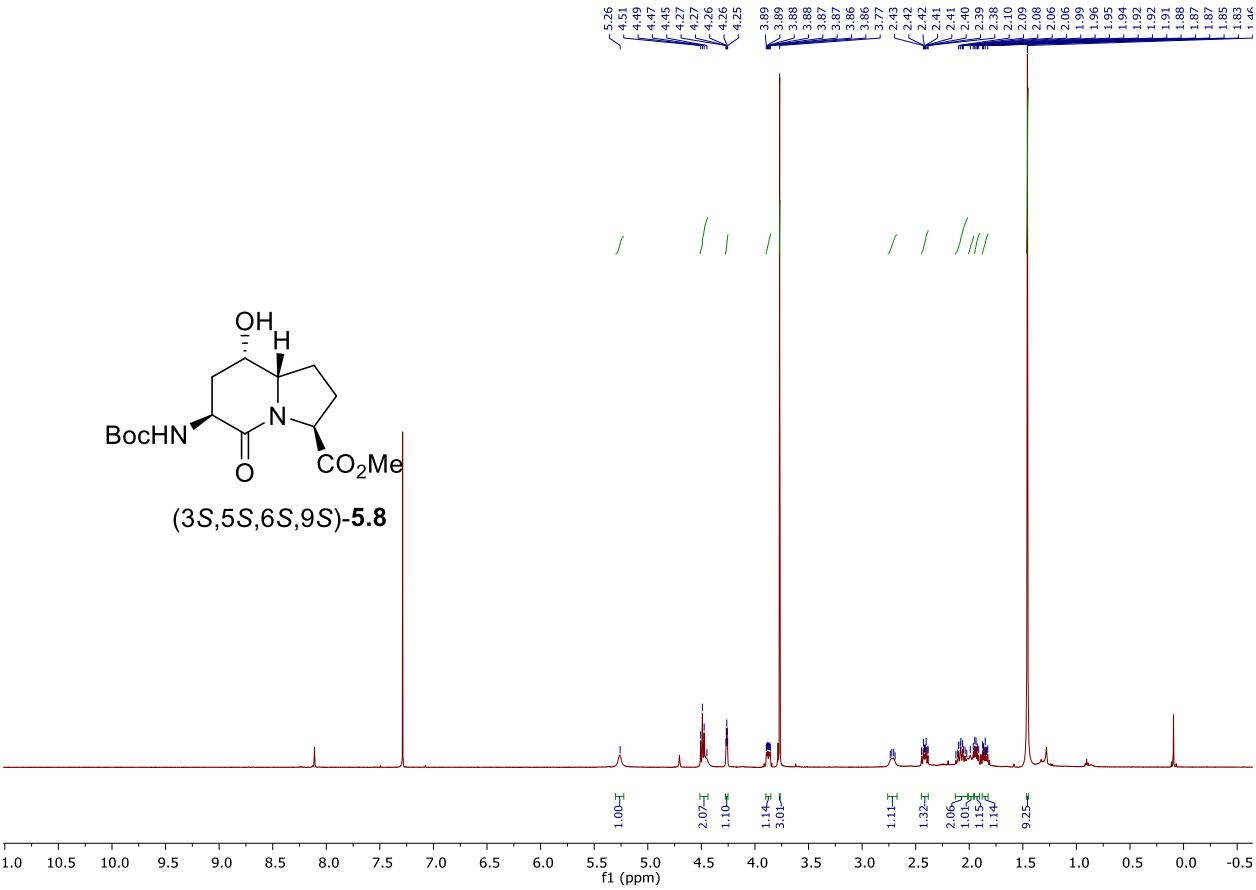

^{13}C NMR, 125 MHz

Solvent: $CDCl_3$

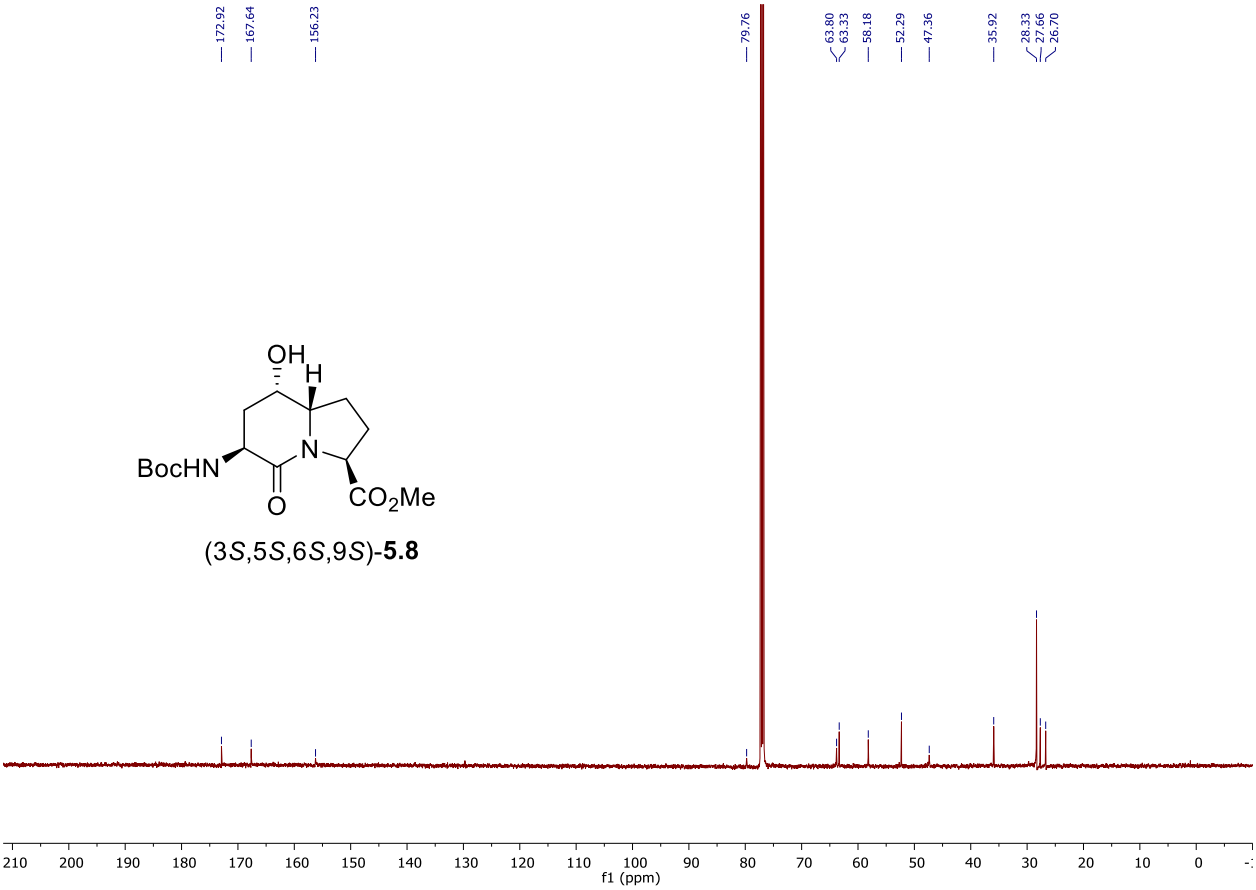

(3*S*,5*S*,6*S*,9*S*)-**5.8**

ed-HSQC, 500 MHz

Solvent: $CDCl_3$

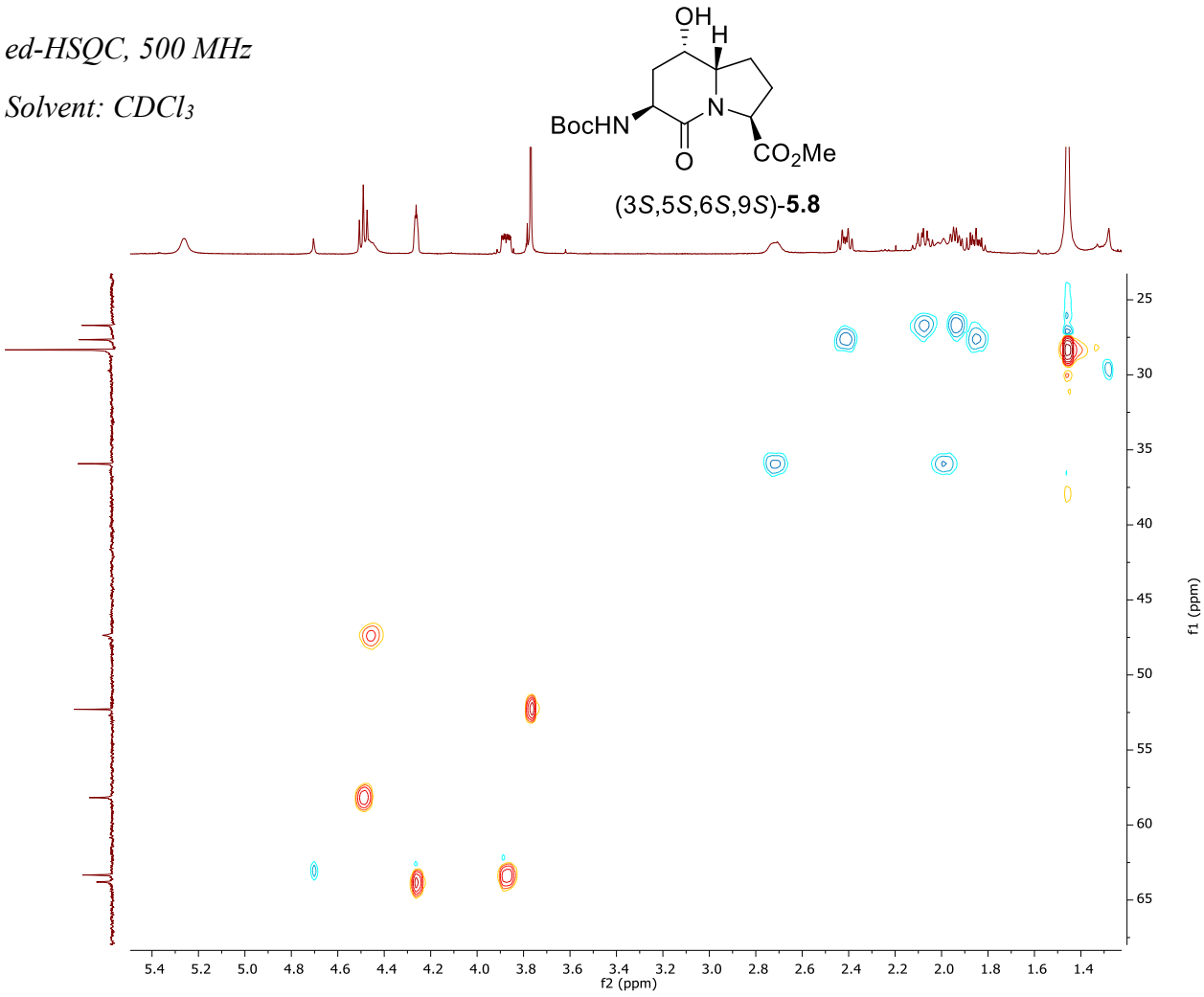

COSY, 500 MHz

Solvent: $CDCl_3$

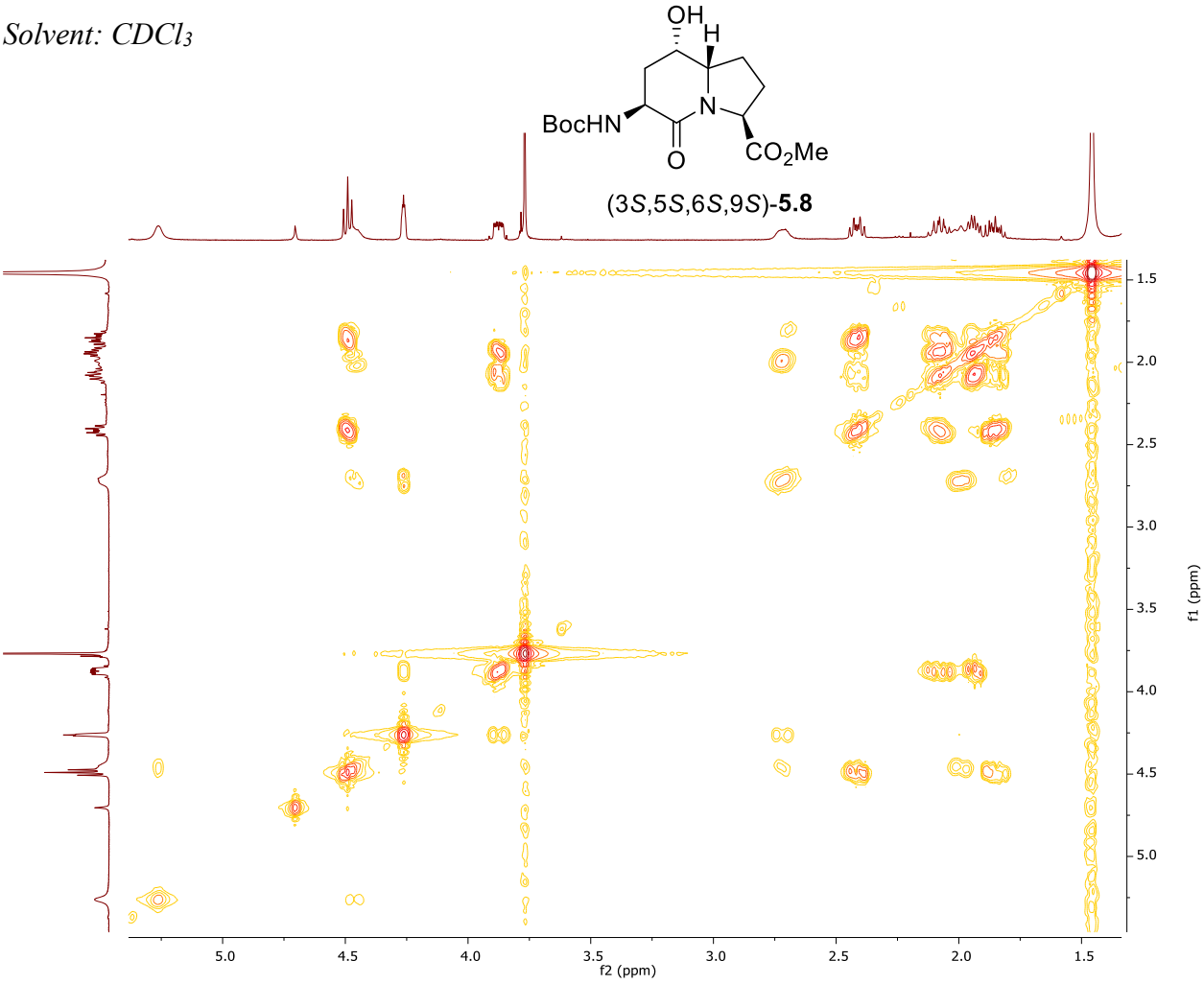

NOESY, 500 MHz

Solvent: $CDCl_3$

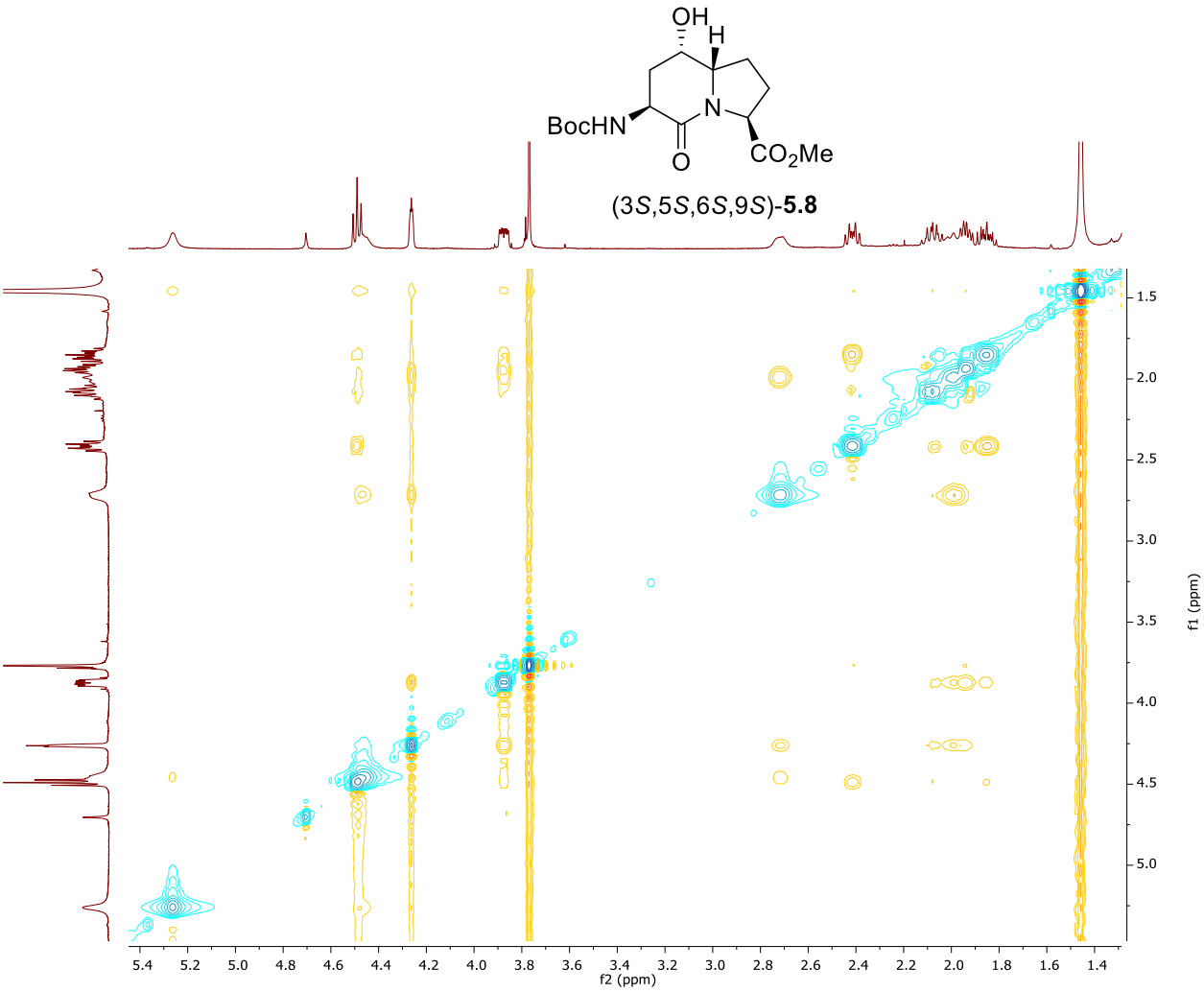

^{1}H NMR, 500 MHz

Solvent: $CDCl_3$

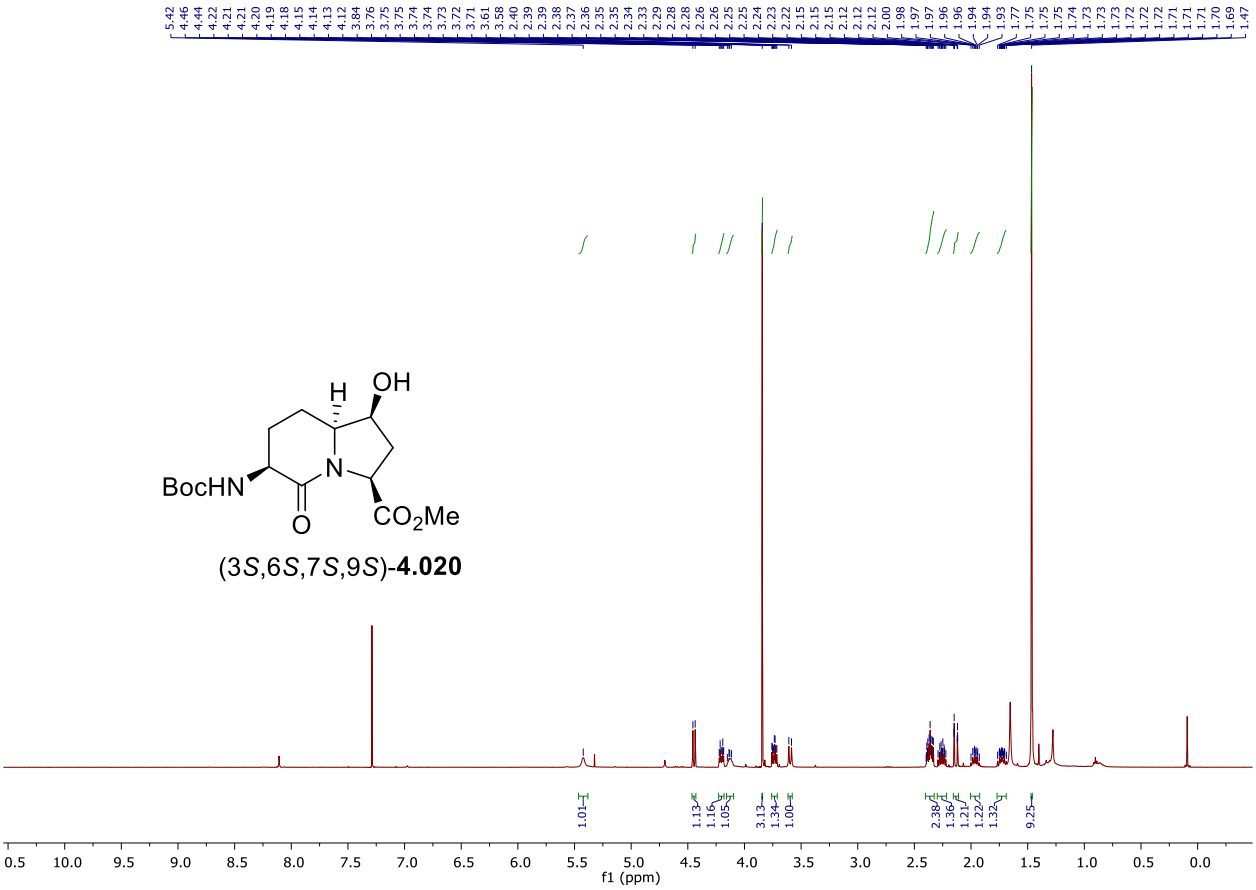

^{13}C NMR, 125 MHz

Solvent: $CDCl_3$

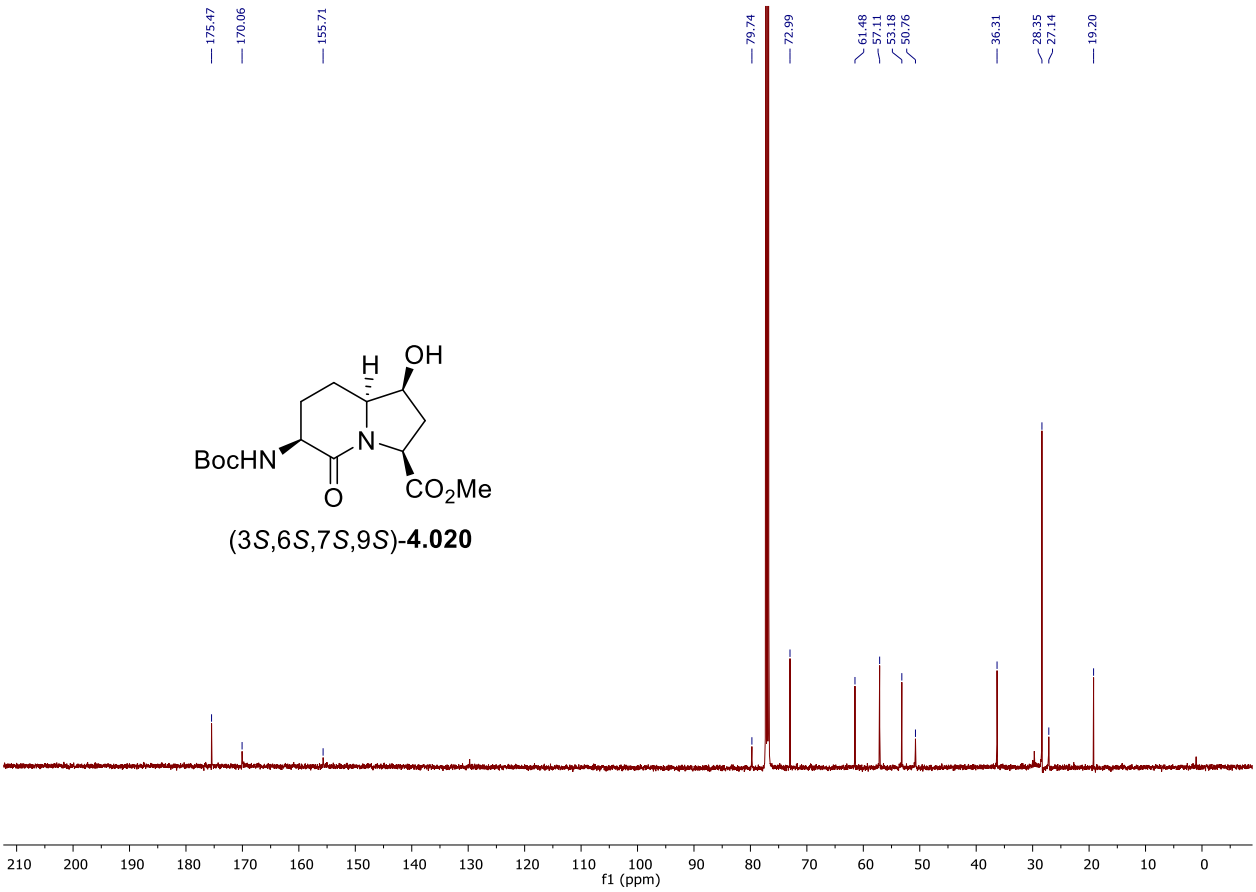

(3*S*,6*S*,7*S*,9*S*)-**4.020**

ed-HSQC, 500 MHz

Solvent: $CDCl_3$

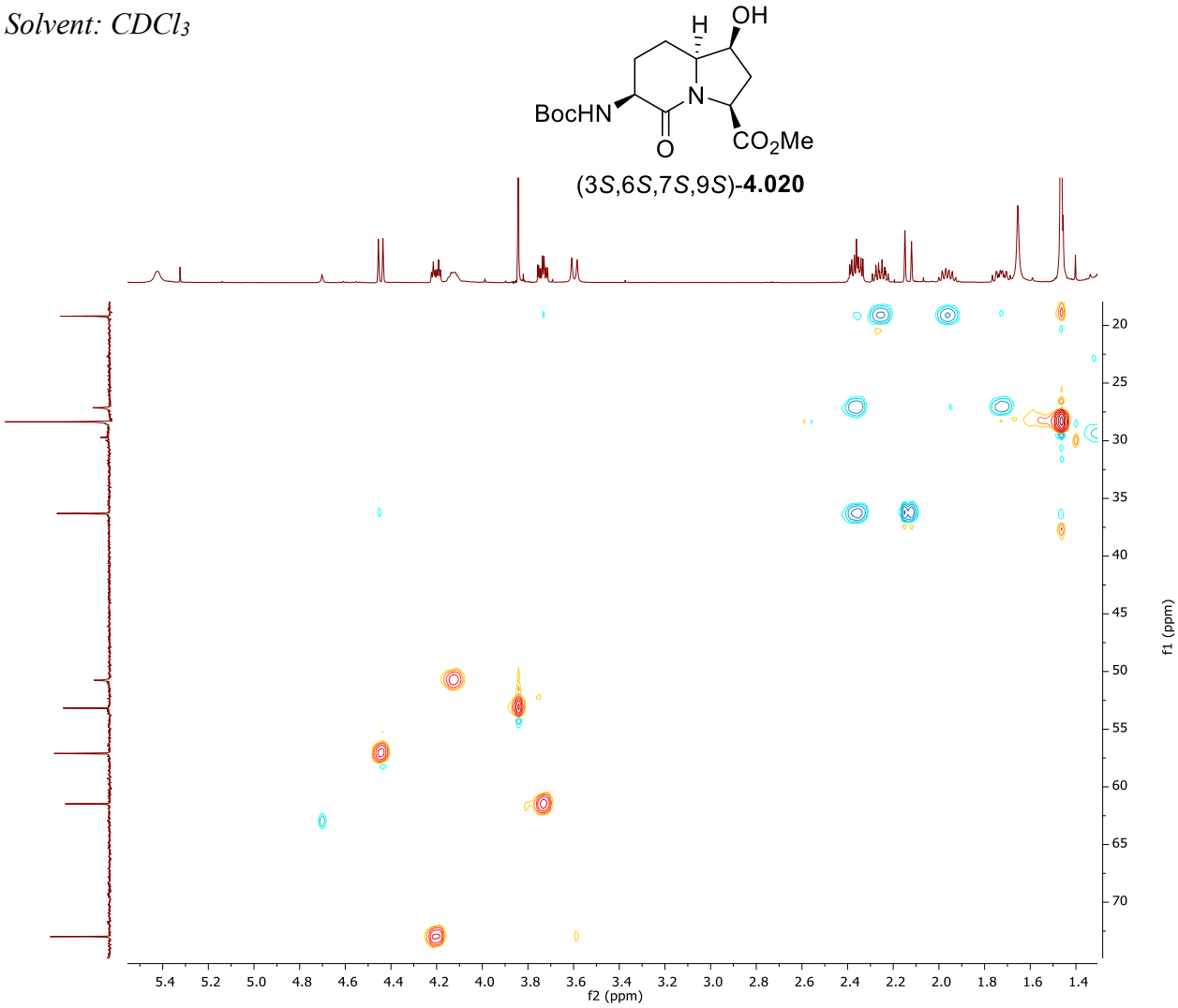

(3*S*,6*S*,7*S*,9*S*)-**4.020**

COSY, 500 MHz

Solvent: $CDCl_3$

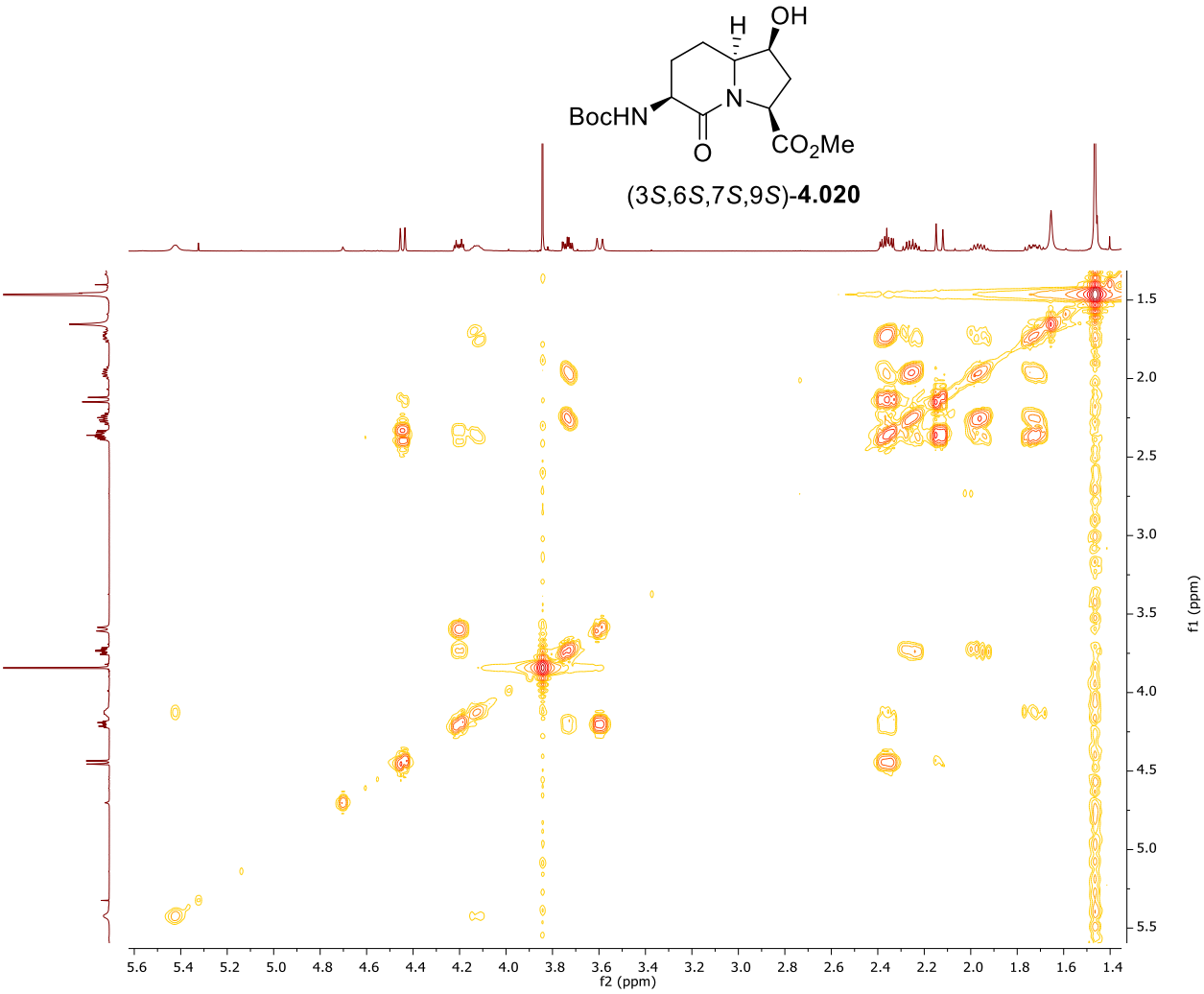

NOESY, 500 MHz

Solvent: $CDCl_3$

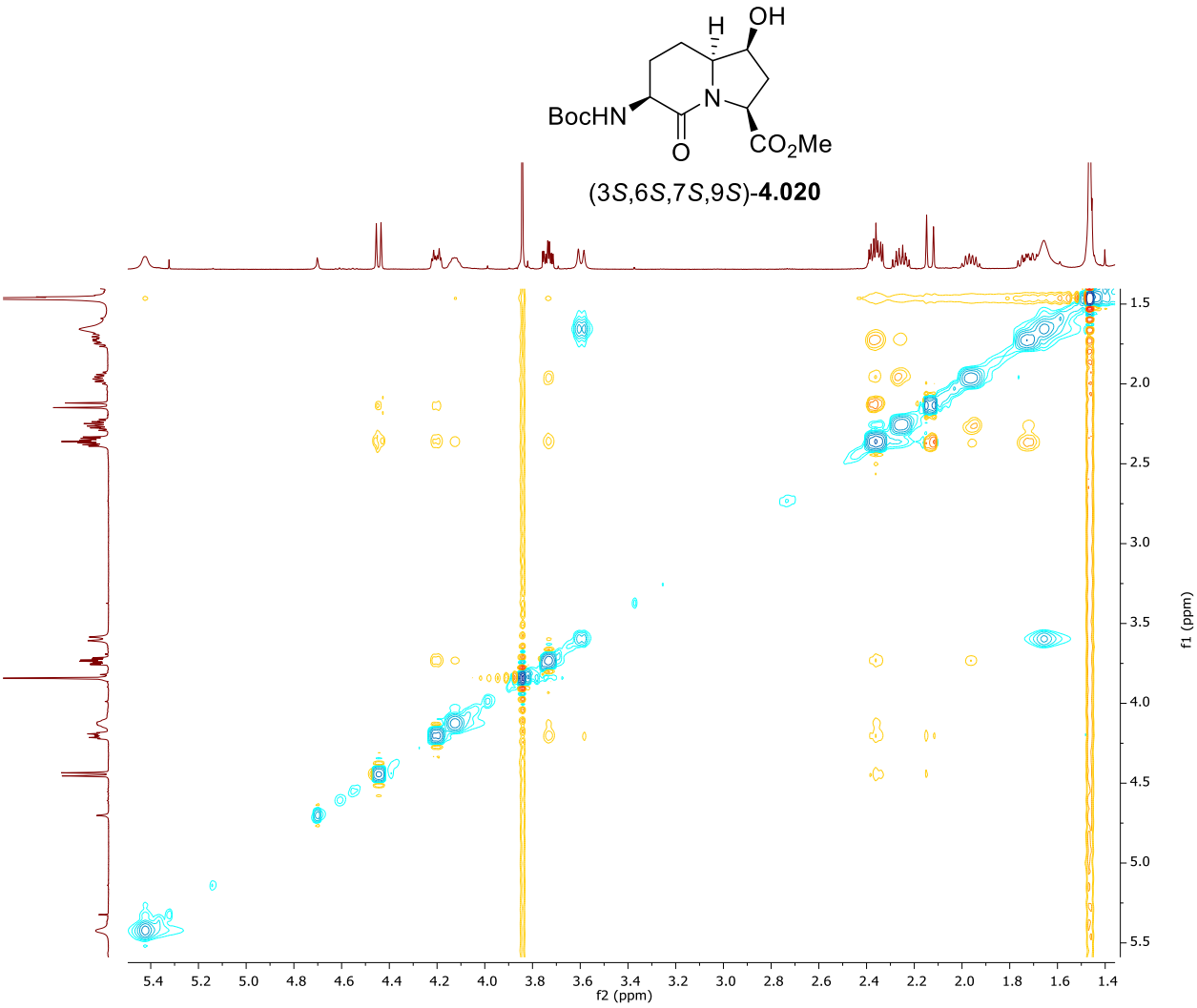

^{1}H NMR, 500 MHz

Solvent: $CDCl_3$

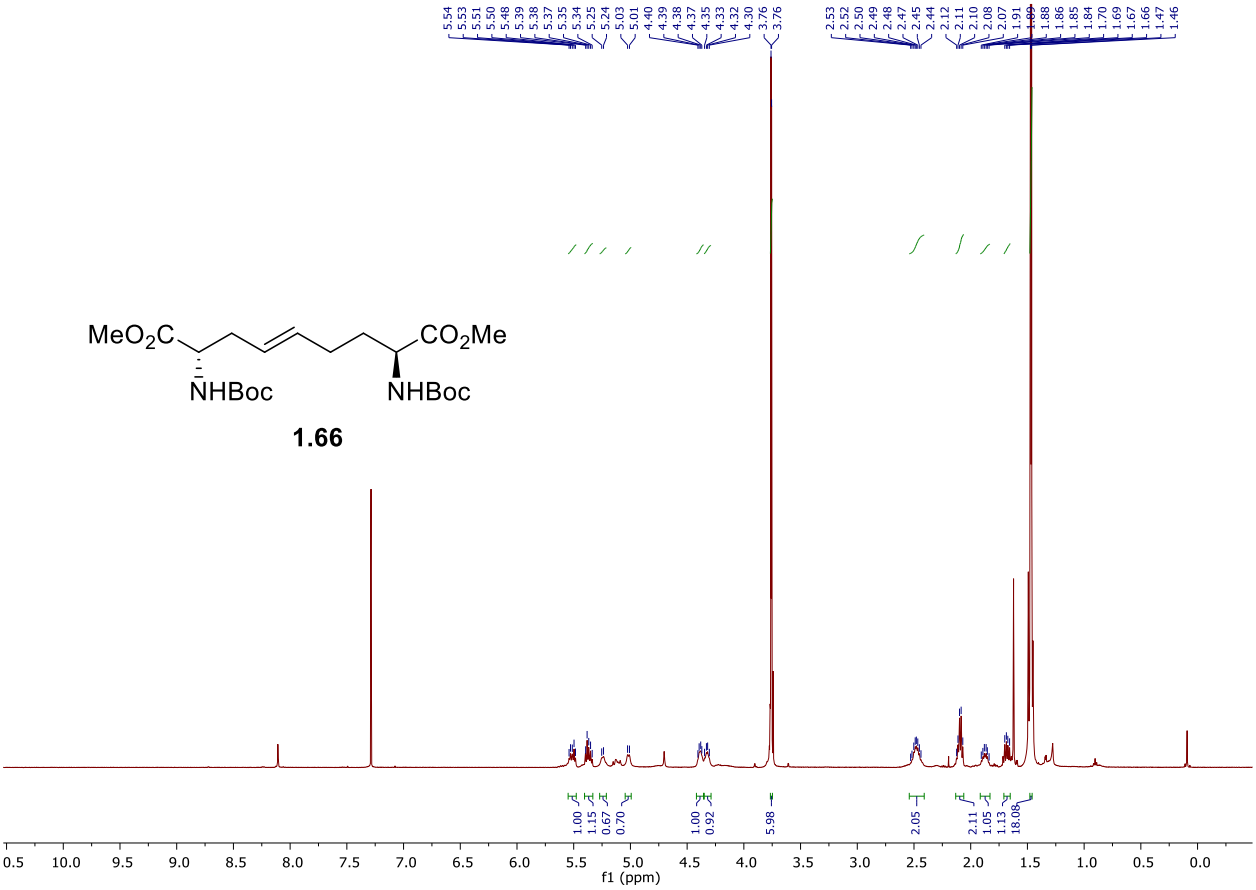

^{13}C NMR, 125 MHz

Solvent: $CDCl_3$

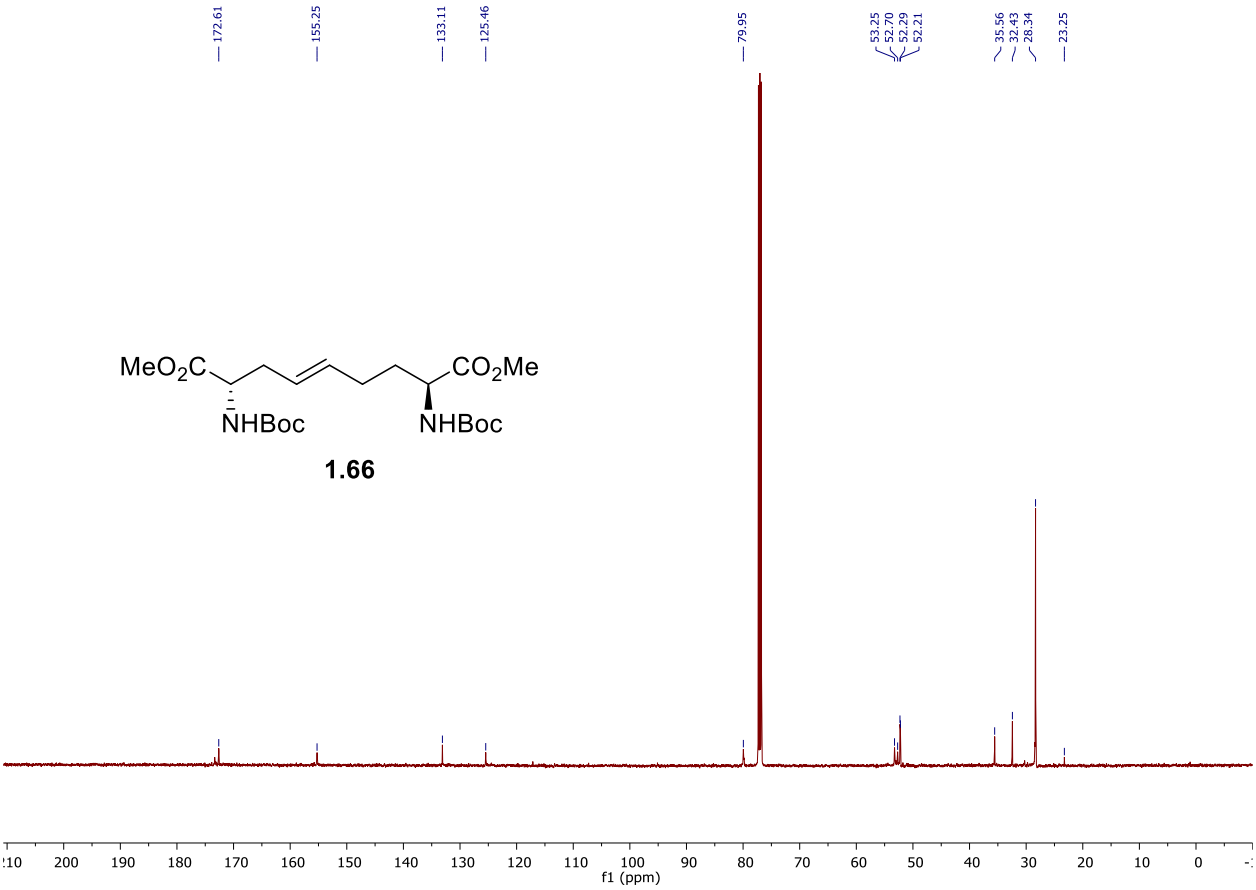

COSY, 500 MHz

Solvent: $CDCl_3$

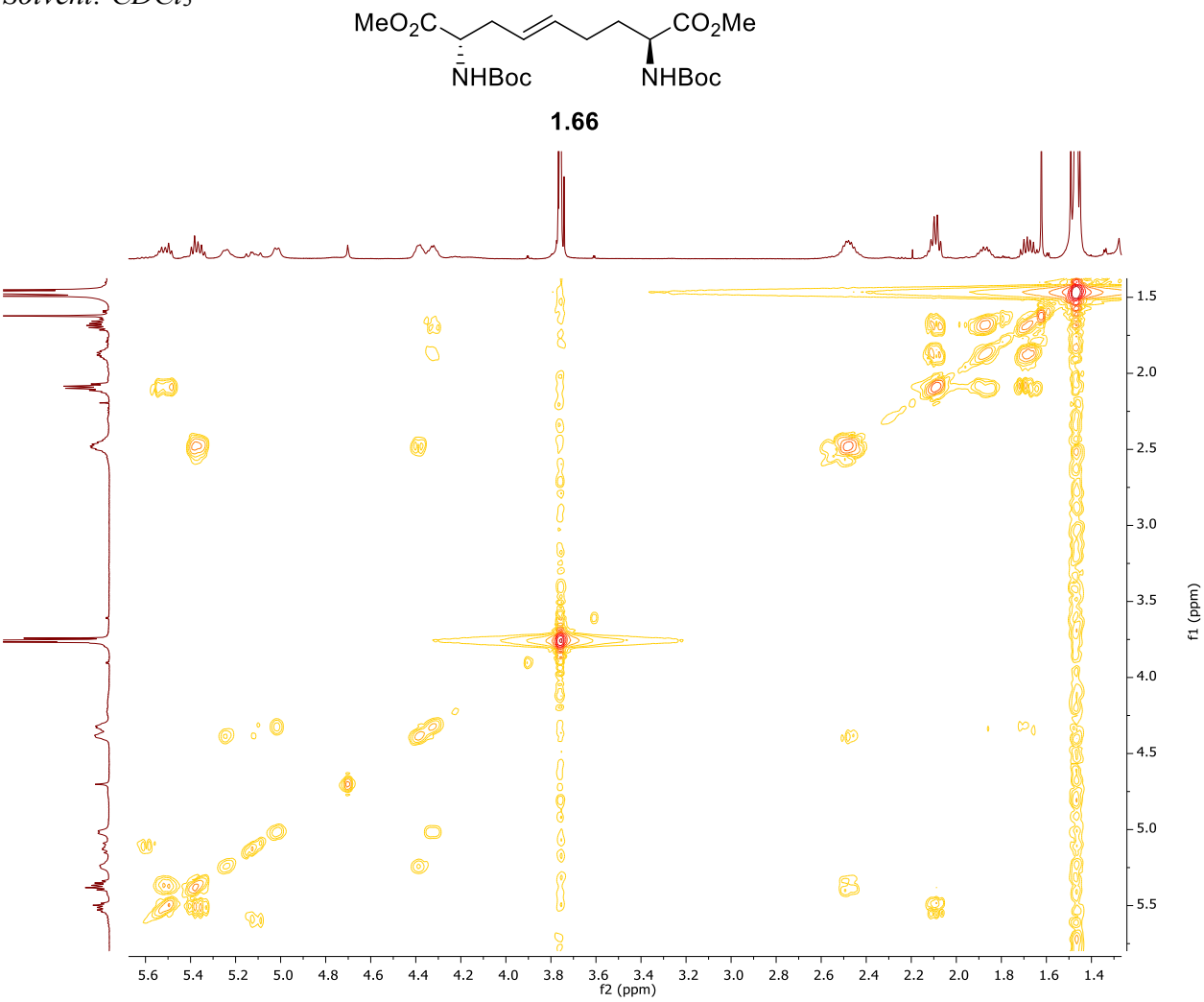

ed-HSQC, 500 MHz

Solvent: $CDCl_3$

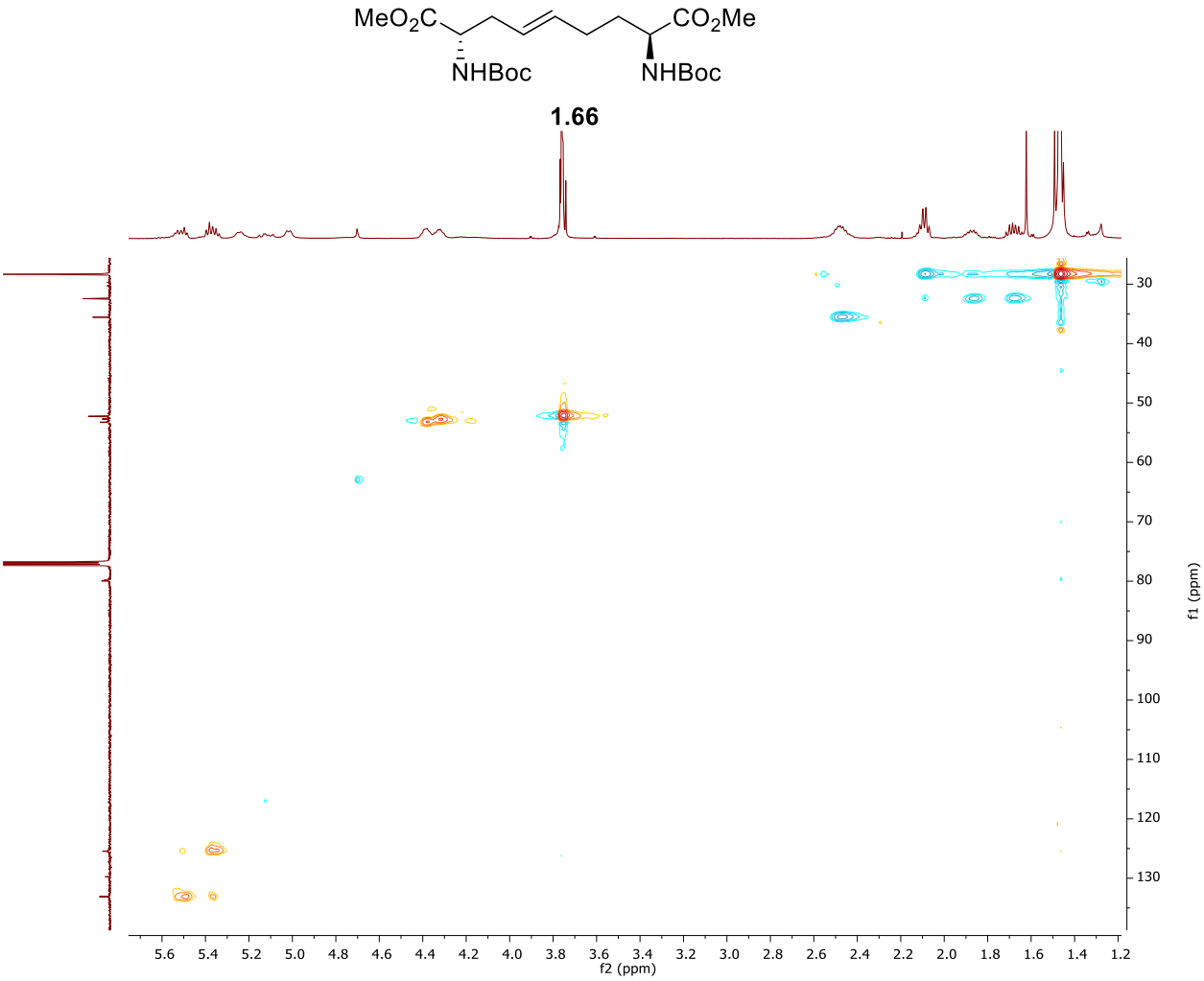

NOESY, 500 MHz

Solvent: $CDCl_3$

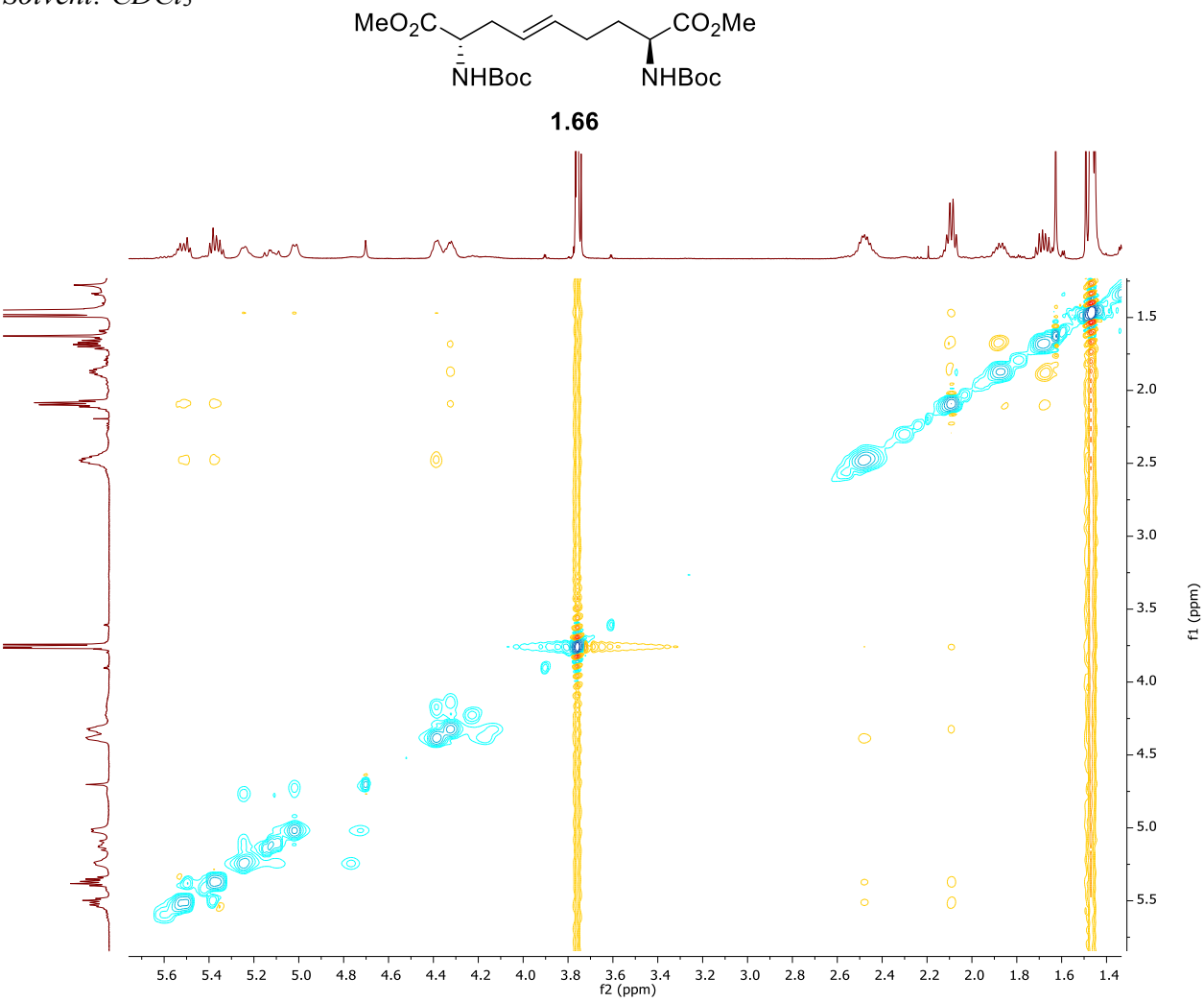

^{1}H NMR, 500 MHz

Solvent: $CDCl_3$

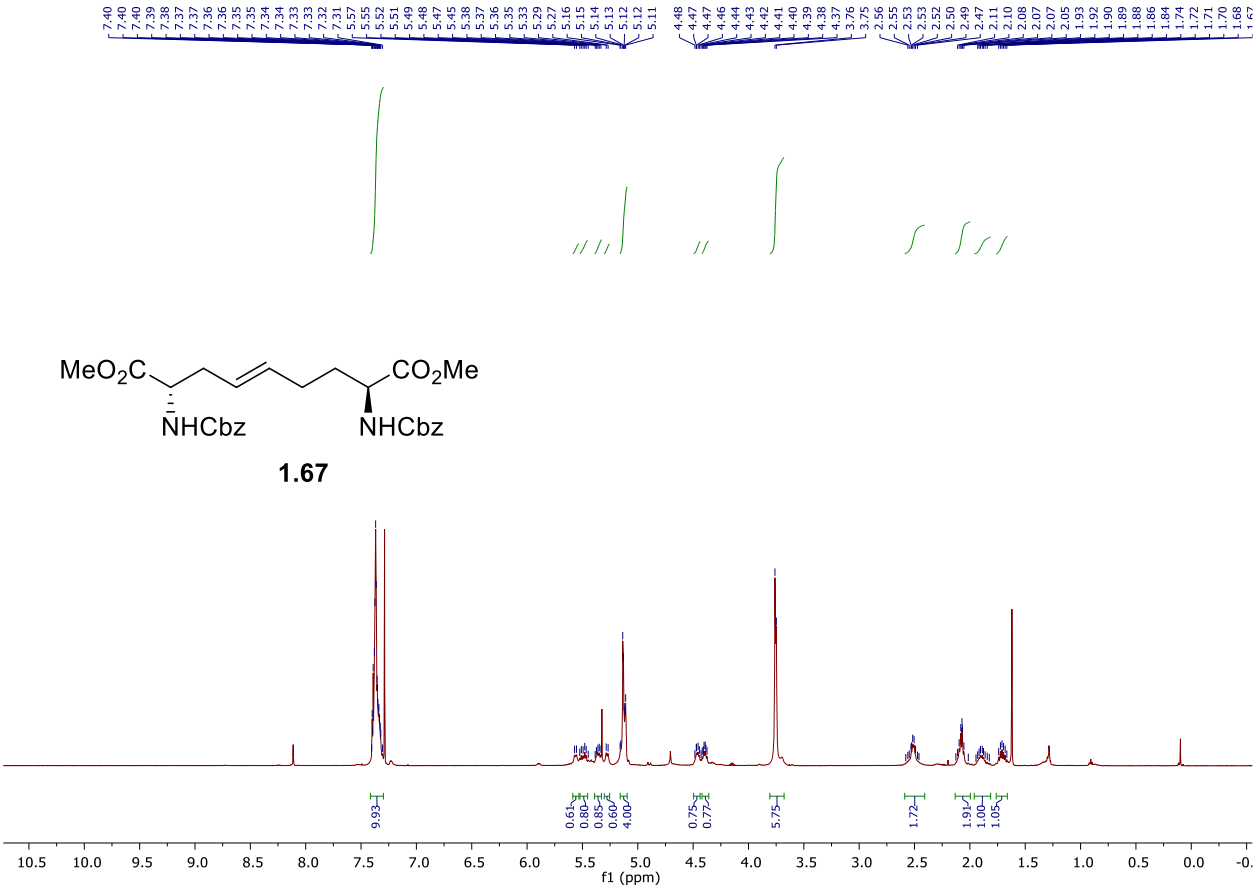

^{13}C NMR, 125 MHz

Solvent: $CDCl_3$

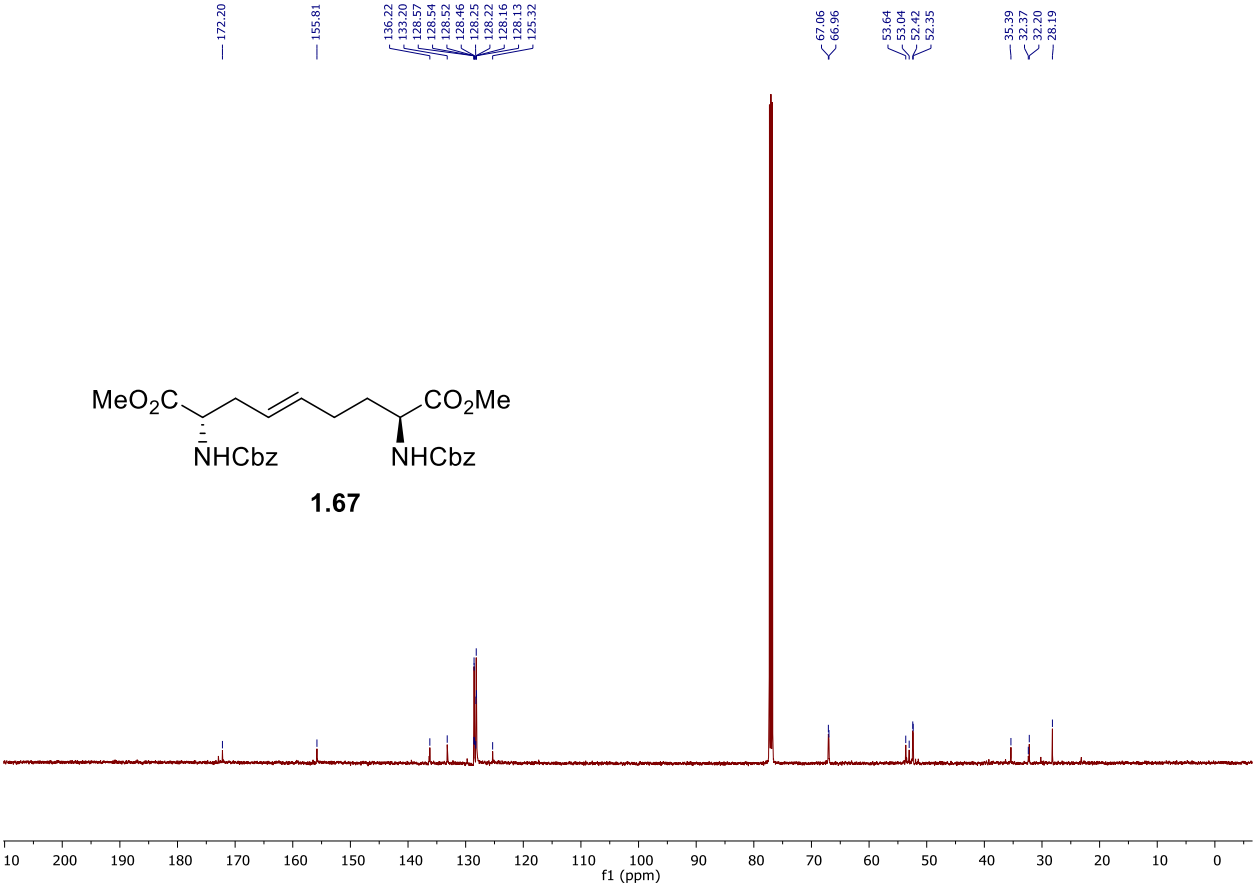

COSY, 500 MHz

Solvent: $CDCl_3$

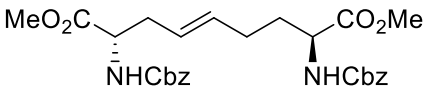

1.67

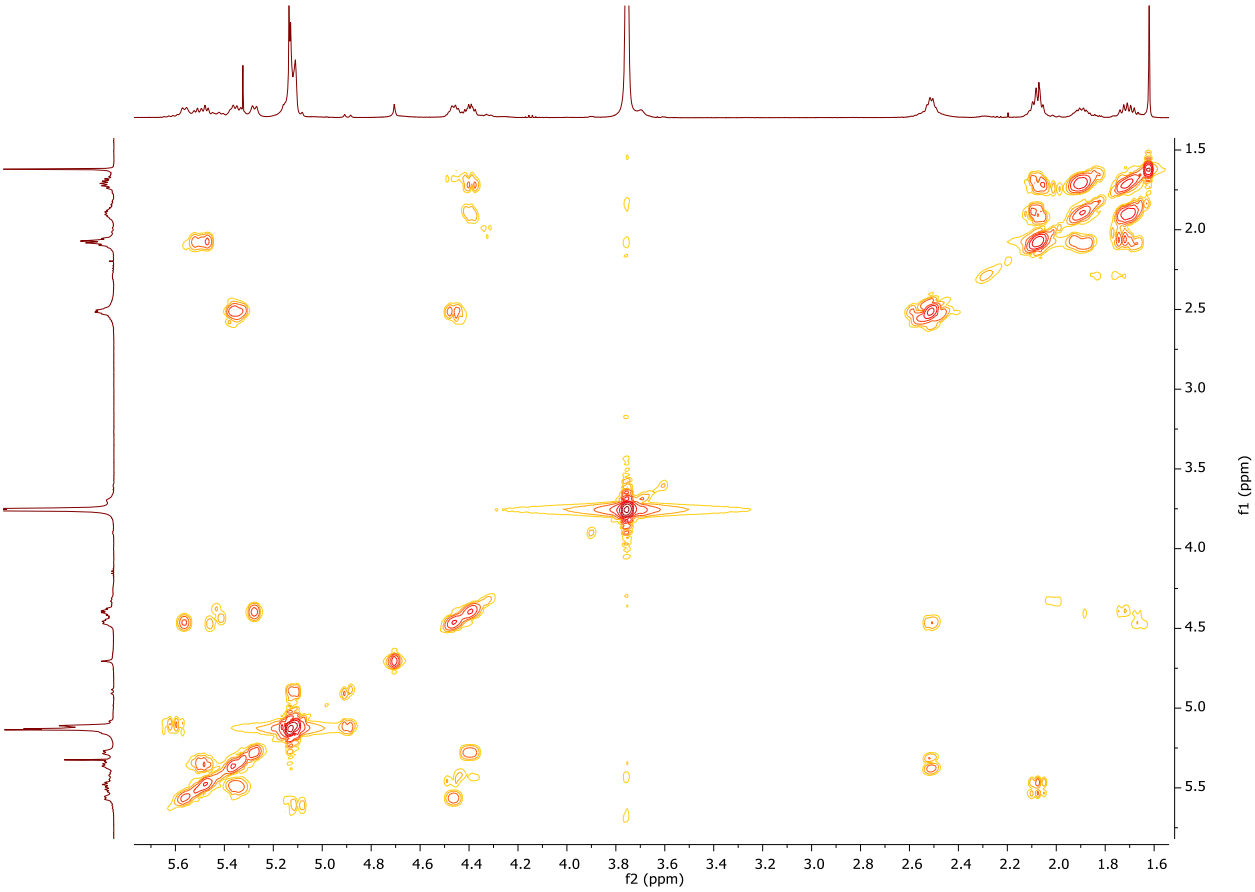

ed-HSQC, 500 MHz

Solvent: $CDCl_3$

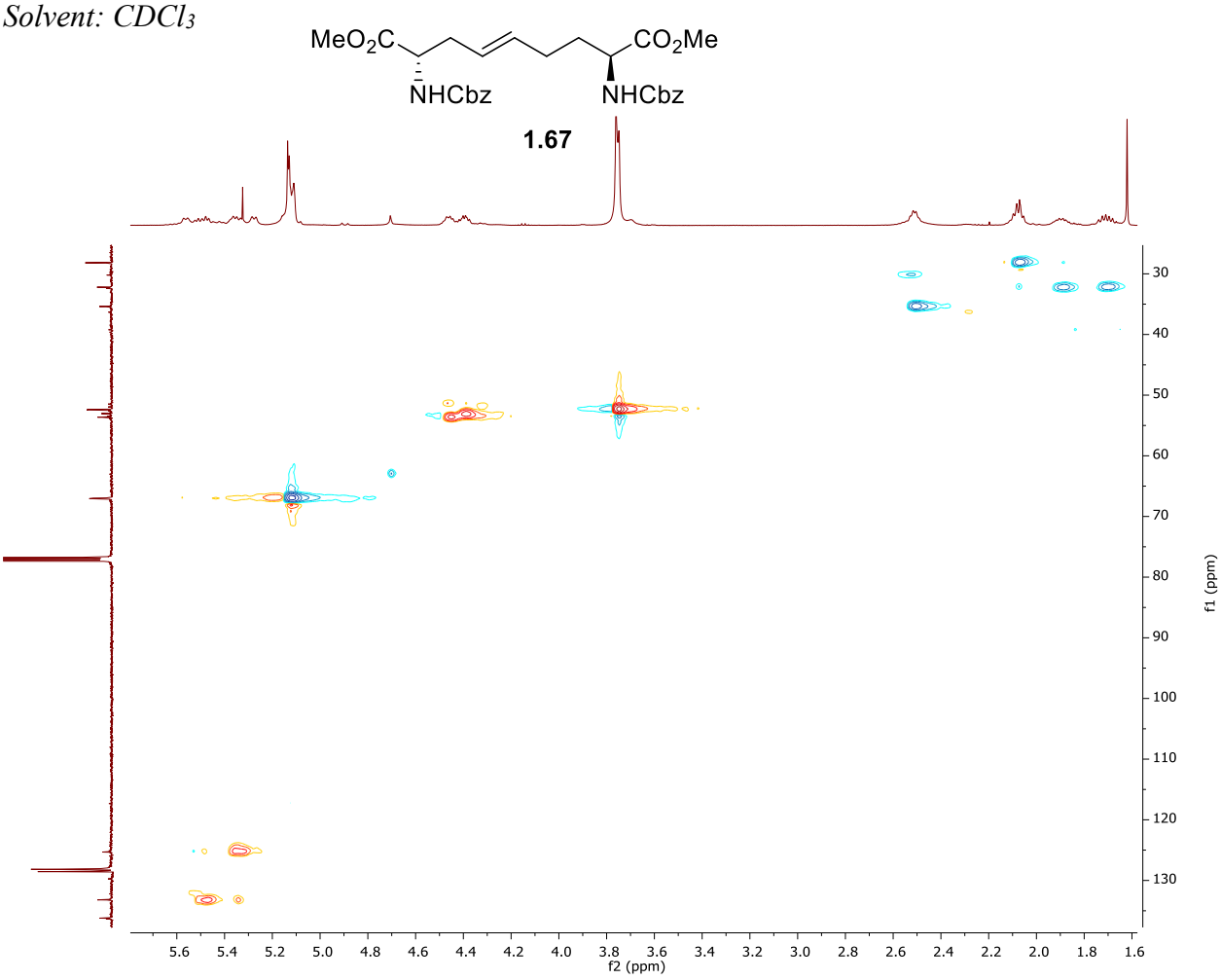

NOESY, 500 MHz

Solvent: $CDCl_3$

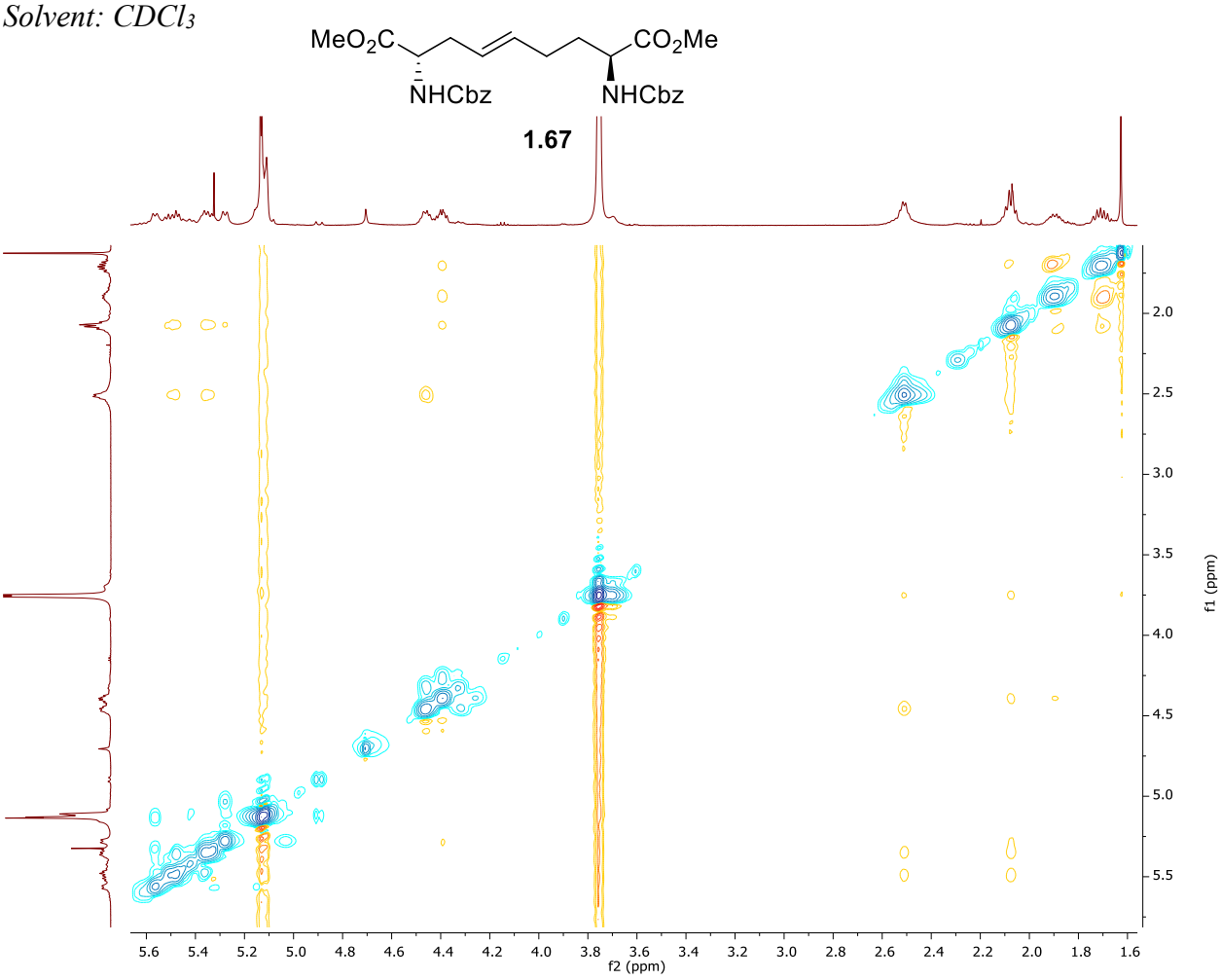

^{1}H NMR, 500 MHz,

Solvent: CD_3OD

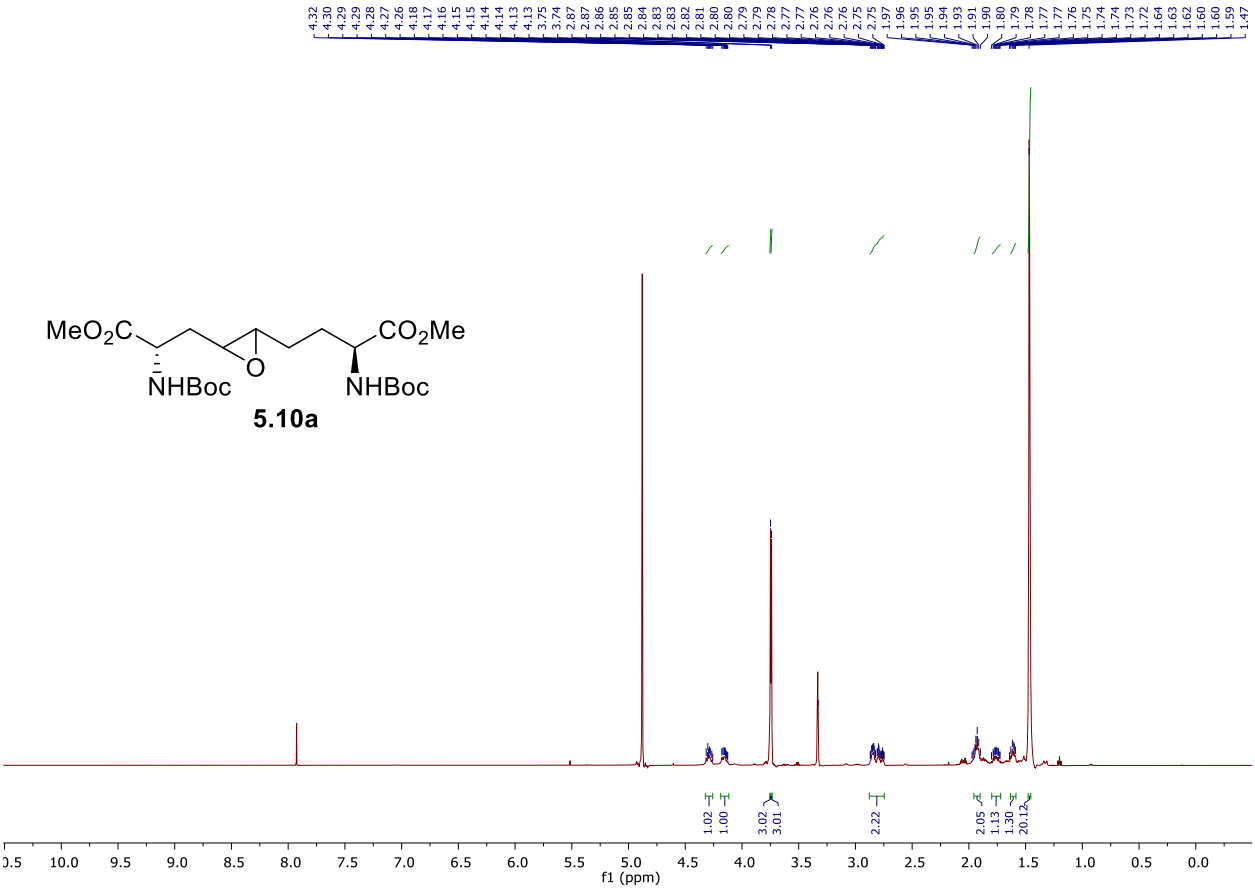

^{13}C NMR, 125 MHz

Solvent: CD_3OD

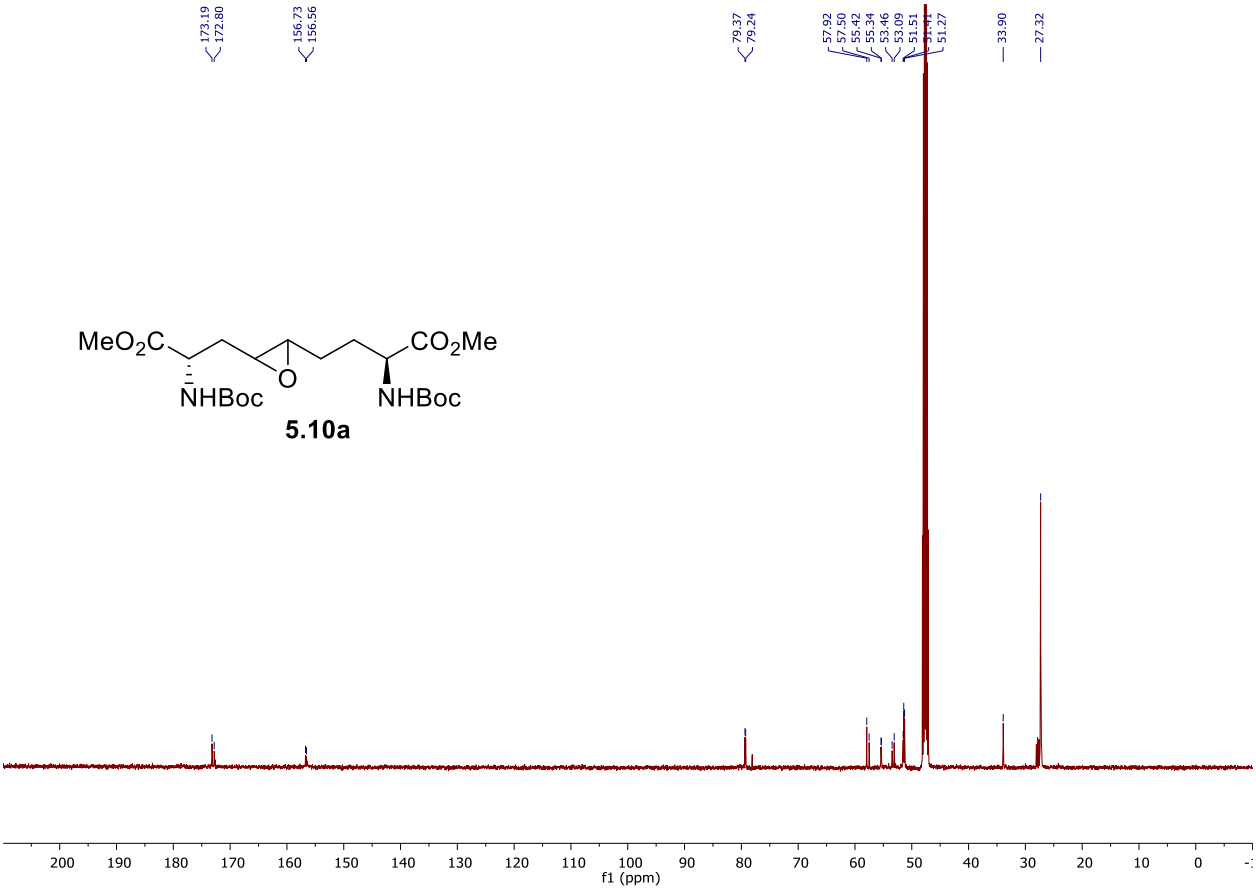

^{1}H NMR, 500 MHz

Solvent: $CDCl_3$

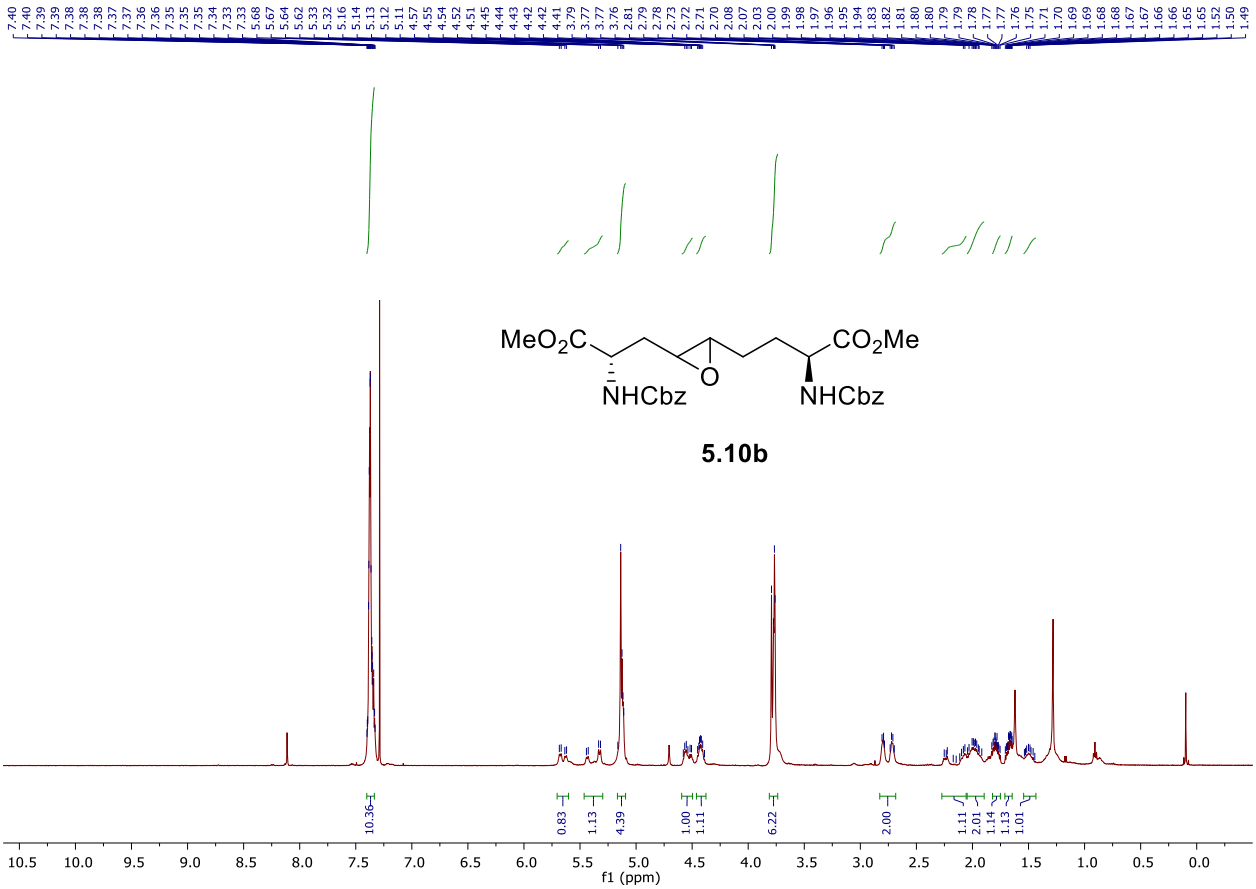

^{13}C NMR, 125 MHz

Solvent: $CDCl_3$

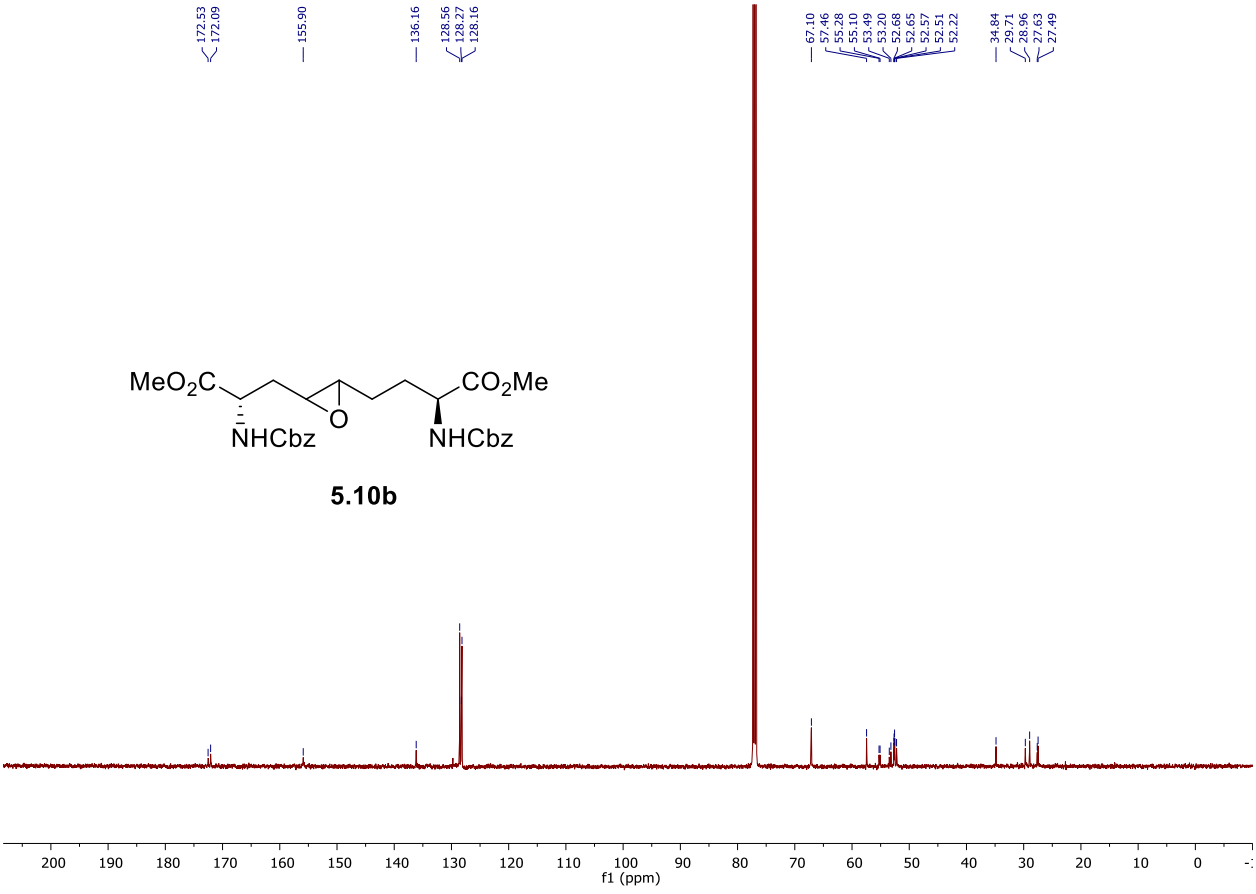

^{1}H NMR, 500 MHz

Solvent: $CDCl_3$

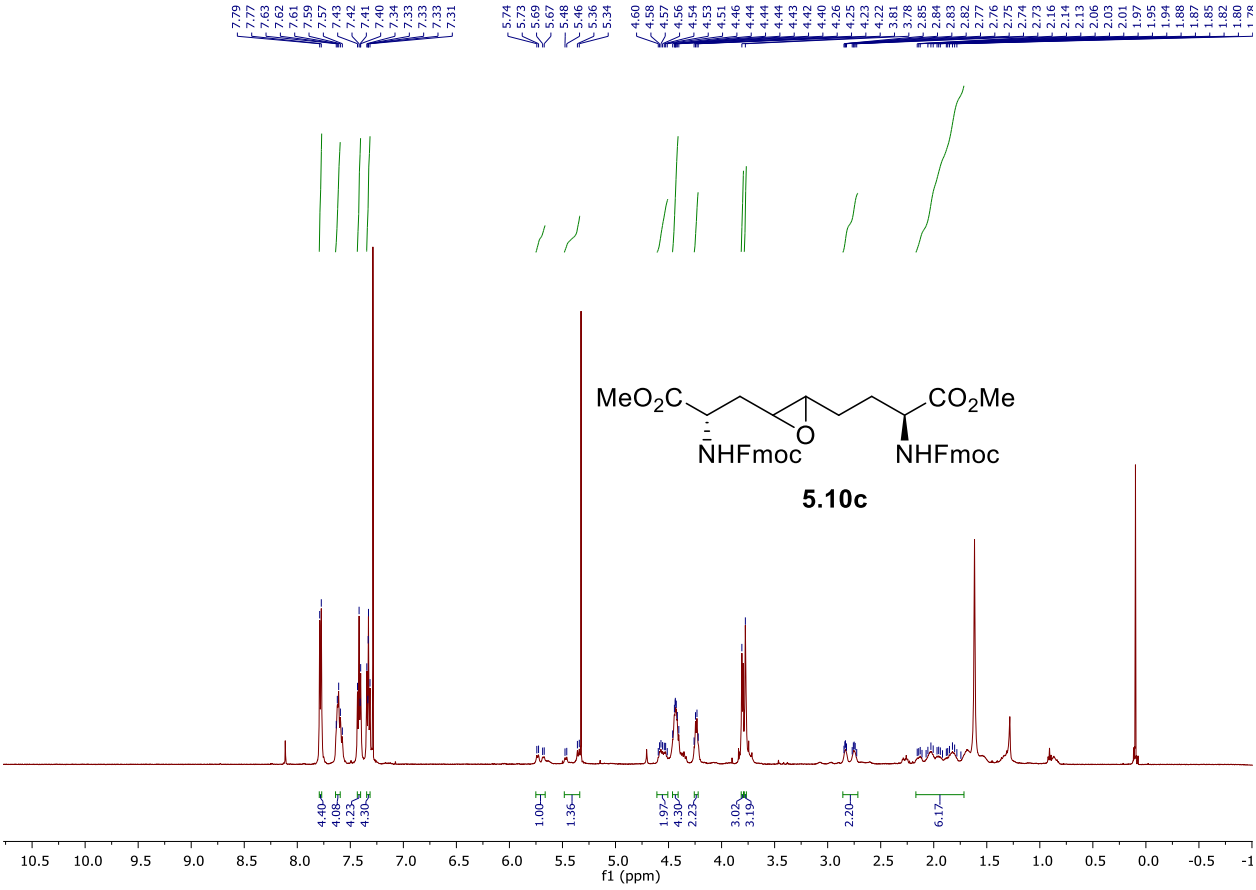

^{13}C NMR, 125 MHz

Solvent: $CDCl_3$

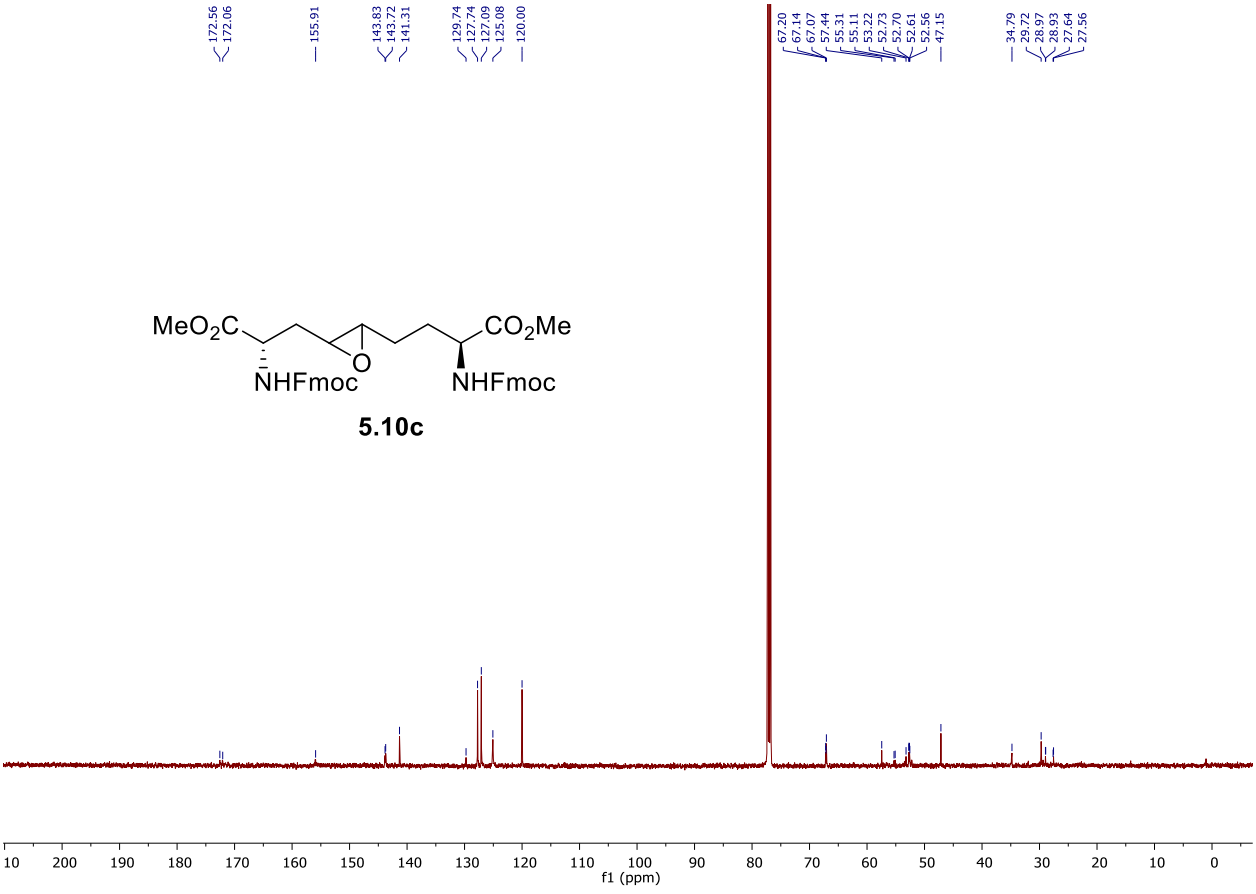

^{1}H NMR, 500 MHz

Solvent: DMSO-D_6

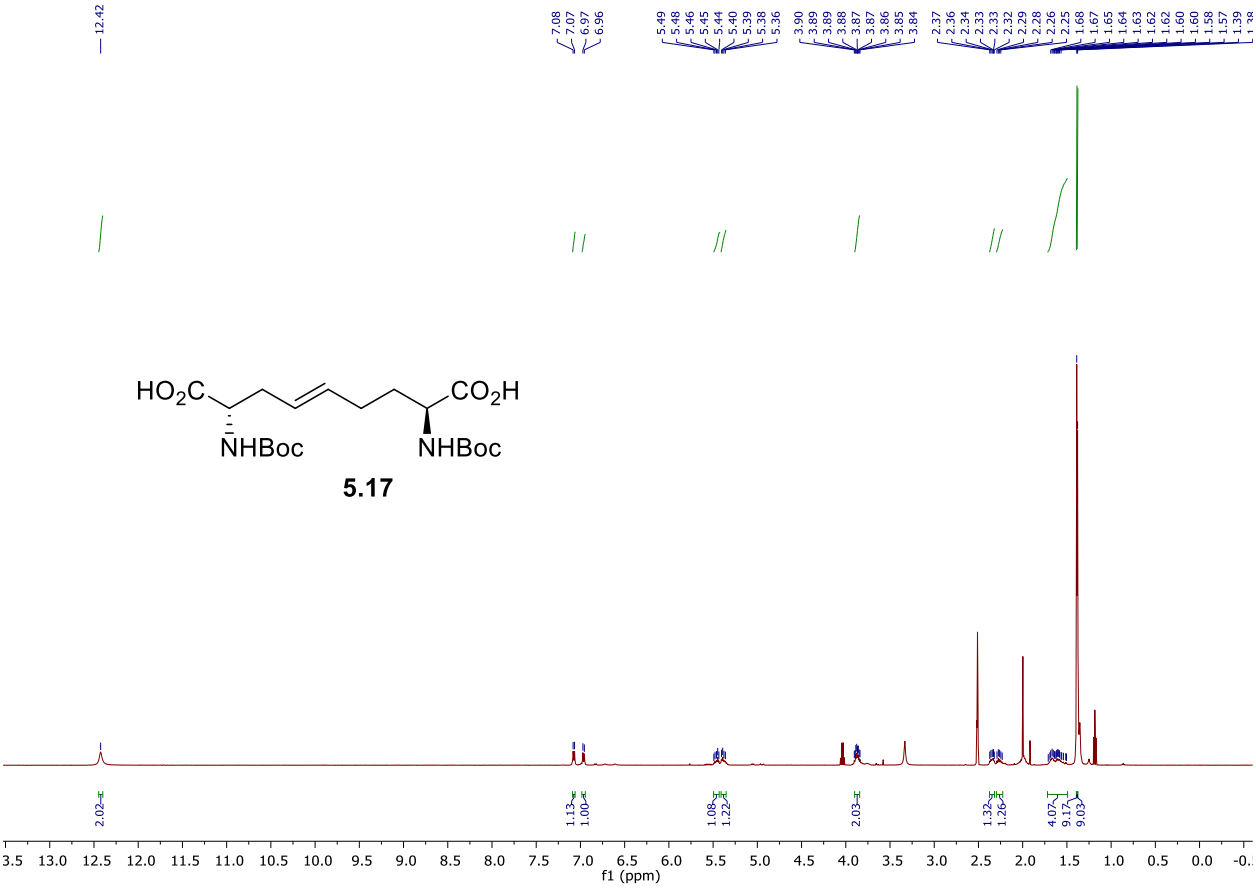

^{13}C NMR, 125 MHz

Solvent: DMSO-D_6

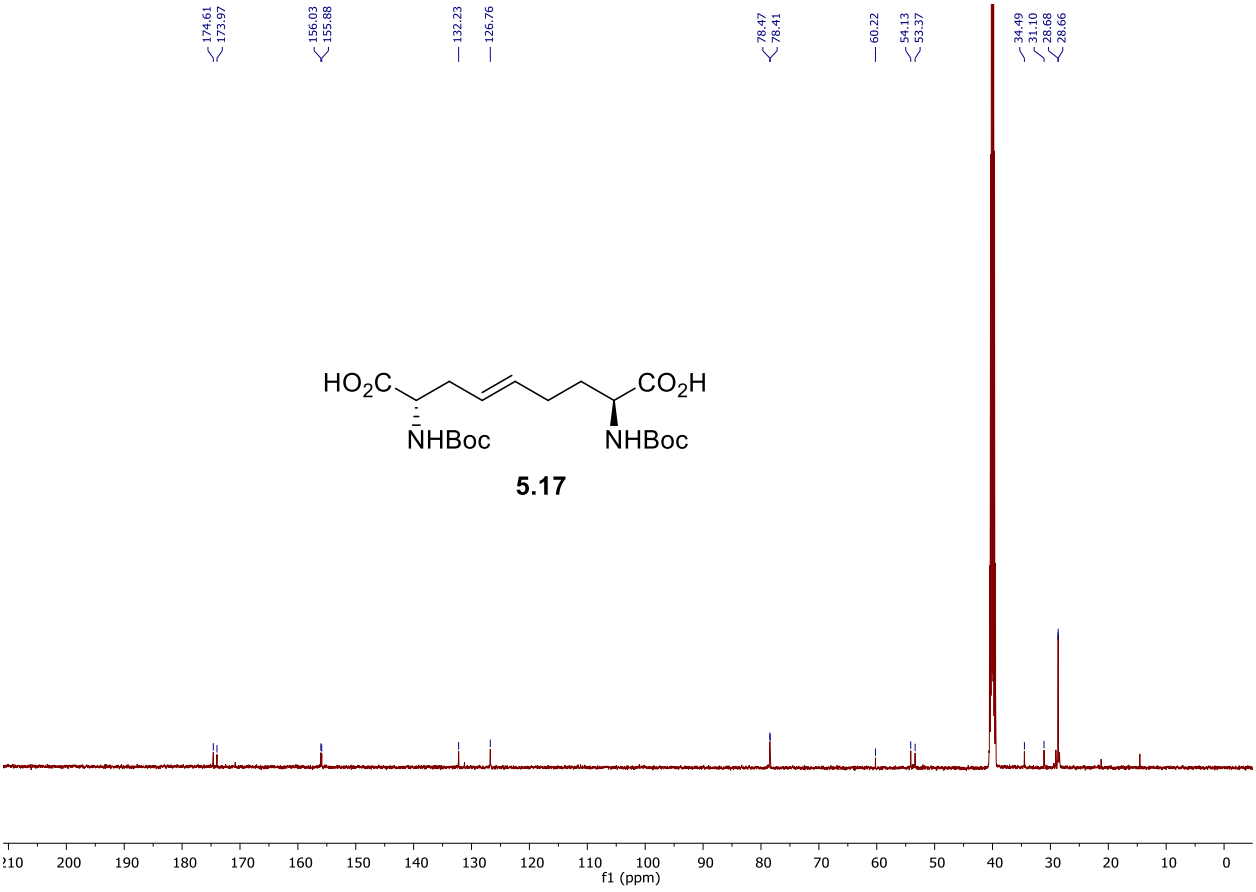

^{1}H NMR, 500 MHz

Solvent: $CDCl_3$

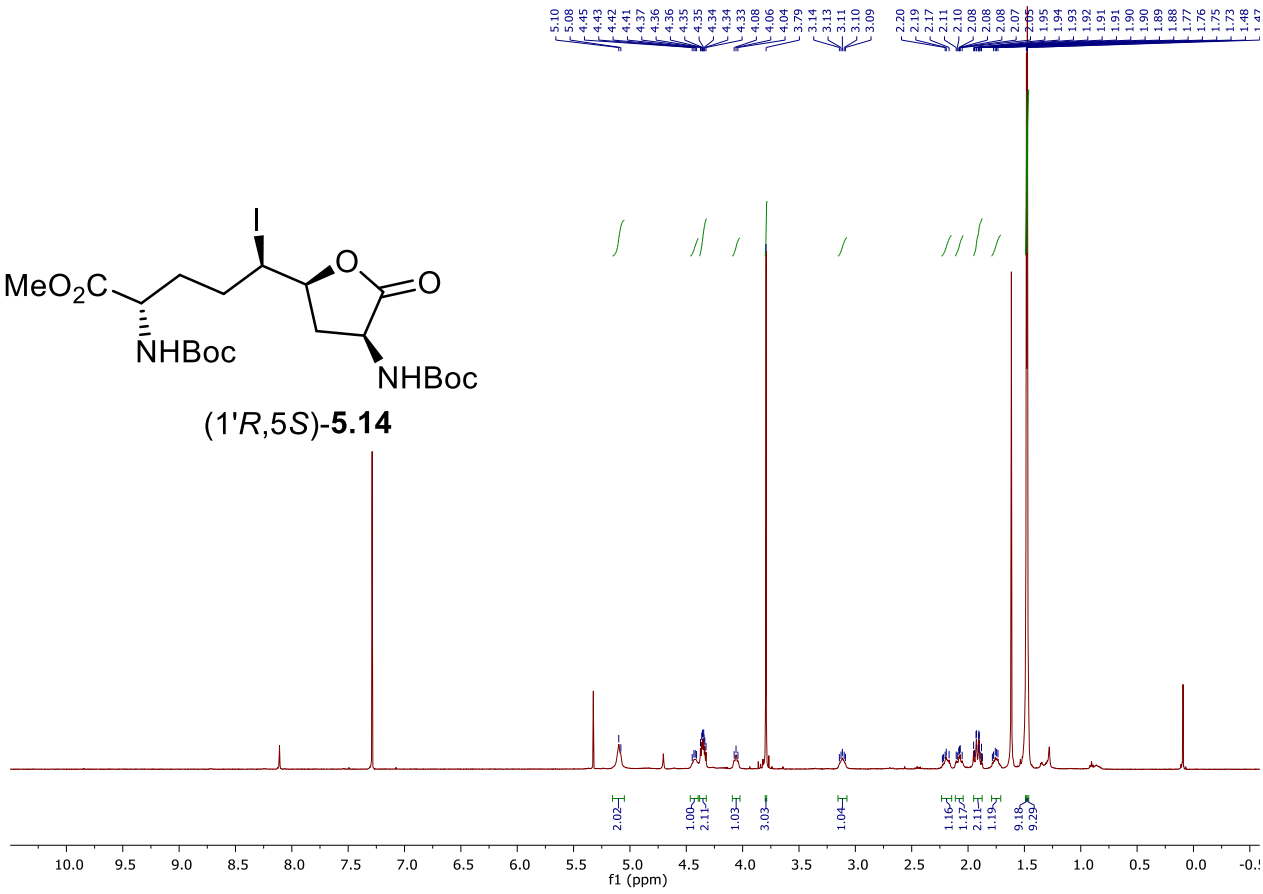

^{13}C NMR, 125 MHz

Solvent: $CDCl_3$

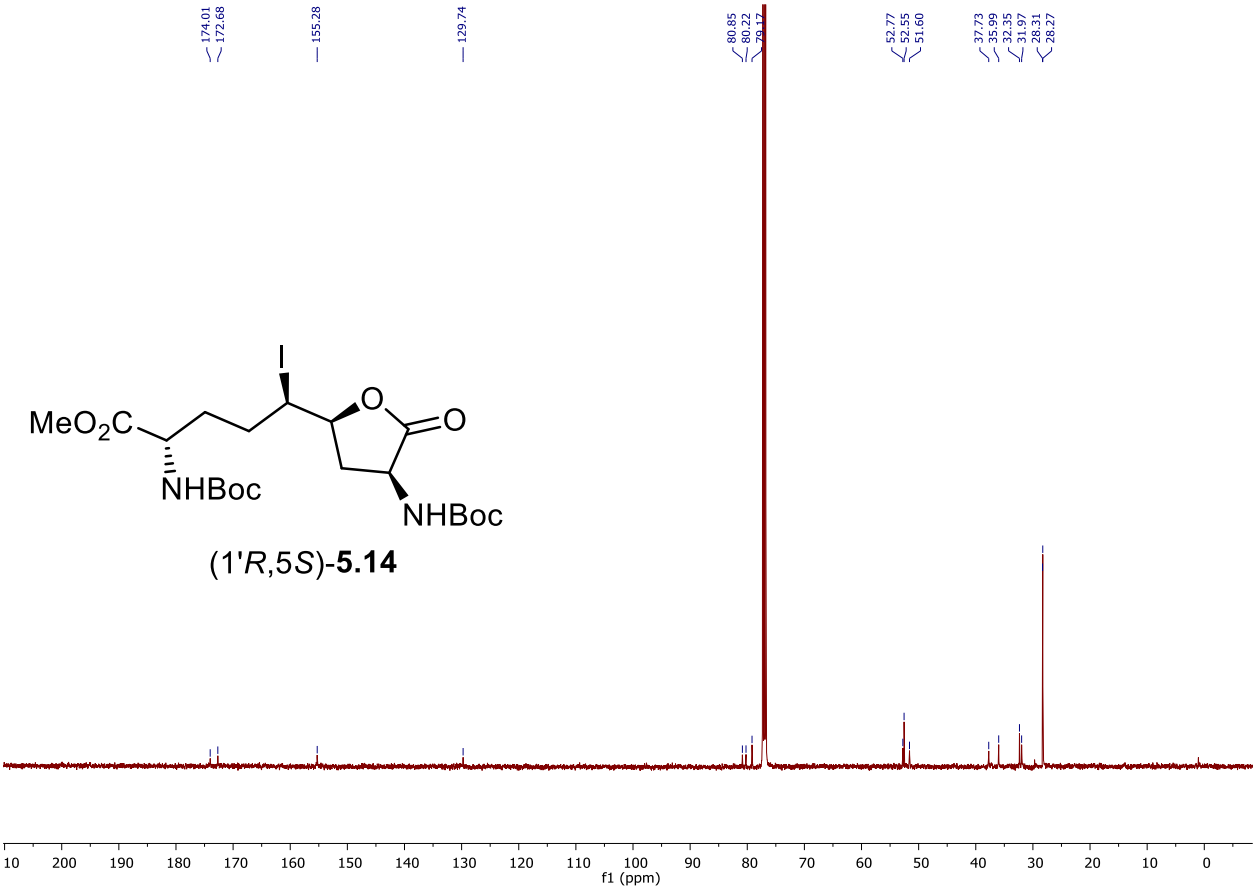

5.9. Crystallography data and molecular structure for compounds

5.9.1. General method for making crystal:

Crystal of azabicyclo[X.Y.Z]alkanones (3*S*,6*S*,7*S*,9*S*)-**5.9** (LUB 1421) was grown from dichloromethane-hexane using the liquid-vapour saturation method.

Methyl 3-*N*-(Boc)amino-7-hydroxy-indolizidin-2-one-9-carboxylate [(3*S*,6*S*,7*S*,9*S*)-5.9, LUB 1421]

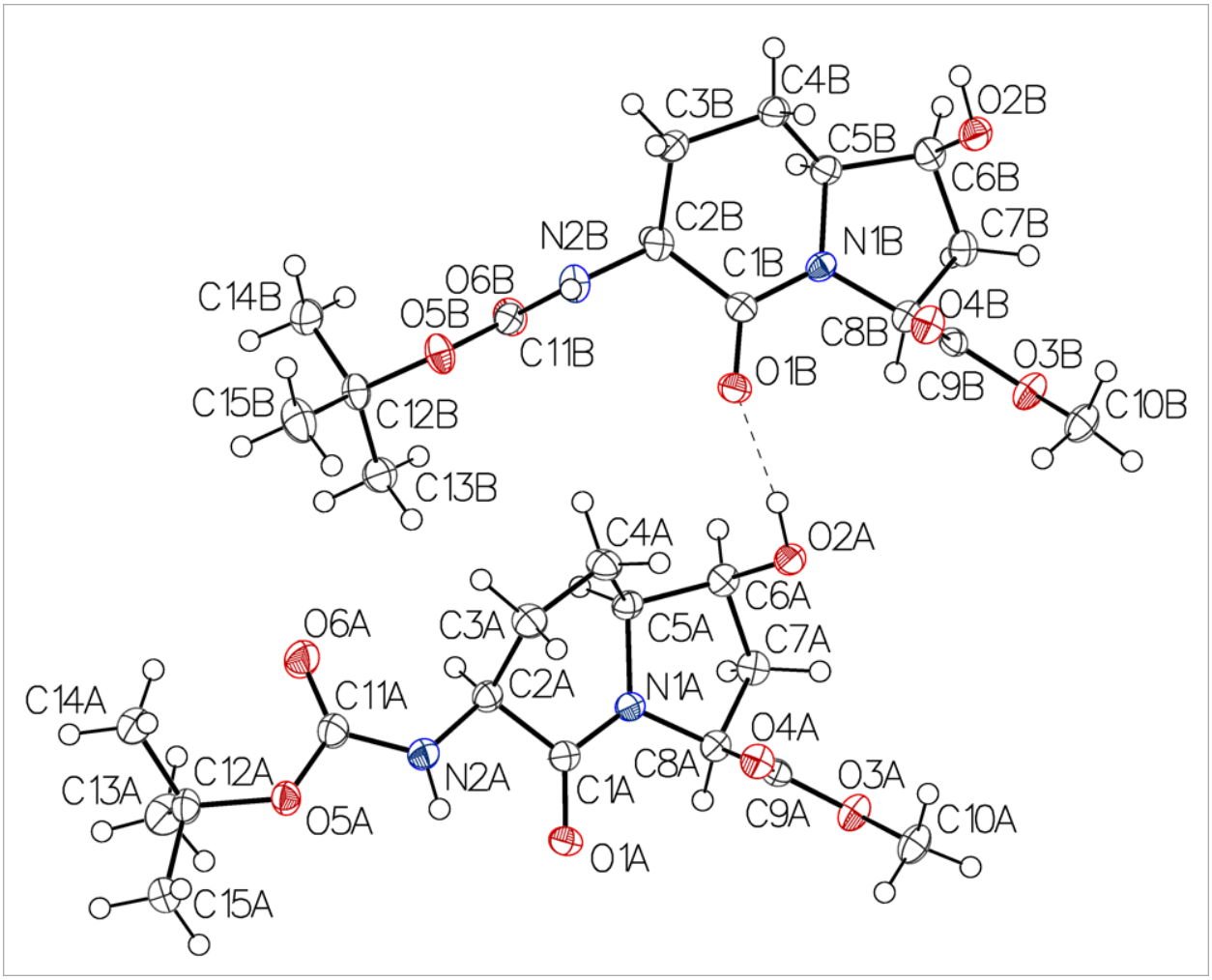

Table 1 Crystal data and structure refinement for lub1421.

Identification code	lub1421

Empirical formula	$C_{15}H_{24}N_2O_6$
Formula weight	328.36
Temperature/K	100
Crystal system	monoclinic
Space group	I2
a/Å	12.8006(6)
b/Å	5.3251(2)
c/Å	48.103(2)
α/°	90
β/°	92.926(2)
γ/°	90
Volume/Å^3	3274.6(2)
Z	8
ρ_{calc}g/cm^3	1.332
μ/mm^{-1}	0.863
F(000)	1408.0
Crystal size/mm^3	0.28 × 0.12 × 0.045
Radiation	Cu Kα (λ = 1.54178)
2Θ range for data collection/°	3.678 to 143.742
Index ranges	$-15 \leq h \leq 15$, $-6 \leq k \leq 5$, $-59 \leq l \leq 59$
Reflections collected	29804
Independent reflections	5590 [R_{int} = 0.0479, R_{sigma} = 0.0375]
Data/restraints/parameters	5590/3/436
Goodness-of-fit on F^2	1.075
Final R indexes [I>=2σ (I)]	R_1 = 0.0355, wR_2 = 0.0887
Final R indexes [all data]	R_1 = 0.0374, wR_2 = 0.0897

Largest diff. peak/hole / e $Å^{-3}$ 0.22/-0.19

Flack parameter 0.05(19)

Table 2 Fractional Atomic Coordinates ($\times 10^4$) and Equivalent Isotropic Displacement Parameters ($Å^2 \times 10^3$) for lub1421. U_{eq} is defined as 1/3 of the trace of the orthogonalised U_{IJ} tensor.

Atom	*x*	*y*	*z*	U(eq)
O1A	7550.5(13)	1894(4)	5970.0(3)	22.0(4)
O4B	1326.4(14)	10777(4)	5623.7(3)	24.2(4)
O2A	3751.2(14)	4584(4)	5634.2(3)	22.6(4)
O1B	2350.8(13)	6095(4)	6002.6(3)	22.9(4)
O6B	1992.0(14)	802(4)	6578.9(4)	24.1(4)
O4A	6277.6(13)	5971(4)	5592.1(3)	22.1(4)
O3B	1325.6(15)	8957(4)	5201.7(3)	24.6(4)
O5A	8555.1(13)	2821(4)	6877.3(3)	23.7(4)
O5B	3065.0(14)	3424(4)	6837.0(3)	24.3(4)
O3A	6095.7(14)	3849(4)	5189.3(3)	24.1(4)
O2B	-1157.5(15)	9343(4)	5610.2(4)	26.0(4)
O6A	6838.2(15)	1781(5)	6924.1(4)	37.4(5)
N1B	633.0(15)	6216(4)	5857.1(4)	18.7(4)
N1A	5775.9(15)	1862(4)	5897.2(4)	18.6(4)
N2B	1860.9(17)	5063(5)	6546.2(4)	22.3(4)
N2A	7440.2(16)	3038(5)	6511.5(4)	24.2(5)
C11B	2285.9(19)	2897(5)	6646.3(5)	19.9(5)
C9B	1163.4(19)	8989(5)	5476.9(5)	18.5(5)

Table 2 Fractional Atomic Coordinates ($\times 10^4$) and Equivalent Isotropic Displacement Parameters ($Å^2 \times 10^3$) for lub1421. U_{eq} is defined as 1/3 of the trace of the orthogonalised U_{IJ} tensor.

Atom	*x*	*y*	*z*	U(eq)
C1A	6657.0(18)	2076(5)	6055.8(5)	18.8(5)
C9A	6063.9(18)	4071(5)	5465.9(5)	18.6(5)
C1B	1418.0(18)	5889(5)	6049.4(5)	18.2(5)
C8A	5756.1(18)	1600(5)	5596.7(5)	19.2(5)
C4B	-658.8(19)	7494(5)	6179.2(5)	22.4(5)
C11A	7547(2)	2444(6)	6785.0(5)	25.3(6)
C12A	8963(2)	1548(5)	7131.2(5)	23.4(5)
C5A	4728.5(18)	2186(5)	6007.3(5)	19.4(5)
C4A	4705(2)	4554(6)	6187.4(5)	24.5(6)
C7A	4623.4(18)	776(5)	5528.7(5)	21.1(5)
C6A	3990.2(19)	2151(5)	5741.2(5)	20.8(5)
C2B	1029.4(19)	5097(5)	6331.4(5)	20.5(5)
C12B	3621(2)	1382(5)	6990.9(5)	23.0(5)
C7B	-311.2(19)	5755(5)	5432.9(5)	21.4(5)
C6B	-1054.4(19)	6698(5)	5647.9(5)	22.5(5)
C2A	6453.0(18)	2637(5)	6358.7(5)	20.9(5)
C8B	783.7(19)	6421(5)	5560.1(5)	18.9(5)
C5B	-473.2(18)	5945(5)	5921.7(5)	19.9(5)
C3A	5719(2)	4906(6)	6371.2(5)	25.1(5)
C3B	98.1(19)	6663(5)	6424.7(5)	21.7(5)
C10A	6431(2)	6085(6)	5048.9(5)	27.7(6)
C14A	8467(2)	2529(6)	7390.1(5)	27.7(6)
C14B	2863(2)	-77(6)	7162.8(5)	29.5(6)

Table 2 Fractional Atomic Coordinates ($\times 10^4$) and Equivalent Isotropic Displacement Parameters ($Å^2 \times 10^3$) for lub1421. U_{eq} is defined as 1/3 of the trace of the orthogonalised U_{IJ} tensor.

Atom	*x*	*y*	*z*	U(eq)
C10B	1712(2)	11258(5)	5087.1(5)	27.1(6)
C15A	10116(2)	2205(6)	7135.9(5)	30.6(6)
C15B	4395(2)	2822(6)	7182.4(6)	33.9(7)
C13B	4199(2)	-272(6)	6793.8(5)	25.7(6)
C13A	8798(3)	-1248(6)	7099.8(6)	34.2(7)

Table 3 Anisotropic Displacement Parameters ($Å^2 \times 10^3$) for lub1421. The Anisotropic displacement factor exponent takes the form: $-2\pi^2[h^2a^{*2}U_{11}+2hka^*b^*U_{12}+\ldots]$.

Atom	U_{11}	U_{22}	U_{33}	U_{23}	U_{13}	U_{12}
O1A	18.2(8)	21.1(10)	26.7(8)	1.1(7)	2.7(6)	1.3(7)
O4B	33.4(10)	16.9(10)	22.4(8)	-0.5(7)	1.9(7)	-2.0(8)
O2A	26.0(9)	19.9(10)	22.3(8)	2.6(7)	5.0(7)	4.5(7)
O1B	19.1(8)	25.5(11)	24.2(8)	-1.2(7)	1.5(6)	2.0(7)
O6B	27.7(9)	16.8(10)	27.3(8)	-0.4(7)	-2.8(7)	-1.4(7)
O4A	26.2(9)	15.5(9)	24.5(8)	-1.0(7)	1.3(6)	-1.2(7)
O3B	35.6(10)	19.3(10)	19.5(8)	0.2(7)	7.4(7)	-2.9(8)
O5A	22.0(9)	26.9(11)	21.9(8)	6.4(8)	-1.3(6)	-3.4(8)
O5B	30.4(10)	16.8(10)	24.9(8)	0.8(7)	-7.4(7)	1.9(8)
O3A	32.8(10)	20.4(10)	19.5(8)	0.0(7)	4.8(7)	-3.1(8)
O2B	29.5(10)	22.8(11)	26.0(9)	5.3(8)	6.2(7)	5.2(8)
O6A	26.8(10)	57.0(15)	28.2(9)	10.1(10)	0.5(7)	-9.5(10)
N1B	20.9(10)	16.8(11)	18.9(9)	0.9(8)	4.1(7)	-1.2(8)

Table 3 Anisotropic Displacement Parameters ($Å^2 \times 10^3$) for lub1421. The Anisotropic displacement factor exponent takes the form: $-2\pi^2[h^2a^{*2}U_{11}+2hka^*b^*U_{12}+\ldots]$.

Atom	U_{11}	U_{22}	U_{33}	U_{23}	U_{13}	U_{12}
N1A	20.0(10)	16.3(11)	19.8(9)	1.4(8)	3.5(7)	1.4(8)
N2B	28.3(11)	16.2(12)	21.8(10)	-0.2(8)	-3.6(8)	-2.2(9)
N2A	20.5(10)	30.0(13)	22.3(10)	3.9(9)	2.0(8)	-2.2(9)
C11B	22.7(12)	19.8(14)	17.4(10)	-0.2(10)	1.9(8)	-0.1(10)
C9B	18.5(11)	17.7(13)	19.1(10)	-0.5(10)	-0.2(8)	3.8(9)
C1A	21.2(12)	12.4(12)	22.9(11)	2.2(9)	3.2(9)	0.1(9)
C9A	17.3(11)	17.1(13)	21.4(11)	-0.4(10)	1.1(8)	2.4(9)
C1B	21.2(12)	12.3(12)	21.2(10)	-2.7(9)	1.5(8)	2.0(9)
C8A	22.4(12)	15.1(13)	20.1(11)	0.0(9)	2.3(9)	-0.1(9)
C4B	22.2(12)	21.2(15)	24.1(11)	4.0(10)	4.5(9)	1.9(10)
C11A	25.3(13)	26.7(16)	23.6(11)	5.3(10)	1.0(9)	-0.8(11)
C12A	27.4(13)	22.9(15)	19.9(11)	3.8(10)	-0.1(9)	1.6(10)
C5A	19.8(11)	17.3(14)	21.3(11)	2.2(10)	4.1(9)	-1.4(9)
C4A	22.6(12)	25.2(16)	25.7(12)	-5.6(11)	1.0(9)	4.1(10)
C7A	24.6(12)	15.5(13)	23.1(11)	-0.9(10)	0.4(9)	-3.2(10)
C6A	22.8(12)	17.4(14)	22.4(11)	0.6(10)	1.9(9)	-2.2(10)
C2B	24.3(12)	15.9(13)	21.1(11)	0.8(9)	0.3(9)	-1.6(10)
C12B	26.8(12)	19.8(15)	22.2(11)	4.4(10)	-2.1(9)	2.2(10)
C7B	25.7(12)	17.8(13)	20.2(11)	1.5(10)	-1.9(9)	-2.6(10)
C6B	21.8(12)	20.0(14)	25.5(11)	3.6(10)	-0.4(9)	-2.9(10)
C2A	21.0(12)	20.9(14)	20.9(11)	2.7(10)	1.6(9)	-2.1(10)
C8B	23.5(12)	15.2(14)	18.0(11)	-0.9(9)	2.3(9)	-0.4(9)
C5B	18.8(11)	17.1(13)	24.1(11)	4.2(10)	3.3(9)	-2.0(10)

Table 3 Anisotropic Displacement Parameters ($Å^2×10^3$) for lub1421. The Anisotropic displacement factor exponent takes the form: $-2π^2[h^2a^{*2}U_{11}+2hka*b*U_{12}+…]$.

Atom	U_{11}	U_{22}	U_{33}	U_{23}	U_{13}	U_{12}
C3A	27.1(13)	23.4(15)	24.7(12)	-5.8(10)	0.4(9)	2.7(11)
C3B	24.5(12)	21.2(14)	19.9(10)	0.7(10)	4.0(9)	0.6(10)
C10A	38.0(14)	23.3(15)	22.3(11)	4.3(11)	6.0(10)	-3.7(12)
C14A	31.6(14)	27.1(16)	24.7(12)	1.0(11)	3.7(10)	-0.5(11)
C14B	32.3(14)	31.0(16)	25.5(12)	6.1(11)	3.8(10)	6.5(12)
C10B	36.7(14)	21.6(15)	23.5(11)	3.5(10)	7.4(10)	-3.3(12)
C15A	27.3(13)	38.5(19)	26.0(12)	5.2(12)	0.5(10)	5.6(12)
C15B	38.6(16)	31.0(17)	30.8(13)	-3.4(13)	-10.1(11)	4.8(13)
C13B	27.2(13)	22.6(15)	27.4(12)	1.5(11)	1.8(10)	1.2(11)
C13A	44.5(17)	24.4(17)	34.2(14)	-0.3(12)	7.6(12)	1.8(13)

Table 4 Bond Lengths for lub1421.

Atom	Atom	Length/Å	Atom	Atom	Length/Å
O1A	C1A	1.239(3)	N2A	C11A	1.353(3)
O4B	C9B	1.197(3)	N2A	C2A	1.445(3)
O2A	C6A	1.421(3)	C9B	C8B	1.512(4)
O1B	C1B	1.231(3)	C1A	C2A	1.523(3)
O6B	C11B	1.216(3)	C9A	C8A	1.519(3)
O4A	C9A	1.204(3)	C1B	C2B	1.528(3)
O3B	C9B	1.351(3)	C8A	C7A	1.534(3)
O3B	C10B	1.441(3)	C4B	C5B	1.517(3)
O5A	C11A	1.358(3)	C4B	C3B	1.553(3)
O5A	C12A	1.469(3)	C12A	C14A	1.519(3)

Table 4 Bond Lengths for lub1421.

Atom	Atom	Length/Å	Atom	Atom	Length/Å
O5B	C11B	1.349(3)	C12A	C15A	1.516(4)
O5B	C12B	1.477(3)	C12A	C13A	1.510(4)
O3A	C9A	1.339(3)	C5A	C4A	1.531(4)
O3A	C10A	1.445(3)	C5A	C6A	1.552(3)
O2B	C6B	1.426(3)	C4A	C3A	1.545(3)
O6A	C11A	1.207(3)	C7A	C6A	1.524(3)
N1B	C1B	1.342(3)	C2B	C3B	1.540(3)
N1B	C8B	1.455(3)	C12B	C14B	1.520(4)
N1B	C5B	1.472(3)	C12B	C15B	1.525(4)
N1A	C1A	1.334(3)	C12B	C13B	1.515(4)
N1A	C8A	1.451(3)	C7B	C6B	1.526(4)
N1A	C5A	1.476(3)	C7B	C8B	1.542(3)
N2B	C11B	1.353(4)	C6B	C5B	1.532(3)
N2B	C2B	1.445(3)	C2A	C3A	1.533(4)

Table 5 Bond Angles for lub1421.

Atom	Atom	Atom	Angle/°	Atom	Atom	Atom	Angle/°
C9B	O3B	C10B	115.9(2)	O5A	C12A	C13A	109.3(2)
C11A	O5A	C12A	119.7(2)	C15A	C12A	C14A	110.9(2)
C11B	O5B	C12B	120.5(2)	C13A	C12A	C14A	111.0(2)
C9A	O3A	C10A	114.6(2)	C13A	C12A	C15A	111.1(2)
C1B	N1B	C8B	123.7(2)	N1A	C5A	C4A	110.1(2)
C1B	N1B	C5B	122.43(19)	N1A	C5A	C6A	103.23(18)

Table 5 Bond Angles for lub1421.

Atom	Atom	Atom	Angle/°	Atom	Atom	Atom	Angle/°
C8B	N1B	C5B	113.05(18)	C4A	C5A	C6A	116.6(2)
C1A	N1A	C8A	123.31(19)	C5A	C4A	C3A	112.5(2)
C1A	N1A	C5A	122.81(19)	C6A	C7A	C8A	104.40(19)
C8A	N1A	C5A	113.47(18)	O2A	C6A	C5A	113.5(2)
C11B	N2B	C2B	122.2(2)	O2A	C6A	C7A	107.89(19)
C11A	N2A	C2A	120.2(2)	C7A	C6A	C5A	103.68(19)
O6B	C11B	O5B	125.4(2)	N2B	C2B	C1B	112.1(2)
O6B	C11B	N2B	125.0(2)	N2B	C2B	C3B	110.6(2)
O5B	C11B	N2B	109.5(2)	C1B	C2B	C3B	113.6(2)
O4B	C9B	O3B	123.9(2)	O5B	C12B	C14B	110.1(2)
O4B	C9B	C8B	127.7(2)	O5B	C12B	C15B	102.4(2)
O3B	C9B	C8B	108.4(2)	O5B	C12B	C13B	110.62(19)
O1A	C1A	N1A	124.8(2)	C14B	C12B	C15B	110.0(2)
O1A	C1A	C2A	122.7(2)	C13B	C12B	C14B	112.9(2)
N1A	C1A	C2A	112.50(19)	C13B	C12B	C15B	110.3(2)
O4A	C9A	O3A	123.9(2)	C6B	C7B	C8B	103.95(19)
O4A	C9A	C8A	125.2(2)	O2B	C6B	C7B	107.2(2)
O3A	C9A	C8A	110.9(2)	O2B	C6B	C5B	113.9(2)
O1B	C1B	N1B	124.1(2)	C7B	C6B	C5B	101.8(2)
O1B	C1B	C2B	123.3(2)	N2A	C2A	C1A	109.12(19)
N1B	C1B	C2B	112.4(2)	N2A	C2A	C3A	112.7(2)
N1A	C8A	C9A	109.7(2)	C1A	C2A	C3A	109.1(2)
N1A	C8A	C7A	102.01(18)	N1B	C8B	C9B	112.8(2)
C9A	C8A	C7A	115.0(2)	N1B	C8B	C7B	102.06(18)

Table 5 Bond Angles for lub1421.

Atom	Atom	Atom	Angle/°	Atom	Atom	Atom	Angle/°
C5B	C4B	C3B	110.4(2)	C9B	C8B	C7B	113.6(2)
O6A	C11A	O5A	126.2(2)	N1B	C5B	C4B	108.2(2)
O6A	C11A	N2A	124.4(2)	N1B	C5B	C6B	102.89(18)
N2A	C11A	O5A	109.3(2)	C4B	C5B	C6B	118.1(2)
O5A	C12A	C14A	112.2(2)	C2A	C3A	C4A	112.4(2)
O5A	C12A	C15A	102.1(2)	C2B	C3B	C4B	113.25(19)

Table 6 Hydrogen Bonds for lub1421.

D	H	A	d(D-H)/Å	d(H-A)/Å	d(D-A)/Å	D-H-A/°
N2B	H2BA	O6B[1]	0.83(3)	2.33(3)	3.065(3)	147(3)
N2A	H2AA	O1A	0.83(3)	2.26(3)	2.686(3)	112(3)
O2A	H2A	O1B	0.92(3)	1.80(3)	2.707(2)	166(4)
O2B	H2B	O1A[2]	0.93(3)	1.88(3)	2.805(3)	172(4)

[1]+X,1+Y,+Z; [2]-1+X,1+Y,+Z

Table 7 Torsion Angles for lub1421.

A	B	C	D	Angle/°	A	B	C	D	Angle/°
O1A	C1A	C2A	N2A	3.2(4)	C8A	C7A	C6A	O2A	85.2(2)
O1A	C1A	C2A	C3A	126.7(3)	C8A	C7A	C6A	C5A	-35.4(2)
O4B	C9B	C8B	N1B	-1.2(4)	C11A	O5A	C12A	C14A	-68.3(3)
O4B	C9B	C8B	C7B	114.4(3)	C11A	O5A	C12A	C15A	173.0(2)
O1B	C1B	C2B	N2B	10.3(4)	C11A	O5A	C12A	C13A	55.3(3)

Table 7 Torsion Angles for lub1421.

A	B	C	D	Angle/°	A	B	C	D	Angle/°
O1B	C1B	C2B	C3B	136.7(3)	C11A	N2A	C2A	C1A	-149.8(3)
O4A	C9A	C8A	N1A	-1.0(3)	C11A	N2A	C2A	C3A	88.9(3)
O4A	C9A	C8A	C7A	113.3(3)	C12A	O5A	C11A	O6A	23.6(4)
O3B	C9B	C8B	N1B	177.18(19)	C12A	O5A	C11A	N2A	-159.2(2)
O3B	C9B	C8B	C7B	-67.2(2)	C5A	N1A	C1A	O1A	-177.7(2)
O3A	C9A	C8A	N1A	177.32(19)	C5A	N1A	C1A	C2A	1.0(3)
O3A	C9A	C8A	C7A	-68.4(3)	C5A	N1A	C8A	C9A	101.5(2)
O2B	C6B	C5B	N1B	-81.6(3)	C5A	N1A	C8A	C7A	-20.8(3)
O2B	C6B	C5B	C4B	37.4(3)	C5A	C4A	C3A	C2A	-7.4(3)
N1B	C1B	C2B	N2B	-172.5(2)	C4A	C5A	C6A	O2A	26.5(3)
N1B	C1B	C2B	C3B	-46.2(3)	C4A	C5A	C6A	C7A	143.3(2)
N1A	C1A	C2A	N2A	-175.5(2)	C6A	C5A	C4A	C3A	-157.1(2)
N1A	C1A	C2A	C3A	-52.0(3)	C2B	N2B	C11B	O6B	-3.6(4)
N1A	C8A	C7A	C6A	34.3(2)	C2B	N2B	C11B	O5B	177.9(2)
N1A	C5A	C4A	C3A	-40.0(3)	C12B	O5B	C11B	O6B	-2.0(4)
N1A	C5A	C6A	O2A	-94.4(2)	C12B	O5B	C11B	N2B	176.4(2)
N1A	C5A	C6A	C7A	22.4(2)	C7B	C6B	C5B	N1B	33.4(3)
N2B	C2B	C3B	C4B	161.7(2)	C7B	C6B	C5B	C4B	152.4(2)
N2A	C2A	C3A	C4A	175.2(2)	C6B	C7B	C8B	N1B	31.5(2)
C11B	O5B	C12B	C14B	-61.8(3)	C6B	C7B	C8B	C9B	-90.3(2)
C11B	O5B	C12B	C15B	-178.8(2)	C2A	N2A	C11A	O5A	175.8(2)
C11B	O5B	C12B	C13B	63.7(3)	C2A	N2A	C11A	O6A	-6.9(5)
C11B	N2B	C2B	C1B	-105.3(3)	C8B	N1B	C1B	O1B	11.2(4)
C11B	N2B	C2B	C3B	126.7(3)	C8B	N1B	C1B	C2B	-165.9(2)

Table 7 Torsion Angles for lub1421.

A	B	C	D	Angle/°	A	B	C	D	Angle/°
C1A	N1A	C8A	C9A	-71.3(3)	C8B	N1B	C5B	C4B	-140.3(2)
C1A	N1A	C8A	C7A	166.4(2)	C8B	N1B	C5B	C6B	-14.7(3)
C1A	N1A	C5A	C4A	46.9(3)	C8B	C7B	C6B	O2B	79.3(2)
C1A	N1A	C5A	C6A	172.0(2)	C8B	C7B	C6B	C5B	-40.6(2)
C1A	C2A	C3A	C4A	53.8(3)	C5B	N1B	C1B	O1B	179.9(2)
C9A	C8A	C7A	C6A	-84.4(2)	C5B	N1B	C1B	C2B	2.8(3)
C1B	N1B	C8B	C9B	-78.4(3)	C5B	N1B	C8B	C9B	112.0(2)
C1B	N1B	C8B	C7B	159.3(2)	C5B	N1B	C8B	C7B	-10.3(3)
C1B	N1B	C5B	C4B	49.9(3)	C5B	C4B	C3B	C2B	16.5(3)
C1B	N1B	C5B	C6B	175.6(2)	C3B	C4B	C5B	N1B	-56.6(3)
C1B	C2B	C3B	C4B	34.5(3)	C3B	C4B	C5B	C6B	-172.8(2)
C8A	N1A	C1A	O1A	-5.5(4)	C10A	O3A	C9A	O4A	1.1(3)
C8A	N1A	C1A	C2A	173.1(2)	C10A	O3A	C9A	C8A	-177.2(2)
C8A	N1A	C5A	C4A	-126.0(2)	C10B	O3B	C9B	O4B	-0.4(4)
C8A	N1A	C5A	C6A	-0.8(3)	C10B	O3B	C9B	C8B	-178.8(2)

Table 8 Hydrogen Atom Coordinates (Å×10^4) and Isotropic Displacement Parameters (Å^2×10^3) for lub1421.

Atom	*x*	*y*	*z*	U(eq)
H8A	6239.25	270.6	5545.35	23
H4BA	-1376.38	7282.16	6230.66	27
H4BB	-549.4	9257.37	6139.45	27
H5A	4573.38	726.23	6122.17	23
H4AA	4114.94	4456.03	6305.87	29

Table 8 Hydrogen Atom Coordinates ($Å \times 10^4$) and Isotropic Displacement Parameters ($Å^2 \times 10^3$) for lub1421.

Atom	*x*	*y*	*z*	U(eq)
H4AB	4602.29	6007.55	6067.62	29
H7AA	4398.15	1255.25	5340.54	25
H7AB	4551.68	-1028.44	5547.83	25
H6A	3346.87	1227.61	5775.02	25
H2BB	779.71	3364.21	6310.28	25
H7BA	-443.64	6592.13	5255.51	26
H7BB	-382.64	3956.39	5405.9	26
H6B	-1735.22	5858.87	5626.53	27
H2AB	6107.62	1179.64	6437.88	25
H8B	1286.8	5146.35	5505.79	23
H5B	-617.82	4176.23	5960.6	24
H3AA	6081.71	6391.69	6310.36	30
H3AB	5539.9	5172.04	6562.42	30
H3BA	363.07	8145.31	6522.03	26
H3BB	-288.87	5681.9	6554.72	26
H10A	6374.44	5821.42	4851.3	42
H10B	7144.83	6446.39	5105.7	42
H10C	5995.74	7472.79	5096.47	42
H14A	8598.73	4297.52	7408.3	42
H14B	8762.57	1670.46	7551.02	42
H14C	7726.12	2238.64	7374.51	42
H14D	2508.48	1060.71	7280.92	44
H14E	3241.47	-1295.14	7275.13	44

Table 8 Hydrogen Atom Coordinates (Å×10^4) and Isotropic Displacement Parameters (Å^2×10^3) for lub1421.

Atom	*x*	*y*	*z*	U(eq)
H14F	2358.9	-917.08	7040.78	44
H10D	1850.96	11005.95	4894.88	41
H10E	2344.96	11746.61	5188.38	41
H10F	1196.57	12555.37	5101.73	41
H15A	10409.41	1603.72	6968.64	46
H15B	10470.36	1432.51	7294.41	46
H15C	10197.73	3994.41	7147.44	46
H15D	4847.79	3804.39	7072.35	51
H15E	4804.45	1656.59	7294.35	51
H15F	4019	3911.96	7301	51
H13D	3703.54	-1105.05	6668.69	39
H13E	4600.66	-1501.31	6898.69	39
H13F	4657.9	742.4	6689.03	39
H13A	8066.14	-1622.85	7106.63	51
H13B	9177.75	-2108.67	7248.39	51
H13C	9045.12	-1789.62	6924.53	51
H2BA	2120(30)	6440(60)	6595(7)	41
H2AA	7960(20)	3080(80)	6414(6)	41
H2A	3290(30)	5360(70)	5748(7)	41
H2B	-1620(30)	10060(80)	5731(7)	41

Experimental

Single crystals of $C_{15}H_{24}N_2O_6$ [lub1421] were []. A suitable crystal was selected and [mounted on a Mitegen microloop (M8-50V)] on a Bruker Smart APEX diffractometer. The crystal was kept at 100 K during data collection. Using Olex2 [1], the structure was solved with

the XT [2] structure solution program using Intrinsic Phasing and refined with the XL [3] refinement package using Least Squares minimisation.

1. Dolomanov, O.V., Bourhis, L.J., Gildea, R.J, Howard, J.A.K. & Puschmann, H. (2009), J. Appl. Cryst. 42, 339-341.
2. Sheldrick, G.M. (2015). Acta Cryst. A71, 3-8.
3. Sheldrick, G.M. (2008). Acta Cryst. A64, 112-122.

Crystal structure determination of [lub1421]

Crystal Data for $C_{15}H_{24}N_2O_6$ (M =328.36 g/mol): monoclinic, space group I2 (no. 5), a = 12.8006(6) Å, b = 5.3251(2) Å, c = 48.103(2) Å, β = 92.926(2)°, V = 3274.6(2) Å^3, Z = 8, T = 100 K, μ(Cu Kα) = 0.863 mm^{-1}, *Dcalc* = 1.332 g/cm^3, 29804 reflections measured (3.678° ≤ 2Θ ≤ 143.742°), 5590 unique (R_{int} = 0.0479, R_{sigma} = 0.0375) which were used in all calculations. The final R_1 was 0.0355 (I > 2σ(I)) and wR_2 was 0.0897 (all data).

Refinement model description

Number of restraints - 3, number of constraints - unknown.

Details:

1. Twinned data refinement
Scales: 0.95(19)
0.05(19)
2. Fixed Uiso
At 1.2 times of:
All C(H) groups, All C(H,H) groups, All C(H,H,H,H) groups
At 1.5 times of:
All C(H,H,H) groups
3. Restrained distances
H2A-O2A ≈ H2B-O2B
with sigma of 0.02
H2BA-N2B ≈ H2AA-N2A
with sigma of 0.02
4.a Ternary CH refined with riding coordinates:

C8A(H8A), C5A(H5A), C6A(H6A), C2B(H2BB), C6B(H6B), C2A(H2AB), C8B(H8B), C5B(H5B)

4.b Secondary CH2 refined with riding coordinates:

C4B(H4BA,H4BB), C4A(H4AA,H4AB), C7A(H7AA,H7AB), C7B(H7BA,H7BB), C3A(H3AA, H3AB), C3B(H3BA,H3BB)

4.c Idealised Me refined as rotating group:

C10A(H10A,H10B,H10C), C14A(H14A,H14B,H14C), C14B(H14D,H14E,H14F), C10B(H10D, H10E,H10F), C15A(H15A,H15B,H15C), C15B(H15D,H15E,H15F), C13B(H13D,H13E,H13F), C13A(H13A,H13B,H13C